Preface

This study was conducted jointly by the Radiation Laboratory of The University of Michigan under the direction of Dr. Thomas B.A. Senior and the supervision of Dr. Valdis V. Liepa, and by Mr. Robert L. Frank, P.E., Consultant, subcontractor to the University of Michigan.

Dr. Surendra Samaddar and Mr. Jack Ligon were successively the USCG Project Engineers. They, as well as Mr. Robert Schellhase, were helpful in providing unpublished and informal Loran-C test data for comparison with model test data. Mr. Burt Gambil and Mr. John Illgen of Kaman-Tempo and Mr. Walter Dean furnished additional information on the Loran-C signal analysis tests. Commander William Schorr, USCG, informally reviewed the bibliography and suggested several listings. Additional information on suspension bridges was supplied by Mr. Thomas Dagnell of the Ambassador Bridge, information on long span power lines by Mr. W. J. Thresher of the Detroit Edison Co. and Mr. R. Broad of Commonwealth Associates, and information on shielding by overhead wires by Dr. D. Deno of the General Electric Company. Information on broadcast band reradiation was provided by Dr. J. S. Belrose of the Communications Research Center, Department of Communications, Canada, and by Mr. O. L. Prestholdt of Ring Associates.

METRIC CONVERSION FACTORS

Approximate Conversions to Metric Measures

Symbol	When You Know	Multiply by	To Find	Symbol
	LENGTH			
in	inches	*2.5	centimeters	cm
ft	feet	30	centimeters	cm
yd	yards	0.9	meters	m
mi	miles	1.6	kilometers	km
	AREA			
in^2	square inches	6.5	square centimeters	cm^2
ft^2	square feet	0.09	square meters	m^2
yd^2	square yards	0.8	square meters	m^2
mi^2	square miles	2.6	square kilometers	km^2
	acres	0.4	hectares	ha
	MASS (weight)			
oz	ounces	28	grams	g
lb	pounds	0.45	kilograms	kg
	short tons (2000 lb)	0.9	tonnes	t
	VOLUME			
tsp	teaspoons	5	milliliters	ml
Tbsp	tablespoons	15	milliliters	ml
fl oz	fluid ounces	30	milliliters	ml
c	cups	0.24	liters	l
pt	pints	0.47	liters	l
qt	quarts	0.95	liters	l
gal	gallons	3.8	liters	l
ft^3	cubic feet	0.03	cubic meters	m^3
yd^3	cubic yards	0.76	cubic meters	m^3
	TEMPERATURE (exact)			
°F	Fahrenheit temperature	5/9 (after subtracting 32)	Celsius temperature	°C

*1 in = 2.54 (exactly). For other exact conversions and more detailed tables, see NBS Misc. Publ. 286, Units of Weights and Measures, Price $2.25, SD Catalog No. C13.10:286.

Approximate Conversions from Metric Measures

Symbol	When You Know	Multiply by	To Find	Symbol
	LENGTH			
mm	millimeters	0.04	inches	in
cm	centimeters	0.4	inches	in
m	meters	3.3	feet	ft
m	meters	1.1	yards	yd
km	kilometers	0.6	miles	mi
	AREA			
cm^2	square centimeters	0.16	square inches	in^2
m^2	square meters	1.2	square yards	yd^2
km^2	square kilometers	0.4	square miles	mi^2
ha	hectares (10,000 m^2)	2.5	acres	
	MASS (weight)			
g	grams	0.035	ounces	oz
kg	kilograms	2.2	pounds	lb
t	tonnes (1000 kg)	1.1	short tons	
	VOLUME			
ml	milliliters	0.03	fluid ounces	fl oz
l	liters	2.1	pints	pt
l	liters	1.06	quarts	qt
l	liters	0.26	gallons	gal
m^3	cubic meters	35	cubic feet	ft^3
m^3	cubic meters	1.3	cubic yards	yd^3
	TEMPERATURE (exact)			
°C	Celsius temperature	9/5 (then add 32)	Fahrenheit temperature	°F

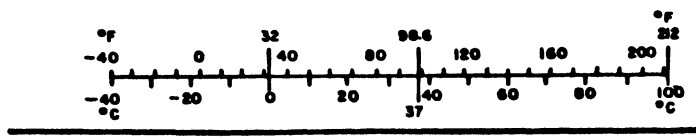

TABLE OF CONTENTS

LIST OF ILLUSTRATIONS

LIST OF TABLES

1. Introduction

As part of the Federal Radio Navigation Plan, Loran-C is being studied and evaluated by the U.S. Coast Guard for use in harbors, harbor approaches and river estuaries. The connecting waters and harbors of the Great Lakes are considered part of this plan.

It has been observed that Loran-C errors of significant magnitude are encountered near large bridges such as the Golden Gate Bridge, with correspondingly smaller and more localized errors near smaller bridges. The errors are attributable to "reradiation" or "scattering" of the signal produced by the currents induced in the conducting structures. The purpose of the present study was to explain and quantify these errors using measurements made with a small scale model of a bridge over a river estuary.

For several years the Radiation Laboratory has operated a specially designed facility for swept-frequency measurements of the amplitude and phase of fields on and near structures illuminated by a plane electromagnetic wave. Since the frequency can be swept over a wide range, one model can simulate a variety of electrical sizes. Continuous waves are used rather than pulses as in the actual Loran-C system, but because of the narrow bandwidth of Loran-C signals, a close correspondence is expected.

In the first part (Chapters 2 through 4) of this report, the facility, bridge model and measurement procedures are described. The results of numerous measurements are then presented in the form of data curves as functions of frequency for various incidence

(illumination) angles and measurement locations with respect to the bridge. The second part (Chapters 5 through 11) starts with a survey of LF and MF reradiation and related effects. Typical bridges and power lines across navigable waters are described, and scale factors are given relating the model to actual bridges at the Loran-C frequency. The model data are then analyzed and discussed, and compared to actual Loran-C observations. Some data for modified bridge models are also presented, and conclusions are drawn. An extensive annotated bibliography and a list of references are provided.

2. Experimental Set-Up

2.1 Facility. The measurements were made in the Radiation Laboratory's surface (and near) field facility, a block diagram of which is shown in Fig. 2.1. The system is a cw one in which the frequency is swept (stepped) over a wide range, and a key part of the facility is a tapered anechoic chamber approximately 50 feet in length. The rectangular test region is 18 feet wide and 12 feet high. The rear wall is covered with 72-inch high-performance pyramidal absorber, with 18-inch material used on the side walls, floor and ceiling. The material in the tapered section (or throat) is 2-inch hairflex absorber. The chamber can be thought of as a lossy-wall horn antenna terminated by the rear wall. The signal is launched from a single exponentially-tapered broadband antenna located at the apex of the chamber. The antenna is fixed and since the radiated signal is horizontally polarized, the pseudo plane wave in the center ('quiet zone') portion of the test region is also horizontally polarized.

The instrumentation is centered around a Hewlett-Packard 8410B network analyzer, and is computer controlled. An HP9830A calculator controls the frequency to be generated, switches in the appropriate power amplifiers and low-pass filters, and reads and stores the amplitude and phase of the signal picked up by the sensor. During a run, the frequencies are typically stepped from 118 to 4400 MHz. Because of the limited memory size of the calculator, this frequency range is recorded in four bands: 118 to 550 MHz (in 4.8 MHz steps), 550 to 1100 MHz (in 4.8 MHz steps),

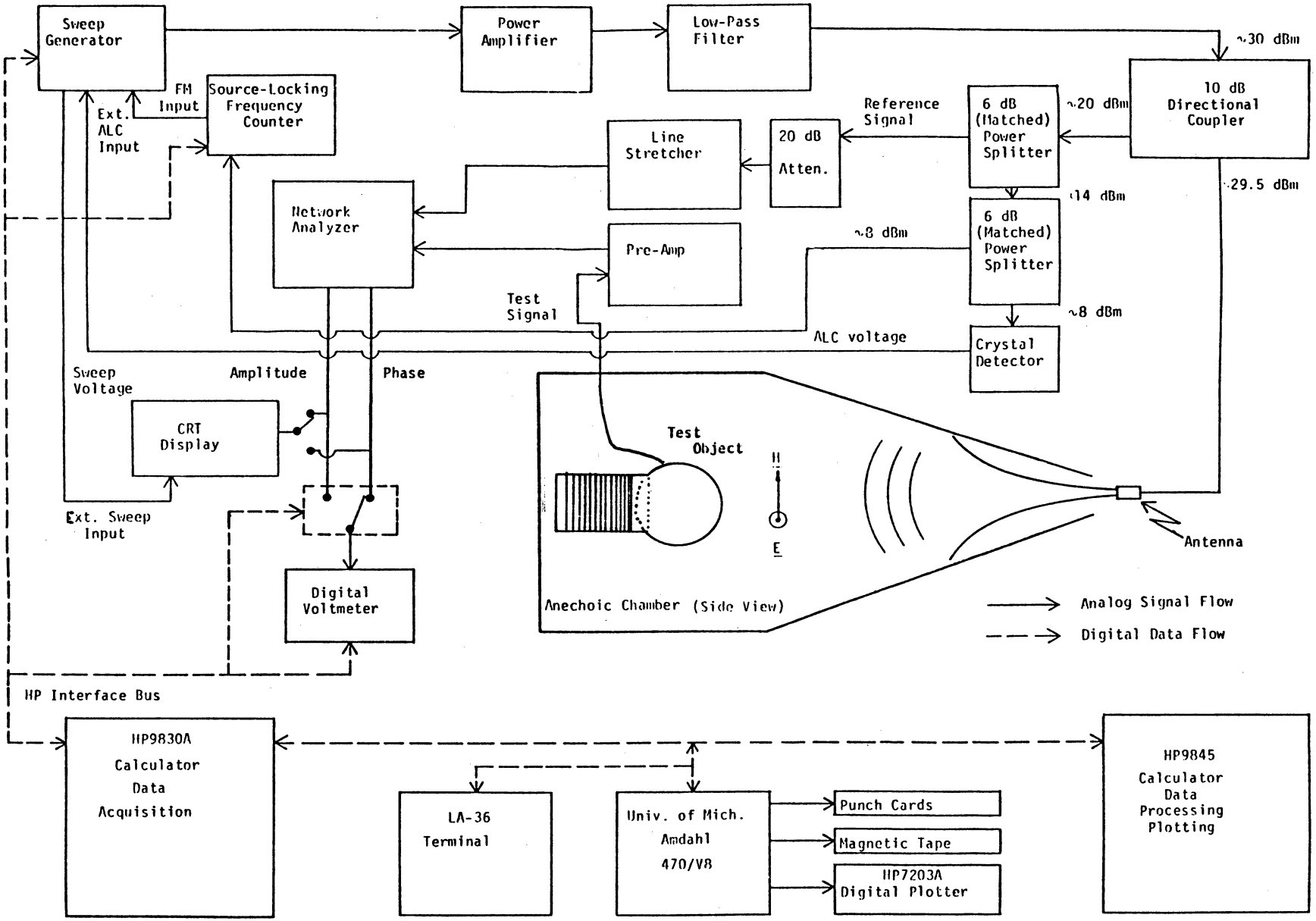

Fig. 2.1: Block diagram of the facility.

1100 to 2000 MHz (in 9.6 MHz steps), and 2000 to 4400 MHz (in 16 MHz steps). The data from each band are stored by the HP9830A calculator on a cassette for later transfer to an HP9845B calculator which processes and plots the data. If substantial processing or computation is involved, or if a need exists to write the data on standard computer tape, the data are transmitted to the central University of Michigan AMDAHL/V8 (IBM compatible) computer.

The signal measured by the network analyzer is a function not only of the model being tested but also of the entire facility, including the probe, chamber, antenna, amplifiers and cabling, and it would be a virtually impossible task to separate and to correct for the contributions of each. The approach taken is to apply an appropriate calibration or normalization whereby the response of the facility and instrumentation are, in principle and practice, eliminated. In short, a measurement is made with the model bridge in place (test measurement) and then repeated without the bridge (calibration); the ratio of the two gives the normalized response of the bridge.

2.2 Modelling. There are two aspects to the modelling: the design and construction of the ground plane and the bridge model itself.

As mentioned above, the anechoic chamber simulates a free space environment, and since it would require considerable modification to create a ground plane chamber, it was necessary to construct a ground plane that could be inserted into the rectangular test region of the present chamber as indicated in Fig.2.1. An actual

Loran-C excitation is vertically polarized, i.e., the incident electric vector is vertical, and its bearing relative to a bridge can be arbitrary. In our chamber, however, the incident field is fixed in direction and is horizontally polarized. It is therefore necessary to have the ground plane vertical, with the capability of rotating the bridge relative to the incident field.

For the reasons given below, we chose a circular aluminum ground plane with a resistive sheet extension as shown in Fig. 2.2. The aluminum disk is 1.53 m (5 ft) in diameter and is supported vertically by a wooden stand at a height midway between the floor and ceiling of the chamber, aligned such that the incident field is almost edge-on to the disk. In Fig. 2.2, the incidence is from the right with the electric vector pointing out of the page. In practice, because of the small stray (scattered) signals that are always present in a measurement situation, the ground plane was rotated five degrees anticlockwise (about a vertical axis) to produce a uniform excitation over the working area of the disk.

It was our original intent to permanently attach the bridge to the ground plane and to produce the different excitations by rotating the aluminum disk about a horizontal axis. This proved to be impractical, partly because of slight warping and irregularities in the ground plane, but more because of the sheer size and weight of the structure. It was therefore decided to keep the disk stationary and permit the rotation of the bridge in discrete amounts.

Although the disk was not rotated as originally planned, it is believed that the circular shape is still desirable. With any

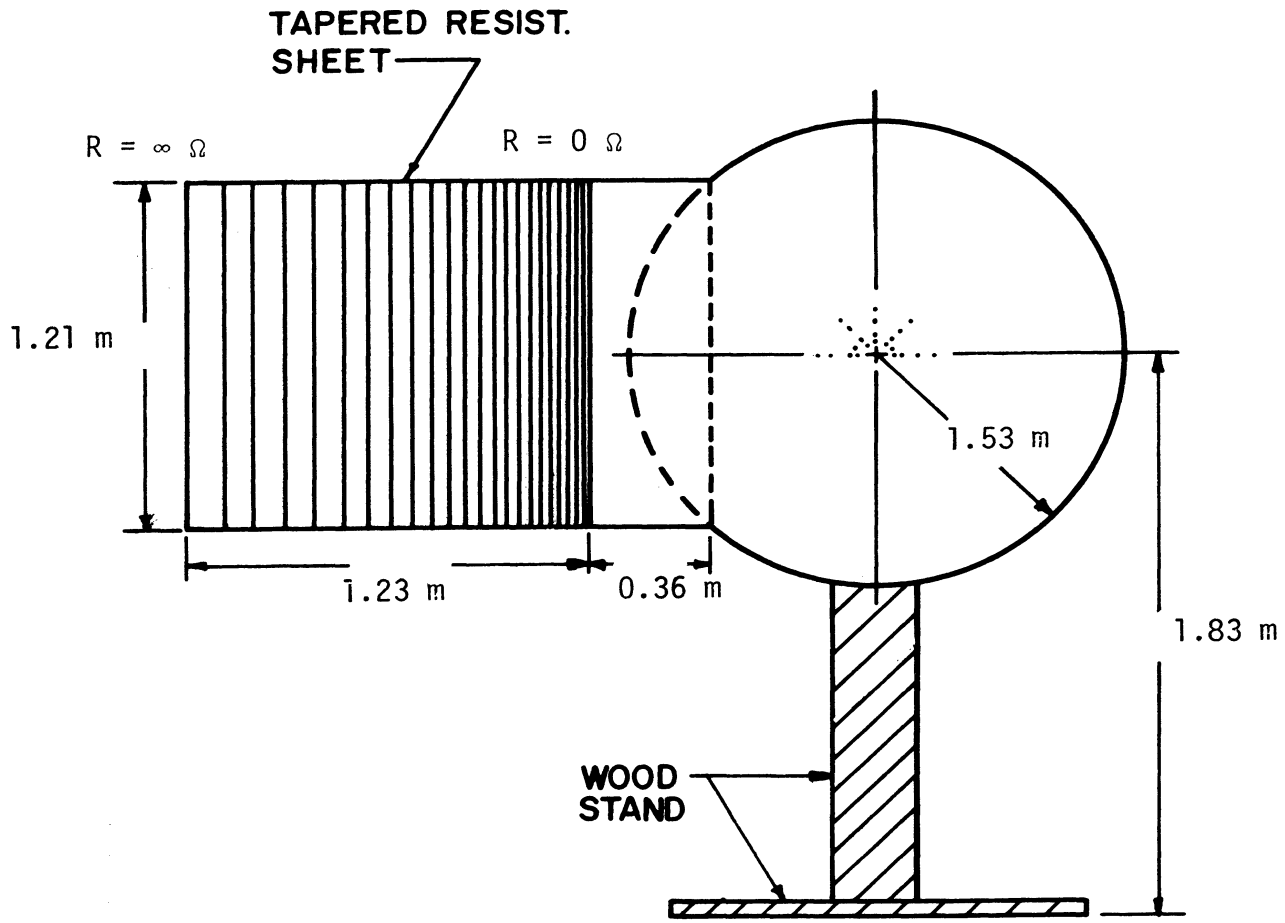

Fig. 2.2: Circular ground plane configuration with resistive sheet extension.

finite ground plane there is the possibility of edge waves which can perturb the uniform field characteristic of an infinite structure, and when the bridge is introduced, an edge-model interaction can occur which would not be eliminated by the field normalization employed. By virtue of the circular geometry, whatever interaction does occur should, to a first order, be independent of the bridge rotation.

The measurements were all performed with the plane wave incident at five degrees to edge-on. Under these circumstances, the main source of any edge-model interaction is the rear edge of the disk which can reflect waves traveling across the surface. To minimize such reflections, a resistive sheet structure was built and attached to the rear edge as shown in Fig. 2.2. The sheet was curved into the page (from right to left) in Fig. 2.2 and was constructed by applying layers of resistive paint to art paper with a wooden support. By varying the paint thickness the resistivity could be controlled, and the final structure had a resistivity which started at about 10 ohms/square at the metal edge and increased linearly to about 1000 ohms/square at the outer (left-hand) edge.

The bridge model is illustrated in Fig. 2.3 which shows the dimensions. It was designed to represent a generic class of large suspension bridges and was chosen to model approximately the Golden Gate Bridge on a scale of 1:4250. The model is 50.56 cm (approximately 20 inches) long and was machined out of 0.25 inch thick aluminum plate. A "solid" bridge, rather than an "open" one built of wires and rods that would model a suspension bridge in more detail,

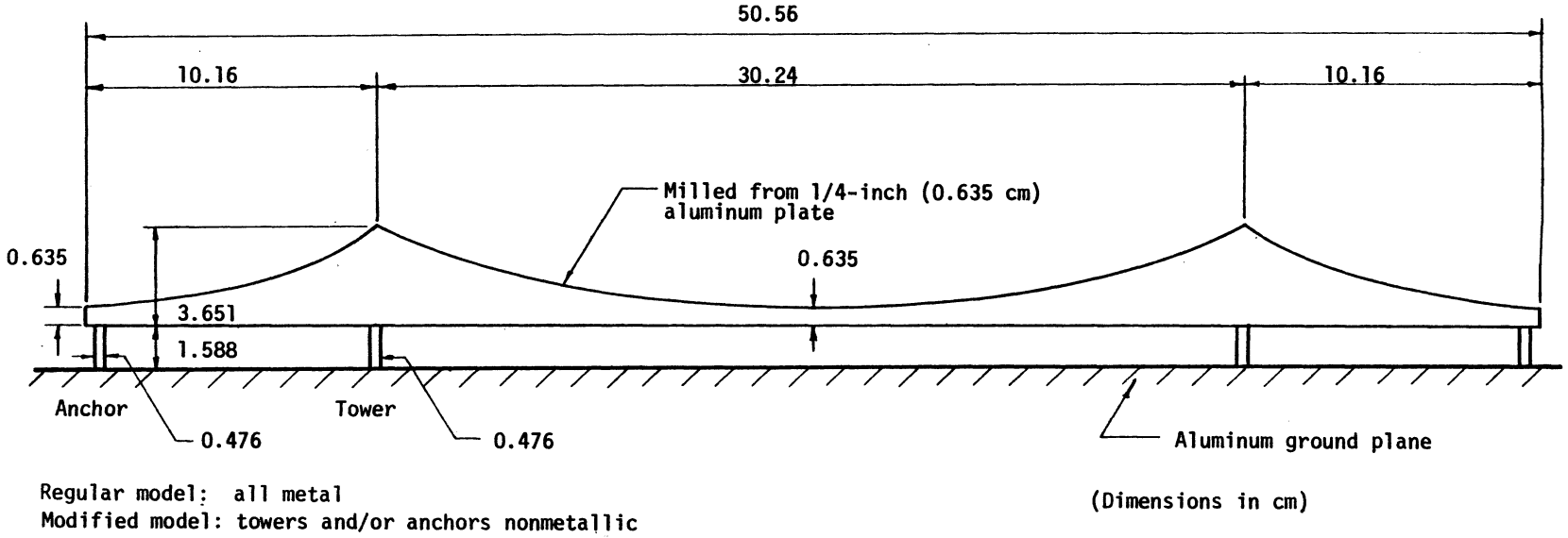

Fig. 2.3: Bridge model used in the measurements.

was chosen for ease of construction and to ensure the ruggedness necessary for frequent re-positioning on the ground plane. At the frequencies of interest there should be no electrical differences between the two since the wire spacing is so small compared with the wavelength. The worst case situation occurs at the highest frequency (550 MHz), and the largest "cell" formed by two adjacent wires, the roadway and the suspension cable is then only 0.05 wavelengths long.

To attach the bridge to the ground plane, the ends of the anchors and towers were threaded and passed through holes drilled in the plane. The bridge was then secured by nuts which bit into the rear of the plane to ensure good electrical contact. In practice it took only a few minutes to remove and then remount the bridge. In addition, a set of nylon towers and anchors was also constructed to produce a modified bridge, all or part of which could be insulated from the ground plane.

3. Measurements

Figure 3.1 depicts the central portion of the ground plane and shows (dashed boxes) the four positions where the bridge was mounted and the holes drilled to accommodate the monopole (field sensing) probe. Because of symmetry it is sufficient to measure the field over a semicircular region only, and no holes were drilled in the lower half of the plane. For any given measurement all holes except that containing the probe were covered with metallic tape to eliminate any effect on the field. A detailed dimensional drawing of the probe is given in Fig. 3.2, and Fig. 3.3 shows the bridge with a probe in place.

Since the direction of illumination is fixed, the four positions of the bridge simulated four different directions of incidence, i.e., positions of the transmitter with respect to the bridge. The measurement procedure is as follows. With the probe mounted at a selected location, the field is recorded without the bridge present to provide the incident field or calibration measurement. The bridge is then attached and the measurement repeated, and in many cases the measurements were performed with the bridge in each of its four positions, with the same calibration run used for all of them. The ratio of the bridge measurements to the calibration data gives the normalized bridge response, i.e., the transfer function of the bridge.

The measurements were all made over the band 118 to 550 MHz sampled 4.8 MHz apart. This is sufficient to embrace most bridges at the Loran-C frequency. When converted to full scale, the data cover bridges from 0.3 to 1.3 times the Golden Gate Bridge in

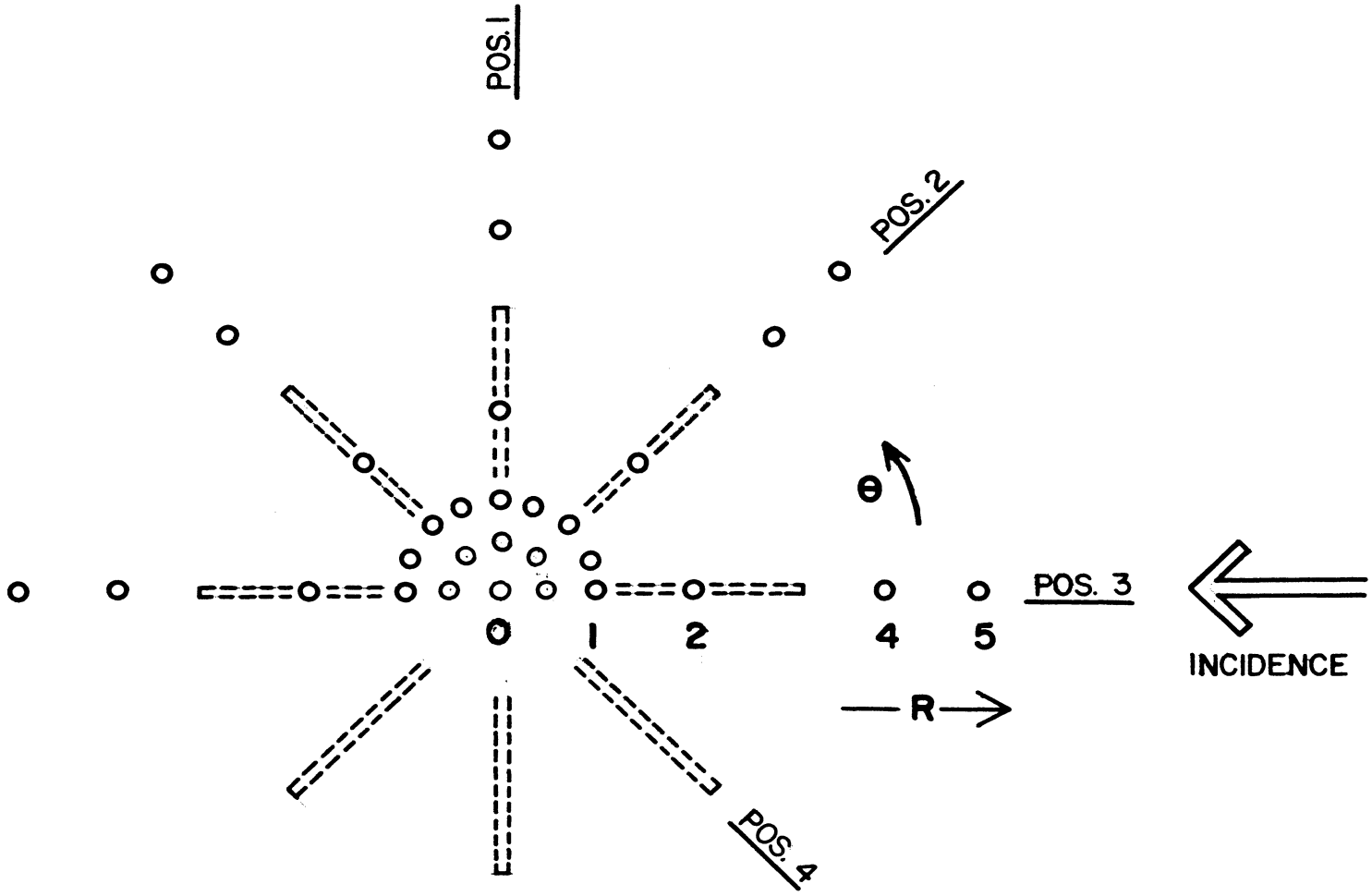

Fig. 3.1: The measurement locations and the permissible bridge positions on the ground plane.
(R = 1 represents 8 cm.)

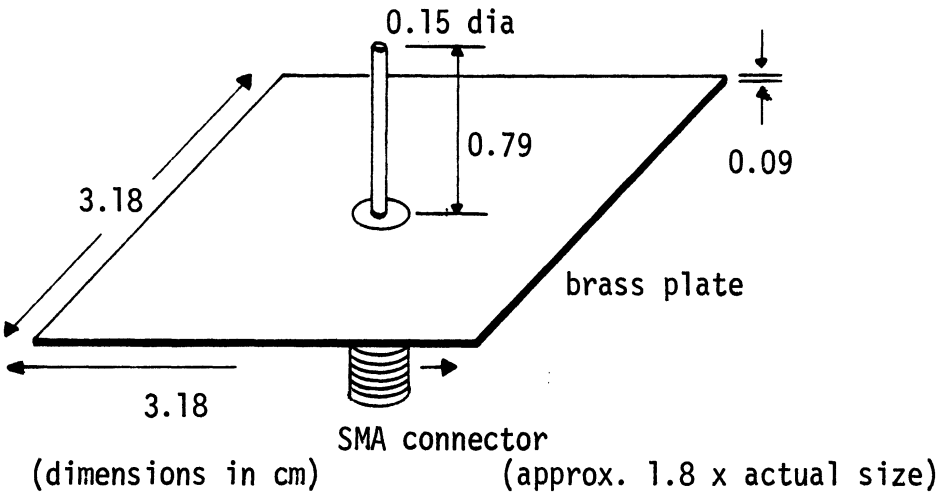

Fig. 3.2: Probe used in measurements. (To mount this probe, holes are drilled in the ground plane to which it is taped.)

Fig. 3.3: The bridge model with a probe mounted on the ground plane. The pencil is included to give an impression of the size.

dimensions (see Chapter 7 to see how the data is applied to a particular size of bridge).

For each measurement, the geometry is defined by (a) the bridge position (see Fig. 3.1), (b) the distance R of the probe from the center, where R = 1 represents 8 cm, and (c) the angle θ (in degrees) of the hole, measured anticlockwise from the positive x axis (see Fig. 3.1). This information is given in the title of each data plot. For example, from p 78, the title is

BR,3,R4,0DEG,EV;BR1301A

and this translates to

Bridge, bridge pos. 3, R = 4, meas. at 0 deg., vert. pol.: data file BR1301.

For ease of interpretation, the angles presented in Tables 4.1 through 4.4 and Chapter 8 are defined in terms of coordinates consistent with those used in navigation.

4. Data Presentation

The magnitude and phase of the electric field component normal to the ground plane were measured in 92 different situations and, by invoking symmetry, have been used to generate 117 plots at a variety of locations relative to the bridge for a number of directions of incidence. The normalization is such that in the absence of the bridge the amplitude is 1.0 and the phase zero degrees. In other words, the plots show the amplitude and phase of E_n/E_{no} where E_n is the normal electric field with the bridge present, and E_{no} is the corresponding field without the bridge.

Most of the measurements are for a "regular" bridge with conducting anchors and towers, but some data are provided for a modified bridge whose anchors and/or towers are replaced by their dielectric (nylon) counterparts. The plots are included in the Appendix in consecutive number order of the file name. Expanded scales having $0 \leq$ amplitude ≤ 2 and $-40 \leq$ phase ≤ 40 degrees are used, with the plots designated by the letter A. Where appropriate, the original plots (designated by the letter B) showing all of the data are also presented. These are placed on facing pages, requiring that some pages be left blank.

Tables 4.1 through 4.4 list the situations for which data are given. The convention used for the description is that the bridge is fixed in a north-south position, with the incidence bearing angle θ_B^i and the measurement location bearing angle θ_B^m measured in degrees clockwise from north. The radial distance R is normalized such that R = 1 corresponds to a (model) distance of 8 cm, representing

15.8 percent of the total bridge length. To locate a particular data set in the Appendix, it is only necessary to determine the plot number from the appropriate table. Tables 4.1, 4.2 and 4.3 are for the regular bridge with incidence angles θ_B^i = 0, 45 and 90 degrees respectively, and Table 4.4 is for the modified bridge.

In addition to the plots, the data have been stored on magnetic tape and are available for qualified users. The data files are identified by the same numbers as the plots, preceded by the letters BR, e.g., BR1301. The format for a data file is as follows:

Line	1	FILENAME (4A4)
	2	Comments (18A4)
	3	Comments (18A4)
	4	TITLE used in plotting (18A4)
	5	FMIN, FMAX, AMPMIN, AMPMAX, PHASEMIN, PHASEMAX, NN (4F8.3, 2F8,2, I5)
	6	F(1) AMP(1) PHASE(1) F(2) AMP(2) PHASE(2) F(3) AMP(3) PHASE(3) 3(2F8.3, F8.2)
	↑	
	data	
	↓	.....F(NN) AMP(NN) PHASE(NN)

where NN is the number of data points in the set. Table 4.5 is an example of a typical data file.

Table 4.1

Data Matrix for End-On Incidence (θ_B^i = 0 Degrees)

(Regular Bridge)

R / θ_B^m(deg)	0	0.5	1	2	4	5
0		3557	1523		1301	
22.5			3473			
45		3569	1705	1715	1555	
90	1669	3545	1505	1515	1475	1449
135		3607	1607	1657	1557	
157.5			3521			
180		3579	1537		1303	
202.5			3521			
225		3607	1607	1657	1557	
270		3545	1505	1515	1475	1449
315		3569	1705	1715	1555	
337.5			3473			

Data plots are in the appendix.

Table 4.2

Data Matrix for Skew Incidence (θ_B^i = 45 degrees)

(Regular Bridge)

θ_B^m(deg) \ R	0	0.5	1	2	4	5
0		3565	1701		1547	
22.5			3503			
45	1667	3529	1519	1531	1327	
90		3571	1707	1711	1559	1719
135		3541	1507	1517	1469	
157.5			3515			
180		3609	1609		1561	
202.5			3517			
225		3577	1631	1675	1325	
270		3605	1605	1653	1549	1651
315		3537	1501	1513	1477	
337.5			3527			

Data plots are in the appendix.

Table 4.3

Data Matrix for Broadside Incidence (θ_B^i = 90 Degrees)

(Regular Bridge)

R / θ_B^m(deg)	0	0.5	1	2	4	5
0		3547	1503		1473	
22.5			3523			
45		3561	1703	1713	1551	
90	1665	3559	1521	1529	1369	1371
135		3561	1703	1713	1551	
157.5			3523			
180		3547	1503		1473	
202.5			3511			
225		3603	1603	1655	1553	
270		3575	1629	1673	1313	1625
315		3603	1603	1655	1553	
337.5			3511			

Data plots are in the appendix.

Table 4.4

Data Matrix for Modified Bridge

θ_B^m (deg)	θ_B^i (deg)	R	Description	Plot No.
0	0	2	Both towers removed; no dielectric supports used.	1725
45	45	2	same as above	1727
90	90	2	same as above	1729
90	90	2	Both towers and both anchors replaced by dielectric ones.	1743
45	45	2	same as above	1745
45	45	2	Aluminum tape shorts from center of bridge to ground; towers and anchors are metal.	1747
90	90	2	same as above	1749

Data plots are in the appendix.

Table 4.5

Example of a Data File

```
  1  BR1701
  2  BR,2,1,45,C/FS,EV...BAND 1
  3  SAMPLE
  4  BR,2,R1,45DEG,EV;BR1701
  5   118.400 545.600    .060  14.962 -177.70  178.70   90
  6   118.400    .177  -16.60 123.200    .097  -23.10 128.000    .087  -13.80
  7   132.800    .094  -22.90 137.600    .101  -25.10 142.400    .103  -29.30
  8   147.200    .095  -31.30 152.000    .096  -35.80 156.800    .090  -36.60
  9   161.600    .088  -41.20 166.400    .087  -43.60 171.200    .077  -51.60
 10   176.000    .072  -56.50 180.800    .067  -50.20 185.600    .076  -76.60
 11   190.400    .088  -75.30 195.200    .065  -69.30 200.000    .070  -73.60
 12   204.800    .060 -136.80 209.600    .065 -111.90 214.400    .071 -119.80
 13   219.200    .069 -125.00 224.000    .076 -138.40 228.800    .083 -156.40
 14   233.600    .086 -166.50 238.400    .089 -167.40 243.200    .097 -169.70
 15   248.000    .110 -171.40 252.800    .121 -173.60 257.600    .136 -173.30
 16   262.400    .153 -177.70 267.200    .171  178.70 272.000    .191  178.10
 17   276.800    .202  175.10 281.600    .216  173.00 286.400    .231  171.90
 18   291.200    .249  171.80 296.000    .272  170.90 300.800    .288  170.70
 19   305.600    .308  171.50 310.400    .339  172.30 315.200    .375  171.90
 20   320.000    .428  171.70 324.800    .484  168.90 329.600    .516  165.30

 31   478.400   9.594  -29.10 483.200   7.211  -10.80 488.000   5.689  -19.20
 32   492.800   4.603  -25.10 497.600   3.873  -28.80 502.400   3.396  -31.40
 33   507.200   2.951  -34.40 512.000   2.624  -35.30 516.800   2.455  -35.80
 34   521.600   2.312  -38.40 526.400   2.168  -39.80 531.200   2.153  -42.30
 35   536.000   2.061  -44.80 540.800   1.954  -47.40 545.600   1.914  -50.70
```

5. Survey of LF and MF Reradiation and Related Effects

Three good existing bibliographies were found [1-3] which contain many references on the subject. The most pertinent have been included here along with those from other sources. The scope of [2,3] which are titled "Direction Finding" is much broader than "direction finding" alone and includes most radio navigation systems in existence at the time. Direction finding effects per se are described [3-6].

Reradiation from vertical monopoles and related phase errors are discussed in [7-10]. The chances of a resonant vertical monopole occurring near the receiver in a harbor/river environment is very small, but the references are included for completeness.

A number of overland measurements were made of low frequency systems including Cytac (the experimental version of Loran-C), Omega, Decca and other LF cw phase measuring systems [11-22] which showed effects due to reradiation from mountains, power lines, telephone lines, towers and trees. Except in the case of mountains, the observed effects were quite localized--extending a distance equal to approximately twice the height of the reradiation object. In general, most of these references do not have the parameters of man-made objects, especially power-line dimensions, well described.

Additional overland measurements are contained in [23-27]. These represent investigations more specifically related to automatic vehicle location work. These tests were in general better controlled than many earlier ones. In [23,24] trouble was reported in high-rise building areas and underneath overhead railroads, but

no difficulty was reported in operating over the Ben Franklin suspension bridge despite the tall towers and suspension cables. These tests did bring out that in the case of high-voltage power lines, an additional source of trouble to Loran-C is the presence of carrier telemetering and communication on frequencies adjacent to or within the Loran-C band. This discovery prompted the investigation reported in [27,28] which resulted in much data both with and without carriers present. In the case of Loran-C, some tests were also made with and without the lines energized. These confirmed that when no carrier is present, the error effects of conventional overland power lines are limited to a distance of a few times the height of the power lines (including height of overhead lightning shield "ground" wires). The difference between energized and de-energized power lines is very slight, provided no carrier is present. The tests were made more difficult to analyze by the use of hard-limiting receivers. Note that the above conclusions for power lines may not apply to very long spans over water, as discussed in the present study.

Actual shipboard measurements of Loran-C performance in the presence of reradiating structures are given in [29-33]. In [29] the errors along the Canadian portion of the St. Lawrence seaway were generally within a few hundred feet, and no large errors were encountered in going under bridges whose spans are relatively short. Difficulties due to loss of synchronization were encountered at one location where there are a number of high voltage power lines crossing within a half-mile stretch.

In [30-33], which are all reports on the same "Loran-C Signal Analysis" program, we have the first observations that the errors when going under bridges are a function of the bridge size. The largest errors were near the Golden Gate Bridge which has a long span (1280 m ≃ 4200 ft). More moderate errors were measured near the Transbay Bridge, which has a medium span (704 m ≃ 2310 ft), and very small errors were measured near the Richmond-San Rafael Bridge which has a much shorter span (305 m = 1000 ft). It was also noted that the error is significantly a function of the direction of incidence of the Loran-C signals. These observations were used in planning the experiments under the present program, and the data from [29-33] will be discussed further in connection with the data from the present program.

Reports of Loran-C measurements on the St. Mary's River in connection with the Loran-C minichain tests were examined, but no measurements near bridges are recorded. The Loran-C calibrations performed in 1980 and 1981 for the U.S. Coast Guard were examined; again, no measurements were made near bridges. (In the case of the Great Lakes, calibrations were made only to within several miles of the Mackinac Bridge and the Blue Water Bridge (across the St. Clair River), since the purpose of the calibrations was for the present use of Loran in open waters).

Additional unpublished observations from the Loran-C Signal Analysis program were obtained from the USCG and from Kaman-Tempo. These reinforced the conclusions of the published

reports. Some unpublished informal observations by the USCG near the Verrazano Narrows Bridge show that the bridge affects Loran-C in much the same way as the Golden Gate Bridge, whose length is similar. Smaller effects were noted in the USCG data near medium length bridges and power lines across the Delaware, where the spans are of the order of 700 m (2300 ft).

An analysis of Loran-C reradiation errors [34,35] was of considerable help in alerting us to the differences in the near field effects with loop antennas and vertical monopole antennas. However, it should be noted that our test data indicate that the analysis in these references appears to be based on over-simplified assumptions about the signal pickup and reradiation phenomena. The differences in near field pickup depending upon the loop or whip antenna configuration have been nicely verified by actual broadcast-band measurements [36].

We remark that the reradiation phenomenon with Loran-C is somewhat related to that in the MF broadcast band. In the latter case, the problem is encountered when directional antennas with deep nulls are used to decrease the transmitted interference to other co-channel broadcast stations. These nulls are reduced when reradiation is present near the transmitter, and one difference between the two cases is that Loran-C is concerned with near-field reradiation and broadcast with far-field.

The problems and solutions when vertical towers are involved are described in [37,38]. Various means of detuning have been used

to reduce reradiation (or scattering, as it is also called), and the first author of the present report has been involved in such investigations [39]. The phenomena when reradiation is from power lines near the transmitter have also been studied [40-44]. In this case, the worst reradiation occurs when the "cells" formed by the overhead ground or shield wires and two adjacent towers are resonant at the broadcast frequency or are harmonically resonant. The cure again is to change the resonant frequency of the "cells" by using series or shunt traps or stubs. It has been found that the reradiation is caused primarily by the closed circuit of the overhead ground (or shield) wires and adjacent towers, and is little affected by the high-voltage conductors, which are insulated from the towers. The usual high-voltage lines have spans of the order of 275 m (900 ft), and these are resonant in the lower part of the broadcast band. This scales to resonance at 100 kHz for bridges only a little longer than the Golden Gate Bridge.

For shorter bridges the present test data suggest that much can be explained by merely considering the effect as due to shielding. References [45-47] are useful in this connection. More information is available on carrier signal radiation [48] and on noise radiation from power lines [49-50], and both must be considered for a thorough examination of the harbor/river Loran-C environment.

6. Description of Bridges and Power Lines

General physical descriptions of bridges are available in encyclopedias and almanacs [51-54], and more detailed descriptions of specific (larger) bridges are also available [57-62]. Some information is also available on navigation charts, particularly with regard to orientation, but charts do not always show bridge piers. Topographic maps omit piers and towers more often than not. Charts, coast pilots and USCG bridge lists [56] consistently show the horizontal clearance for navigation rather than the total span between piers, and only occasionally is total span given. Such information is insufficient for the purposes of the present report where the total span is required to calculate electrical effects.

Physical data for bridges is summarized in Table 6.1. (Only areas where Loran test data are available are covered, and the list is incomplete as regards bridges below 2800 ft. span in the United States, and below 3500 ft. in foreign countries).

The electrical characteristics of bridges are harder to find. Although no definitive information was obtained, it can be expected that bridge towers and cable anchorages are gounded for lightning protection. Cables of suspension bridges are uniformly of steel, usually galvanized, and roadway suspension cables are hung from main suspension cables over steel saddles which surround the suspension cables. All structural steel is painted rather than galvanized [55].

Typical roadway dimensions are summarized in Table 6.2. To the accuracy required for scaling, all the large bridges have

Table 6.1

Long-Span Bridges

Name Location	Center Span	Side Spans (each)	Vertical Clearance (center or central portion)	Tower Height
Humber Hull, England	1410 m	530/280 m		
Verrazano-Narrows New York	1300 m	370 m	70 m	210 m
Golden Gate San Francisco, CA	1280 m	343 m	67 m	226 m
Mackinac Michigan	1200 m	549 m	46 m	161 m
South Bisan Seto Japan (compl. 1987)	1098 m	270 m		
Bosphorus Turkey	1074 m	243 m	64 m	165 m
George Washington New York, NY	1067 m	198 m	65 m	194 m
Forth Road Scotland	1006 m	408 m		156 m
Commodore Barry Chester, PA	854 m		58 m	
Tacoma Narrows Tacoma, WA	853 m		55 m	
Transbay San Francisco, CA	704 m	534 m	57 m	149 m
Delaware Memorial (Twin Span 300' separation Wilmington, PA	655 m	213 m	57 m	
Bronx-Whitestone New York, NY	690 m		41 m	
Throgs Neck New York, NY	522 m		42 m	

Table 6.1 (cont.)

Name Location	Center Span	Side Spans (each)	Vertical Clearance (center or central portion)	Tower Height
Walt Whitman Philadelphia, PA	610 m		46 m	
Benjamin Franklin Philadelphia, PA	514 m		41 m	
Chesapeake (Twin Span 400' separation)	457 m (main channel)		56 m	
Richmond-San Rafael California	296/305 m		41/56 m	
Seaway International Medina, NY (St. Lawrence Seaway)	244 m		37 m	
(Twin Span) Groton, CT	152 m		41 m	

Blank space denotes that missing entry information was not readily available to us at this time.

Table 6.2

Suspension Span Roadway Dimensions

Golden Gate: Single deck, 6 lanes, width 90 ft; open truss on each edge of roadway, 25 ft high, with approximately 3 x 3 ft box girder at top and bottom edges.

Transbay: Double deck, 6 lanes each, width 66 ft. Box girders each edge of each deck approximately 3 x 3 ft (scaled from drawing). Overall height of roadway structure, 30 ft.

Verrazano-Narrows: Double deck, 6 lanes each, width 74 ft. Box girders each edge of deck approximately 3 x 3 ft; overall height of side trusses, 24 ft.

Mackinac: Single deck, width 68 ft. Open trusses each edge 38 ft high. Box girders at top and bottom of truss approximately 3 ft high.

For other bridges, see [61, pp 175 and 203].

remarkably similar roadway dimensions and construction features. The side trusses on the roadways, which form the principle lengthwise electrical path, are all open trusses with similar box girders at top and bottom. The truss dimensions are primarily determined by the roadway stiffness needed for stability under high wind conditions.

The suspension cables may be expected to have low conductivity at 100 kHz because of the surrounding steel saddles for roadway suspension even with galvanizing. In any event, the box girders at the four corners of the roadway structure have much lower inductance than the suspension cables because they are closer to the return path through the water and also are much shorter.

An investigation of power cables over navigable harbor/river waters was not included in the present program, but as the study proceeded it became apparent that much of the scale model and real-world work was applicable to power cables as well as bridges, and that an understanding of one would help the other.

In the United States power lines over navigable waters are controlled by the U.S. Army Corps of Engineers, but as with bridges, most of their records, as well as most chart and Coast Pilot information, concern navigation clearances and not actual spans. There does not seem to be any publication for power lines similar to the USCG list of bridges, but charts are better than for bridges in showing actual tower locations. General information about power lines construction dimensions are given in [63,64], and many water crossings can be located from [65] as well as on charts and Coast Pilot publications. Water crossings are often larger

than standard spans [66,70] and involve special construction designs for the towers and conductors.

Some noteworthy power line spans are tabulated in Table 6.3. The listing makes no pretense of being complete for the United States, but is reasonably complete for the rivers listed for the large spans. The variability of conditions affecting Loran-C are greater for power lines than for bridges, and some power line construction features are listed in Table 6.4. This illustrates the type of information which should be obtained for a thorough interpretation of full-scale field test data.

Table 6.3

Notable Power Line Water Spans

Location	Span	Vertical Clearance	Towers	Miscellaneous
Sange Fiord Norway	4888 m			[62]
Strait of Messina Italy	3628 m		225 m	[62]
Genissiat to Malgovert line	2088 m			may not be over water [67]
"There are spans over one mile across fiords in British Columbia"				[69]
St. Lawrence Seaway Eisenhower Locks	396 m	43 m		many lines crossing 900' along canal
Line from Shawinigan Falls to Quebec City	1463 m	52 m	107 m	
Saguenay River Quebec	1792 m	91 m	Uses mountains (sag 122 m)	no shield (ground) wires on water spans
Detroit River Detroit, MI	728 m	56 m	92 m	2 grounds, 3 conductors, carriers
St. Clair River, MI	707 m	54 m*	84 m	same
St. Clair River, MI	665 m	50 m*	102 m	same
St. Clair River, MI	730 m	47 m*	98 m	same

*These are actual mechanical clearances, and the same as the "reported" and "authorized" clearances on NOS charts. Apparently there is no allowance on charts for any high voltage additional clearance. Similar information for other spans was not verified.

(cont.)

Table 6.3 (cont.)

Location	Span	Vertical Clearance	Towers	Miscellaneous
New Castle, PA Pub. Service Elec./Gas	823 m	68 m	149 m	2 shields, 3 conductors
Chester, PA Pub. Service Elec./Gas	853 m	64 m	149 m	2 shields 3 conductors
Potomac River Quantico 77°16'W38"N	457 m	52 m		
Mississippi River				
Multz/Laplace 90°38'W,30°00°N	1006/1143 m	46 m	149 m	2 circuits 1006 m apart
Bridge City 90°11'W,29°56'N	1189 m	45 m	149 m	
Point Pleasant Willow Glen 91°08°W,30°16°N	1219 m	51 m	149 m	
Lakesville (?) 3 mi below Baton Rouge	1234 m	46 m	143 m	
Nine-Man Point	823 m			
Below New Orleans	1000 m	53 m		
Memphis	732 m			
Lake Ponchatrain	579 m	27 m		also many 274 m spans in tandem

Blank space denotes that missing entry information is not readily available to us at this time.

Table 6.4

Power Line Variables

A. Ground (Shield) Wire Configuration

(a) None (e.g., Saguenay River crossing 1792 m 735 kV)

(b) Grounded at each tower

(c) Insulated (with spark gaps) and used also for power-line carrier transmission (e.g., especially in higher voltage systems such as 500 kV), or as phase-wire also.

B. Ground (Shield) Wire Material

(a) Steel (usually galvanized).

(b) ACSR (aluminum covered steel, reinforced).

C. Ground (Shield) Wire Number

Zero to two.

D. Tower Height

Up to 225 m.

E. Span

Up to 4900 m or more. Should be resonant at slightly lower frequencies than a suspension bridge due to the longer path, tower-span-tower.

F. Carrier or Random Noise May be Present on the Line

7. Scaling for Model Measurements

The theory of scale modeling is well known [71]: if the model dimensions are 1/n, the model frequencies must be multiplied by n; the dielectric constant and permeability are unaffected, and the model conductivity should be increased by n.

The model bridge is shown in Fig. 2.3 and was chosen to represent a class of suspension bridges. Its form was prompted by that of the Golden Gate Bridge and, as regards its main (central) span, it models this on a scale of 1:4250. 425 MHz therefore corresponds to 100 kHz full scale. The side-span to main-span ratio for the Golden Gate Bridge is 0.27, but this ratio varies from one bridge to another. Some examples are:

Golden Gage Bridge	0.27
Verrazano-Narrows	0.29
Delaware Memorial	0.35
Transbay	0.52
Mackinac	0.47

The ratio selected for the scale model was 0.37.

For the reasons described in Chapter 2, an aluminum plate five feet in diameter and 1/8 inch thick was chosen as the ground plane. Since the bridge had to be moved to achieve the different directions of illumination, and had to be removed to make the calibration measurement for each probe location, it was necessary to have the model rugged. We chose to use a piece of solid aluminum plate 1/4 inch thick cut in the overall outline of the bridge.

In scale model work it is generally difficult to properly scale the conductivity, but we were quite fortunate. The approximate properties of the full scale and model materials are given as follows [73,74]:

Material	Conductivity (σ)	Permeability (μ_r)
Steel	8.0×10^6 S/m *	450
Aluminum	3.6×10^7 S/m	1
Sea water	4.0 S/m	1
Fresh water	0.002 S/m	1

At 100 kHz, the depth of penetration of the current is about one meter in sea water and 0.02 cm in aluminum. In both the full scale and model situations we are therefore dealing with surface currents only. The solid model may have a proportionally lower resistance than the real bridge (which has many openings), but proximity effects should make most of the current flow along the lower surface, and the difference due to the solid model should not be great.

The ratio of the conductivities of aluminum and steel is $3.6 \times 10^7/8 \times 10^6 = 4.5$. The resistance ratio times the permability ratio gives a scaling ratio of $4.5 \times 450 = 2025$, which is reasonably close to the model ratio 4250.

In the case of scaling for the ground conductivity, the ratio of the conductances for sea water is $3.6 \times 10^7/4 = 9 \times 10^6$, but the ground plane has a much larger surface than the bridge, and should contribute relatively little to the resistance of the bridge-ground circulating current circuit. Thus, the excessively high model

*S/m is Siemens/meter (mhos/m).

conductivity should not greatly affect the overall results, and for fresh water the scaling is better.

In studies [40-44] of the effect of power lines on nulls in broadcast station directivity patterns, it has been found that the overhead shield or "ground" wires, which are usually grounded at each tower, are the primary factors in determining the resonance and other effects of a power line. To evaluate the modeling of a power line by the bridge, let us consider the current-carrying cross-section of overhead shield wires compared to the current-carrying cross-section of the bridge. The current-carrying circumference of a typical pair of shield wires of 5/8 inch diameter is 20 cm. The current-carrying equivalent of the real bridge is primarily the outside surface of the box-girders supporting the roadway. With 3 x 3 ft girders, the width of the current sheet is approximately 730 cm. The ratio of these two is 20/1 in favor of the bridge, but the bridge has poorer conductivity and higher permeability which increase the skin effect. Taking into account that the skin effect varies as the square root of these quantities, there is a factor $\sqrt{2000} = 45$ in favor of the power cables. Thus, the better conductivity and lower permeability of the power cables almost balances out the greater current-carrying cross section of the bridge, and the bridge model can therefore serve as an approximate model of a power line.

The dimensions of the bridge model are shown in Fig. 2.3. The distances of the measurement points are scaled in units of R, where R = 8 cm. The center span of the bridge is 11.91 inches = 30.24 cm,

i.e., 3.78 R. The clearance height is 5/8 inch = 1.59 cm = 0.20 R, and other scaling factors are given in Table 8.1.

8. Data Analysis: Regular Bridge

To get a better understanding of the measured data, summaries were made at several frequencies, corresponding to different classes of bridges, as indicated in Table 8.1.

At all angles of incidence, the model resonated at about 470 MHz. This corresponds to a bridge span of 1417 meters (4650 ft) which is very close to the length of the Humber Bridge at Hull, England, the largest span bridge in the world. Three other bridge sizes were analyzed, the size being determined by the particular frequency of the measurements.

Examination of the data indicates that the choice R = 5 for the maximum distance at which measurements were made was a good one, large enough to show the range of errors even at resonance. For smaller bridges, some more measurements for R < 1 corresponding to shorter distances would have been desirable. Nevertheless, the range of distances and angles measured does give a reasonably satisfying overall picture.

Inspection of the data indicates that the random error of measurement is roughly one degree in angle and 0.04 in amplitude (ratio), so that values twice these amounts can be considered a serious indication of relevant phenomena.

For each of the three non-resonant bridge sizes, consolidated plots of the measured data were made for three directions of incidence of the radio signal: broadside, skew (45 degrees), and end-on. At each point the amplitude ratio and the error angle of

Table 8.1

Scaling Factors for Bridge Sizes

Size	Model Frequency	Span Length (3.78 R)	Span Height (0.20 R)	Distance Scale (1 R)	Representative Bridges
Resonant	470 MHz	1417 m (4650')	75 m (246')	0.12 λ, 376 m (1233')	Humber (Hull, England)
"Large"	425 MHz	1280 m (4200')	68 m (223')	0.11 λ, 340 m (1115')	Golden Gate Verrazano-Narrows
"Medium"	225 MHz	678 m (2225')	36 m (118')	0.06 λ, 180 m (590')	Transbay Delaware Memorial
"Small"	125 MHz	376 m (1235')	20 m (65')	0.03 λ, 100 m (328')	Richmond-San Rafael

the resulting field are shown (conditions with the bridge model removed are $1.0/\underline{0°}$). The results are presented in Figs. 8.1 through 8.7. For the large bridge, parts of the same data are replotted in Figs. 8.8 through 8.10, with phase error shown as a function of angle of incidence, parametric in R. The smaller amount of data with significant errors did not permit plotting the results for medium and small bridges in the same manner. For the resonant bridge case, the results are summarized in Table 8.2. The errors for small R are so large that a detailed plot does not have much significance.

For the large size bridge, large errors up to 180 degrees exist directly under the bridge and even at some other points. The errors drop to near negligible values at R = 4. The errors are significantly a function of the angle of incidence, with the largest errors for broadside incidence and for broadside measurement points, and the smallest for end-on incidence or end-on measurement points.

For the medium and small bridges the above directional pattern is maintained, but the errors become much smaller, and are least for the small bridge. Directly underneath the bridge, the errors are fairly erratic as a function of frequency (the error vector is the result of the near cancellation of the bridge-free field by the reradiation field). It is apparent that for broadside incidence any current induced in the two towers of the bridge must be in phase, i.e., the bridge is acting as two adjacent top-loaded inverted-L antennas [72] and not as a loop antenna. The length of the span (0.3025 m) plus the height of the span (0.0159 m) is 0.318 m

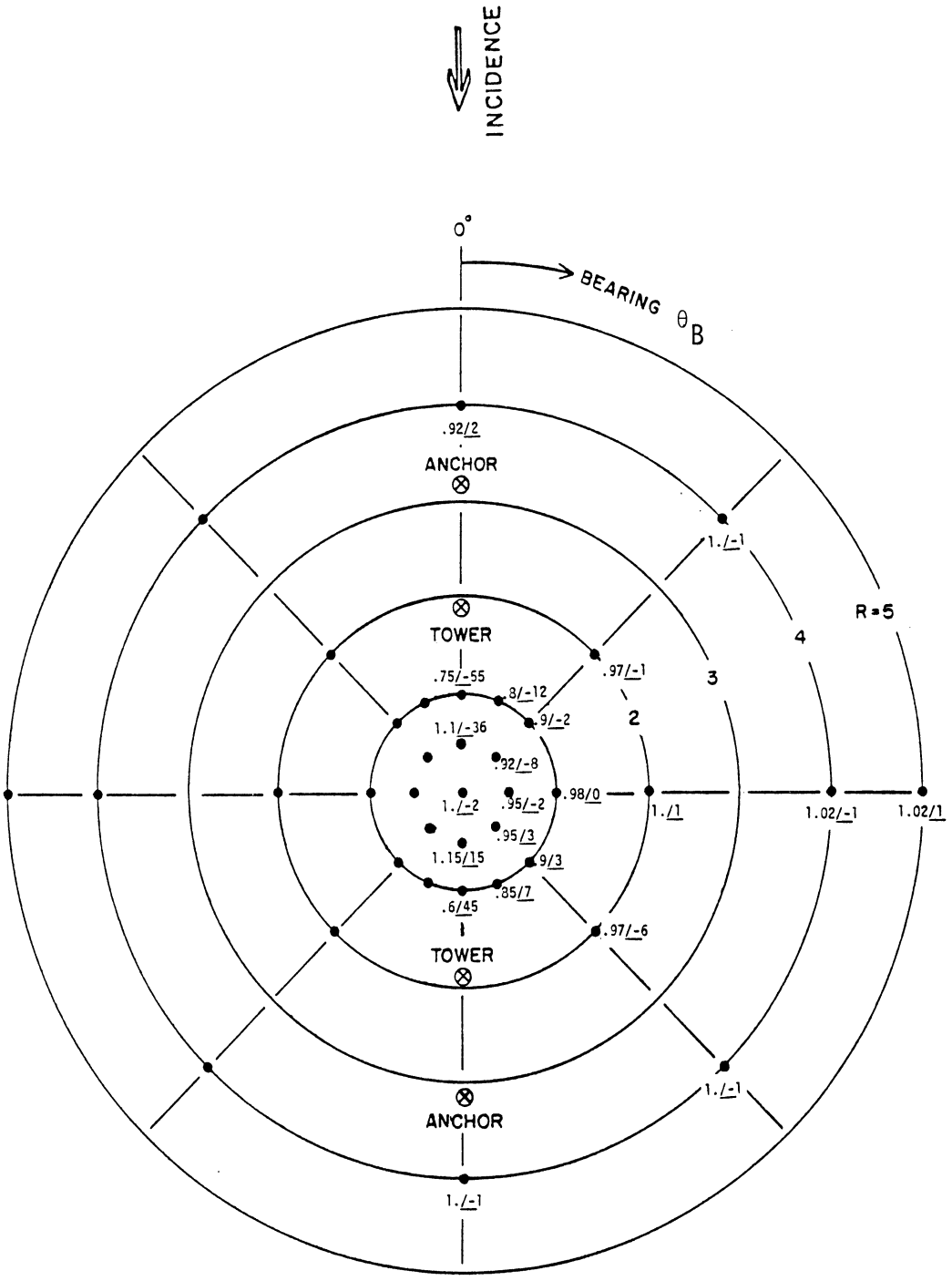

Fig. 8.1 Signal amplitude ratio and phase angle error.

Large bridge (model at 425 MHz)
Span 1280 m (4200 ft)
End-on incidence ($\theta_B^1 = 0°$)

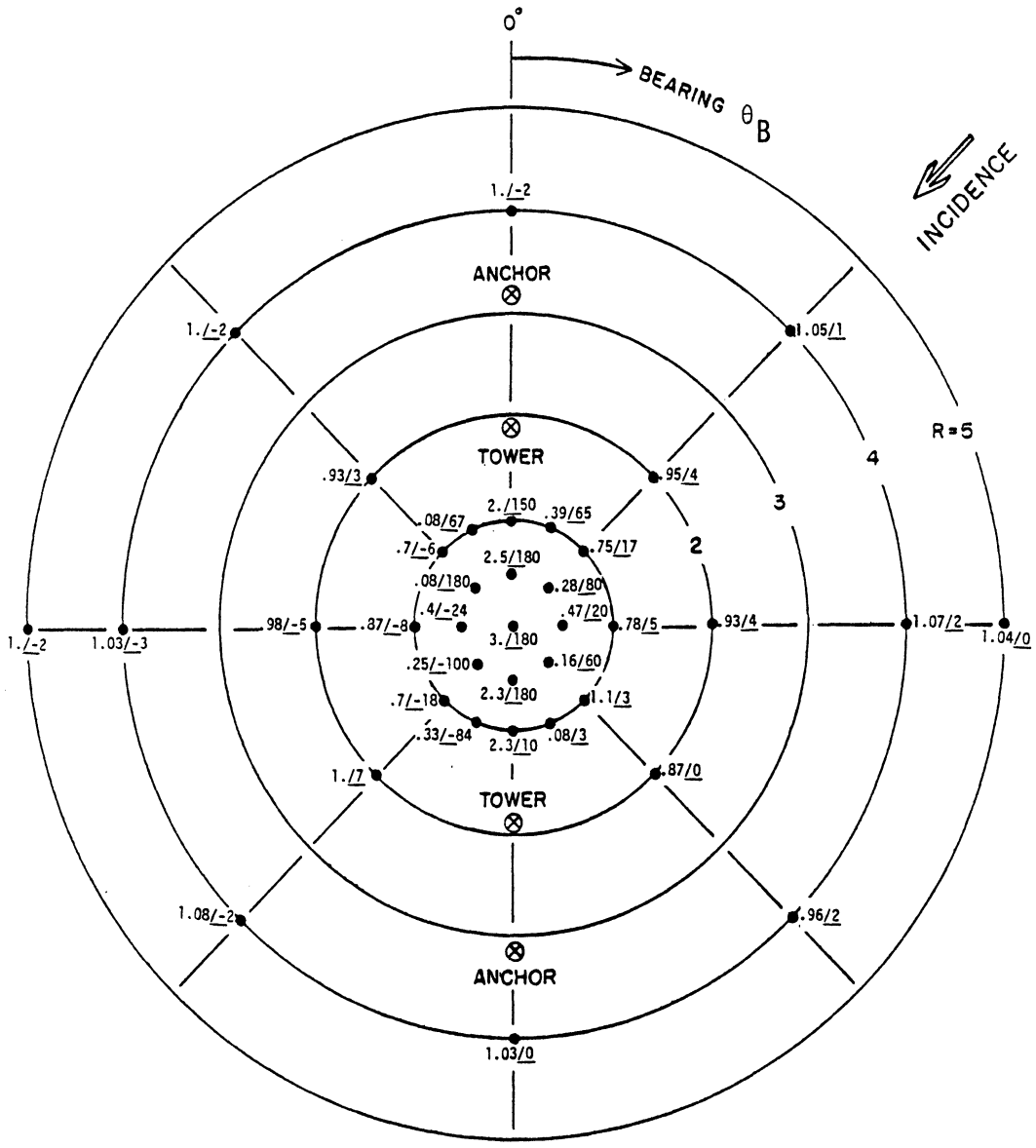

Fig. 8.2: Signal amplitude ratio and phase angle error.

Large bridge (model at 425 MHz)
Span 1280 m (4200 ft)
Skew incidence (θ_B^i = 45°)

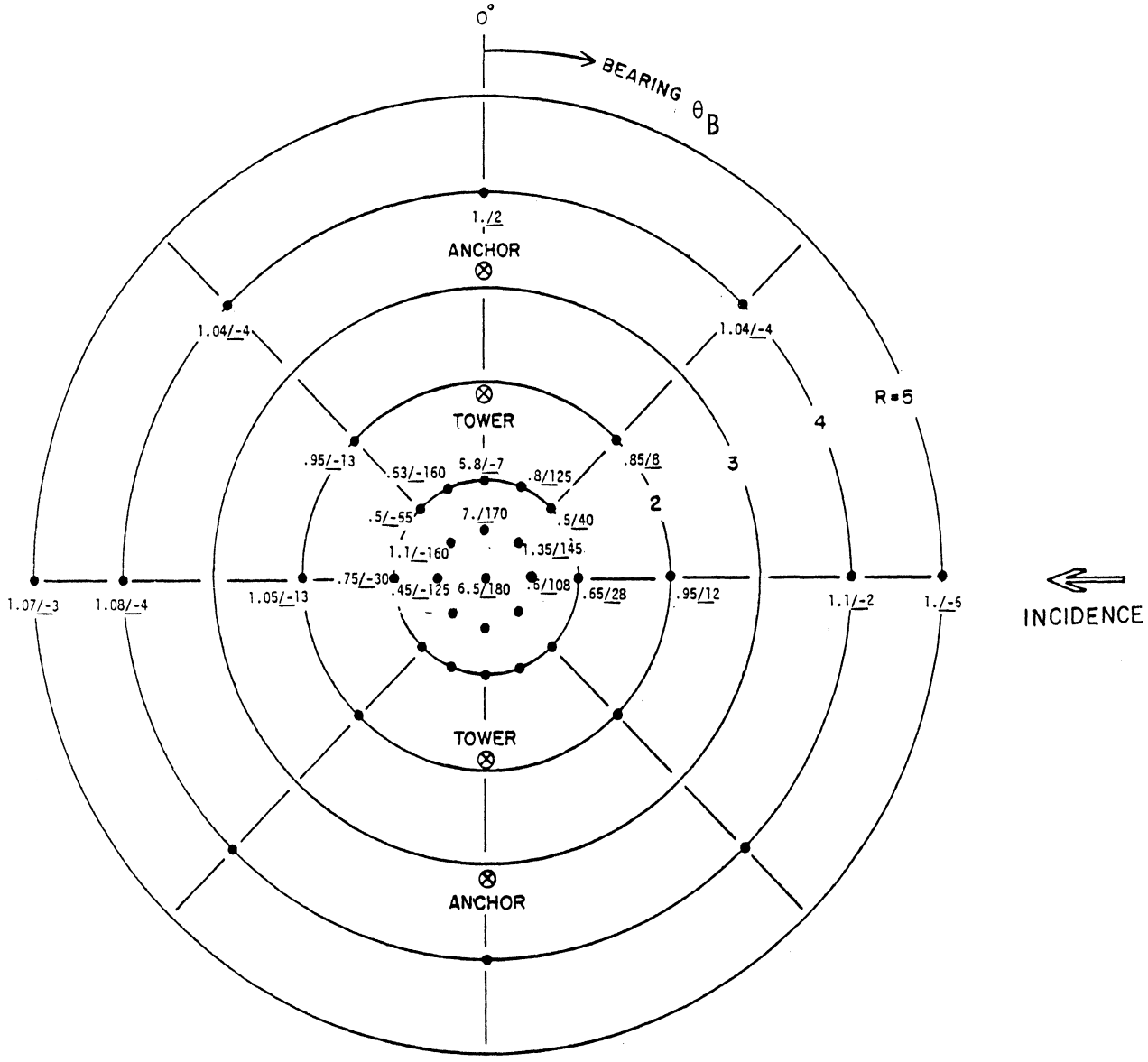

Fig. 8.3 Signal amplitude ratio and phase angle error.

Large bridge (model at 425 MHz)
Span 1280 m (4200 ft)
Broadside incidence (θ_B^i = 90°)

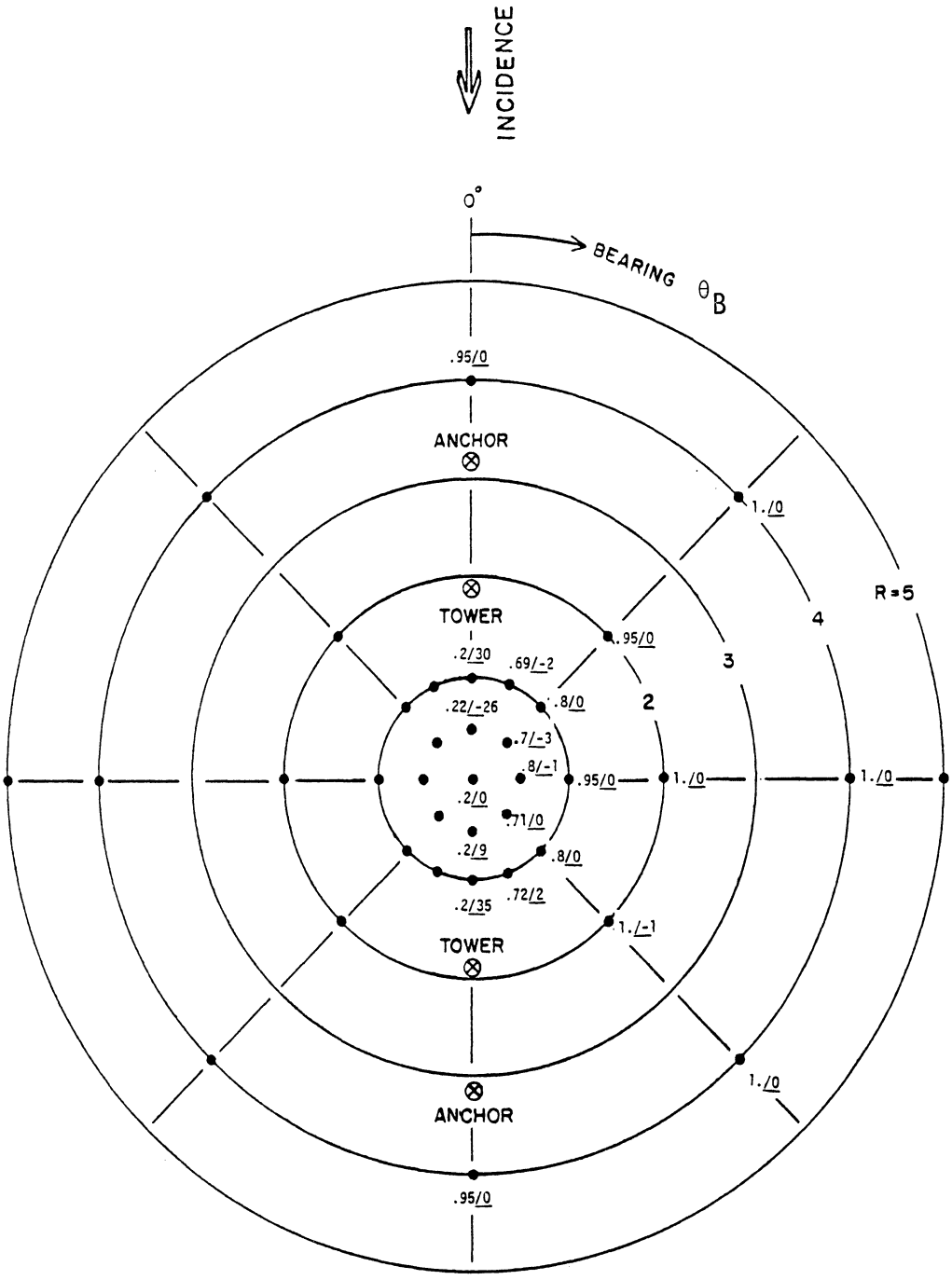

Fig. 8.4 Signal amplitude ratio and phase angle error.

Medium bridge (model at 225 MHz)
Span 678 m (2235 ft)
End-on incidence (θ_B^1 = 0°)

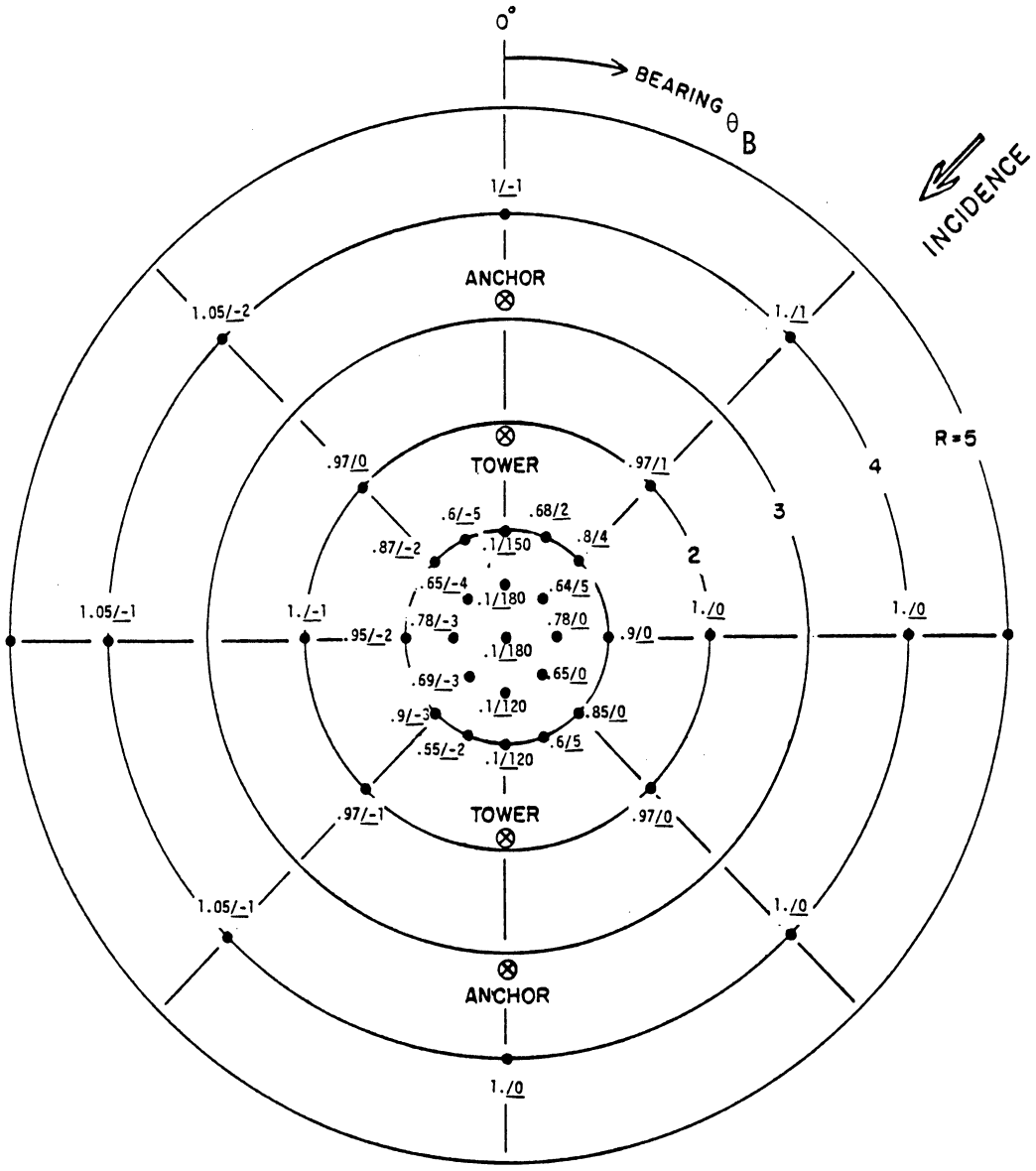

Fig. 8.5: Signal amplitude ratio and phase angle error.

Medium bridge (model at 225 MHz)
Span 678 m (2235 ft)
Skew incidence (θ_B = 45°)

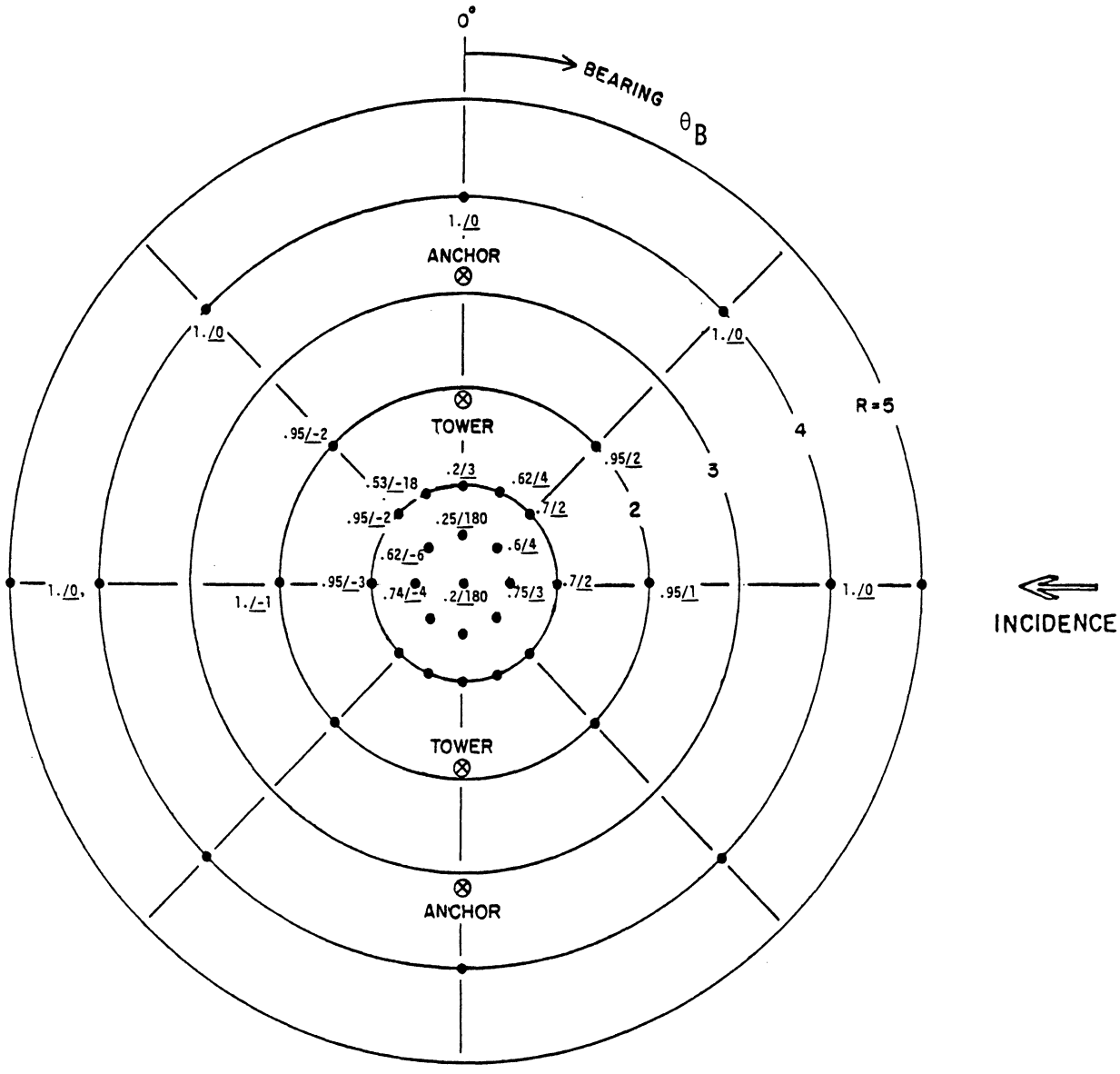

Fig. 8.6 Signal amplitude ratio and phase angle error.

Medium bridge (model at 225 MHz)
Span 678 m (2235 ft)
Broadside incidence (i_B = 90°)

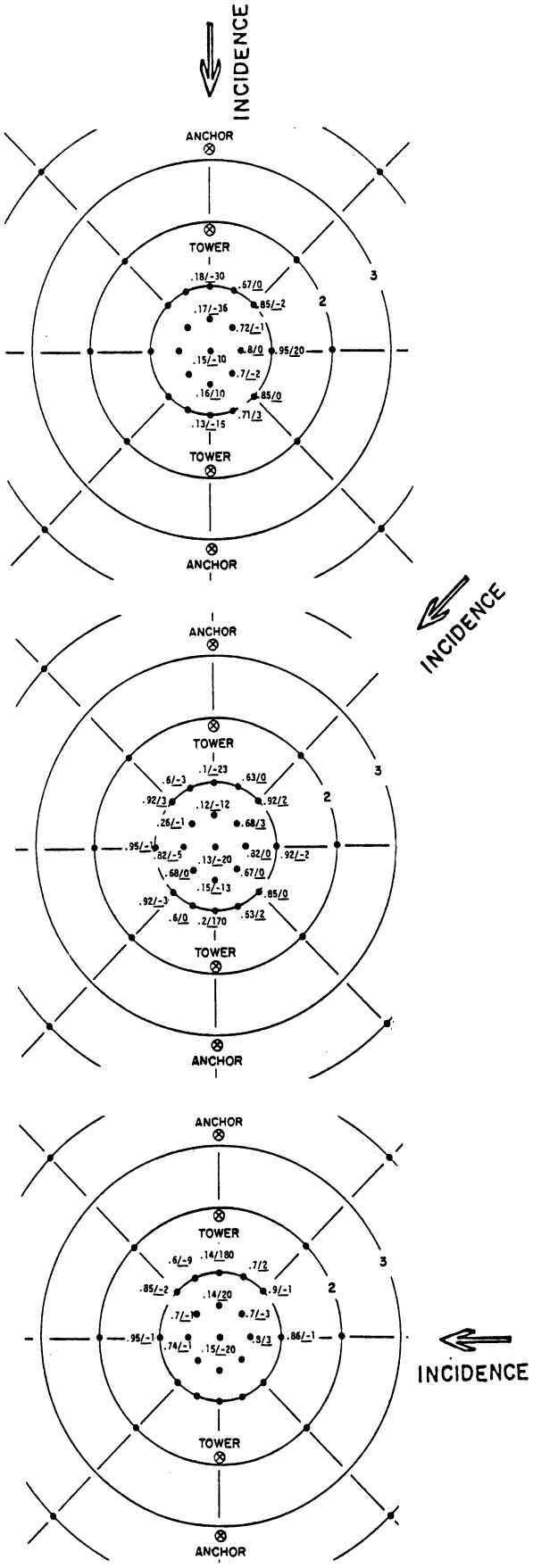

Fig. 8.7: Signal amplitude ratio and phase angle error.

Small bridge (model at 125 MHz)
Span 376 m (1235 ft)
End-on, skew, and broadside incidence (θ_B^i = 0°, 45°, 90°)

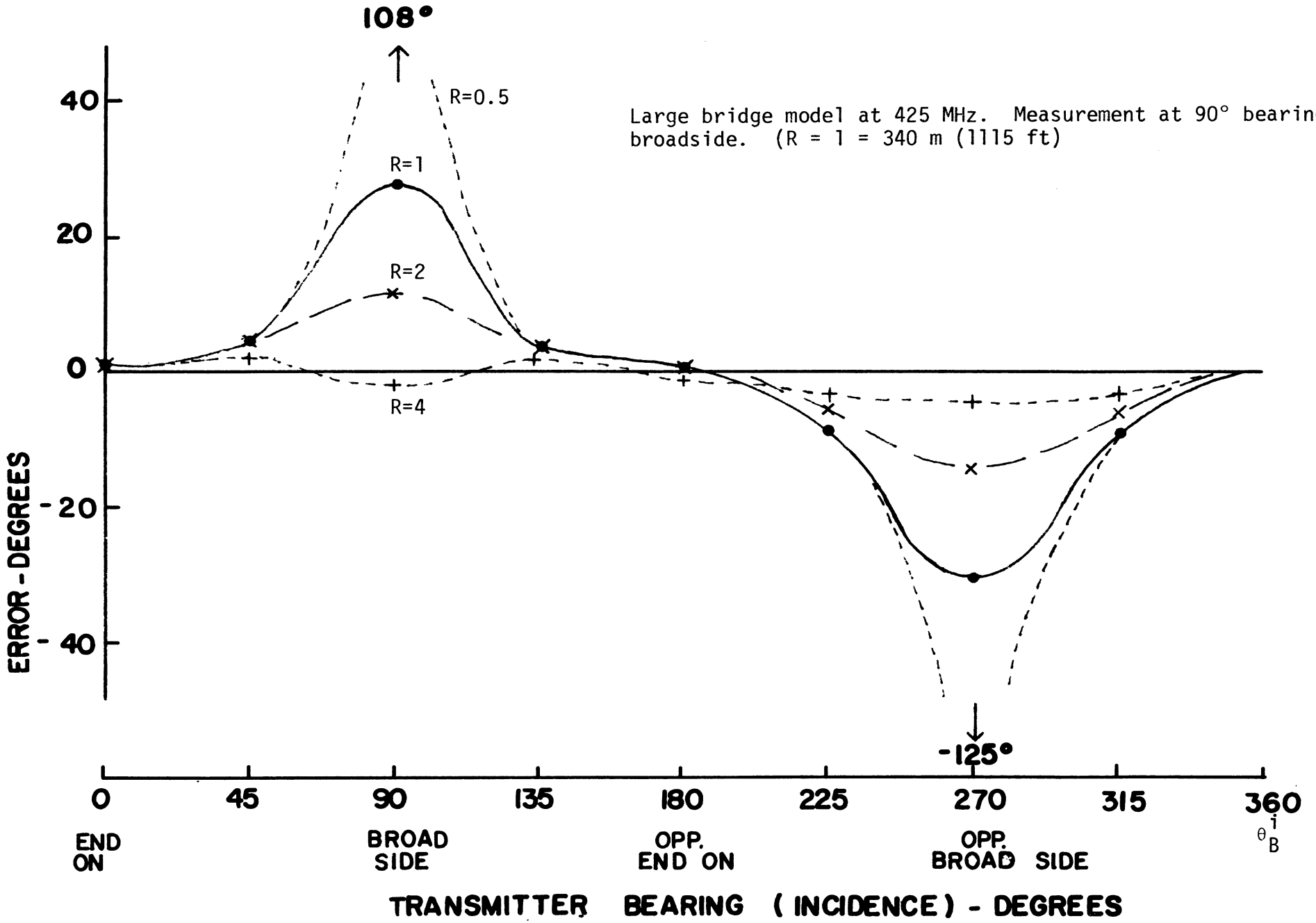

Fig. 8.8: Phase error vs incidence.

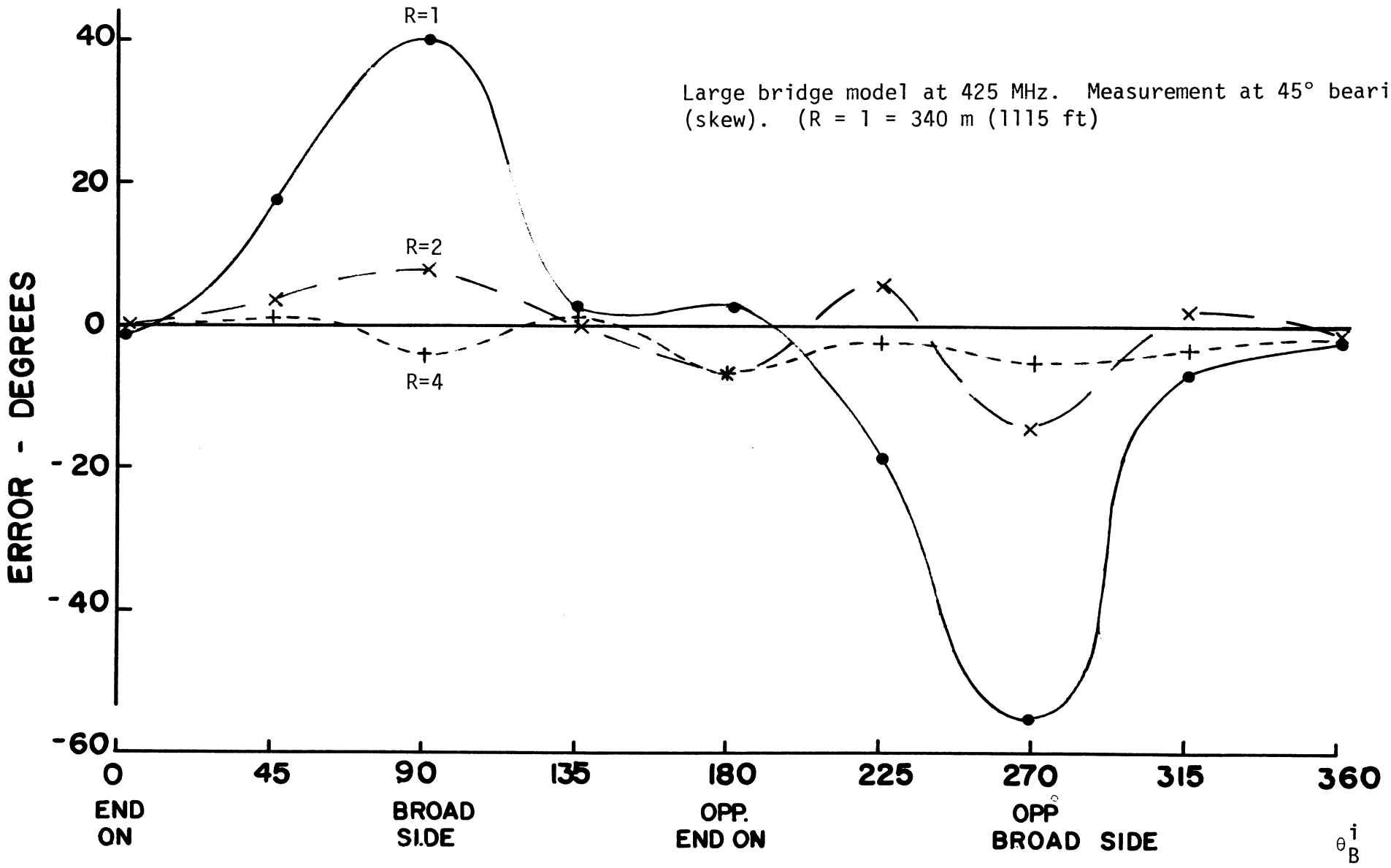

Fig. 8.9: Phase error vs incidence.

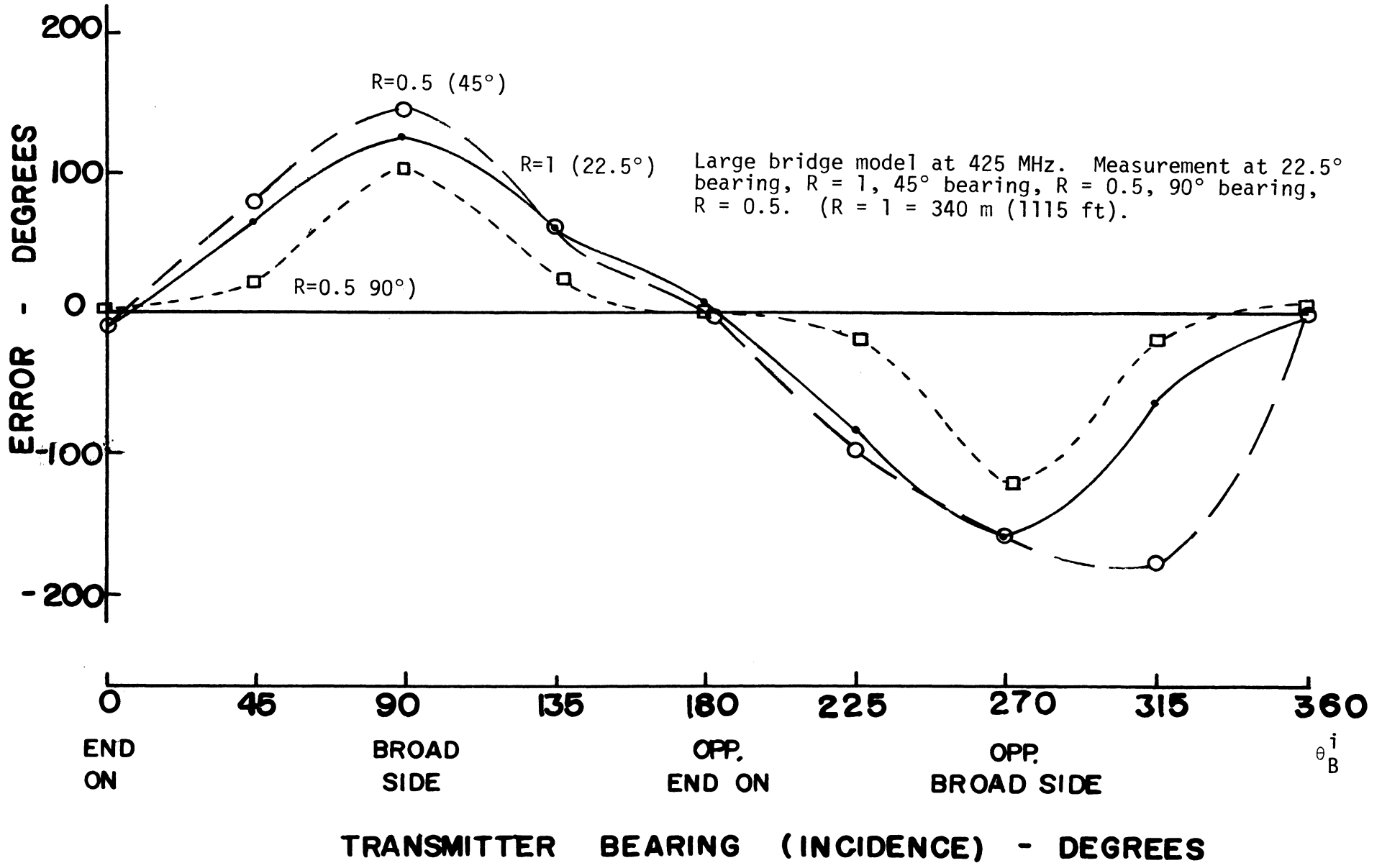

Fig. 8.10: Phase error vs. incidence.

Table 8.2

Errors at Resonance

Incidence	Measurement	Most deviant ratio and largest phase error
R = 4 (1353 m = 4840 ft)		
broadside	broadside	1.3 - 0.05/70°
skew	skew or broadside	0.7/15°
end-on	broadside	0.85/8°
R = 1 (340 m = 1115 ft) excluding points under bridge		
broadside	skew	7.5/180°
skew, broadside	skew	0.2 - 3.0/120°
end-on	skew	1.8/80°
R = 0.5 (169 m = 555 ft)		
broadside	broadside	11.0/130°
	skew	18.4/145°
skew	broadside	4.0/100°
	skew	7.0/180°
end-on	broadside	2.3/110°
	skew	3.0/180°
broadside	under bridge	32.0/90°
end-on	under bridge	24.0/50°
R = 0 (under bridge at center)		
broadside		22.0/180°
skew		18.0/180°
end-on		12.0/180°

and should then correspond to one half wavelength at resonance. At resonance (470 MHz) the half-wavelength is 300/(470 x 2) = 0.319 m, and the agreement is almost exact.

This explanation could be verified if data were available with the center of the model span insulated. A previous analysis of Loran-C reradiation based on bridges acting as loops [35] predicts that the maximum errors occur for end-on incidence and for observations in the end-on direction (bearing 0°). But even with the small size bridge (measurements at 125 MHz) the errors are larger for broadside incidence. In other words, the unspoken assumption in [35] that loop effects predominate over vertical antenna effects seems to be incorrect.

It is also apparent that the large oscillatory nature of the error polarity suggested by [32, Fig. 6.6] and [33, Fig. 7.5] is not supported by either the data in these reports or by the scale model measurements of the present investigation. This is so because the error due to reradiation falls off faster as a function of distance than those figures suggest. In the present data there is a mere suggestion of oscillatory data polarity as a function of distance from the bridge.

For the small size bridges (under about 1500 ft = 457 m) the bridge apparently can be analyzed as an overhead grounded shield, since the distance from the bridge center to ground at the tower is 2 R = 0.06 λ. The theoretical shielding effect of an overhead conductor has been calculated in [46, Fig. 3] as a function of shield height H, and horizontal distance x. The amplitude is

0.87 of normal at x/H = 2.5, which corresponds to a distance of R = 0.5 in the model. The measured amplitude at R = 0.5 varies from 0.74 to 0.82. Directly under the bridge (at x/H = -0.2) the calculated amplitude ratio is 0.21, and the measured ratio varies from 0.10 to 0.20. The agreement between simple theory and model measurements is thus quite good. Measurements of Loran signals near overhead high-voltage power lines are also available [27]. A number of the measurements in [27] have the power line de-energized or energized with no carrier communications present. This also should be expected to model the small bridge situation since the spans are of the order of 275 meters (900 ft). The height of the ground wires in [27] is about 35 meters and the amplitude of the Loran-C signal is reduced in amplitude out to about 70 meters--which also agrees with the analysis of the overhead conductor shield effect.

The fact that the large bridges are quite near resonance makes the resistance (and hence the Q of the resonance) a significant factor. As we saw in the previous section, the resistance is also the hardest model parameter to scale accurately. We do not have any Q measurements for real structures nor any Loran-C signal amplitude measurements near them, and [27] contains only signal-to-noise ratio measurements, made using hard-limiting receivers. However, we can use time difference errors near the Golden Gate Bridge [33, Fig. 7.13] and similar unpublished data near the Verrazano-Narrows Bridge. These figures show a combination of bridge errors and secondary phase factor errors. Near the bridges, the bridge errors predominate. The shore-to-shore span of the

Golden Gate Bridge is roughly 5 R (the northern pier is at the shore line but the southern pier at 1 R from the shore.*) In [33, Fig. 7.13] the TDX error at 2 R is 0.33 microseconds = 12 degrees, and this agrees very closely with the model measurements (e.g., Fig. 8.3). We therefore conclude that the Q of the model is a reasonably good approximation to that of the real bridge.

The orientation and Loran station bearing of some of the bridges under discussion are shown in Table 8.3. It is noteworthy that the X-secondary station has a relative bearing almost end-on to both the Golden Gate Bridge and the Verrazano-Narrows Bridge. Full scale time difference data [33, p. 83] show greater errors in the M-X time difference than in the M-Y time difference; this is ascribed in that report to cancellation of nearly equal M and Y errors but not of unequal M and X errors. In the case of measurements of time-of-arrival (TOA) of individual station signals [31] a similar conclusion is drawn, but is supported only by some of the data. In other data, and in unpublished informal USCG data taken near the Verrazano-Narrows Bridge, the X error is not substantially smaller than the other station's errors, but it is of opposite polarity. In the latter data, the agreement with the present scale model measurements is not good. Possible reasons are that the full scale measurements were made under dynamic conditions and that the full scale measurements were made (at least in some

*Figure 1 of [31] is incorrect and misleading in this respect.

Table 8.3

Bridge Orientation and Loran-C Incidence Bearing Absolute and Relative to Bridge

Bridge Name	Bridge Orientation	Station Incidence Bearing M	W	X	Y	Z
Golden Gage	356°	60°	-	0°	110°	-
	(0°)	(64°)	-	(4°)	(114°)	-
Transbay	41°	59°		355°	110°	
	(0°)	(342°)		(314°)	(69°)	
Richmond-SanRafael	95°	61°		355°	111°	
	(0°)	(326°)		(260°)	(16°)	
Verrazano-Narrows	67°	320°	21°	76°	205°	270°
	(0°)	(253°)	(314°)	(9°)	(138°)	(203°)

cases) near the bridge towers. The exact locations of the runs were not stated.

Some advance data were obtained from the USCG from work in progress on evaluating the PLAD (portable Loran assist device) system. These data were taken near the Verrazano-Narrows Bridge and in the Delaware River. All were taken on moving boats and indicated errors smaller than the static errors found in model testing. The Delaware River area south of Philadelphia has two "medium" length bridge spans and two medium length power line crossings. Cross track errors of 50 meters were noticeable due to both, with one case of loss of lock near a power line crossing.

9. Data Analysis: Modified Bridge Configuration

Three runs were made with the inner tower bases from the roadway to the water removed. This corresponds to insulating the towers from the ground, but leaving the cable anchorages grounded.

Run No.	Incidence	Measurement	Corresponding Regular Bridge
BR 1729	broadside	R = 2, broadside	BR 1259
BR 1727	skew	R = 2, skew	BR 1531
BR 1725	end-on	R = 2, end-on	none (tower in way)

In all the runs, the frequency at which resonance occurs is reduced from the normal 470 MHz to 280 MHz; i.e., the resonant wavelength is increased by a factor 470/280 = 1.68. The center span length plus height is increased from 30.24 + 1.59 = 31.83 cm to 50.56 + 1.59 = 52.15 cm. The ratio of the two is 52.15/31.83 = 1.64, which is very close to the factor for the resonant wavelength. We conclude from this that the resonance of the regular bridge configuration is primarily due to the center span and is not greatly influenced by the shorter end spans.

The errors at 425 MHz were greatly reduced, compared to the regular bridge model at the same measurement points.

Two runs were made where a short metallic connection was made from the center of the model span to the nearest ground point beneath the span.

Run No.	Incidence	Measurement
BR 1749	broadside	R = 2, broadside
BR 1747	skew	R = 2, skew

In these two runs no resonance or significant errors appear. This is reasonable since the lowest resonance is now doubled by adding the shorting wire, and the resonance should occur at a frequency beyond those covered by the measurements.

Two runs, BR 1743 and BR 1745, were made with both the tower bottoms and anchorages of the model replaced by dielectric spacers. No significant errors or resonances appeared. (The small spikes are believed to be measurement artifacts.) This is consistent with the elimination of any current flow in the bridge model by insertion of dielectric spacers.

The analysis previously given which indicates that the current must be in-phase in the two towers at broadside incidence also forces the conclusion that insulation inserted at the center of the span would be ineffectual in changing the current flow and, hence, the errors for broadside incidence--the case of largest errors.

We can conclude from the above measurements and analyses that the resonant effects are indeed due to the critical bridge dimensions, particularly the length of the middle span. The insulating effects modeled might be achieved practically in real bridges using shunt stubs as has been done for power lines [37,38, 40,44]. The addition of a shorting cable from the span center to ground does greatly reduce the errors and might be a useful experimental technique for separating site errors (secondary phase factor) from bridge errors. It is doubtful that such a cable would be acceptable by navigators for a permanent installation, even where traffic separation is practiced. Note that the

reduced errors resulting in the model tests were all at R = 2, that is, at distances from the bridge equal to about one half of the bridge span. Substantial errors may still exist within distances of about twice the span clearance height.

10. Conclusions

Scale models appear to provide a very good means for examining reradiation phenomena. The achievable model parameters permit sufficiently accurate scaling at about 1:4000 scale, and the model measurements agree quite well with the available real-world measurements. With vertical whip antennas (E-field), the greatest errors are for signals arriving broadside to the bridge, and smallest errors are for end-on arrival. The predominant phenomena in bridge-produced errors appear attributable to reradiation from pairs of vertically polarized top-loaded antennas, rather than reradiation from a closed loop antenna as previously assumed. This applied at least to bridges over 300 m (1000 ft) in length.

Large suspension bridges, such as the Golden Gate and the Verrazano-Narrows, are only ten percent below resonance at 100 kHz. This provides a good explanation for the much greater errors experienced near bridges such as these, compared to the errors with smaller bridges. The world's longest bridge over the Humber estuary near Hull in England is expected to be almost exactly resonant at the Loran-C frequency.

The results for shorter bridges (under 500 m = 1600 ft in length) seem to be explainable by considering the bridge as an overhead grounded shield conductor, and using static (dc) field theory. From rough calculations, high voltage power line spans are closely represented by similar-length bridge models, and comparable reradiation errors are to be expected. In the case of power lines, the arrangement of the overhead lightning shield ("ground") wires

is expected to be the controlling factor. Of course, there may be additional errors from power line carrier communication radiation, and corona noise radiation should also be examined. No actual models of power lines were tested.

11. Recommendations for Future Work

Promising preliminary approaches to reduce the effects of near-resonant bridges on Loran-C signals should be explored further, and the investigation extended to cover bridges which are not near resonance.

Additional measurements or computer simulations should be made near bridges, and an explanation sought for the 180 degree phase reversal underneath bridges. The effect of variations in receiving antenna height on the phase errors should be examined.

Some data on H-field reception should also be obtained.

12. Bibliography and References

A. Reradiation and Related Effects

1. C. Veronda, Bibliography and comments on Loran-C ground wave propagation, DOT-TSC-RSPD-77-2 Final Report, December 1977. NTIS PB 279463.
2. D. N. Travers, Abstracts of the available literature on radio direction finding 1899-1965, Southwest Research Institute Report (487 pages), July 1966. NTIS AD 800 110. [Covers the whole field of navigation systems. It has been verified (1981) that no update of this bibliography exists].
3. R. Keen, Wireless direction finding, Iliffe and Sons, London (4th Ed.), 1947. [Extensive bibliography; discussion of errors due to reradiation and cures thereof (pp 110-113, 478-483, 491-505)].
4. L. E. Whitemore, Objects that distort radio waves, Radio Broadcast Vol. 1, pp 101-106, 1922. [Direction finder errors due to reradiation, including resonant structures. Some material also in Bureau of Standards Scientific Paper No. 428, 1922].
5. R. L. Smith-Rose and R. H. Barfied, The effect of local conditions on radio direction-finding installations, J. IEE (London) Vol. 61, pp 179-196, 1923.
6. R. H. Barfield, The attenuation of wireless waves over land, J. IEE (London) Vol. 66, pp 204-218, 1928.
7. R. Bateman, E. F. Florman and A. Tait, A source of error in radio phase measuring systems, Proc. IRE Vol. 38, pp 612-614, 1950. For discussion, see Proc. IRE Vol. 39, pp 436-438, 1951.
8. G. A. Hufford, An analysis of some anomalous properties of equiphase contours, Proc. IRE Vol. 38, pp 614-618, 1950. [The above two

references discuss singularities in the field produced by reradiation from vertical antennas, and possible cycle-skip. Tests on 300 kHz systems].

9. H. C. Forbes, Reradiation from tuned antenna systems, Proc. IRE Vol. 14, pp 363-382, 1925. [Considers only vertical monopoles. Measurements at MF].

10. D. A. Feldman and W. H. Hayes, On the characteristics of reradiation from 625' Loran-C transmitter antennas, USCG EECEN Final Report on Project W0763-A4, July 1975. [Considers monopole only; includes actual transmitter driving impedances].

11. L. G. Reynolds, An examination of some site and transmission path errors of the Decca navigator system when used over land, Proc. IEE (London), Pt. III, Vol. 100, 1953, pp 29-35. [Power lines, trees, etc.].

12. R. F. Linfield, R. H. Doherty and G. Hefley, Evaluation of the propagation aspects of the CYTAC system, National Bureau of Standards Report 4CB101, March 1957. NTIS AD 128228. [Most data also in the next reference].

13. G. Hefley, The development of Loran-C navigation and timing, National Bureau of Standards Monograph 129, 1972. [Describes errors due to power lines, etc]. U.S. Govt. Printing Office.

14. J. Evans and J. O'Day, Low-frequency anomalies due to man-made electrical conductors, University of Michigan Willow Run Laboratory Report No. 2900-72-R, July 1959. NTIS AD 219 852. [Errors under and over power and phone lines. Power lines are low (22 ft), telephone lines are open wire (24 ft). Errors occur within distances equal to twice the height of the wires].

15. J. O'Day, W. Porter and J. Sullivan, An experimental investigation of the calibration of errors in predicted lines of position of low-frequency hyperbolic navigation system, University of Michigan IST Report No. 2900-244-R, June 1961. NTIS AD 258 221.

16. J. M. Ross and J. E. Kirch, A few observations of the perturbations in the phase of the low-frequency radio ground, J. Research, National Bureau of Standards Vol. 65-D, pp. 393-396, July-August 1961. [Discusses errors due to isolated mountains and due to power lines in cw phase measurement systems at 450 kHz. Observation of "Beverage Antenna" effect due to power lines was inconclusive].

17. J. O. Day, Errors in the field of a low-frequency hyperbolic navigation system in mountainous terrain, Fifth IEEE MIL-E-CON Conf. Proc. pp 521-530, June 1961. [Analysis of mountains as scatterers].

18. E. R. Swanson, R. H. Gimber and J. E. Britt, Calibrated VLF phase measurements: simultaneous remote and local measurements of 10.2 kHz carrier phase using Cesium standards, Proc. Fourth Precision Time and Time Interval Meeting, pp 232-248 (paging irregular), November 1972. [Analyses errors from capacitive coupling. Slightly more detail in next reference].

19. E. R. Swanson, R. H. Gimber and J. E. Britt, Calibrated VLF phase measurements: simultaneous remote and local measurements of 10.2 kHz carrier phase using Cesium standards, Naval Electronics Laboratory Center Technical Note NELC-1778, December 1970. NTIS AD 892 1531.

20. "Raymondville interference signal investigations," submitted to USCG under contract DTCG 23-80-P-01499 (circa 1980) Austron Navigation Inc. [Verifies reflection of Loran-C from mountain range].

21. D. A. Hendley, Notes on reflections from high ridge, Racal Decca Navigation Limited (circa 1980). [Comments on Austron Raymondville investigation].

22. J. R. Johler et al., Some comments on experimental data collection for west coast Loran-C chain, Colorado Research and Prediction Laboratory, Inc. Report 78-8, August 1978. [Includes comments on various older experiments and unpublished data on power line reradiation measurements on Loran-D at Eglin AFB].

23. Loran-C automatic vehicle monitoring system Vol. 1, Teledyne Systems, Inc., UMTA-IT-06-0041-72-1. NTIS PB-216322, July 1972. [First Philadelphia tests. Includes tests underneath overhead railroads and on suspension bridge roadway].

24. Loran automatic vehicle monitoring system, Phase 1, Vol. 1, Teledyne Systems, Inc., UMTA-MA-06-0041-77-10, NTIS PB-274955, August 1977. [Second Philadelphia tests. Includes tests on suspension bridge roadway].

25. M. C. Poppe, Jr., Observations regarding usability of Loran-C signals in the Nashville area, in Cambridge Engineering Monthly Report Activity for April 1978, pp 5-7. [Reprinted in next reference].

26. P. S. Brown, Evaluation of Loran-C for the accurate location and documentation of highway events, features, elements, Tenn. D.O.T. Final Report TN/DOT/RP/79-01, July 1979.

27. P. E. Mauro and J. D. Gakin, The effects of primary power transmission lines on the performance of Loran-C receivers in terrestrial applications, Final Report No. DOT-TSC-RSPA-79-8, July 1979. [Tests on TVA system with and without carrier present on 161 kV and 500 kV power lines]. NTIS PB 301 367.

28. W. A. Kissick, Power line carrier radiation and the low-frequency aeronautical radio compass, Report FAA-RD-80-31, May 1980 (available from NTIS). [Includes minor information on reradiation from power lines].

29. M. C. Day, An automatic vessel traffic control system utilizing Loran-C, Proc. 2nd Annual Technical Symposium of the Wild Goose Assoc., 3-5 October 1972. [Publication only by preprint: Amecom Div., Litton Systems, Inc., College Park, MD. Tests on Canadian portion of St. Lawrence Seaway; objective was 250 ft accuracy (95%)].

30. J. D. Illgen and D. A. Feldman, Loran-C signal analysis experiments--an overview, Proc. 7th Annual Technical Symposium of the Wild Goose Assoc., New Orleans, 18-20 October 1978.

31. W. N. Dean, Phase measurements near Golden Gate Bridge, Proc. 7th Annual Technical Symposium of the Wild Goose Assoc., New Orleans 18-20 October 1978. [Time of arrival measurements].

32. B. Gambill and K. Schwartz, Loran-C signal analysis propagation model evaluation, General Electric--TEMPO, Report No. CG-D-20-80, July 1979. NTIS AD-A084338. [Includes San Francisco Harbor tests, time difference measurements].

33. L. W. Nelson and B. Gambill, Loran-C signal analysis, General Electric--TEMPO Report No. CG-D-4-80, December 1979. NTIS AD-A084239. [Includes San Francisco Harbor tests, time difference measurements].

34. F. H. Raub and R. G. Olsen, Detection of Loran-C anomalies caused by man-made structures, Proc. 7th Annual Technical Symposium of the Wild Goose Assoc., New Orleans, 18-20 October 1978. [Slightly more detail in next reference].

35. F. H. Raub and R. G. Olsen, Application of three-axis magnetic field reception to Loran-C, Polhemus Navigation Sciences, Inc. Final Report under USCG Contract T4, 42, B/WDC, December 1977. [Emphasizes differences between loop and dipole near fields].

36. H. C. Turnage, Highway advisory radio, IEEE Trans. Vehicular Technology, Vol. VT-29, No. 2, pp 183-191, May 1980. [Measurements on MF near field loop and whip antenna reception from radiating cable. Loop antenna is greater].

37. O. L. Prestholdt, The effects of re-radiation from television towers and other structures upon directional antennas, NAB 1958 Broadcast Engineering Conference (CBS Engineering Department Publication).

38. O. J. Sather, Construction of the WOR transmitter and directional antenna system, IEEE Trans. Broadcasting, Vol. BC-15, p 65, September 1969. [Reduction of reradiation from towers].

39. K. M. Chen and V. V. Liepa, The minimization of the backscattering of a cylinder by central loading, IEEE Trans. Antennas Propag., Vol. AP-12, pp 576-582, September 1964.

40. D. F. Jones and R. L. Hicks, Effect of power lines on radiation patterns of broadcast antennas, Ontario Hydro Research Quarterly, pp 7-13, 1971, Fourth Quarter.

41. K. G. Balmain and J. S. Belrose, AM broadcast re-radiation from buildings and power lines, IEEE Conf. Publ. No. 169, Antennas and Propagation, Part 1, pp 268-272, November 1978.

42. J. S. Belrose et al, The effects of re-radiation from highrise buildings and transmission lines upon the radiation pattern of MF broadcast antenna arrays, NATO-AGARD/FPP Specialist Meeting on Terrain Profiles and Contours in EM Propagation, Norway, 11-14 September 1979, pp 2-1 to 2-11.

43. C. W. Trueman et al, The prediction of re-radiation from power lines at MF frequencies, IEEE International Symposium on Electromagnetic Compatability, Baltimore MD, 7-9 October 1980.

44. J. S. Belrose, On minimizing the effect of re-radiation from power transmission lines on the radiation patterns of MF-AM broadcasting antenna arrays, IEE Second International Conference on Antennas and Propagation, University of York, UK, 13-16 April 1981.

45. A. A. Smith Jr., Attenuation of electric and magnetic fields by buildings, IEEE Trans. Electromagnetic Compatibility, Vol. EMC-20, pp 411-418, August 1978. [Quantitative data, 20 kHz to 500 MHz: large attenuation of 100 kHz electric field inside steel-frame buildings].

46. D. Deno, UHV transmission line electric field reduction with a set of horizontal wires, IEEE Trans. Power Apparatus and Systems, Vol. PAS-96, September/October 1977. [Shielding effect of single and multiple wires].

47. J. E. Bridges, Biological influence of power frequency electric fields (Tutorial Review), Proc. IEEE Vol. 69, pp 1092-1120, September 1981. [Figure 2 shows shielding due to towers].

48. W. Chugoy et al, Petition of rule making of the Utilities Telecommunications Council before FCC [relative amendment of rules to provide regulatory recognition and protection for power line carrier operation of electric utilities in band 10-490 kHz), September 30, 1980. [Includes C.I.G.R.E. memorandum on power line carrier systems 1973].

49. IEEE Committee Report: Review of technical considerations on limits to interference from power lines and stations, IEEE Trans. Power Apparatus and Systems, Vol. PAS-99, pp 365-388, March/April 1980. [Considers primarily noise due to corona discharge].

50. W. R. Vincent and G. Sage, Loran-C RFI measured in Los Angeles, California, Report UMTA-MA-06-0041-80-1, October 1980. NTIS PB81-151300.

B. Bridge and Power Line Physical Information

51. Encyclopedia Americana, 1981 (see bridges).

52. The World Almanac, 1981.

53. Information Please Almanac, 1981.

54. Hammond Almanac, 1982.

55. T. Dagnall, private communication from superintendent of maintenance, Ambassador Bridge, Detroit, MI, 27 July 1981.

56. USCG (GNBR) COMDTINST M16590.3, Bridges over navigable waters of the United States, 15 December 1980.

57. R. Dillon, High steel: building the bridges across San Francisco Bay, Millbrae, CA: Celestial Arts, 1979. [Golden Gate and Transbay Bridges].

58. L. A. Rubin, Mighty Mac: The official picture history of the Mackinac Bridge, Wayne State University Press, Detroit, 1958.

59. E. Cohen and B. Birdsdale (eds), Long span bridges, O. H. Ammann Centennial Conference, Annals of N. Y. Academy of Sciences, Vol. 352, 1980. [Good information on Verrazano Narrows Bridge].

60. J. H. Stevens, Towers and Bridges and Other Structures, Sterling Publishing Co., New York NY, 1976.

61. H. S. Smith, The World's great bridges, Harper and Row, New York, N.Y., 1964. [Good detailed dimensions].

62. Guinness Book of World Records, New York: Bantam, 1982, pp 276 and 344. [Large bridges and power lines].

63. Transmission Line Reference Book - 345 kV and Above, Electric Power Research Institute, Palo Alto, CA, 1975. [Second edition to be available 1982].

64. EVH Transmission Line Reference Book, Edison Electric Institute, New York, 1968.

65. Principle Electrical Facilities, Dept. of Energy, Energy Information Administration DOE/EIA 0057, 1978. [Map: 10 sheets cover continental U.S.].

66. Highest Voltage Commercial Transmission in the World, IEEE Trans. Power Apparatus and Systems, Vol. PAS-85, pp 562-564, June 1966. [Describes Hydro-Quebec 735 kV transmission with spans up to 5880 feet; overhead grounded shield wires omitted on water span].

67. V. List, Mechanical Design of Overhead Transmission Lines, SNTL; Prague; English Edition, 1963. [Describes spans over 5 km, towers over 225 meters; location unspecified].

68. W. J. Thrasher, Detroit Edison Co., Detroit, personal communication, 24 June 1981. [Information on Detroit river and St. Clair river power line crossings].

69. R. Broad, Commonwealth Associates, Jackson, MI., personal communication, 7 July 1981. [Information on Mississippi river crossings].

70. J. D. Phillips and F. A. Denbrook, 1160 miles of EHV transmission optimized, IEEE Trans. on Power Apparatus and Systems, Vol. PAS-85, pp. 566-570, June 1960. [Describes south central USA river spans].

71. G. Sinclair, Theory of models of electromagnetic systems, Proc. IRE Vol. 36, pp 1364-1370, November 1948.

72. E. D. Sunde, Earth Conduction Effects in Transmission Systems, Van Nostrand Co., New York, 1949; Chapter II.

73. Reference Data for Engineers, 5th Edition, H. W. Sams Co., New York, 1968, pp 4-32.

74. A. D. Watt, VLF Engineering, Pergamon Press, New York, 1967; pp 52, 92 and 183.

75. W. Dean et al, Cytac long range tactical bombing system, Sperry Gyroscope Co., Final Engineering Report 5223-1307-14, March 1956. NTIS AD 125 048. [Figure N-4 describes a scale model test of the resonant L-antenna].

APPENDIX

MODEL BRIDGE DATA

Summary of these data are given in Chapter 4, Tables 4.1 through 4.4.

The data plots are identified by a plot number (e.g., 1301A) given in the upper right-hand corner of each plot. Data are plotted on scales $0 \leq$ amplitude ≤ 2 and $-40 \leq$ phase ≤ 40 degrees, with the plot designated by the letter A. Where appropriate, plots (designated by the letter B) showing all the data are also presented. These are placed on facing pages, requiring that some pages be left blank.

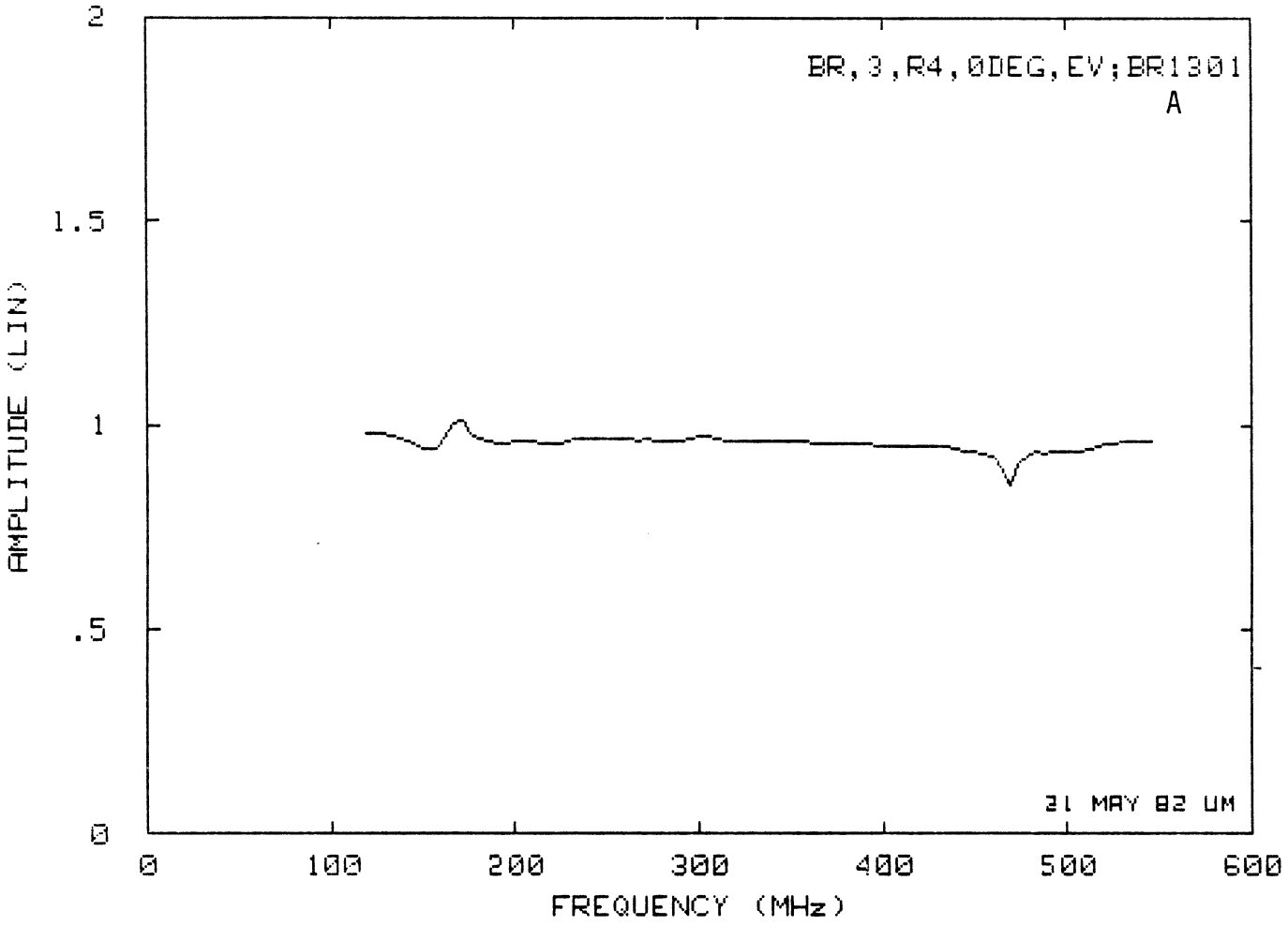
BR,3,R4,0DEG,EV;BR1301
A
21 MAY 82 UM
AMPLITUDE (LIN)
2
1.5
1
.5
0
0
100
200
300
400
500
600
FREQUENCY (MHz)

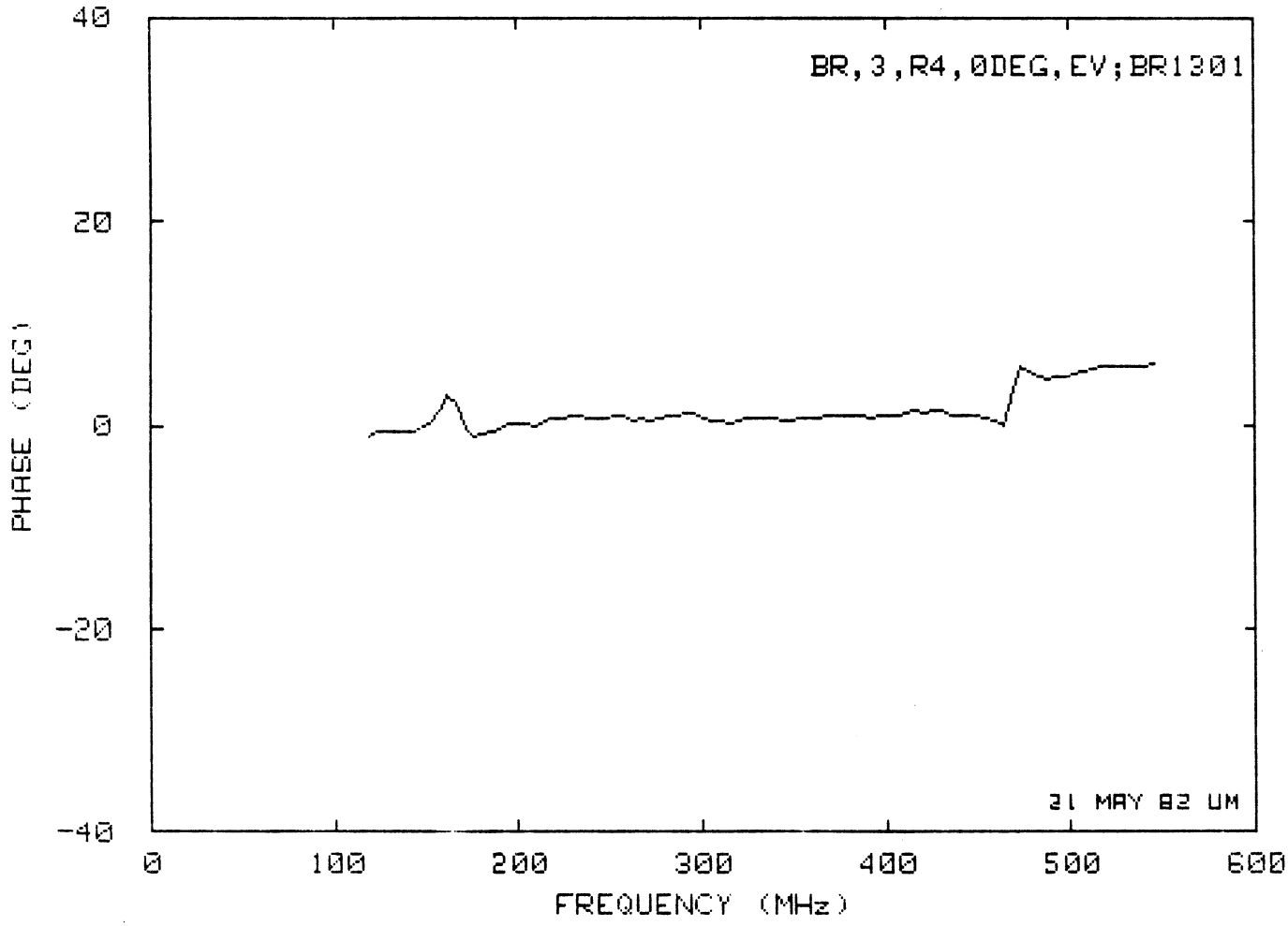
BR,3,R4,0DEG,EV;BR1301
21 MAY 82 UM
PHASE (DEG)
40
20
0
-20
-40
0
100
200
300
400
500
600
FREQUENCY (MHz)

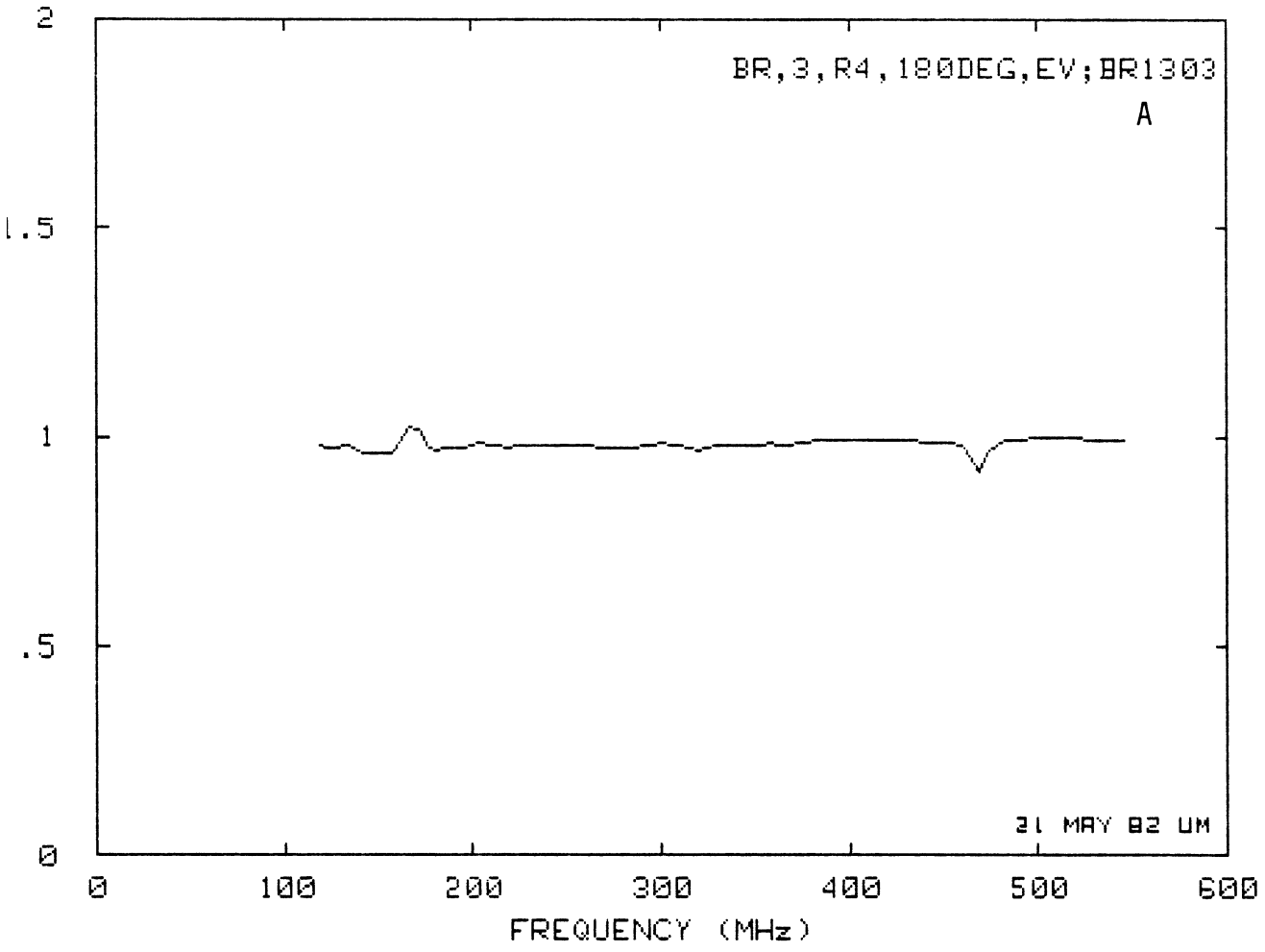
BR,3,R4,180DEG,EV;BR1303
A
21 MAY 82 UM
2
1.5
1
.5
0
0
100
200
300
400
500
600
FREQUENCY (MHz)

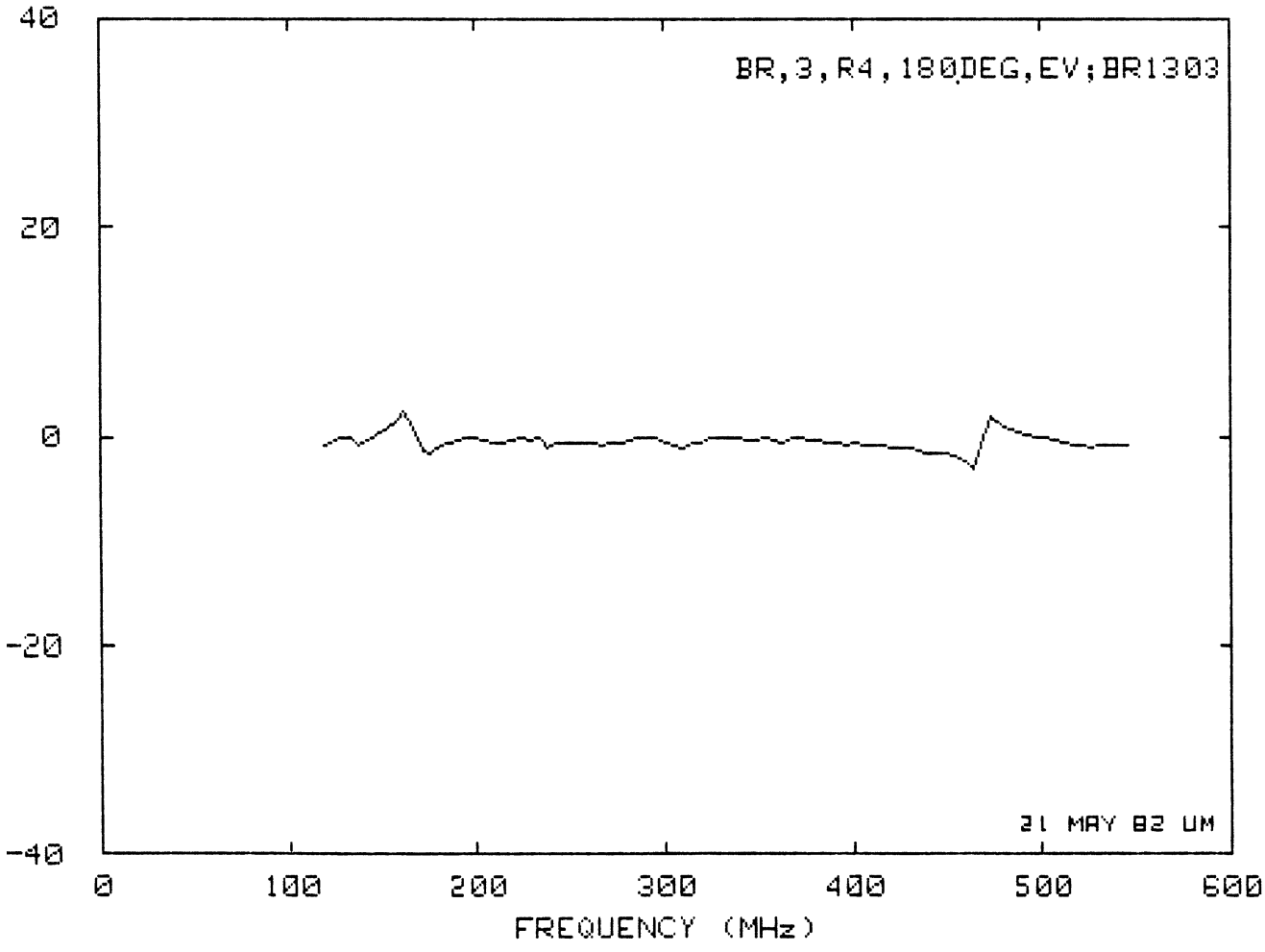
BR,3,R4,180DEG,EV;BR1303
21 MAY 82 UM
40
20
0
-20
-40
0
100
200
300
400
500
600
FREQUENCY (MHz)

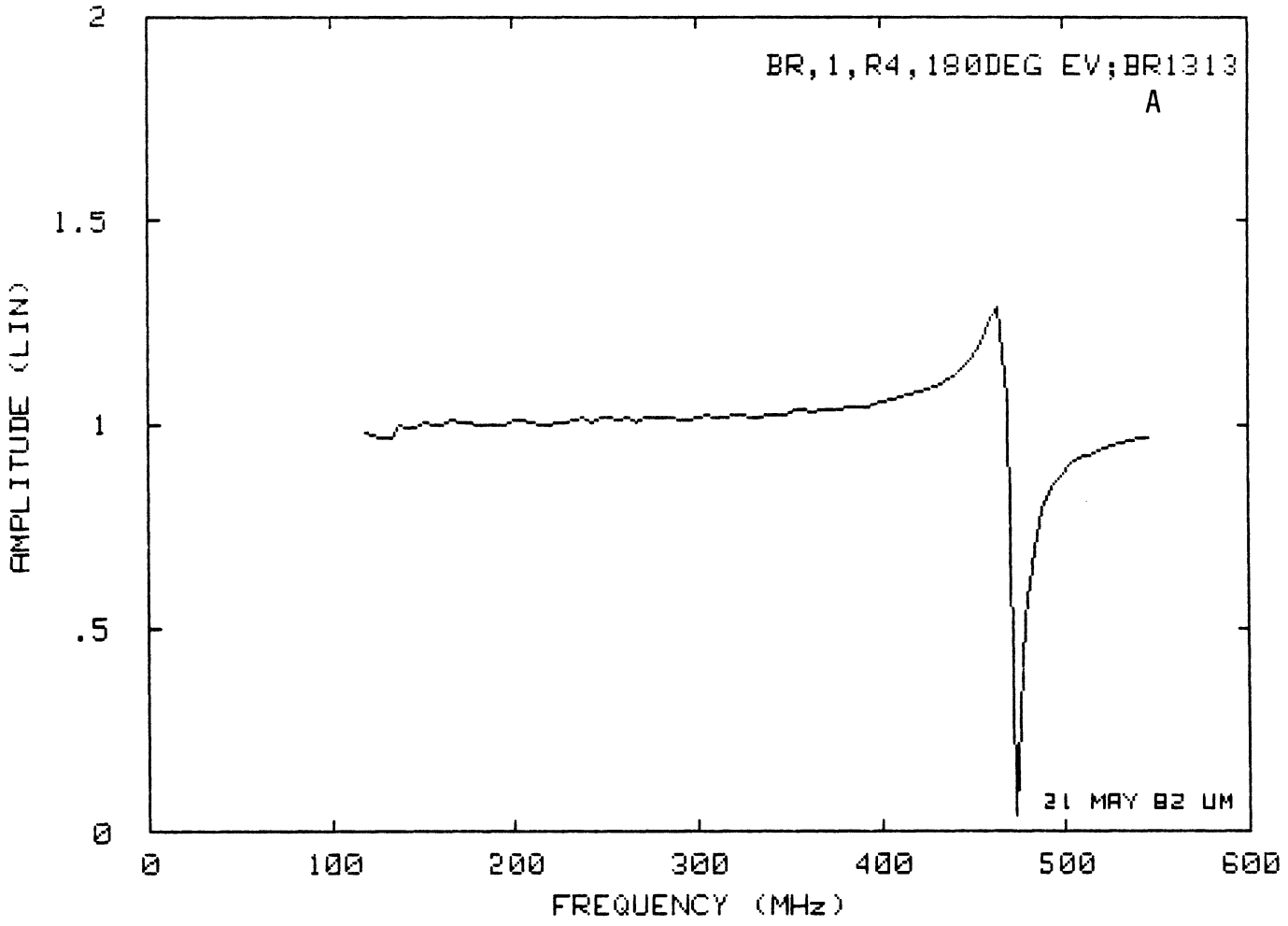
BR,1,R4,180DEG EV;BR1313
A
21 MAY 82 UM
AMPLITUDE (LIN)
2
1.5
1
.5
0
0
100
200
300
400
500
600
FREQUENCY (MHz)

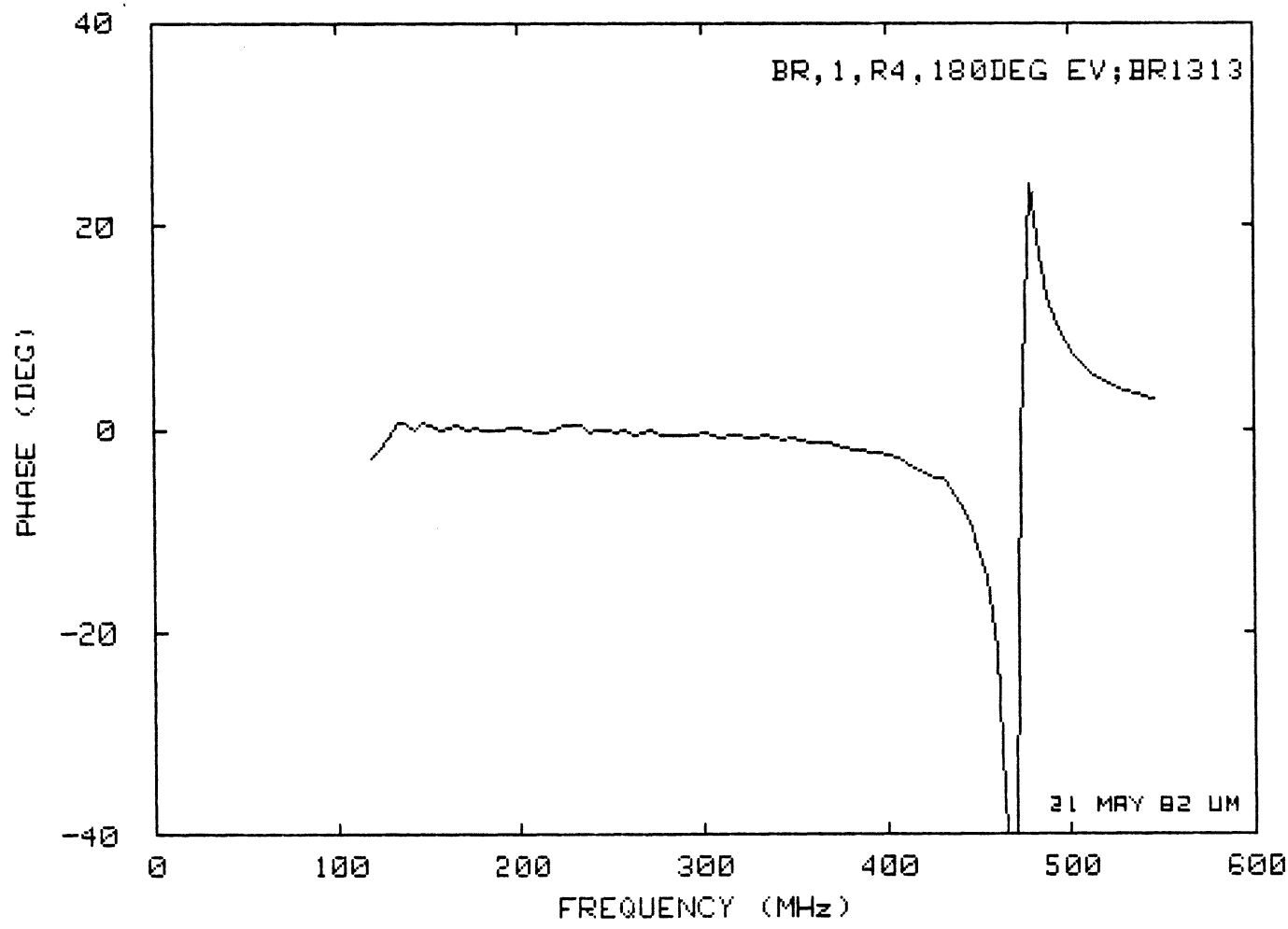
BR,1,R4,180DEG EV;BR1313
21 MAY 82 UM
PHASE (DEG)
40
20
0
-20
-40
0
100
200
300
400
500
600
FREQUENCY (MHz)

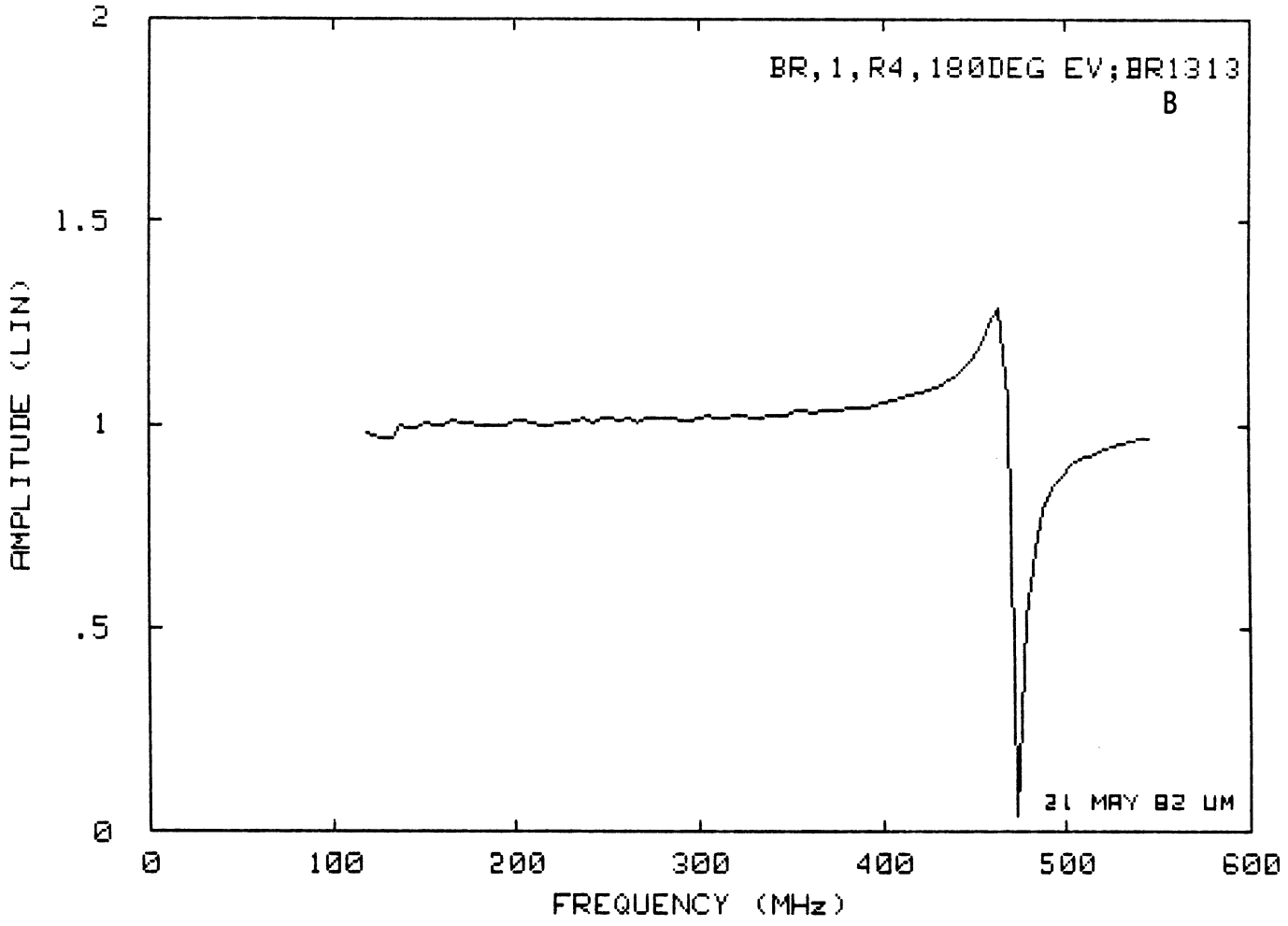
BR,1,R4,180DEG EV;BR1313
B
21 MAY 82 UM
AMPLITUDE (LIN)
2
1.5
1
.5
0
0
100
200
300
400
500
600
FREQUENCY (MHz)

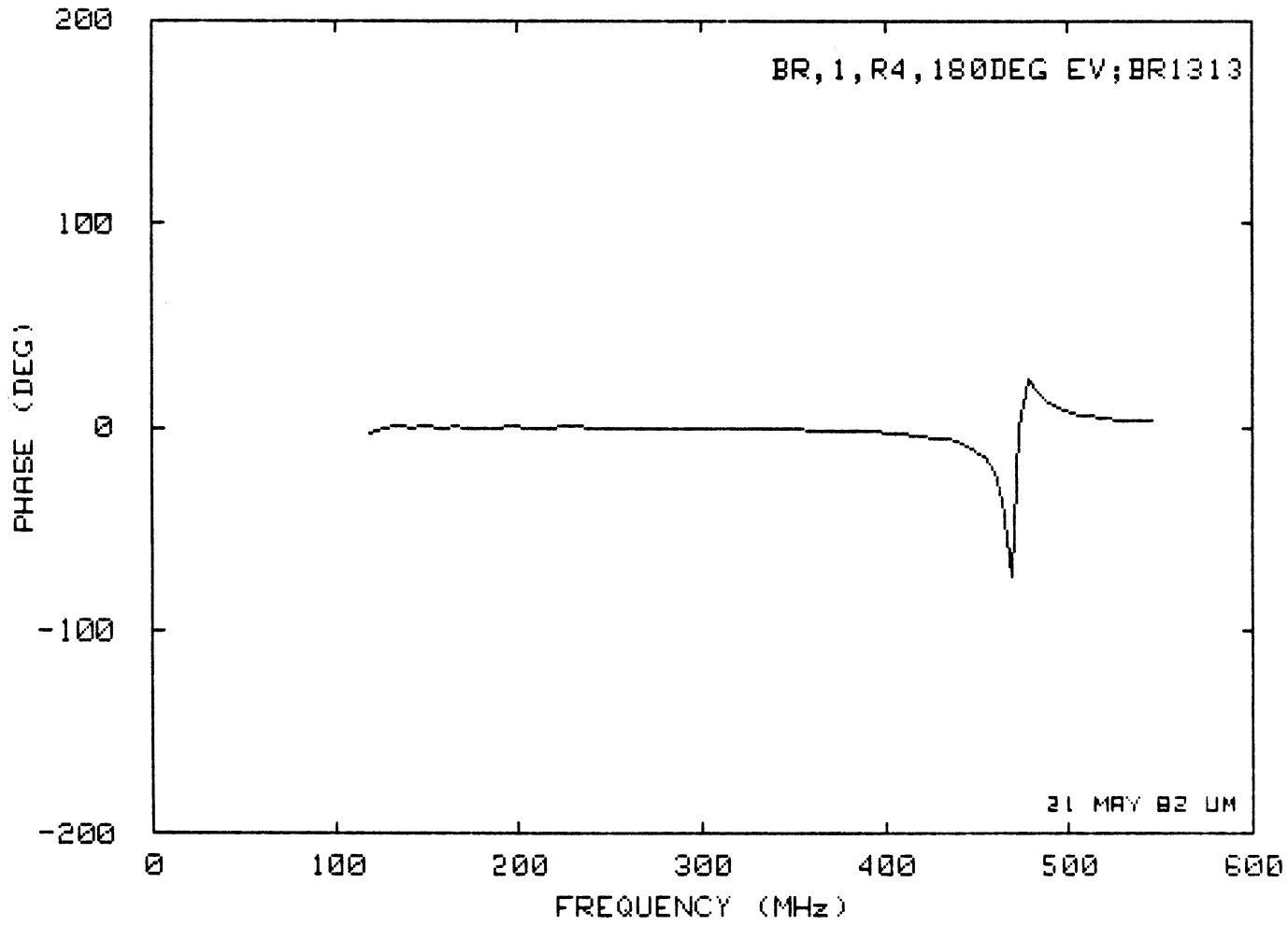
BR,1,R4,180DEG EV;BR1313
21 MAY 82 UM
PHASE (DEG)
200
100
0
-100
-200
0
100
200
300
400
500
600
FREQUENCY (MHz)

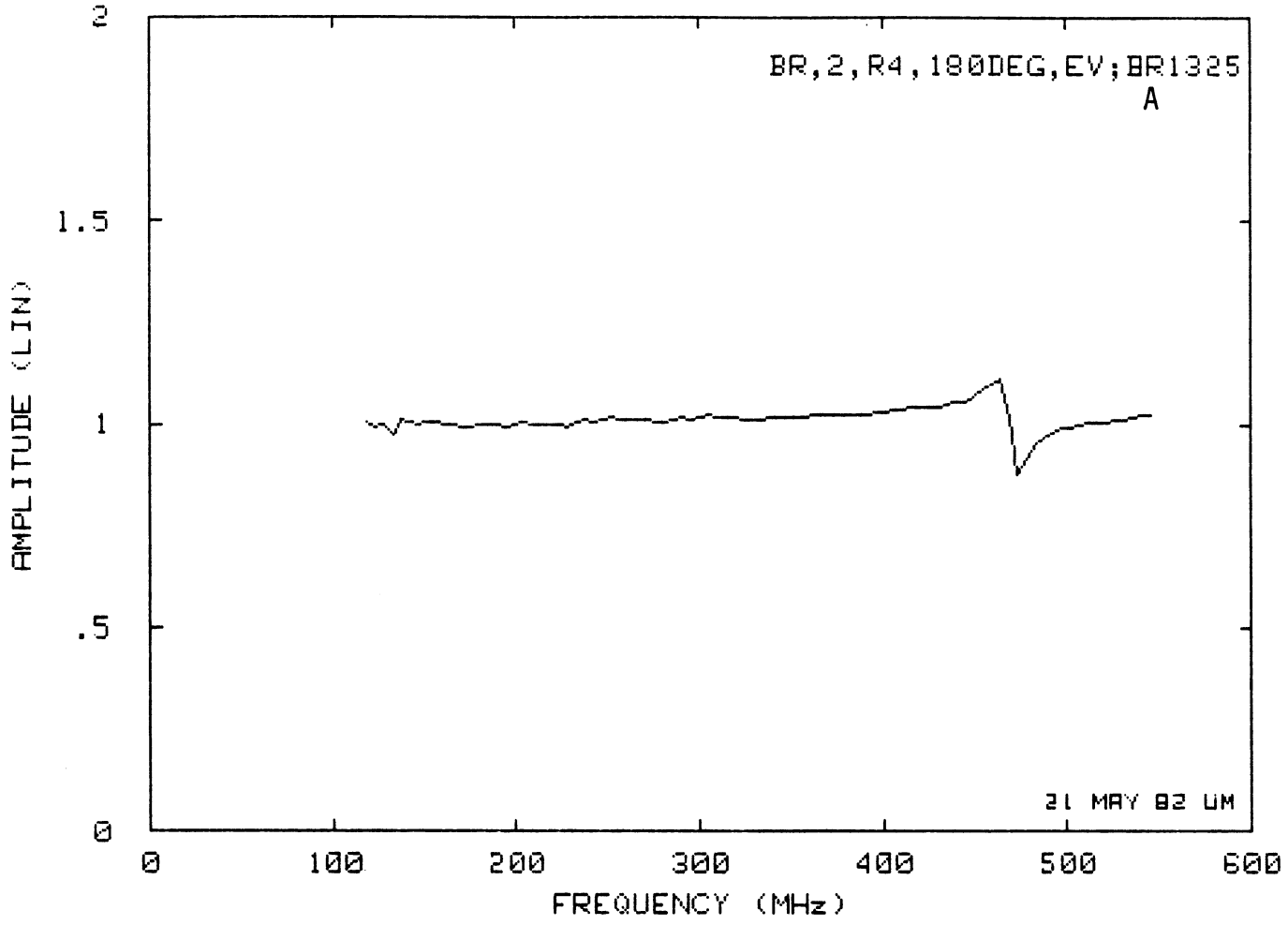
BR,2,R4,180DEG,EV;BR1325
A
21 MAY 82 UM
AMPLITUDE (LIN)
2
1.5
1
.5
0
0
100
200
300
400
500
600
FREQUENCY (MHz)

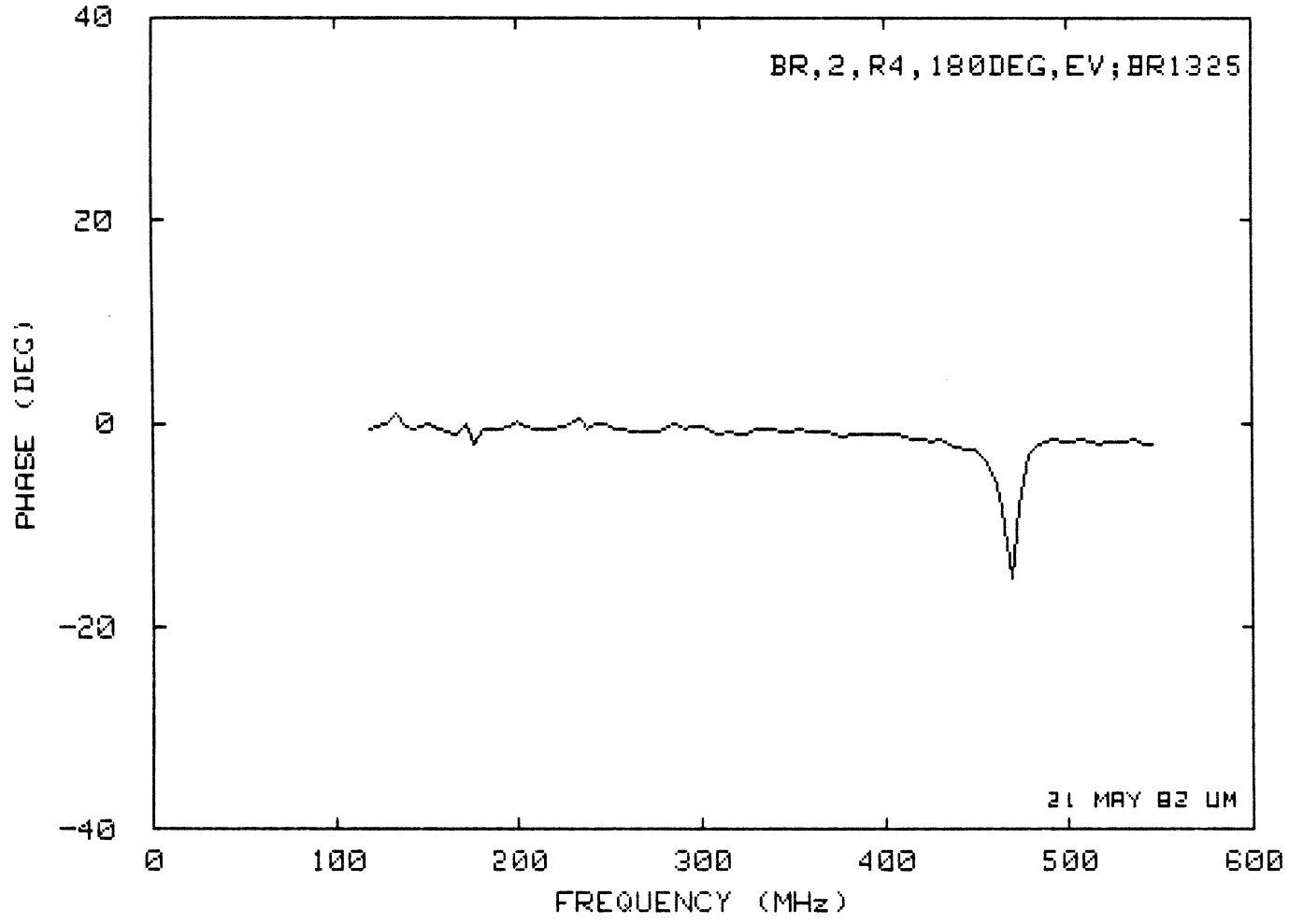
BR,2,R4,180DEG,EV;BR1325
21 MAY 82 UM
PHASE (DEG)
40
20
0
-20
-40
0
100
200
300
400
500
600
FREQUENCY (MHz)

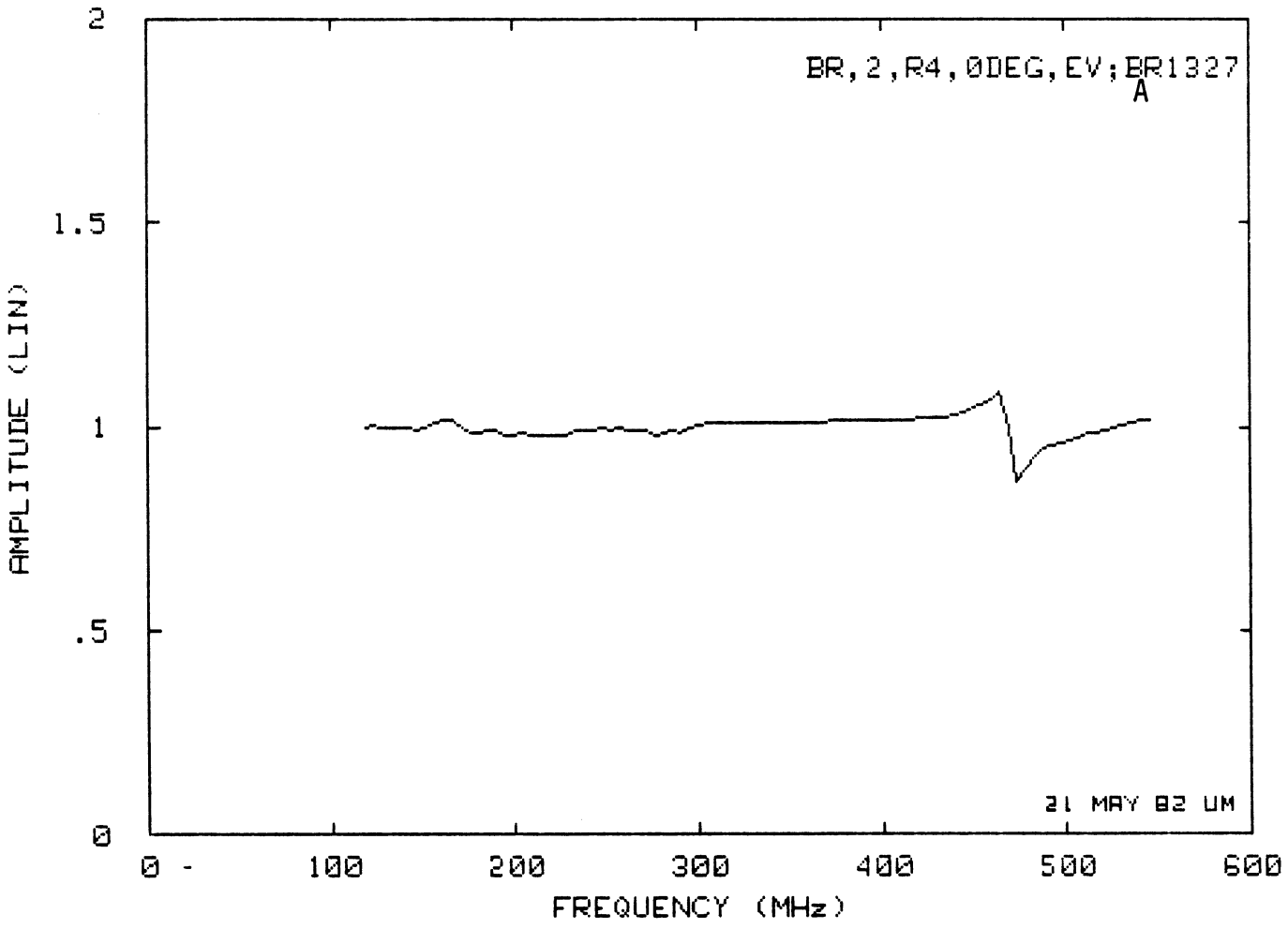
BR,2,R4,0DEG,EV;BR1327
A
21 MAY 82 UM
AMPLITUDE (LIN)
2
1.5
1
.5
0
0 -
100
200
300
400
500
600
FREQUENCY (MHz)

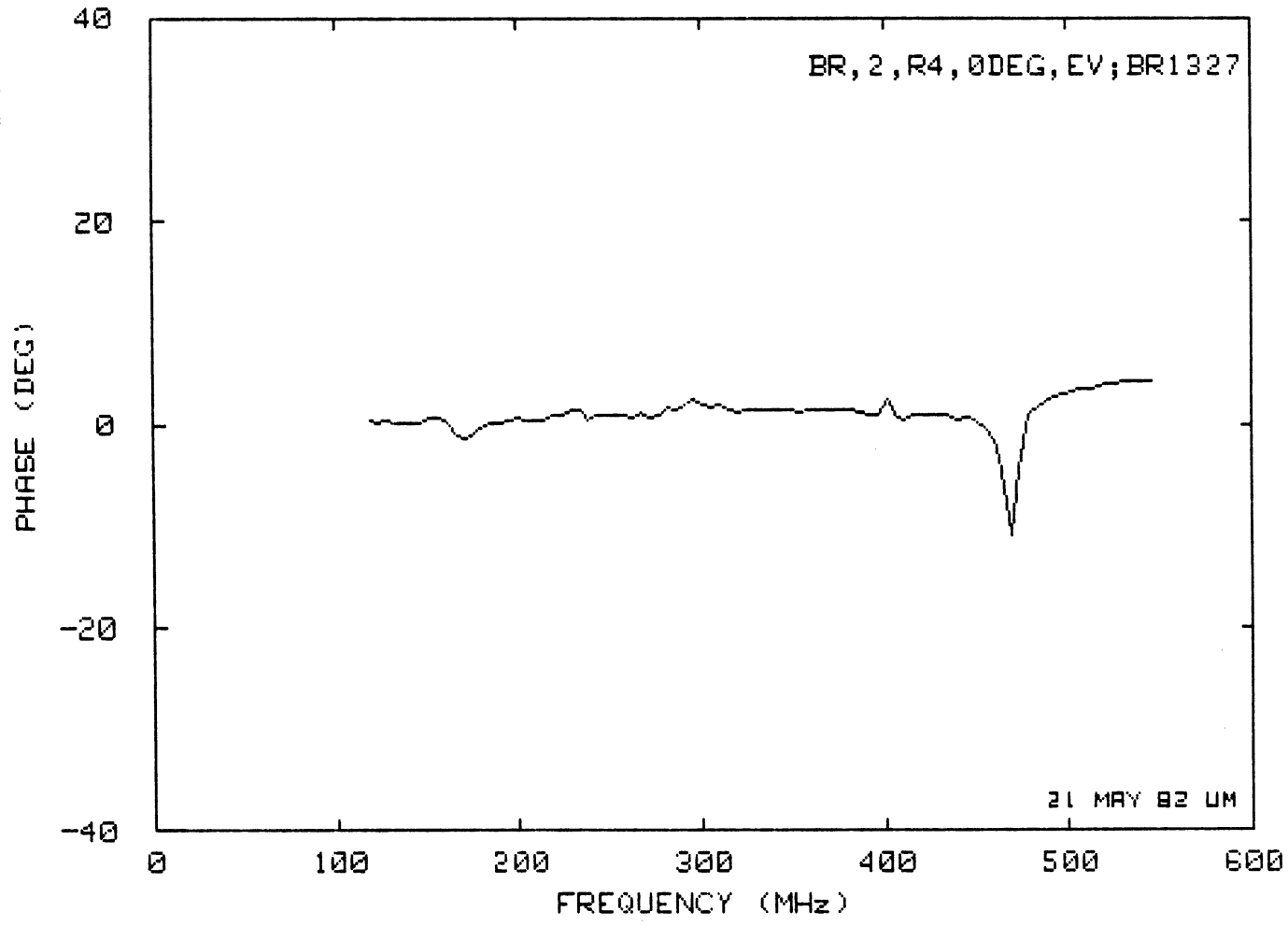
BR,2,R4,0DEG,EV;BR1327
21 MAY 82 UM
PHASE (DEG)
40
20
0
-20
-40
0
100
200
300
400
500
600
FREQUENCY (MHz)

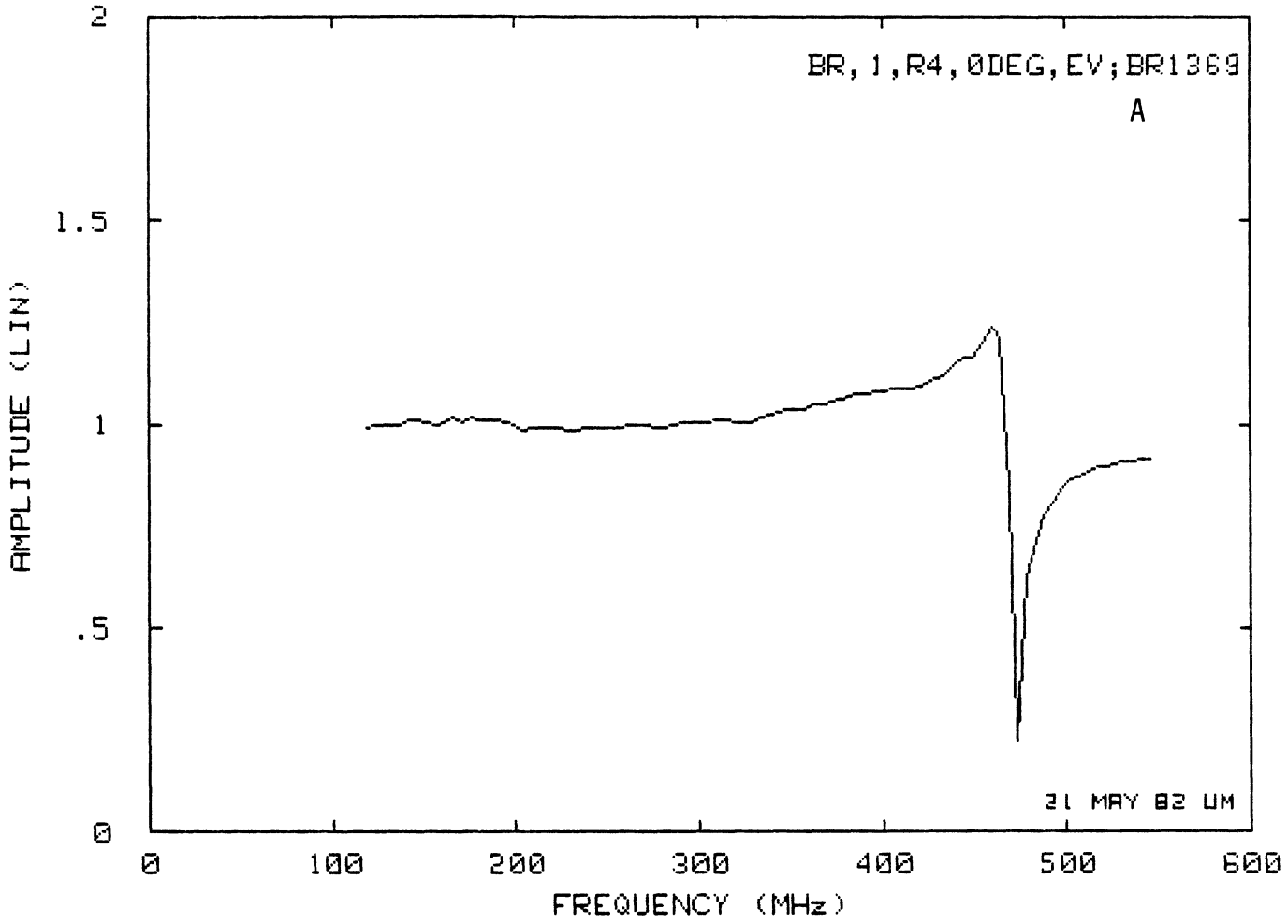
BR,1,R4,0DEG,EV;BR1369
A
21 MAY 82 UM
AMPLITUDE (LIN)
2
1.5
1
.5
0
0
100
200
300
400
500
600
FREQUENCY (MHz)

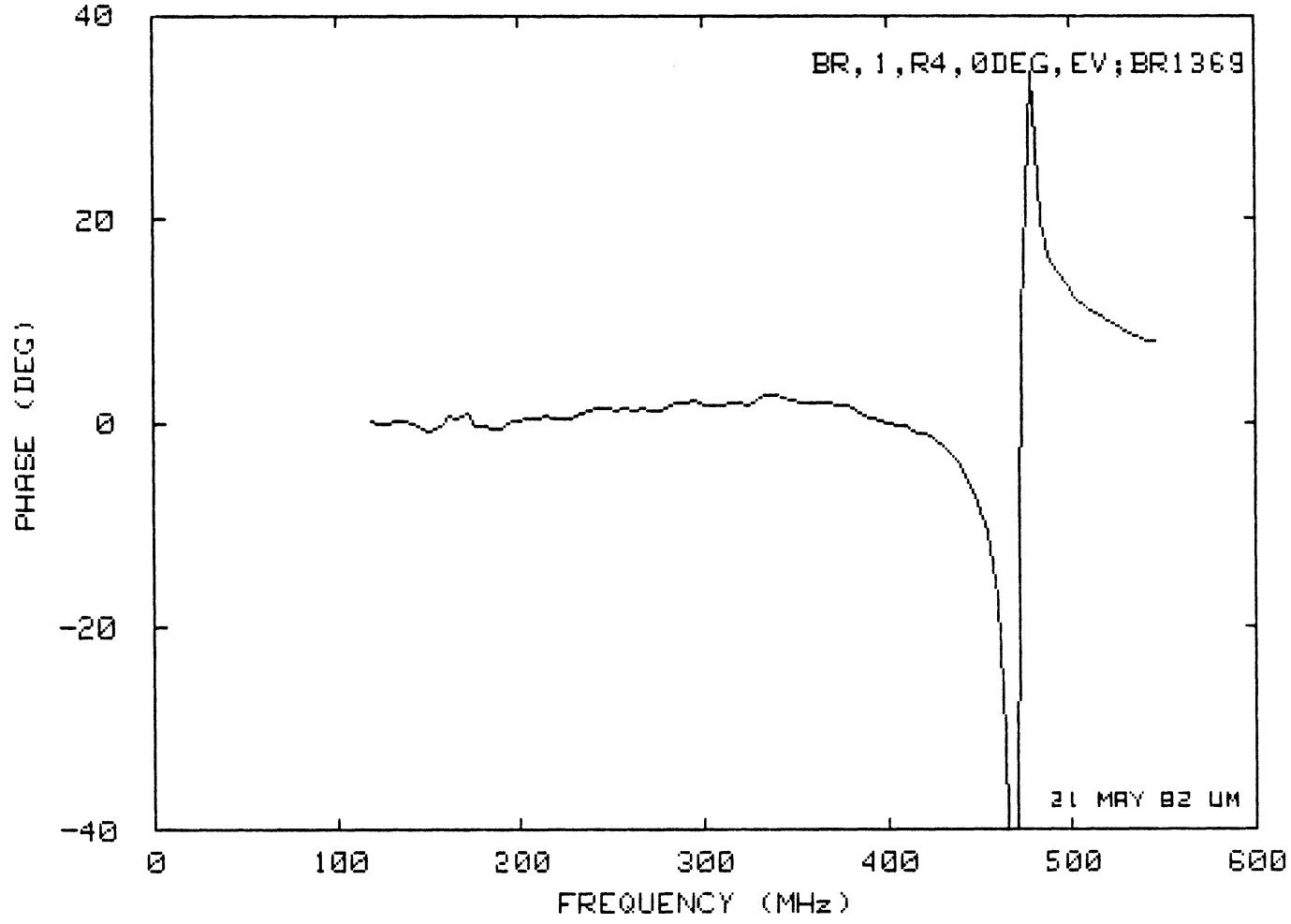
BR,1,R4,0DEG,EV;BR1369
21 MAY 82 UM
PHASE (DEG)
40
20
0
-20
-40
0
100
200
300
400
500
600
FREQUENCY (MHz)

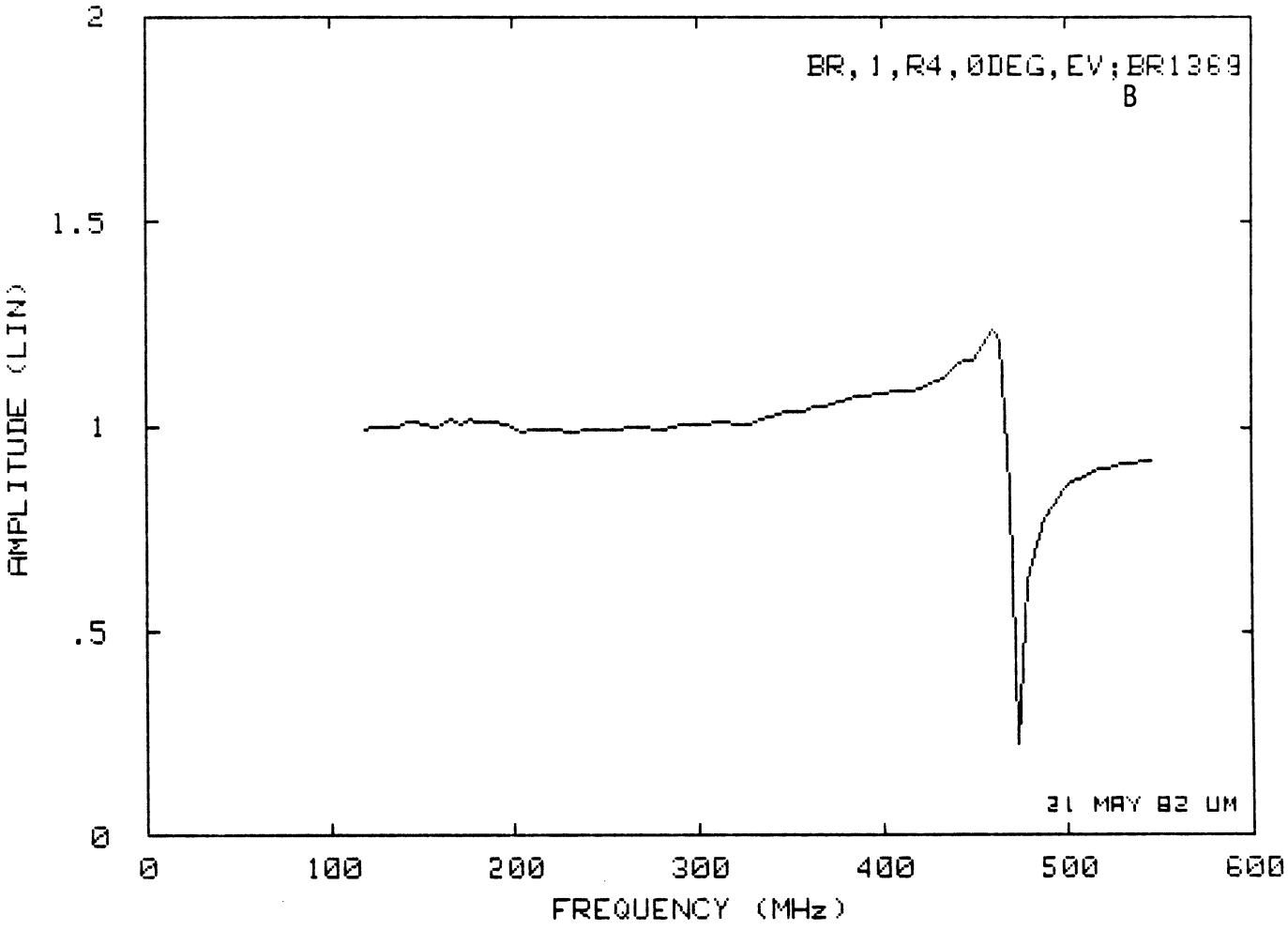
BR,1,R4,0DEG,EV;BR1369
B
21 MAY 82 UM
AMPLITUDE (LIN)
2
1.5
1
.5
0
0
100
200
300
400
500
600
FREQUENCY (MHz)

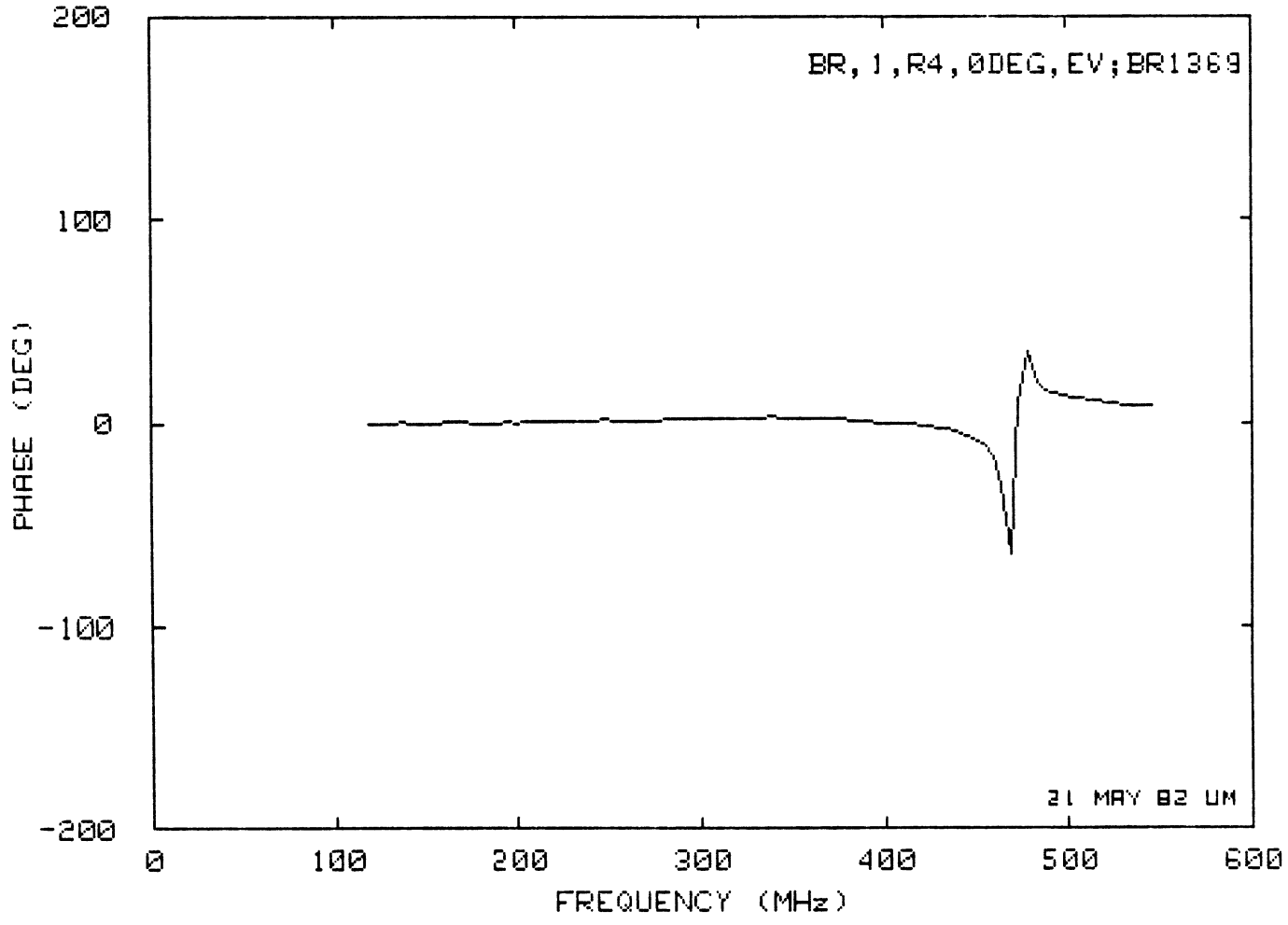
BR,1,R4,0DEG,EV;BR1369
21 MAY 82 UM
PHASE (DEG)
200
100
0
-100
-200
0
100
200
300
400
500
600
FREQUENCY (MHz)

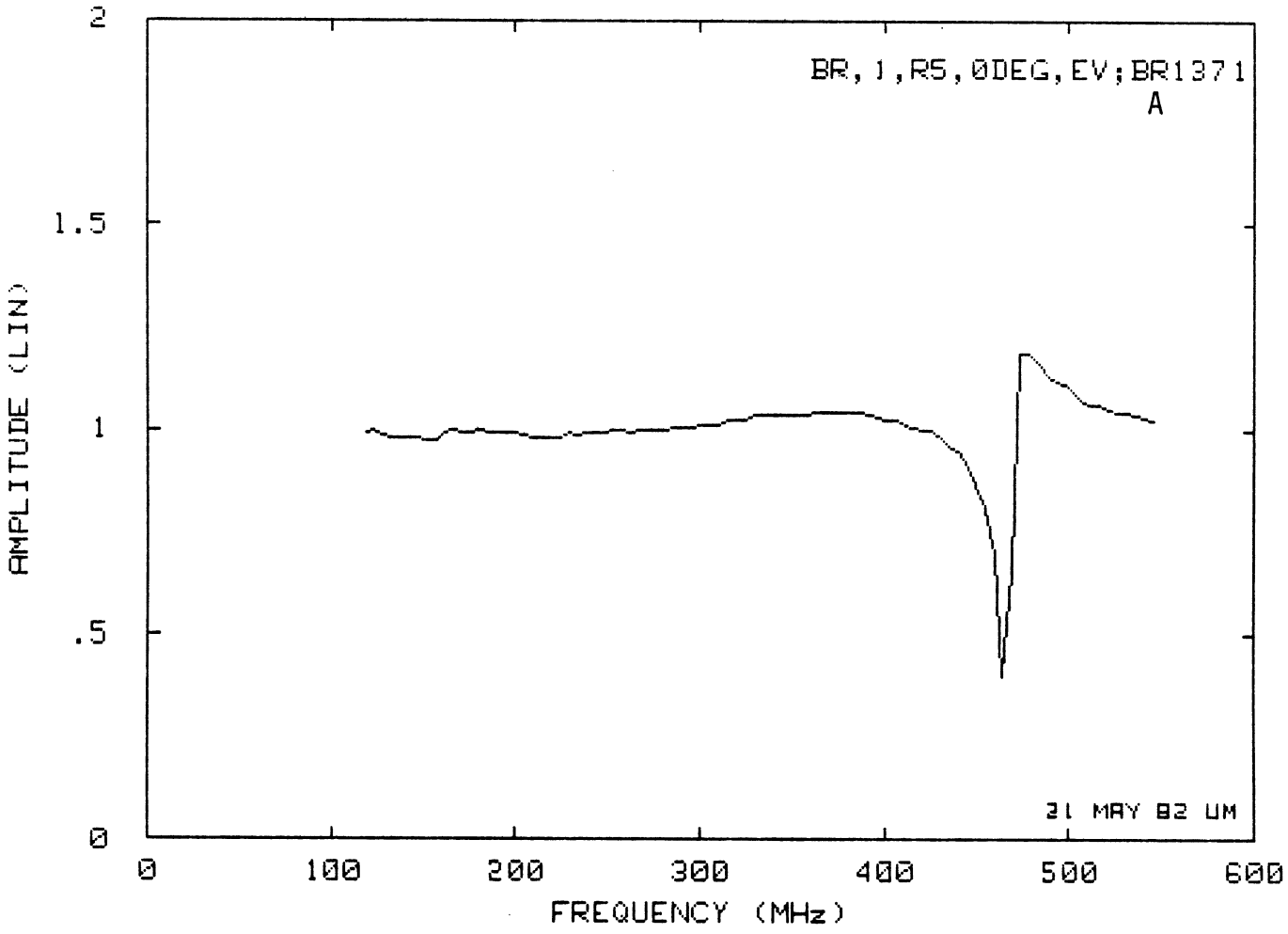
BR,1,RS,0DEG,EV;BR1371
A
21 MAY 82 UM
AMPLITUDE (LIN)
2
1.5
1
.5
0
0
100
200
300
400
500
600
FREQUENCY (MHz)

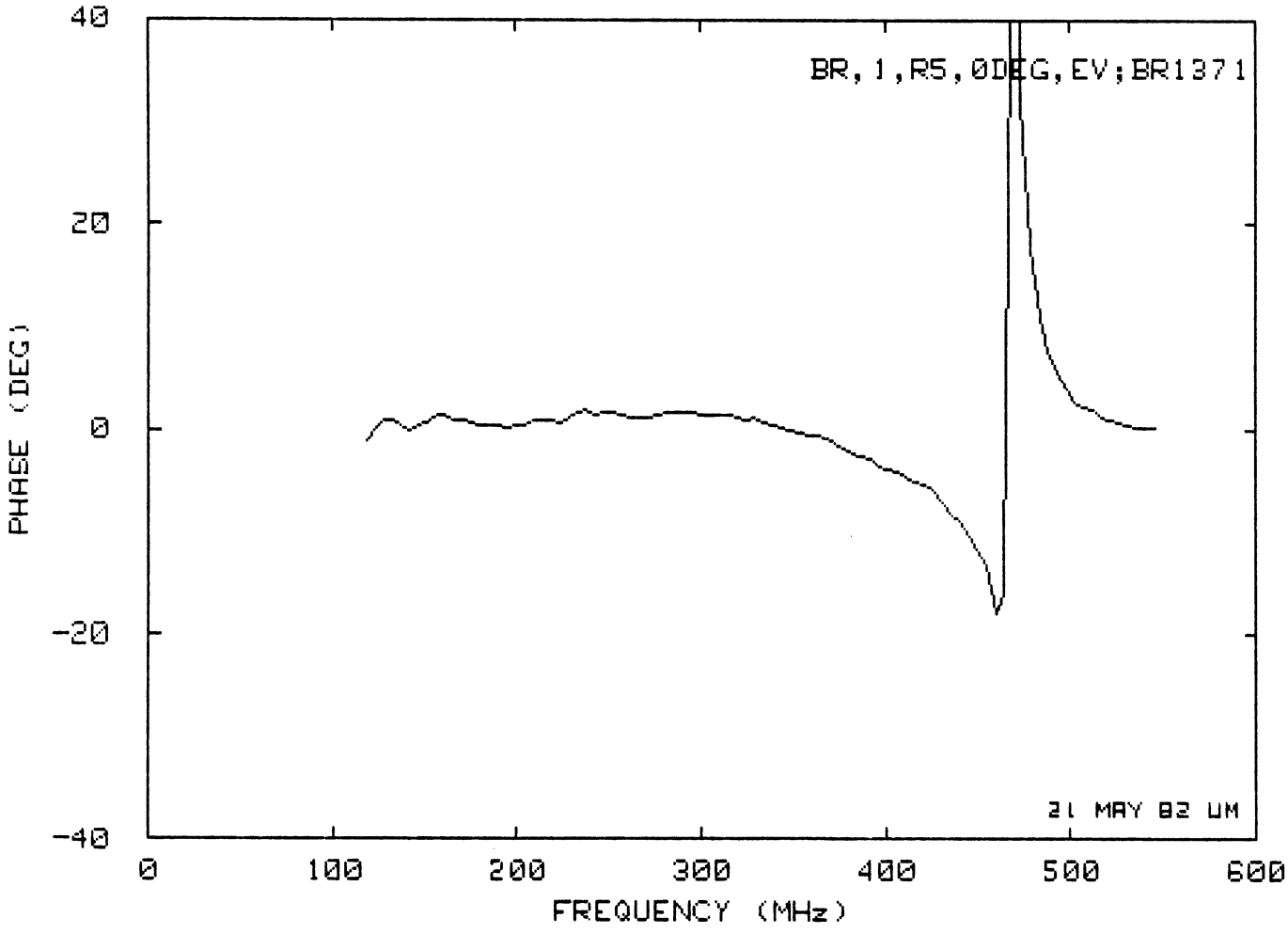
BR,1,RS,0DEG,EV;BR1371
21 MAY 82 UM
PHASE (DEG)
40
20
0
-20
-40
0
100
200
300
400
500
600
FREQUENCY (MHz)

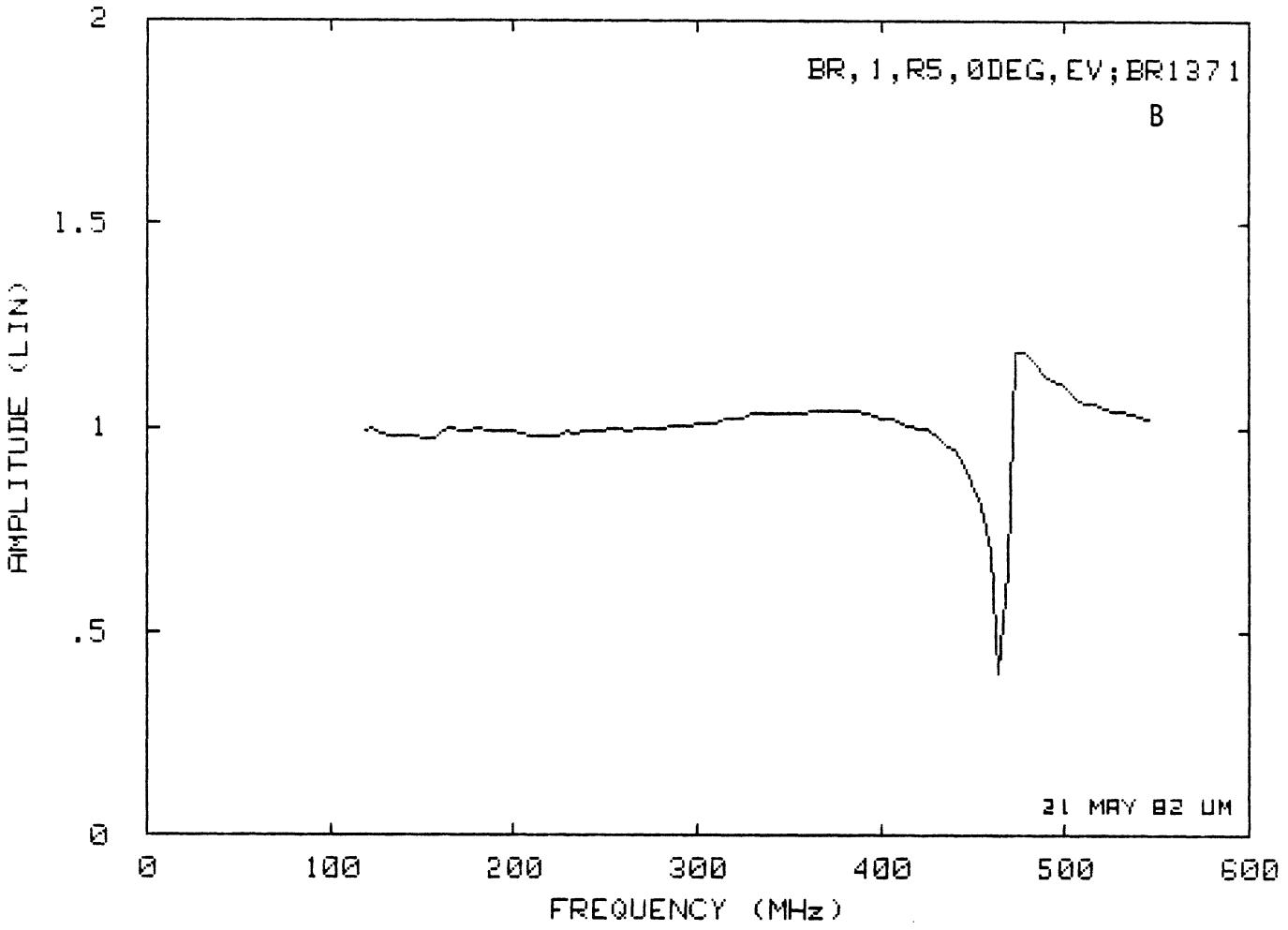
BR,1,R5,0DEG,EV;BR1371
B
21 MAY 82 UM
AMPLITUDE (LIN)
2
1.5
1
.5
0
0
100
200
300
400
500
600
FREQUENCY (MHz)

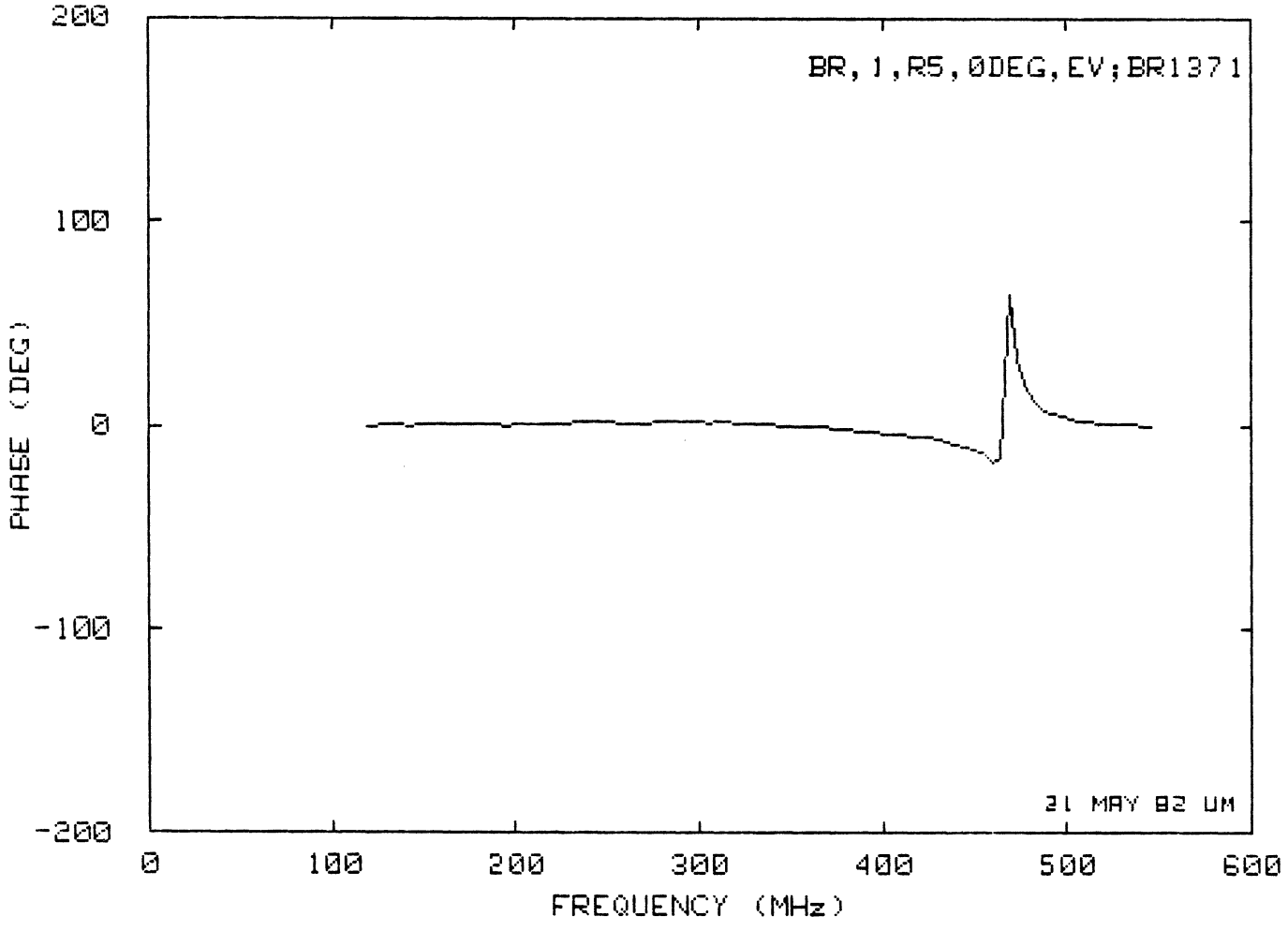
BR,1,R5,0DEG,EV;BR1371
21 MAY 82 UM
PHASE (DEG)
200
100
0
-100
-200
0
100
200
300
400
500
600
FREQUENCY (MHz)

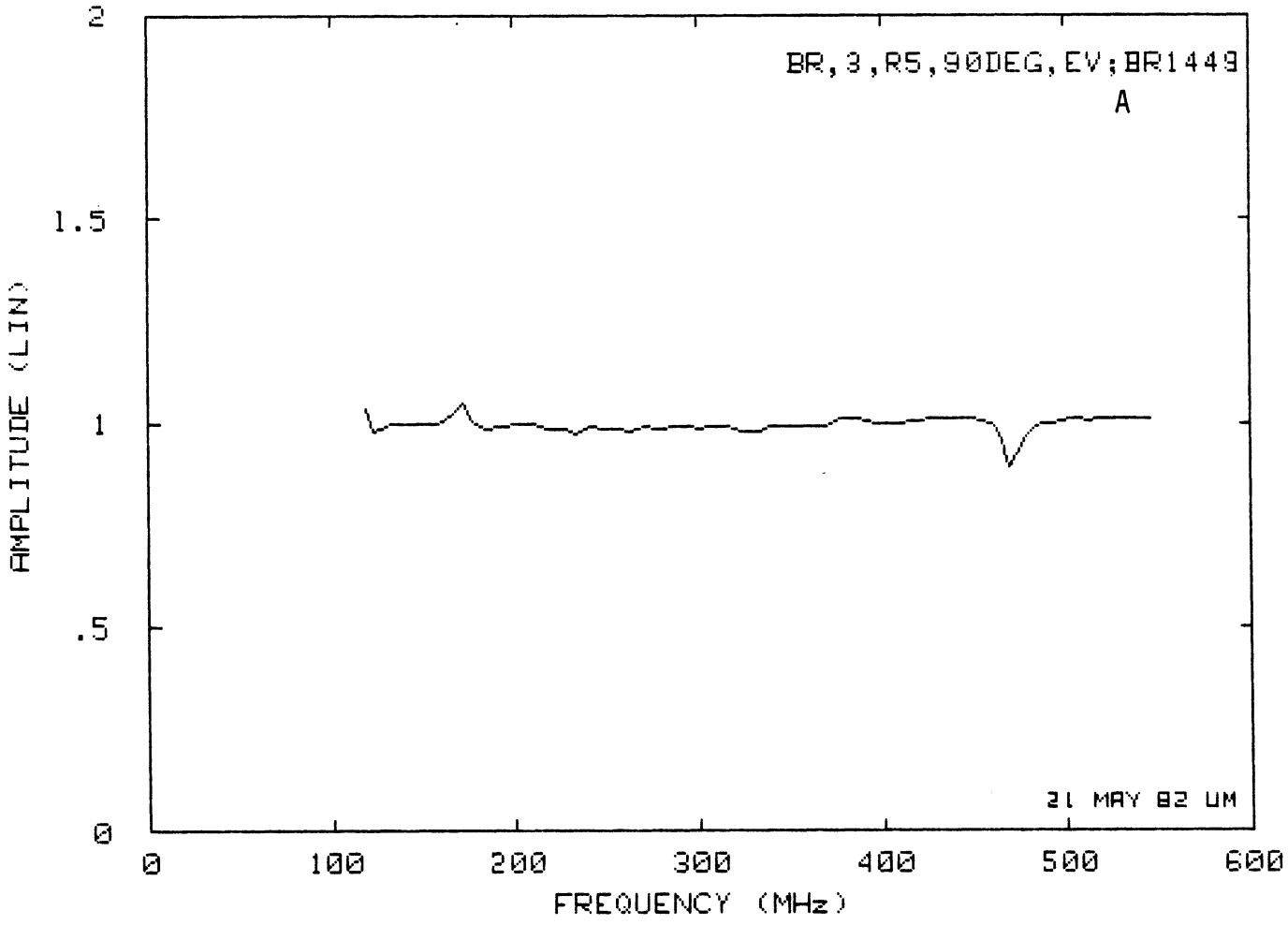
BR,3,R5,90DEG,EV;BR1449
A
21 MAY 82 UM
AMPLITUDE (LIN)
2
1.5
1
.5
0
0
100
200
300
400
500
600
FREQUENCY (MHz)

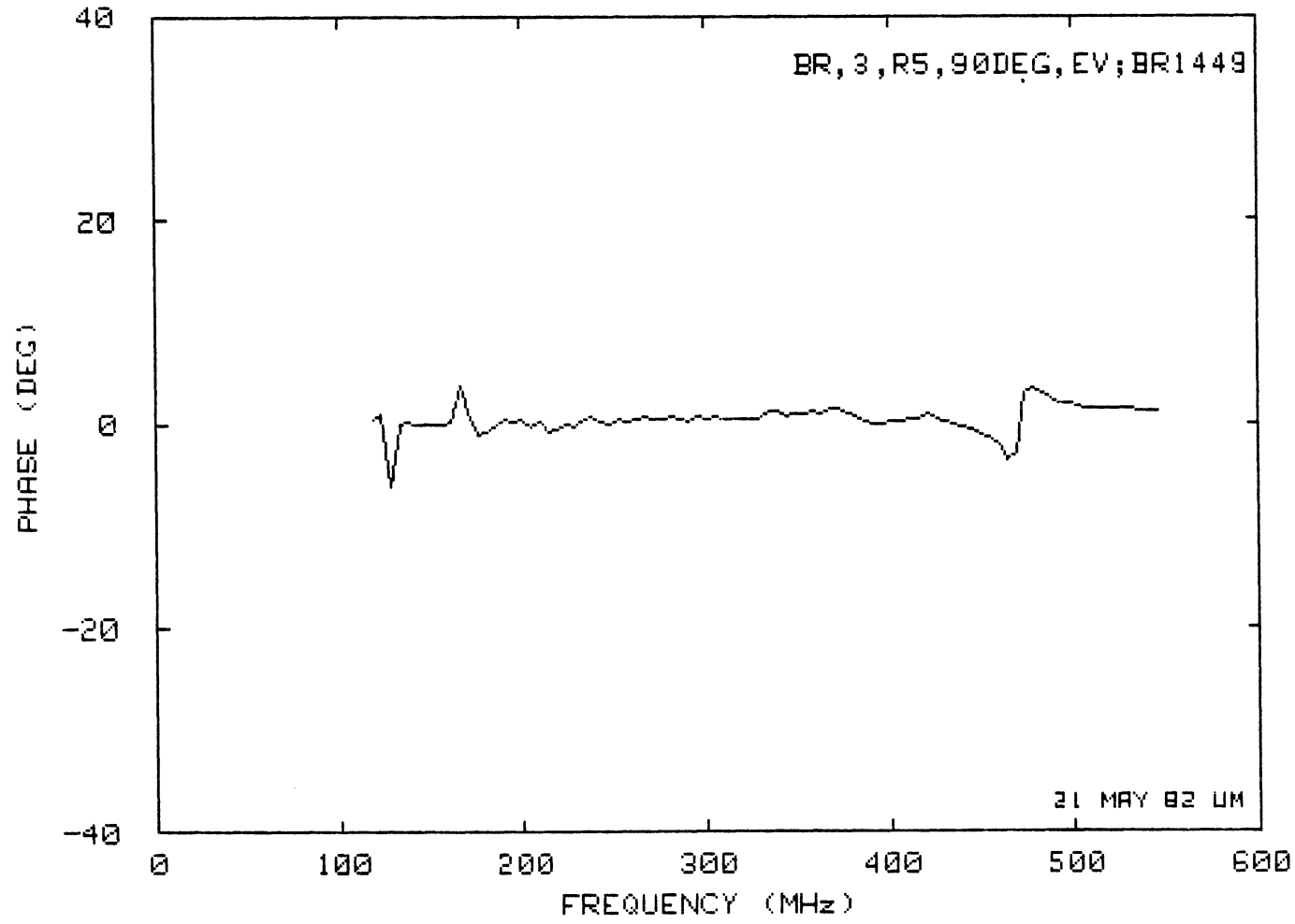
BR,3,R5,90DEG,EV;BR1449
21 MAY 82 UM
PHASE (DEG)
40
20
0
-20
-40
0
100
200
300
400
500
600
FREQUENCY (MHz)

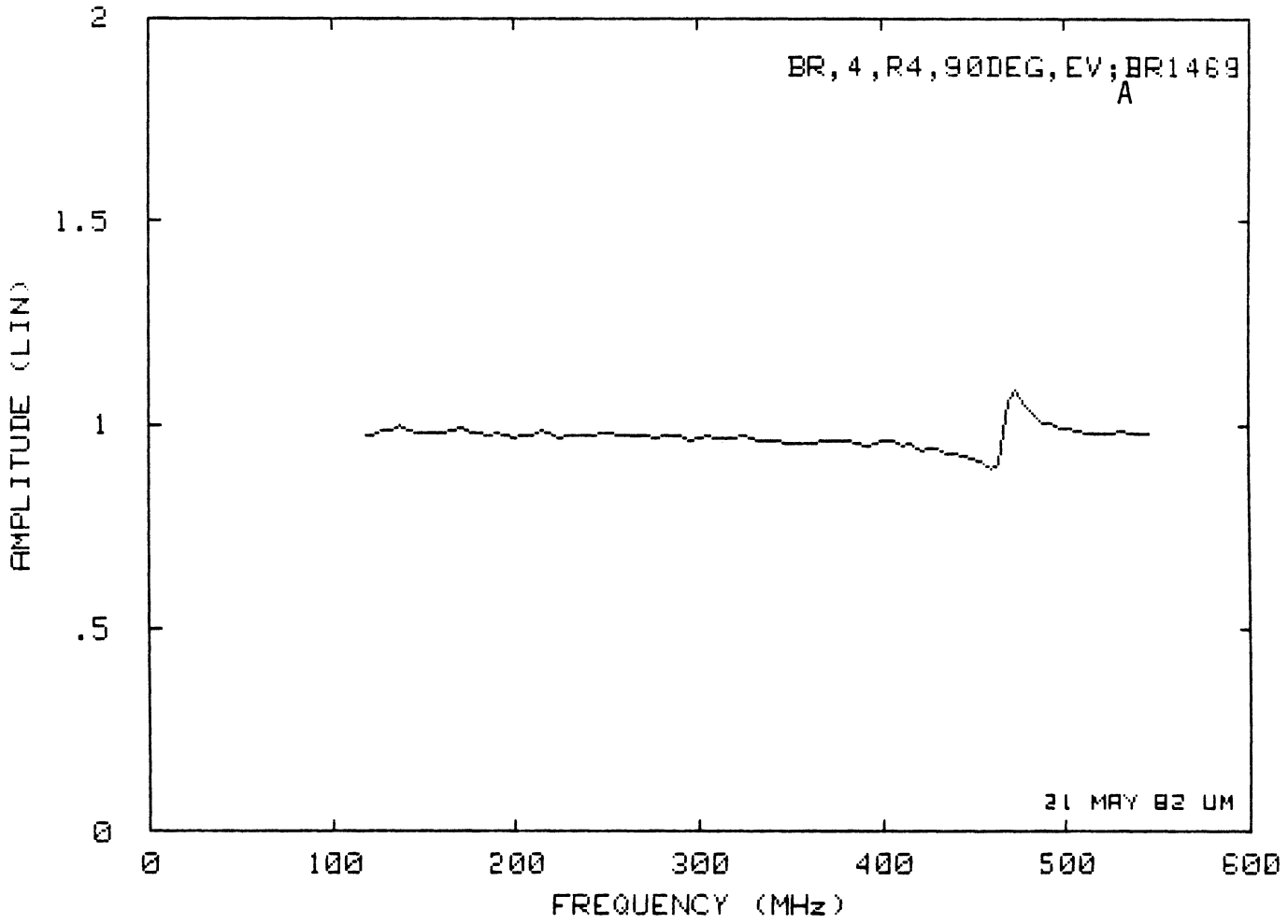
BR,4,R4,90DEG,EV;BR1469
A
21 MAY 82 UM
AMPLITUDE (LIN)
2
1.5
1
.5
0
0
100
200
300
400
500
600
FREQUENCY (MHz)

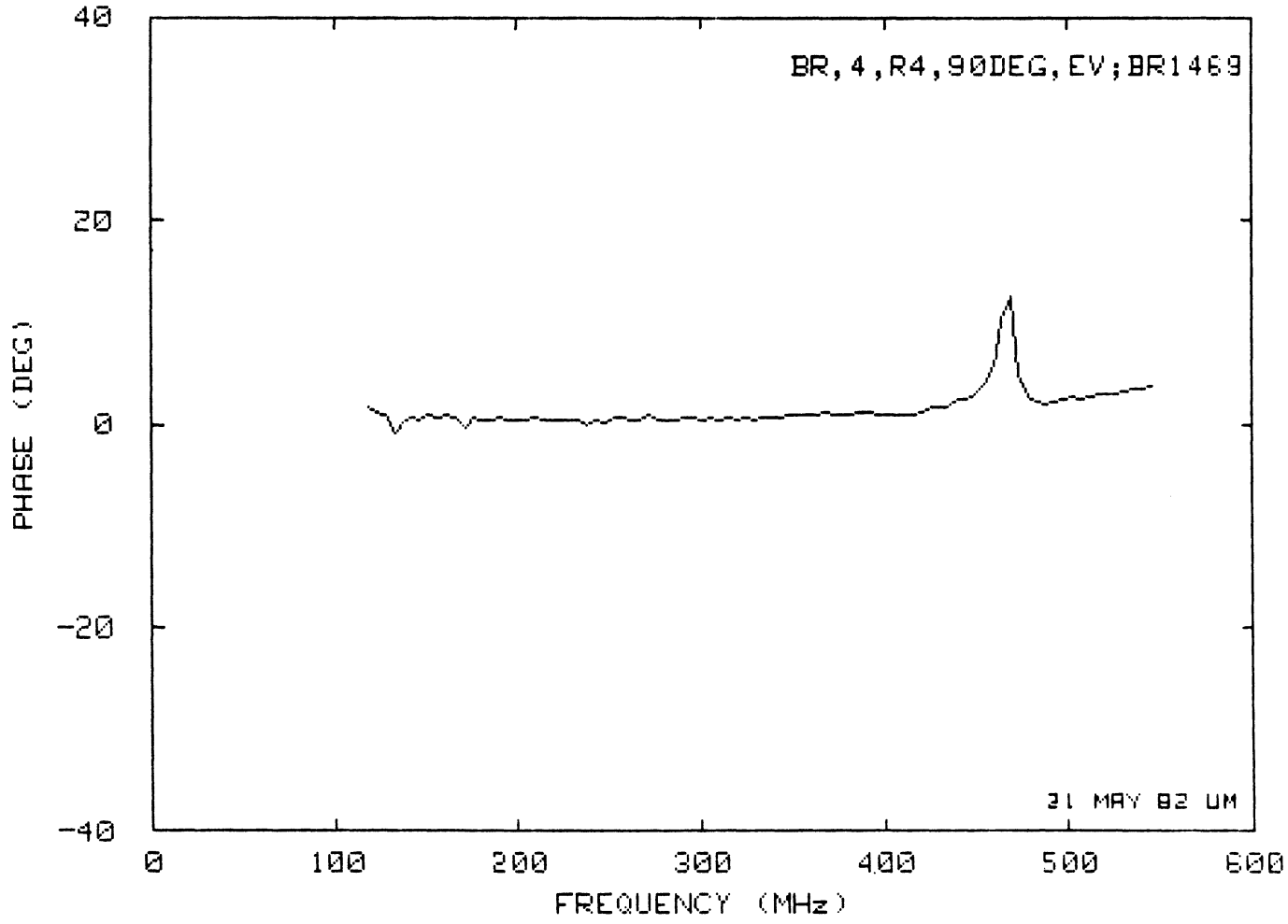
BR,4,R4,90DEG,EV;BR1469
21 MAY 82 UM
PHASE (DEG)
40
20
0
-20
-40
0
100
200
300
400
500
600
FREQUENCY (MHz)

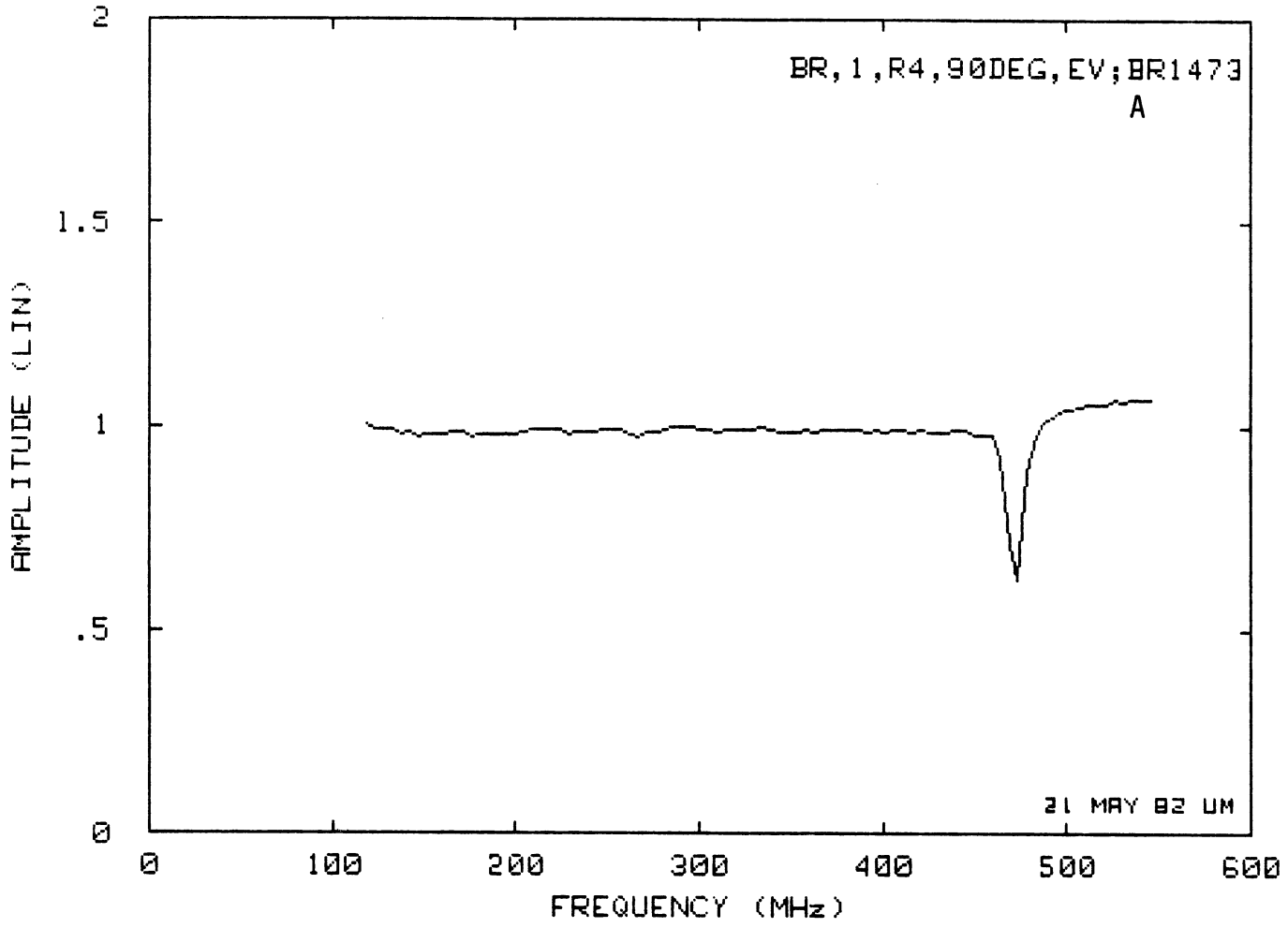
BR,1,R4,90DEG,EV;BR1473
A
21 MAY 82 UM
AMPLITUDE (LIN)
2
1.5
1
.5
0
0
100
200
300
400
500
600
FREQUENCY (MHz)

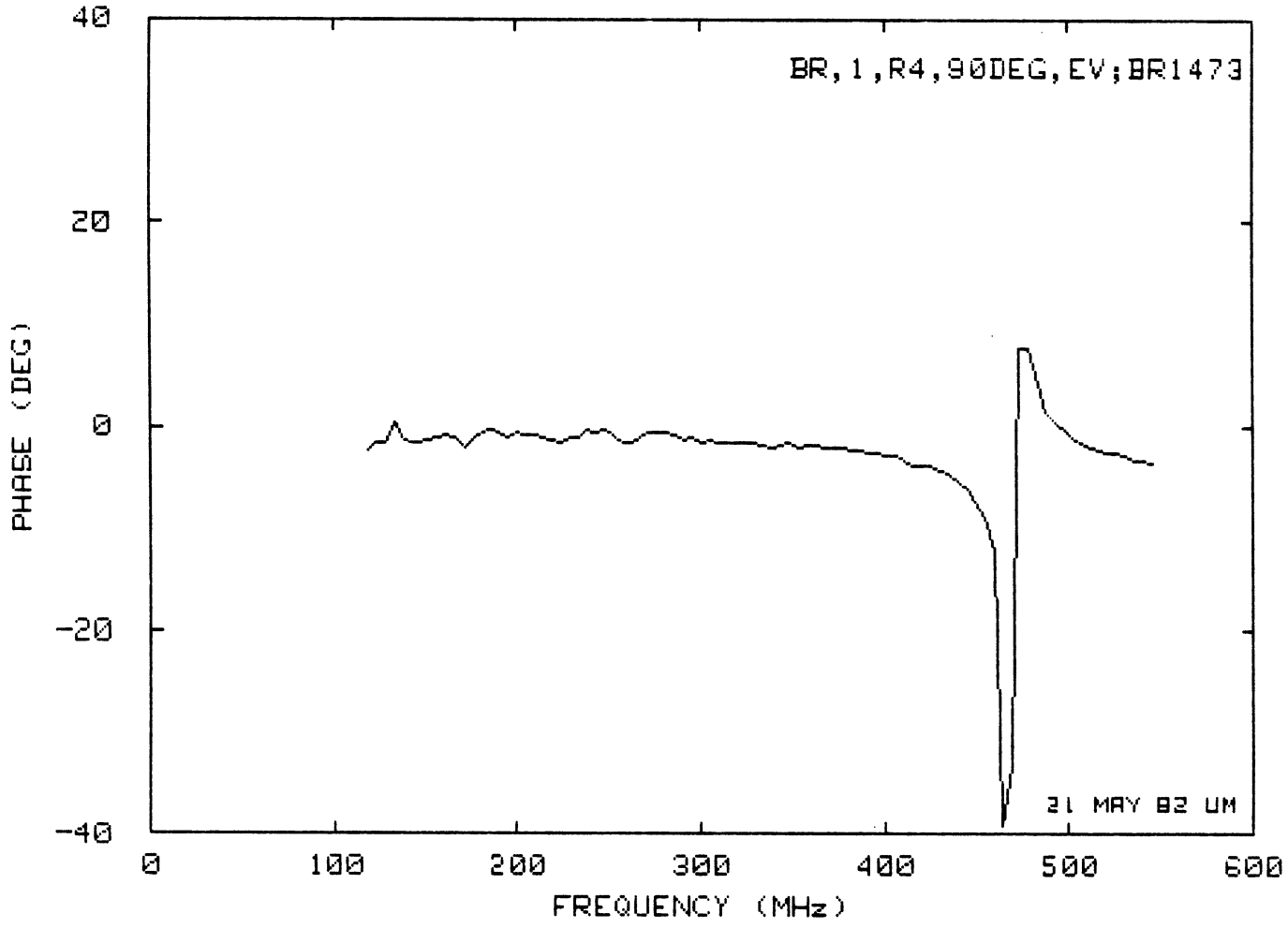
BR,1,R4,90DEG,EV;BR1473
21 MAY 82 UM
PHASE (DEG)
40
20
0
-20
-40
0
100
200
300
400
500
600
FREQUENCY (MHz)

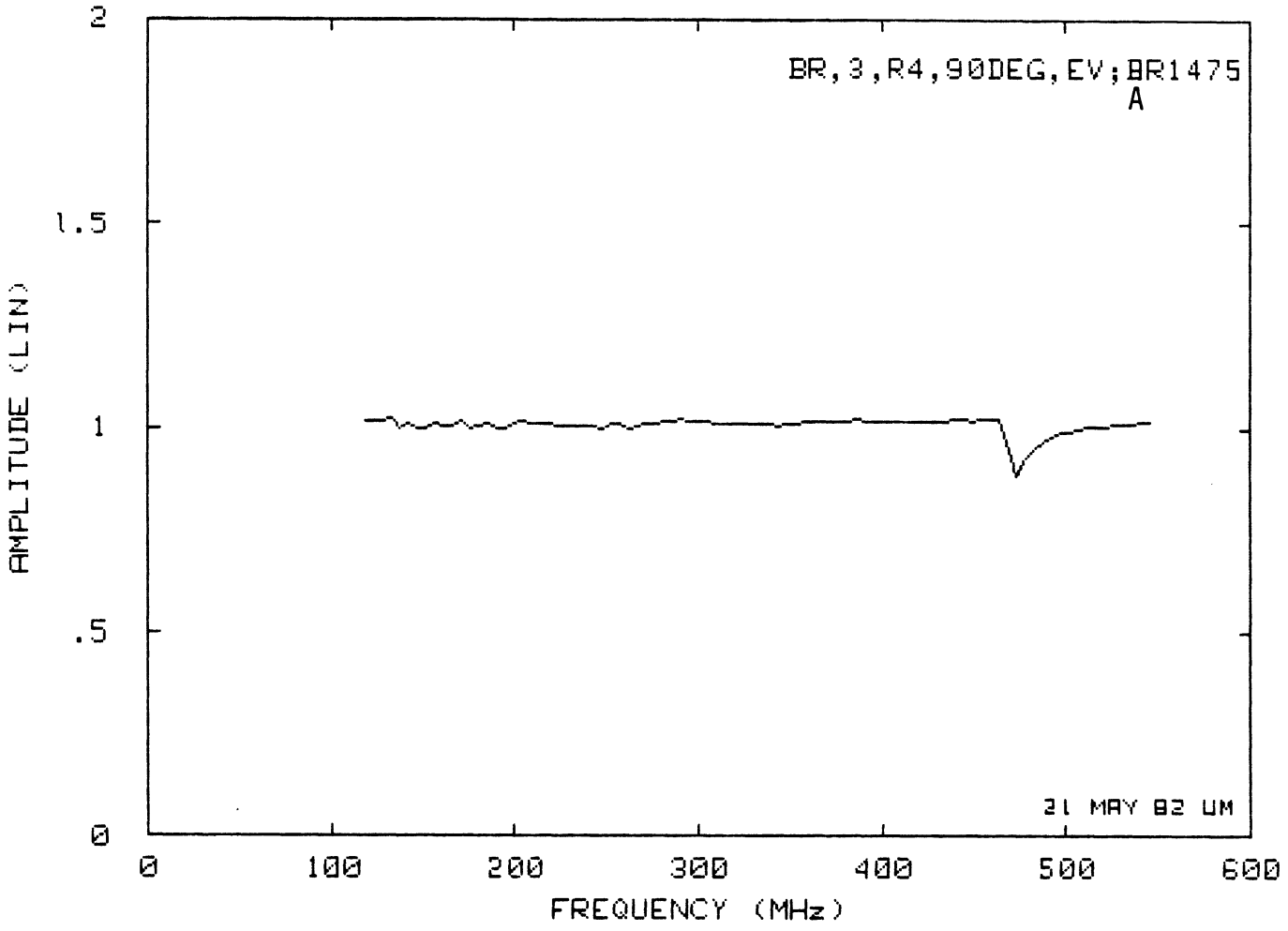
BR,3,R4,90DEG,EV;BR1475
A
21 MAY 82 UM
AMPLITUDE (LIN)
2
1.5
1
.5
0
0
100
200
300
400
500
600
FREQUENCY (MHz)

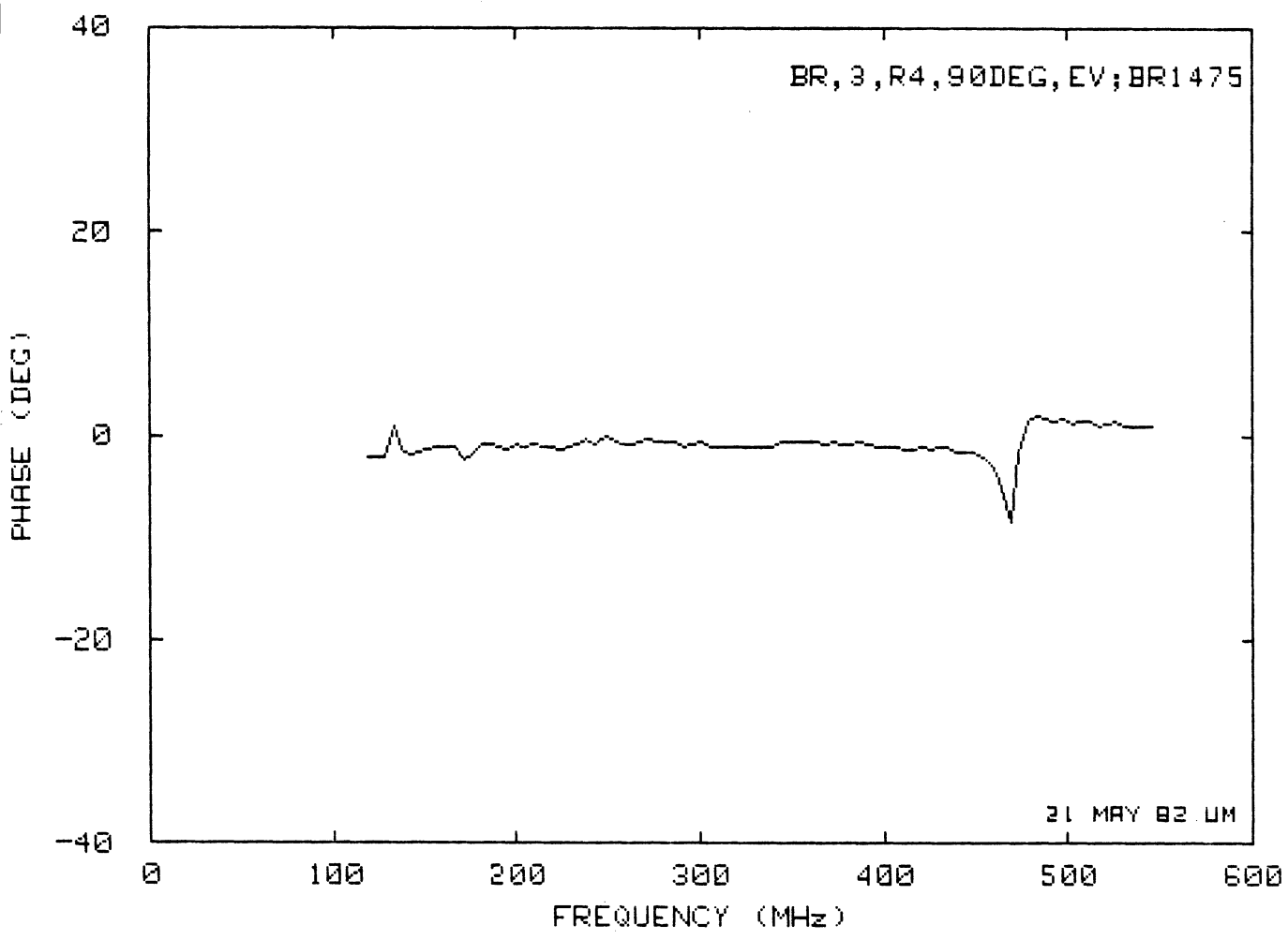
BR,3,R4,90DEG,EV;BR1475
21 MAY 82 UM
PHASE (DEG)
40
20
0
-20
-40
0
100
200
300
400
500
600
FREQUENCY (MHz)

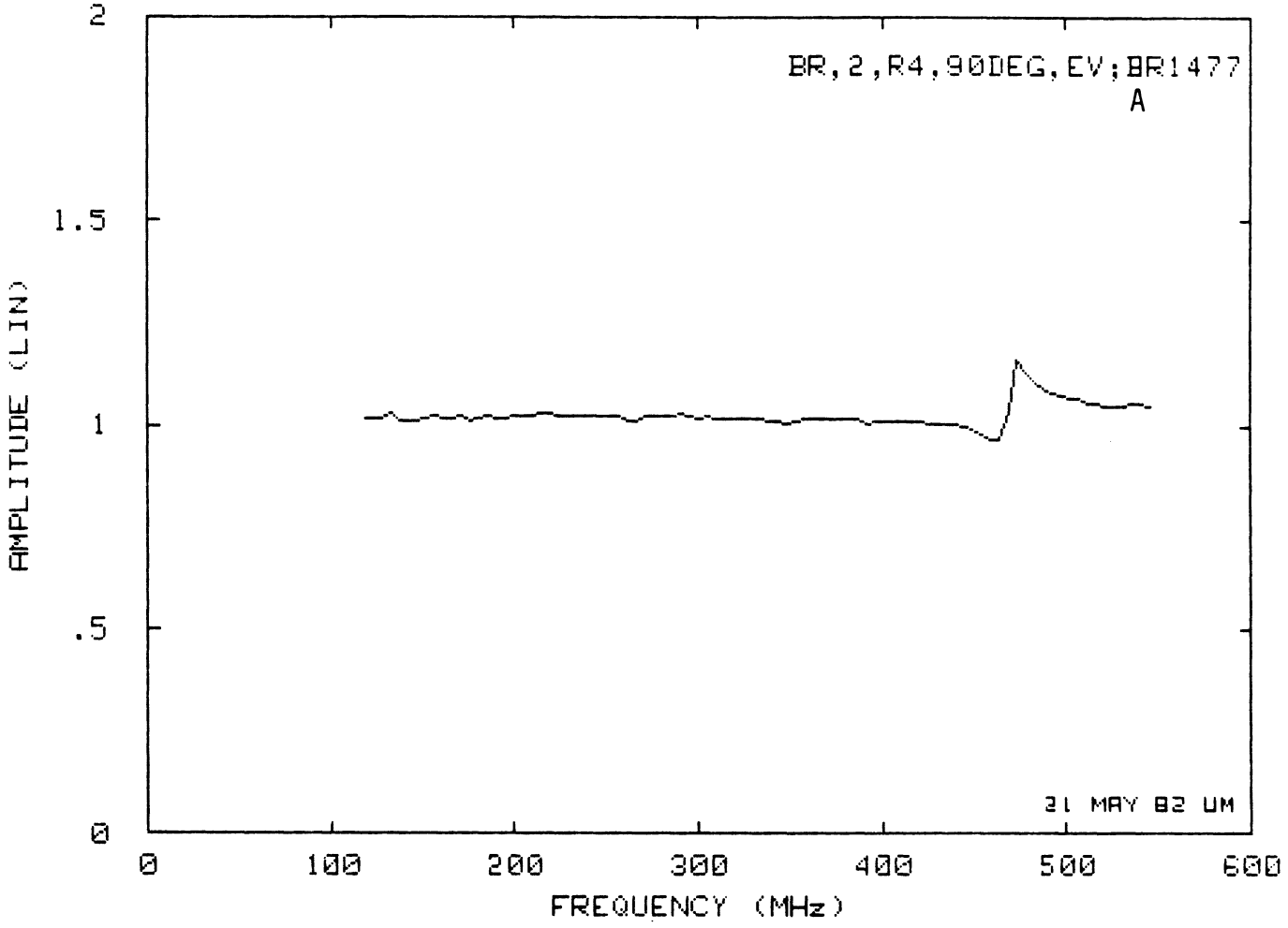
BR,2,R4,90DEG,EV;BR1477
A
21 MAY 82 UM
AMPLITUDE (LIN)
2
1.5
1
.5
0
0
100
200
300
400
500
600
FREQUENCY (MHz)

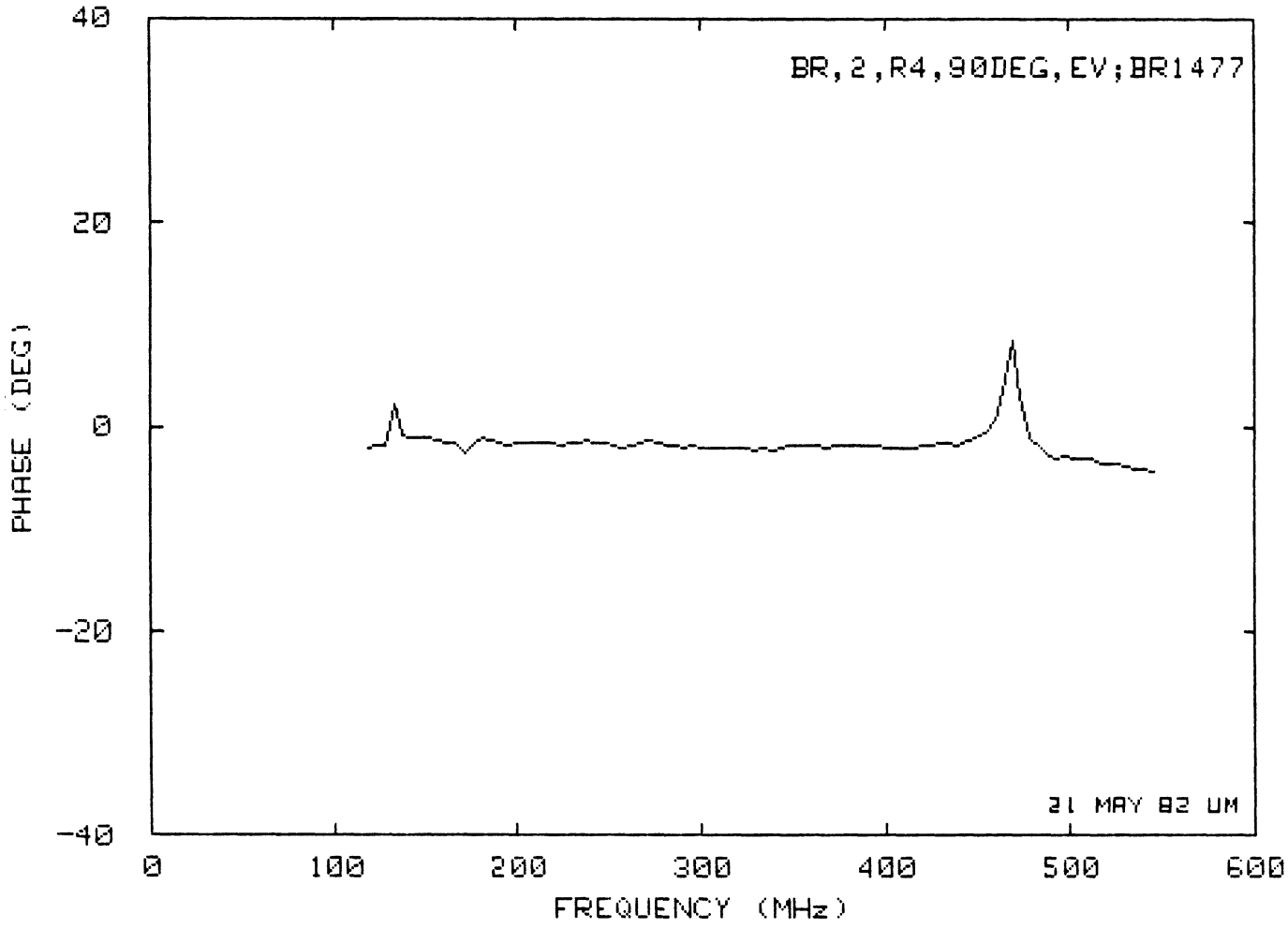
BR,2,R4,90DEG,EV;BR1477
21 MAY 82 UM
PHASE (DEG)
40
20
0
-20
-40
0
100
200
300
400
500
600
FREQUENCY (MHz)

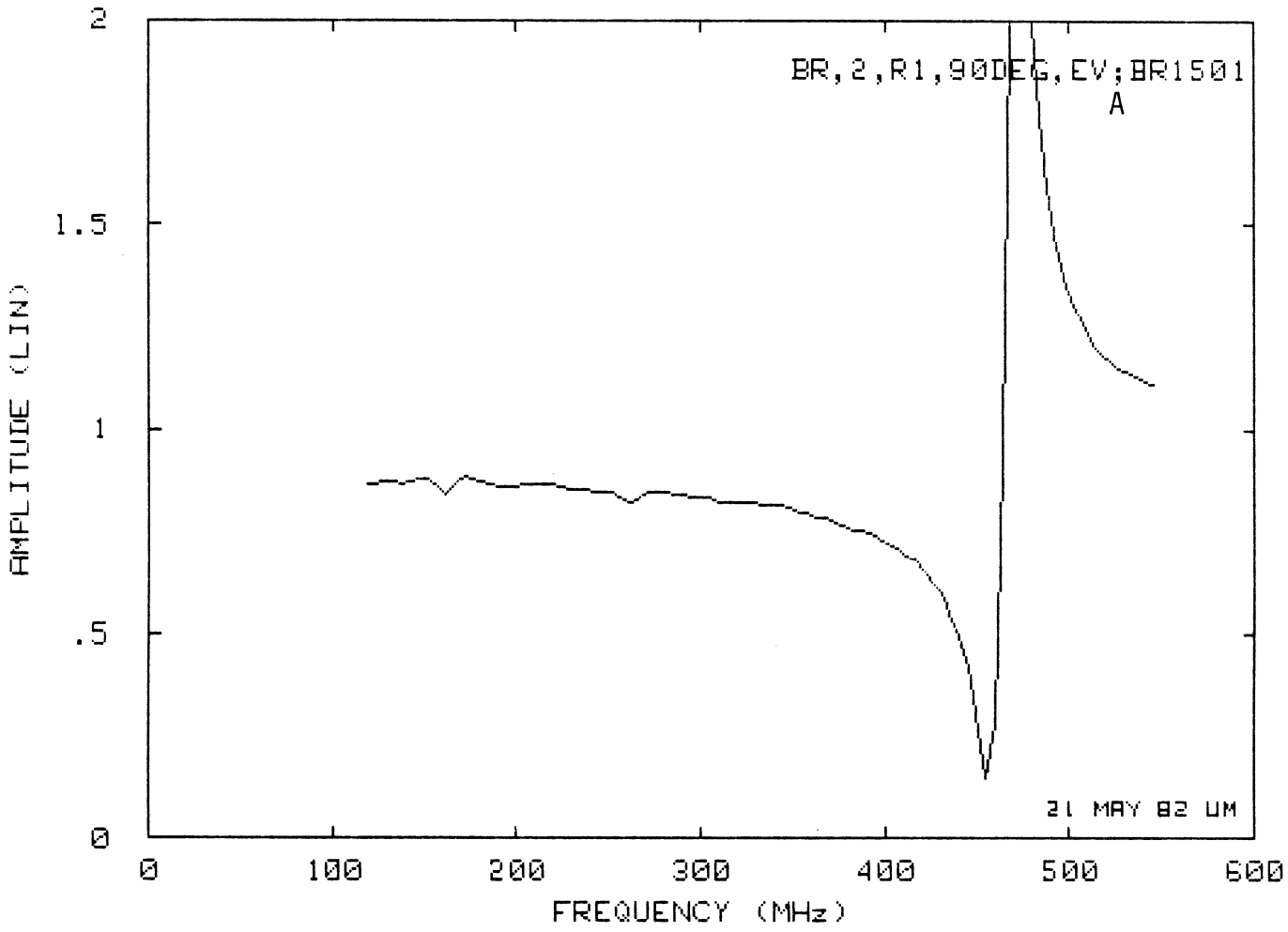
BR,2,R1,90DEG,EV;BR1501
A
21 MAY 82 UM
AMPLITUDE (LIN)
2
1.5
1
.5
0
0
100
200
300
400
500
600
FREQUENCY (MHz)

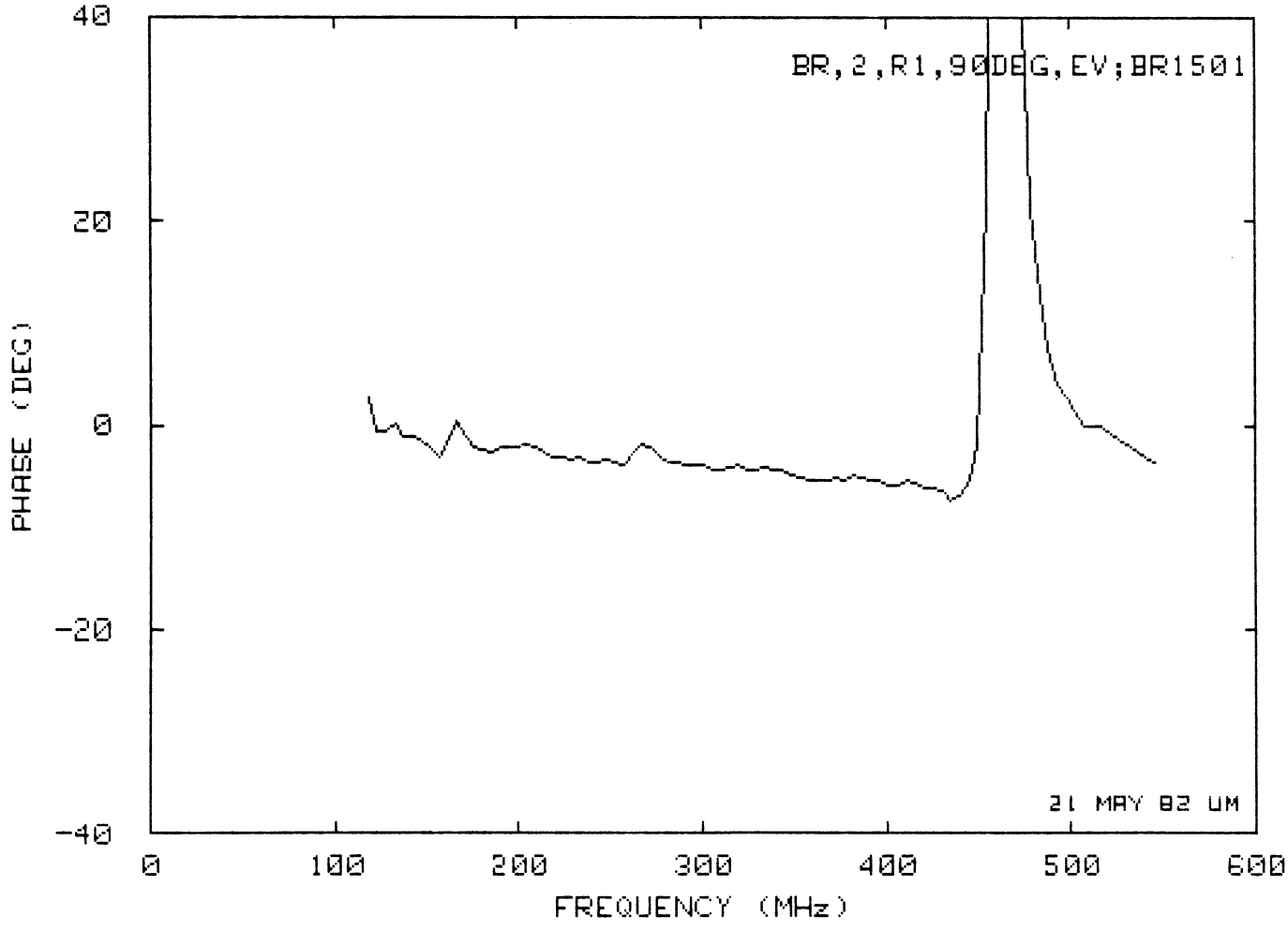
BR,2,R1,90DEG,EV;BR1501
21 MAY 82 UM
PHASE (DEG)
40
20
0
-20
-40
0
100
200
300
400
500
600
FREQUENCY (MHz)

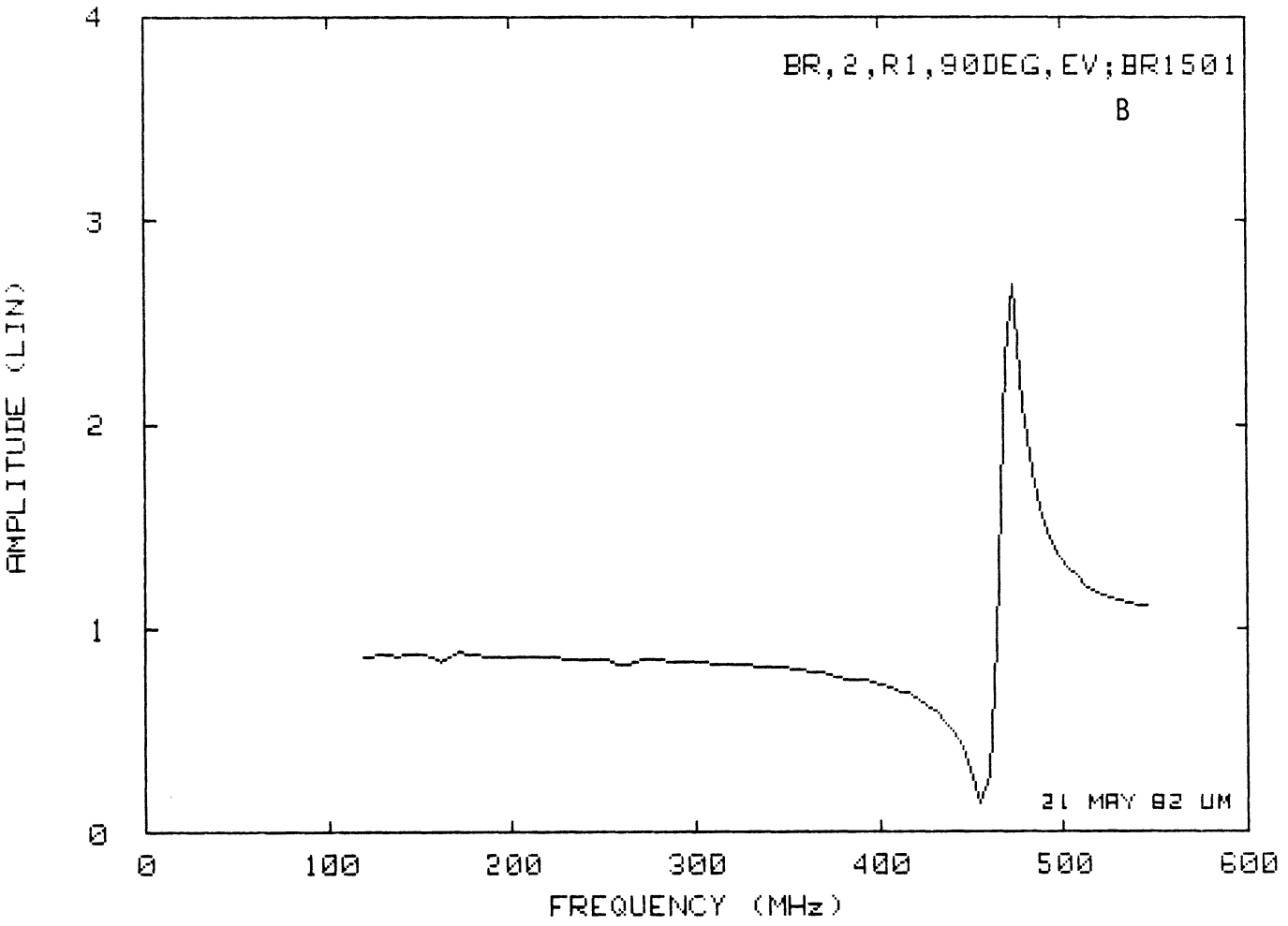
BR,2,R1,90DEG,EV;BR1501
B
21 MAY 82 UM
AMPLITUDE (LIN)
4
3
2
1
0
0
100
200
300
400
500
600
FREQUENCY (MHz)

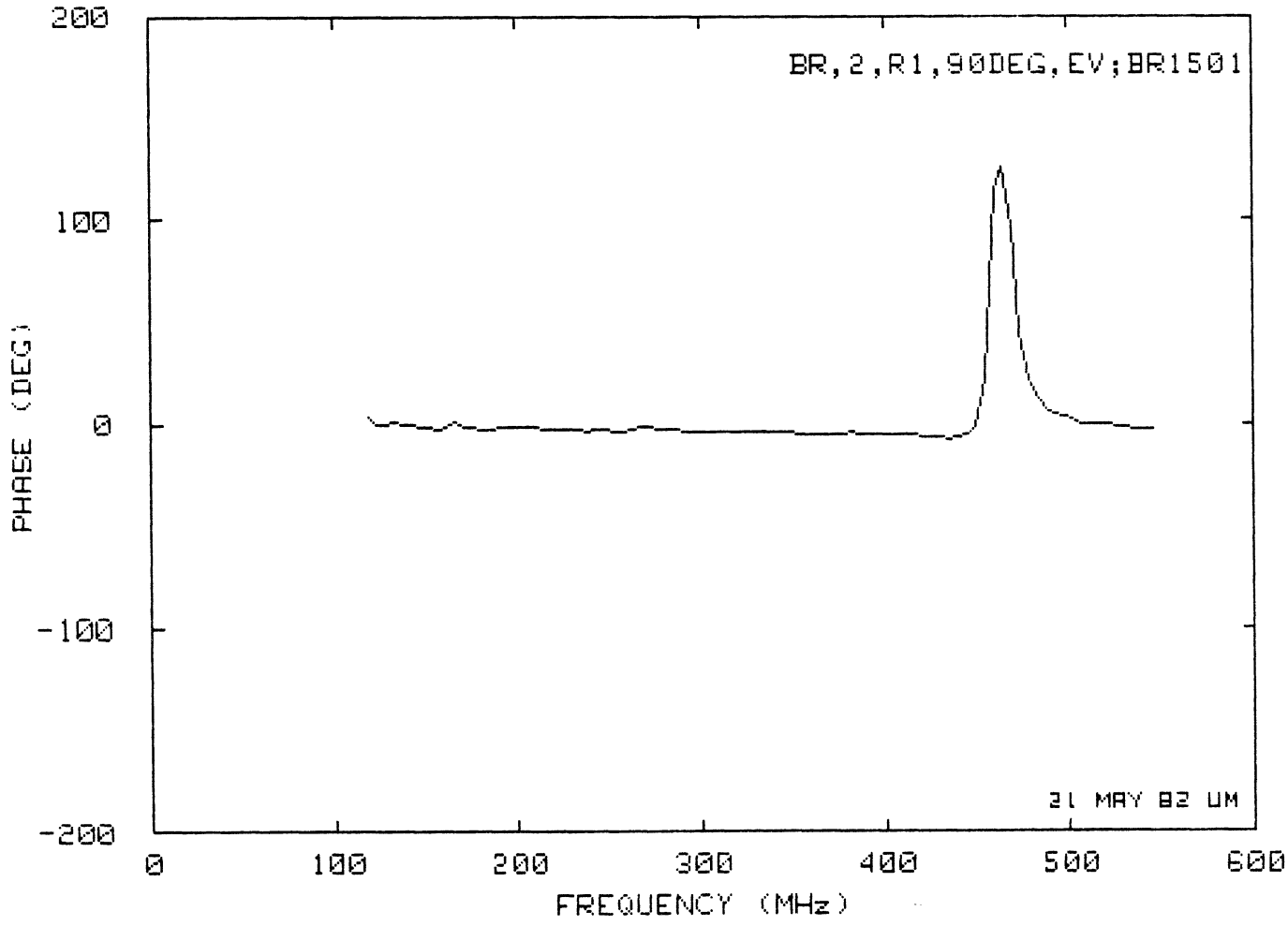
BR,2,R1,90DEG,EV;BR1501
21 MAY 82 UM
PHASE (DEG)
200
100
0
-100
-200
0
100
200
300
400
500
600
FREQUENCY (MHz)

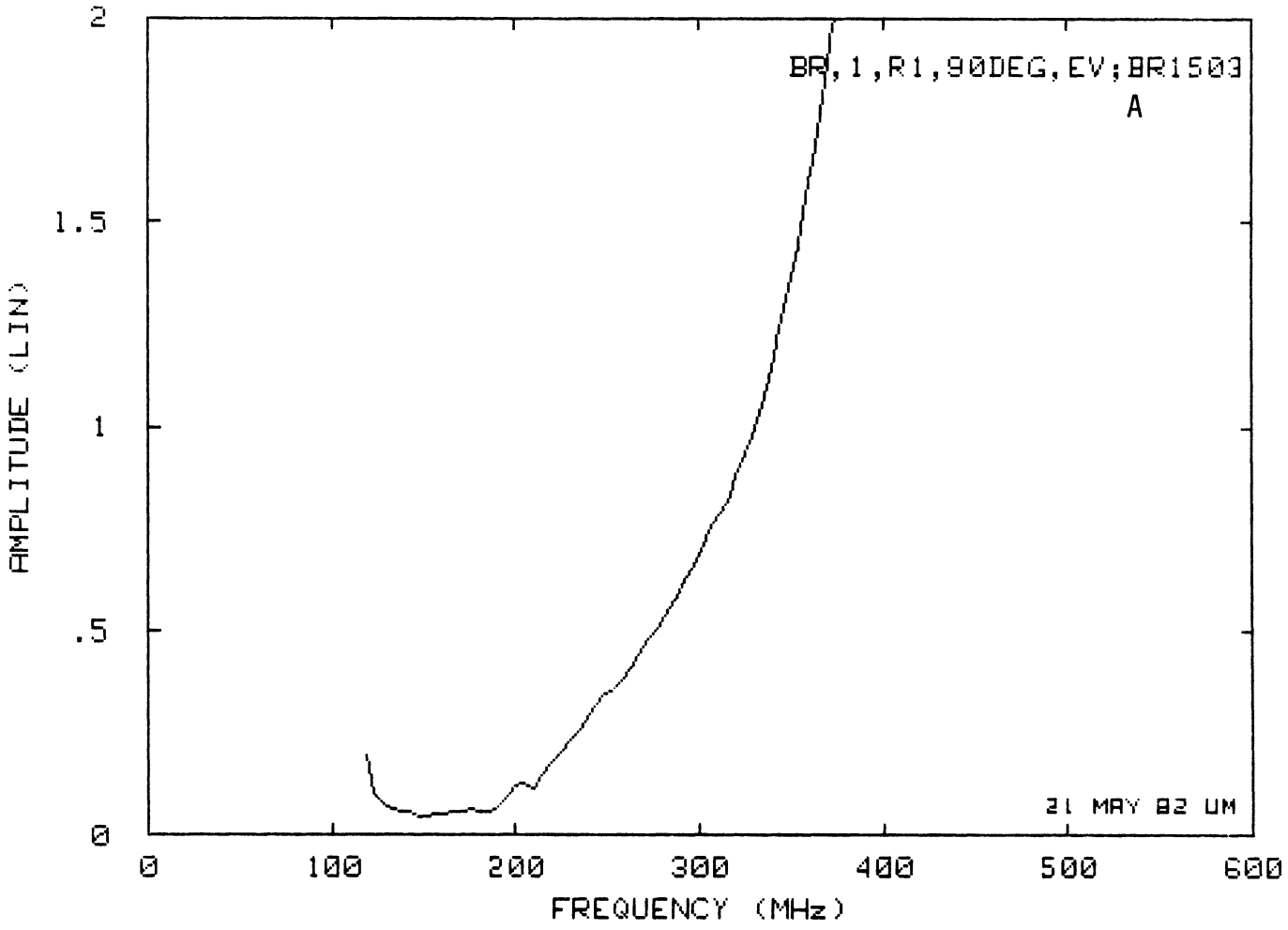
BR,1,R1,90DEG,EV;BR1503
A
21 MAY 82 UM
AMPLITUDE (LIN)
2
1.5
1
.5
0
0
100
200
300
400
500
600
FREQUENCY (MHz)

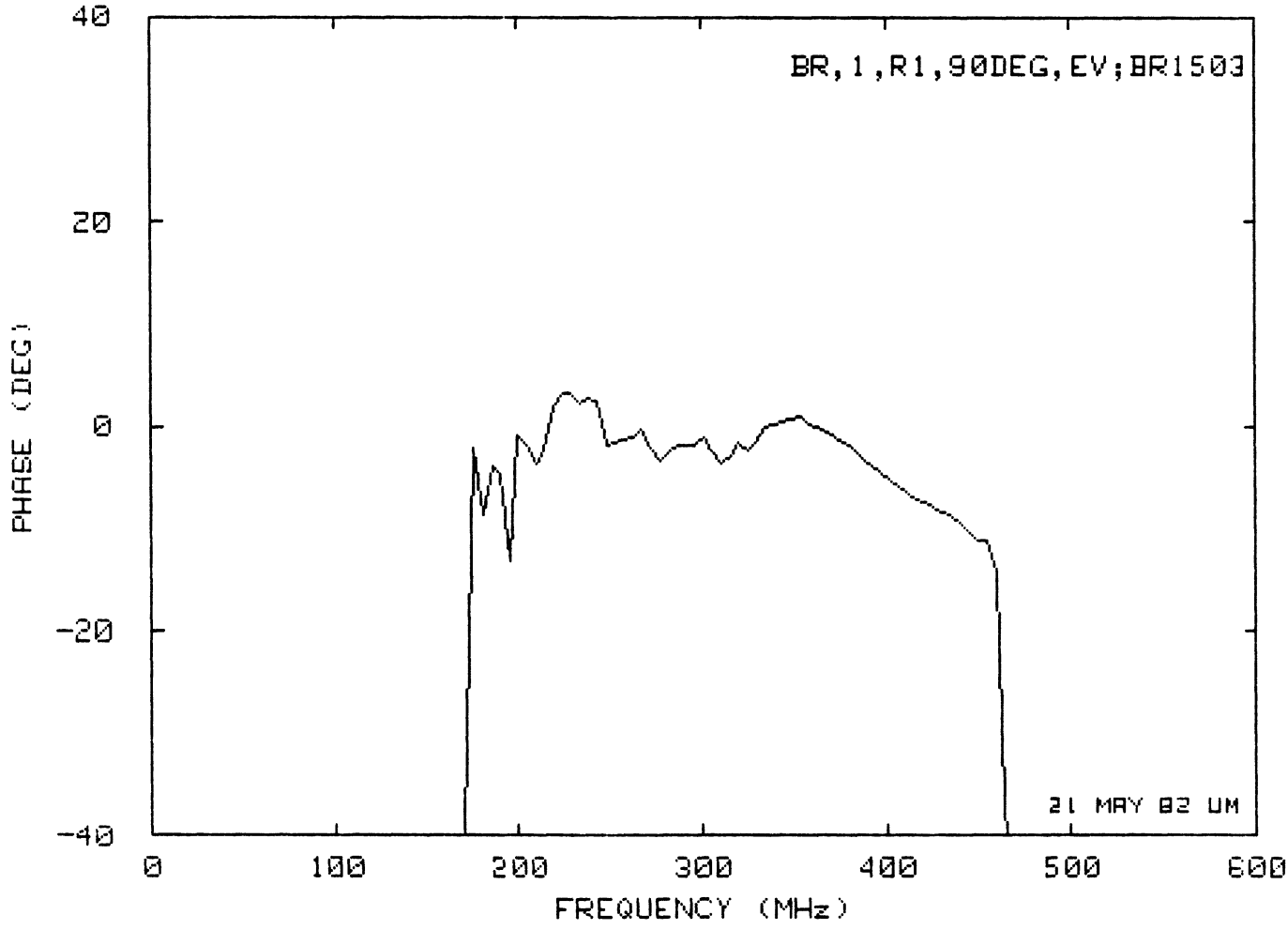
BR,1,R1,90DEG,EV;BR1503
21 MAY 82 UM
PHASE (DEG)
40
20
0
-20
-40
0
100
200
300
400
500
600
FREQUENCY (MHz)

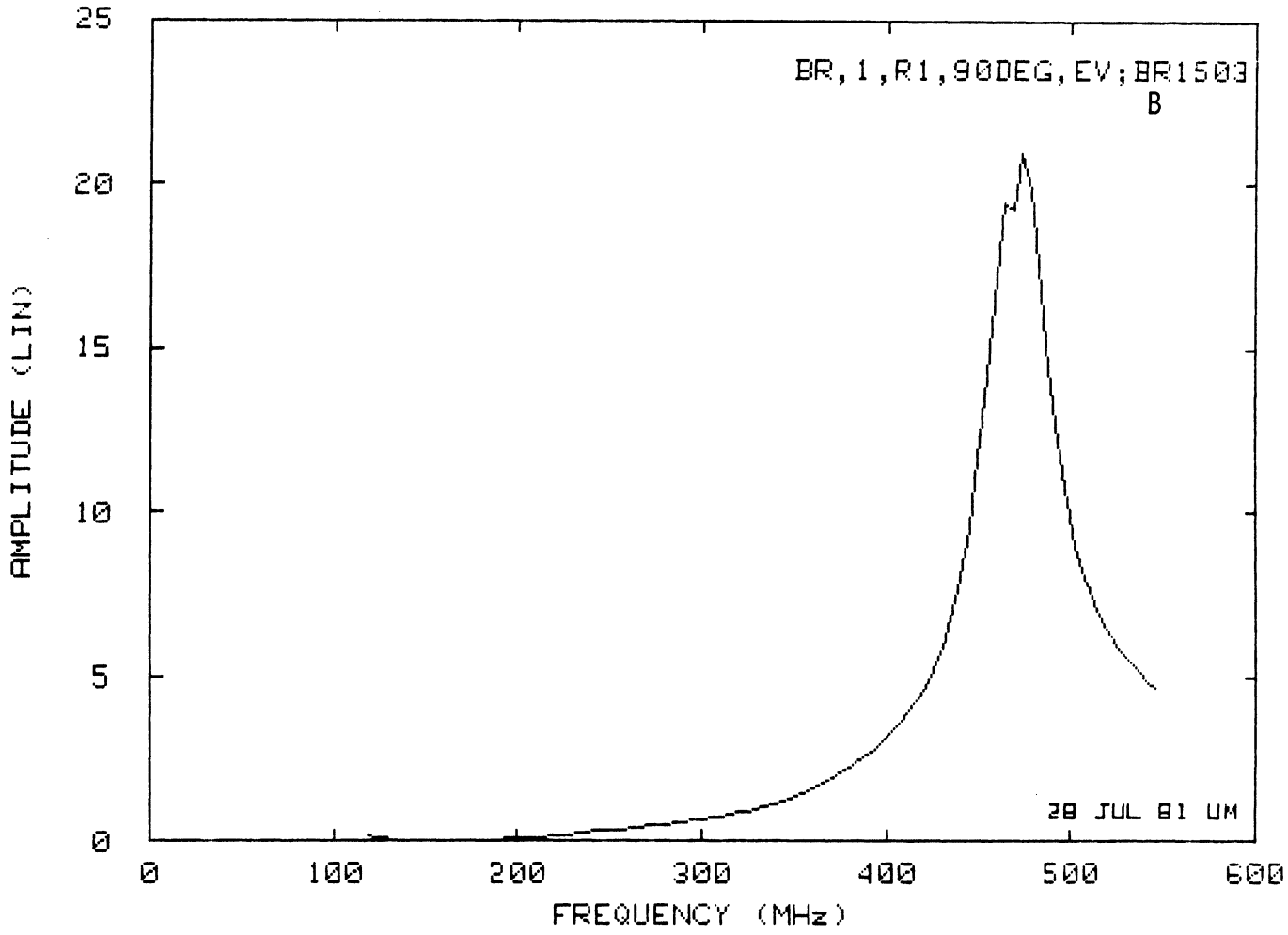
BR,1,R1,90DEG,EV;BR1503
B
28 JUL 81 UM
AMPLITUDE (LIN)
25
20
15
10
5
0
0
100
200
300
400
500
600
FREQUENCY (MHz)

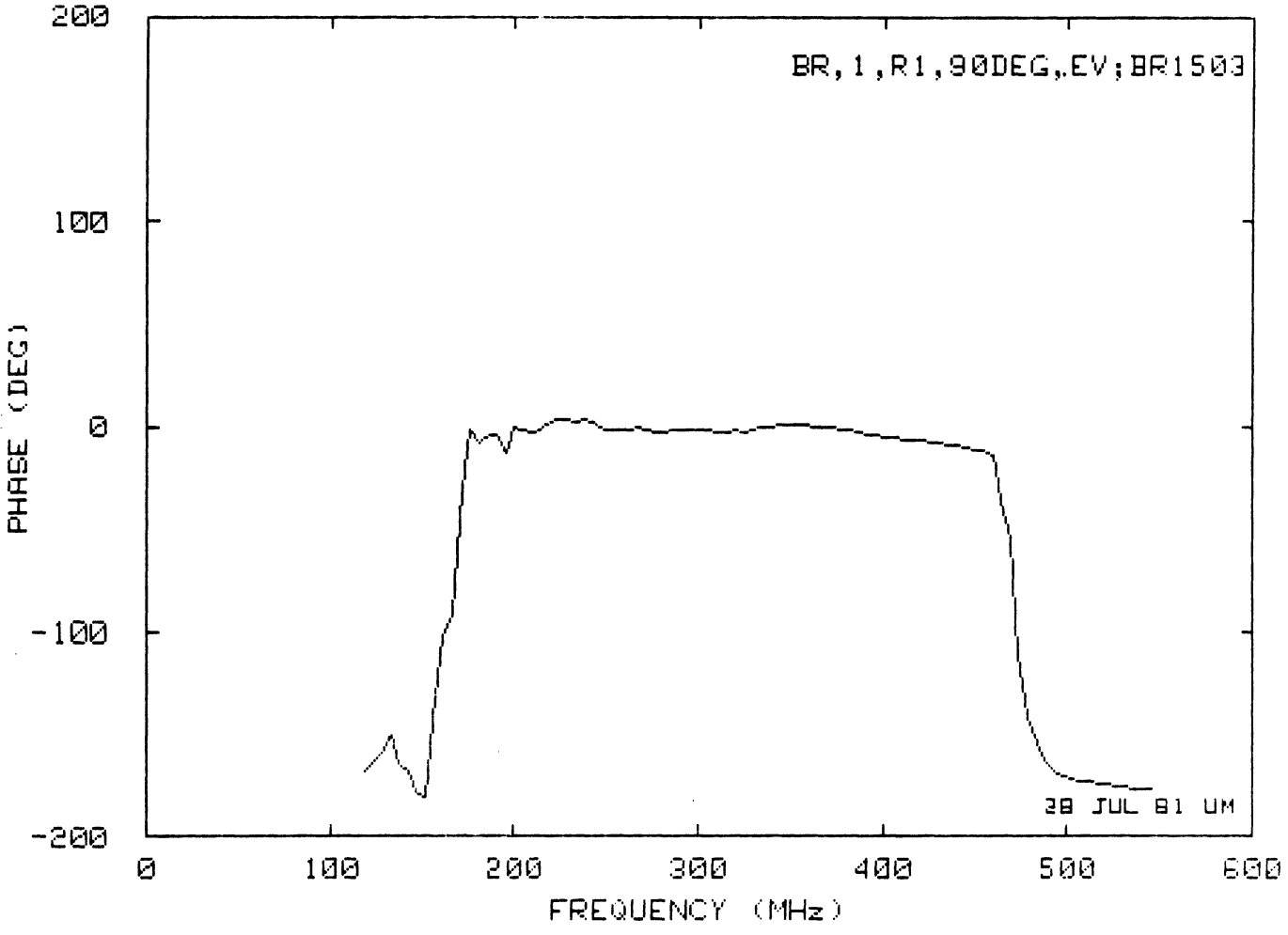
BR,1,R1,90DEG,.EV;BR1503
28 JUL 81 UM
PHASE (DEG)
200
100
0
-100
-200
0
100
200
300
400
500
600
FREQUENCY (MHz)

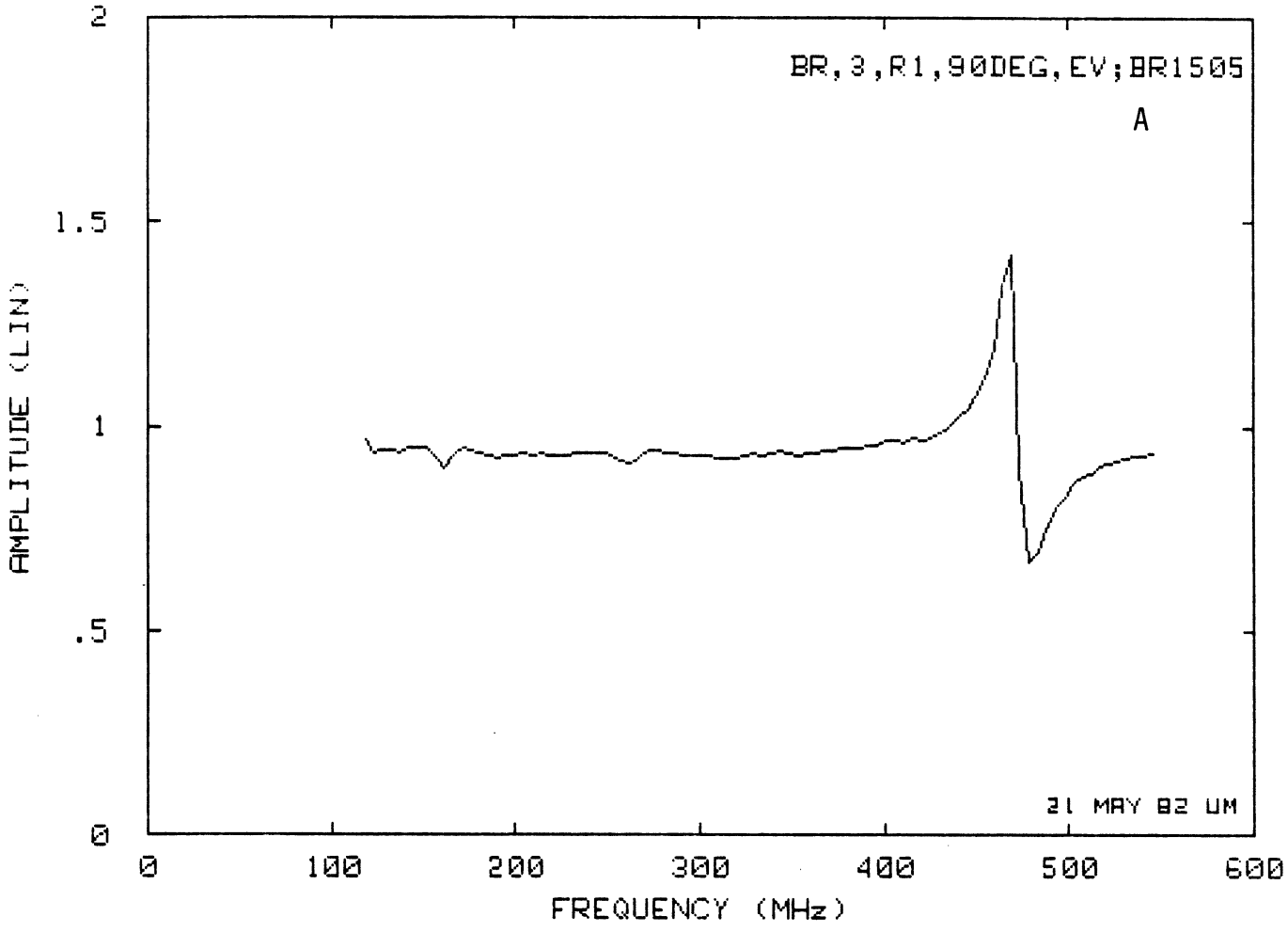
BR,3,R1,90DEG,EV;BR1505
A
21 MAY 82 UM
AMPLITUDE (LIN)
2
1.5
1
.5
0
0
100
200
300
400
500
600
FREQUENCY (MHz)

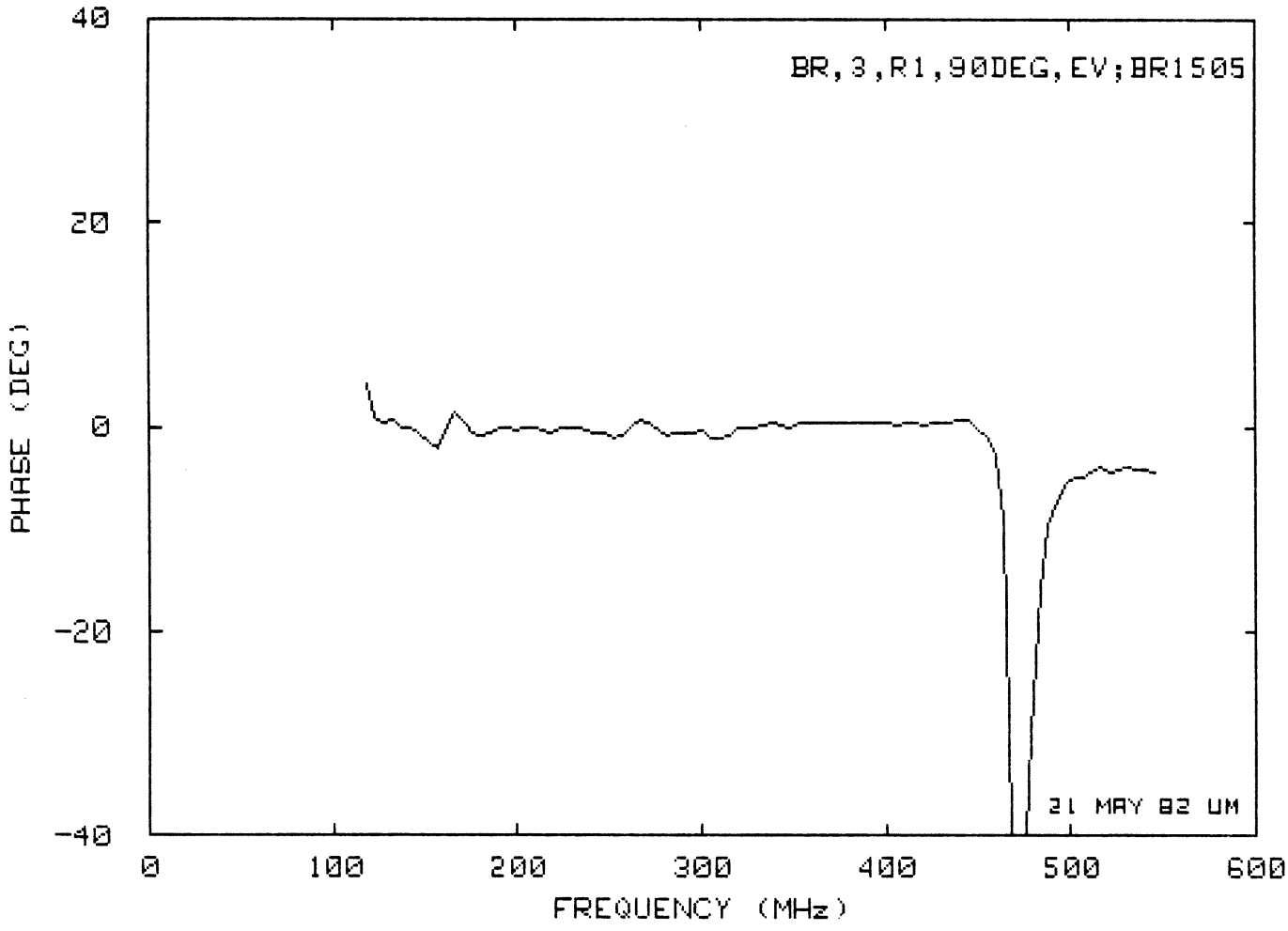
BR,3,R1,90DEG,EV;BR1505
21 MAY 82 UM
PHASE (DEG)
40
20
0
-20
-40
0
100
200
300
400
500
600
FREQUENCY (MHz)

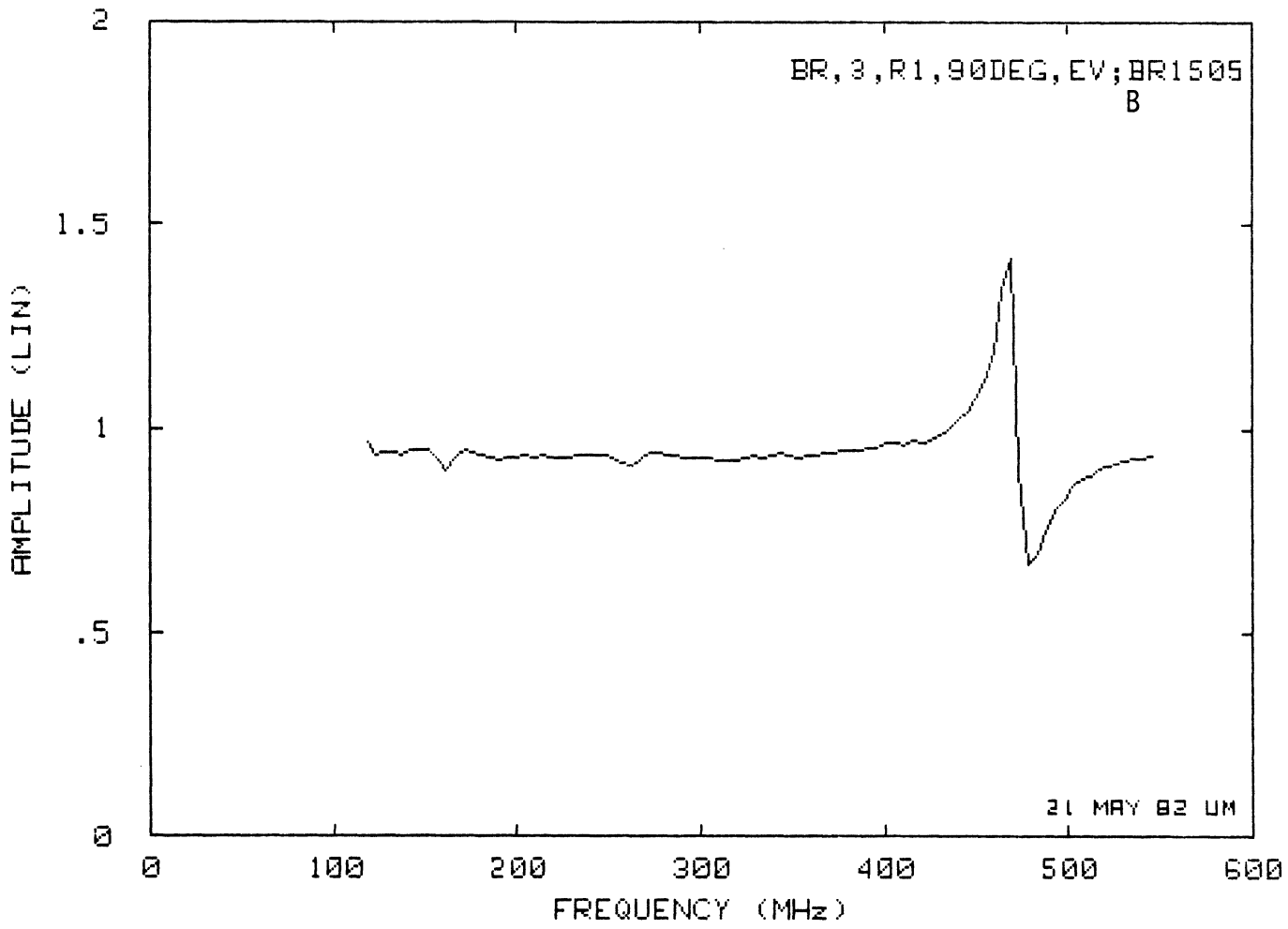
BR,3,R1,90DEG,EV;BR150S
B
21 MAY 82 UM
AMPLITUDE (LIN)
2
1.5
1
.5
0
0
100
200
300
400
500
600
FREQUENCY (MHz)

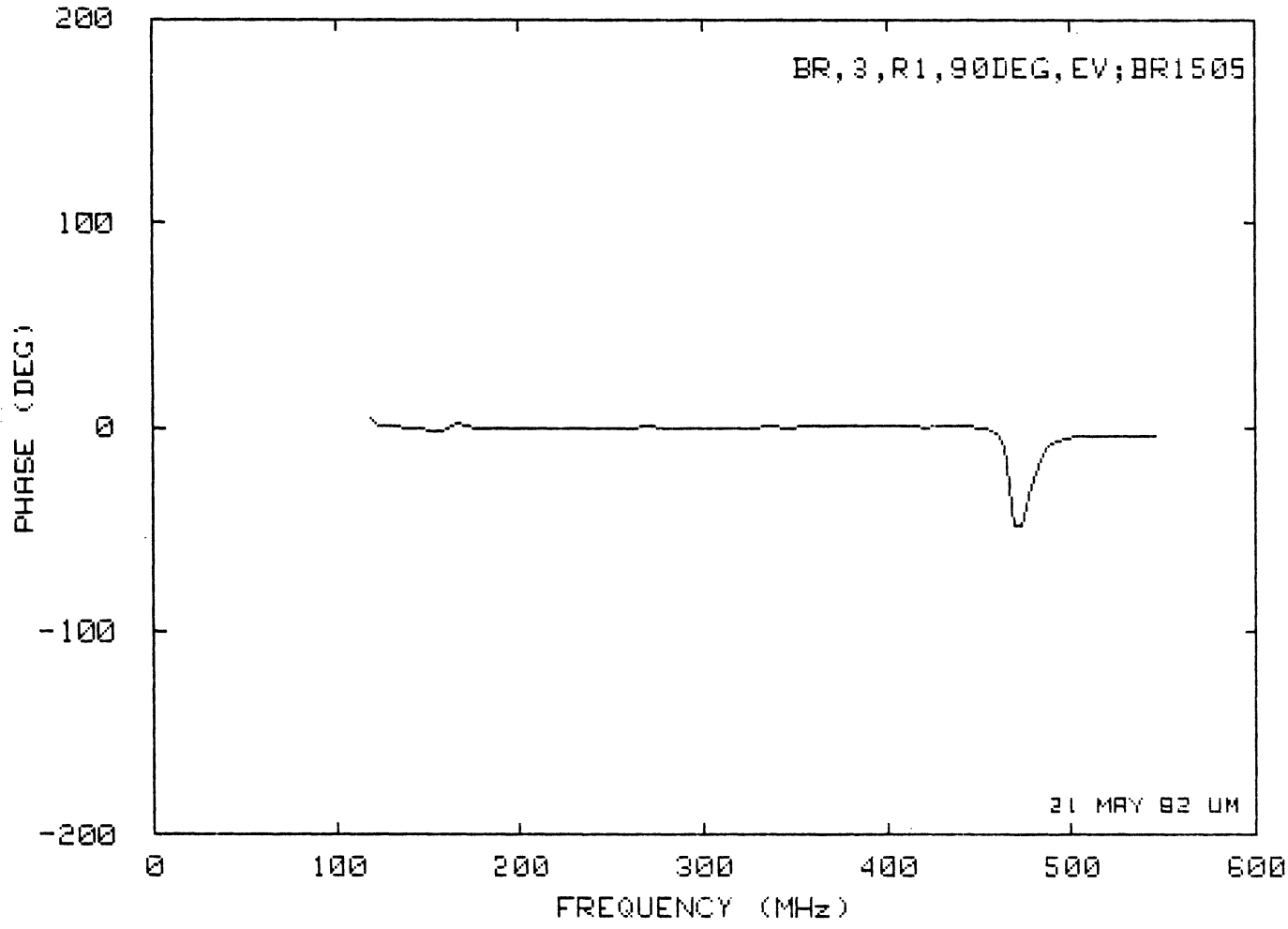
BR,3,R1,90DEG,EV;BR150S
21 MAY 82 UM
PHASE (DEG)
200
100
0
-100
-200
0
100
200
300
400
500
600
FREQUENCY (MHz)

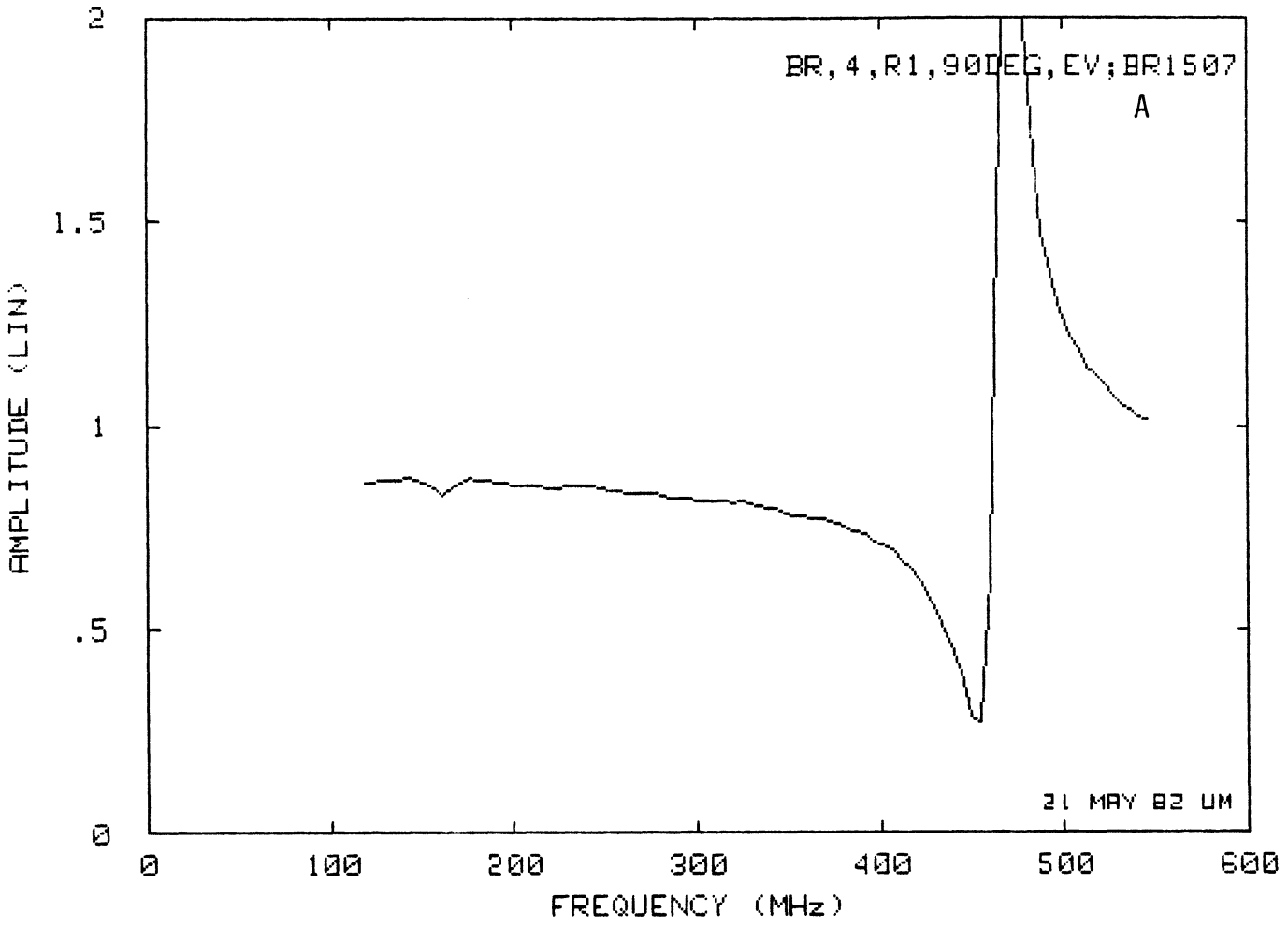
BR,4,R1,90DEG,EV;BR1507
A
21 MAY 82 UM
AMPLITUDE (LIN)
2
1.5
1
.5
0
0
100
200
300
400
500
600
FREQUENCY (MHz)

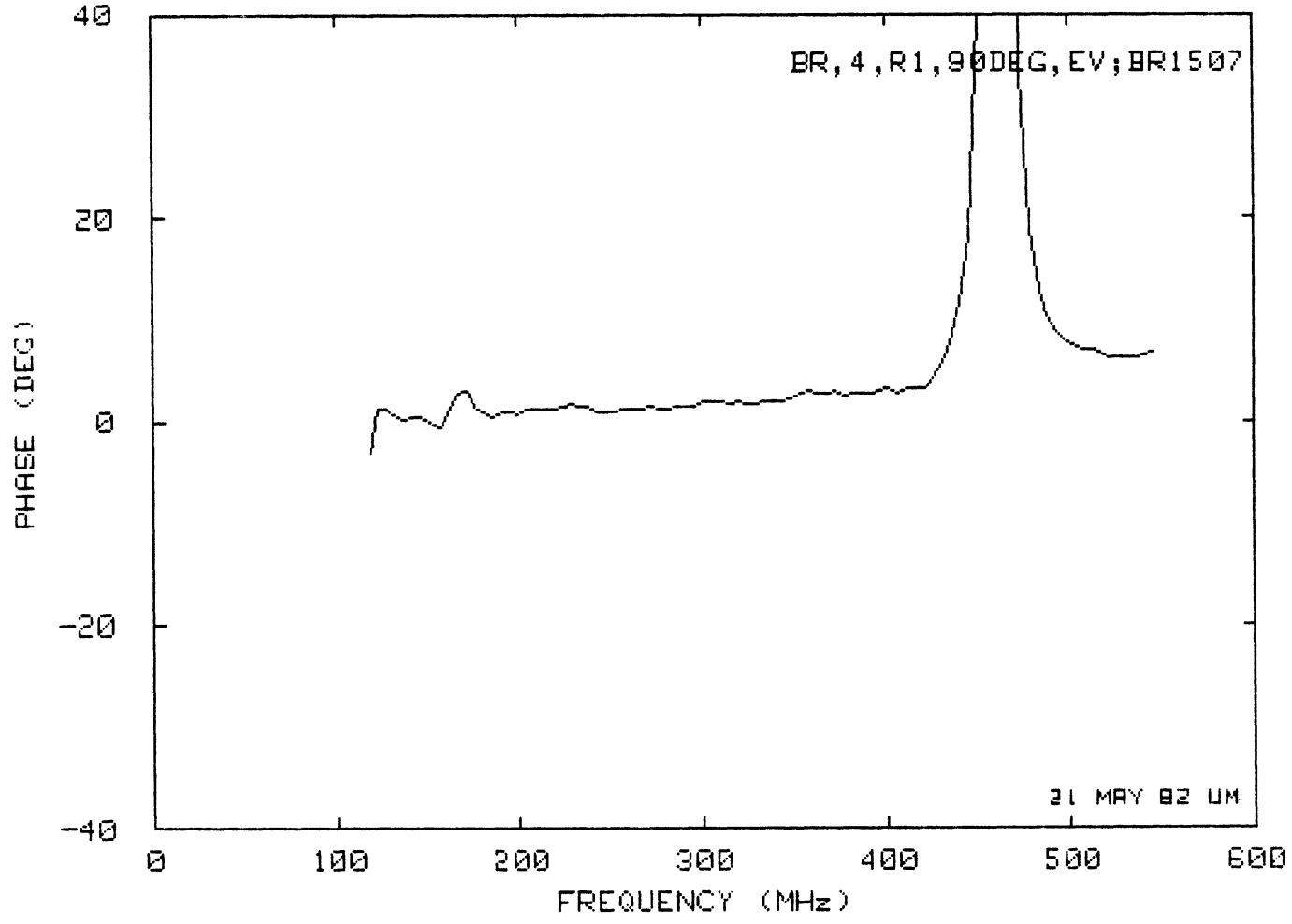
BR,4,R1,90DEG,EV;BR1507
21 MAY 82 UM
PHASE (DEG)
40
20
0
-20
-40
0
100
200
300
400
500
600
FREQUENCY (MHz)

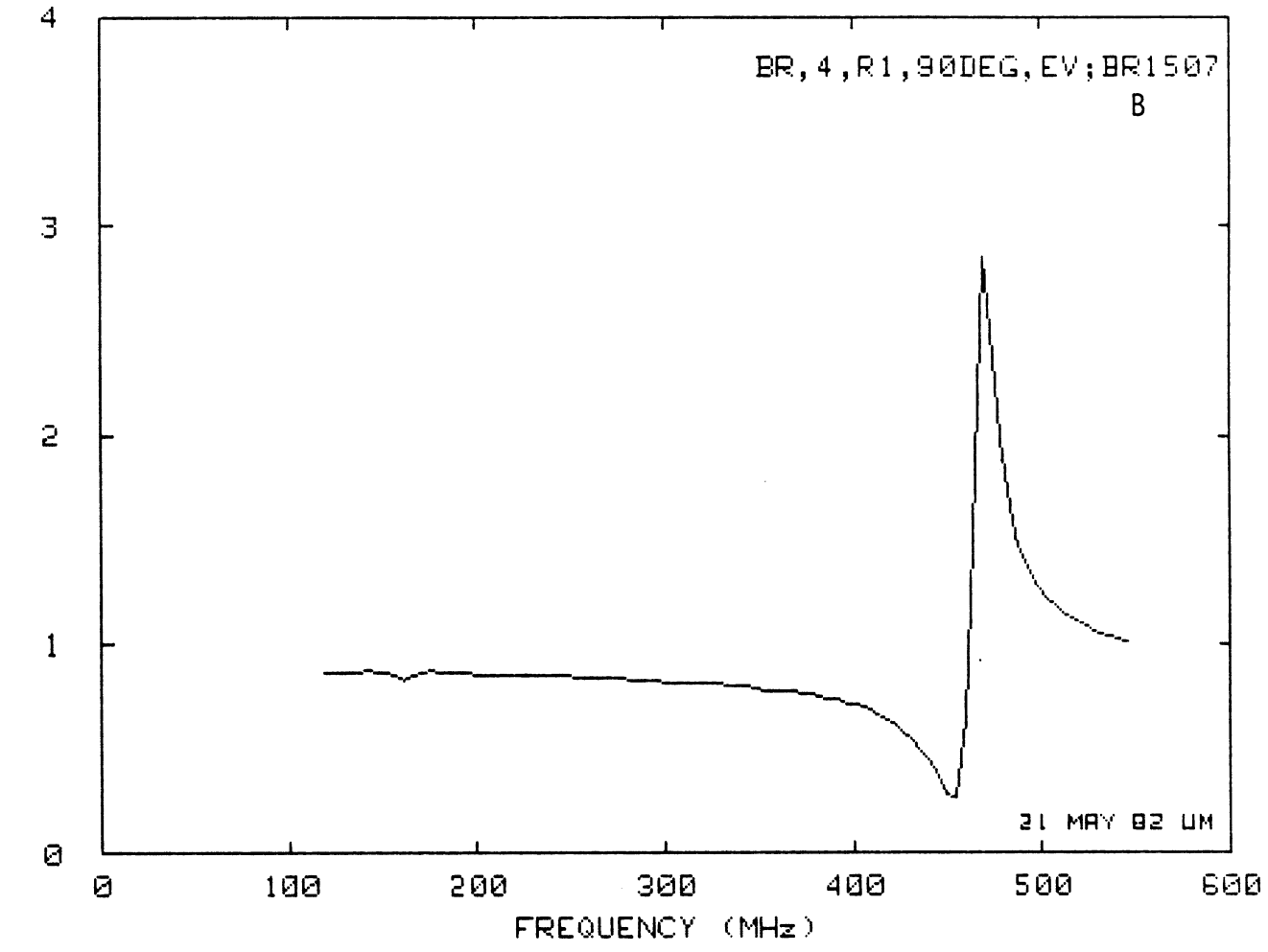
BR,4,R1,90DEG,EV;BR1507
B
21 MAY 82 UM
4
3
2
1
0
0
100
200
300
400
500
600
FREQUENCY (MHz)

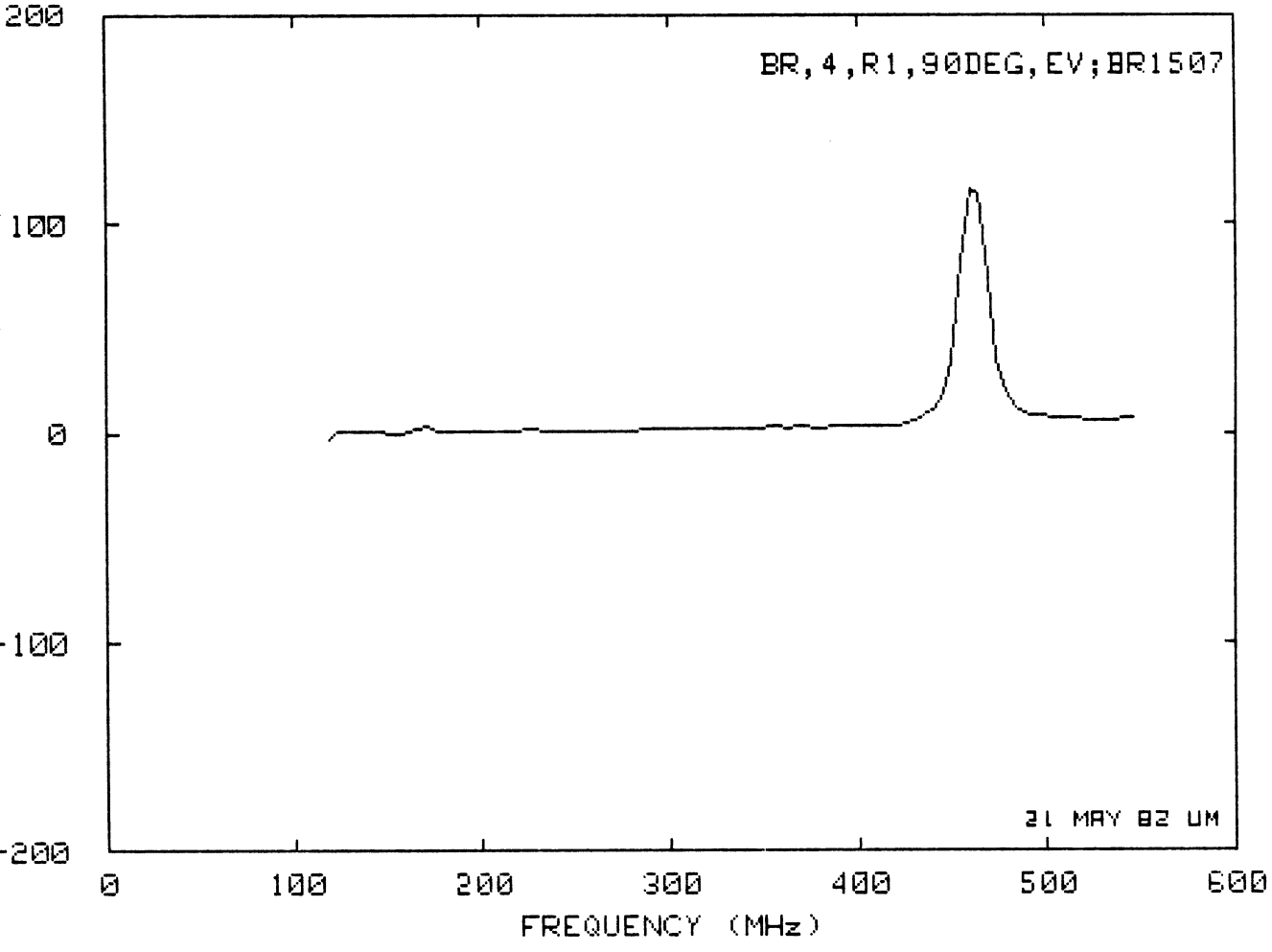
BR,4,R1,90DEG,EV;BR1507
21 MAY 82 UM
200
100
0
-100
-200
0
100
200
300
400
500
600
FREQUENCY (MHz)

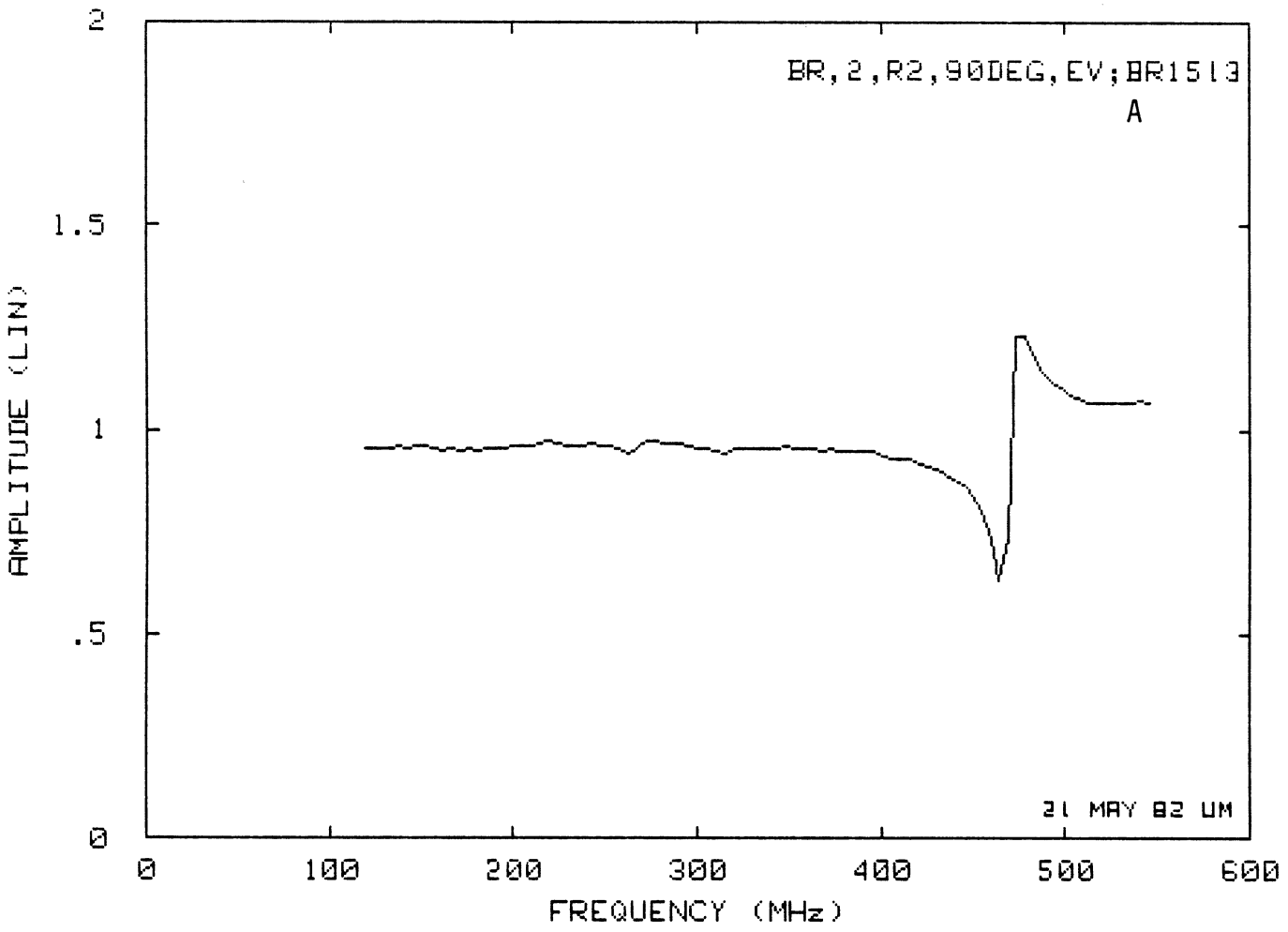
BR,2,R2,90DEG,EV;BR1513
A
21 MAY 82 UM
AMPLITUDE (LIN)
2
1.5
1
.5
0
0
100
200
300
400
500
600
FREQUENCY (MHz)

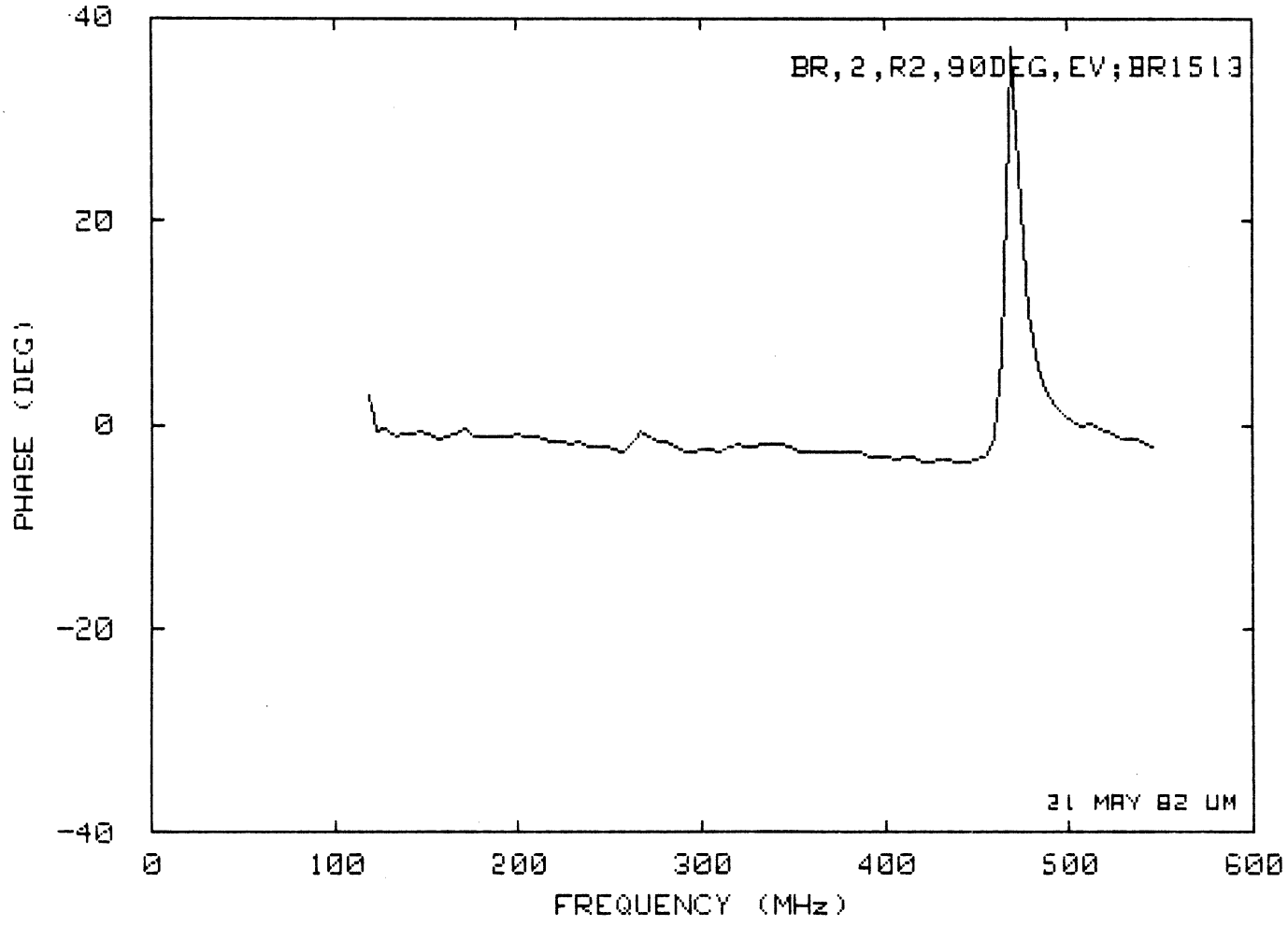
BR,2,R2,90DEG,EV;BR1513
21 MAY 82 UM
PHASE (DEG)
40
20
0
-20
-40
0
100
200
300
400
500
600
FREQUENCY (MHz)

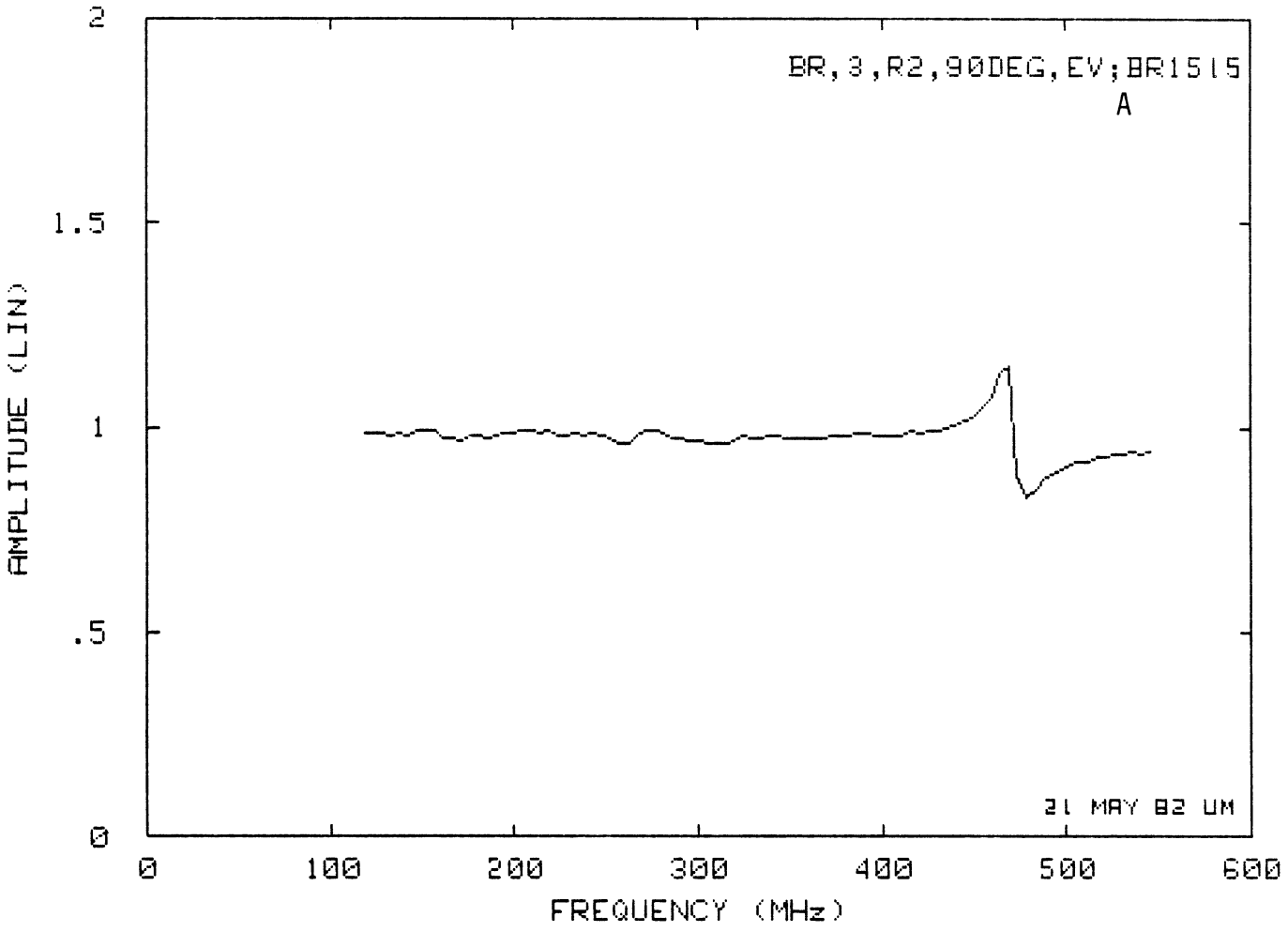
BR,3,R2,90DEG,EV;BR15|5
A
21 MAY 82 UM
AMPLITUDE (LIN)
2
1.5
1
.5
0
0
100
200
300
400
500
600
FREQUENCY (MHz)

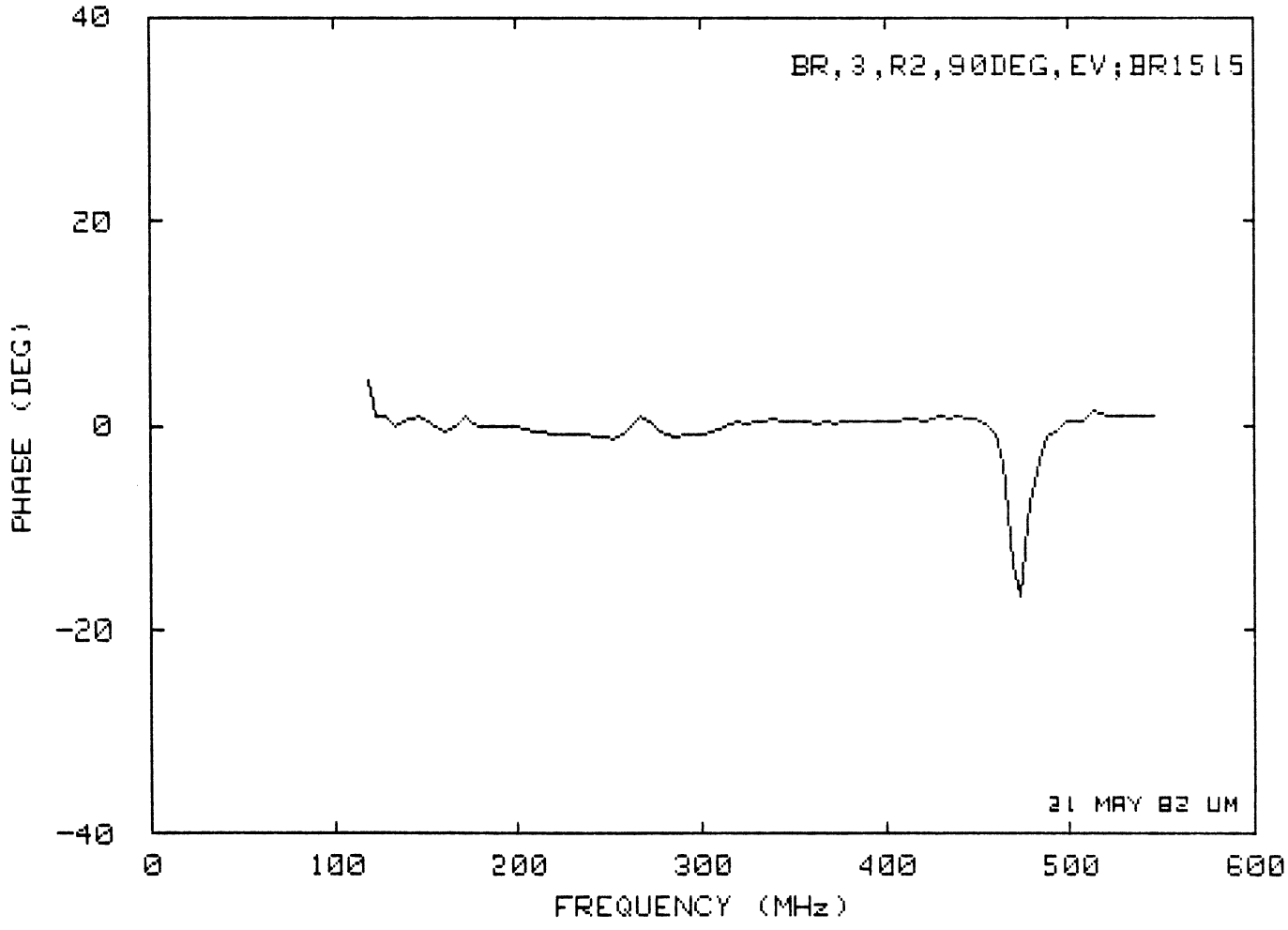
BR,3,R2,90DEG,EV;BR15|5
21 MAY 82 UM
PHASE (DEG)
40
20
0
-20
-40
0
100
200
300
400
500
600
FREQUENCY (MHz)

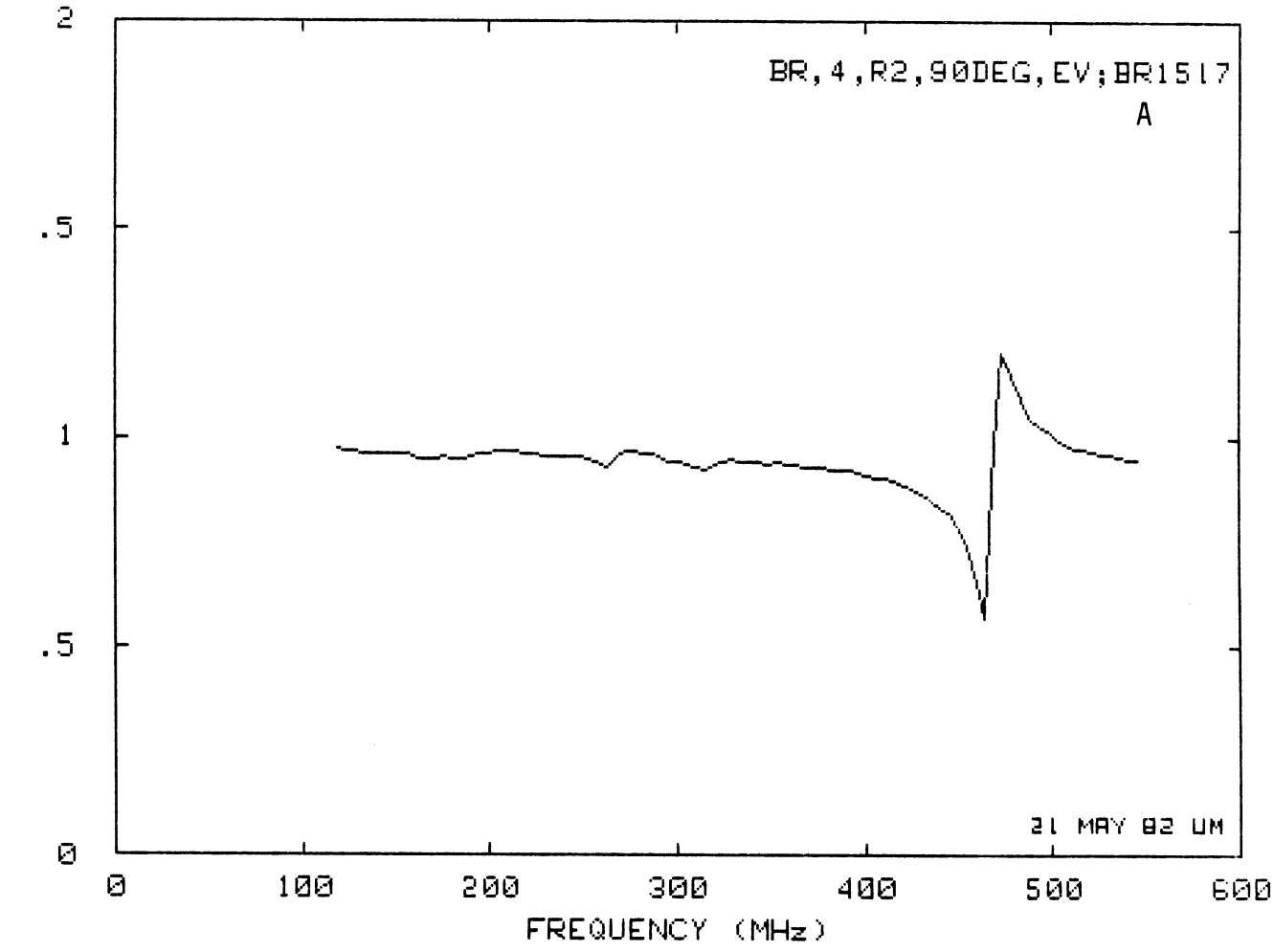
BR,4,R2,90DEG,EV;BR1517
A
21 MAY 82 UM
2
.5
1
.5
0
0
100
200
300
400
500
600
FREQUENCY (MHz)

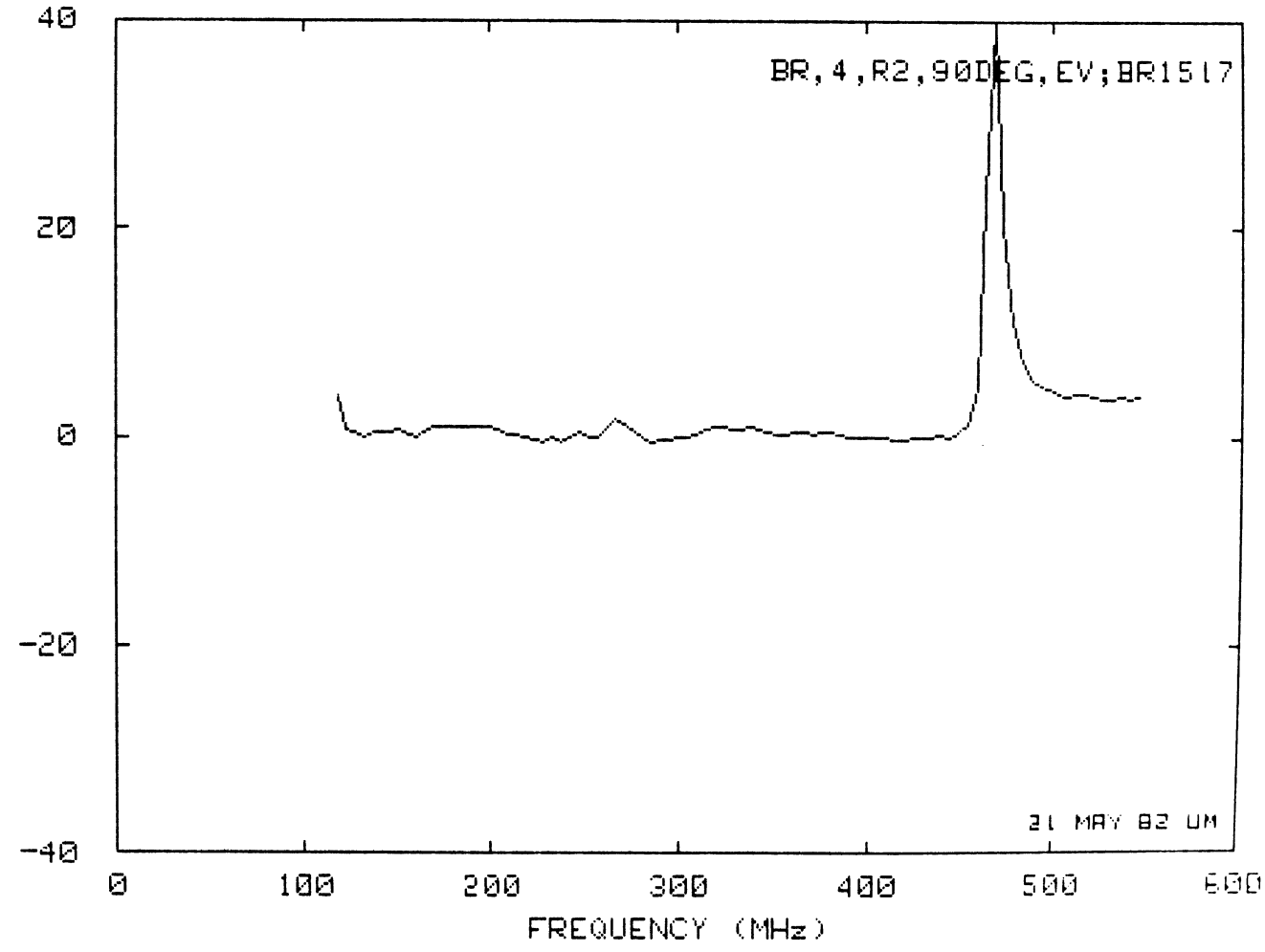
BR,4,R2,90DEG,EV;BR1517
21 MAY 82 UM
40
20
0
-20
-40
0
100
200
300
400
500
600
FREQUENCY (MHz)

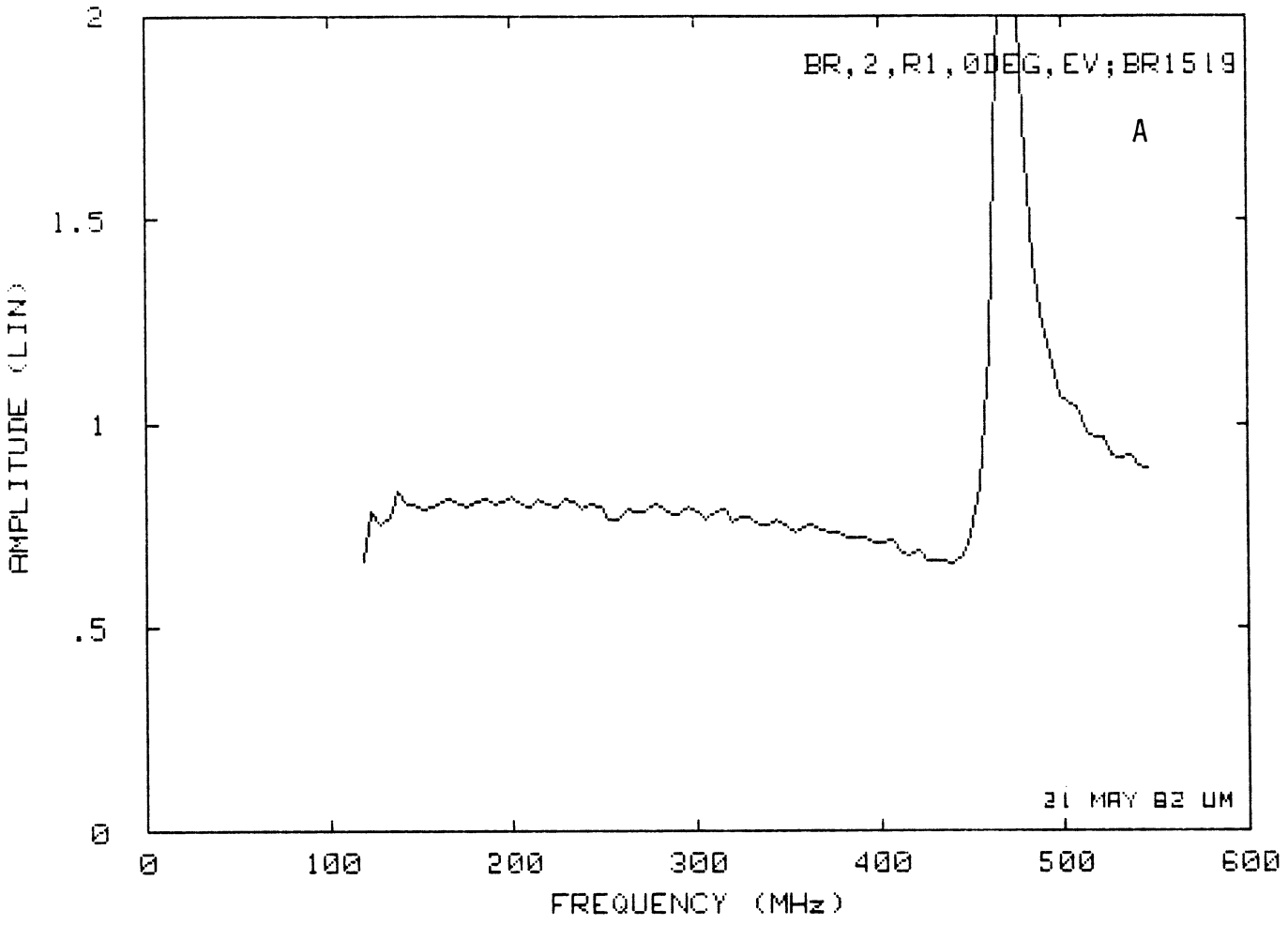
BR,2,R1,0DEG,EV;BR1519
A
21 MAY 82 UM
AMPLITUDE (LIN)
2
1.5
1
.5
0
0
100
200
300
400
500
600
FREQUENCY (MHz)

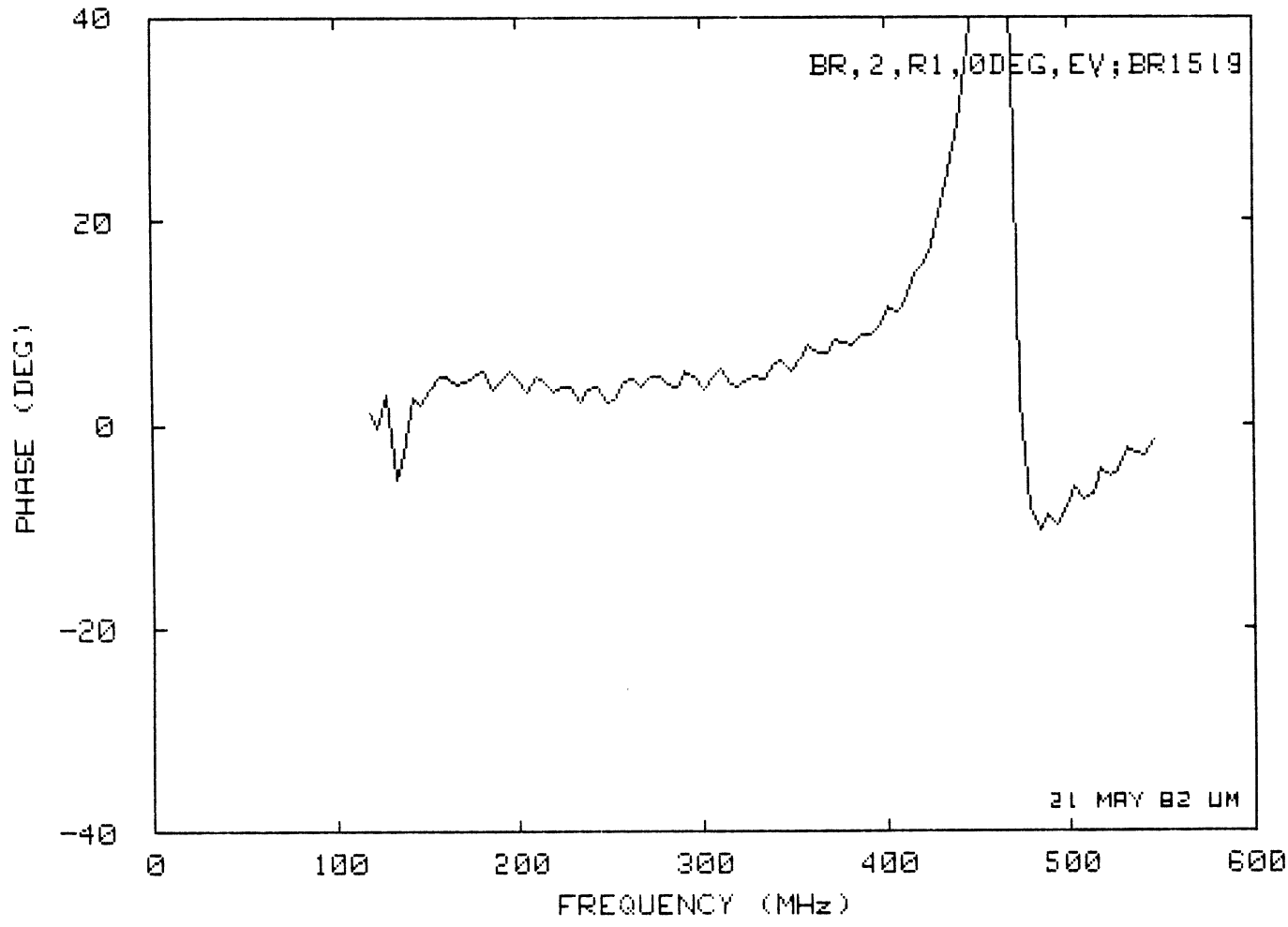
BR,2,R1,0DEG,EV;BR1519
21 MAY 82 UM
PHASE (DEG)
40
20
0
-20
-40
0
100
200
300
400
500
600
FREQUENCY (MHz)

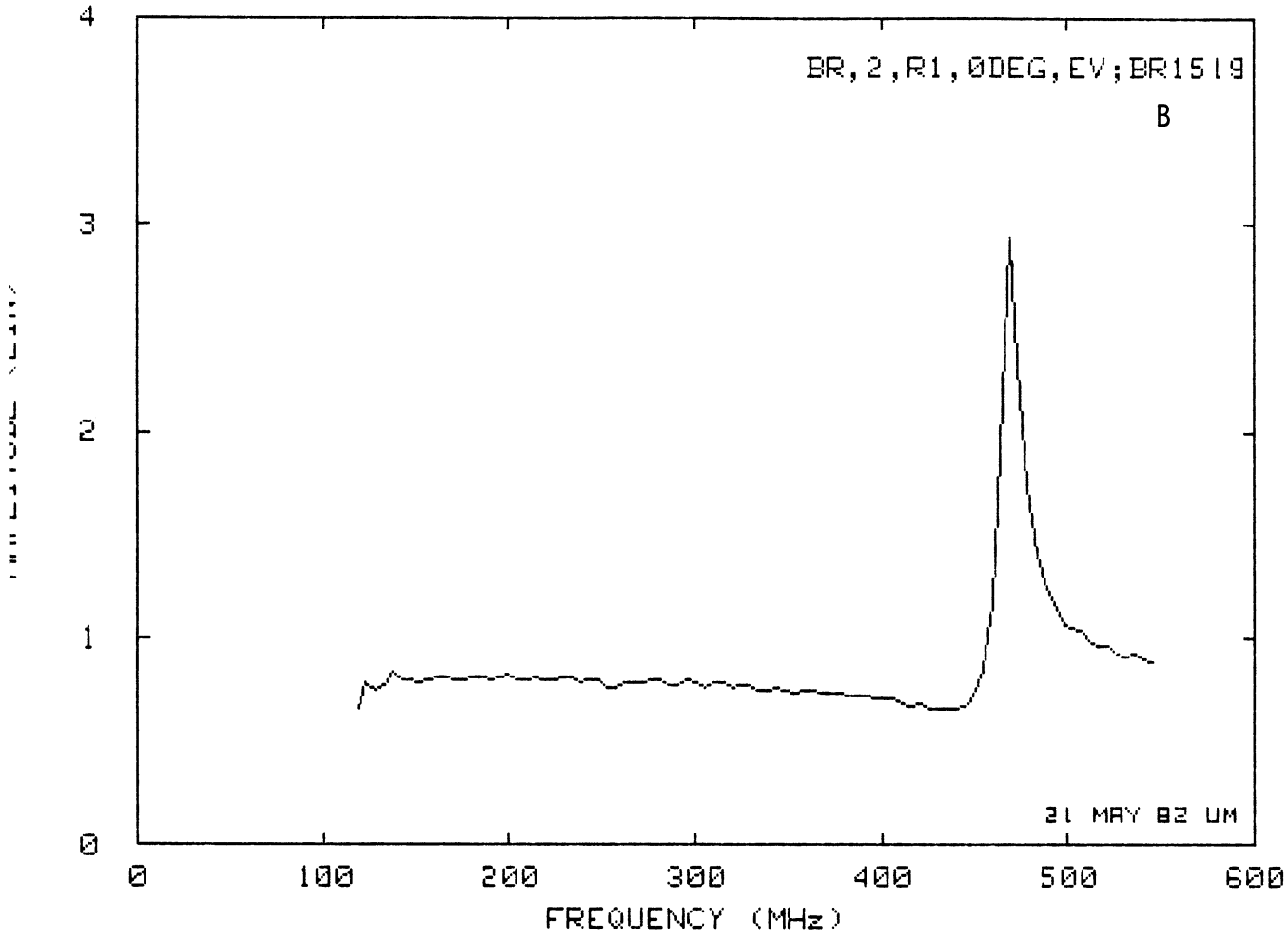
BR,2,R1,0DEG,EV;BR1519
B
21 MAY 82 UM
4
3
2
1
0
0
100
200
300
400
500
600
FREQUENCY (MHz)

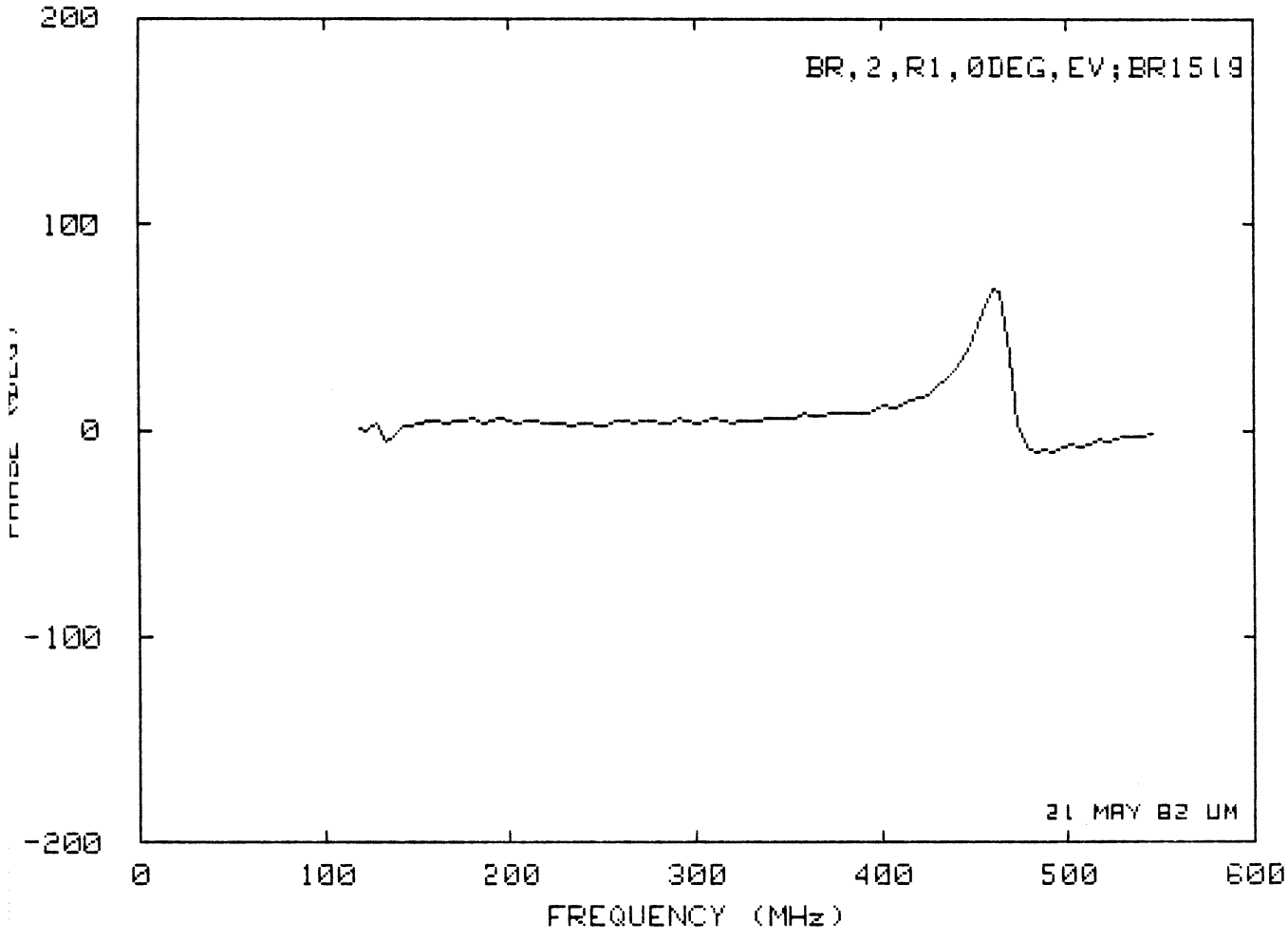
BR,2,R1,0DEG,EV;BR1519
21 MAY 82 UM
200
100
0
-100
-200
0
100
200
300
400
500
600
FREQUENCY (MHz)

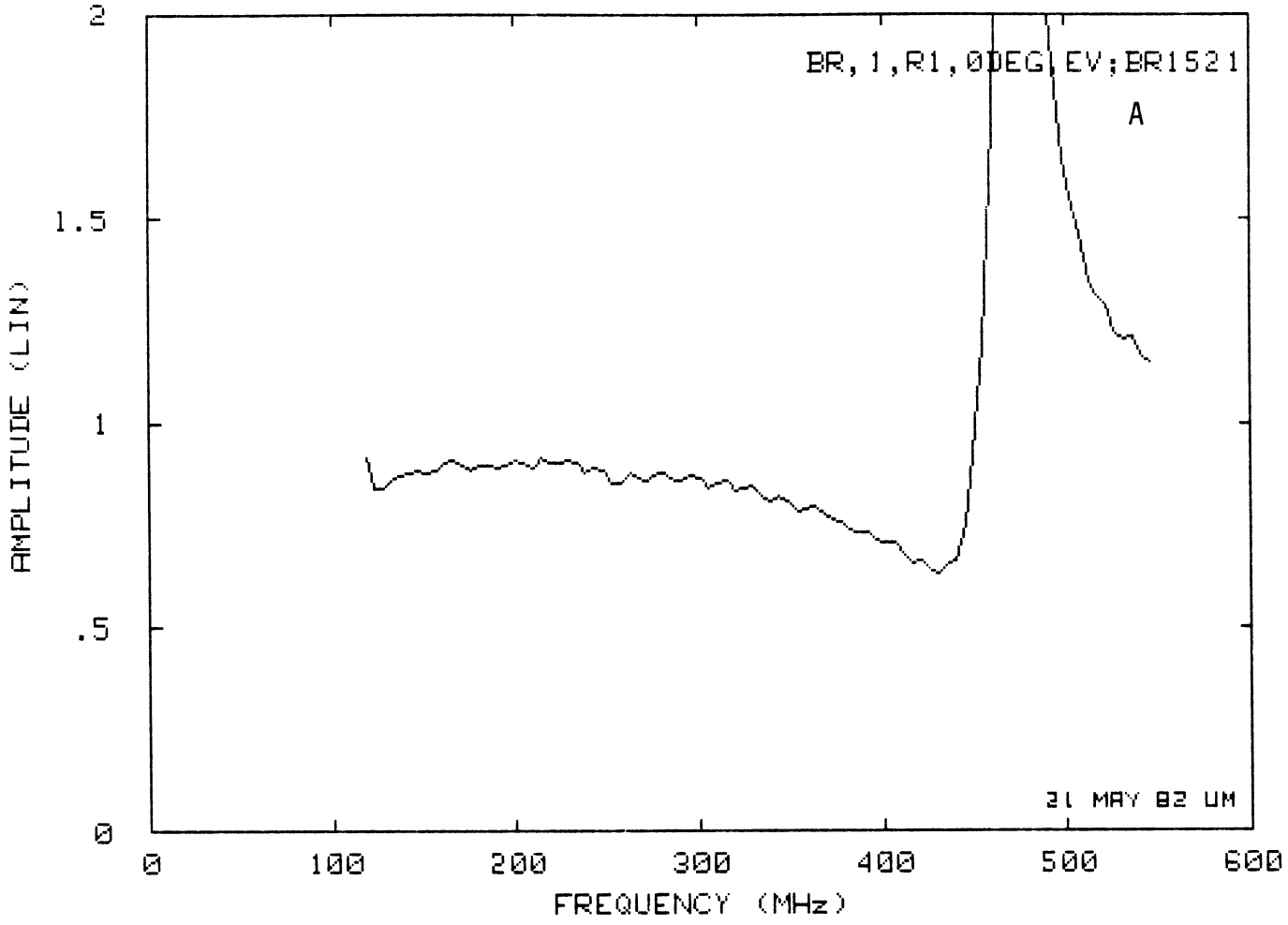
BR,1,R1,0DEG,EV;BR1521
A
21 MAY 82 UM
AMPLITUDE (LIN)
2
1.5
1
.5
0
0
100
200
300
400
500
600
FREQUENCY (MHz)

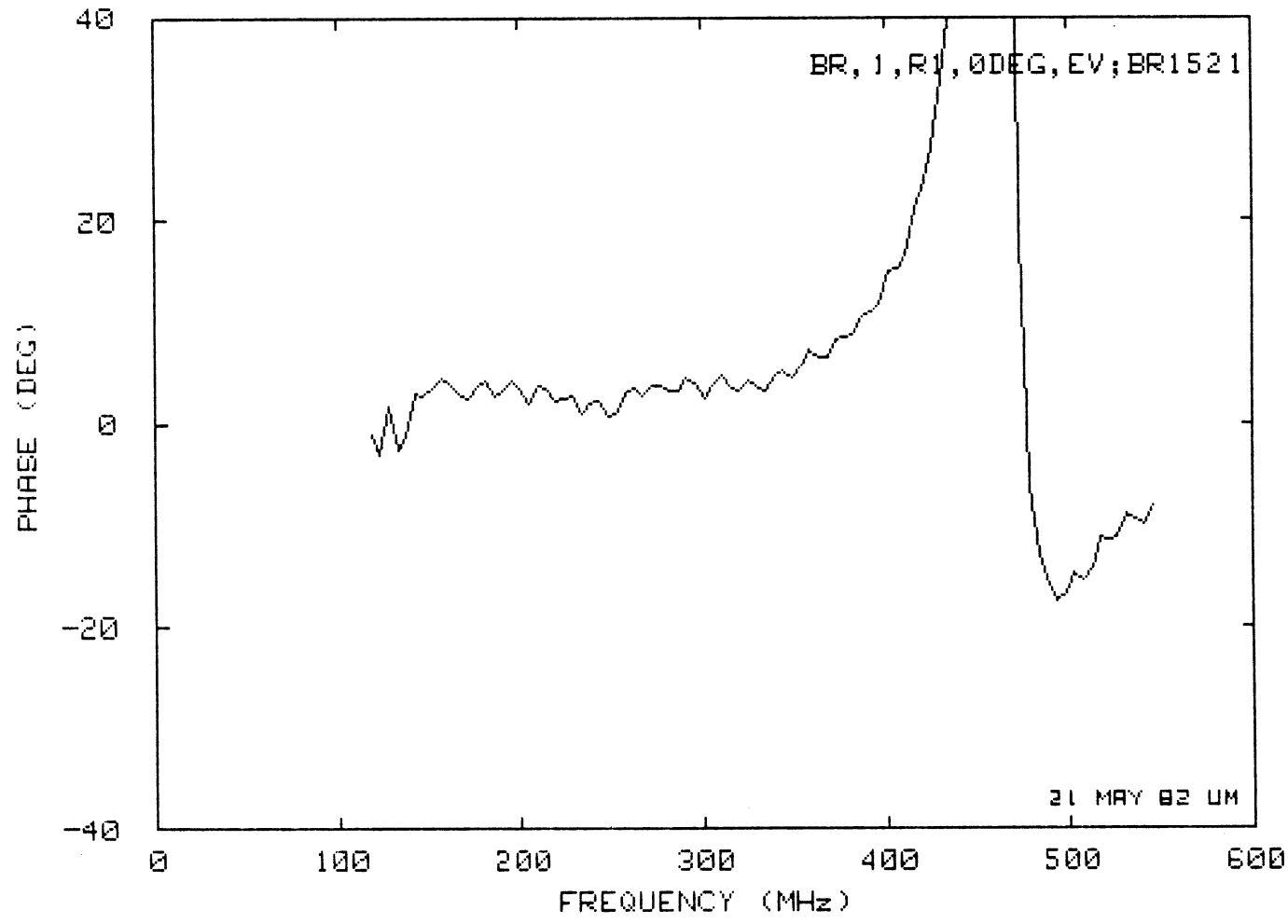
BR,1,R1,0DEG,EV;BR1521
21 MAY 82 UM
PHASE (DEG)
40
20
0
-20
-40
0
100
200
300
400
500
600
FREQUENCY (MHz)

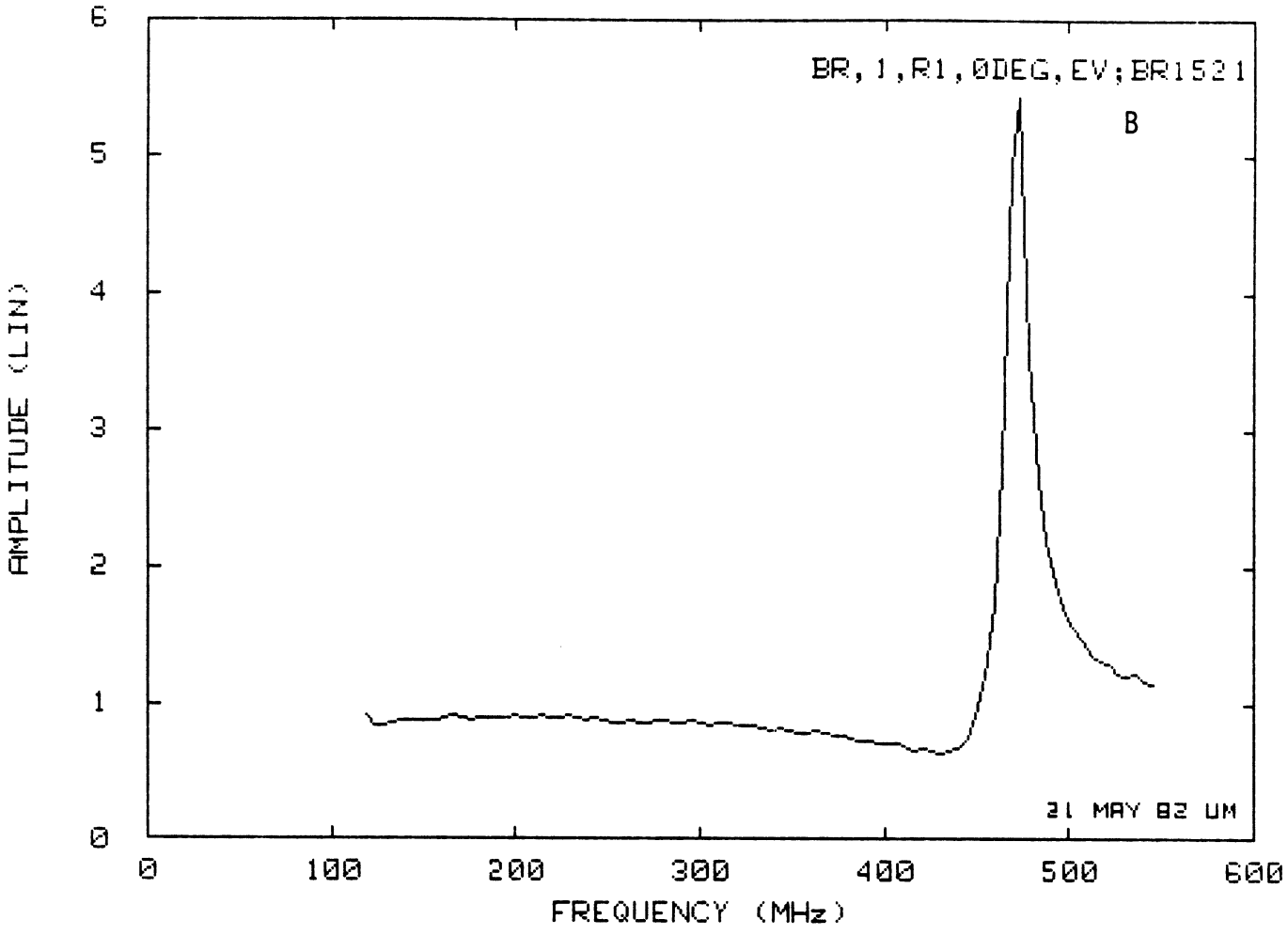
BR,1,R1,0DEG,EV;BR1521
B
21 MAY 82 UM
AMPLITUDE (LIN)
0
1
2
3
4
5
6
0
100
200
300
400
500
600
FREQUENCY (MHz)

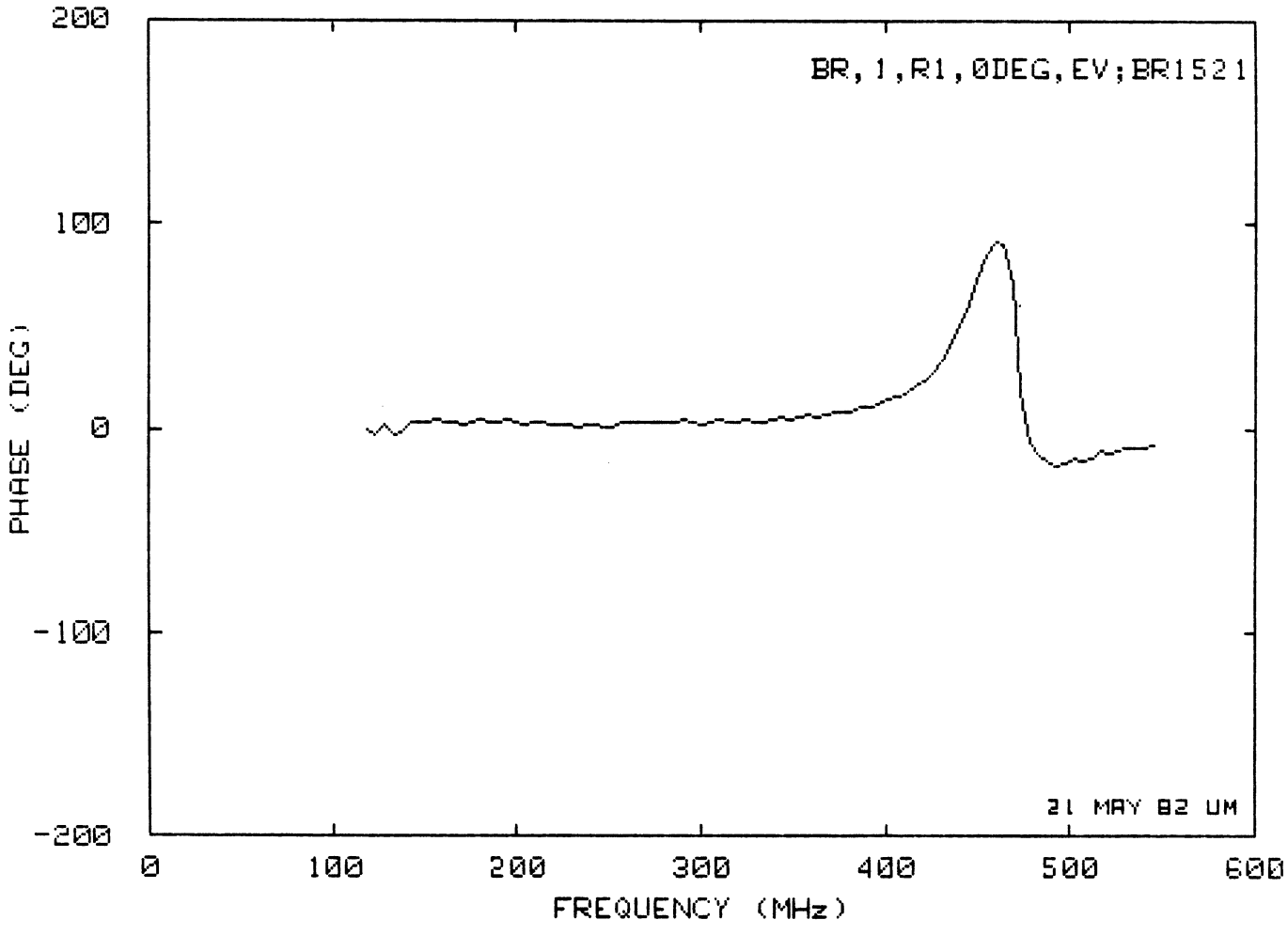
BR,1,R1,0DEG,EV;BR1521
21 MAY 82 UM
PHASE (DEG)
200
100
0
-100
-200
0
100
200
300
400
500
600
FREQUENCY (MHz)

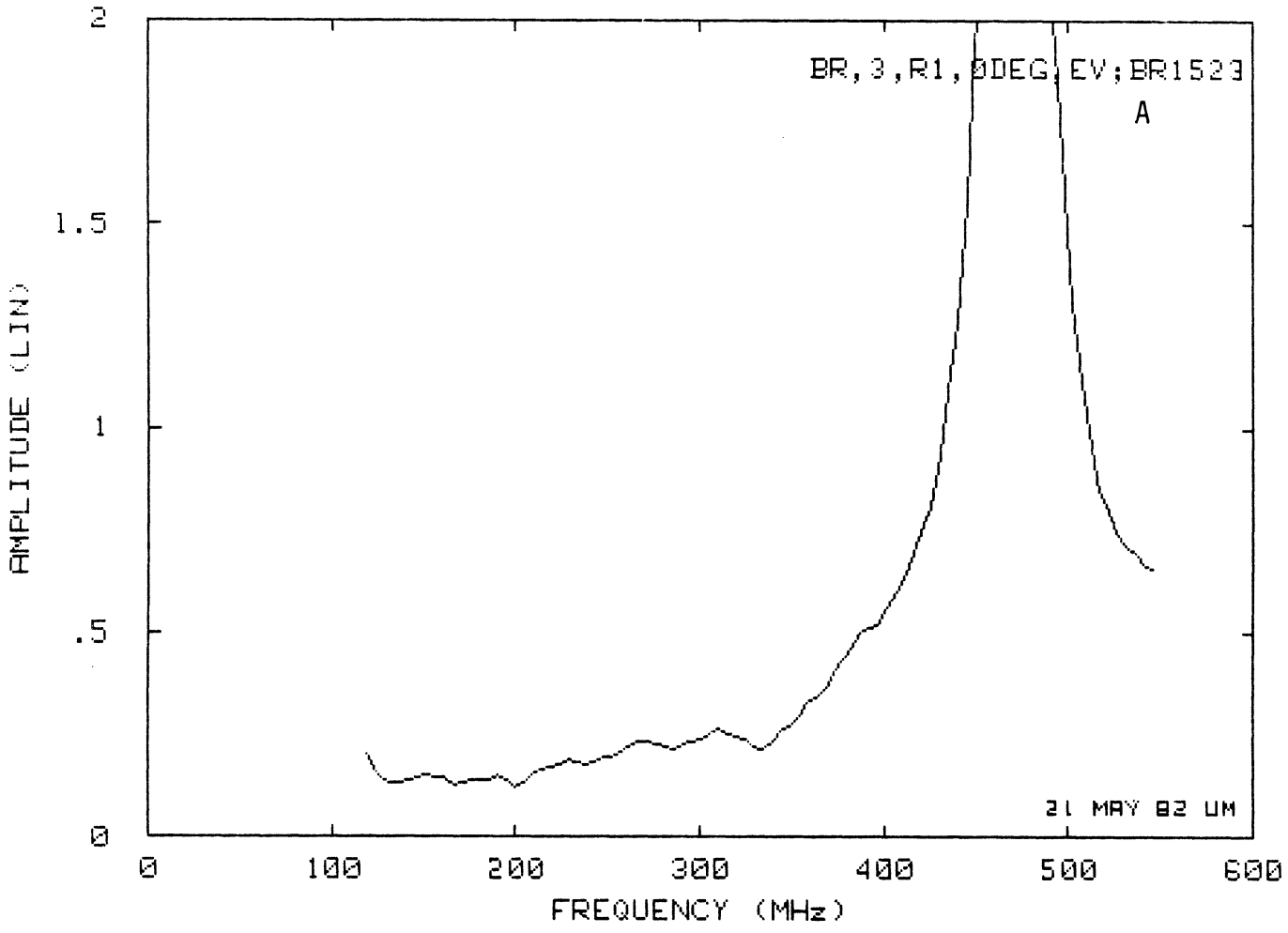
BR,3,R1,0DEG,EV;BR1523
A
21 MAY 82 UM
AMPLITUDE (LIN)
2
1.5
1
.5
0
0
100
200
300
400
500
600
FREQUENCY (MHz)

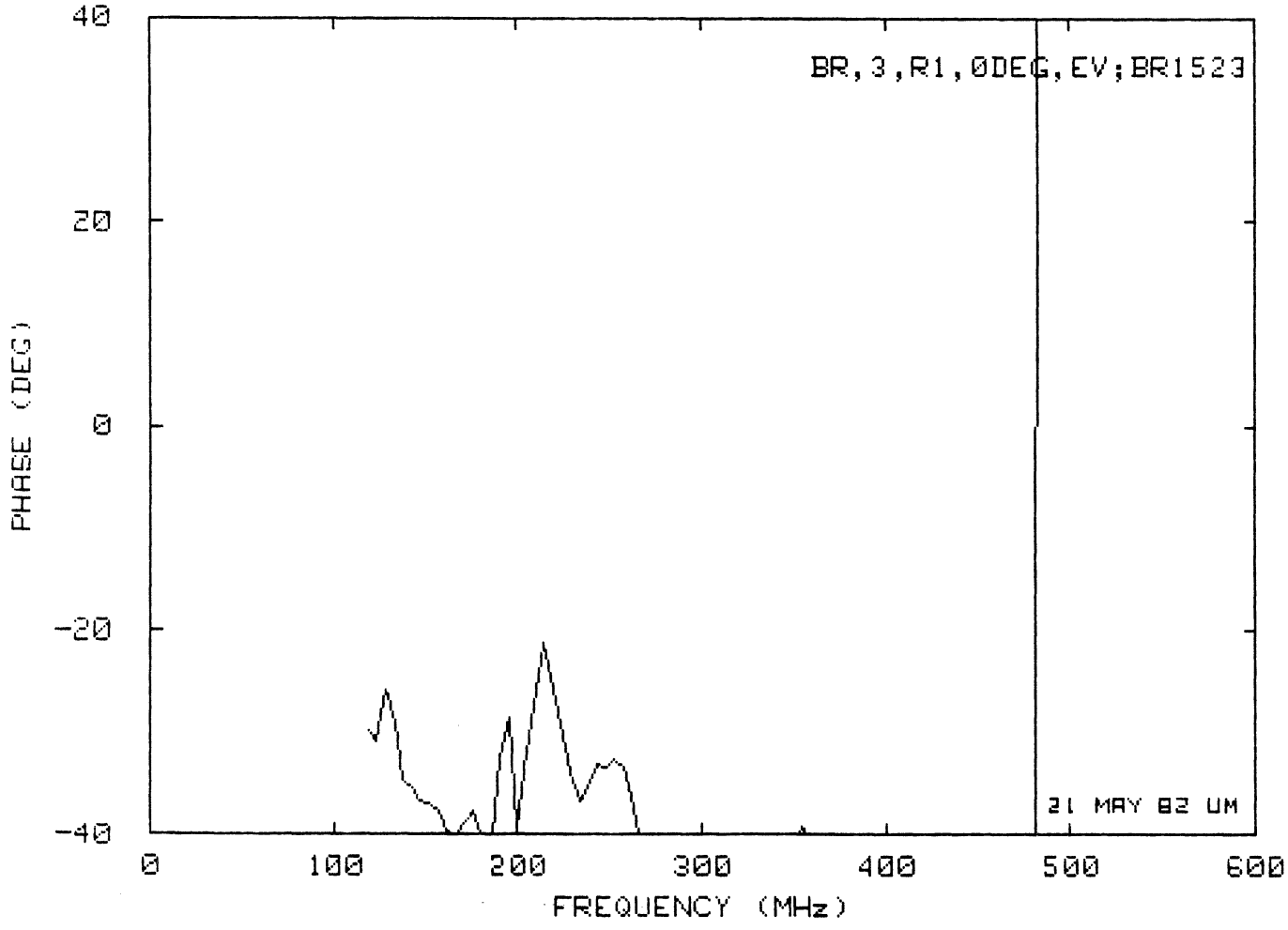
BR,3,R1,0DEG,EV;BR1523
21 MAY 82 UM
PHASE (DEG)
40
20
0
-20
-40
0
100
200
300
400
500
600
FREQUENCY (MHz)

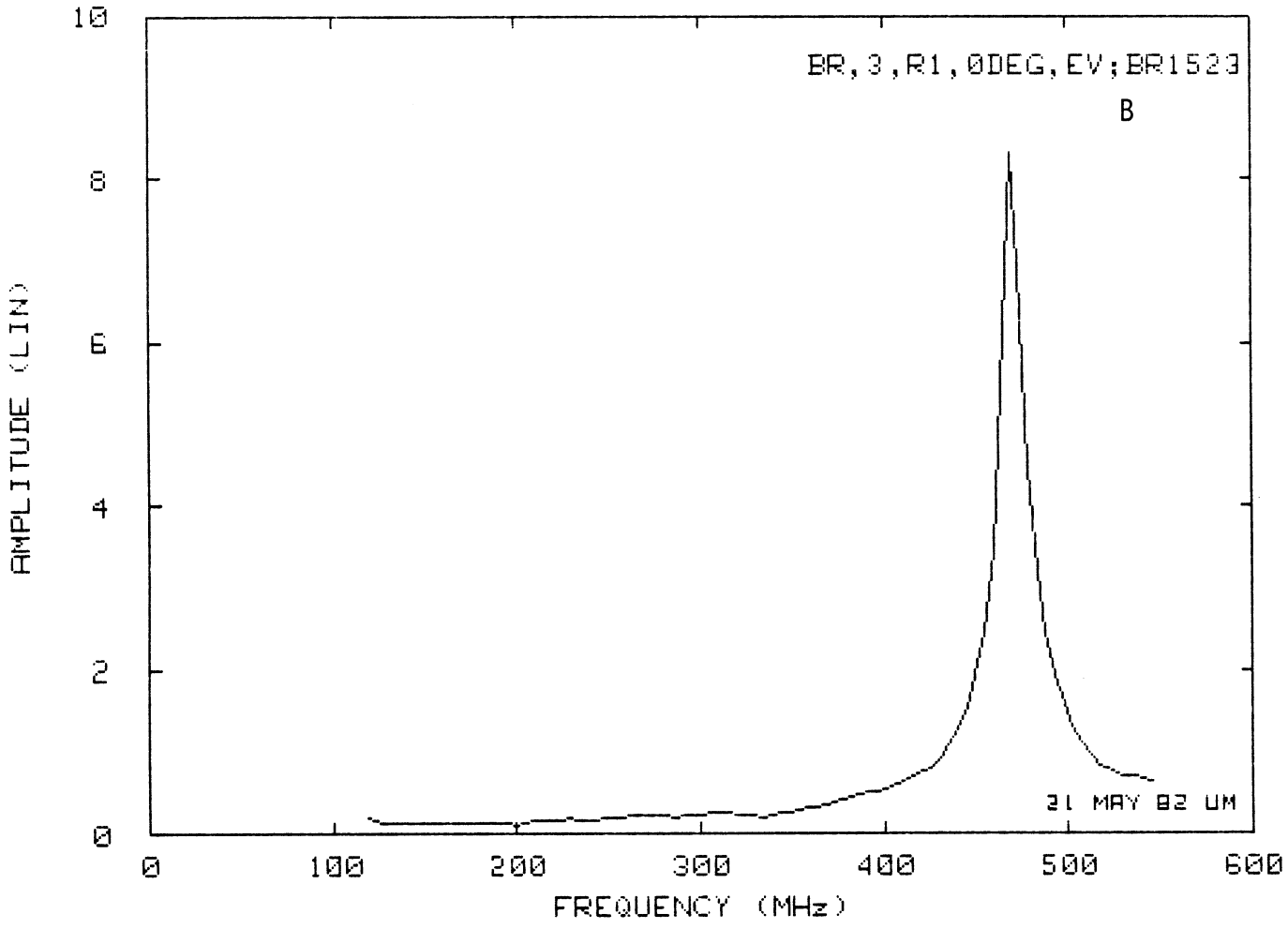
BR,3,R1,0DEG,EV;BR1523
B
21 MAY 82 UM
AMPLITUDE (LIN)
10
8
6
4
2
0
0
100
200
300
400
500
600
FREQUENCY (MHz)

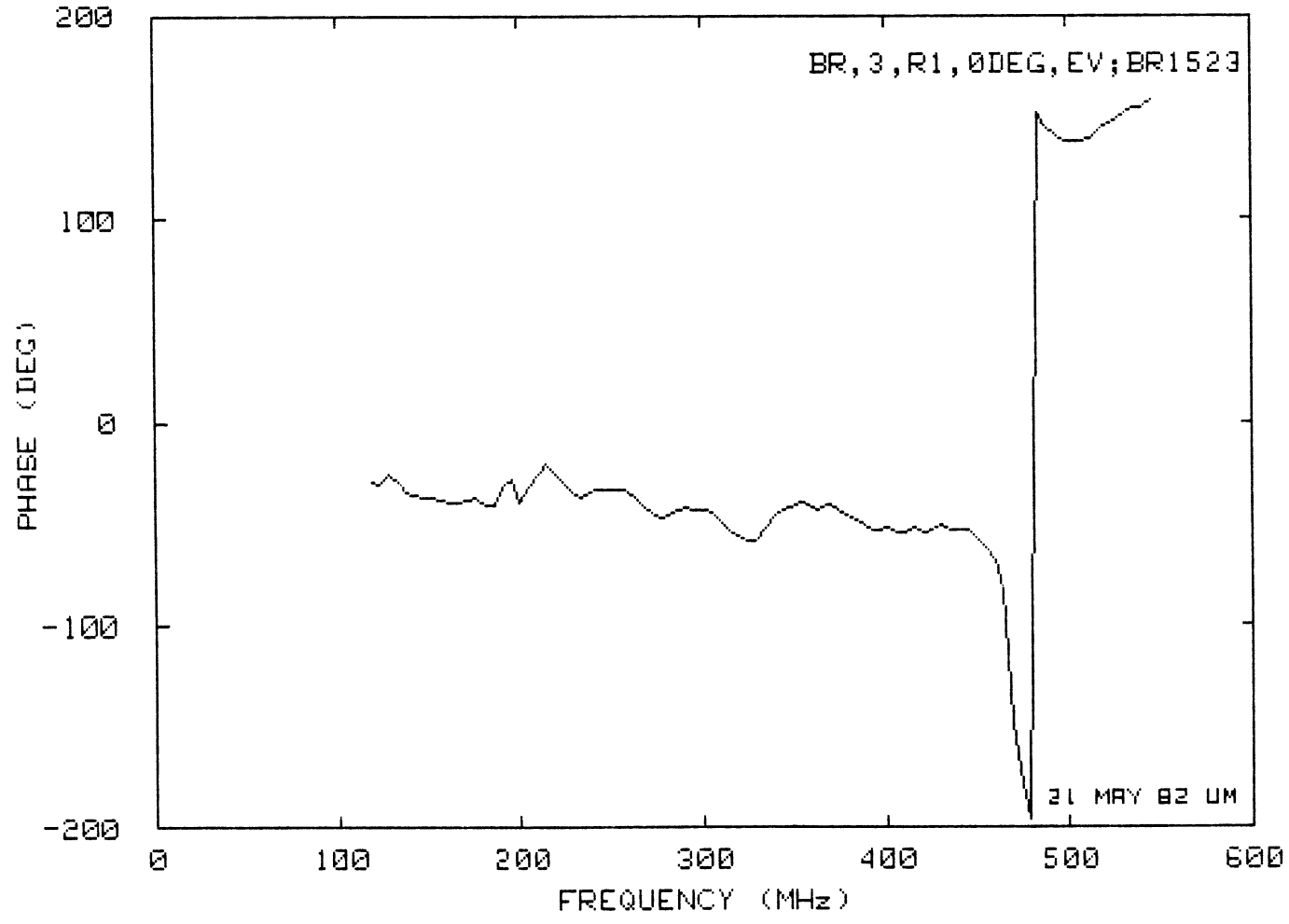
BR,3,R1,0DEG,EV;BR1523
21 MAY 82 UM
PHASE (DEG)
200
100
0
-100
-200
0
100
200
300
400
500
600
FREQUENCY (MHz)

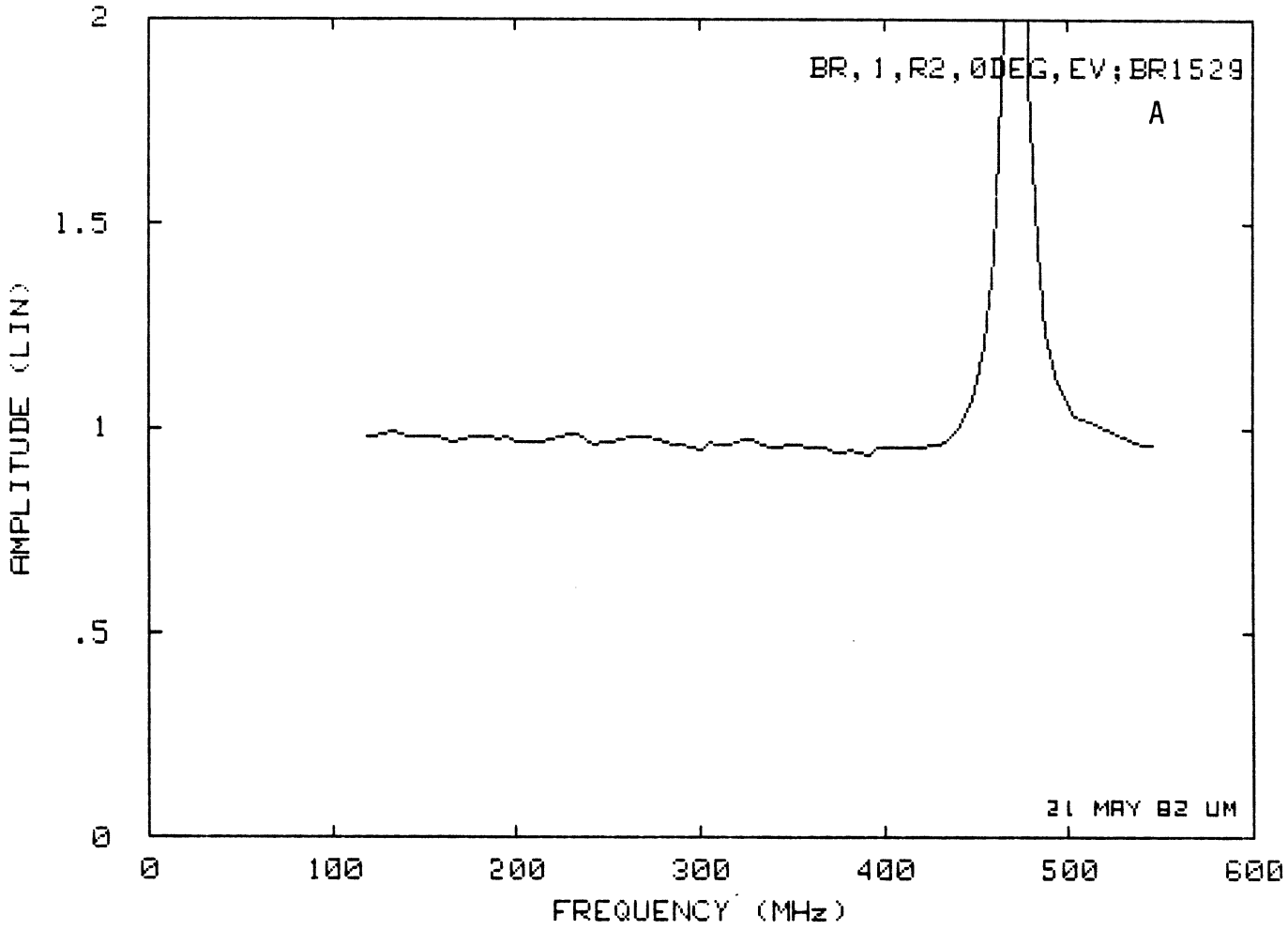
BR,1,R2,0DEG,EV;BR1529
A
21 MAY 82 UM
AMPLITUDE (LIN)
2
1.5
1
.5
0
0
100
200
300
400
500
600
FREQUENCY (MHz)

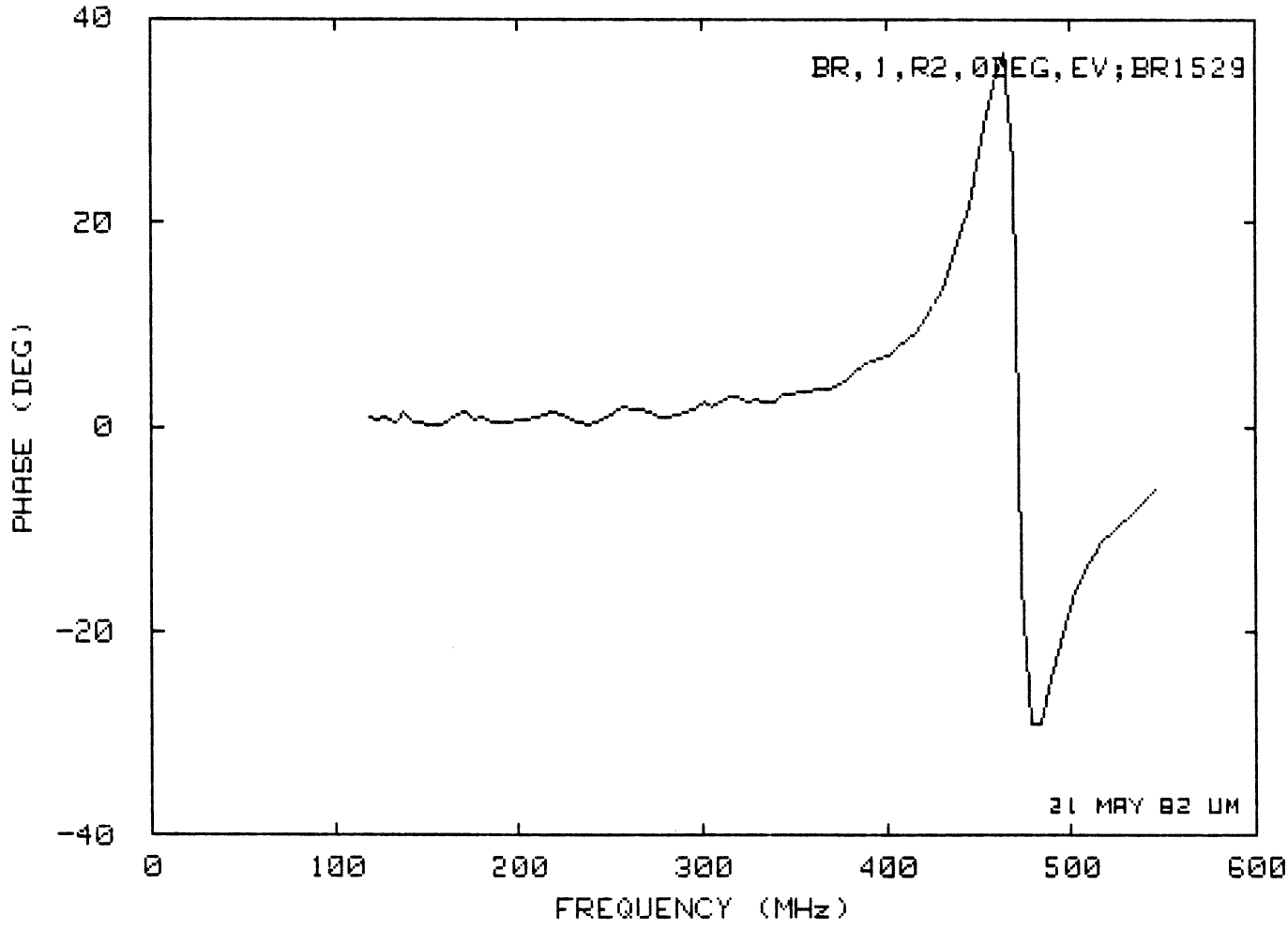
BR,1,R2,0DEG,EV;BR1529
21 MAY 82 UM
PHASE (DEG)
40
20
0
-20
-40
0
100
200
300
400
500
600
FREQUENCY (MHz)

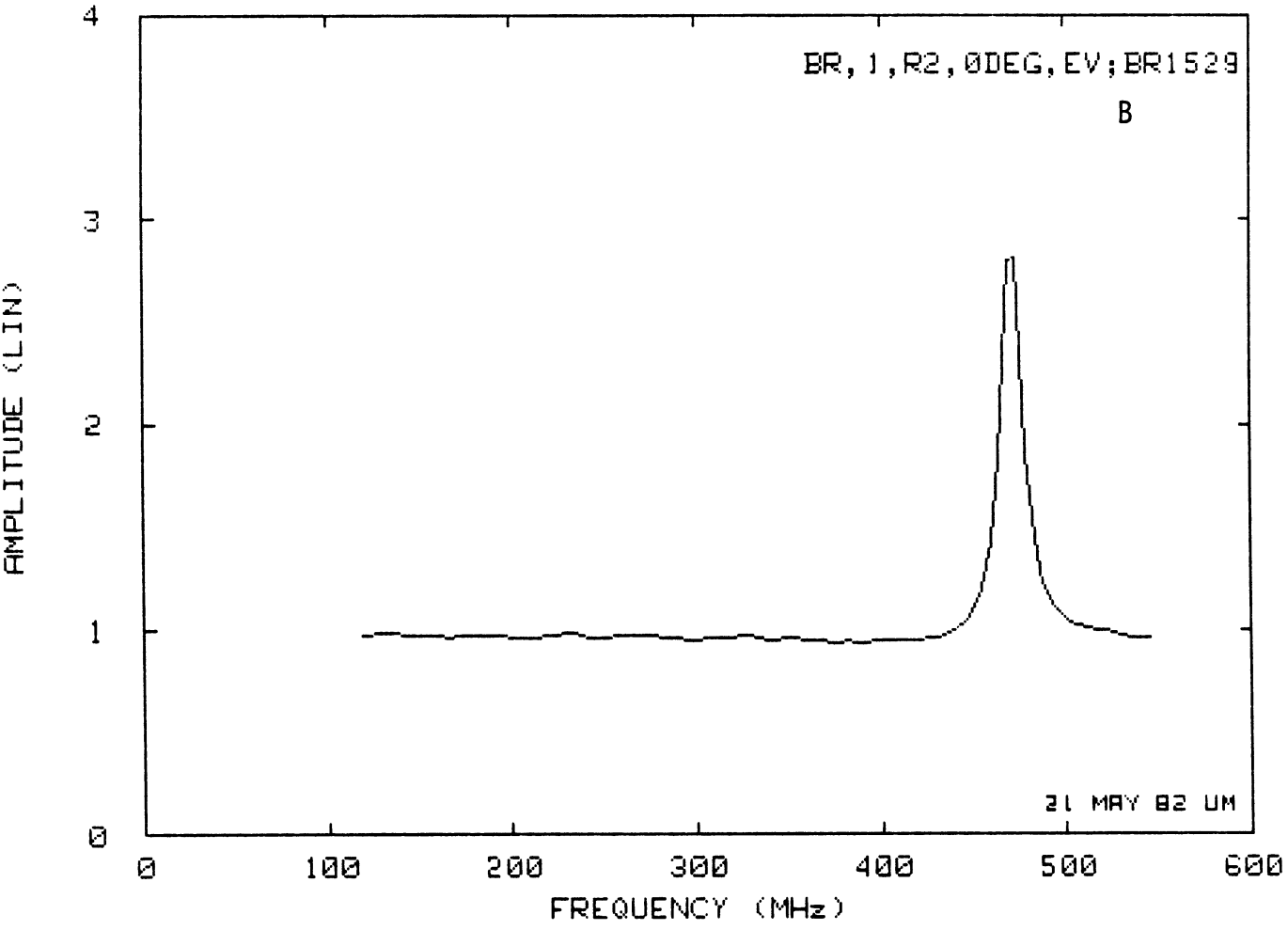
BR,1,R2,0DEG,EV;BR1529
B
21 MAY 82 UM
AMPLITUDE (LIN)
4
3
2
1
0
0
100
200
300
400
500
600
FREQUENCY (MHz)

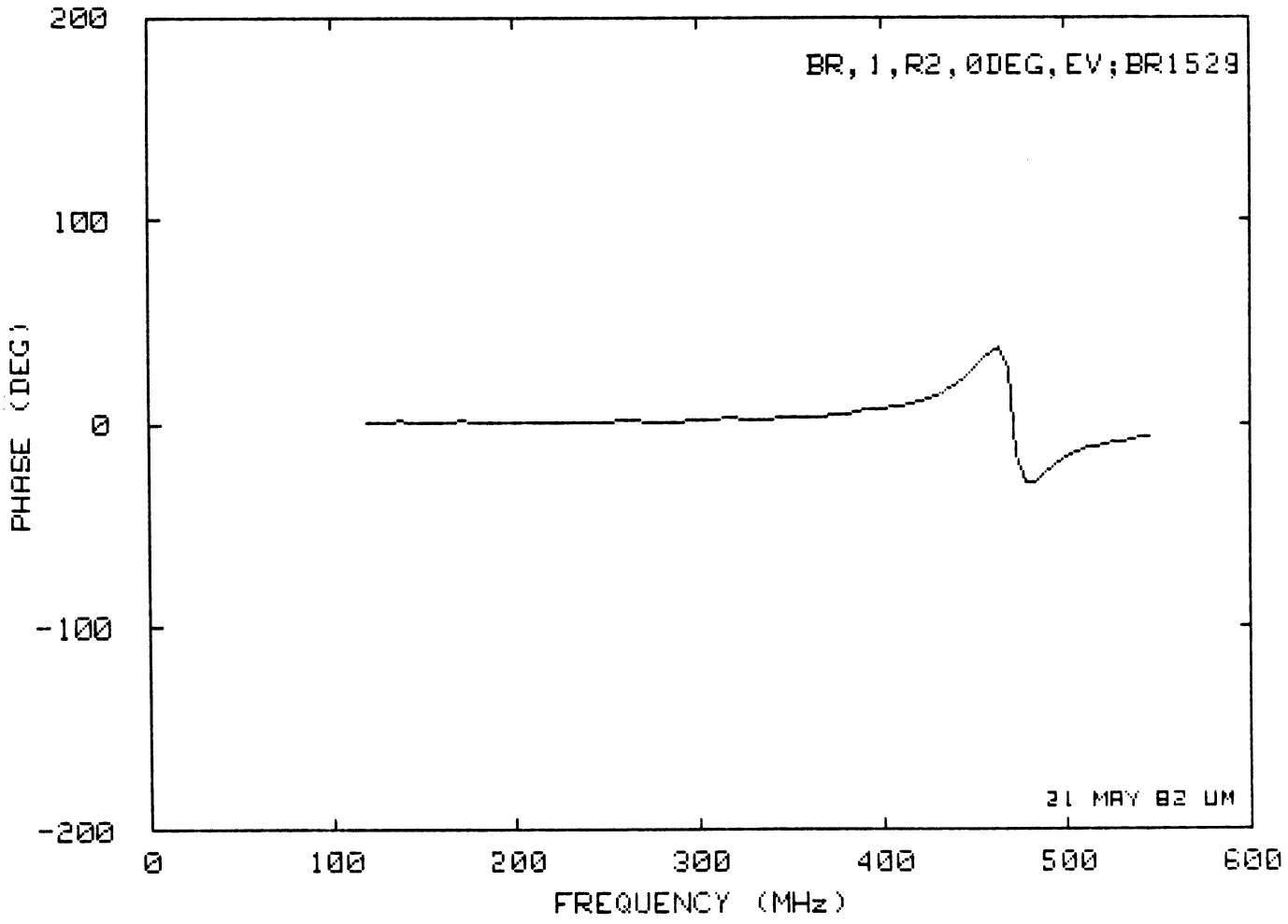
BR,1,R2,0DEG,EV;BR1529
21 MAY 82 UM
PHASE (DEG)
200
100
0
-100
-200
0
100
200
300
400
500
600
FREQUENCY (MHz)

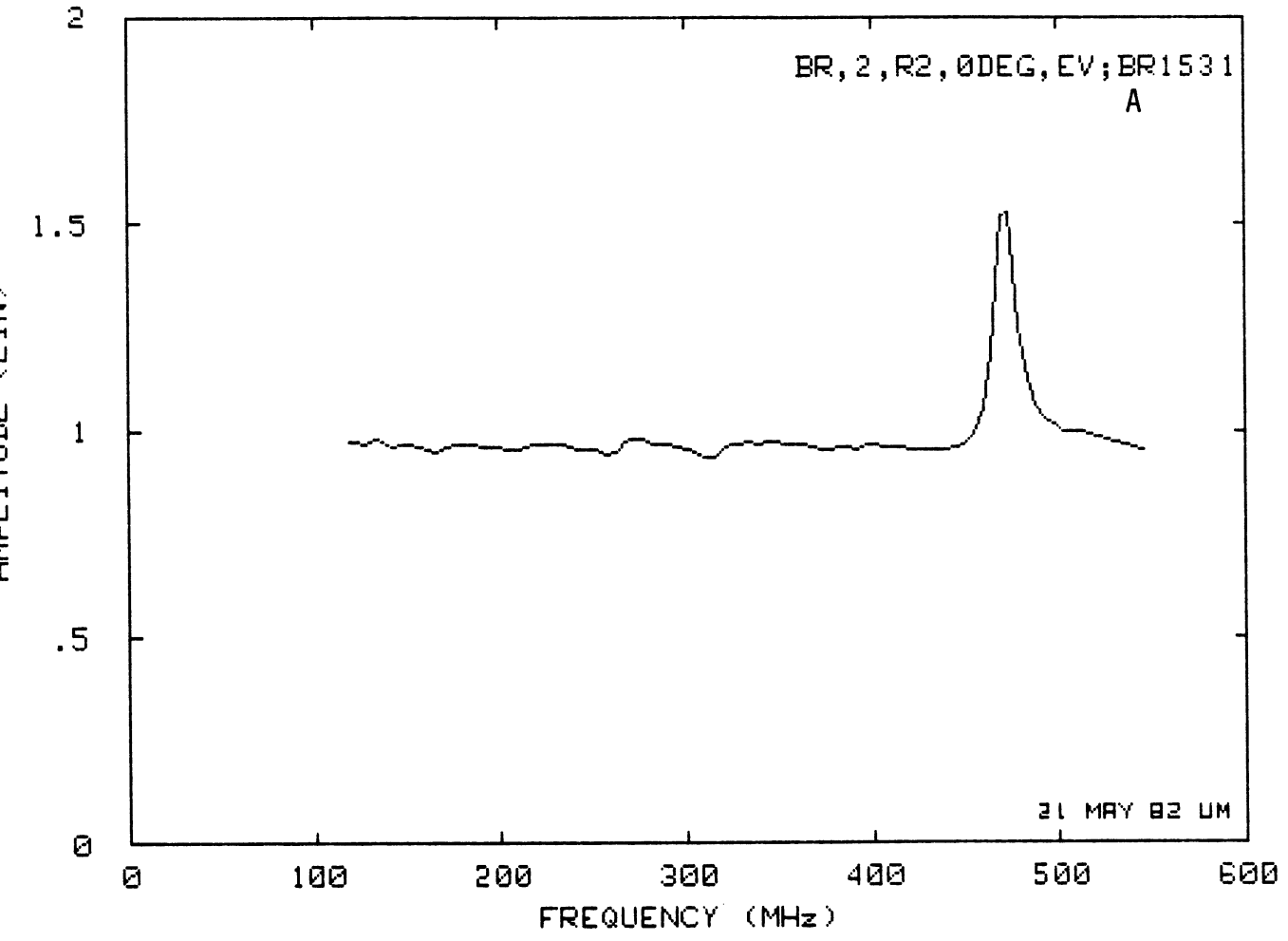
BR,2,R2,0DEG,EV;BR1531
A
21 MAY 82 UM
2
1.5
1
.5
0
0
100
200
300
400
500
600
FREQUENCY (MHz)

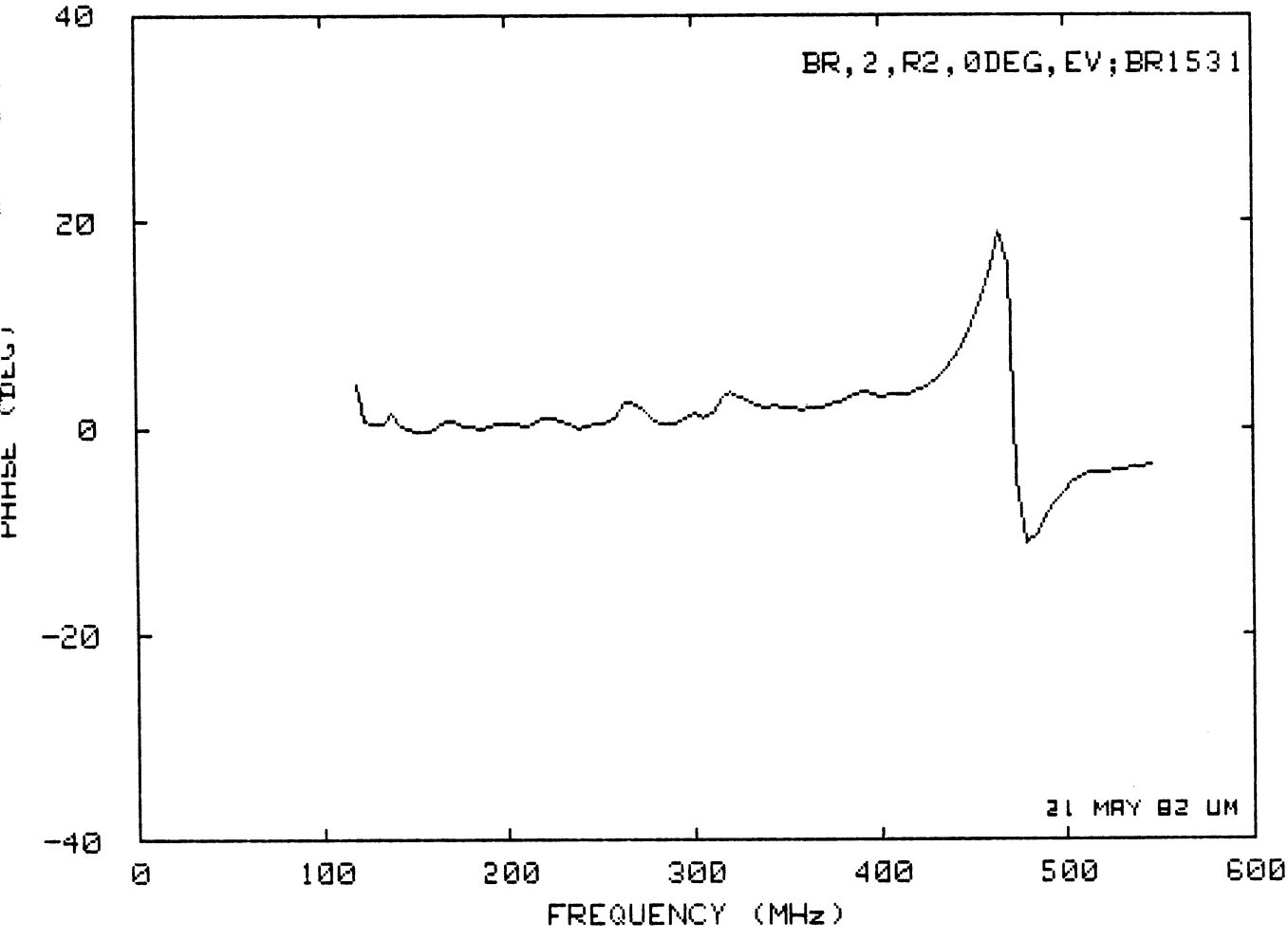
BR,2,R2,0DEG,EV;BR1531
21 MAY 82 UM
40
20
0
-20
-40
0
100
200
300
400
500
600
FREQUENCY (MHz)

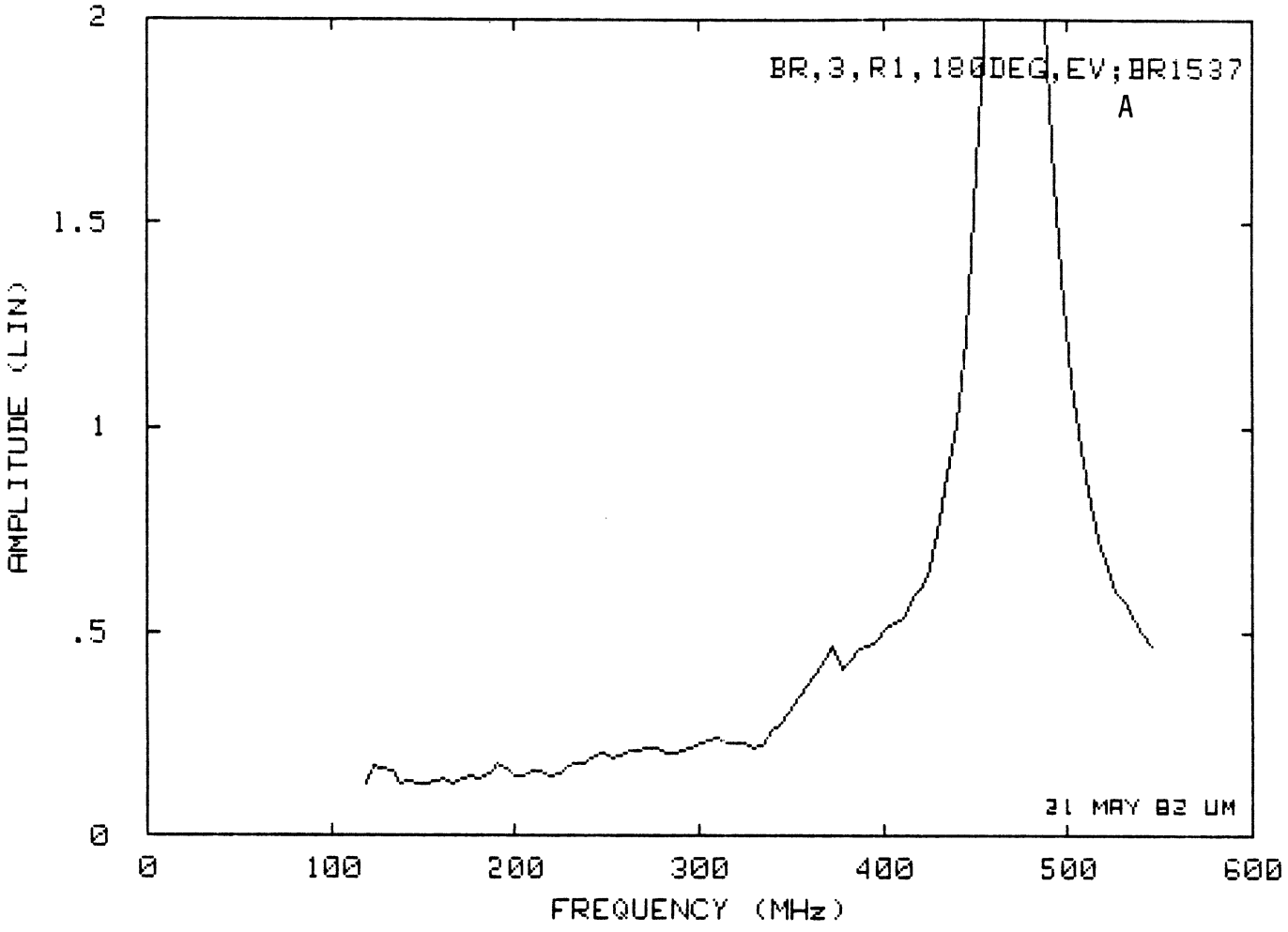
BR,3,R1,180DEG,EV;BR1537
A
21 MAY 82 UM
AMPLITUDE (LIN)
2
1.5
1
.5
0
0
100
200
300
400
500
600
FREQUENCY (MHz)

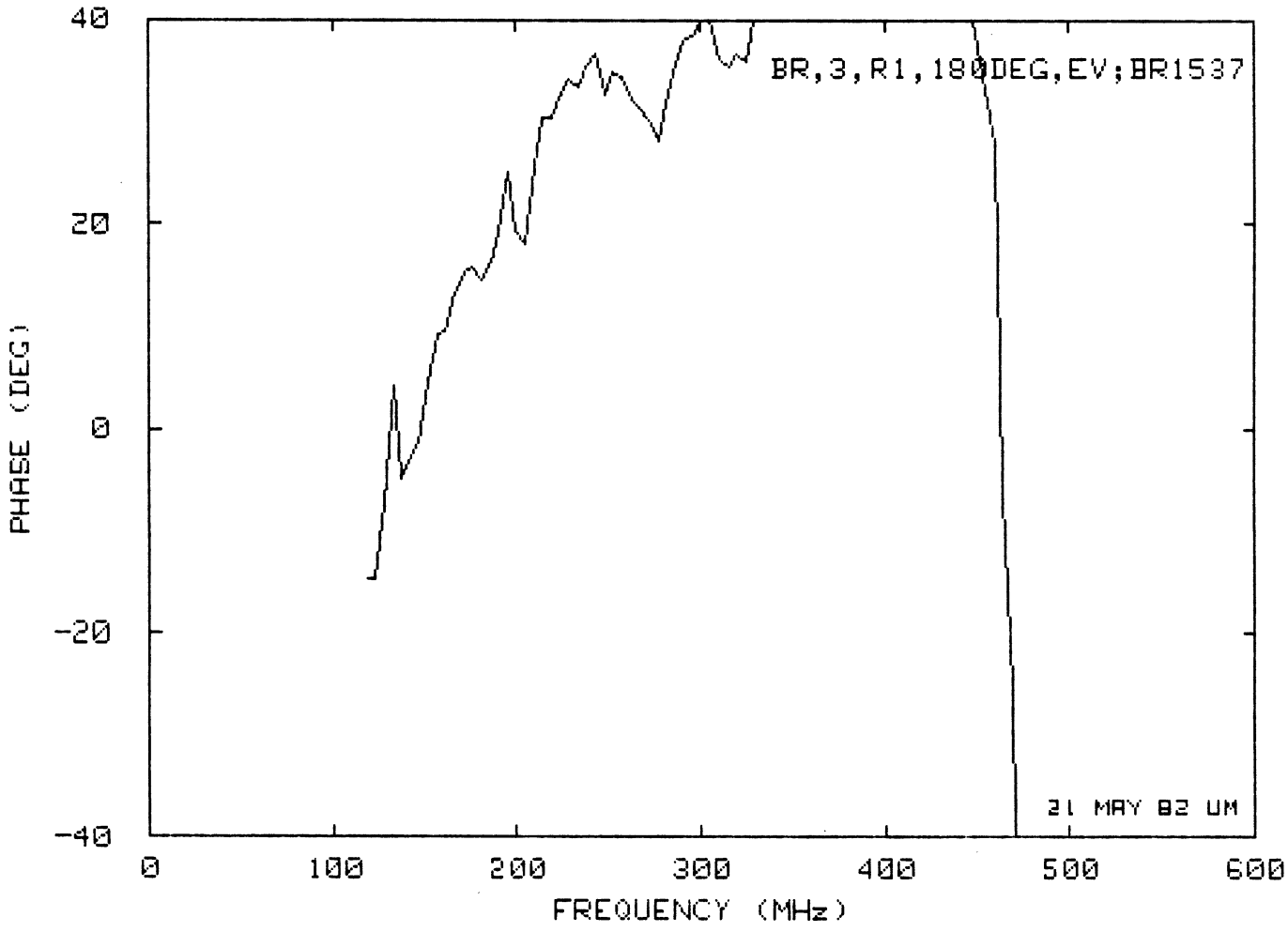
BR,3,R1,180DEG,EV;BR1537
21 MAY 82 UM
PHASE (DEG)
40
20
0
-20
-40
0
100
200
300
400
500
600
FREQUENCY (MHz)

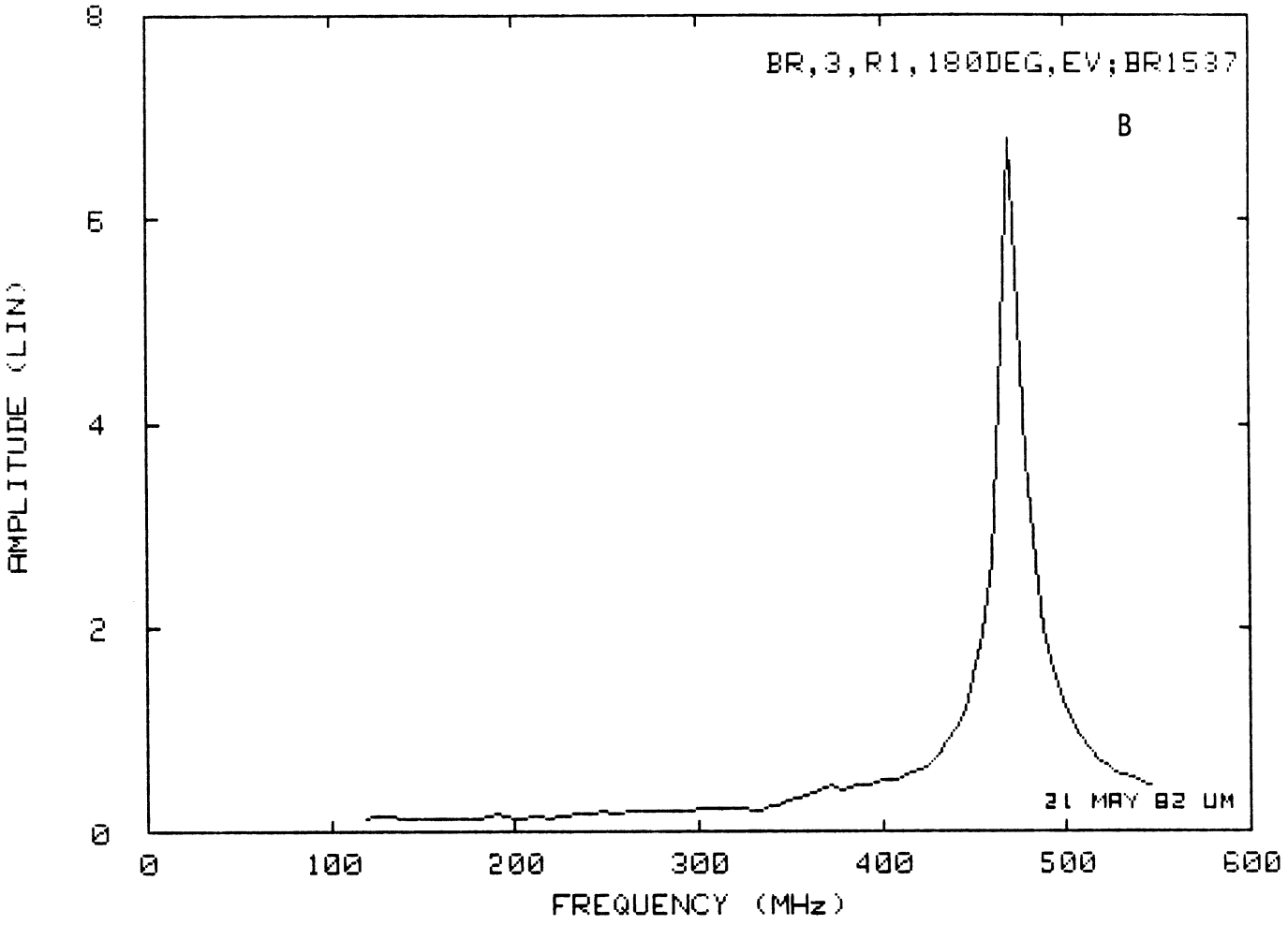
BR,3,R1,180DEG,EV;BR1537
B
21 MAY 82 UM
AMPLITUDE (LIN)
8
6
4
2
0
0
100
200
300
400
500
600
FREQUENCY (MHz)

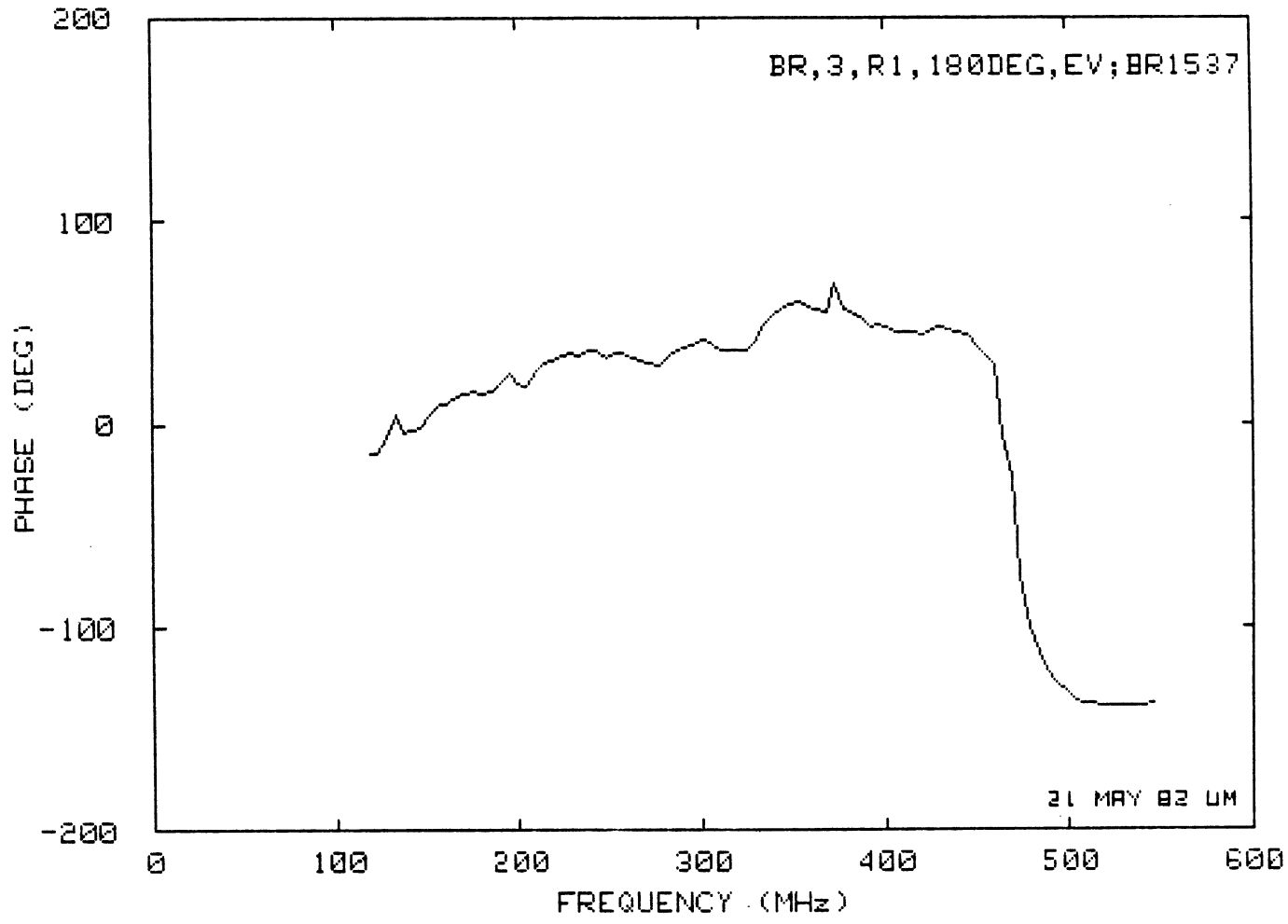
BR,3,R1,180DEG,EV;BR1537
21 MAY 82 UM
PHASE (DEG)
200
100
0
-100
-200
0
100
200
300
400
500
600
FREQUENCY (MHz)

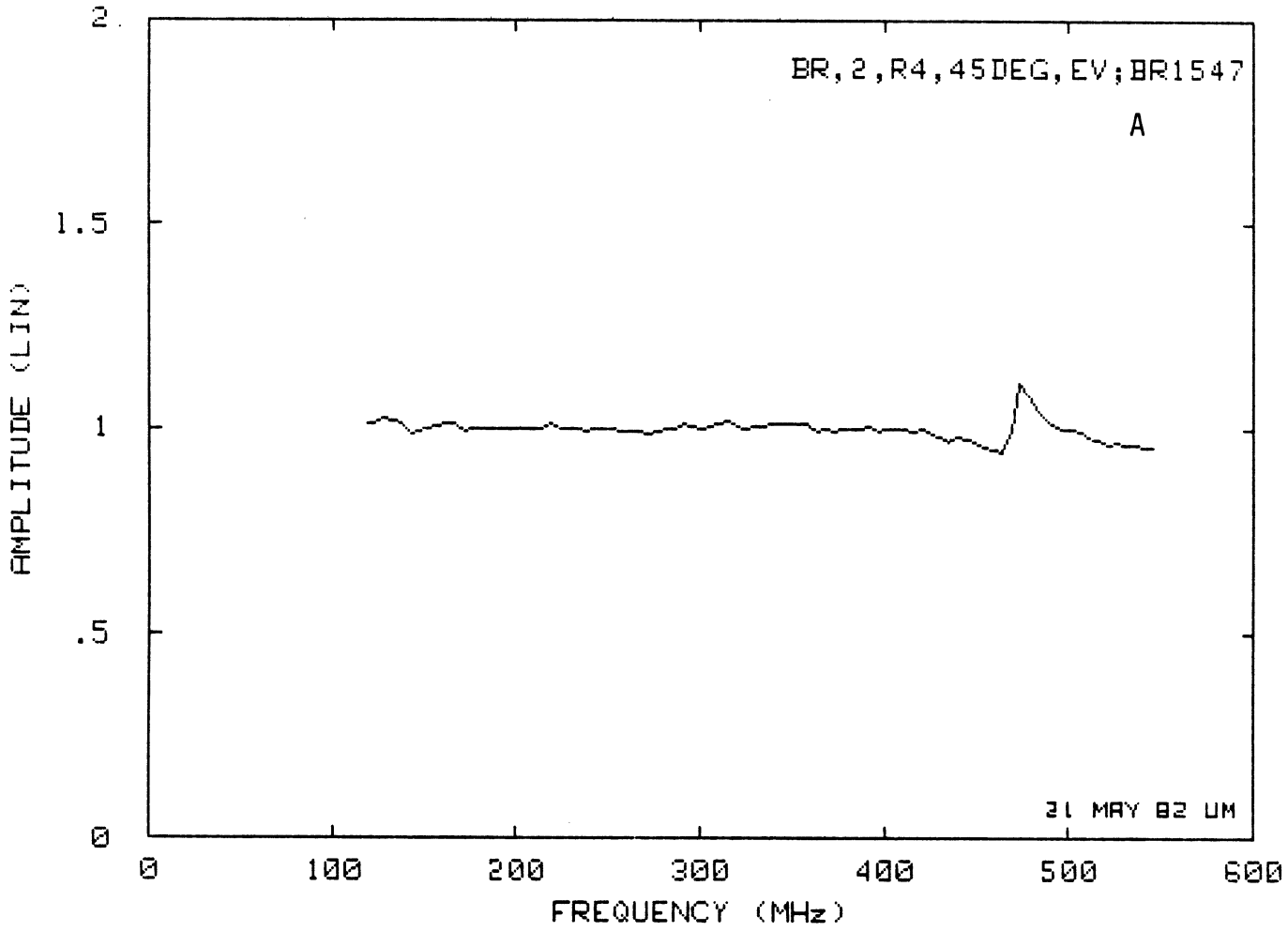
BR,2,R4,45DEG,EV;BR1547
A
21 MAY 82 UM
AMPLITUDE (LIN)
2
1.5
1
.5
0
0
100
200
300
400
500
600
FREQUENCY (MHz)

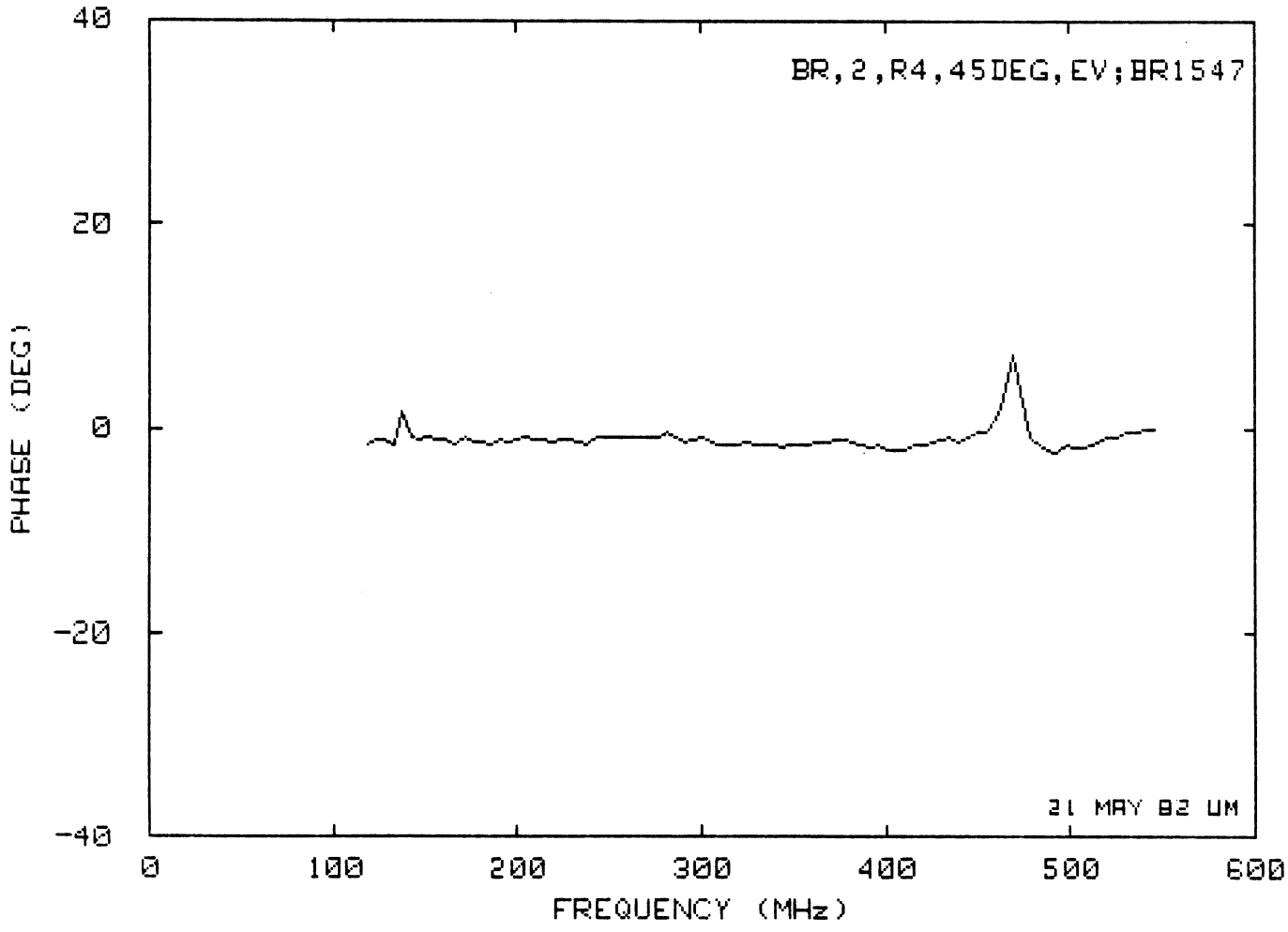
BR,2,R4,45DEG,EV;BR1547
21 MAY 82 UM
PHASE (DEG)
40
20
0
-20
-40
0
100
200
300
400
500
600
FREQUENCY (MHz)

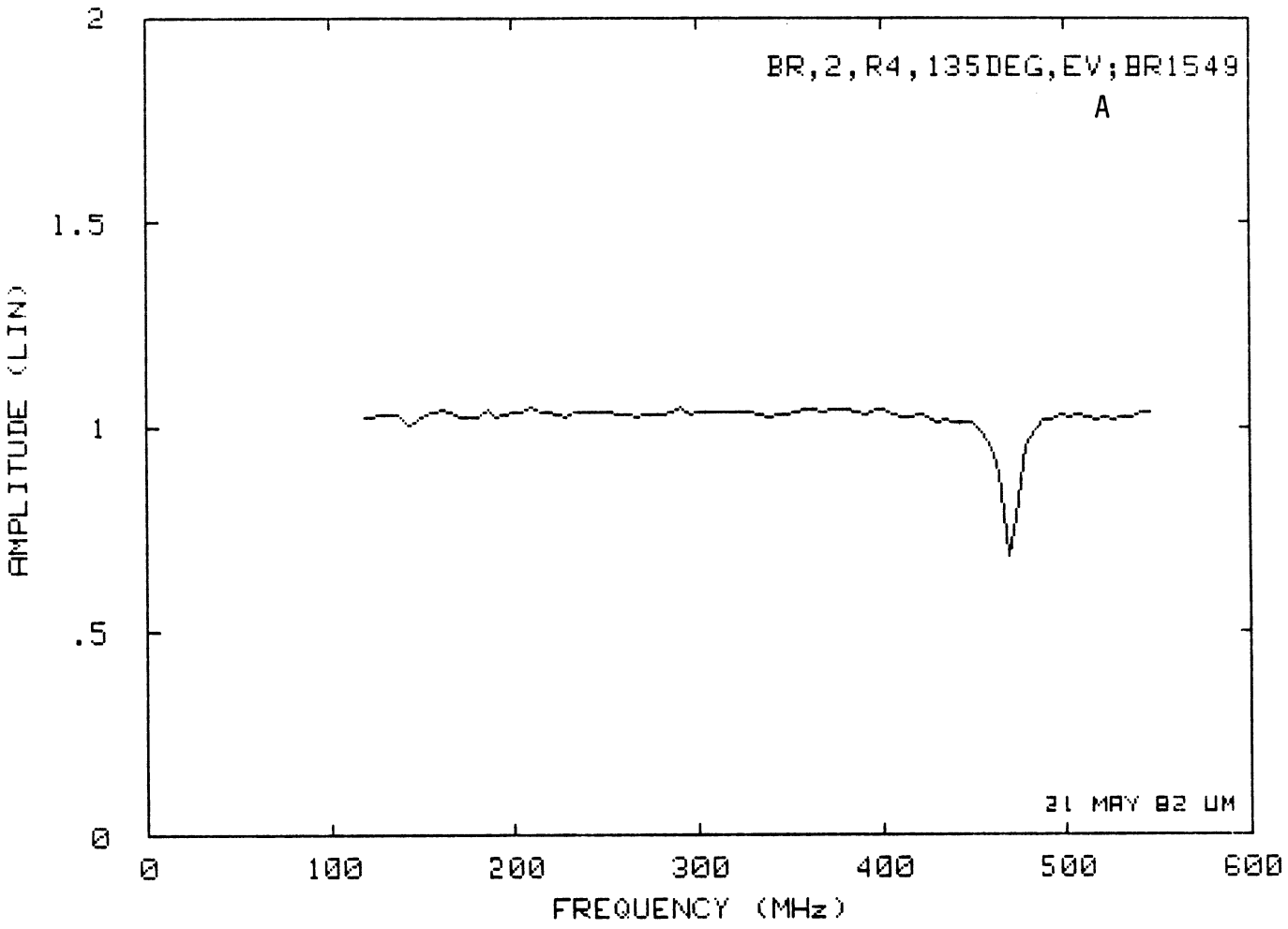
BR,2,R4,135DEG,EV;BR1549
A
21 MAY 82 UM
AMPLITUDE (LIN)
2
1.5
1
.5
0
0
100
200
300
400
500
600
FREQUENCY (MHz)

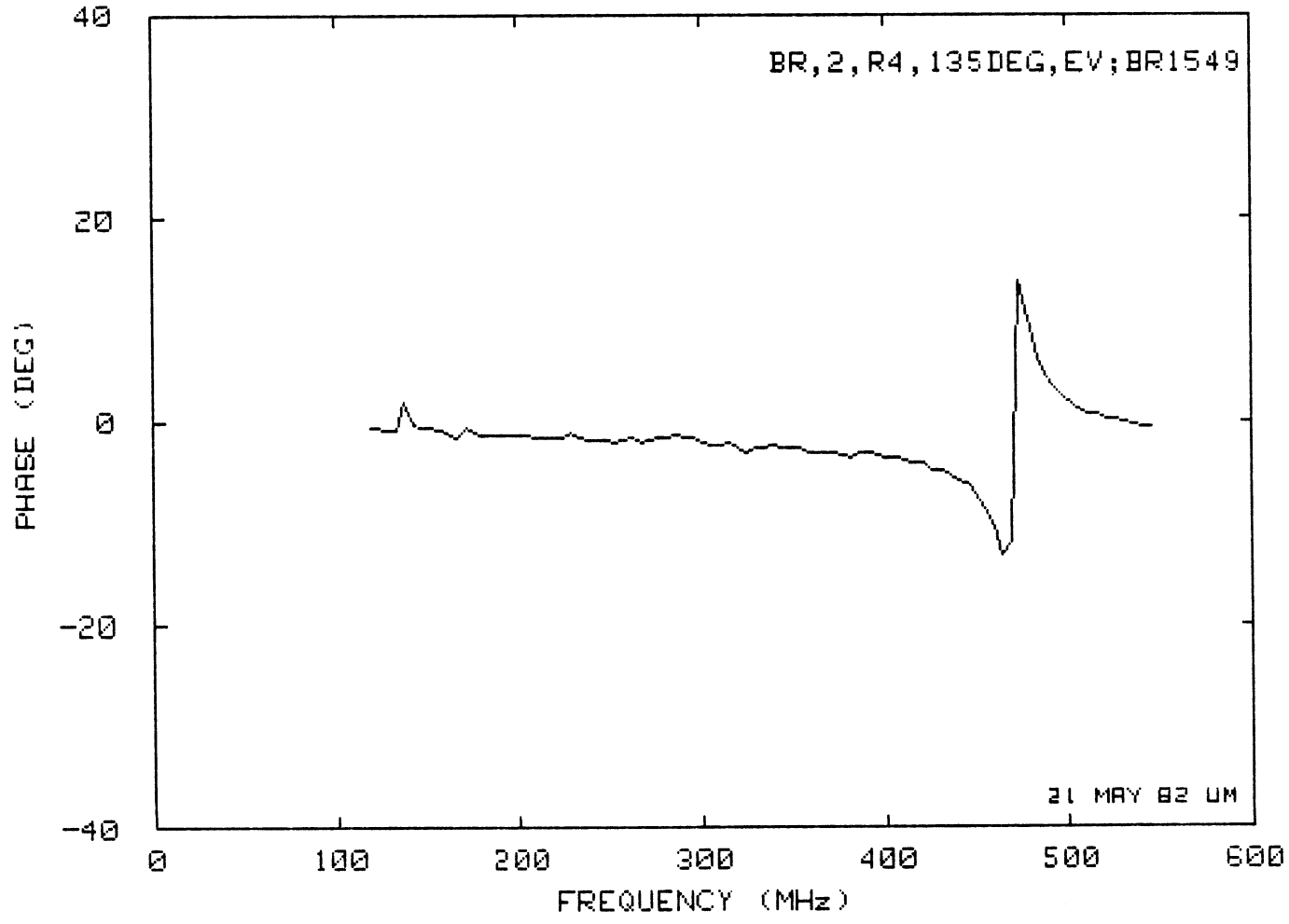
BR,2,R4,135DEG,EV;BR1549
21 MAY 82 UM
PHASE (DEG)
40
20
0
-20
-40
0
100
200
300
400
500
600
FREQUENCY (MHz)

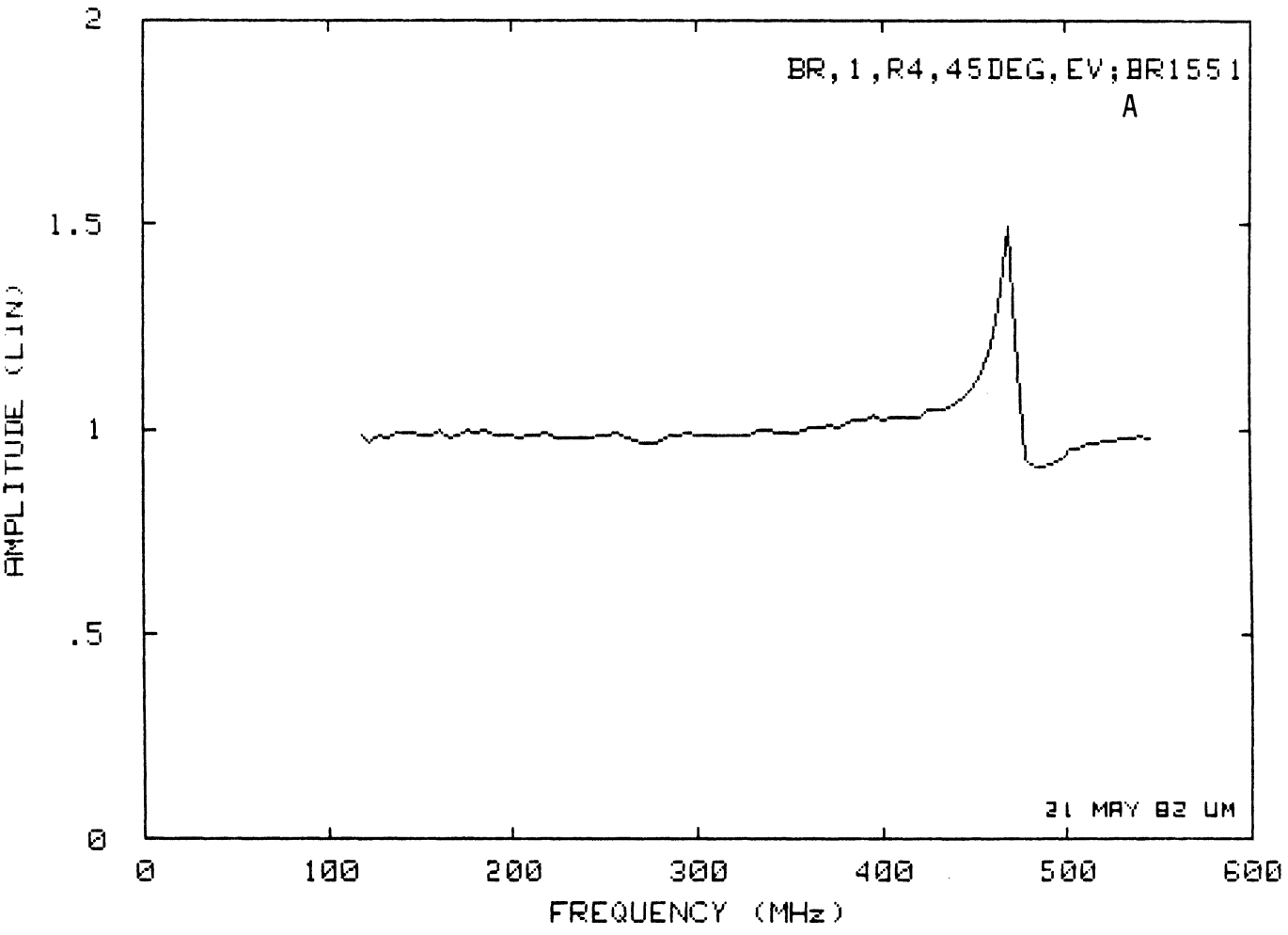
BR,1,R4,45DEG,EV;BR1551
A
21 MAY 82 UM
AMPLITUDE (LIN)
2
1.5
1
.5
0
0
100
200
300
400
500
600
FREQUENCY (MHz)

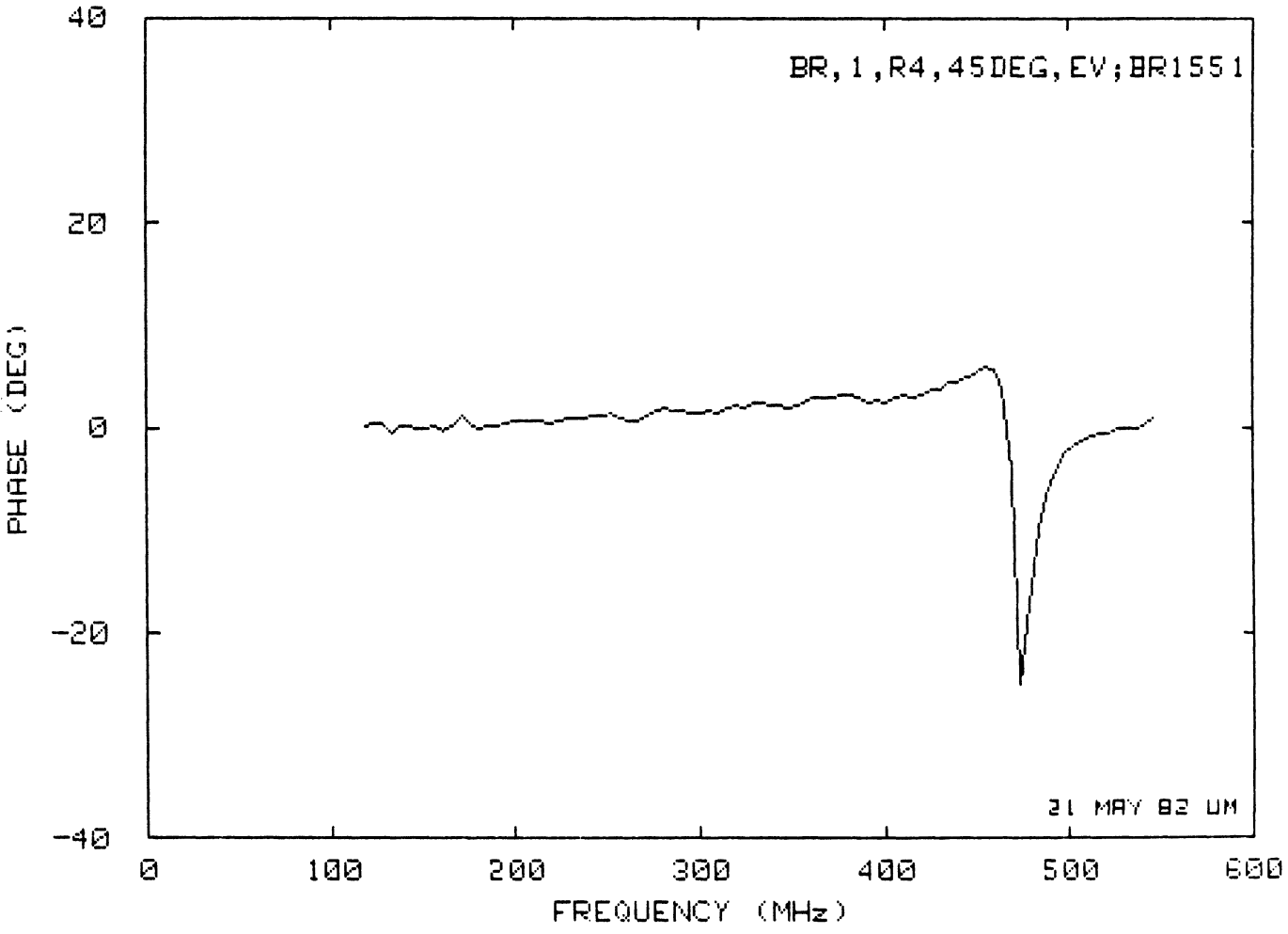
BR,1,R4,45DEG,EV;BR1551
21 MAY 82 UM
PHASE (DEG)
40
20
0
-20
-40
0
100
200
300
400
500
600
FREQUENCY (MHz)

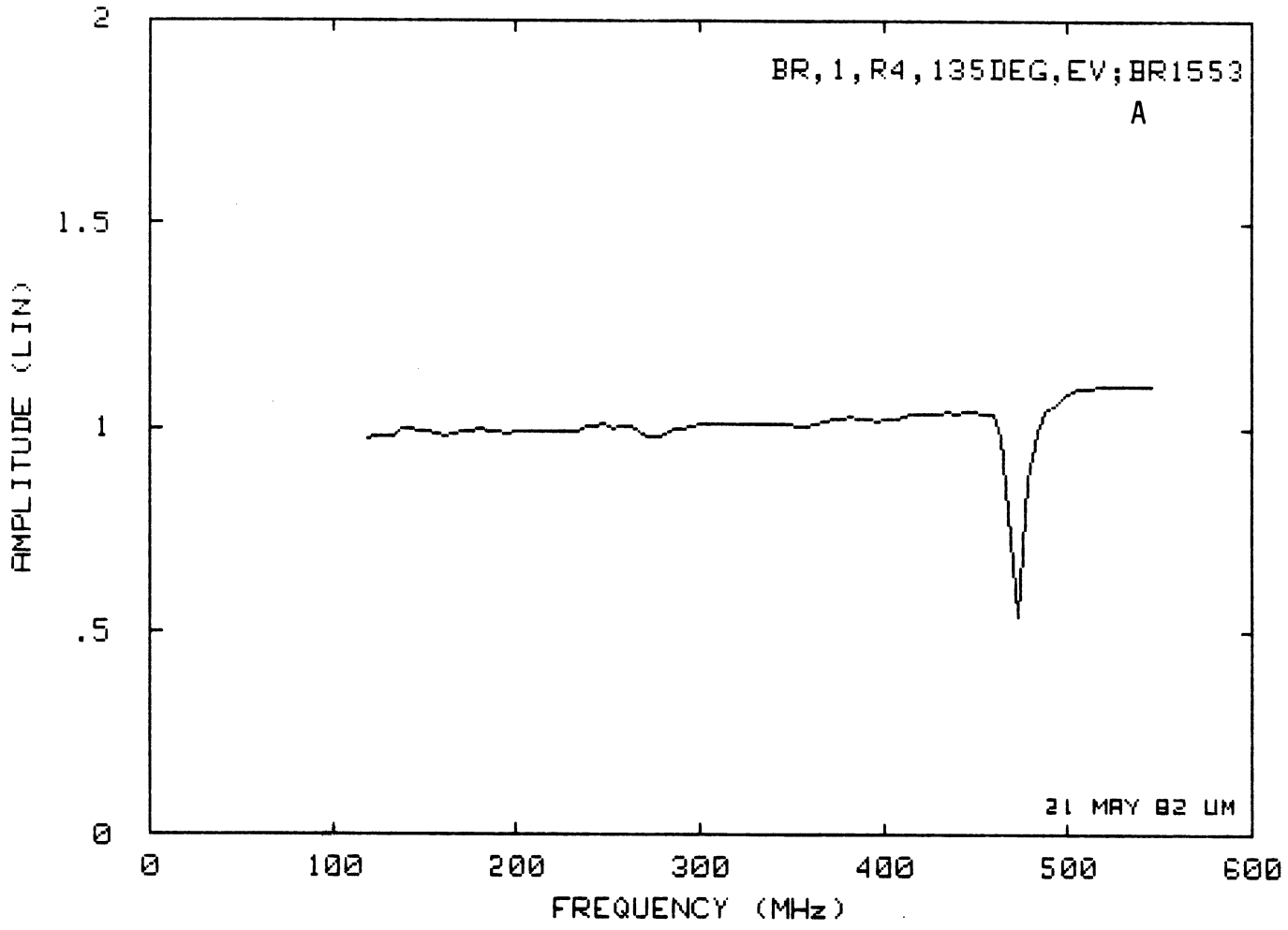
BR,1,R4,135DEG,EV;BR1553
A
21 MAY 82 UM
AMPLITUDE (LIN)
2
1.5
1
.5
0
0
100
200
300
400
500
600
FREQUENCY (MHz)

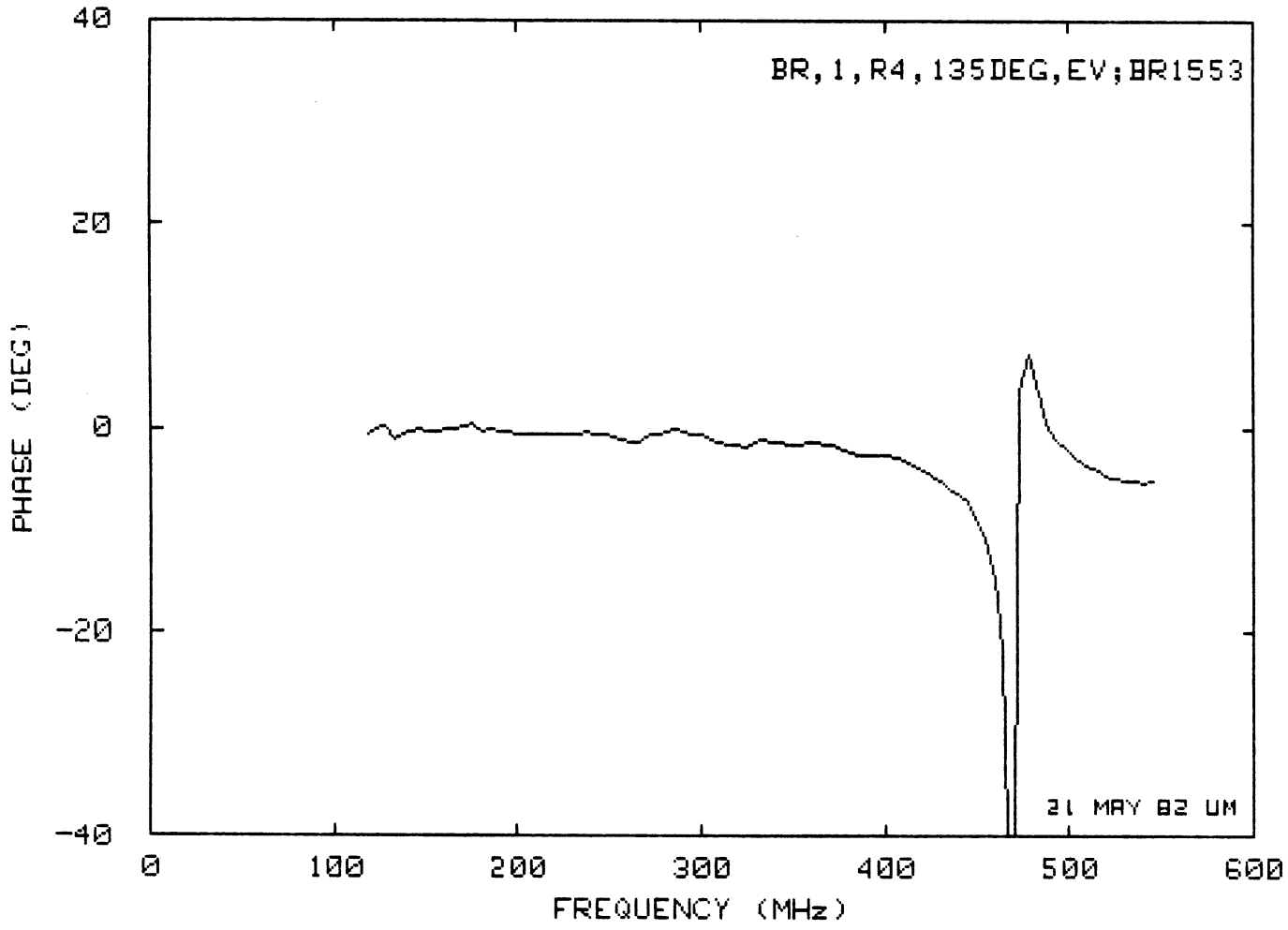
BR,1,R4,135DEG,EV;BR1553
21 MAY 82 UM
PHASE (DEG)
40
20
0
-20
-40
0
100
200
300
400
500
600
FREQUENCY (MHz)

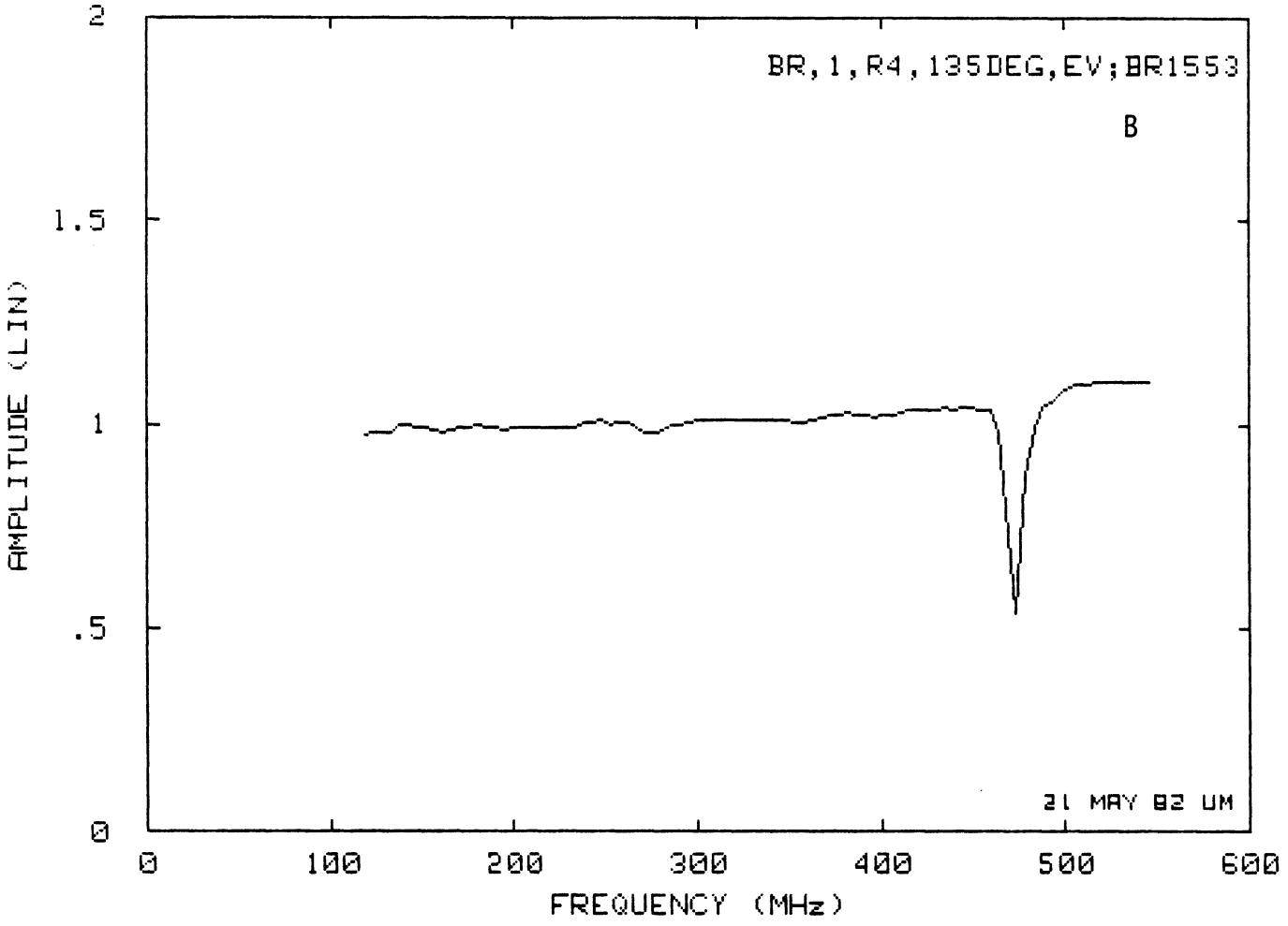
BR,1,R4,135DEG,EV;BR1553
B
21 MAY 82 UM
AMPLITUDE (LIN)
2
1.5
1
.5
0
0
100
200
300
400
500
600
FREQUENCY (MHz)

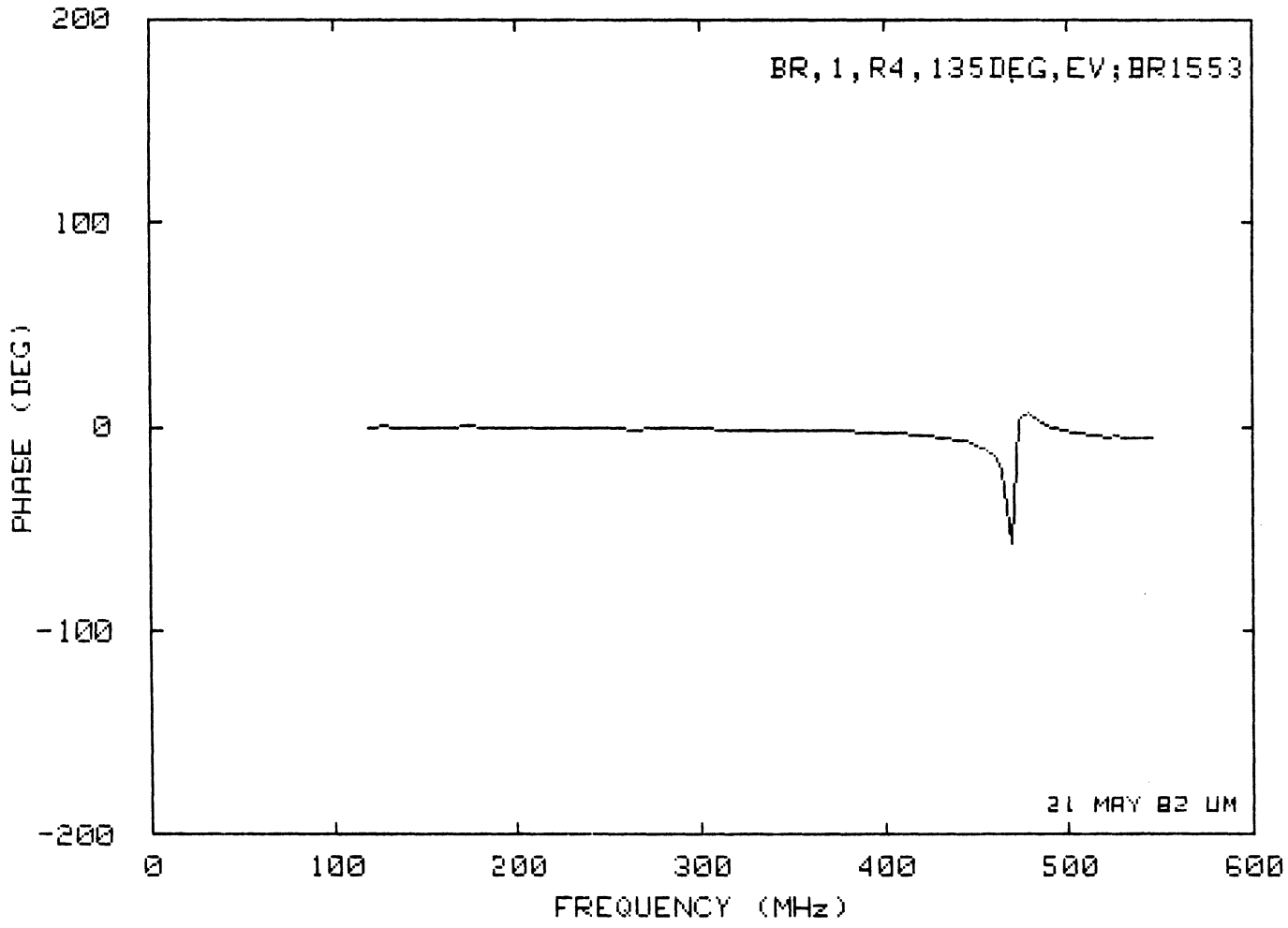
BR,1,R4,135DEG,EV;BR1553
21 MAY 82 UM
PHASE (DEG)
200
100
0
-100
-200
0
100
200
300
400
500
600
FREQUENCY (MHz)

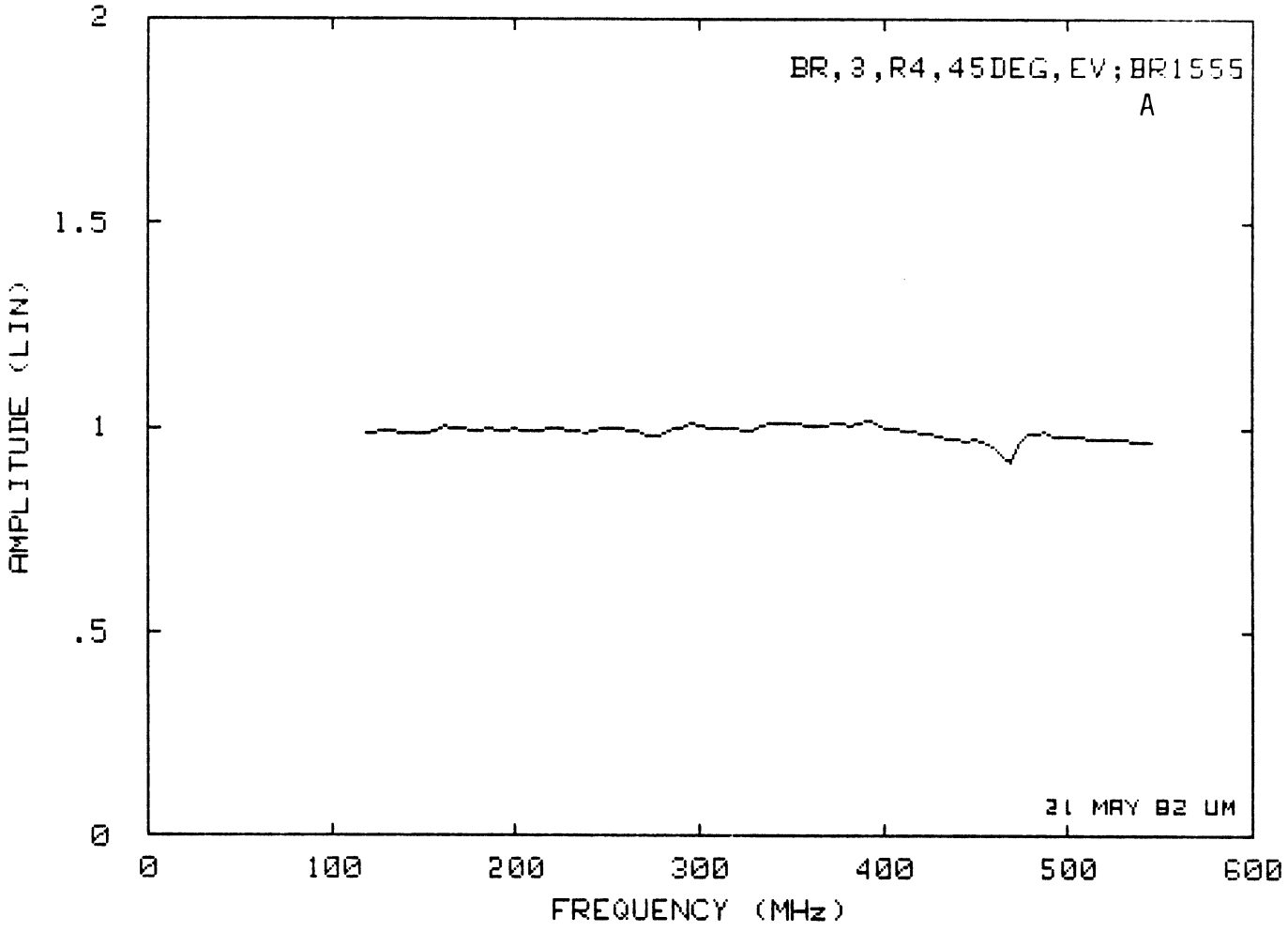
BR,3,R4,45DEG,EV;BR1555
A
21 MAY 82 UM
AMPLITUDE (LIN)
2
1.5
1
.5
0
0
100
200
300
400
500
600
FREQUENCY (MHz)

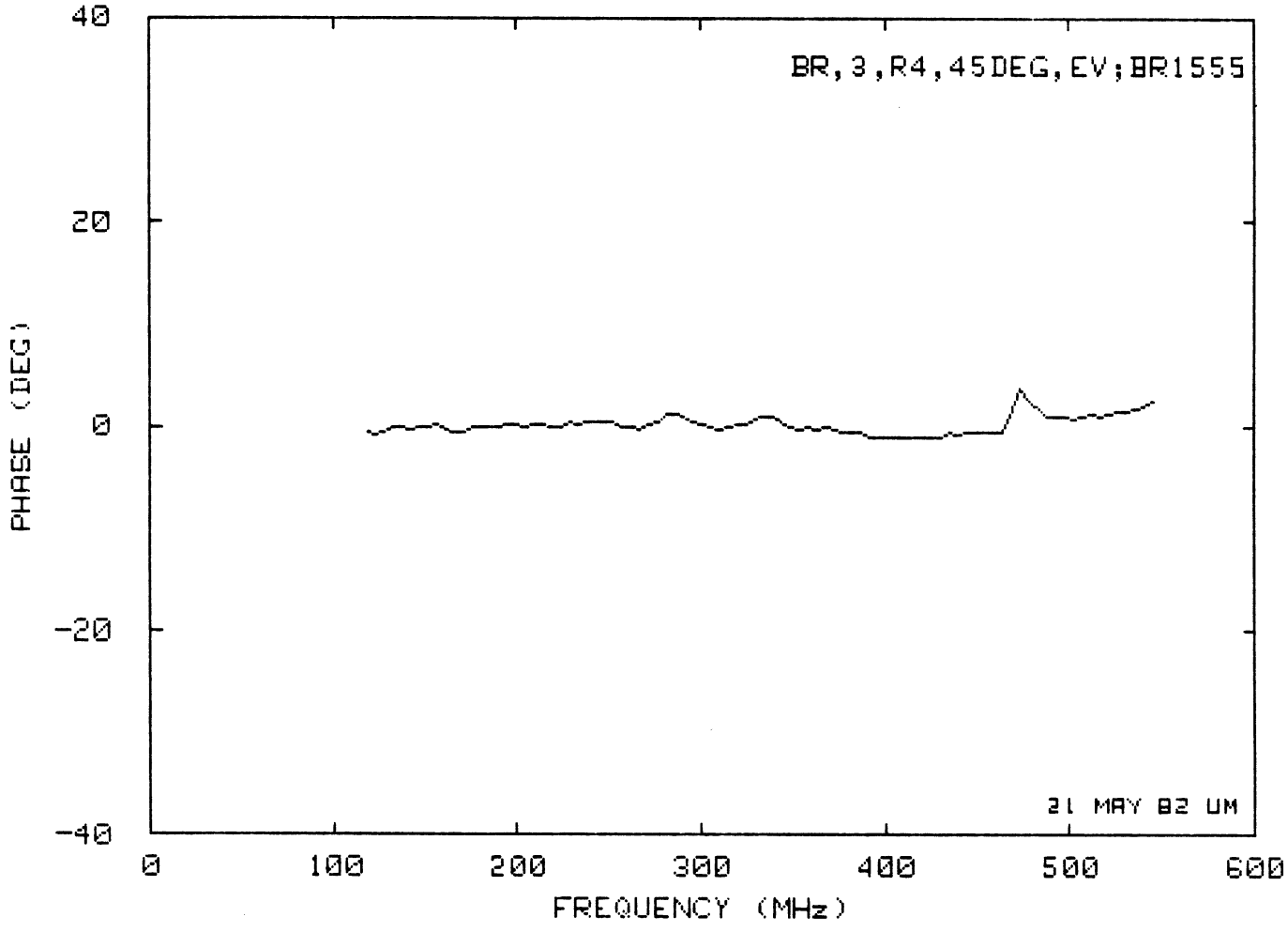
BR,3,R4,45DEG,EV;BR1555
21 MAY 82 UM
PHASE (DEG)
40
20
0
-20
-40
0
100
200
300
400
500
600
FREQUENCY (MHz)

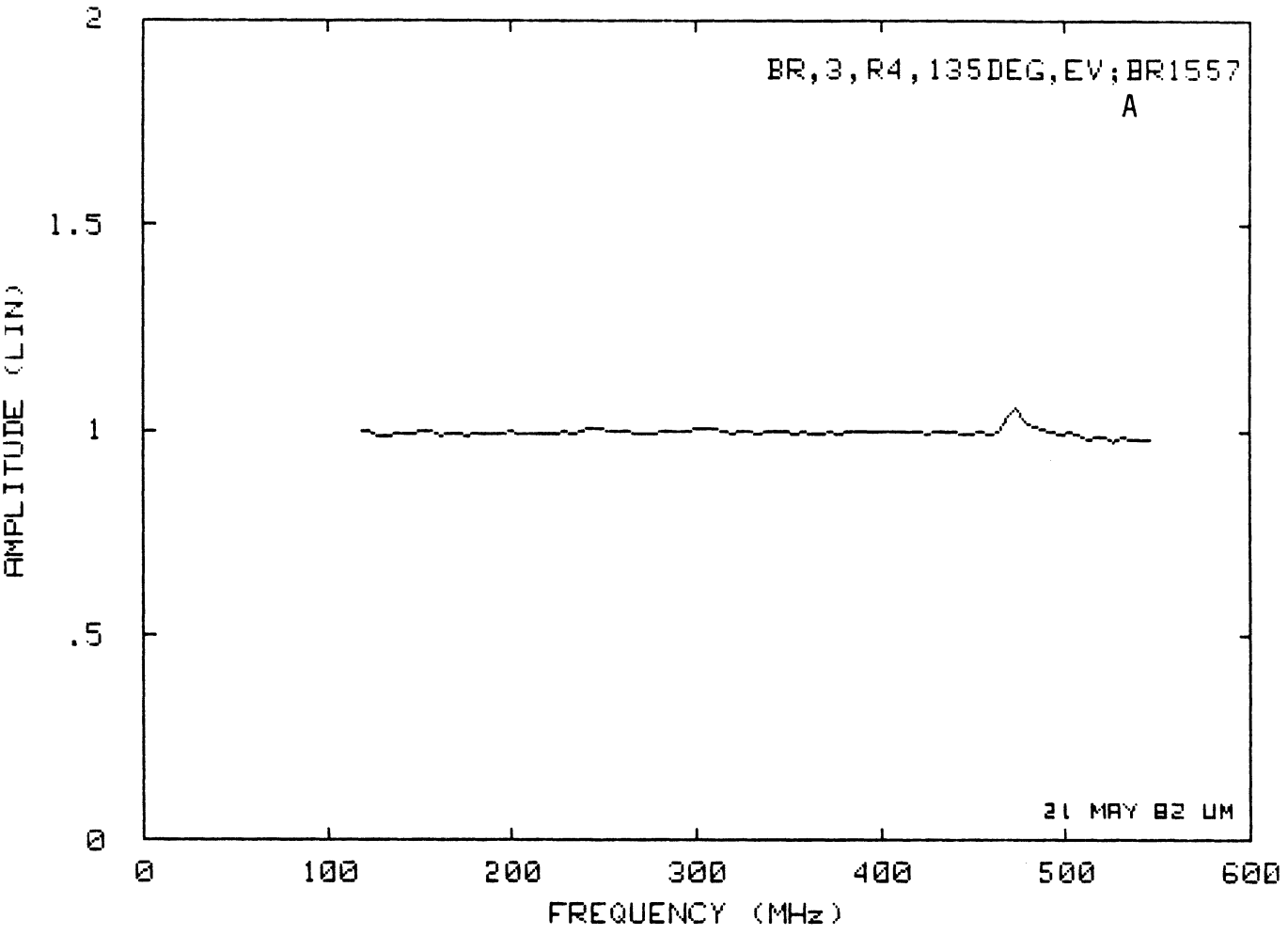
BR,3,R4,135DEG,EV;BR1557
A
21 MAY 82 UM
AMPLITUDE (LIN)
2
1.5
1
.5
0
0
100
200
300
400
500
600
FREQUENCY (MHz)

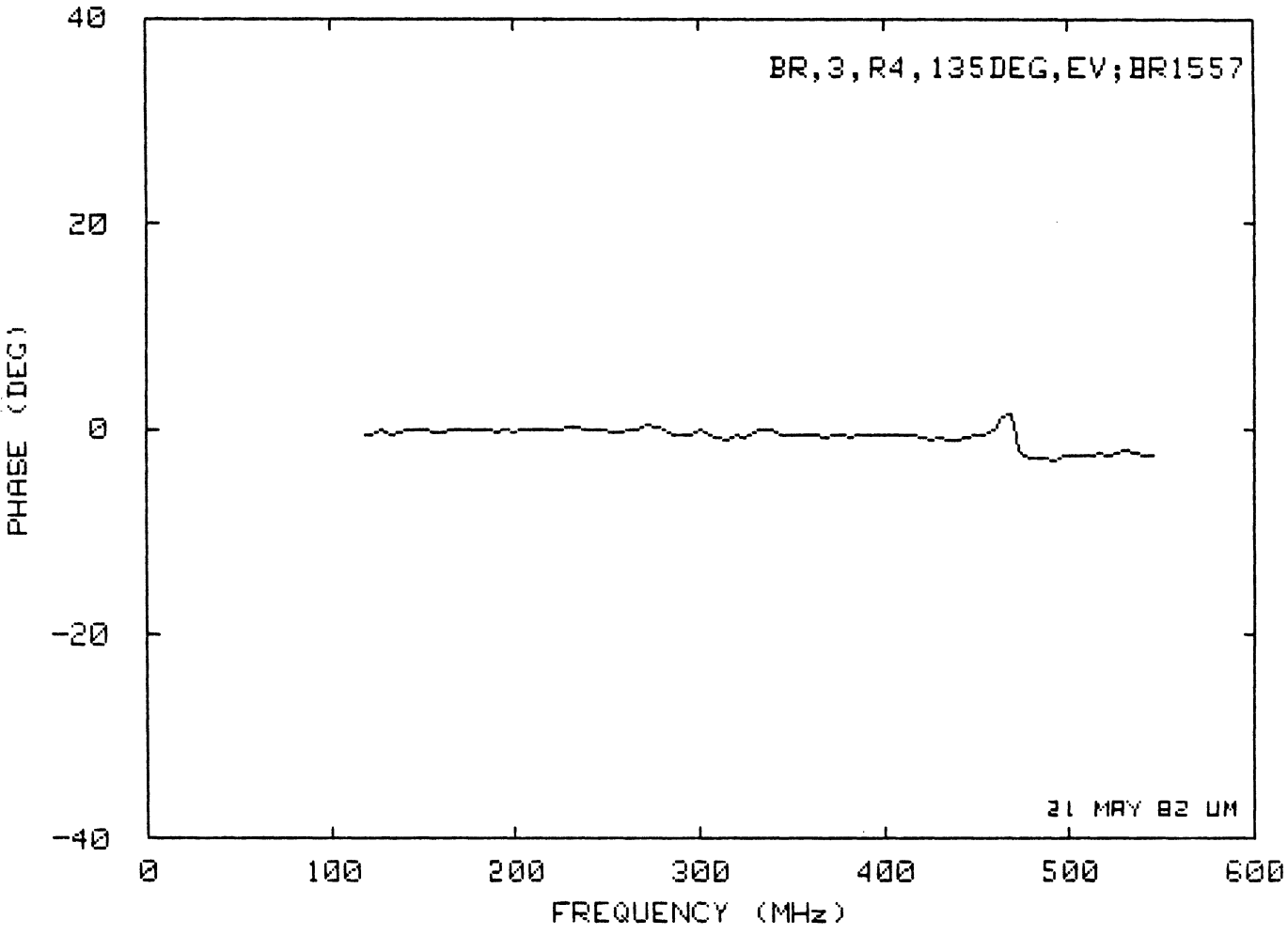
BR,3,R4,135DEG,EV;BR1557
21 MAY 82 UM
PHASE (DEG)
40
20
0
-20
-40
0
100
200
300
400
500
600
FREQUENCY (MHz)

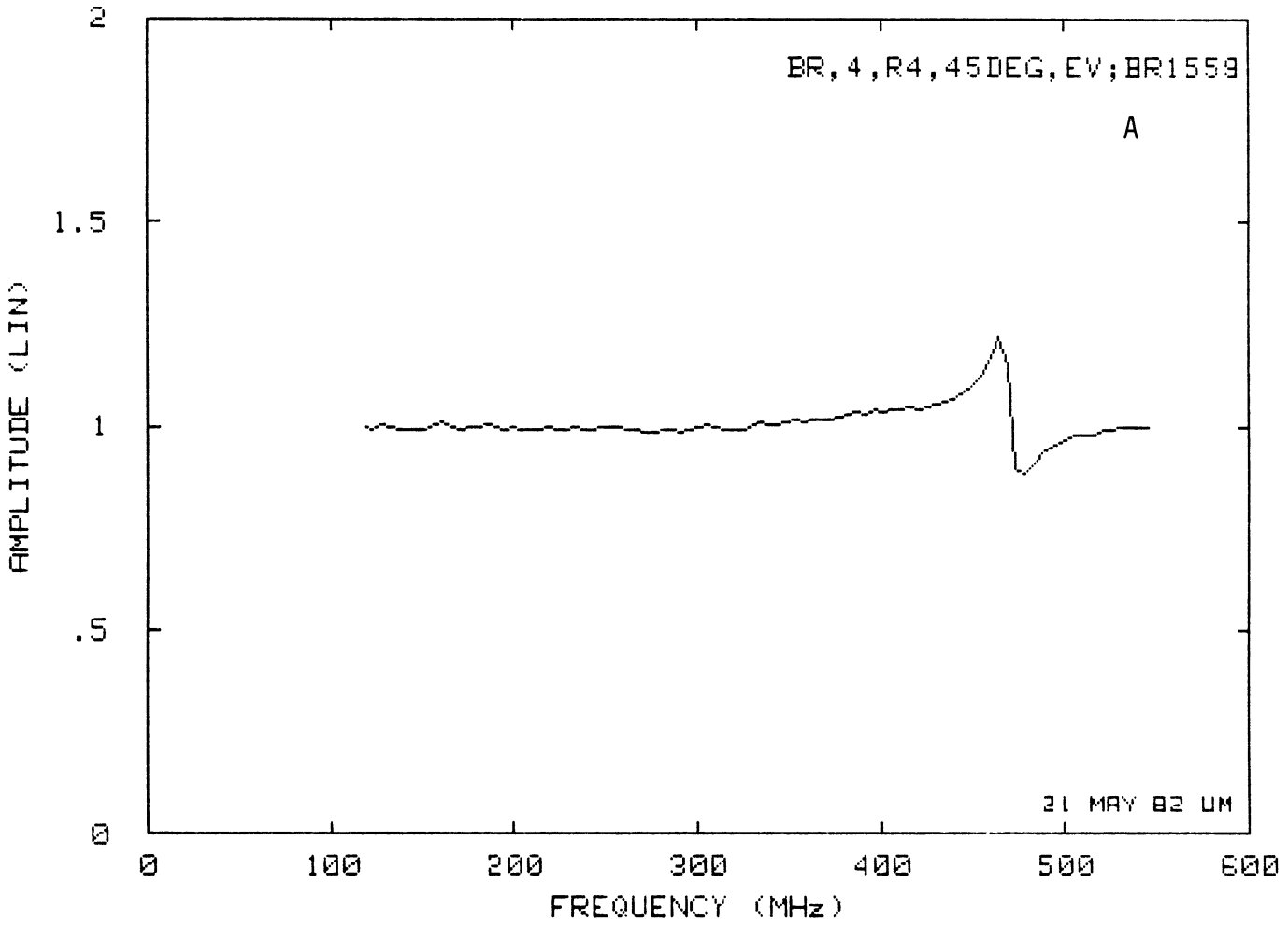
BR,4,R4,45DEG,EV;BR1559
A
21 MAY 82 UM
AMPLITUDE (LIN)
2
1.5
1
.5
0
0
100
200
300
400
500
600
FREQUENCY (MHz)

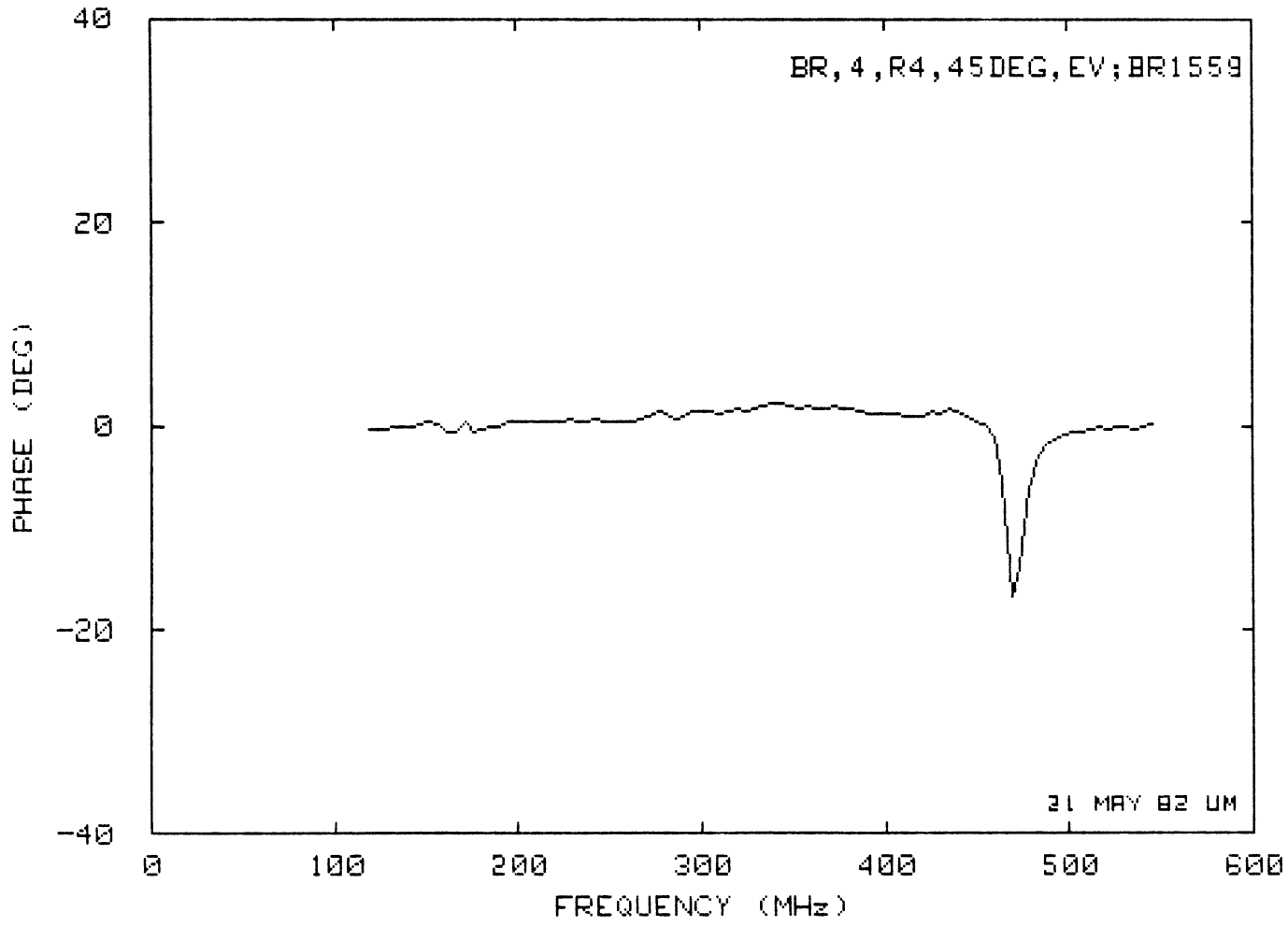
BR,4,R4,45DEG,EV;BR1559
21 MAY 82 UM
PHASE (DEG)
40
20
0
-20
-40
0
100
200
300
400
500
600
FREQUENCY (MHz)

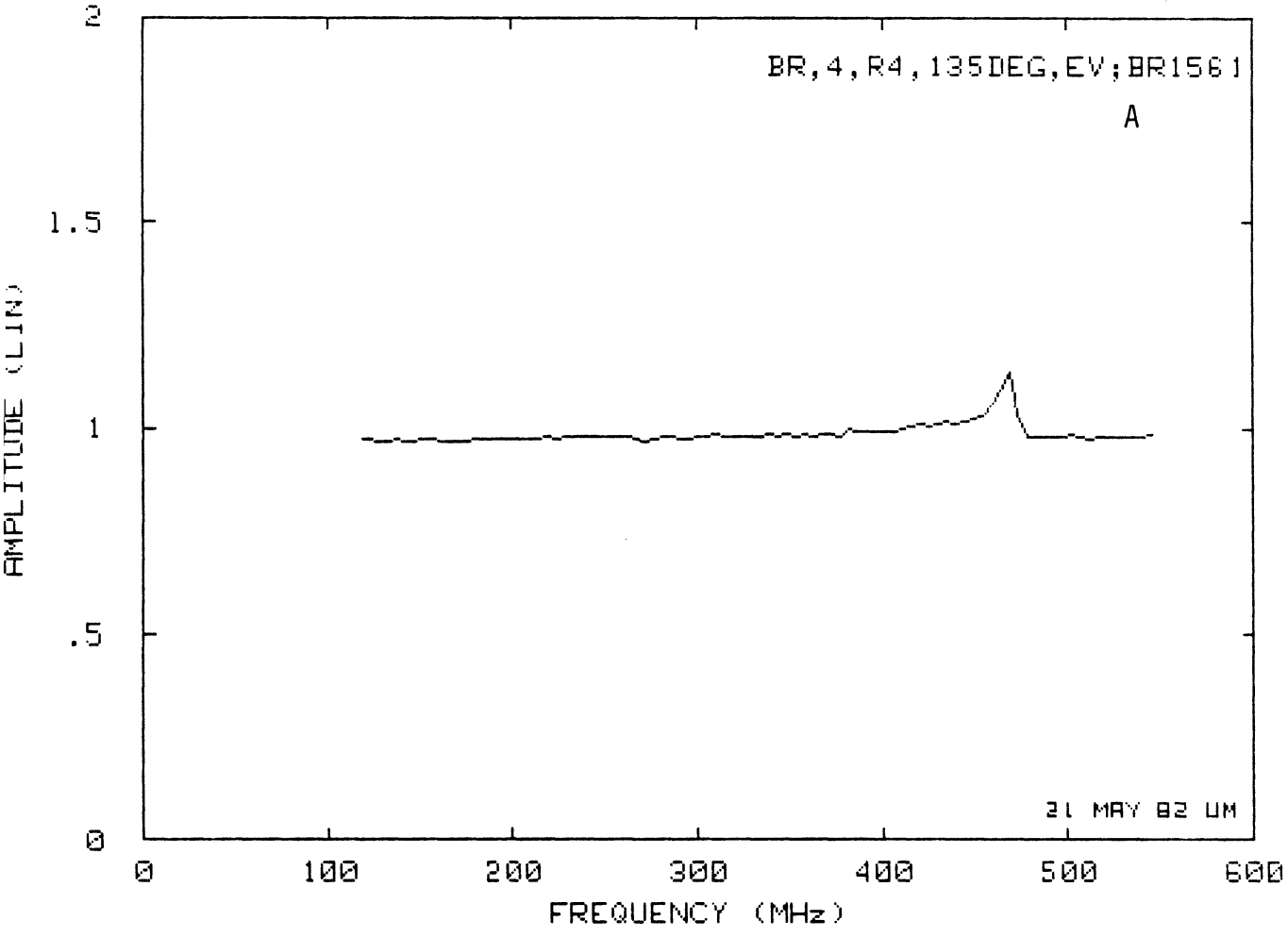
BR,4,R4,135DEG,EV;BR1561
A
21 MAY 82 UM
AMPLITUDE (LIN)
2
1.5
1
.5
0
0
100
200
300
400
500
600
FREQUENCY (MHz)

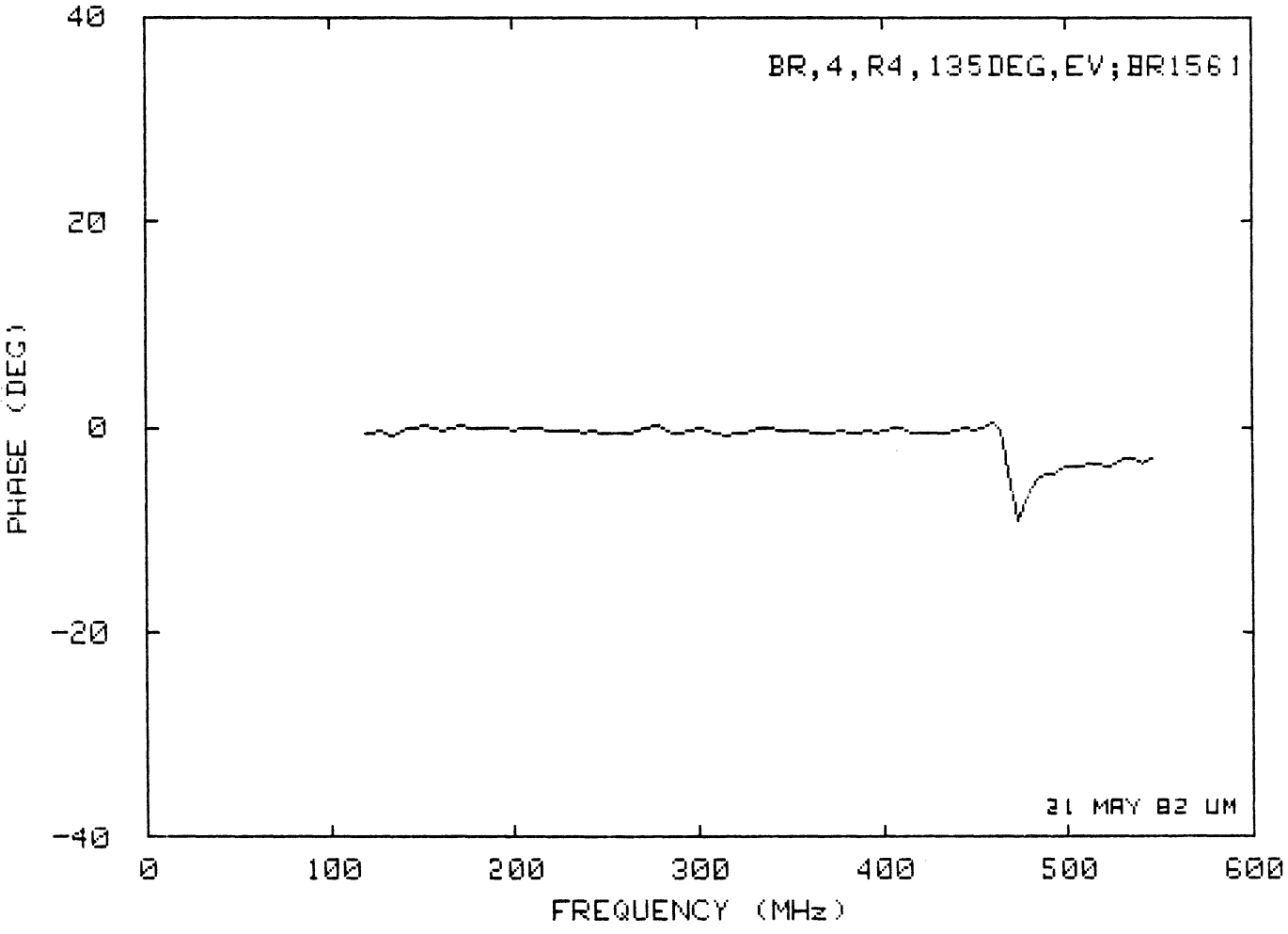
BR,4,R4,135DEG,EV;BR1561
21 MAY 82 UM
PHASE (DEG)
40
20
0
-20
-40
0
100
200
300
400
500
600
FREQUENCY (MHz)

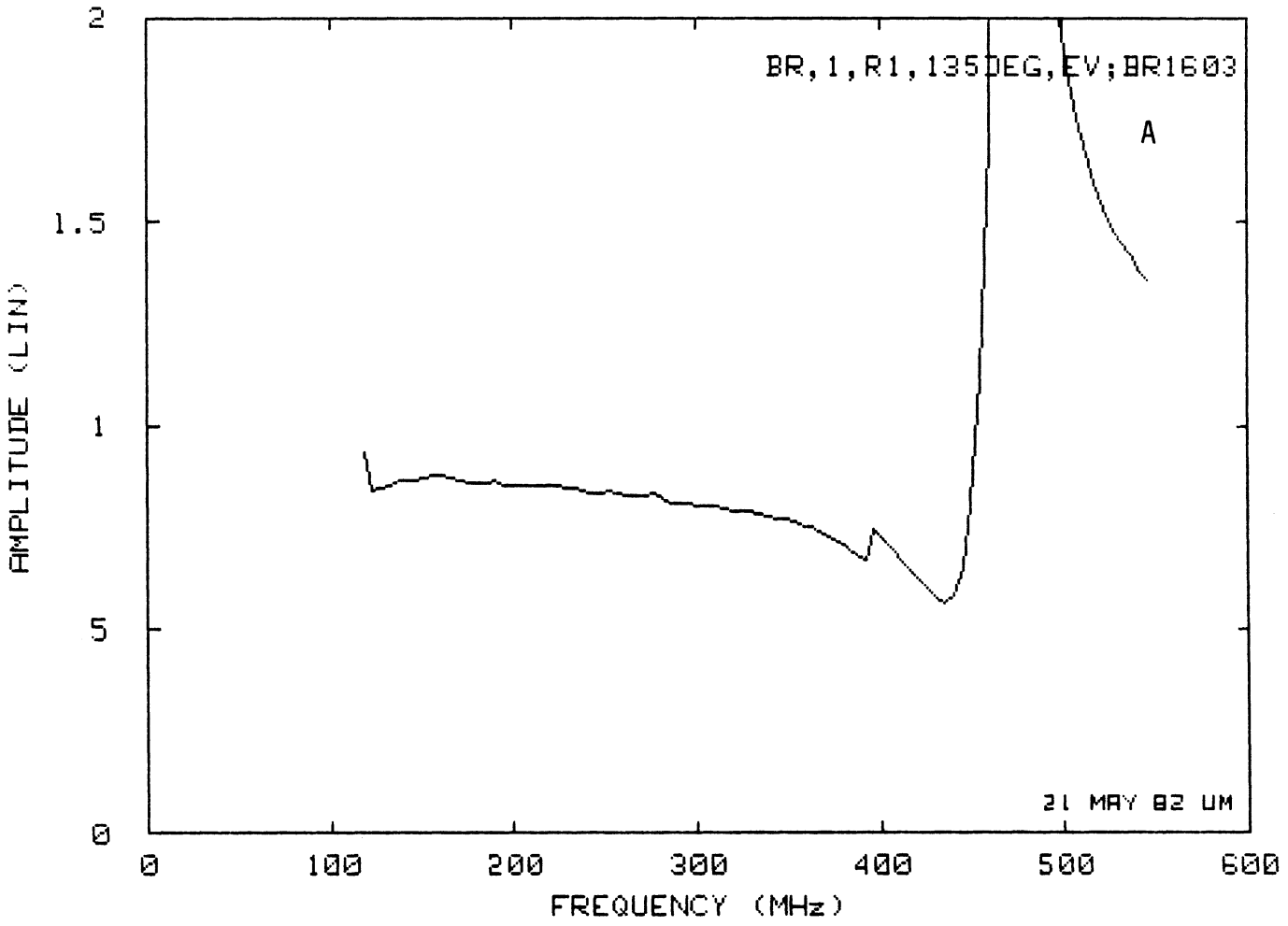
BR,1,R1,135DEG,EV;BR1603
A
21 MAY 82 UM
AMPLITUDE (LIN)
2
1.5
1
5
0
0
100
200
300
400
500
600
FREQUENCY (MHz)

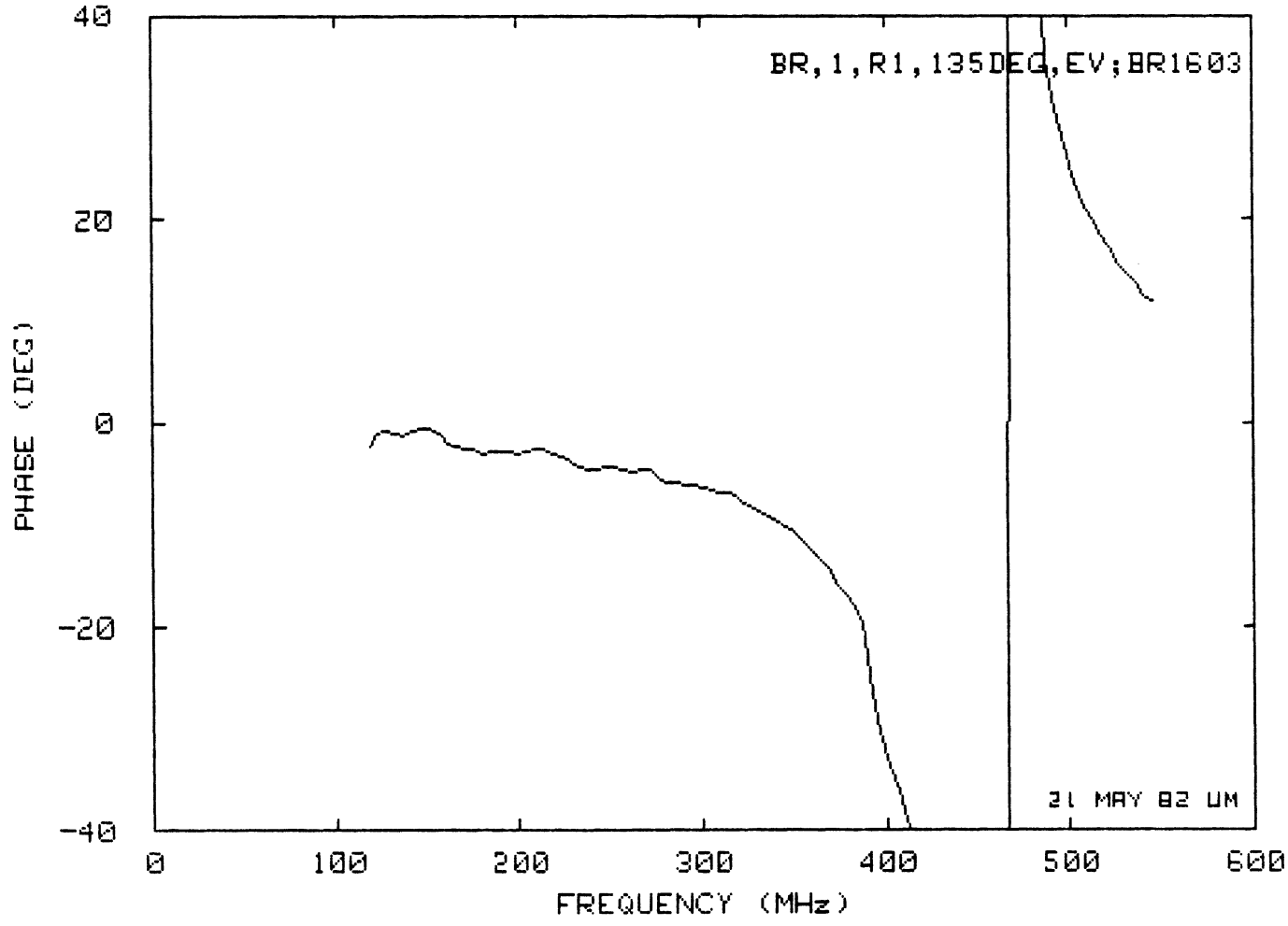
BR,1,R1,135DEG,EV;BR1603
21 MAY 82 UM
PHASE (DEG)
40
20
0
-20
-40
0
100
200
300
400
500
600
FREQUENCY (MHz)

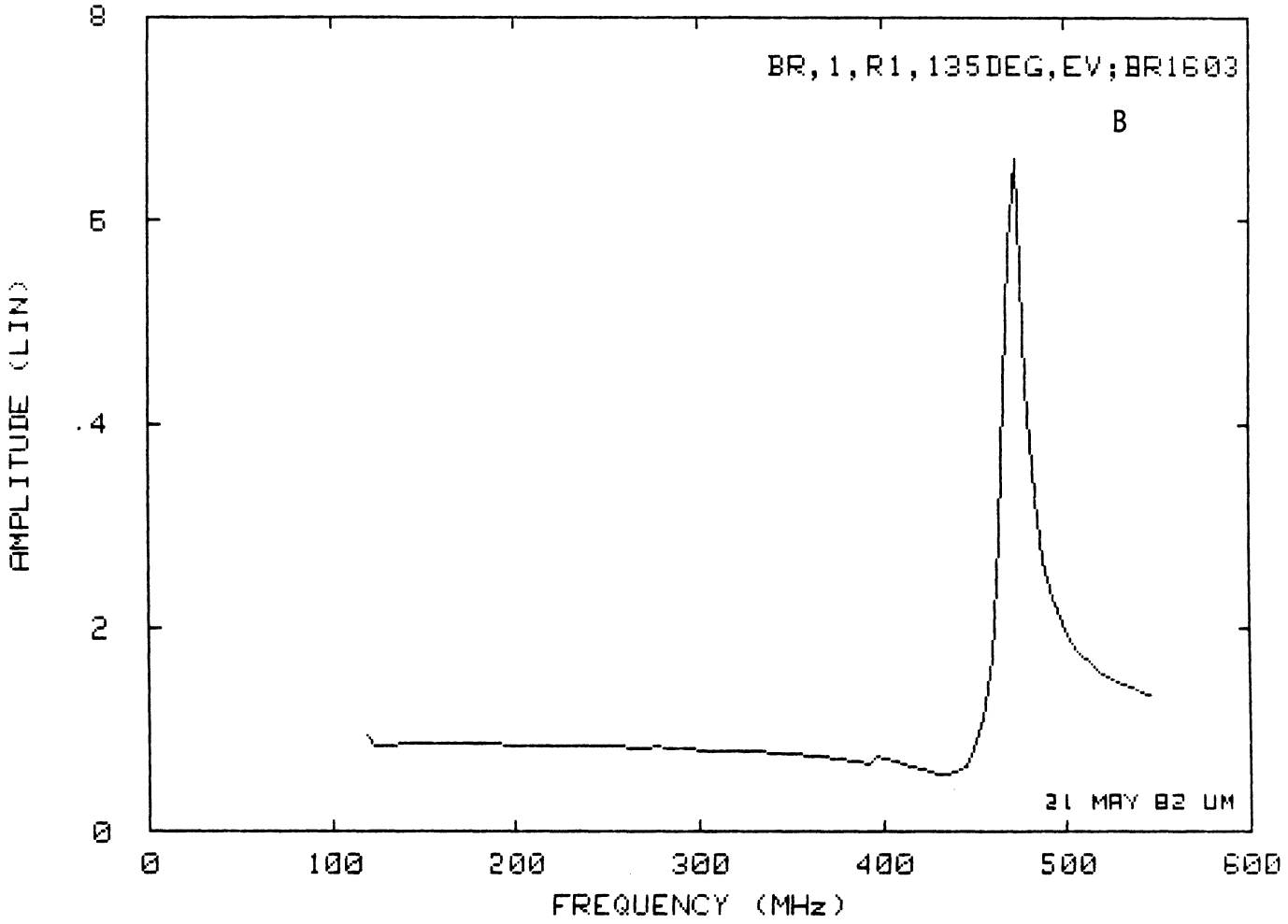
BR,1,R1,135DEG,EV;BR1603
B
21 MAY 82 UM
AMPLITUDE (LIN)
8
6
.4
2
0
0
100
200
300
400
500
600
FREQUENCY (MHz)

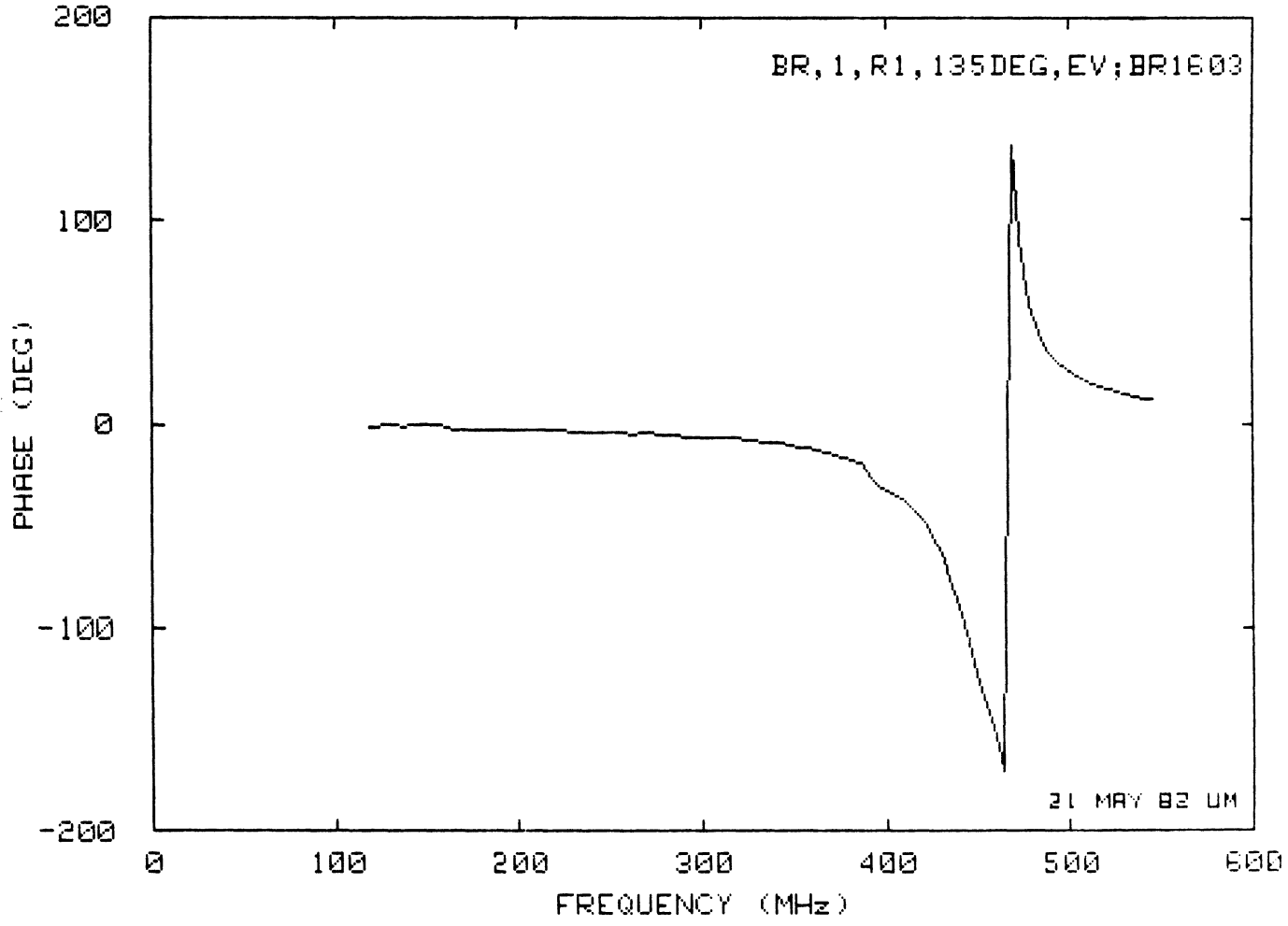
BR,1,R1,135DEG,EV;BR1603
21 MAY 82 UM
PHASE (DEG)
200
100
0
-100
-200
0
100
200
300
400
500
600
FREQUENCY (MHz)

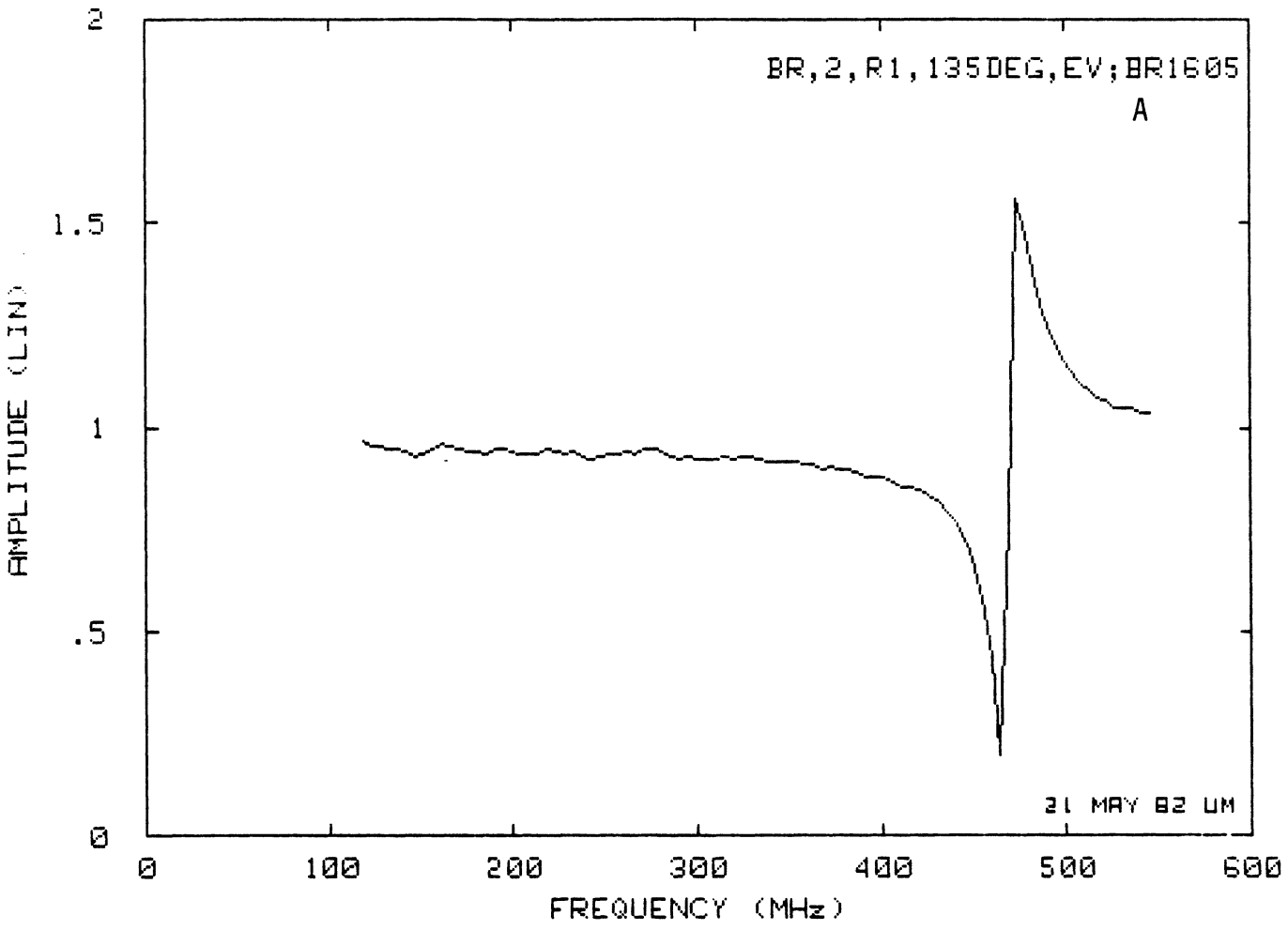
BR,2,R1,135DEG,EV;BR1605
A
21 MAY 82 UM
AMPLITUDE (LIN)
2
1.5
1
.5
0
0
100
200
300
400
500
600
FREQUENCY (MHz)

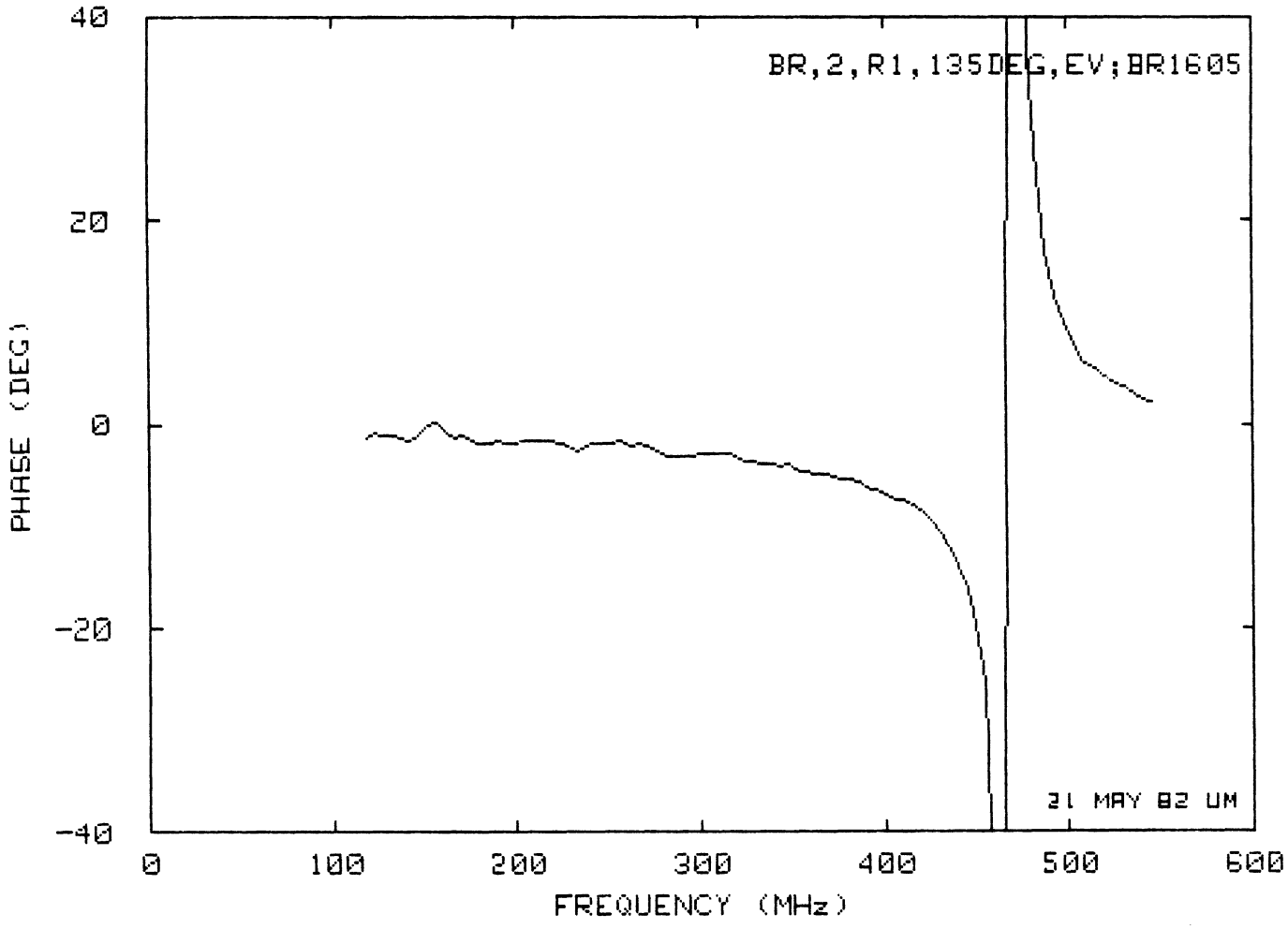
BR,2,R1,135DEG,EV;BR1605
21 MAY 82 UM
PHASE (DEG)
40
20
0
-20
-40
0
100
200
300
400
500
600
FREQUENCY (MHz)

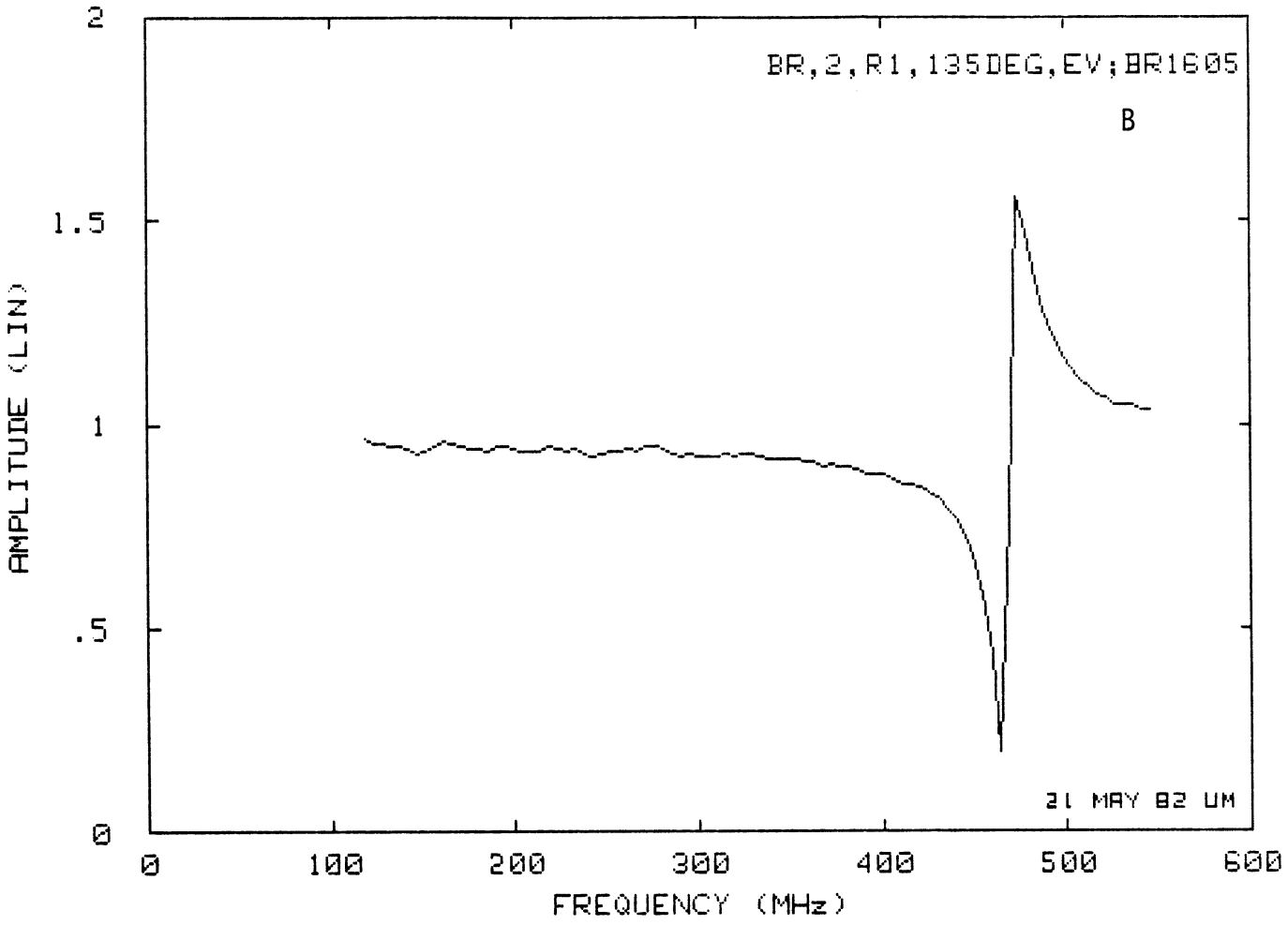
BR,2,R1,135DEG,EV;BR1605
B
21 MAY 82 UM
AMPLITUDE (LIN)
2
1.5
1
.5
0
0
100
200
300
400
500
600
FREQUENCY (MHz)

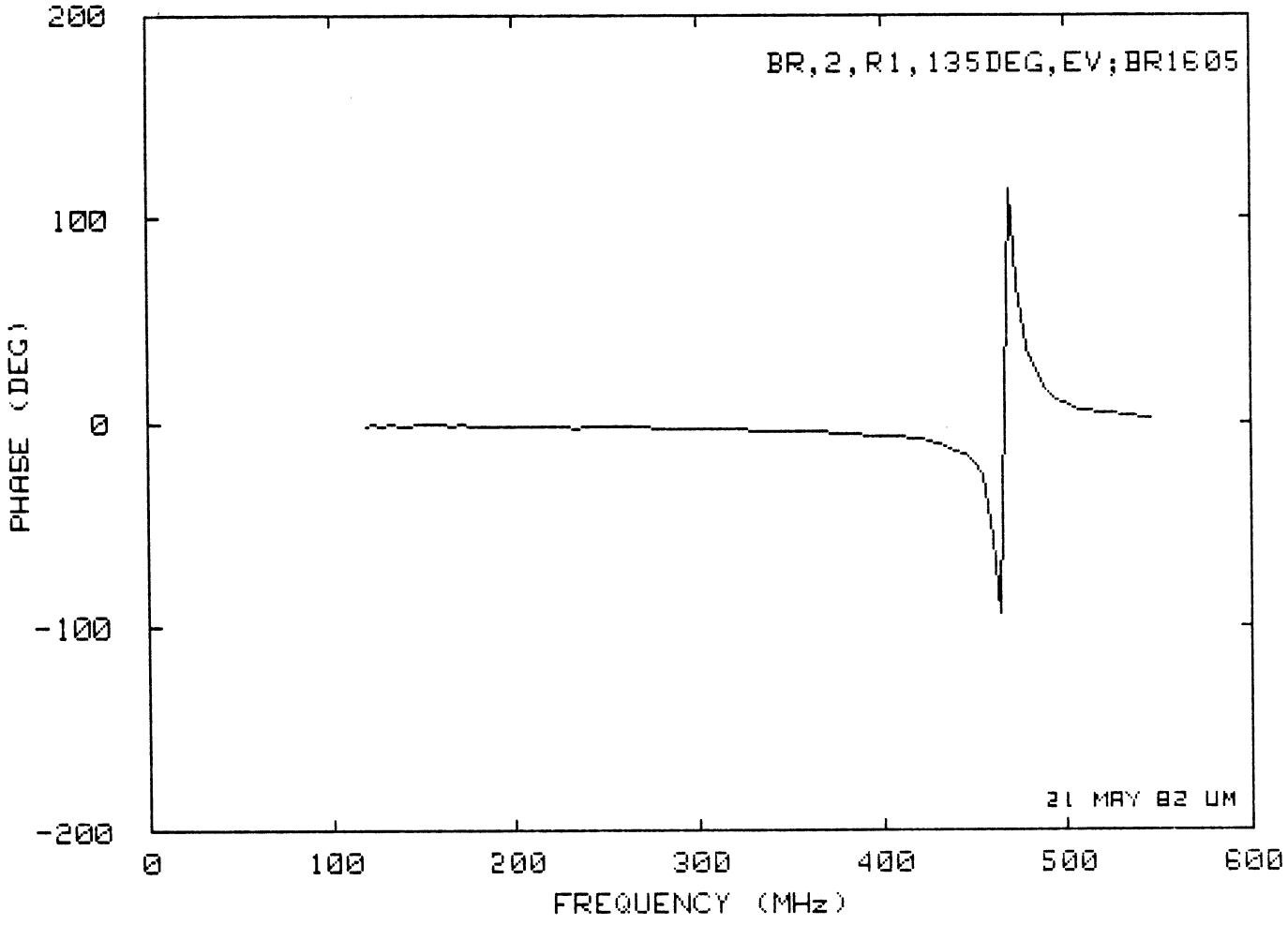
BR,2,R1,135DEG,EV;BR1605
21 MAY 82 UM
PHASE (DEG)
200
100
0
-100
-200
0
100
200
300
400
500
600
FREQUENCY (MHz)

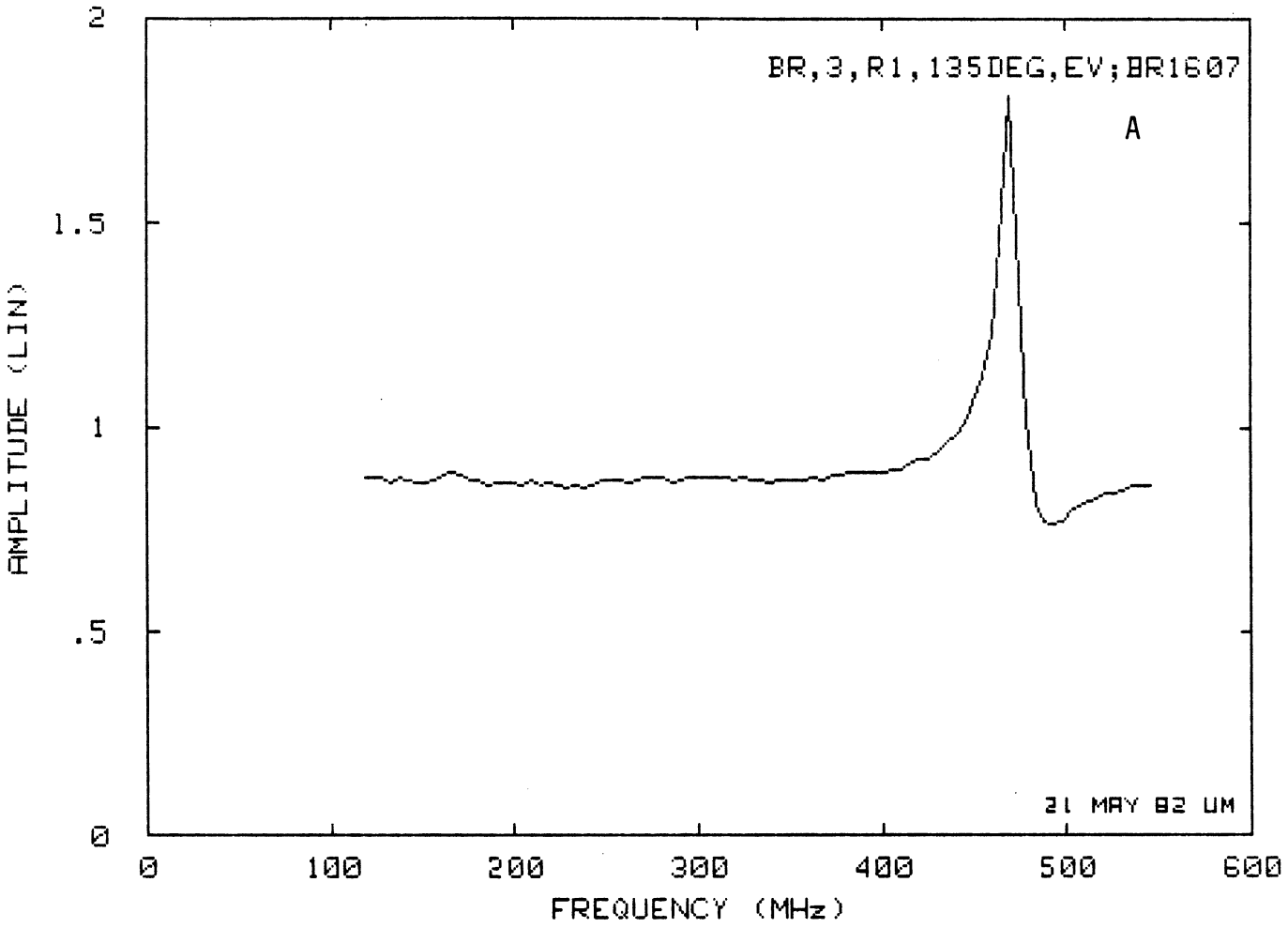
BR,3,R1,135DEG,EV;BR1607
A
21 MAY 82 UM
AMPLITUDE (LIN)
2
1.5
1
.5
0
0
100
200
300
400
500
600
FREQUENCY (MHz)

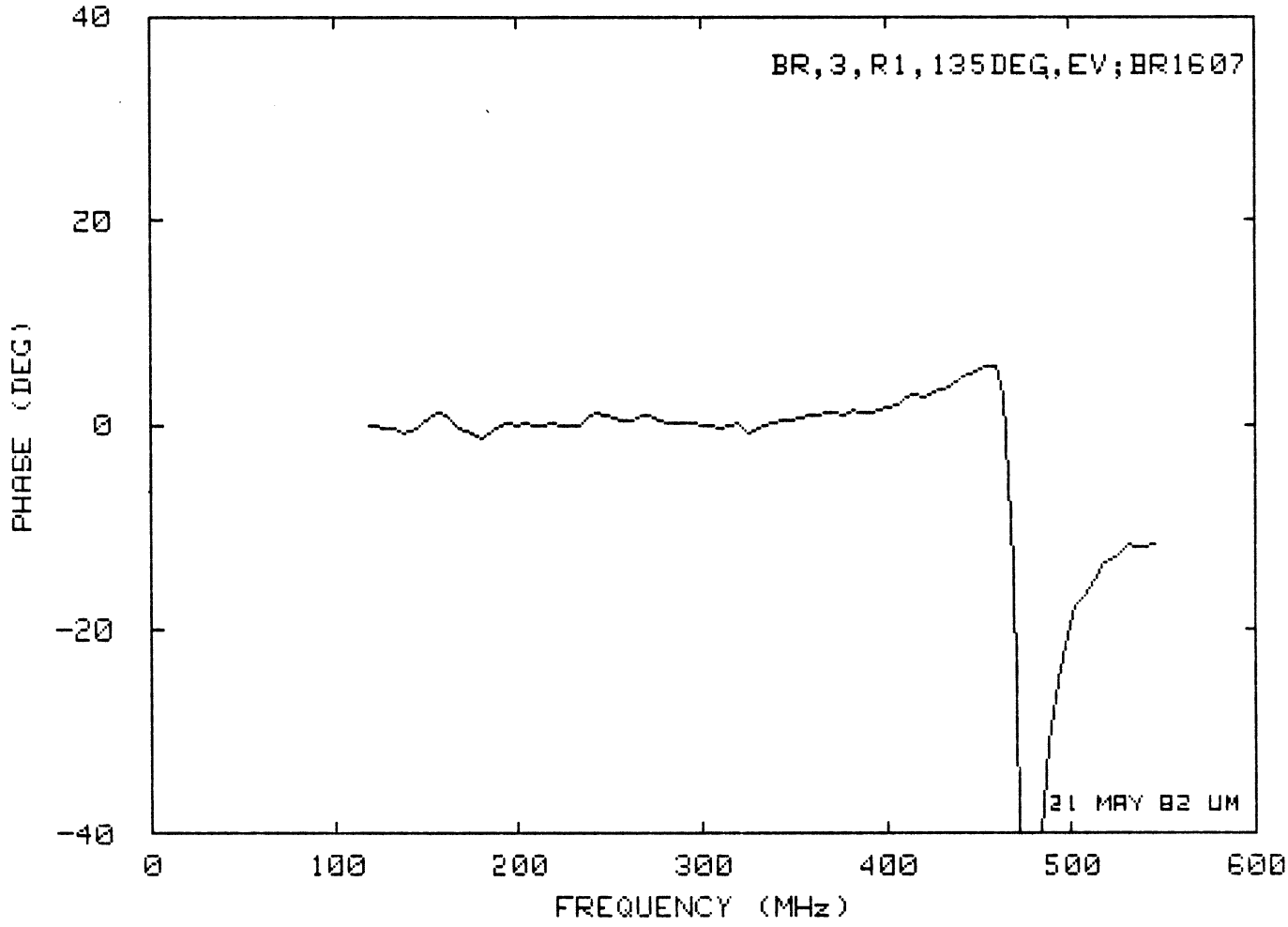
BR,3,R1,135DEG,EV;BR1607
21 MAY 82 UM
PHASE (DEG)
40
20
0
-20
-40
0
100
200
300
400
500
600
FREQUENCY (MHz)

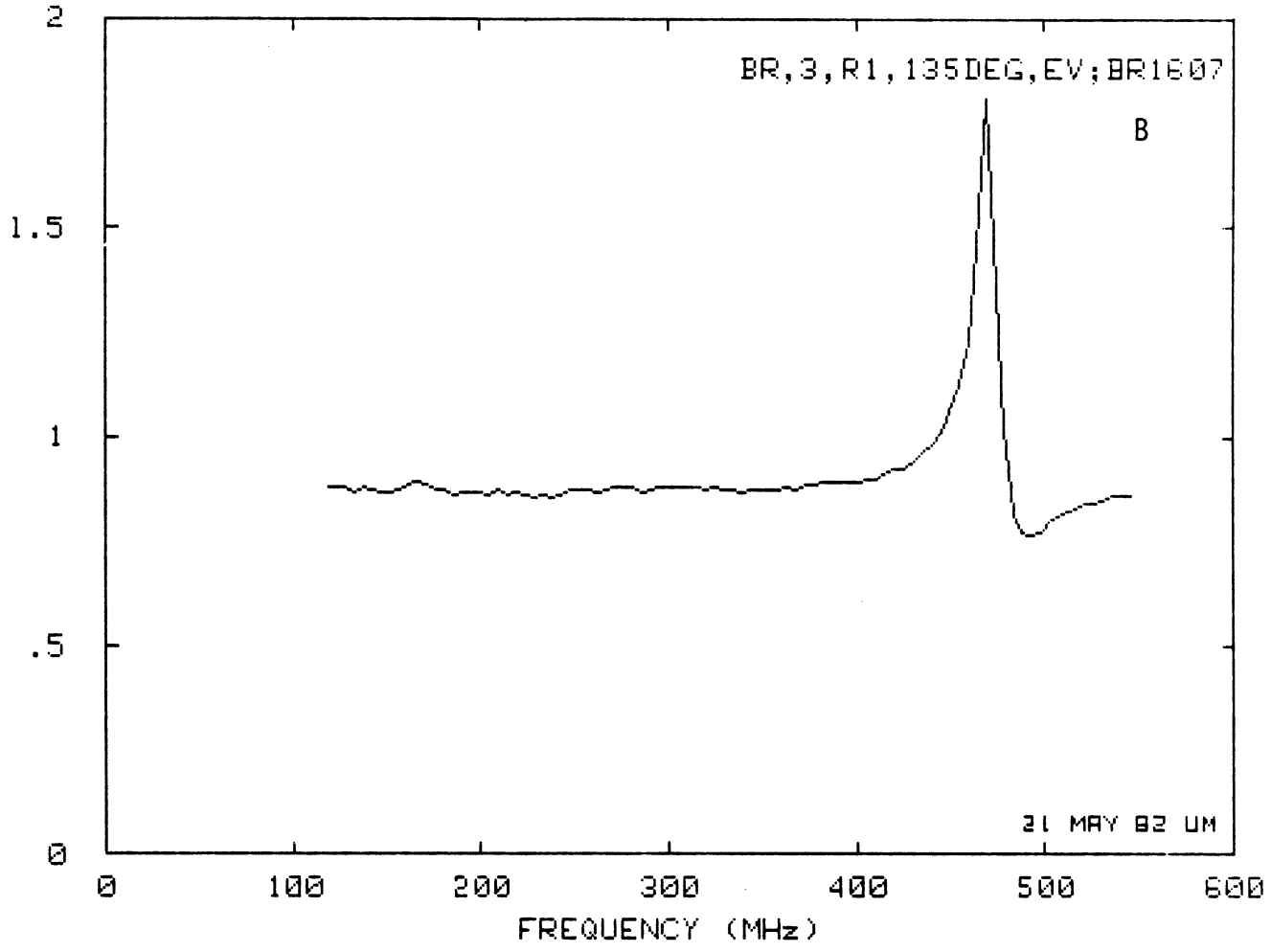
BR,3,R1,135DEG,EV;BR1607
B
21 MAY 82 UM
2
1.5
1
.5
0
0
100
200
300
400
500
600
FREQUENCY (MHz)

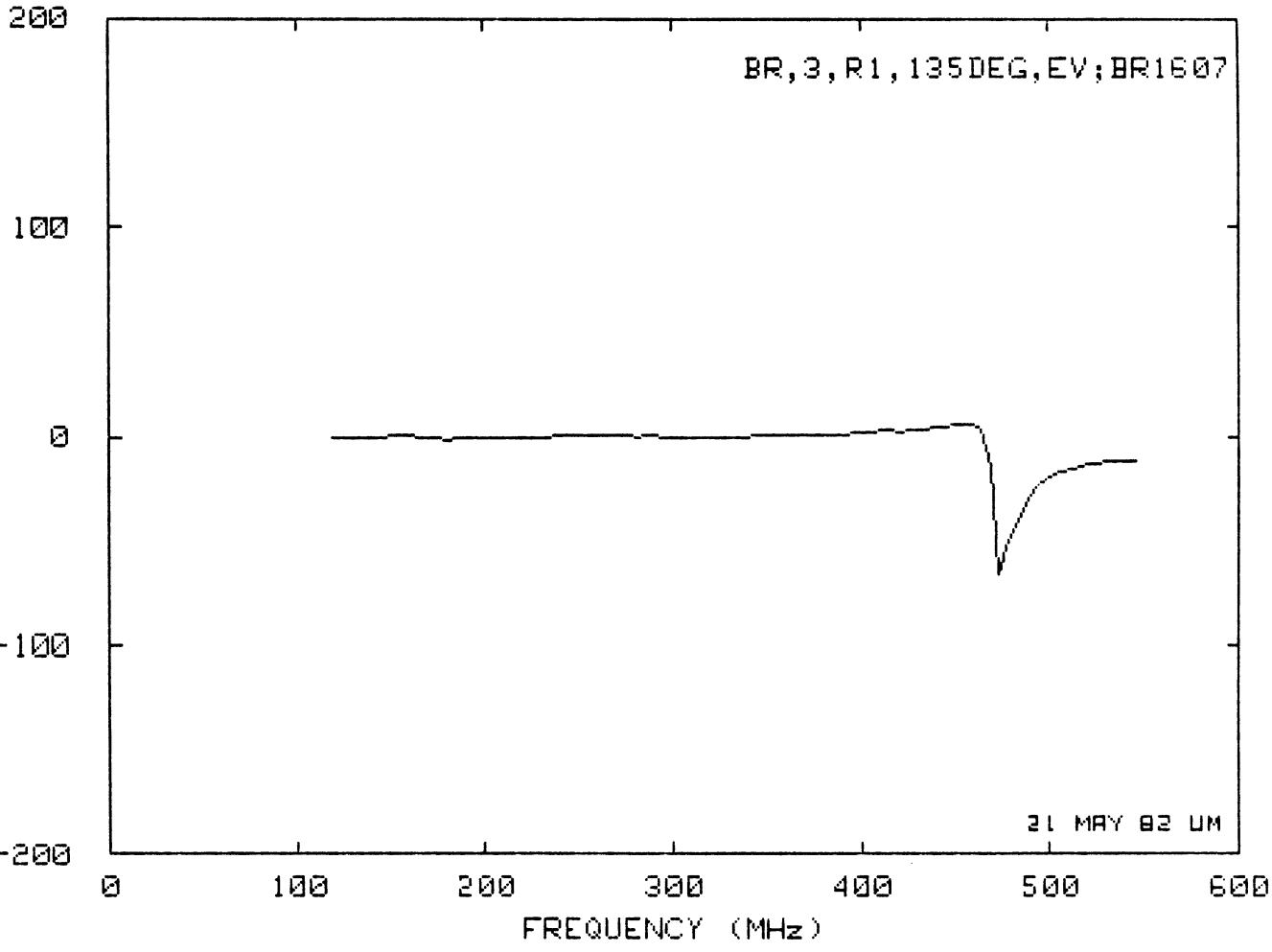
BR,3,R1,135DEG,EV;BR1607
21 MAY 82 UM
200
100
0
-100
-200
0
100
200
300
400
500
600
FREQUENCY (MHz)

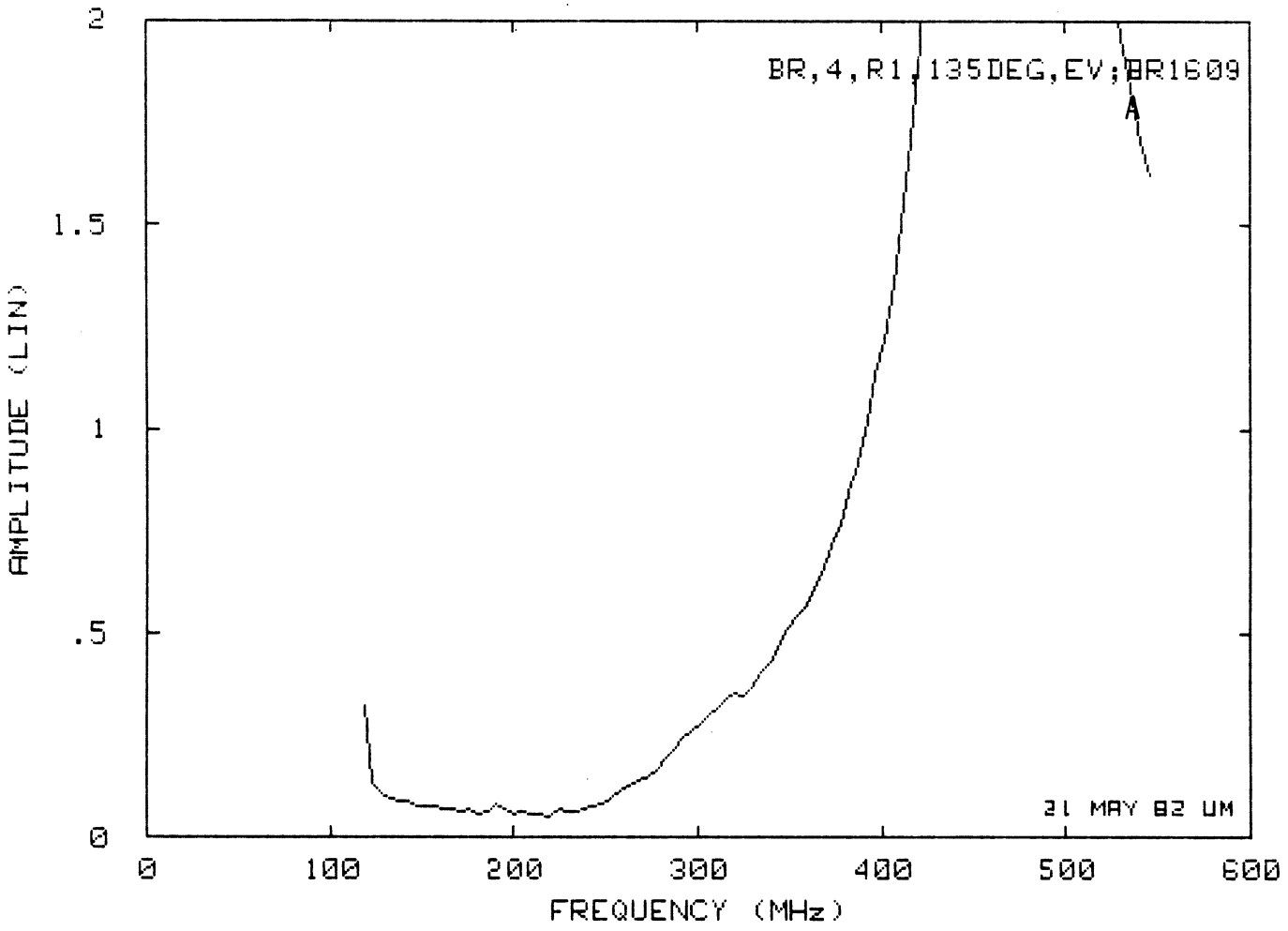
BR,4,R1,135DEG,EV;BR1609
A
21 MAY 82 UM
AMPLITUDE (LIN)
2
1.5
1
.5
0
0
100
200
300
400
500
600
FREQUENCY (MHz)

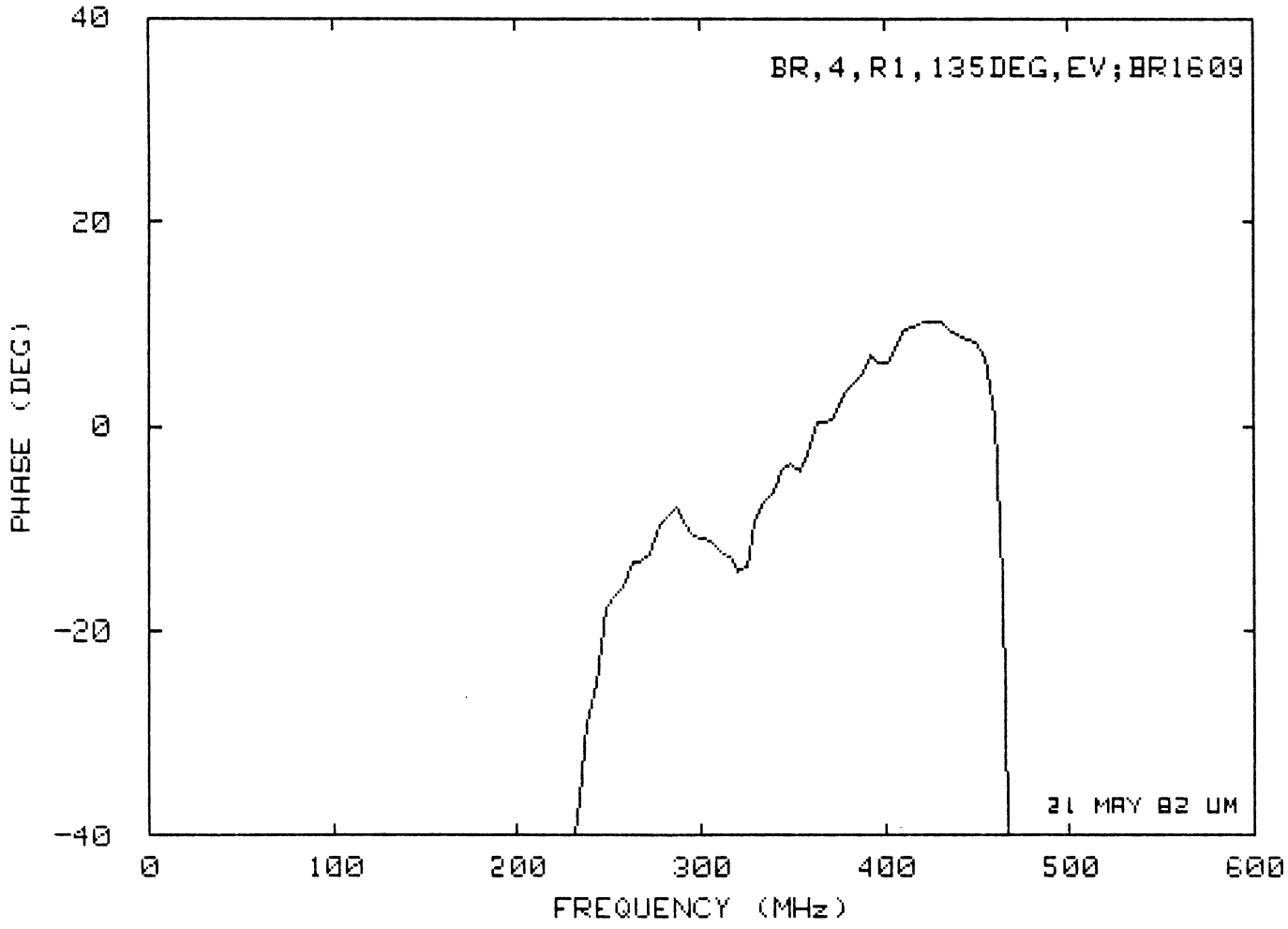
BR,4,R1,135DEG,EV;BR1609
21 MAY 82 UM
PHASE (DEG)
40
20
0
-20
-40
0
100
200
300
400
500
600
FREQUENCY (MHz)

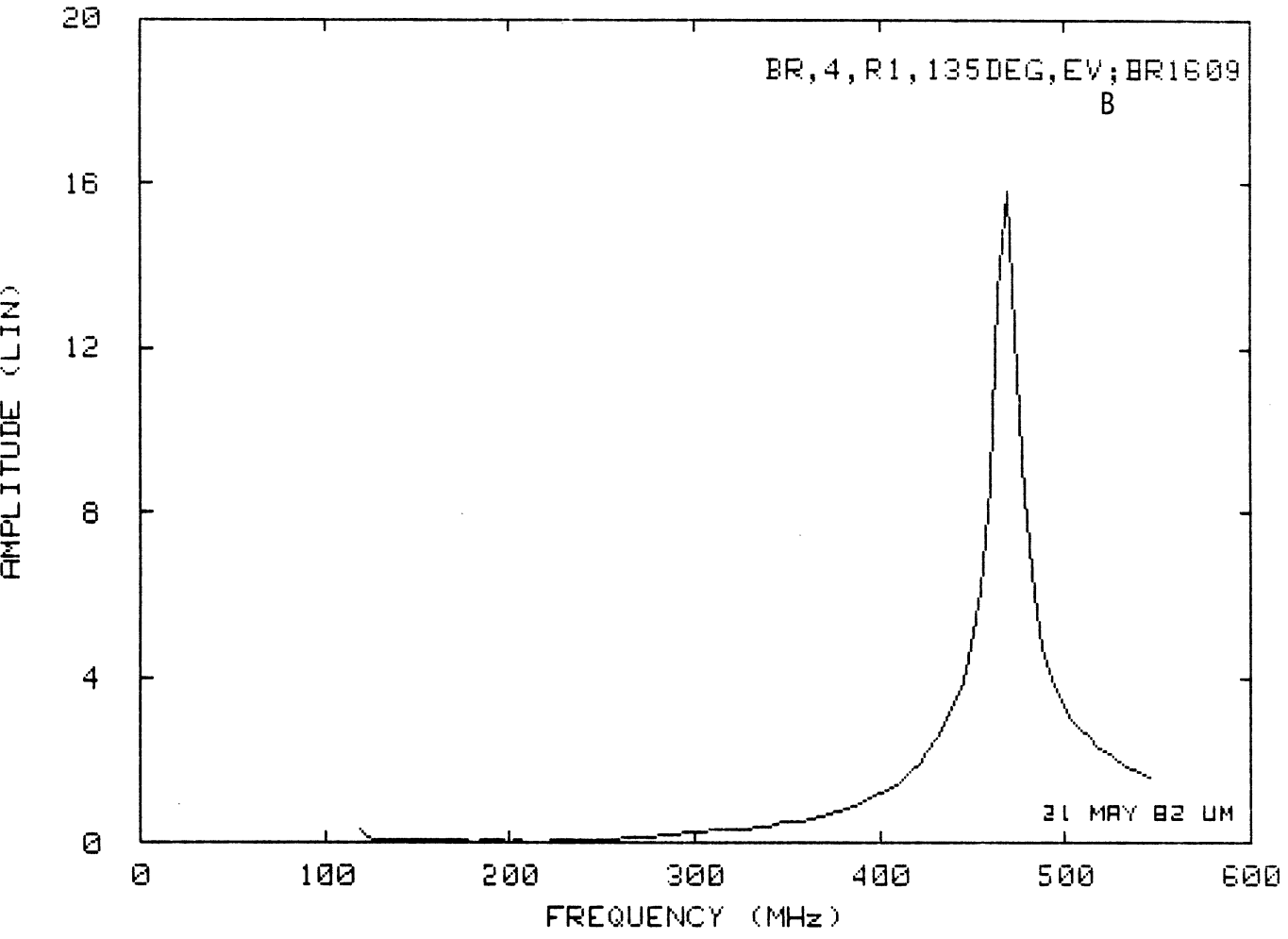
BR,4,R1,135DEG,EV;BR1609
B
21 MAY 82 UM
AMPLITUDE (LIN)
20
16
12
8
4
0
0
100
200
300
400
500
600
FREQUENCY (MHz)

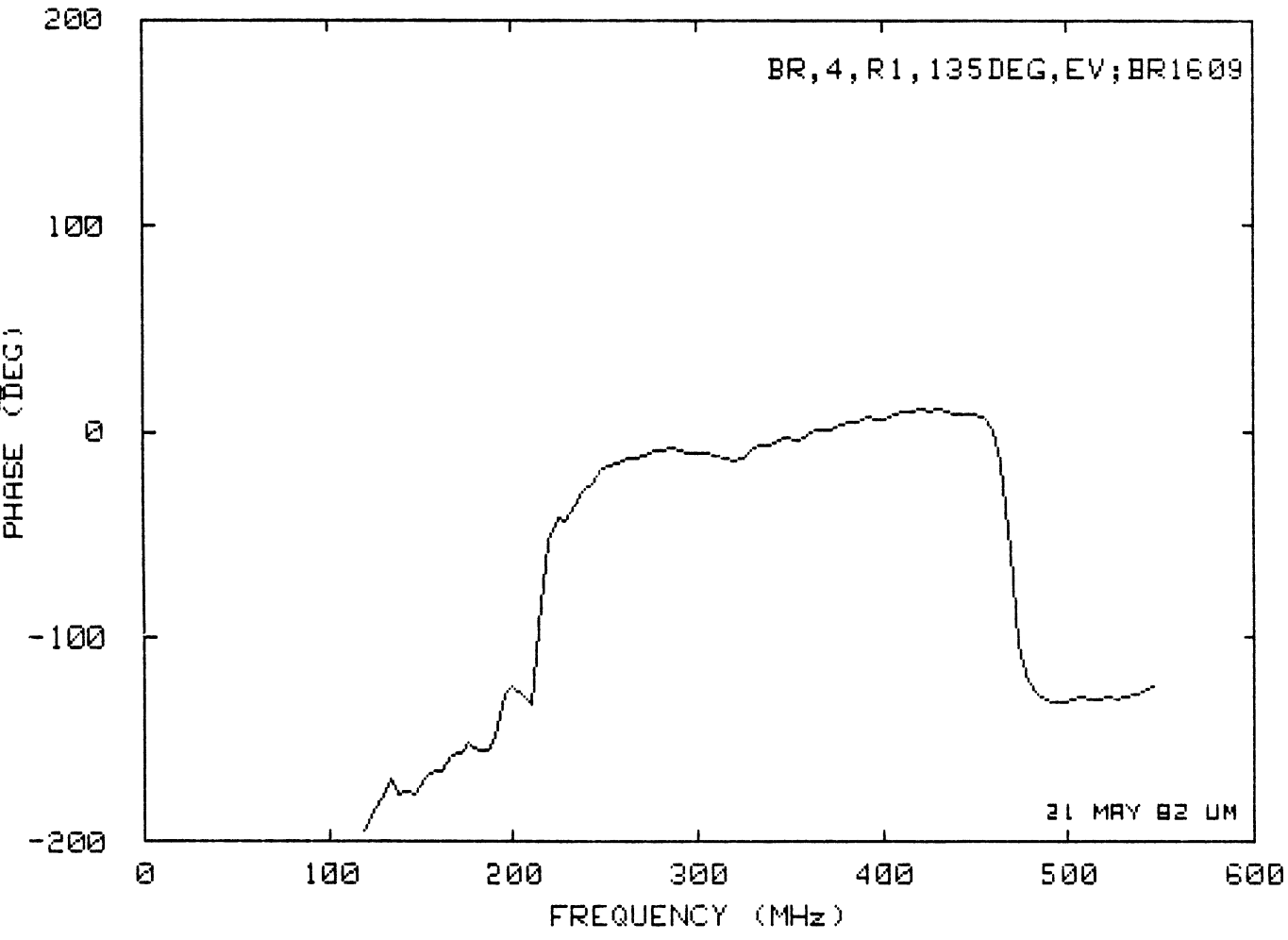
BR,4,R1,135DEG,EV;BR1609
21 MAY 82 UM
PHASE (DEG)
200
100
0
-100
-200
0
100
200
300
400
500
600
FREQUENCY (MHz)

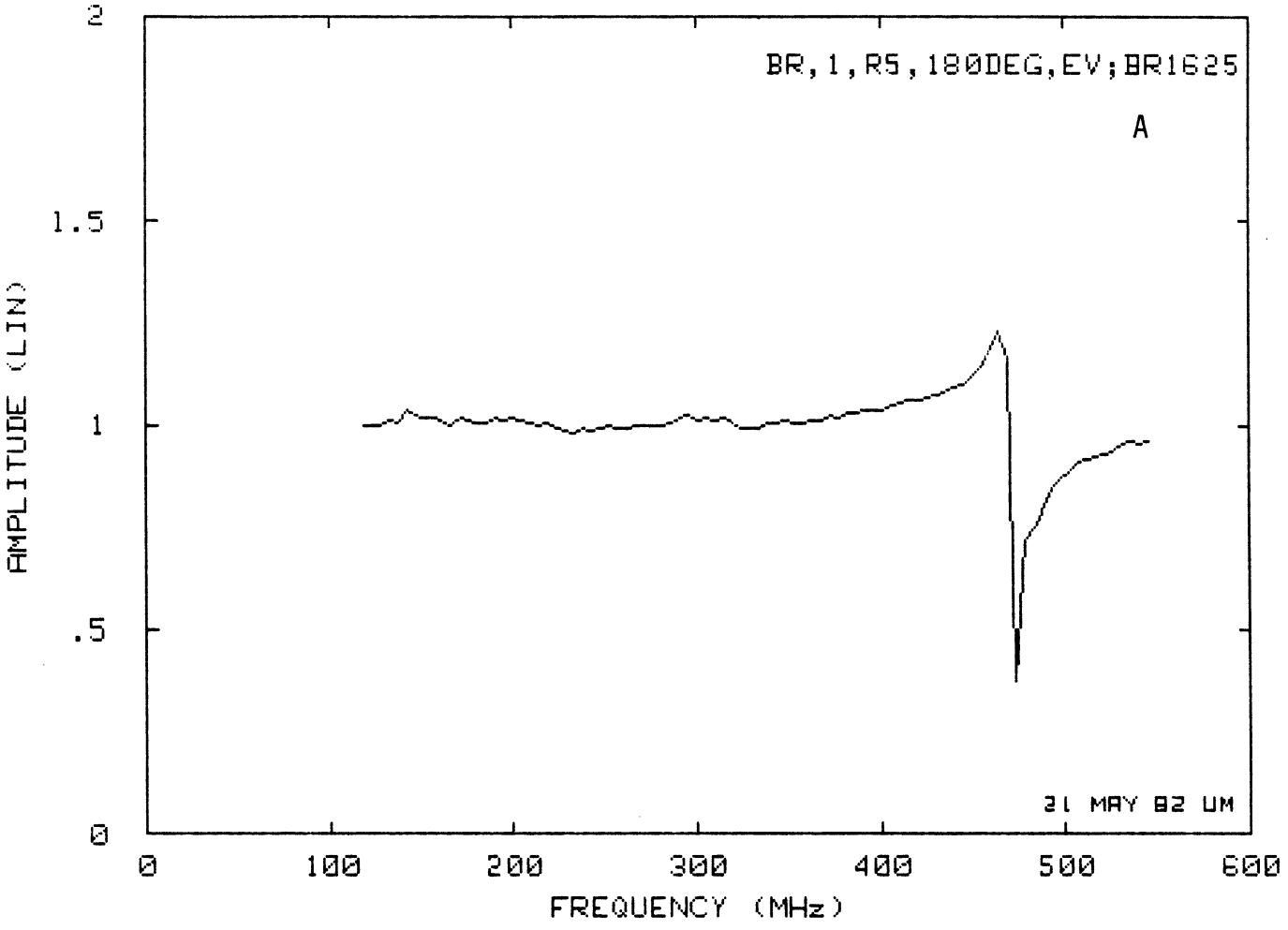
BR,1,R5,180DEG,EV;BR1625
A
21 MAY 82 UM
AMPLITUDE (LIN)
2
1.5
1
.5
0
0
100
200
300
400
500
600
FREQUENCY (MHz)

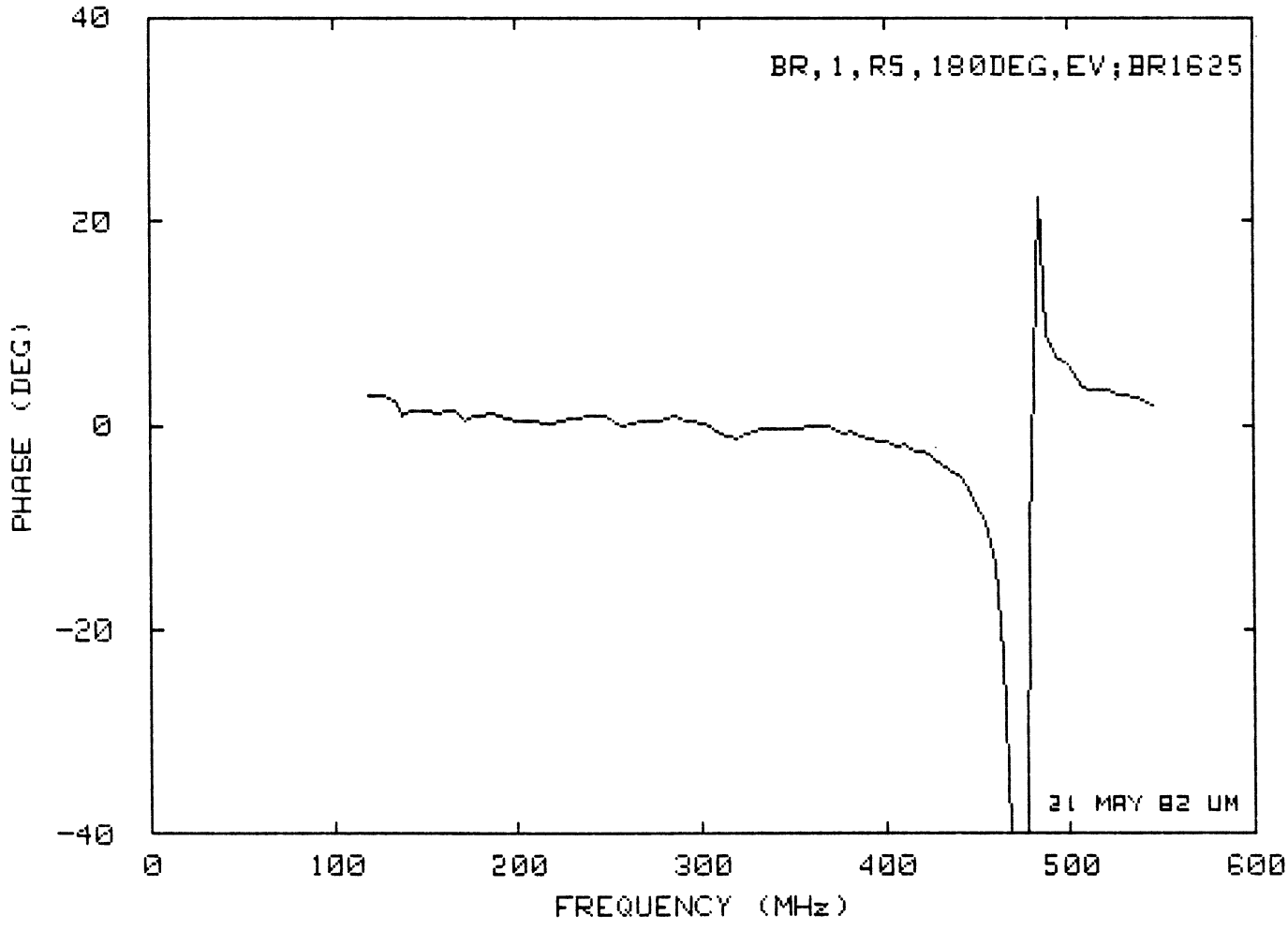
BR,1,R5,180DEG,EV;BR1625
21 MAY 82 UM
PHASE (DEG)
40
20
0
-20
-40
0
100
200
300
400
500
600
FREQUENCY (MHz)

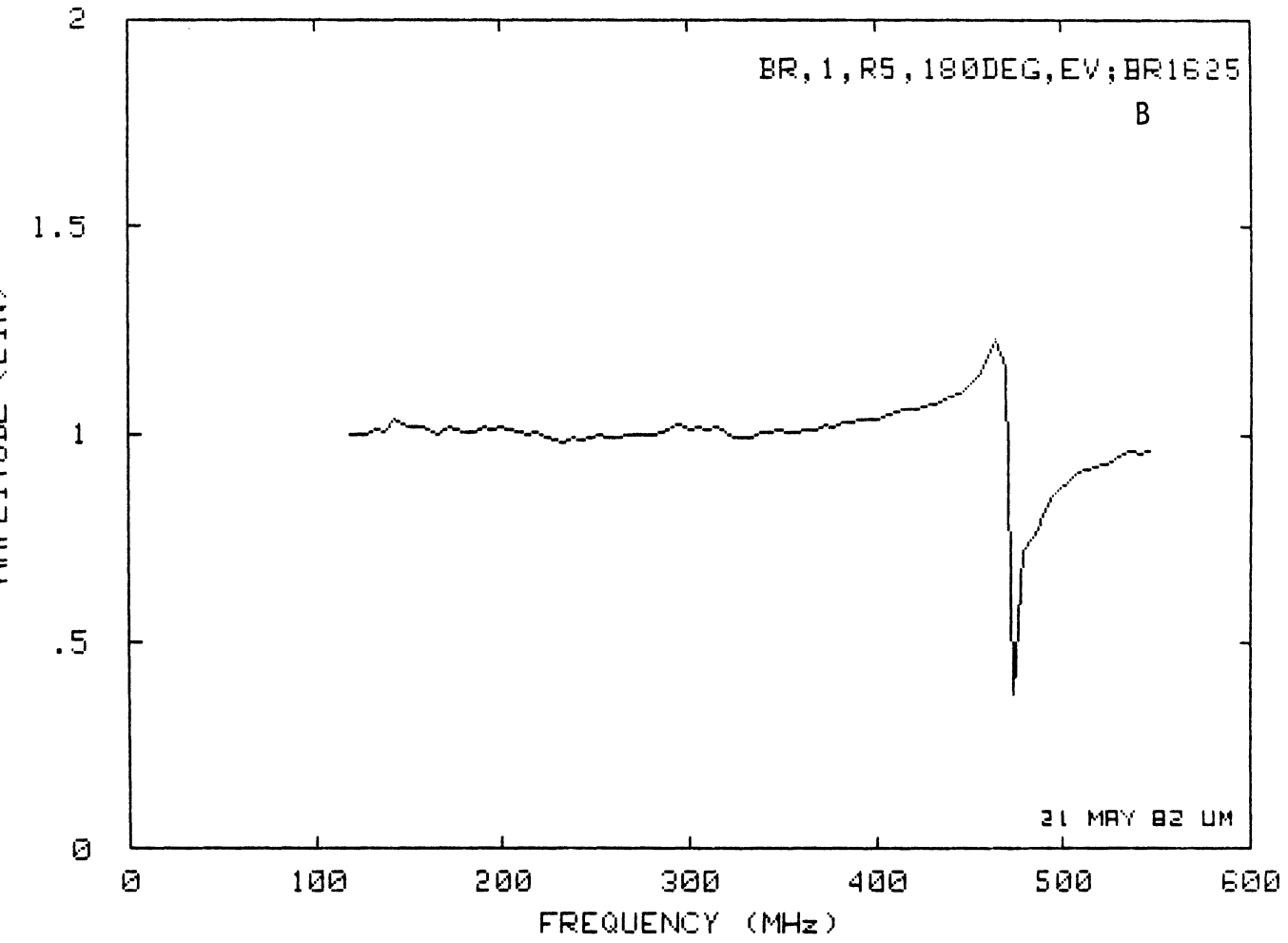
BR,1,R5,180DEG,EV;BR1625
B
21 MAY 82 UM
2
1.5
1
.5
0
0
100
200
300
400
500
600
FREQUENCY (MHz)

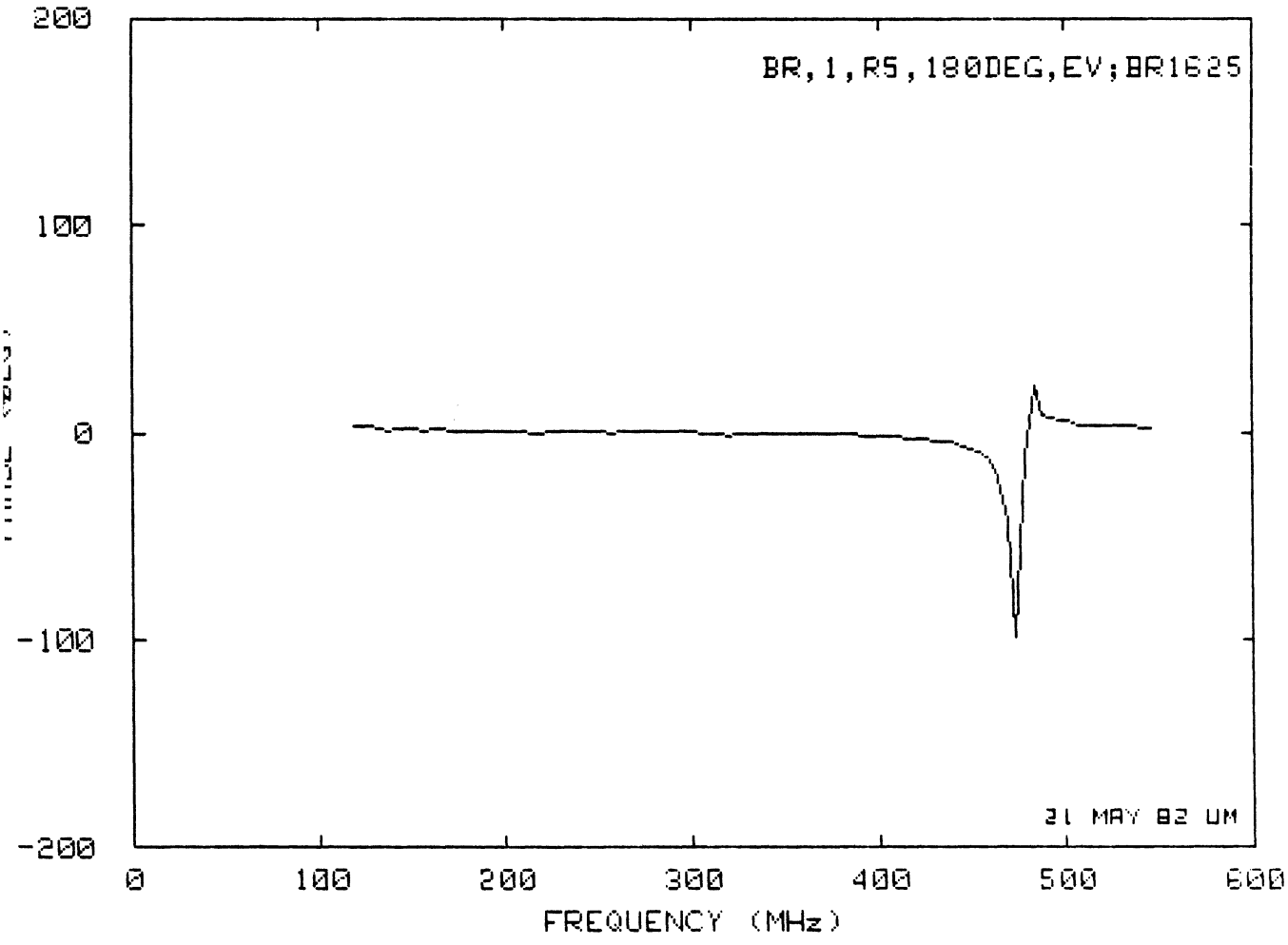
BR,1,R5,180DEG,EV;BR1625
21 MAY 82 UM
200
100
0
-100
-200
0
100
200
300
400
500
600
FREQUENCY (MHz)

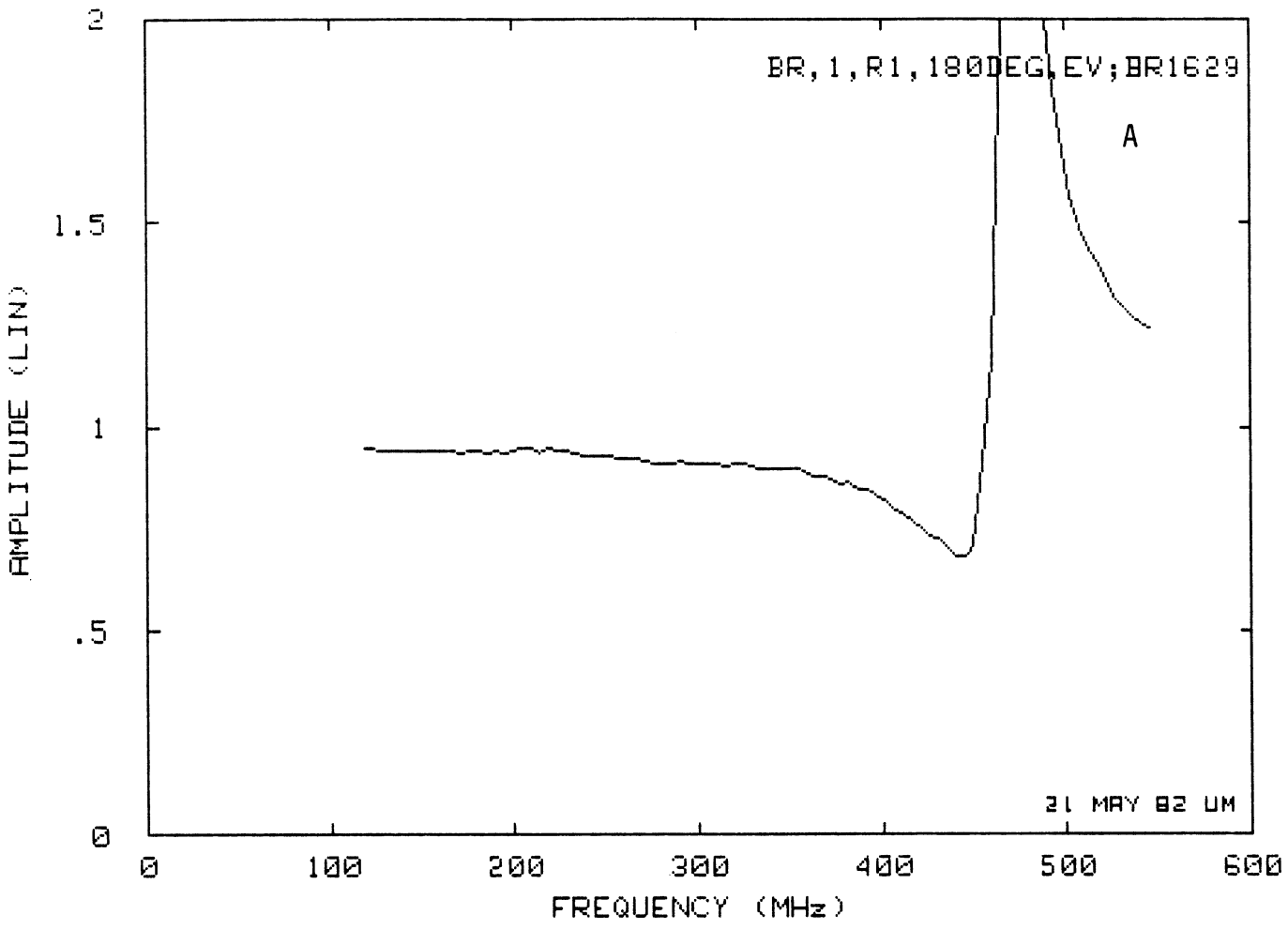
BR,1,R1,180DEG,EV;BR1629
A
21 MAY 82 UM
AMPLITUDE (LIN)
2
1.5
1
.5
0
0
100
200
300
400
500
600
FREQUENCY (MHz)

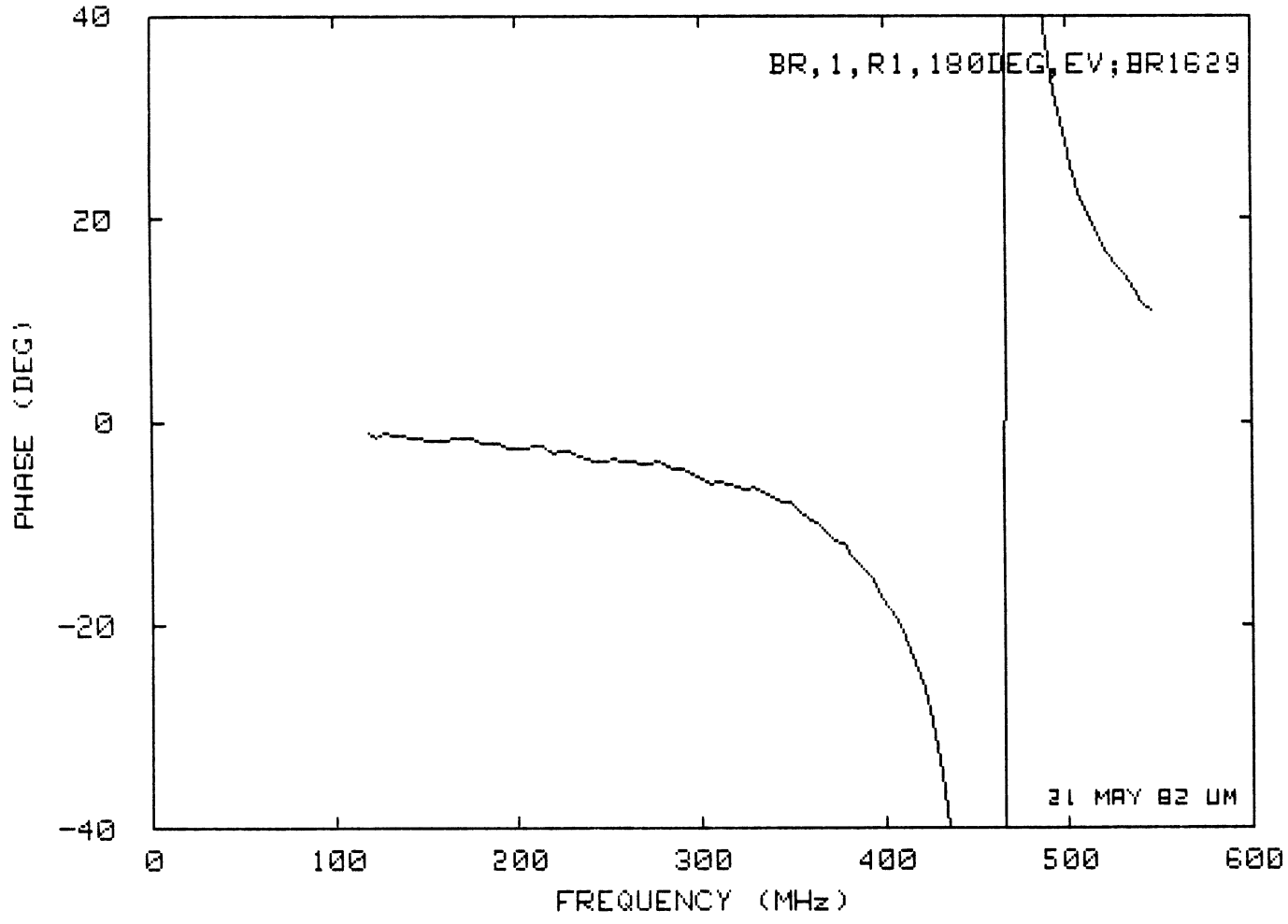
BR,1,R1,180DEG,EV;BR1629
21 MAY 82 UM
PHASE (DEG)
40
20
0
-20
-40
0
100
200
300
400
500
600
FREQUENCY (MHz)

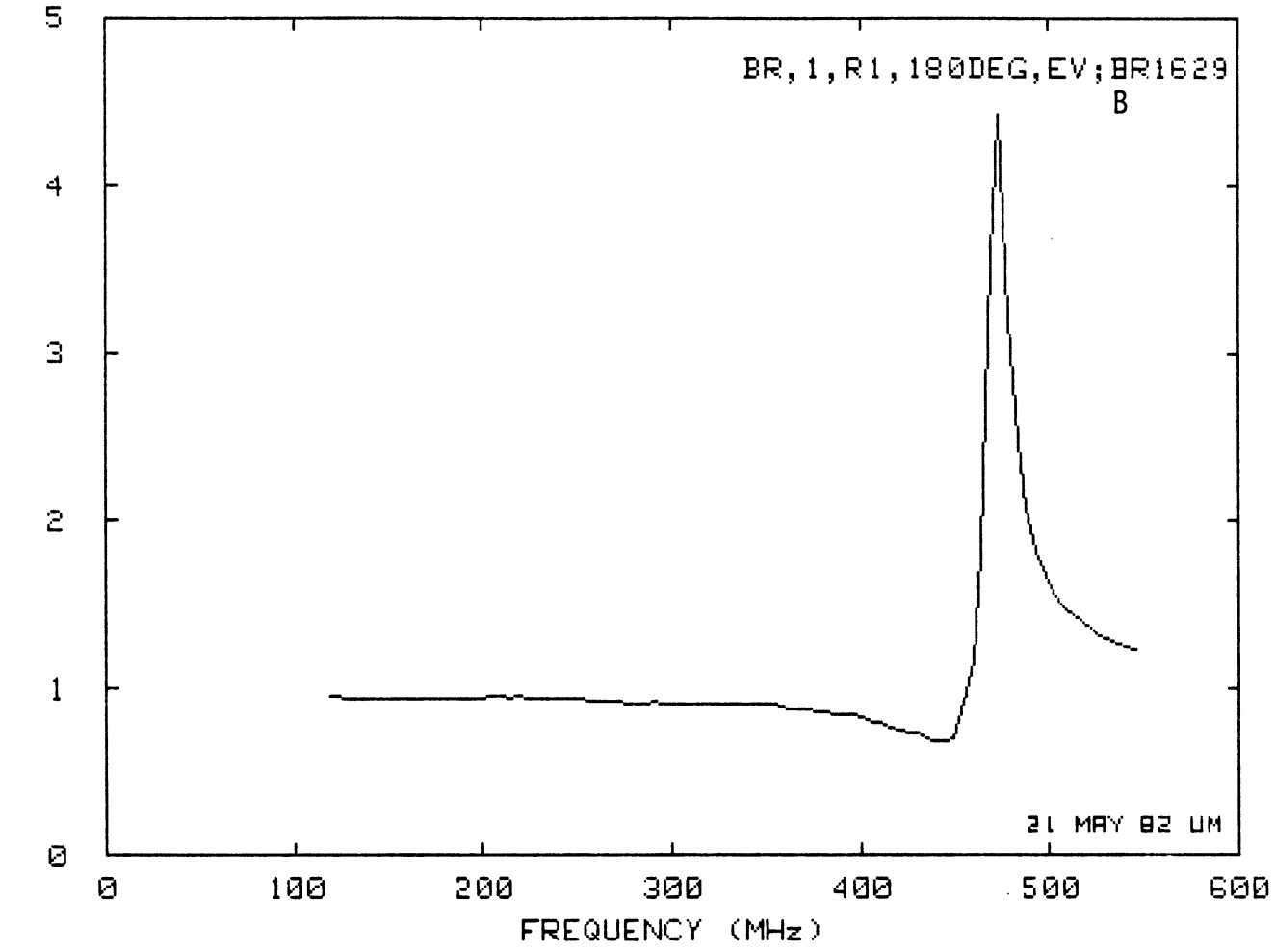
BR,1,R1,180DEG,EV;BR1629
B
21 MAY 82 UM
5
4
3
2
1
0
0
100
200
300
400
500
600
FREQUENCY (MHz)

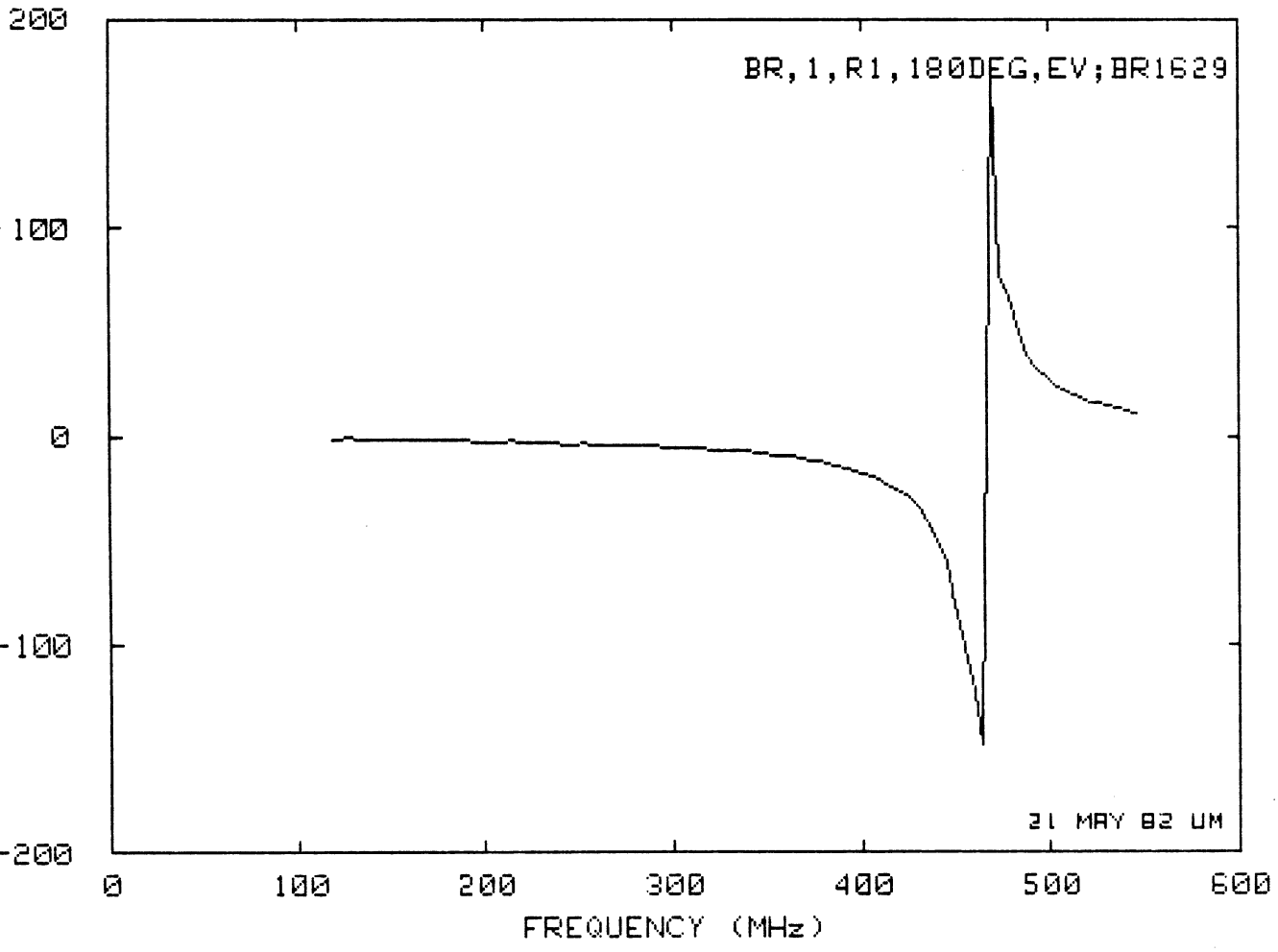
BR,1,R1,180DEG,EV;BR1629
21 MAY 82 UM
200
100
0
-100
-200
0
100
200
300
400
500
600
FREQUENCY (MHz)

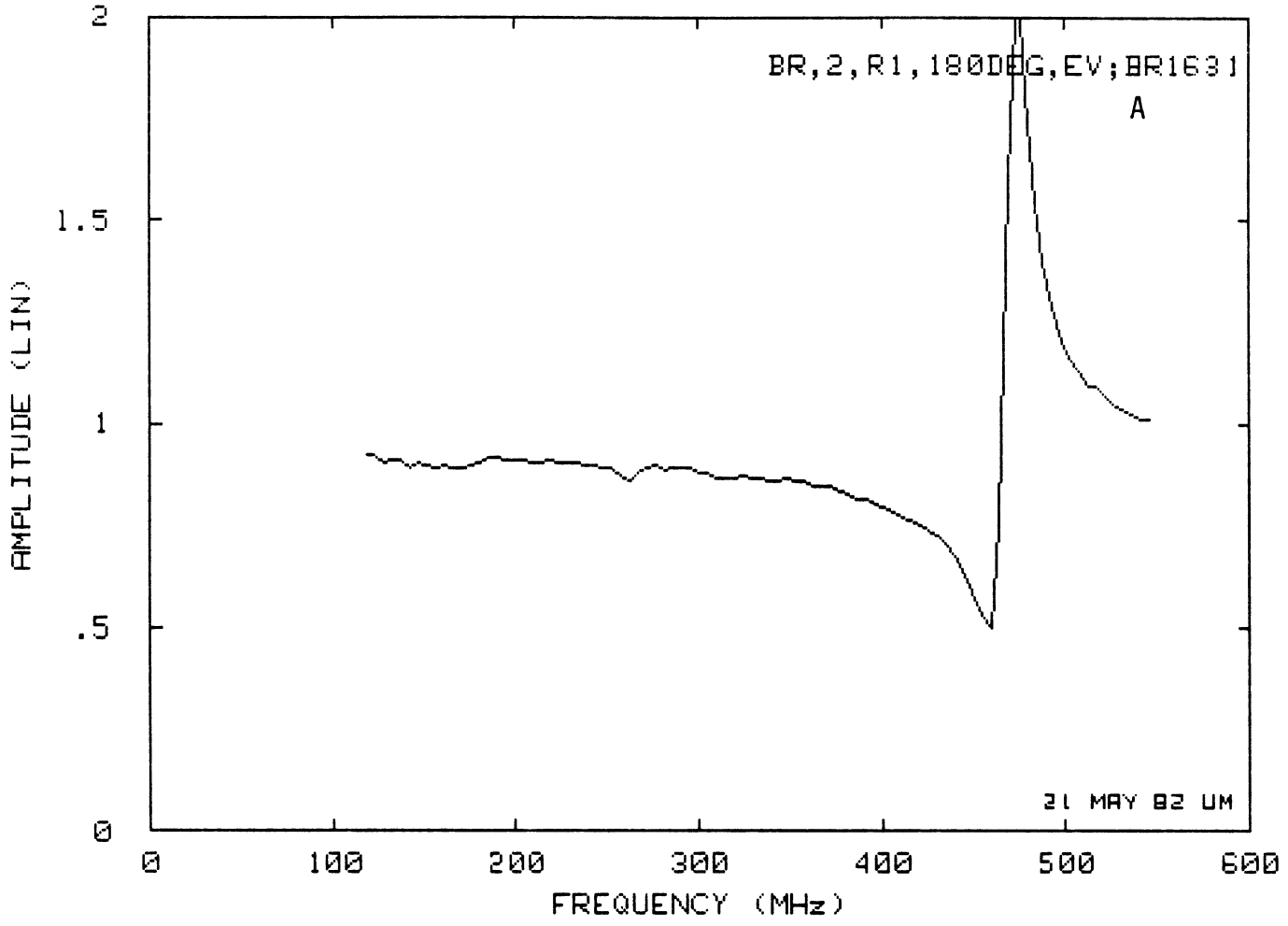
BR,2,R1,180DEG,EV;BR1631
A
21 MAY 82 UM
AMPLITUDE (LIN)
2
1.5
1
.5
0
0
100
200
300
400
500
600
FREQUENCY (MHz)

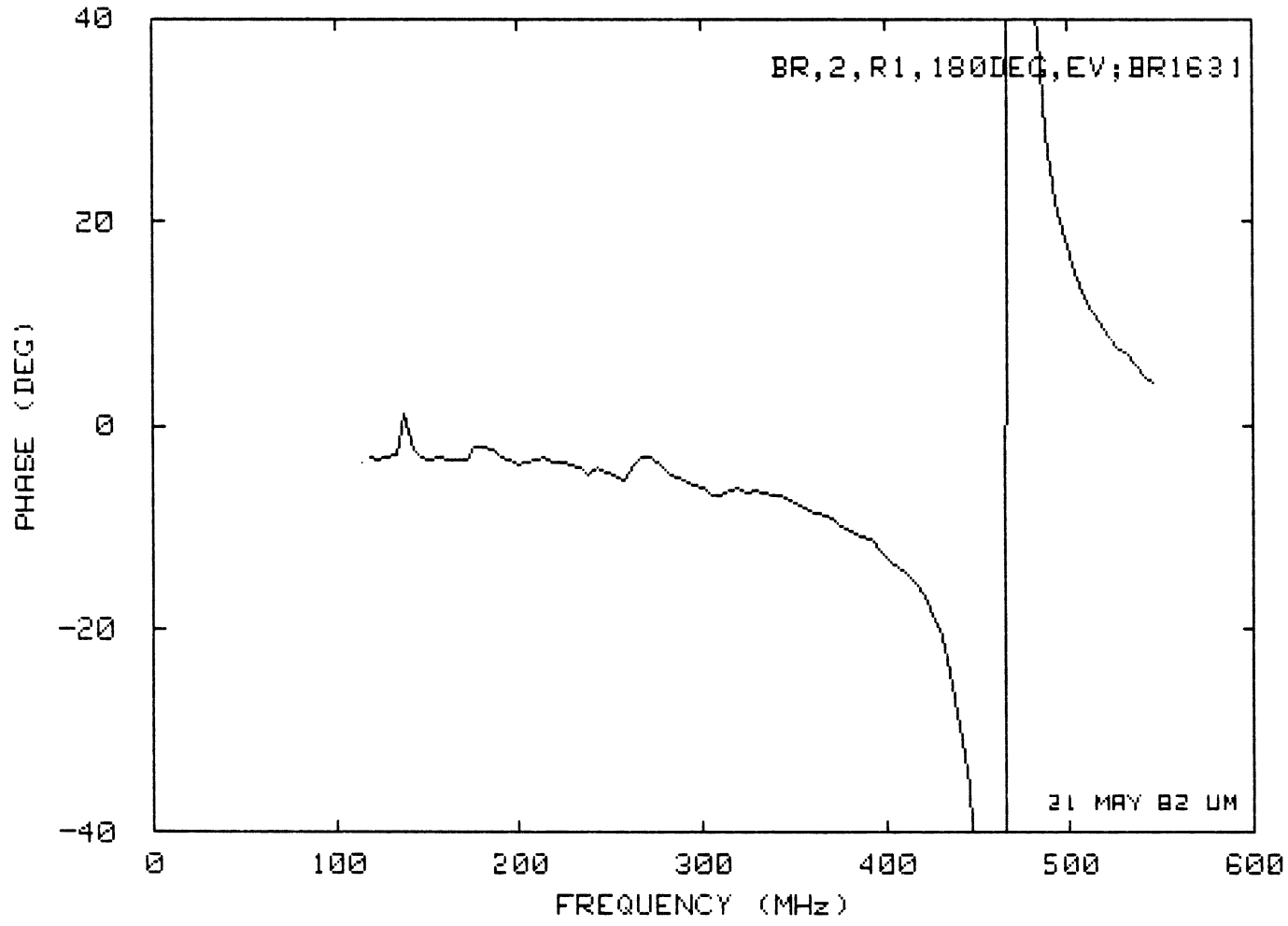
BR,2,R1,180DEG,EV;BR1631
21 MAY 82 UM
PHASE (DEG)
40
20
0
-20
-40
0
100
200
300
400
500
600
FREQUENCY (MHz)

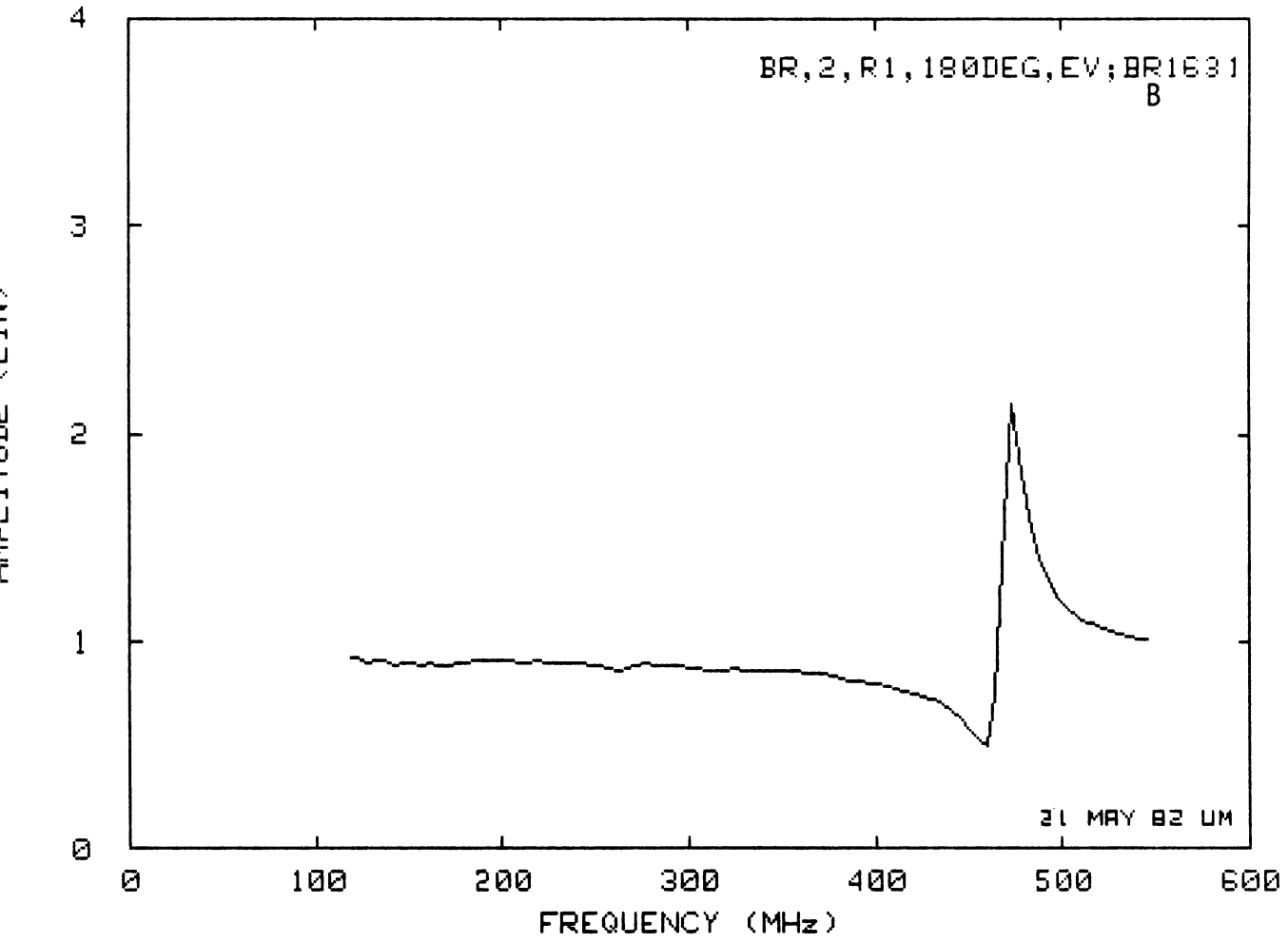
BR,2,R1,180DEG,EV;BR1631
B
21 MAY 82 UM
4
3
2
1
0
0
100
200
300
400
500
600
FREQUENCY (MHz)

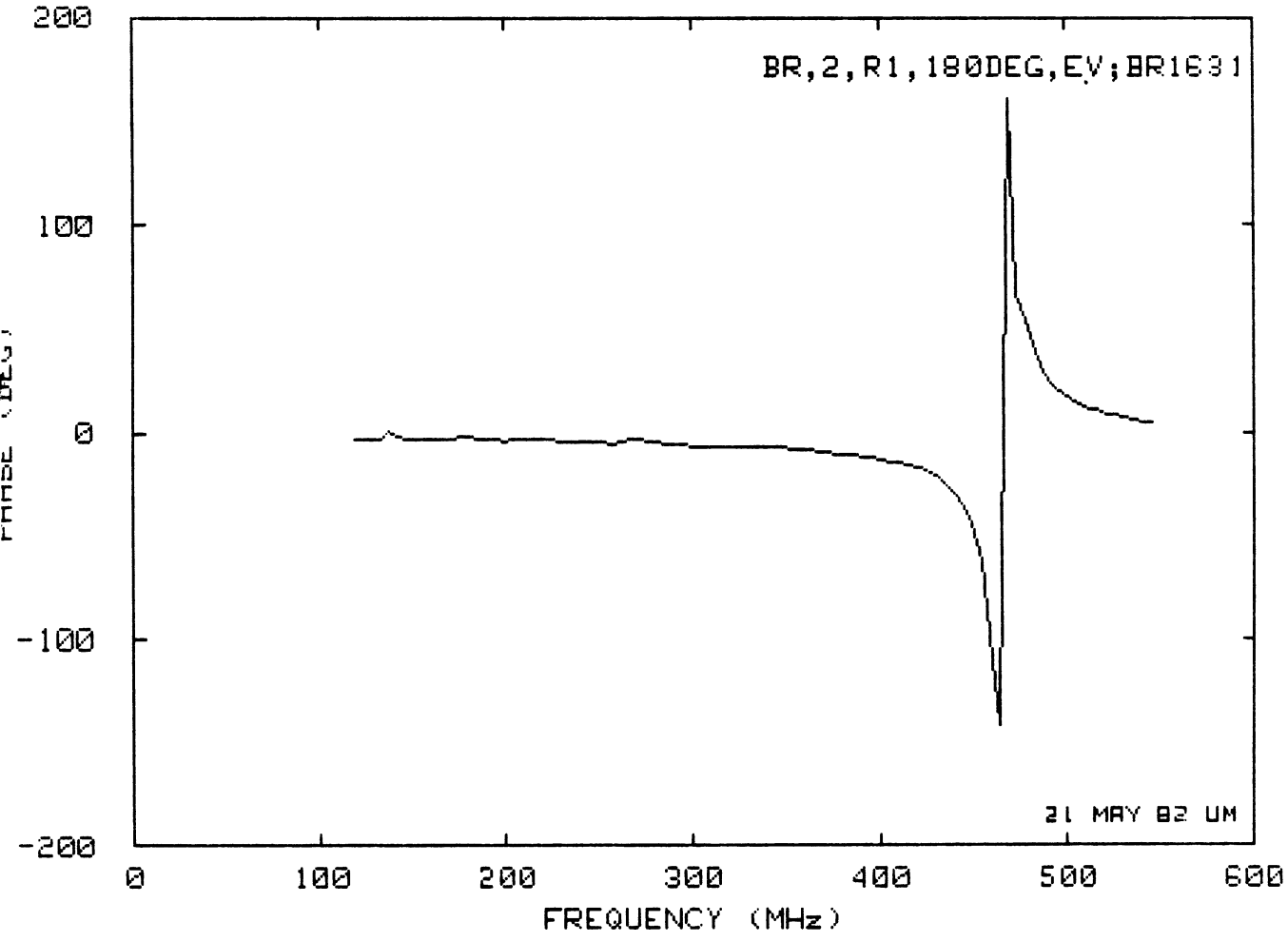
BR,2,R1,180DEG,EV;BR1631
21 MAY 82 UM
200
100
0
-100
-200
0
100
200
300
400
500
600
FREQUENCY (MHz)

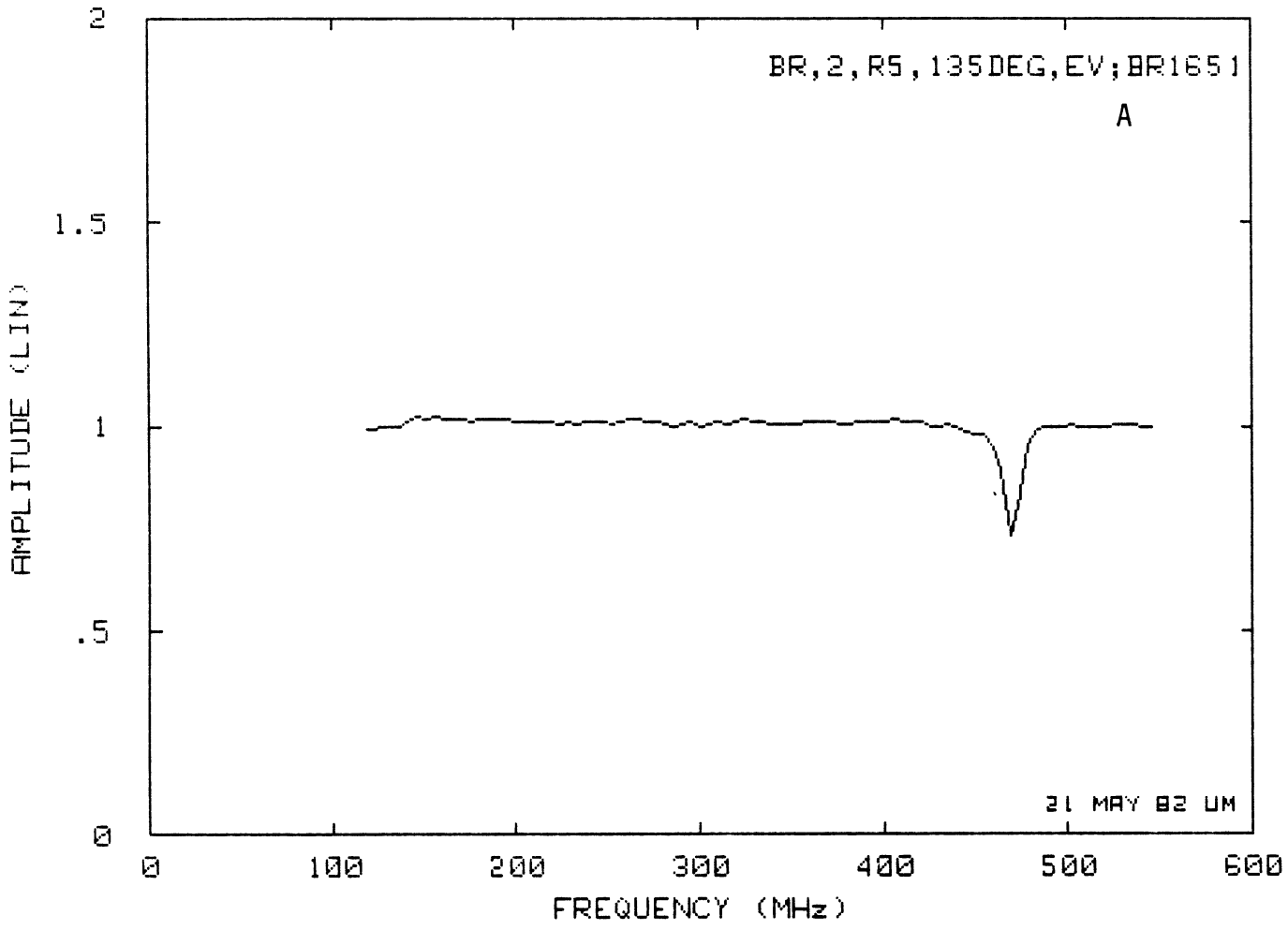
BR,2,R5,135DEG,EV;BR1651
A
21 MAY 82 UM
AMPLITUDE (LIN)
2
1.5
1
.5
0
0
100
200
300
400
500
600
FREQUENCY (MHz)

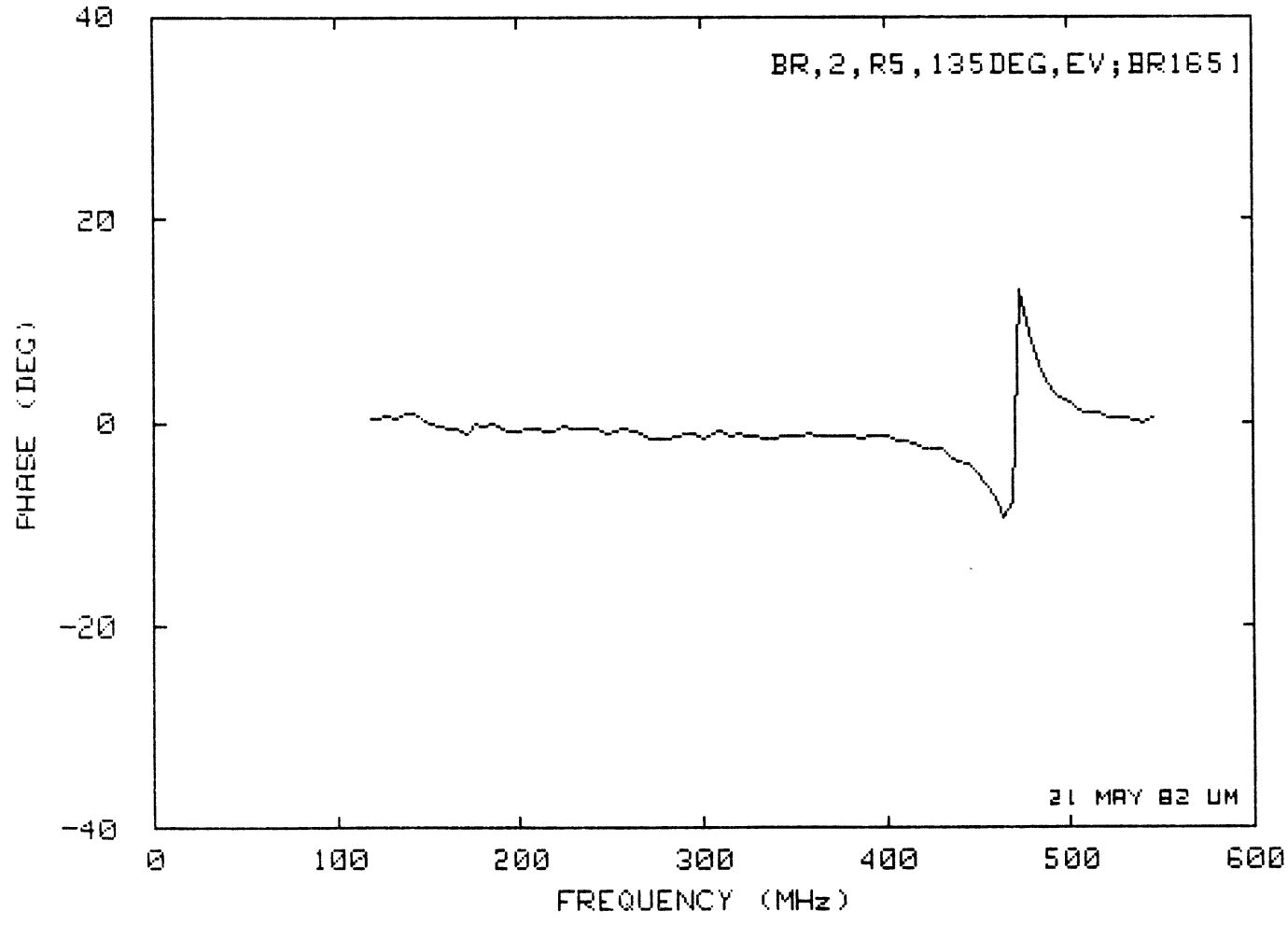
BR,2,R5,135DEG,EV;BR1651
21 MAY 82 UM
PHASE (DEG)
40
20
0
-20
-40
0
100
200
300
400
500
600
FREQUENCY (MHz)

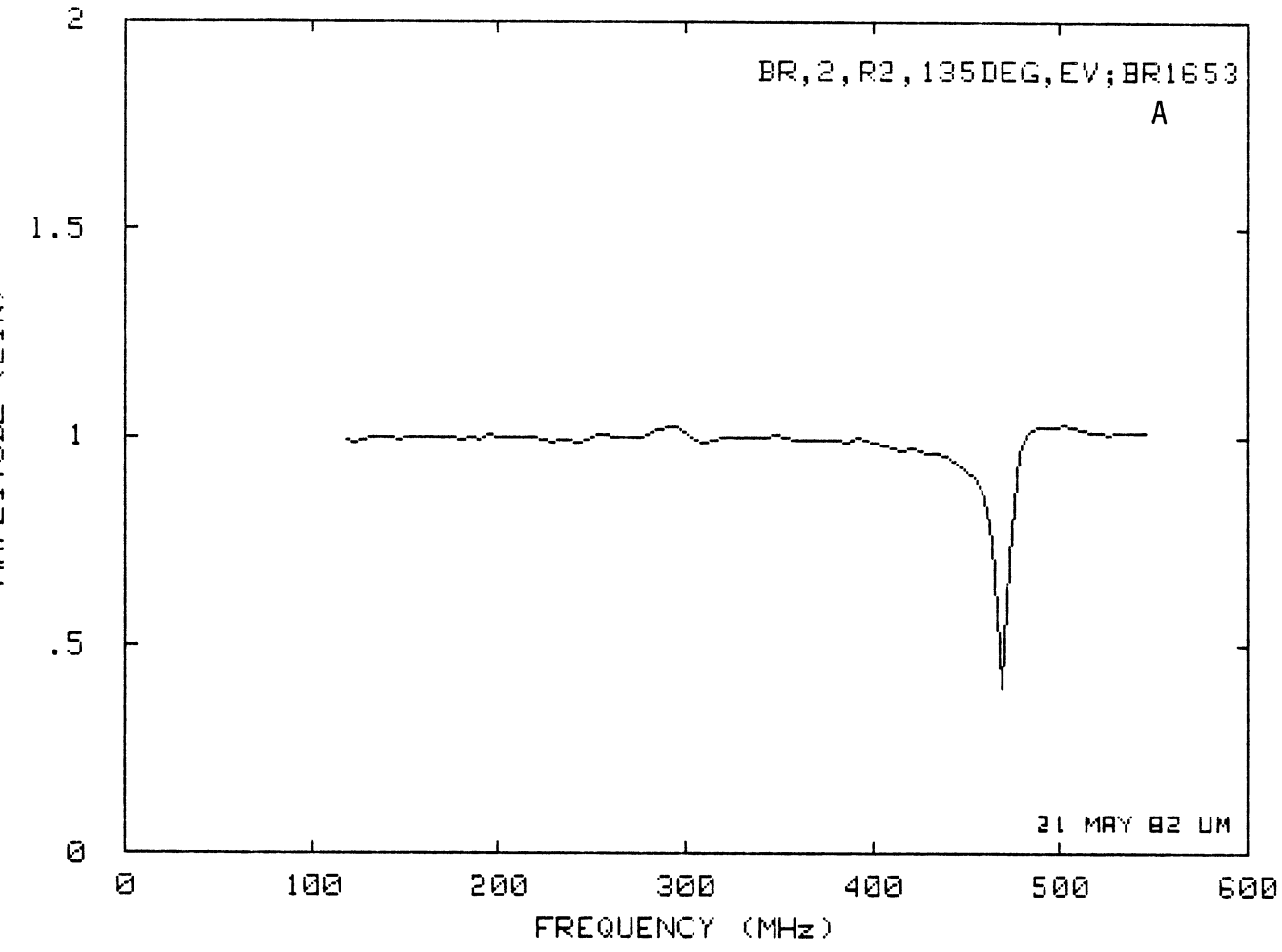
BR,2,R2,135DEG,EV;BR1653
A
21 MAY 82 UM
2
1.5
1
.5
0
0
100
200
300
400
500
600
FREQUENCY (MHz)

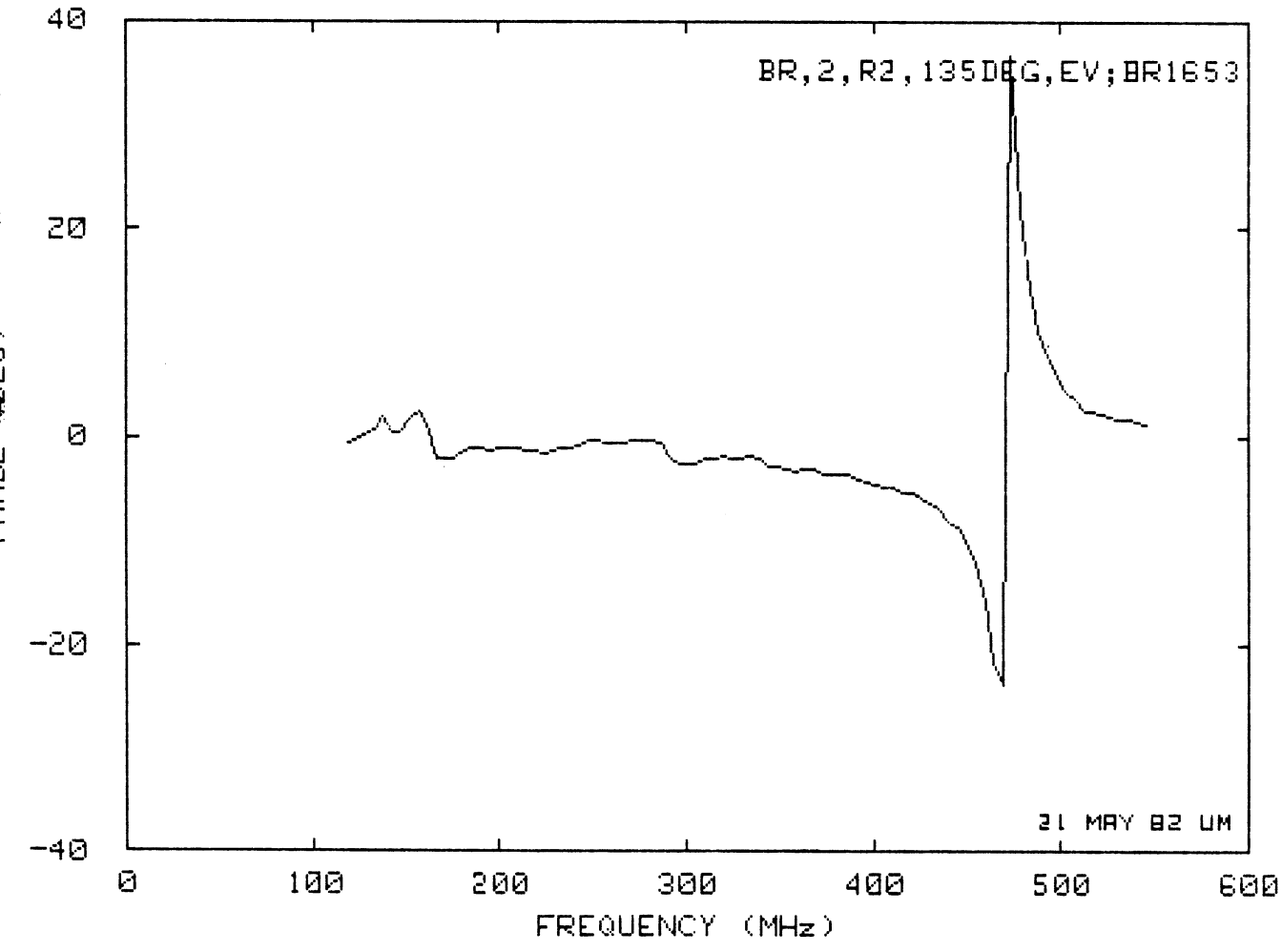
BR,2,R2,135DEG,EV;BR1653
21 MAY 82 UM
40
20
0
-20
-40
0
100
200
300
400
500
600
FREQUENCY (MHz)

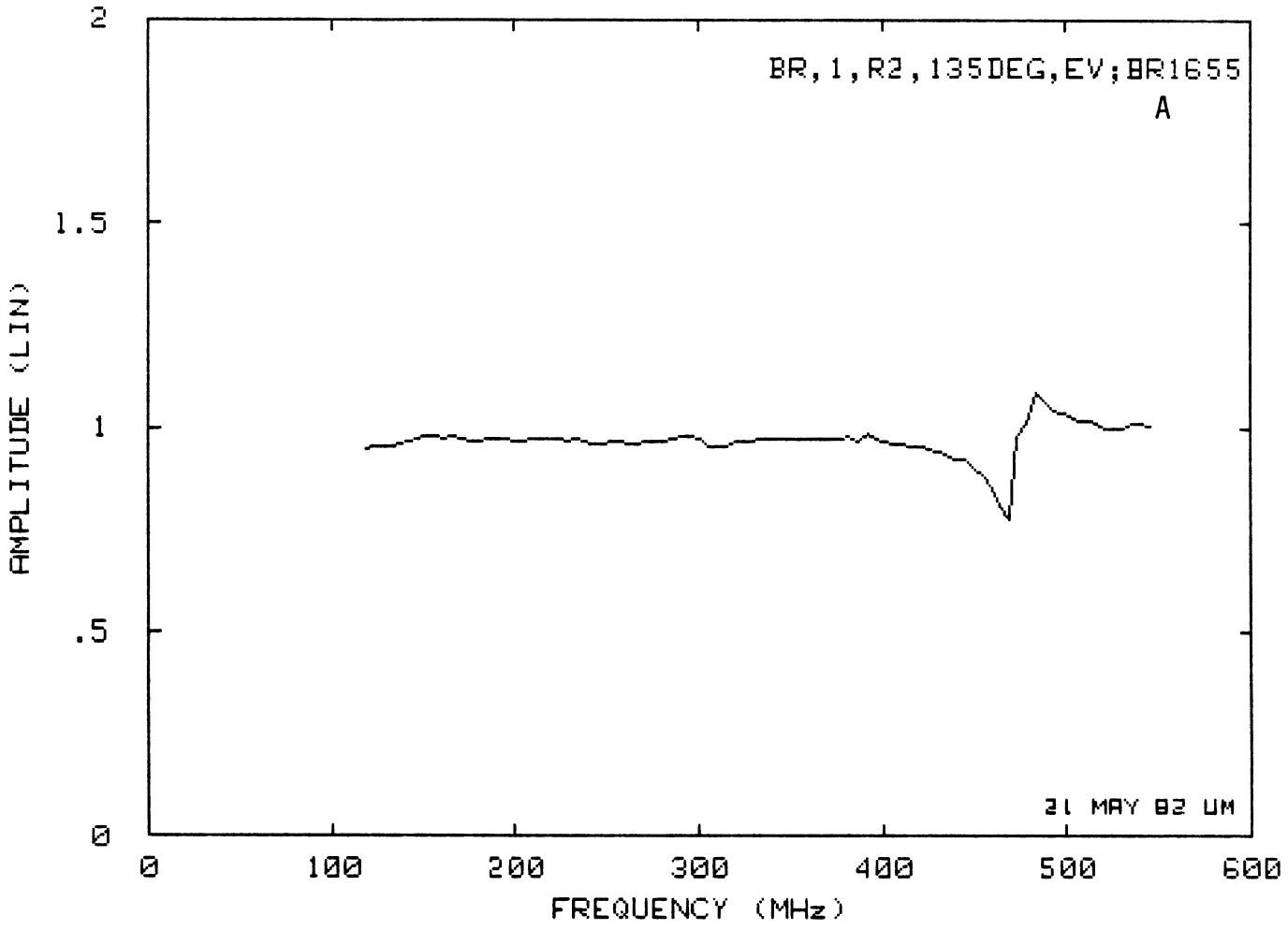
BR,1,R2,135DEG,EV;BR1655
A
21 MAY 82 UM
AMPLITUDE (LIN)
2
1.5
1
.5
0
0
100
200
300
400
500
600
FREQUENCY (MHz)

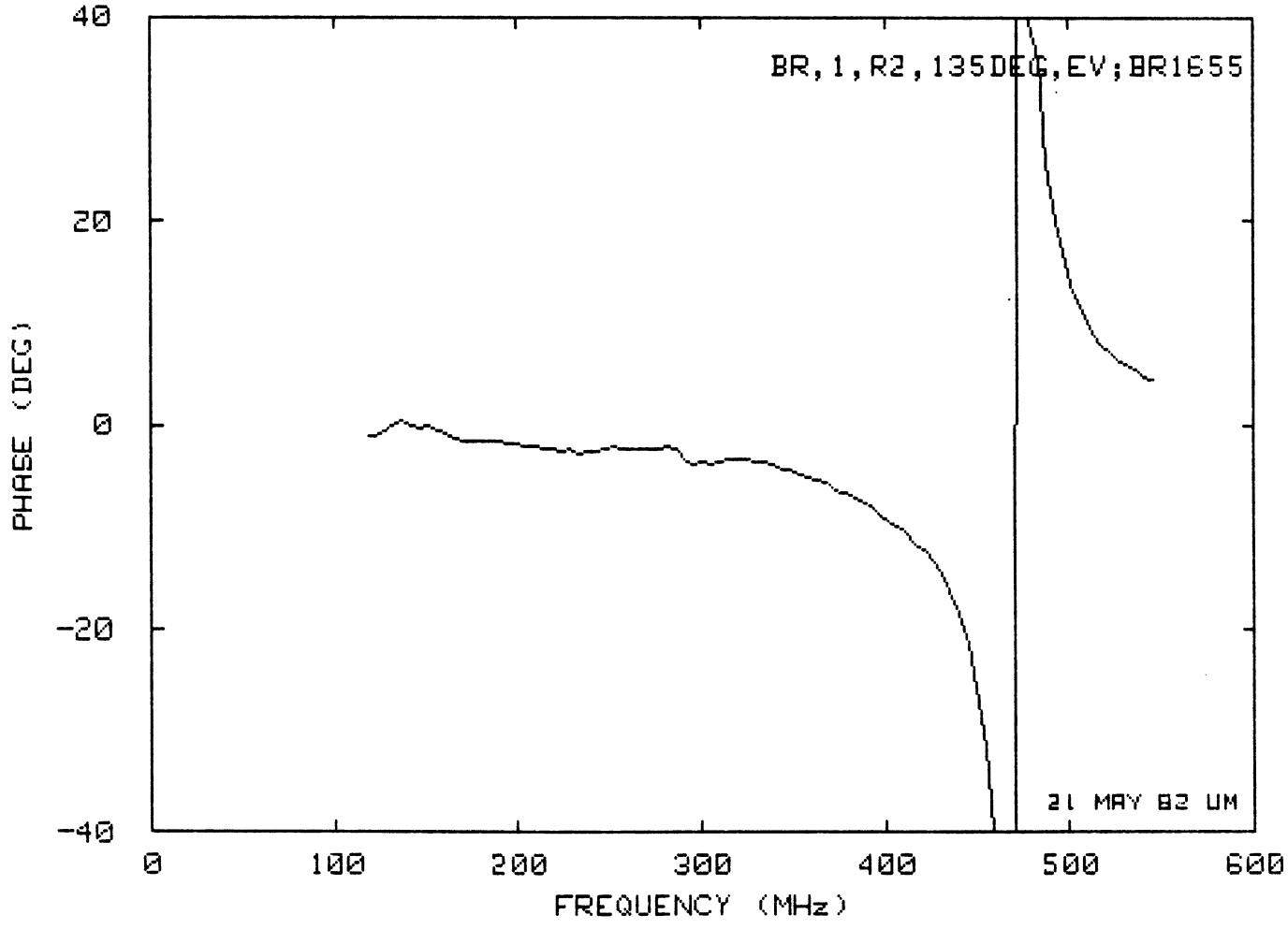
BR,1,R2,135DEG,EV;BR1655
21 MAY 82 UM
PHASE (DEG)
40
20
0
-20
-40
0
100
200
300
400
500
600
FREQUENCY (MHz)

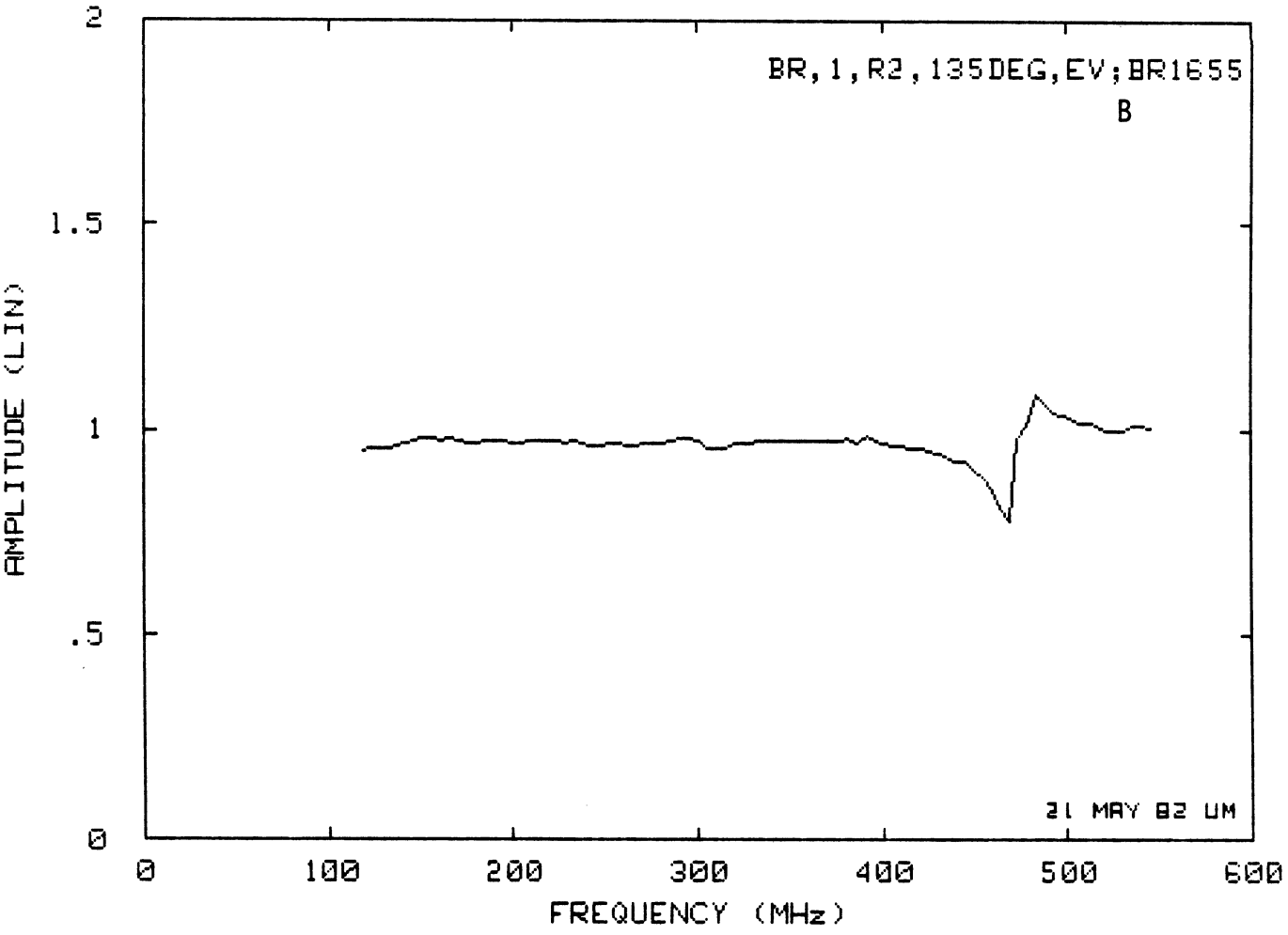
BR,1,R2,135DEG,EV;BR1655
B
21 MAY 82 UM
AMPLITUDE (LIN)
2
1.5
1
.5
0
0
100
200
300
400
500
600
FREQUENCY (MHz)

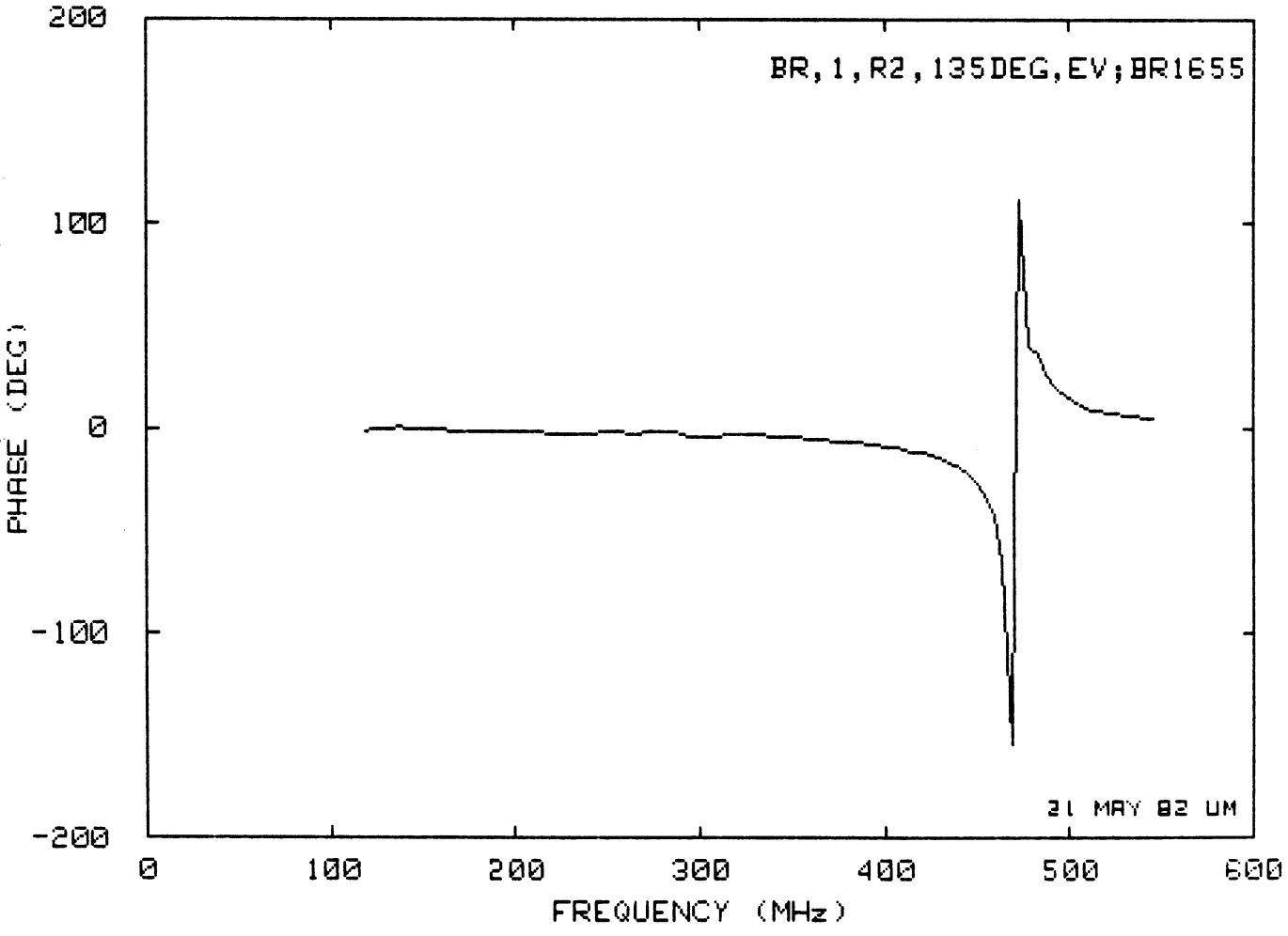
BR,1,R2,135DEG,EV;BR1655
21 MAY 82 UM
PHASE (DEG)
200
100
0
-100
-200
0
100
200
300
400
500
600
FREQUENCY (MHz)

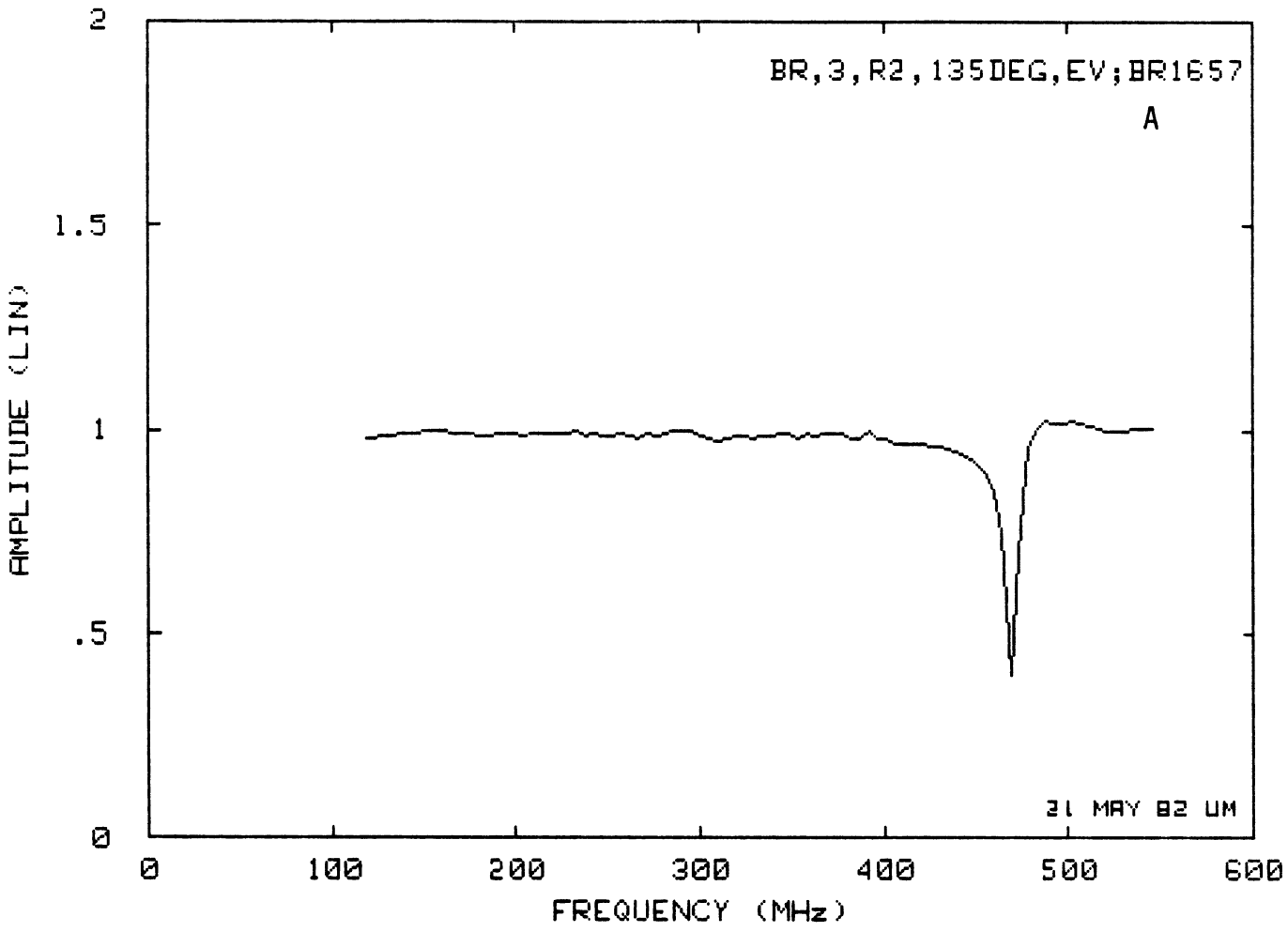
BR,3,R2,135DEG,EV;BR1657
A
21 MAY 82 UM
AMPLITUDE (LIN)
2
1.5
1
.5
0
0
100
200
300
400
500
600
FREQUENCY (MHz)

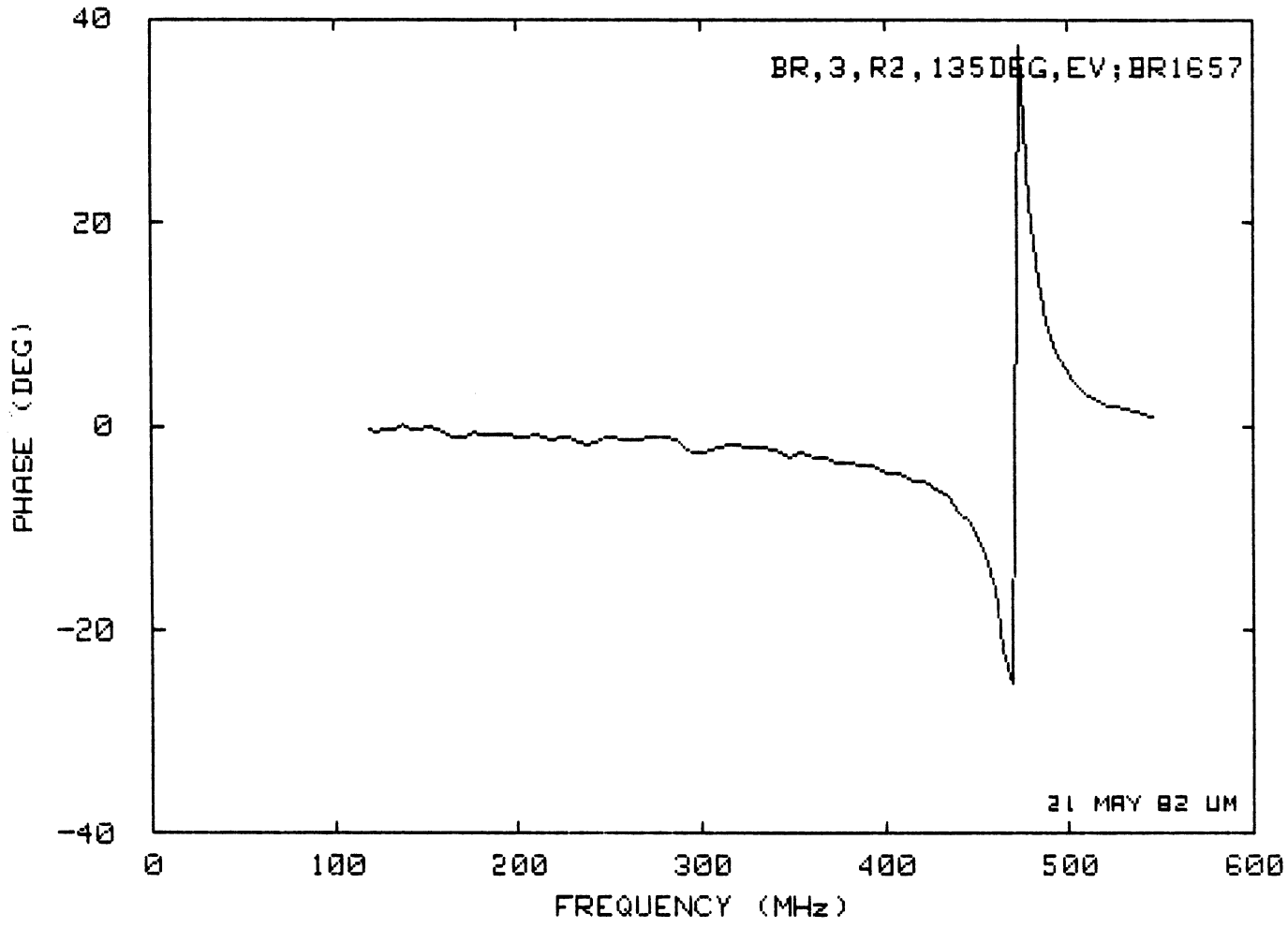
BR,3,R2,135DEG,EV;BR1657
21 MAY 82 UM
PHASE (DEG)
40
20
0
-20
-40
0
100
200
300
400
500
600
FREQUENCY (MHz)

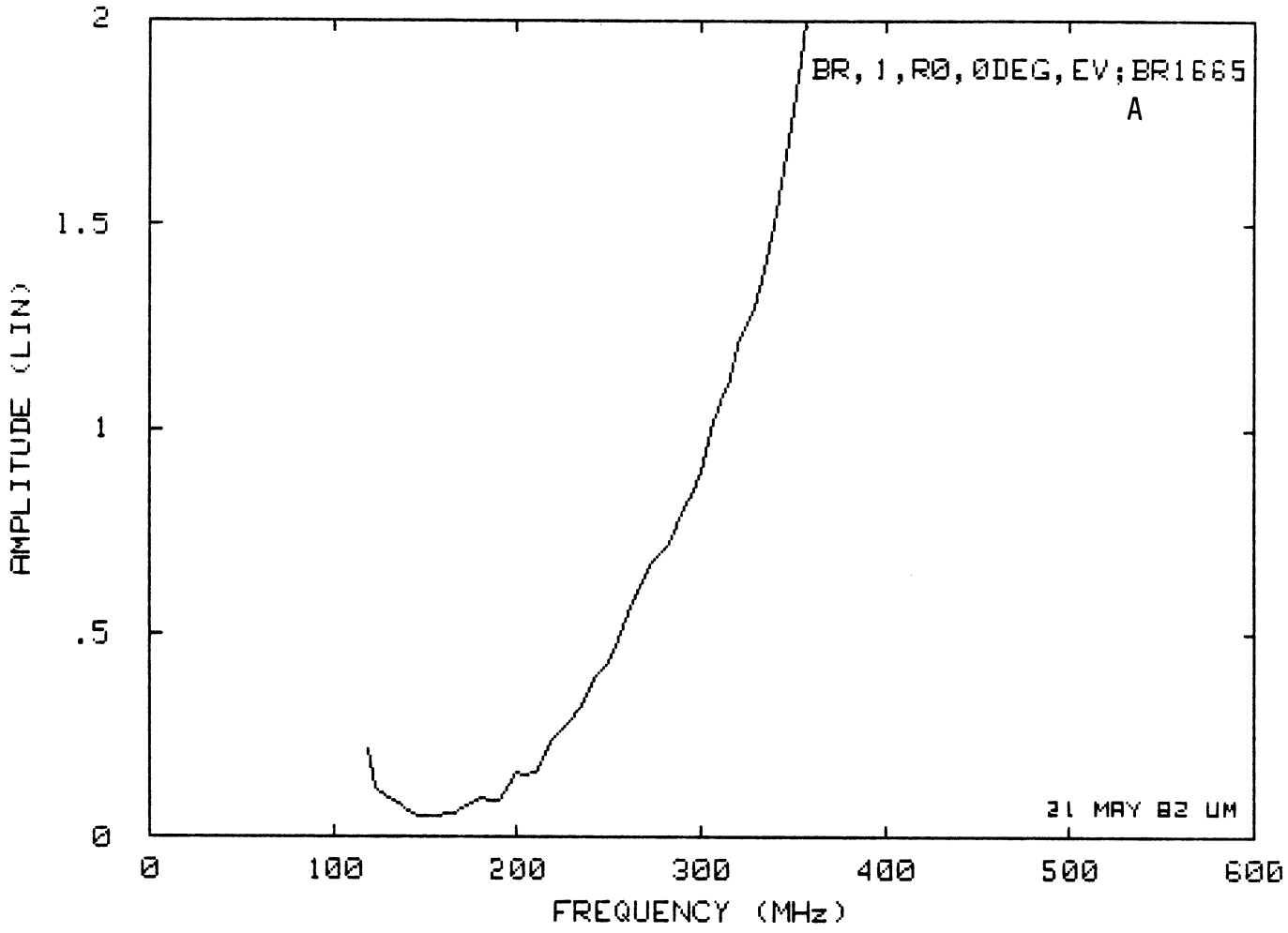
BR,1,R0,0DEG,EV;BR1665
A
21 MAY 82 UM
AMPLITUDE (LIN)
2
1.5
1
.5
0
0
100
200
300
400
500
600
FREQUENCY (MHz)

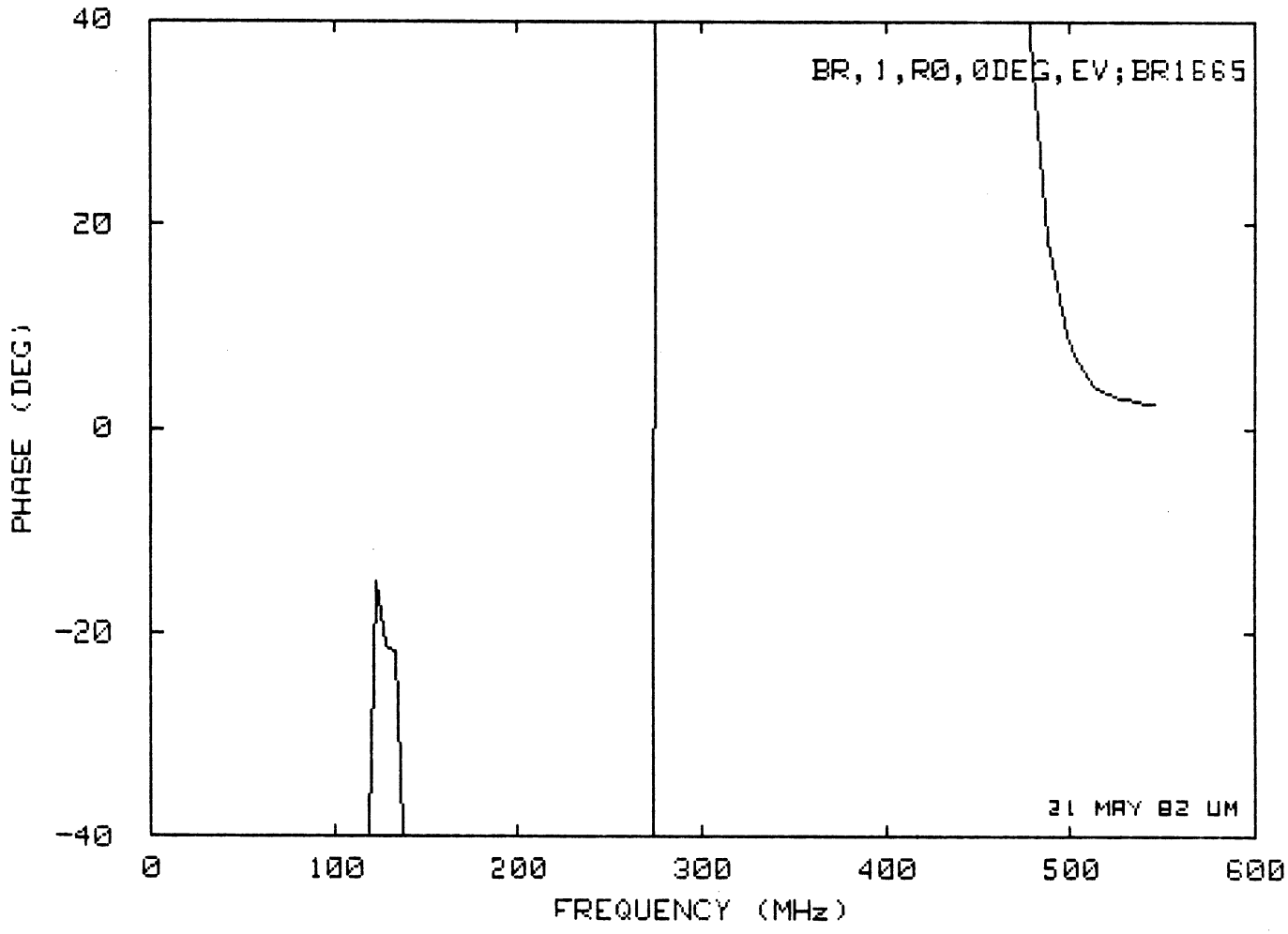
BR,1,R0,0DEG,EV;BR1665
21 MAY 82 UM
PHASE (DEG)
40
20
0
-20
-40
0
100
200
300
400
500
600
FREQUENCY (MHz)

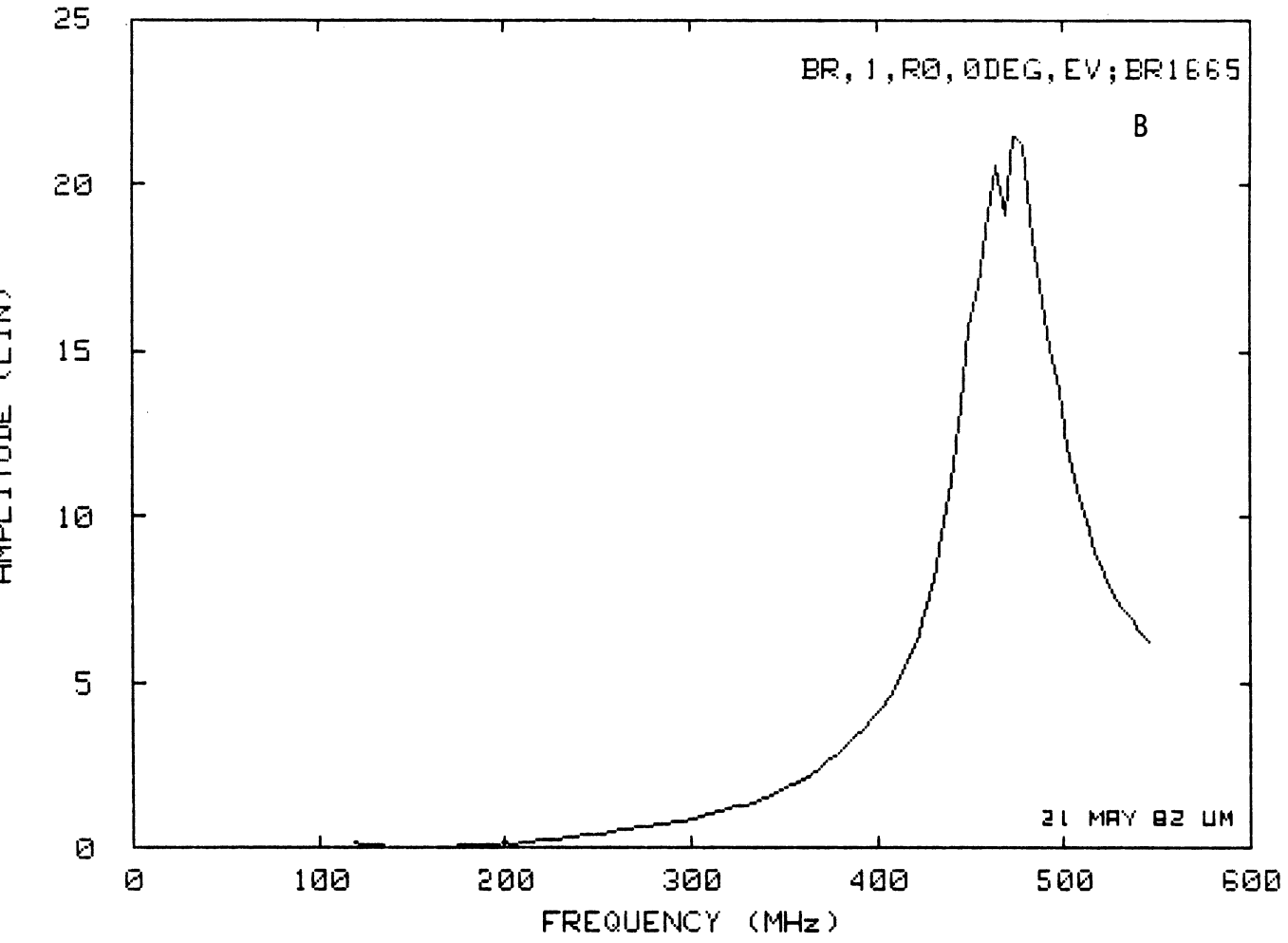
BR,1,R0,0DEG,EV;BR1665
B
21 MAY 82 UM
AMPLITUDE (LIN)
25
20
15
10
5
0
0
100
200
300
400
500
600
FREQUENCY (MHz)

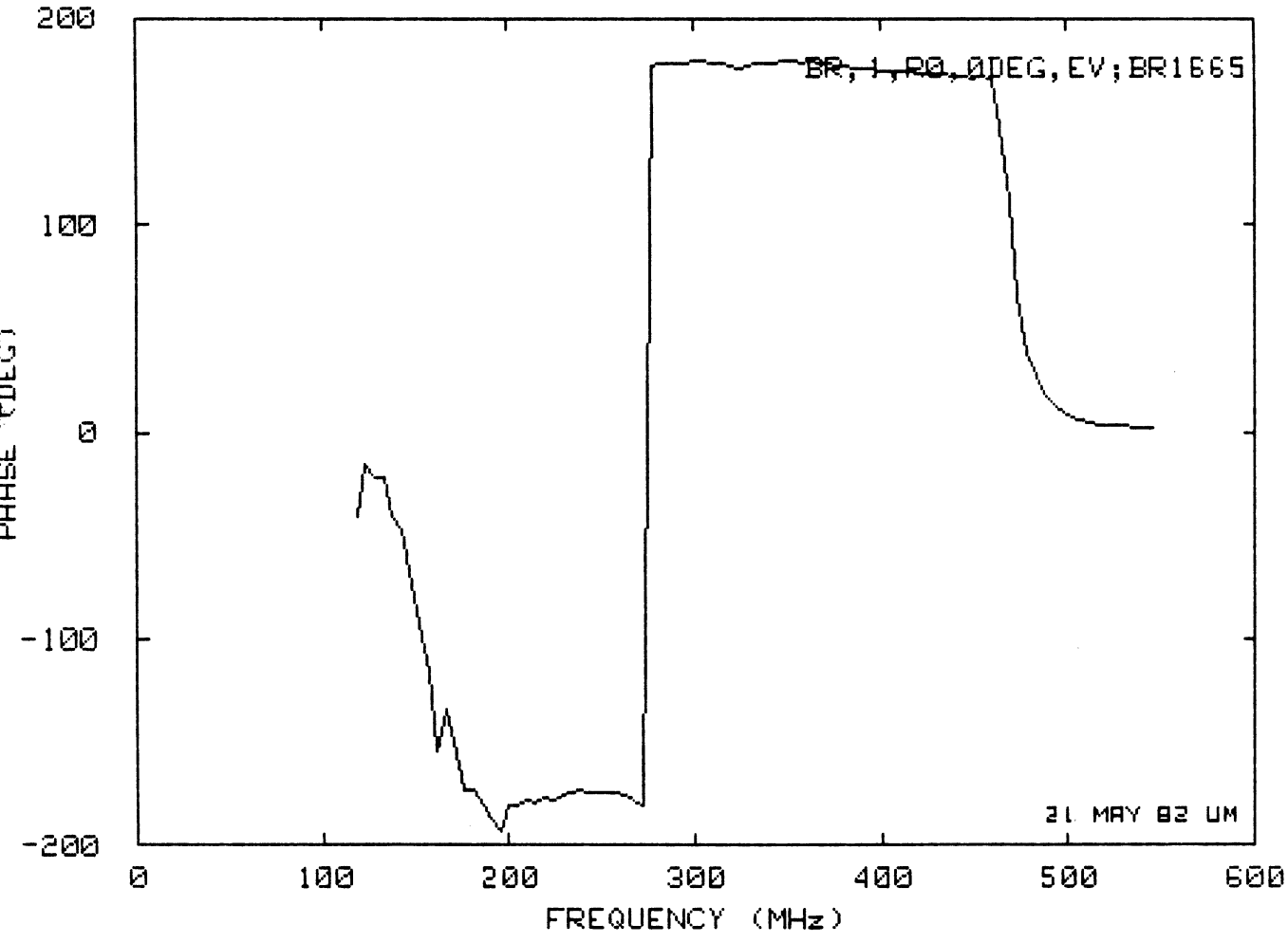
BR,1,R0,0DEG,EV;BR1665
21 MAY 82 UM
PHASE (DEG)
200
100
0
-100
-200
0
100
200
300
400
500
600
FREQUENCY (MHz)

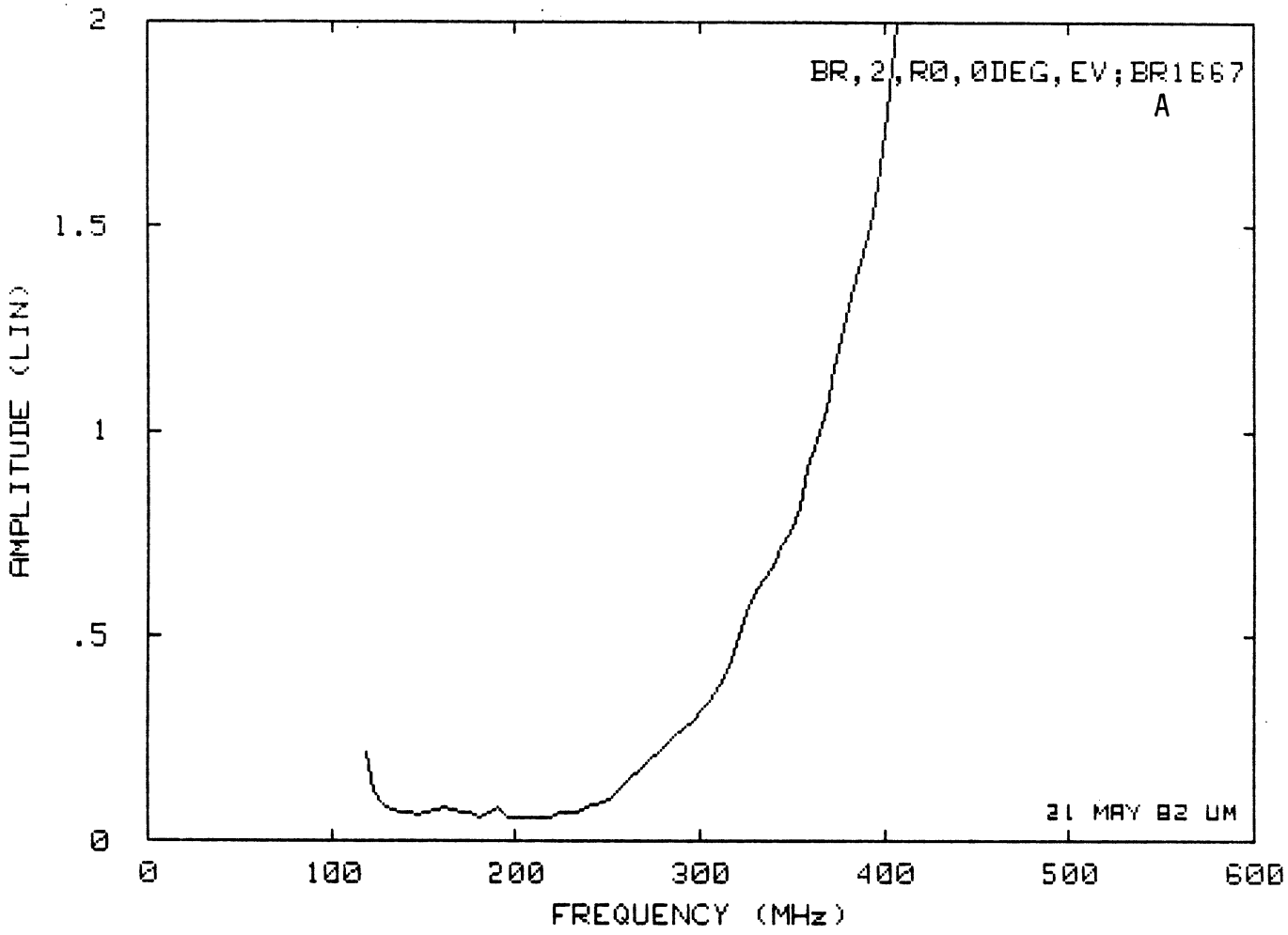
BR,2,R0,0DEG,EV;BR1667
A
21 MAY 82 UM
AMPLITUDE (LIN)
2
1.5
1
.5
0
0
100
200
300
400
500
600
FREQUENCY (MHz)

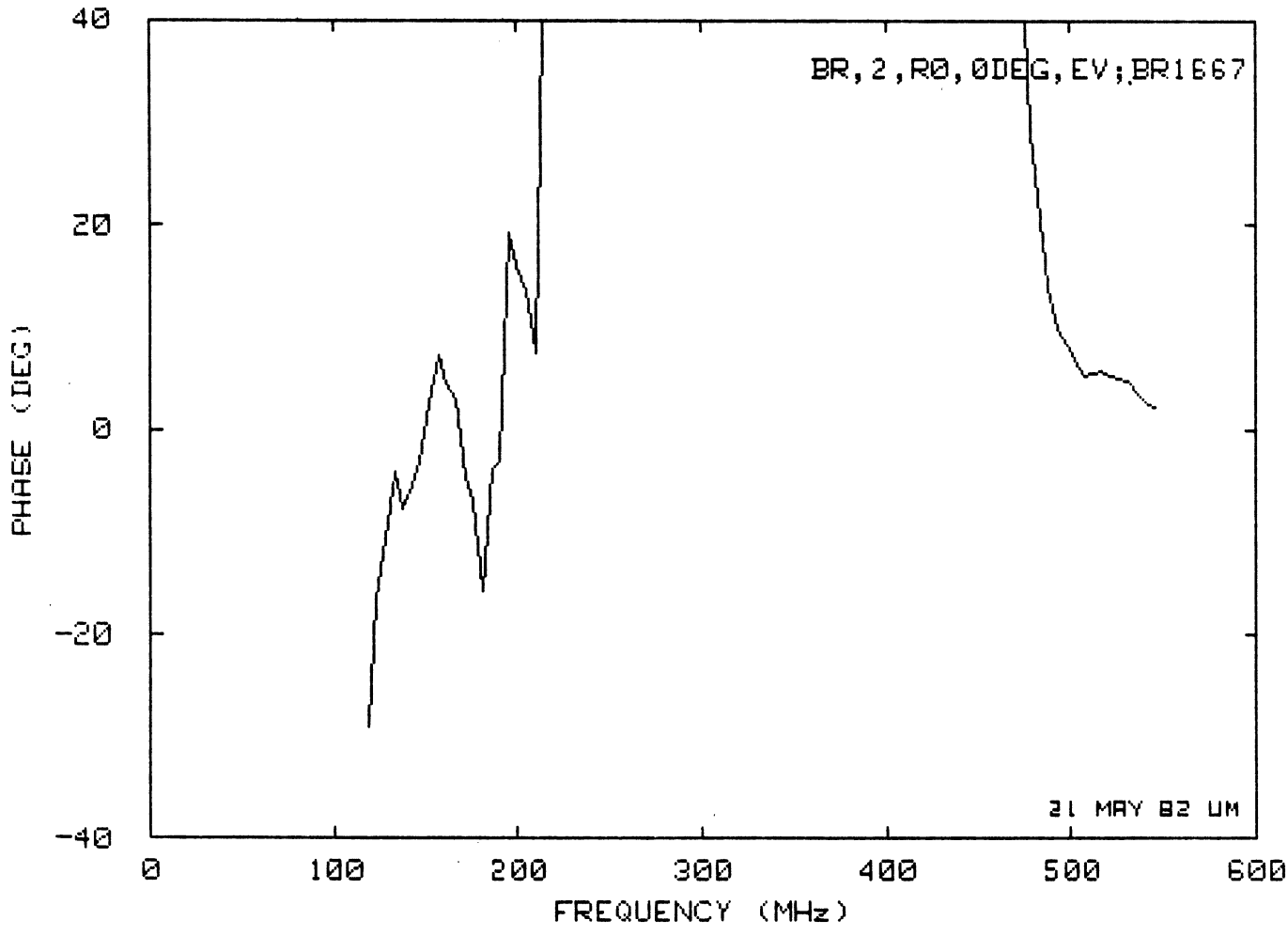
BR,2,R0,0DEG,EV;BR1667
21 MAY 82 UM
PHASE (DEG)
40
20
0
-20
-40
0
100
200
300
400
500
600
FREQUENCY (MHz)

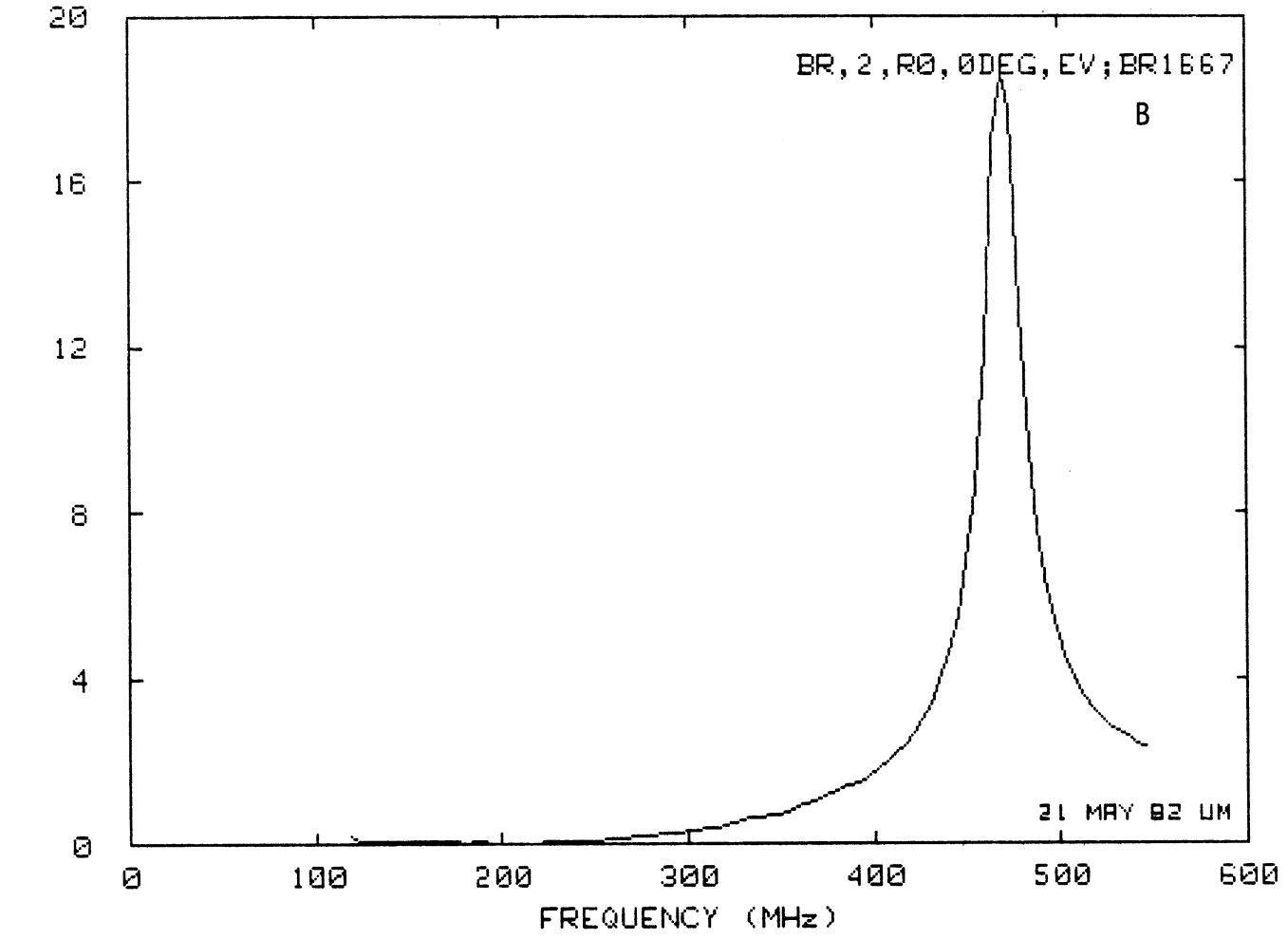
BR,2,R0,0DEG,EV;BR1667
B
21 MAY 82 UM
20
16
12
8
4
0
0
100
200
300
400
500
600
FREQUENCY (MHz)

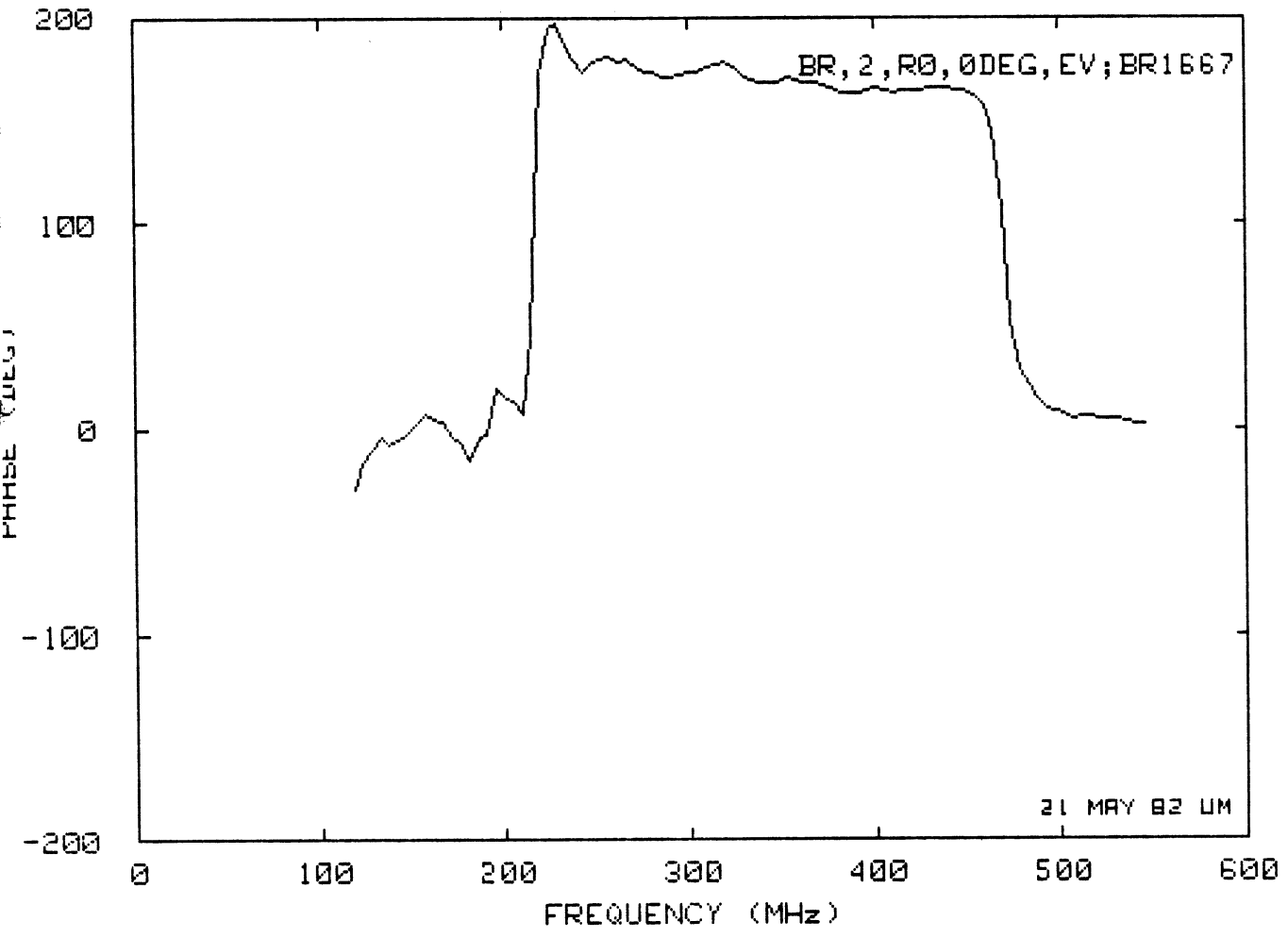
BR,2,R0,0DEG,EV;BR1667
21 MAY 82 UM
200
100
0
-100
-200
0
100
200
300
400
500
600
FREQUENCY (MHz)

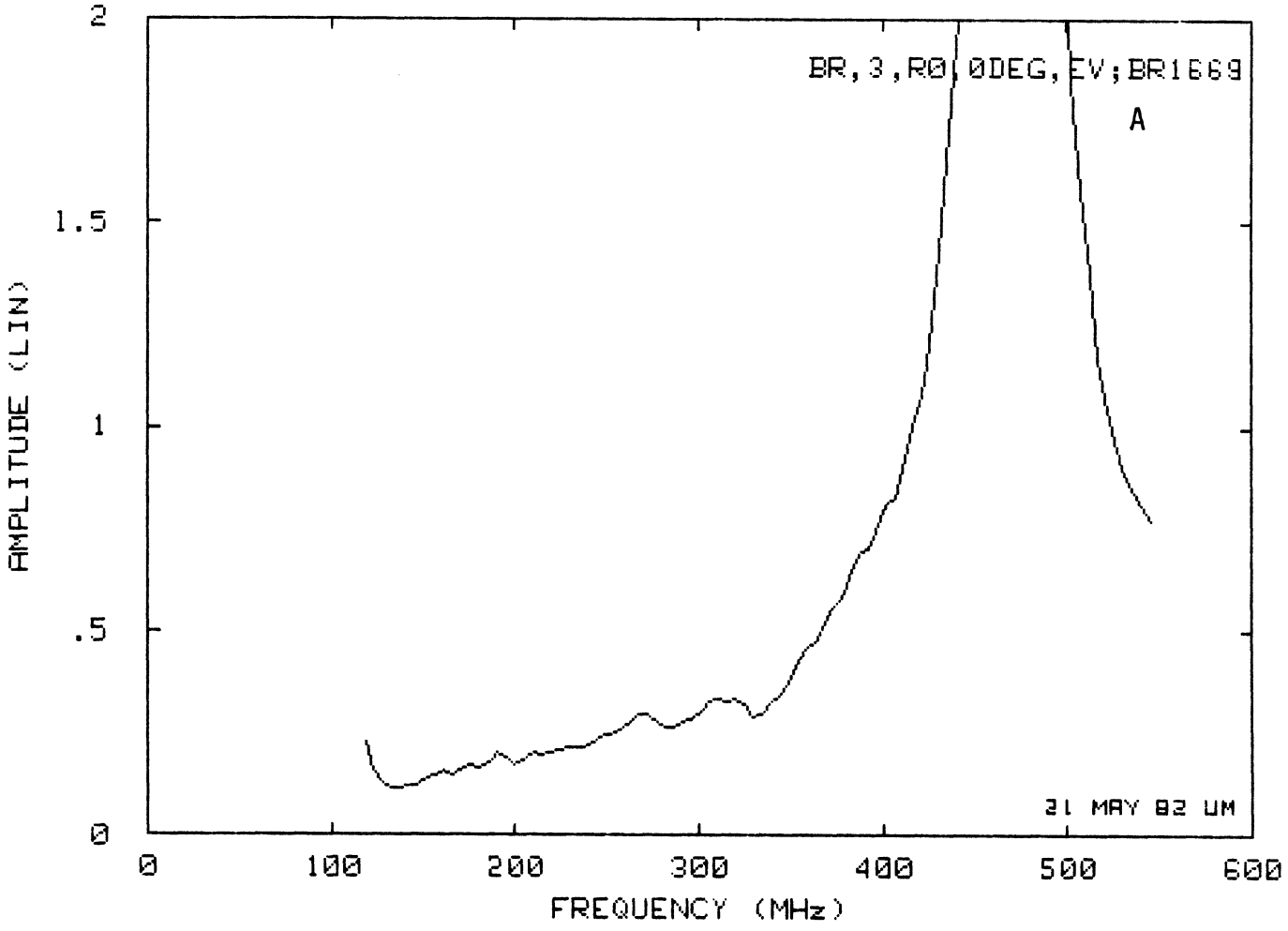
BR,3,R0,0DEG,EV;BR1669
A
21 MAY 82 UM
AMPLITUDE (LIN)
2
1.5
1
.5
0
0
100
200
300
400
500
600
FREQUENCY (MHz)

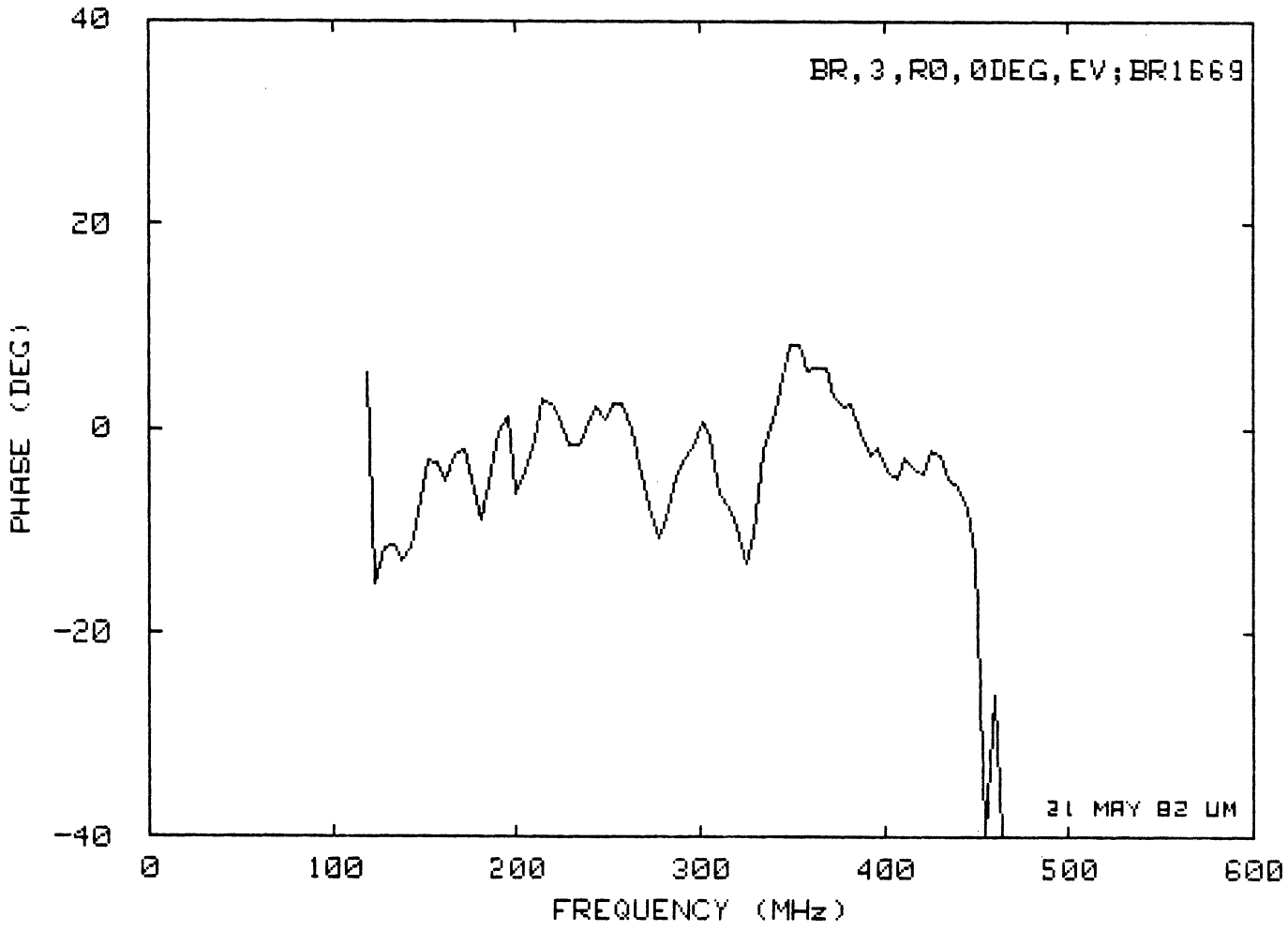
BR,3,R0,0DEG,EV;BR1669
21 MAY 82 UM
PHASE (DEG)
40
20
0
-20
-40
0
100
200
300
400
500
600
FREQUENCY (MHz)

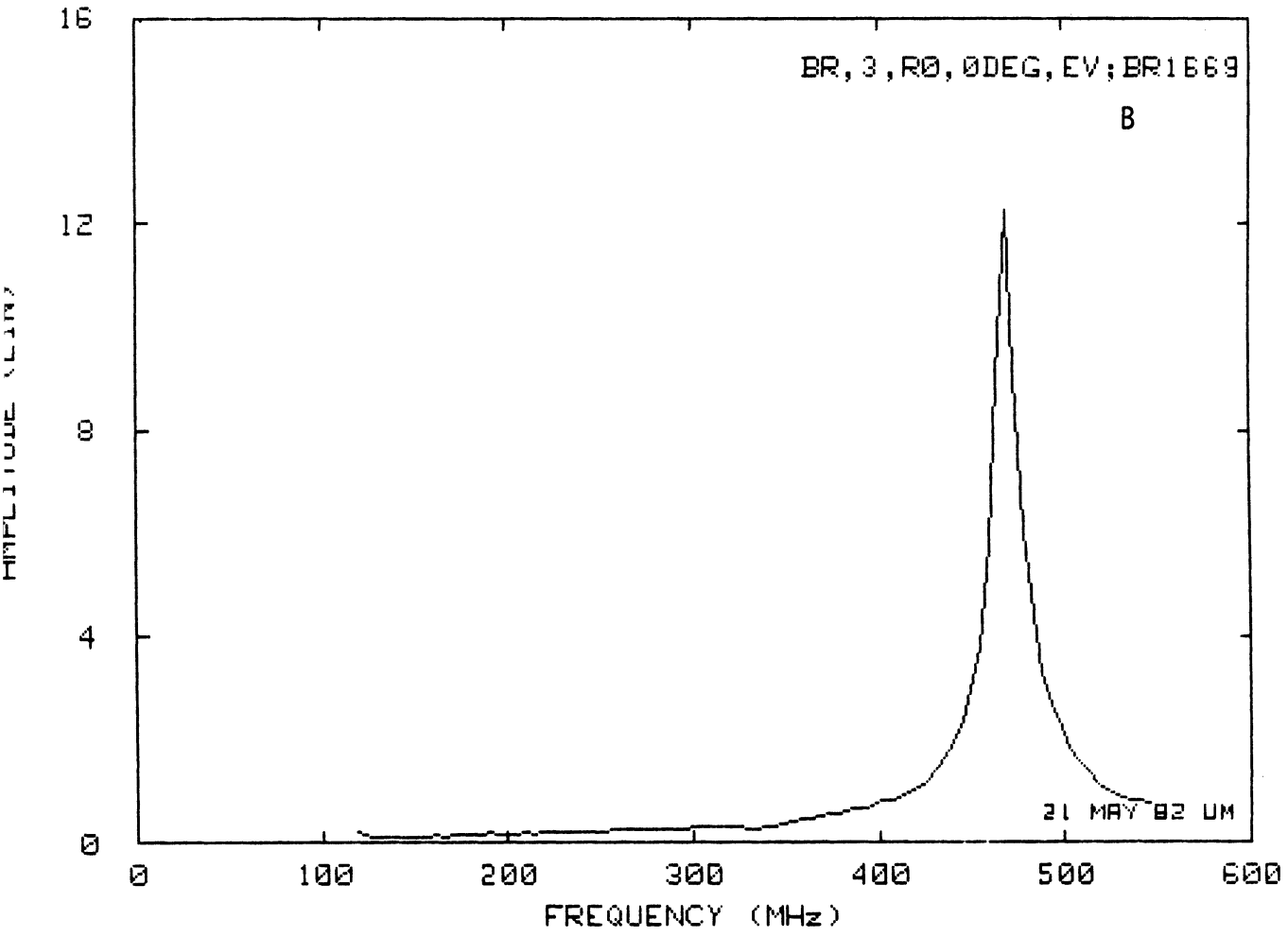
BR,3,R0,0DEG,EV;BR1669
B
21 MAY 82 UM
16
12
8
4
0
0
100
200
300
400
500
600
FREQUENCY (MHz)

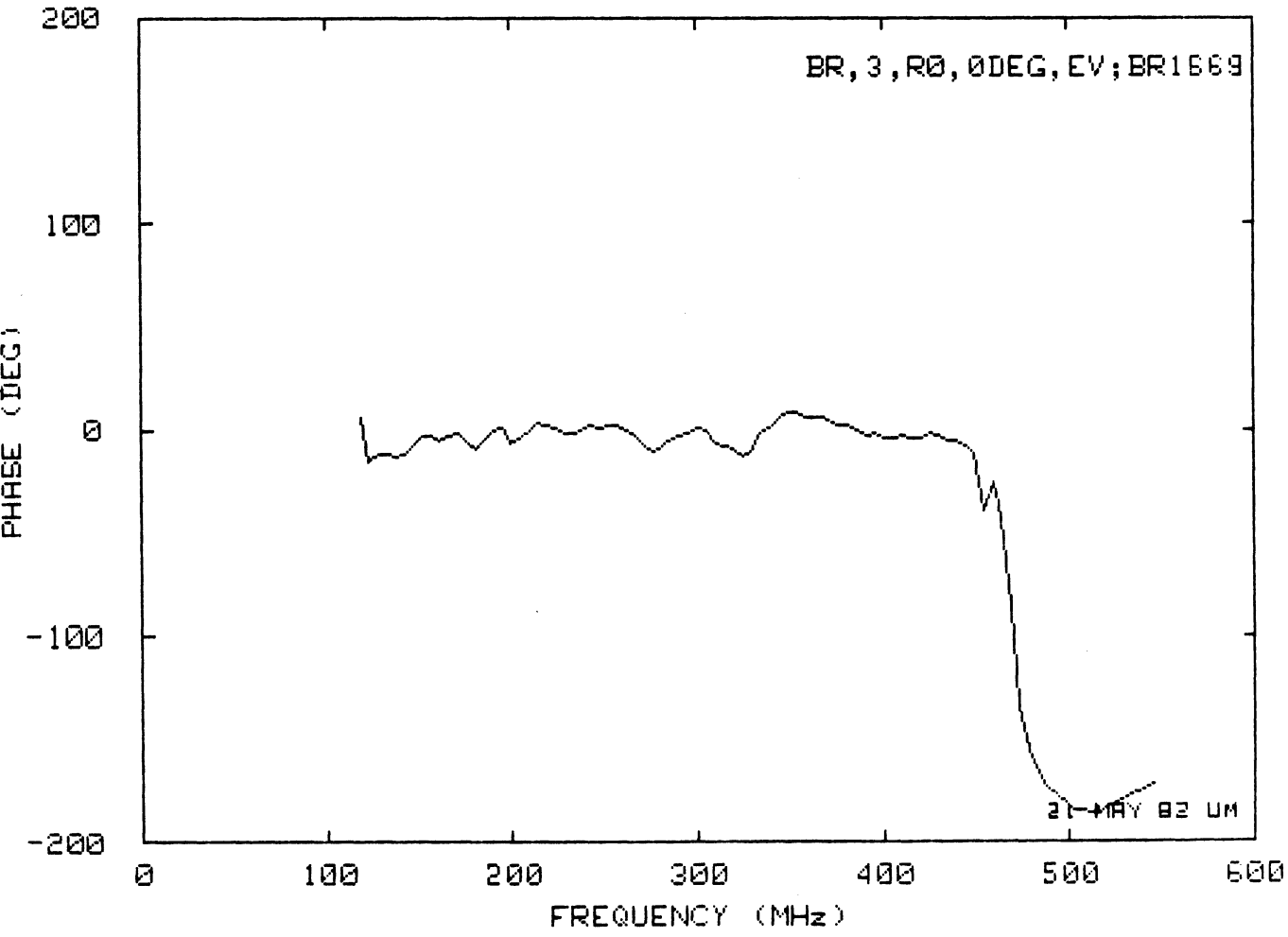
BR,3,R0,0DEG,EV;BR1669
21 MAY 82 UM
200
100
0
-100
-200
PHASE (DEG)
0
100
200
300
400
500
600
FREQUENCY (MHz)

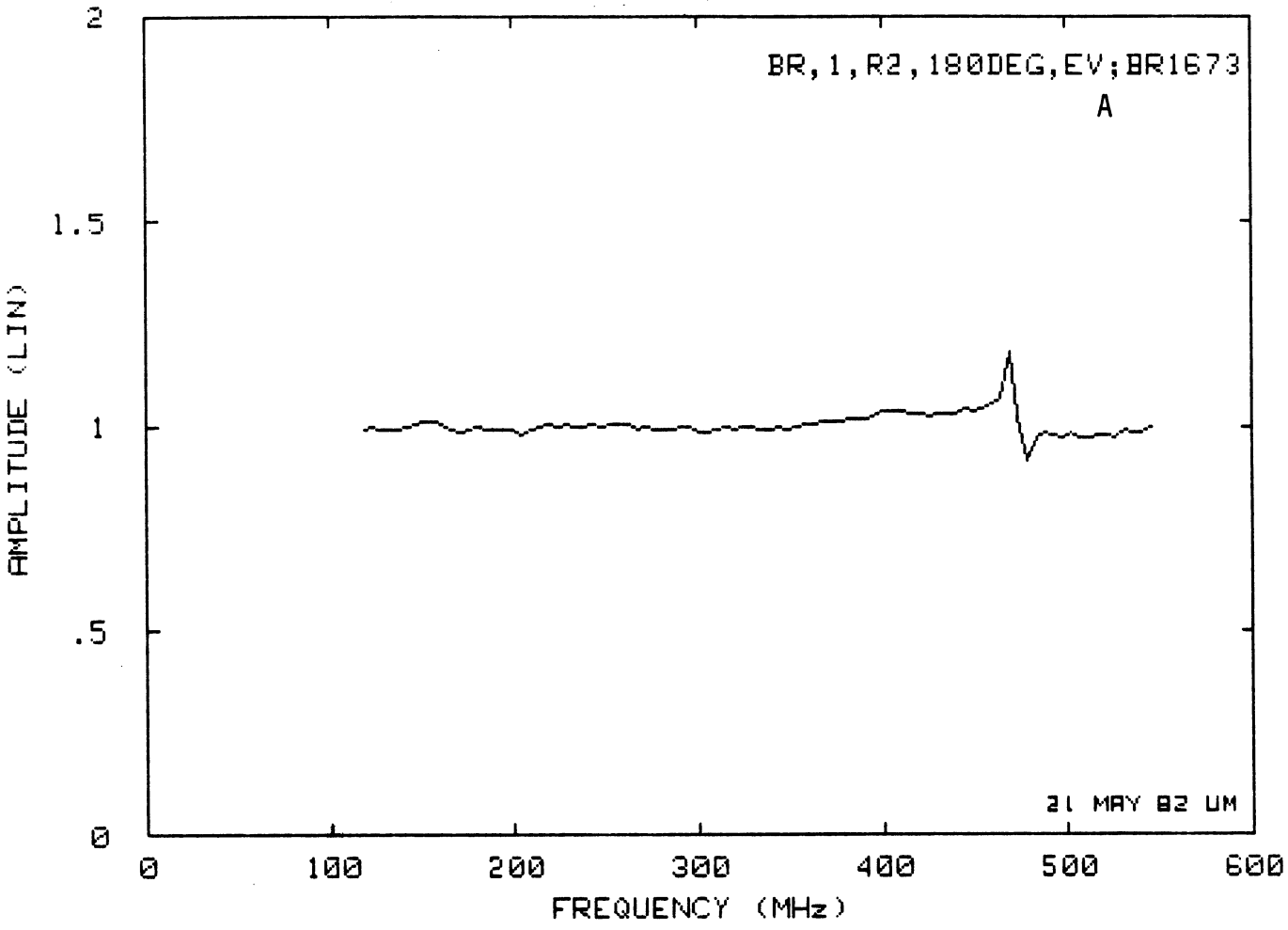
BR,1,R2,180DEG,EV;BR1673
A
21 MAY 82 UM
AMPLITUDE (LIN)
2
1.5
1
.5
0
0
100
200
300
400
500
600
FREQUENCY (MHz)

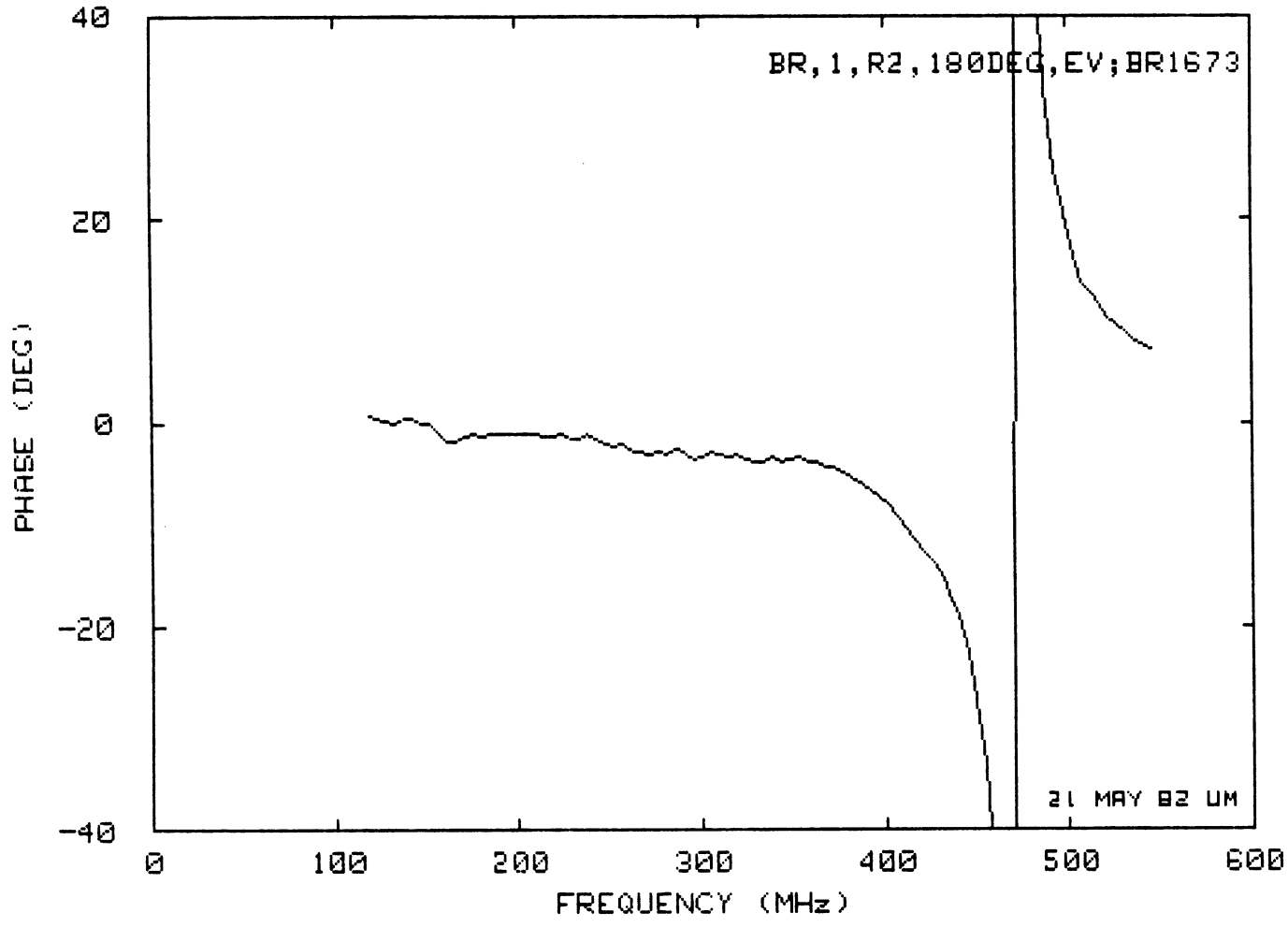
BR,1,R2,180DEG,EV;BR1673
21 MAY 82 UM
PHASE (DEG)
40
20
0
-20
-40
0
100
200
300
400
500
600
FREQUENCY (MHz)

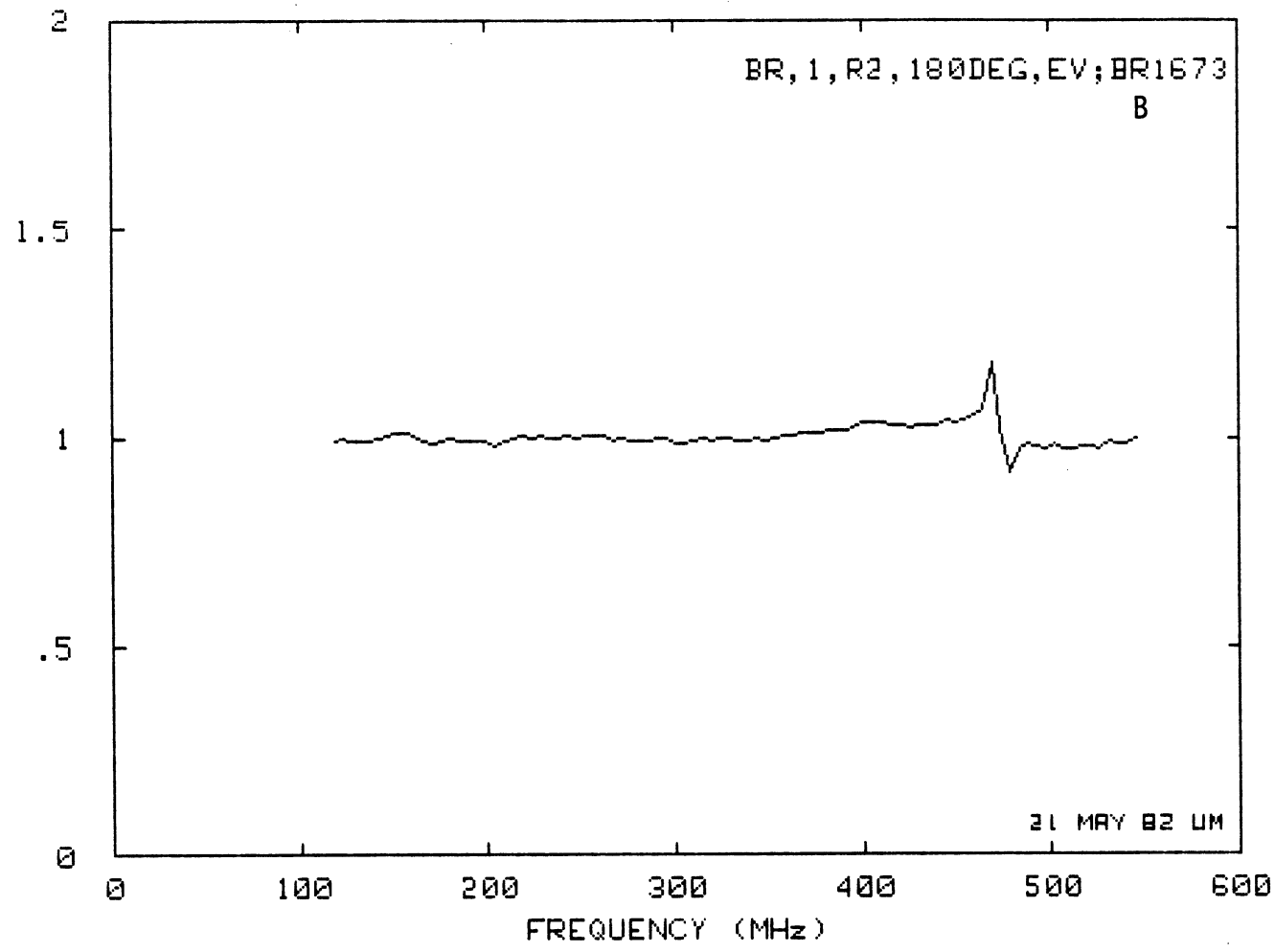
BR,1,R2,180DEG,EV;BR1673
B
21 MAY 82 UM
2
1.5
1
.5
0
0
100
200
300
400
500
600
FREQUENCY (MHz)

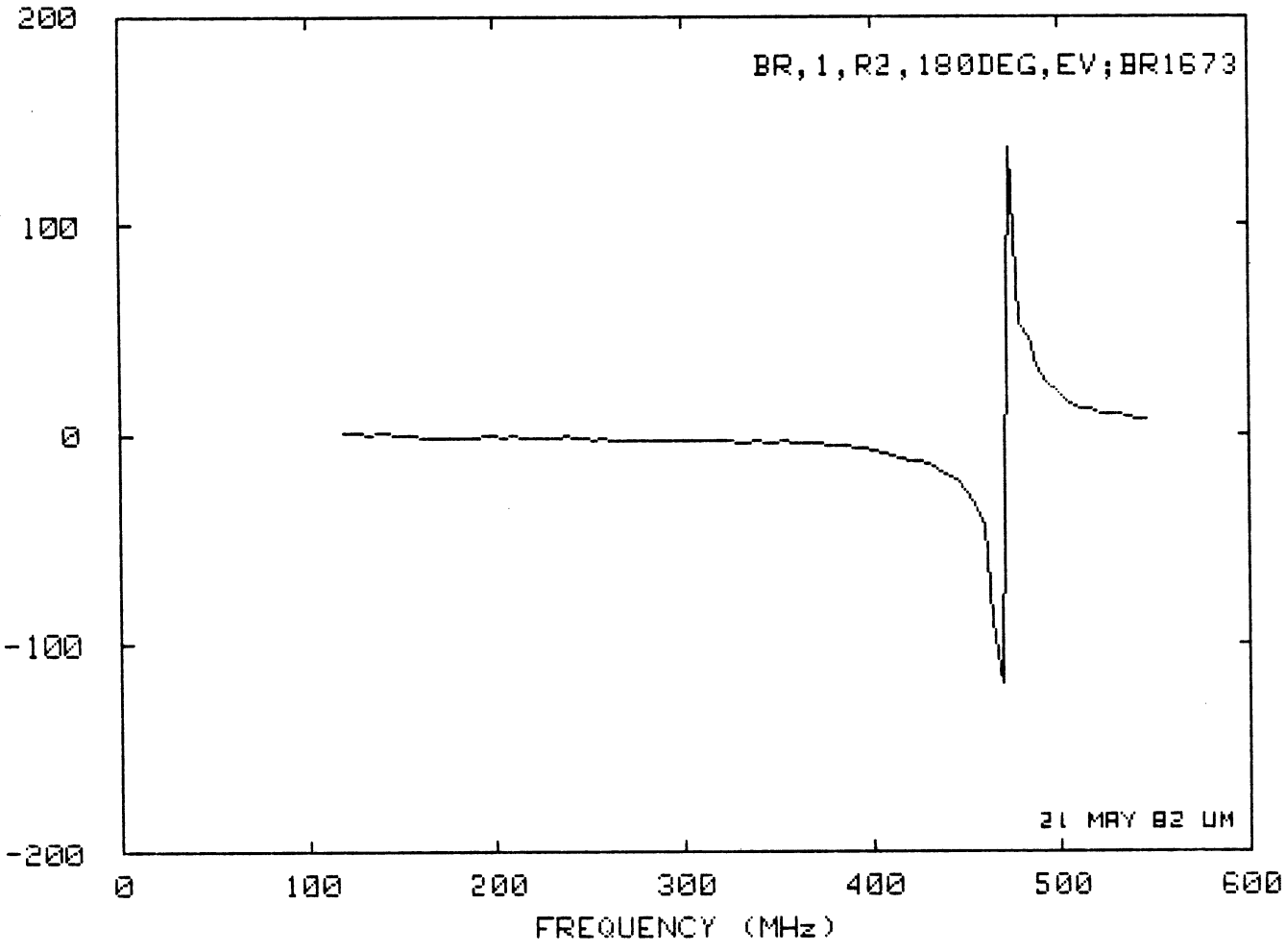
BR,1,R2,180DEG,EV;BR1673
21 MAY 82 UM
200
100
0
-100
-200
0
100
200
300
400
500
600
FREQUENCY (MHz)

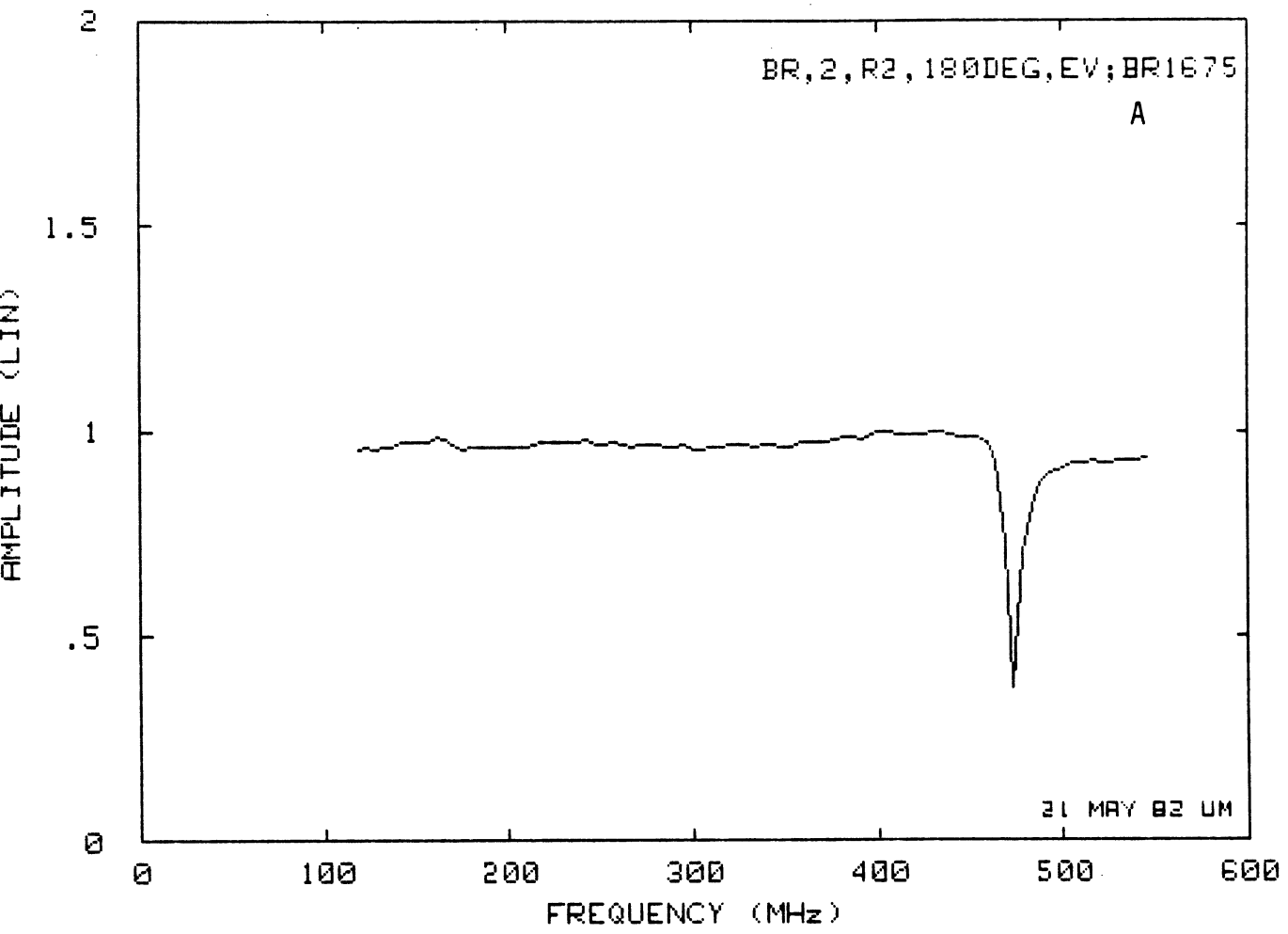
BR,2,R2,180DEG,EV;BR1675
A
21 MAY 82 UM
AMPLITUDE (LIN)
2
1.5
1
.5
0
0
100
200
300
400
500
600
FREQUENCY (MHz)

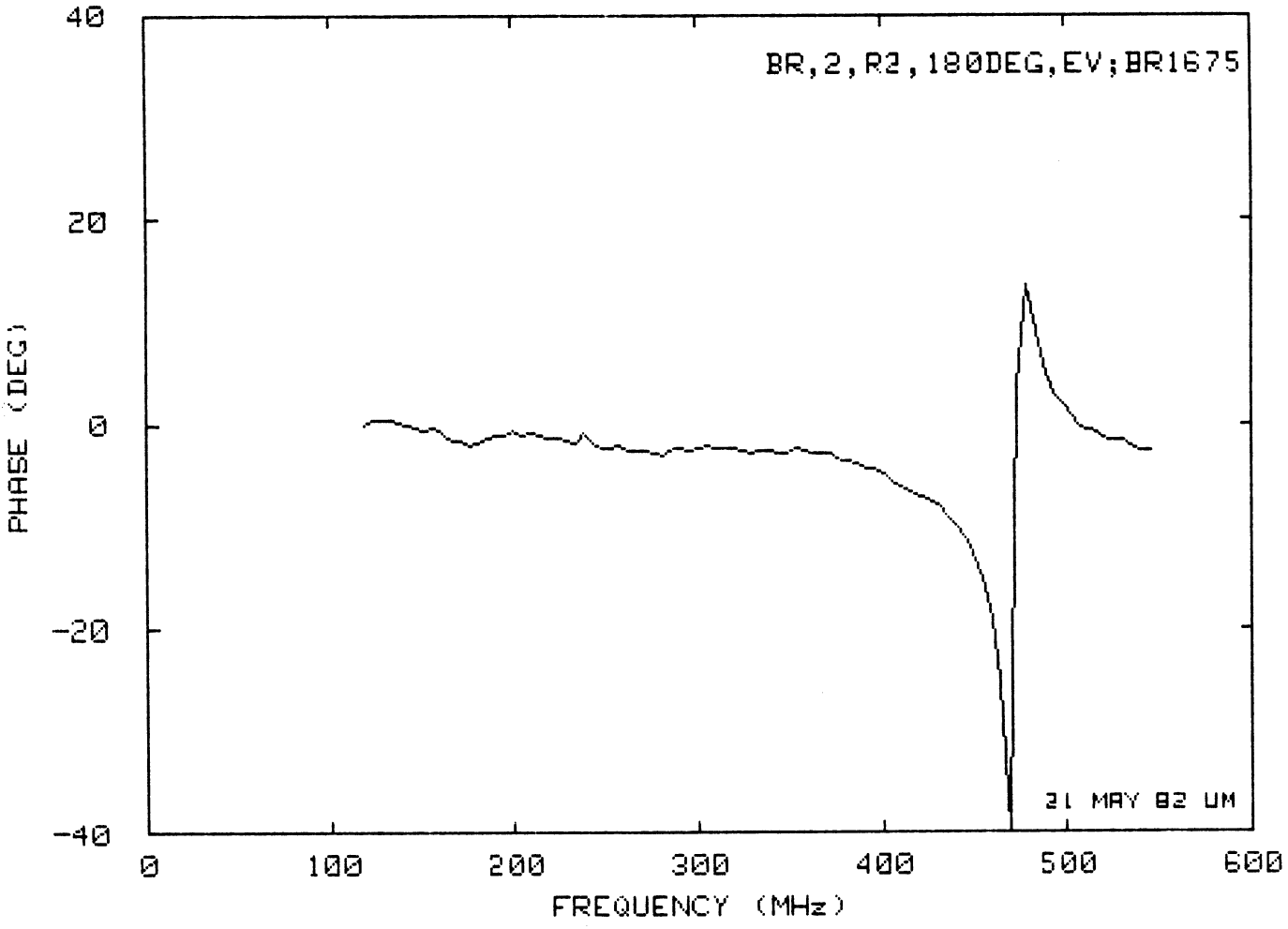
BR,2,R2,180DEG,EV;BR1675
21 MAY 82 UM
PHASE (DEG)
40
20
0
-20
-40
0
100
200
300
400
500
600
FREQUENCY (MHz)

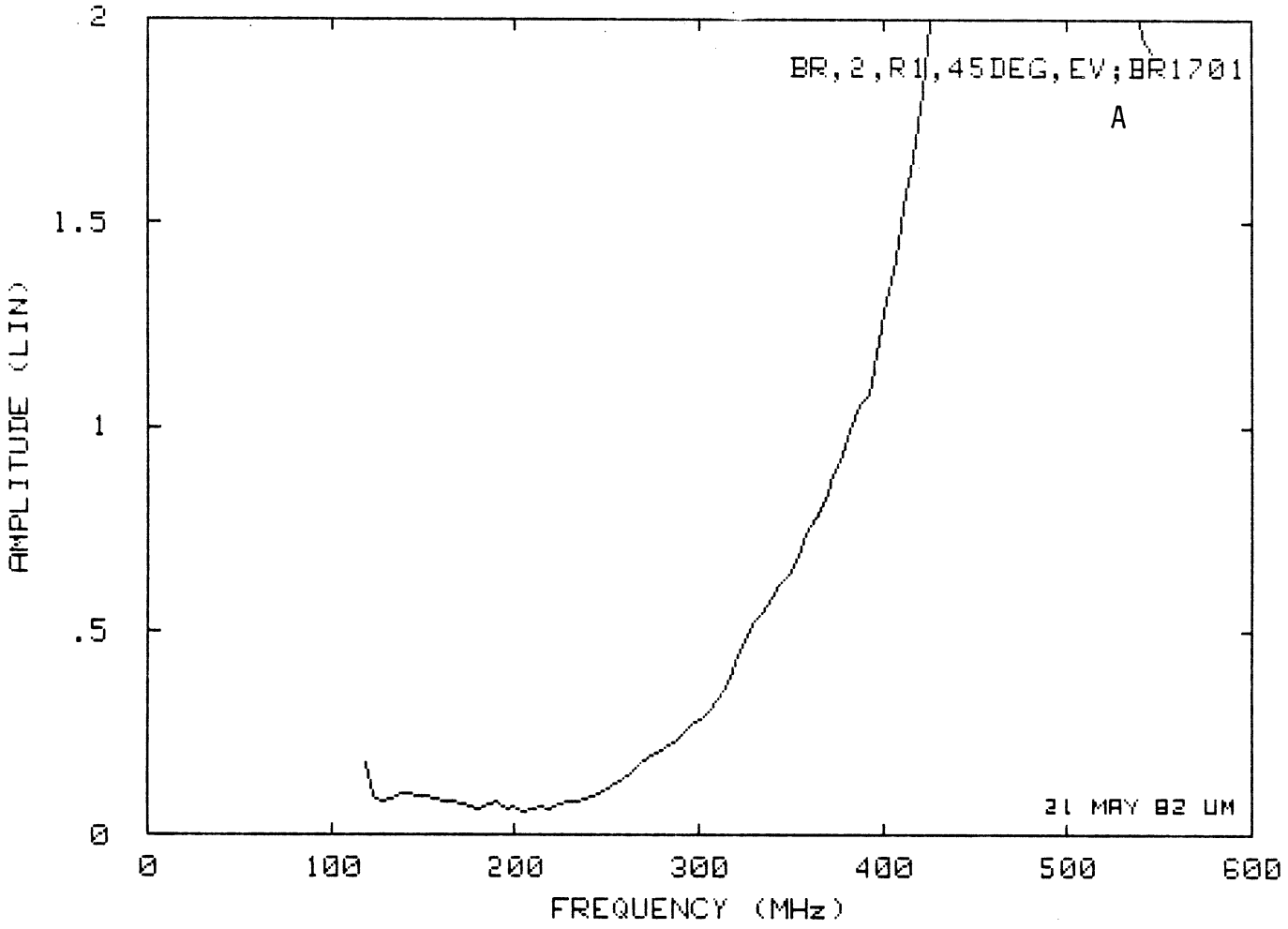
BR,2,R1,45DEG,EV;BR1701
A
21 MAY 82 UM
AMPLITUDE (LIN)
2
1.5
1
.5
0
0
100
200
300
400
500
600
FREQUENCY (MHz)

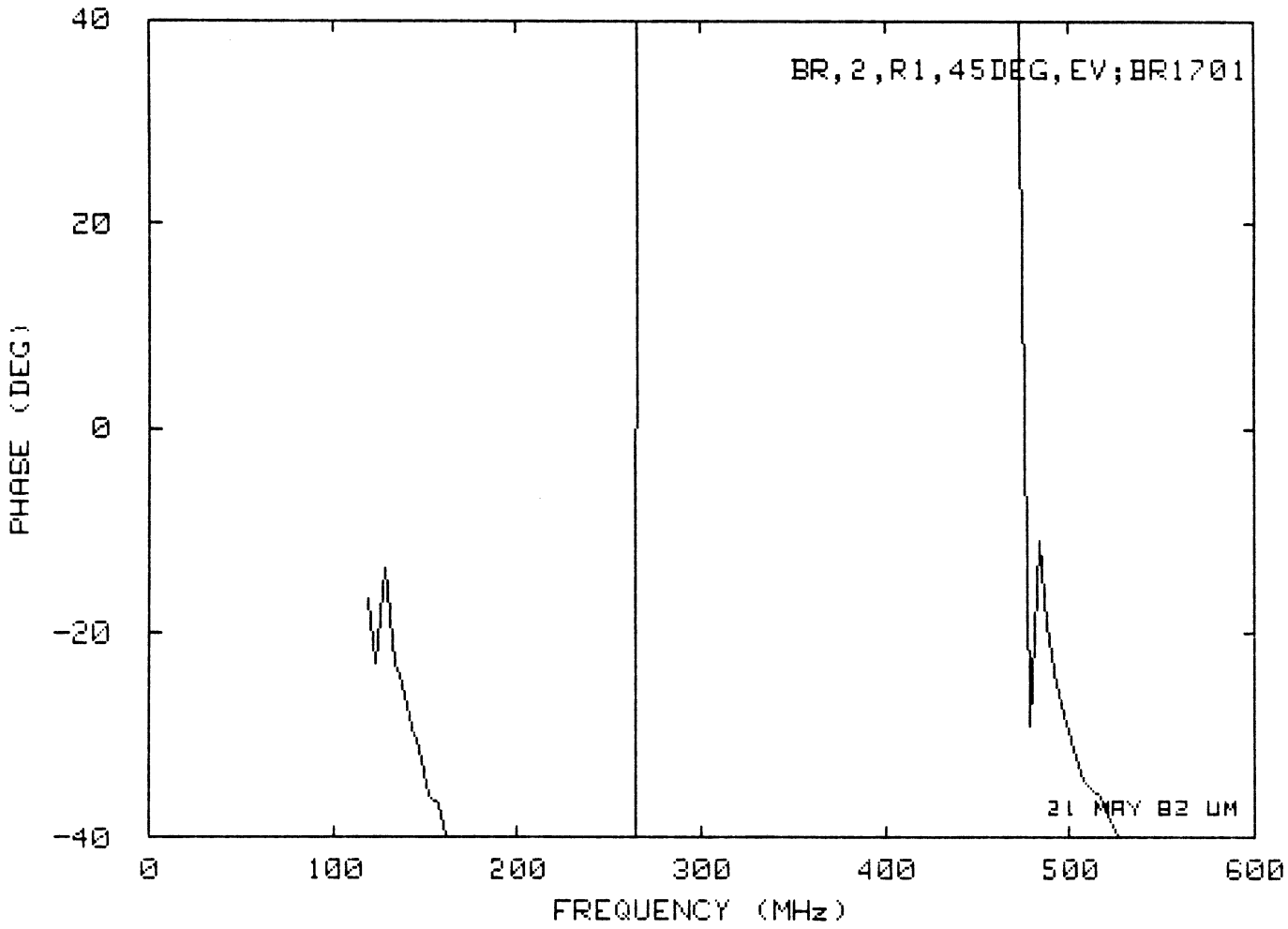
BR,2,R1,45DEG,EV;BR1701
21 MAY 82 UM
PHASE (DEG)
40
20
0
-20
-40
0
100
200
300
400
500
600
FREQUENCY (MHz)

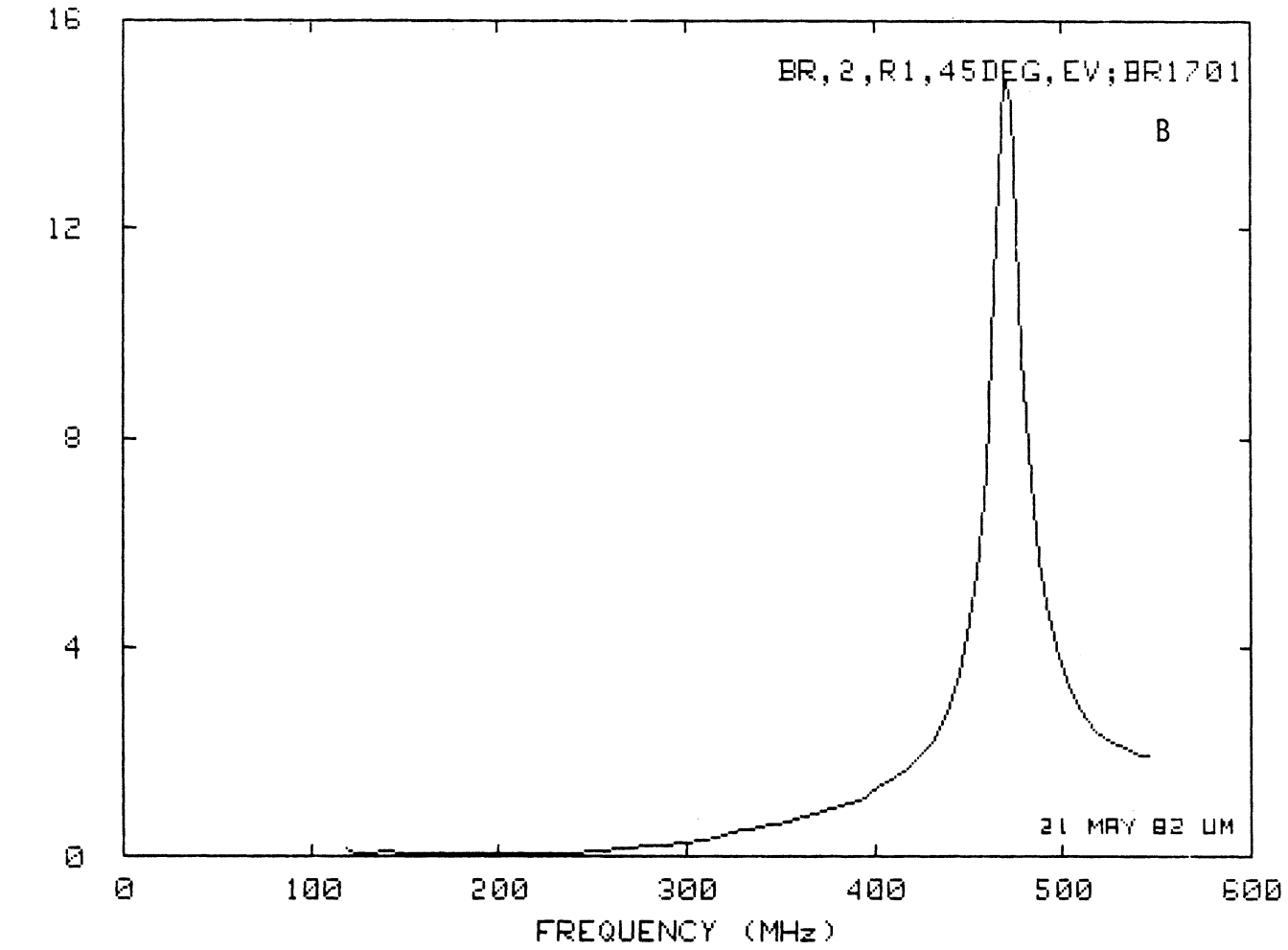
BR,2,R1,45DEG,EV;BR1701
B
21 MAY 82 UM
16
12
8
4
0
0
100
200
300
400
500
600
FREQUENCY (MHz)

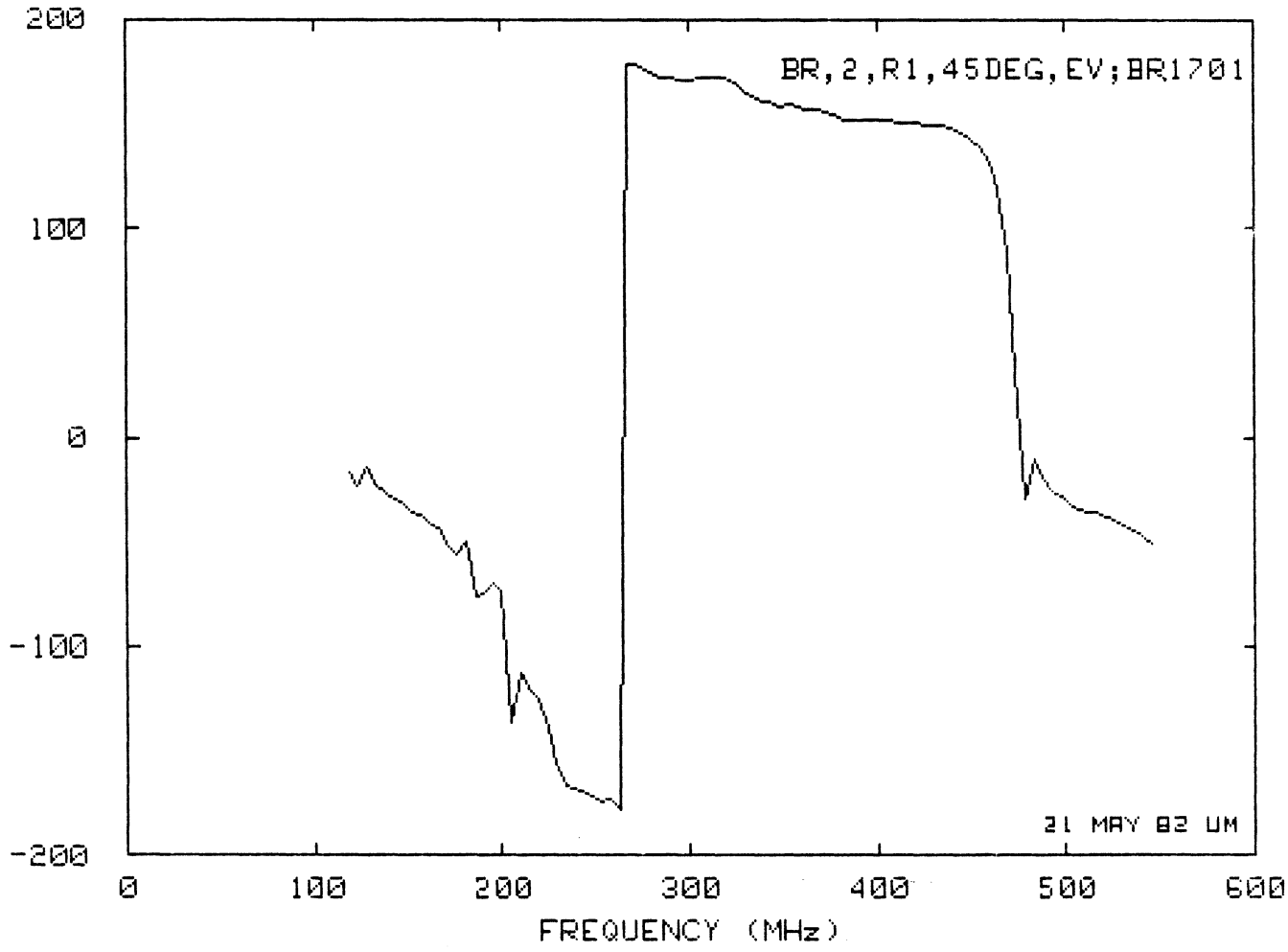
BR,2,R1,45DEG,EV;BR1701
21 MAY 82 UM
200
100
0
-100
-200
0
100
200
300
400
500
600
FREQUENCY (MHz)

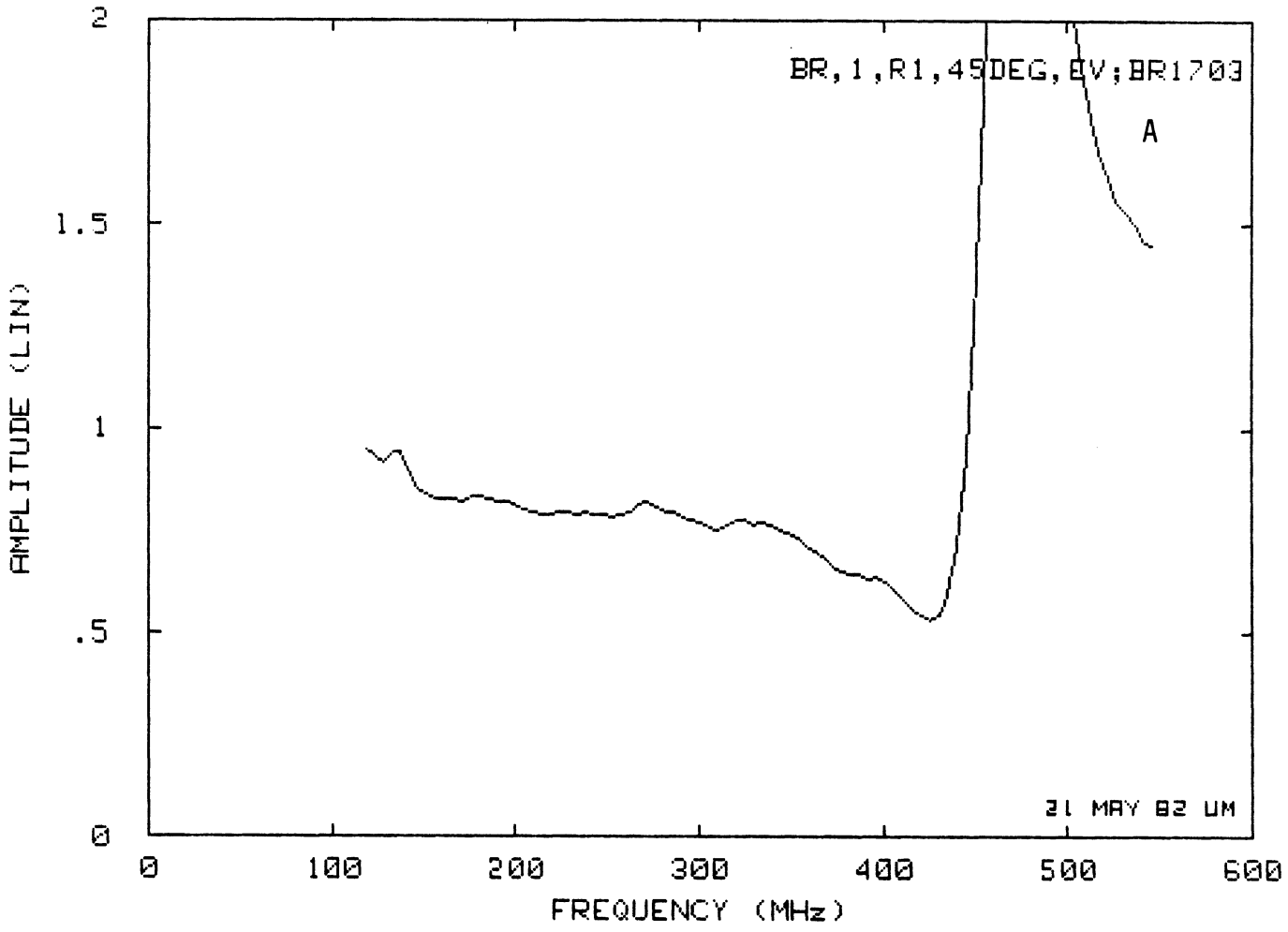
BR,1,R1,45DEG,EV;BR1703
A
21 MAY 82 UM
AMPLITUDE (LIN)
2
1.5
1
.5
0
0
100
200
300
400
500
600
FREQUENCY (MHz)

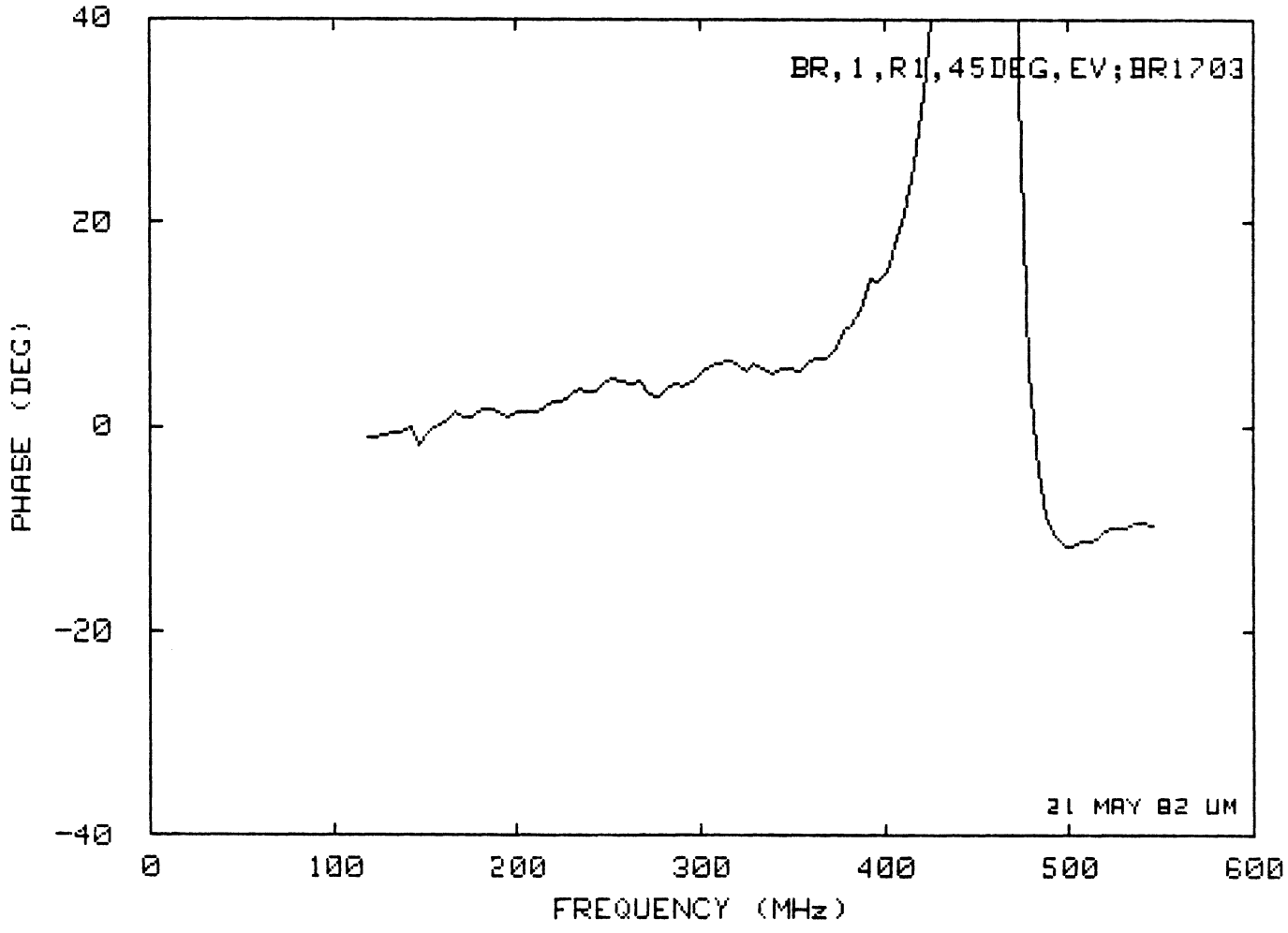
BR,1,R1,45DEG,EV;BR1703
21 MAY 82 UM
PHASE (DEG)
40
20
0
-20
-40
0
100
200
300
400
500
600
FREQUENCY (MHz)

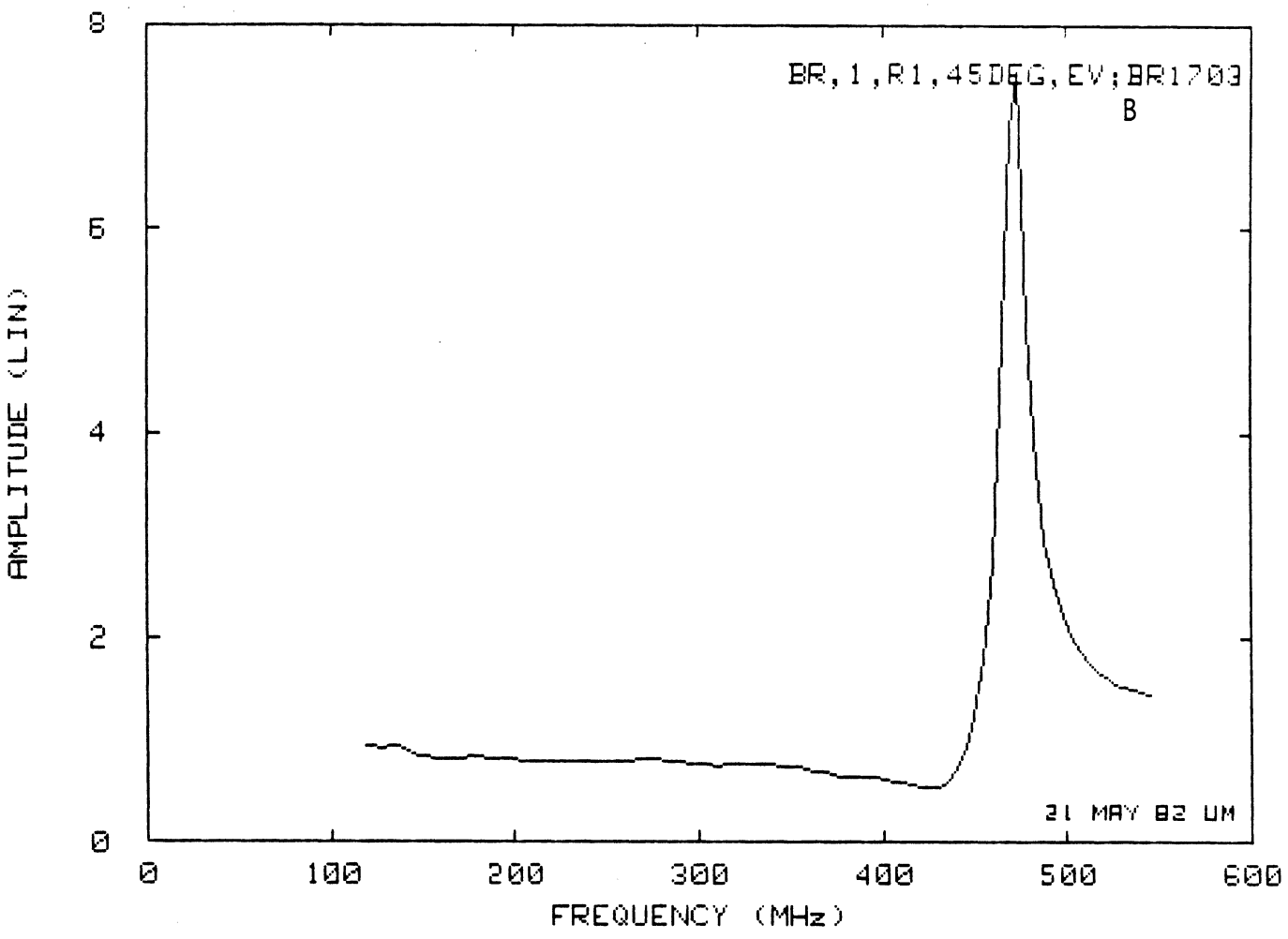
BR,1,R1,45DEG,EV;BR1703
B
21 MAY 82 UM
AMPLITUDE (LIN)
8
6
4
2
0
0
100
200
300
400
500
600
FREQUENCY (MHz)

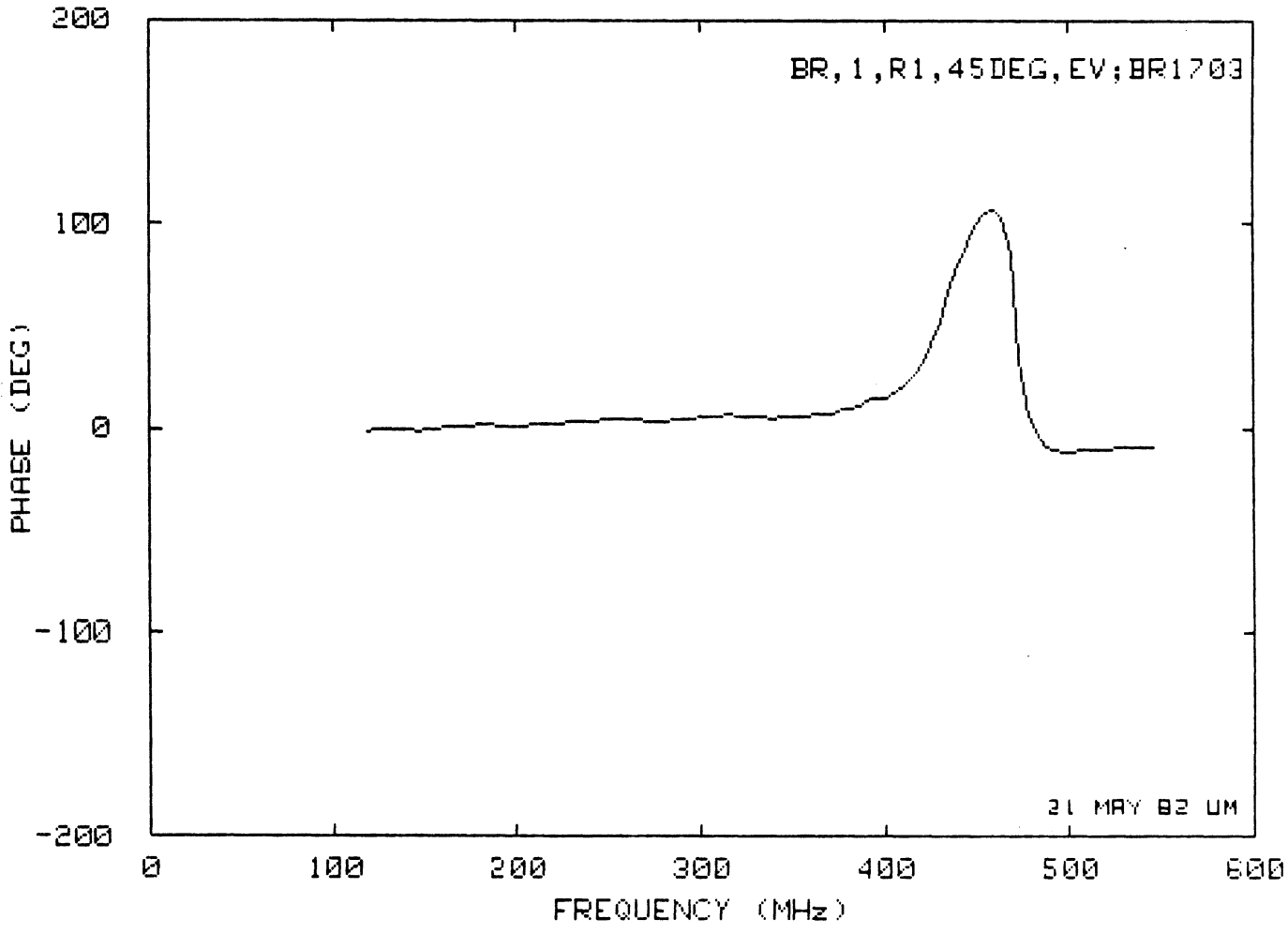
BR,1,R1,45DEG,EV;BR1703
21 MAY 82 UM
PHASE (DEG)
200
100
0
-100
-200
0
100
200
300
400
500
600
FREQUENCY (MHz)

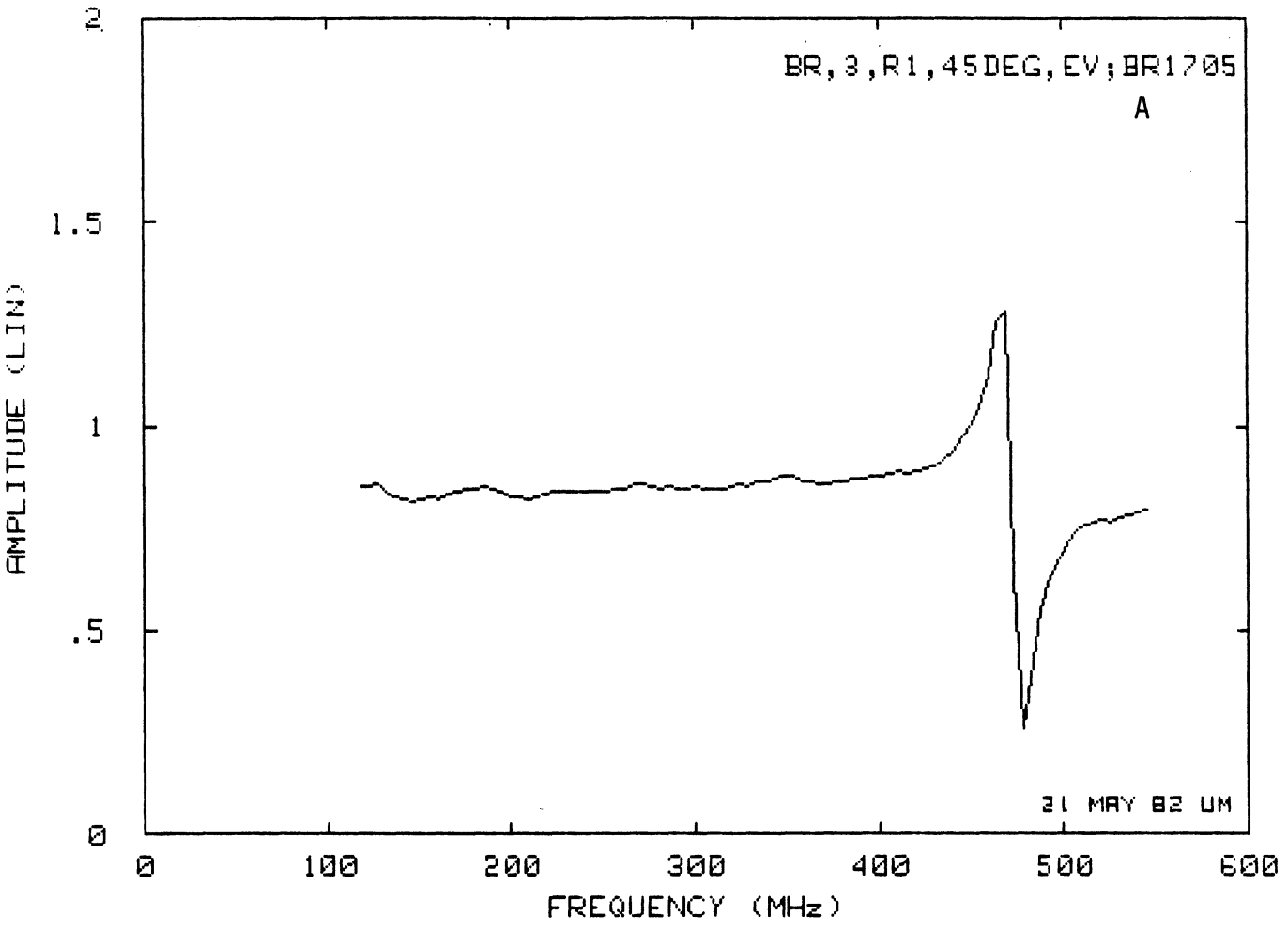
BR,3,R1,45DEG,EV;BR1705
A
21 MAY 82 UM
AMPLITUDE (LIN)
2
1.5
1
.5
0
0
100
200
300
400
500
600
FREQUENCY (MHz)

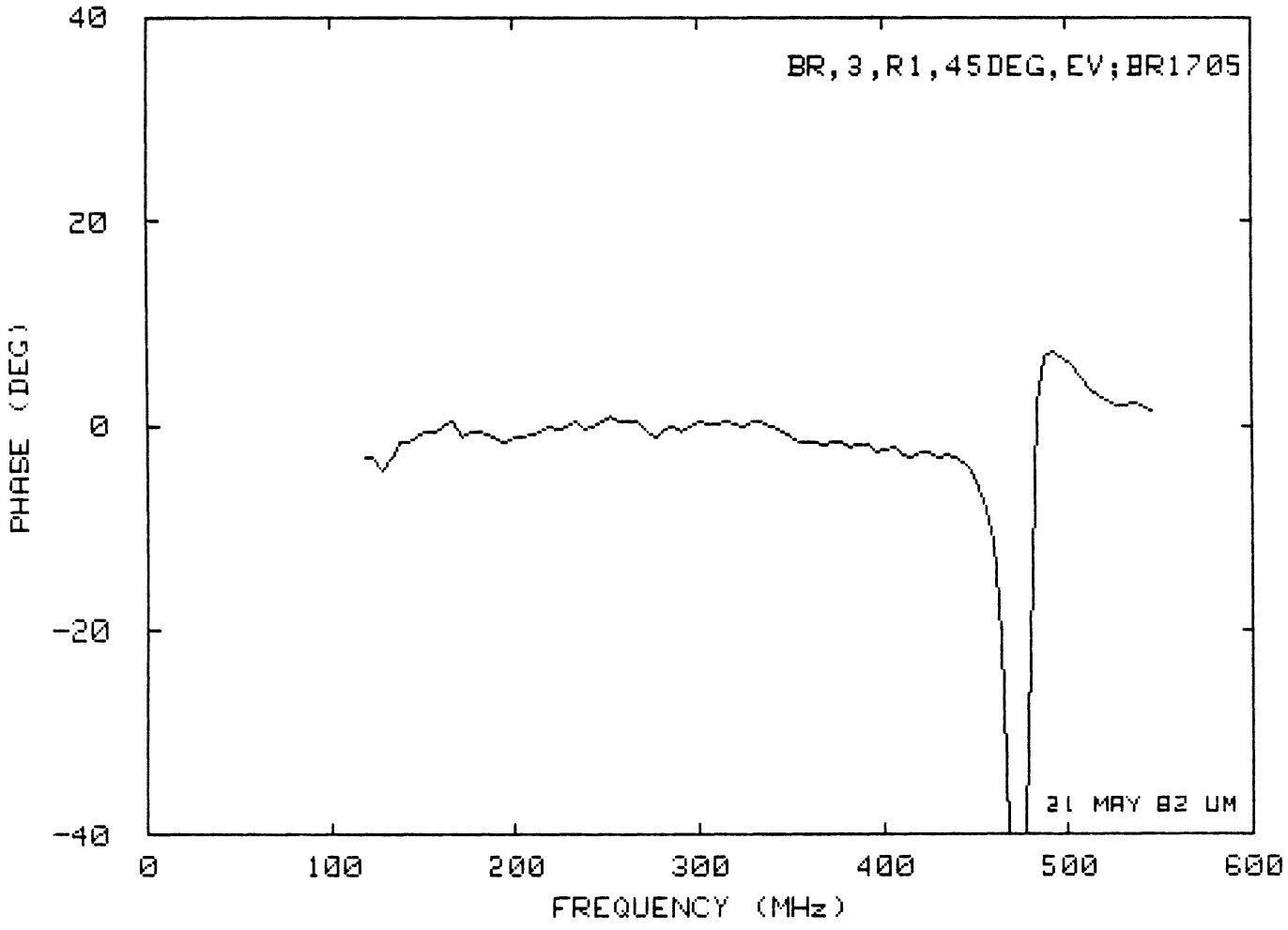
BR,3,R1,45DEG,EV;BR1705
21 MAY 82 UM
PHASE (DEG)
40
20
0
-20
-40
0
100
200
300
400
500
600
FREQUENCY (MHz)

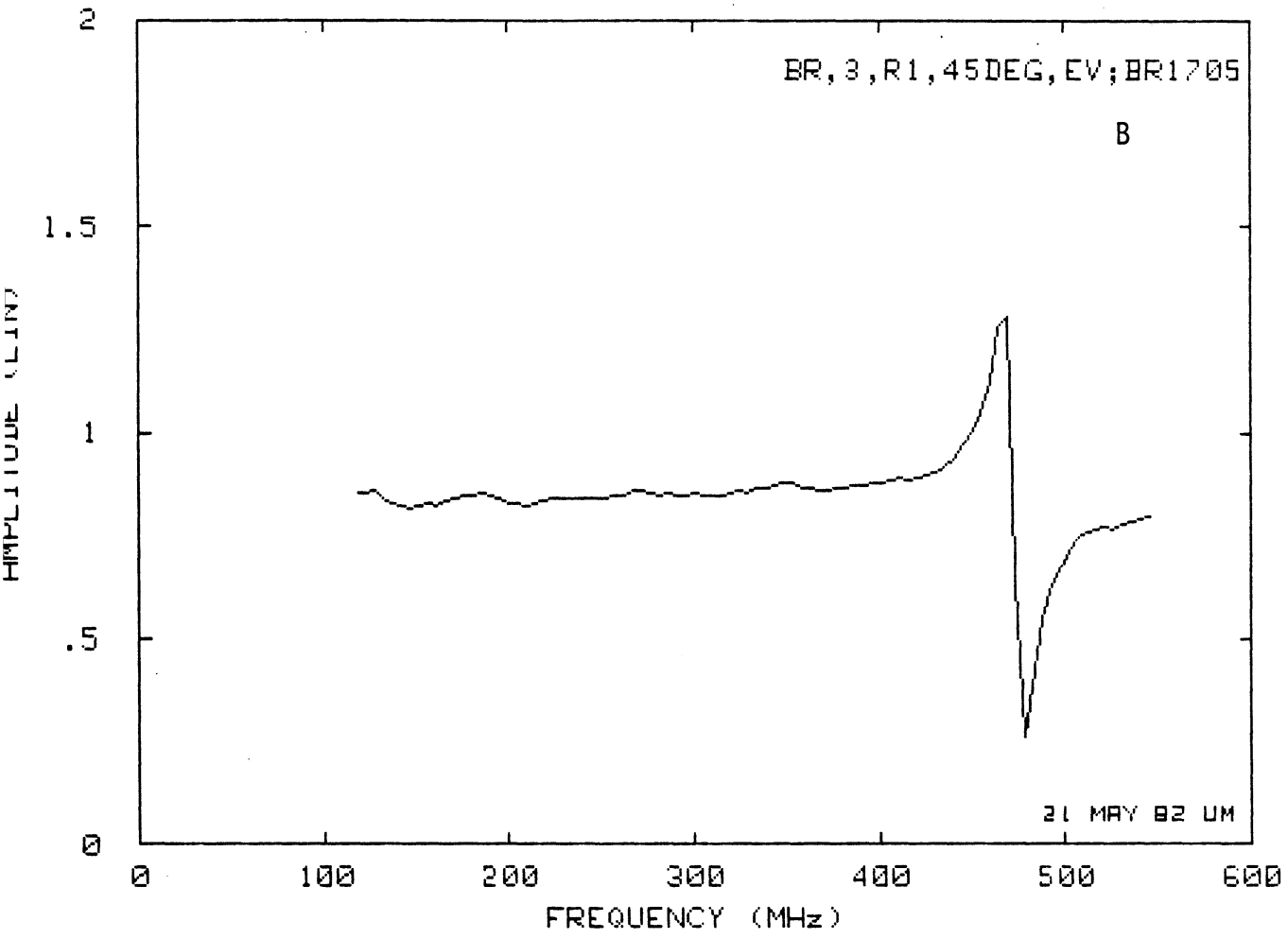
BR,3,R1,45DEG,EV;BR1705
B
21 MAY 82 UM
2
1.5
1
.5
0
0
100
200
300
400
500
600
FREQUENCY (MHz)

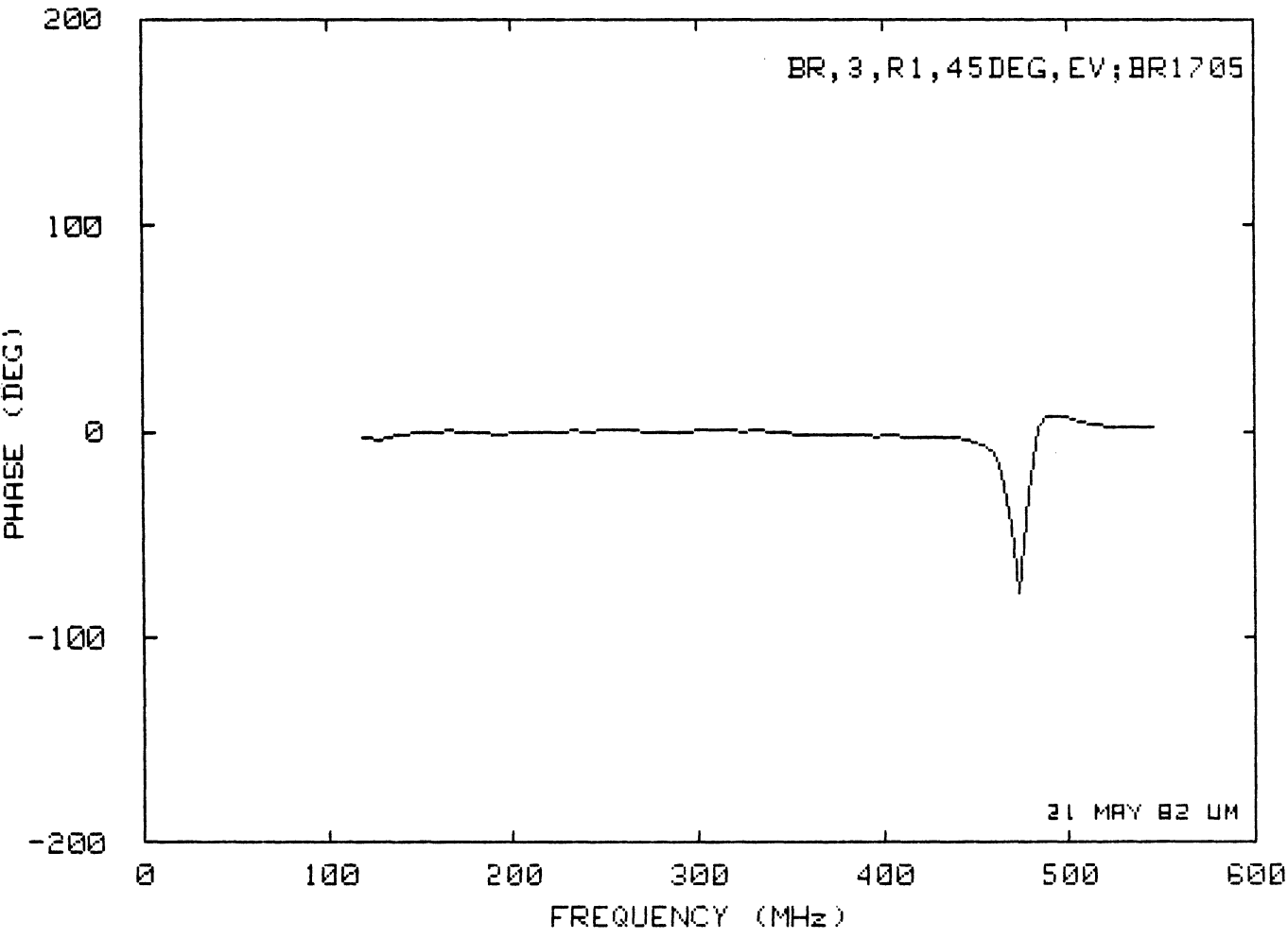
BR,3,R1,45DEG,EV;BR1705
21 MAY 82 UM
200
100
0
-100
-200
PHASE (DEG)
0
100
200
300
400
500
600
FREQUENCY (MHz)

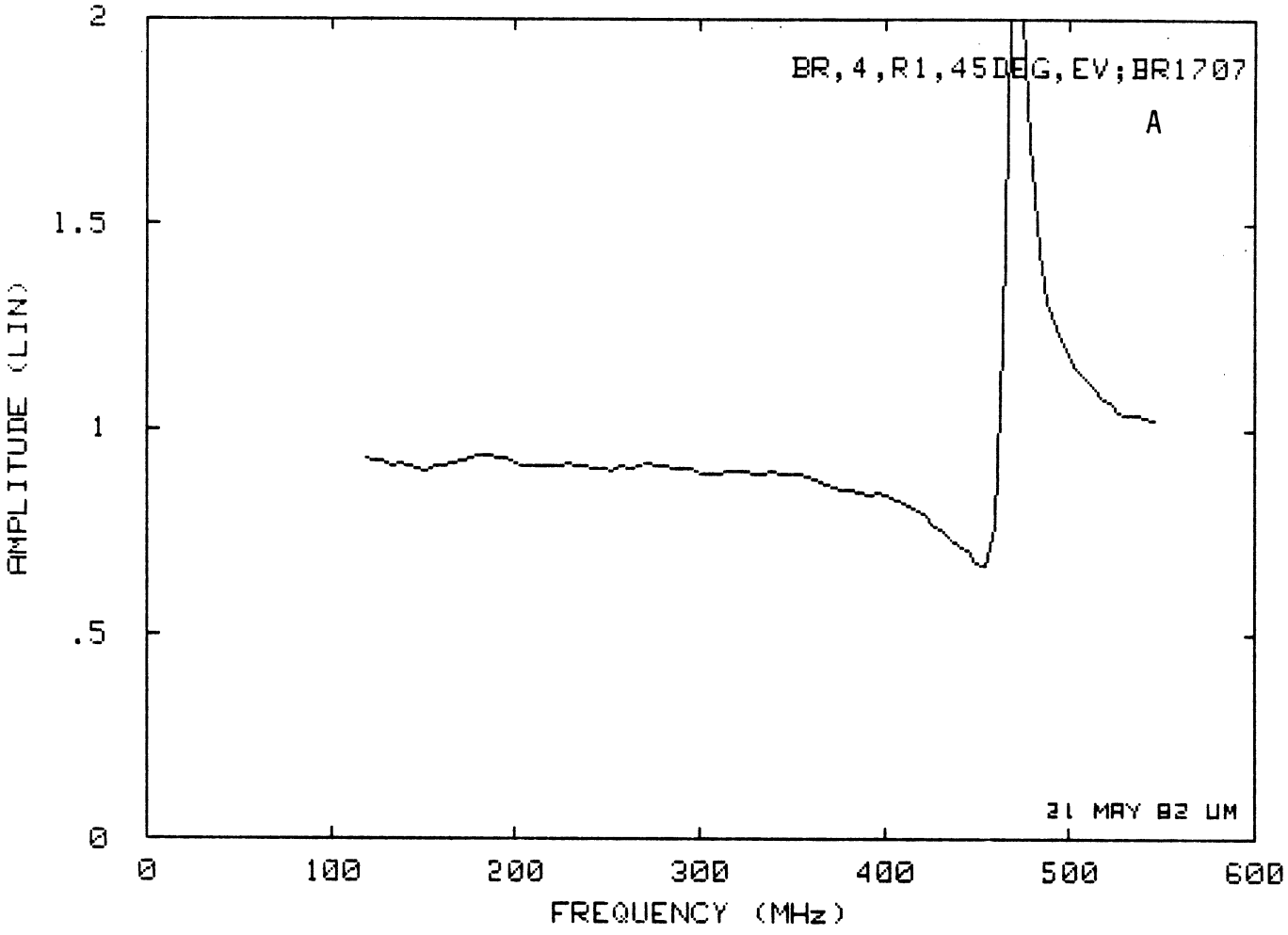
BR,4,R1,45DEG,EV;BR1707
A
21 MAY 82 UM
AMPLITUDE (LIN)
2
1.5
1
.5
0
0
100
200
300
400
500
600
FREQUENCY (MHz)

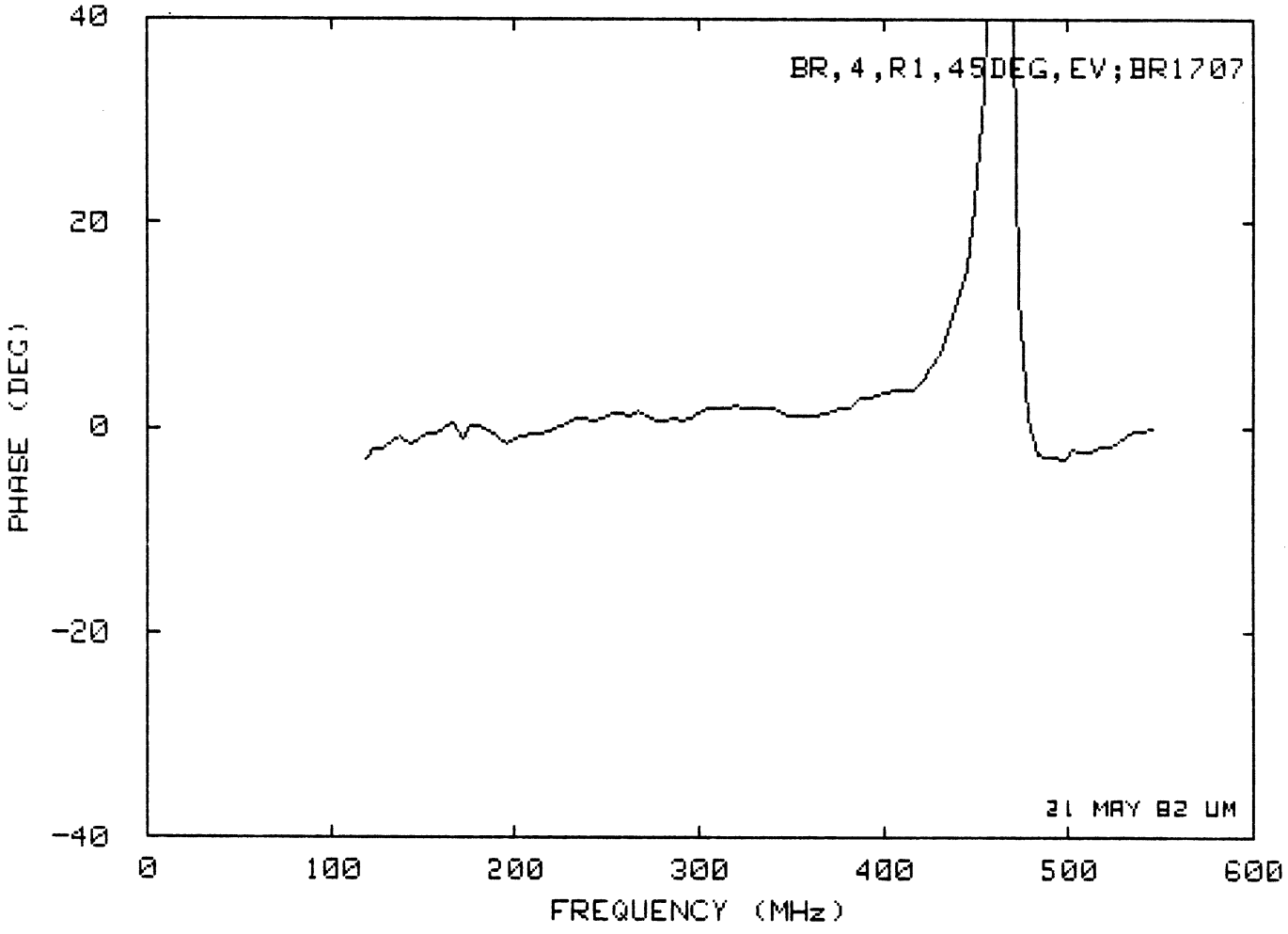
BR,4,R1,45DEG,EV;BR1707
21 MAY 82 UM
PHASE (DEG)
40
20
0
-20
-40
0
100
200
300
400
500
600
FREQUENCY (MHz)

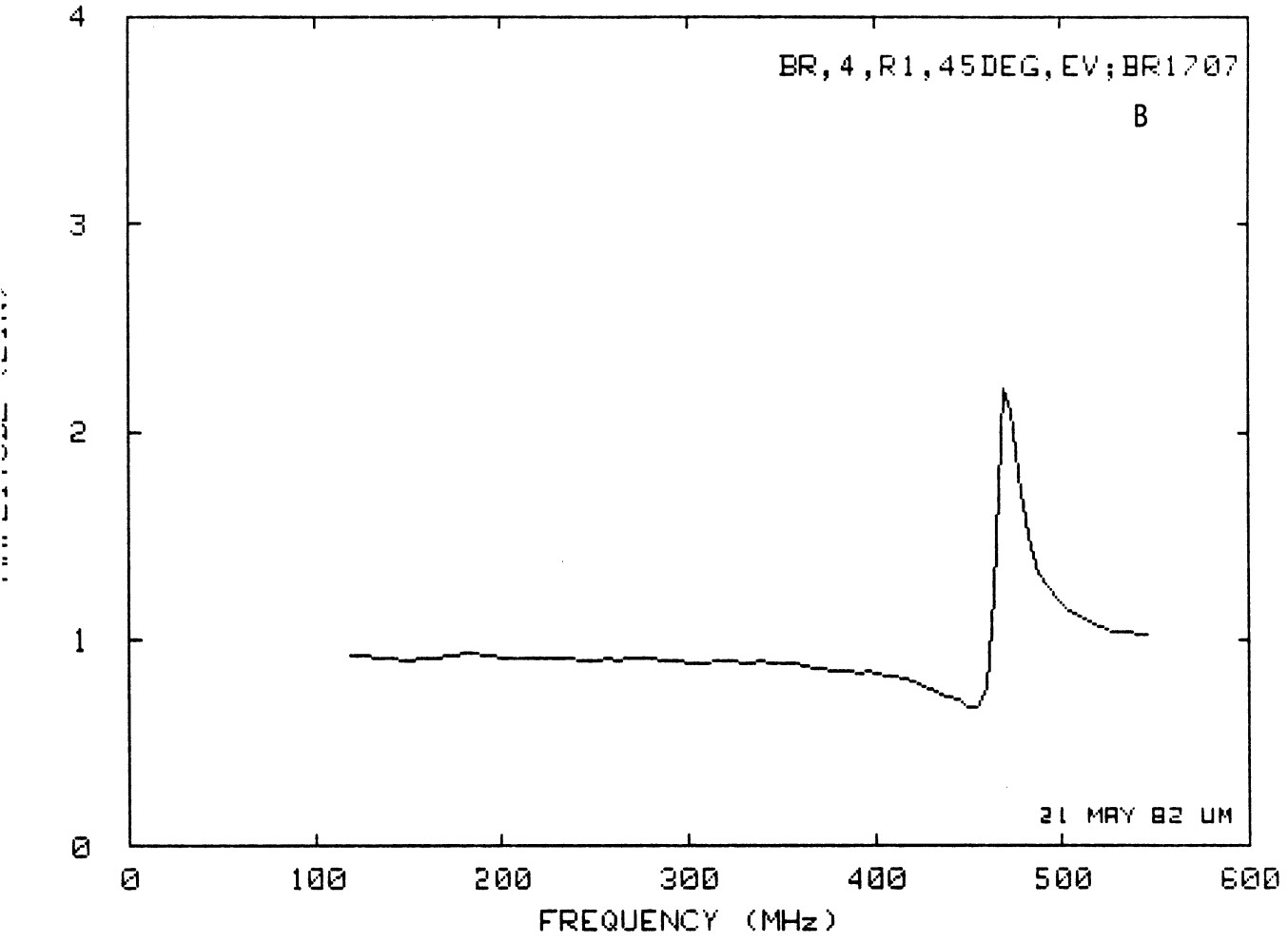
BR,4,R1,45DEG,EV;BR1707
B
21 MAY 82 UM
4
3
2
1
0
0
100
200
300
400
500
600
FREQUENCY (MHz)

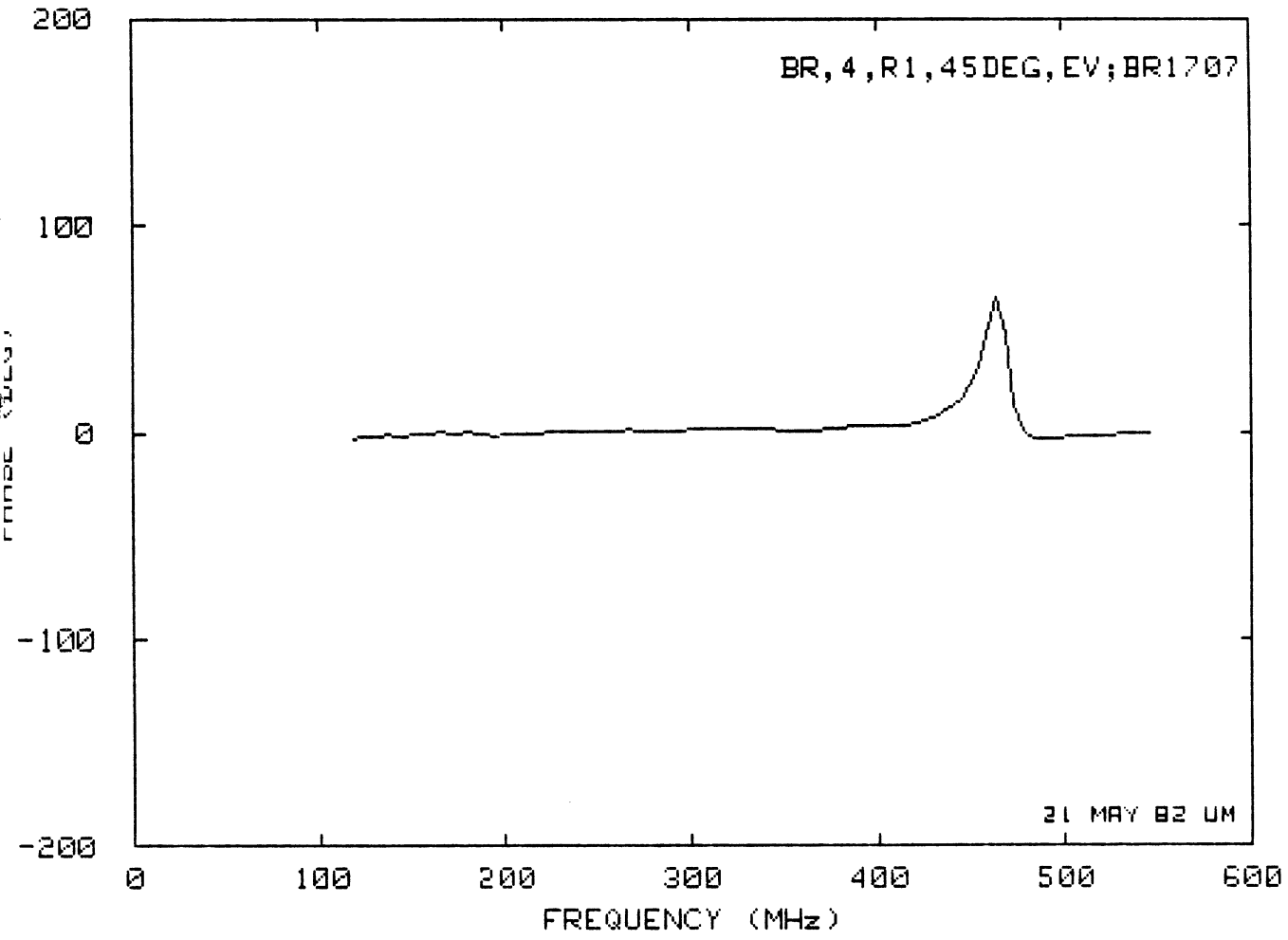
BR,4,R1,45DEG,EV;BR1707
21 MAY 82 UM
200
100
0
-100
-200
0
100
200
300
400
500
600
FREQUENCY (MHz)

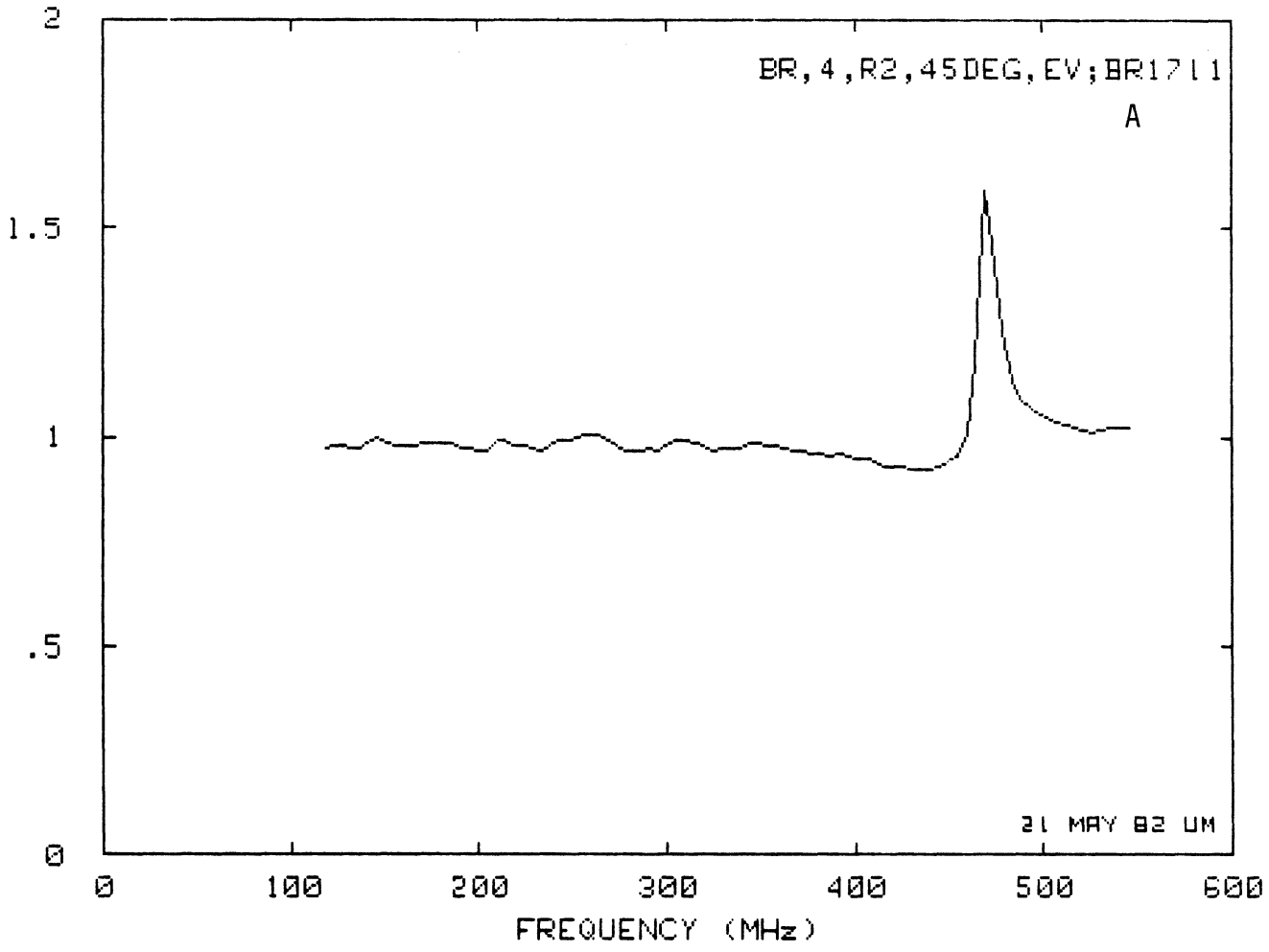
BR,4,R2,45DEG,EV;BR1711
A
21 MAY 82 UM
2
1.5
1
.5
0
0
100
200
300
400
500
600
FREQUENCY (MHz)

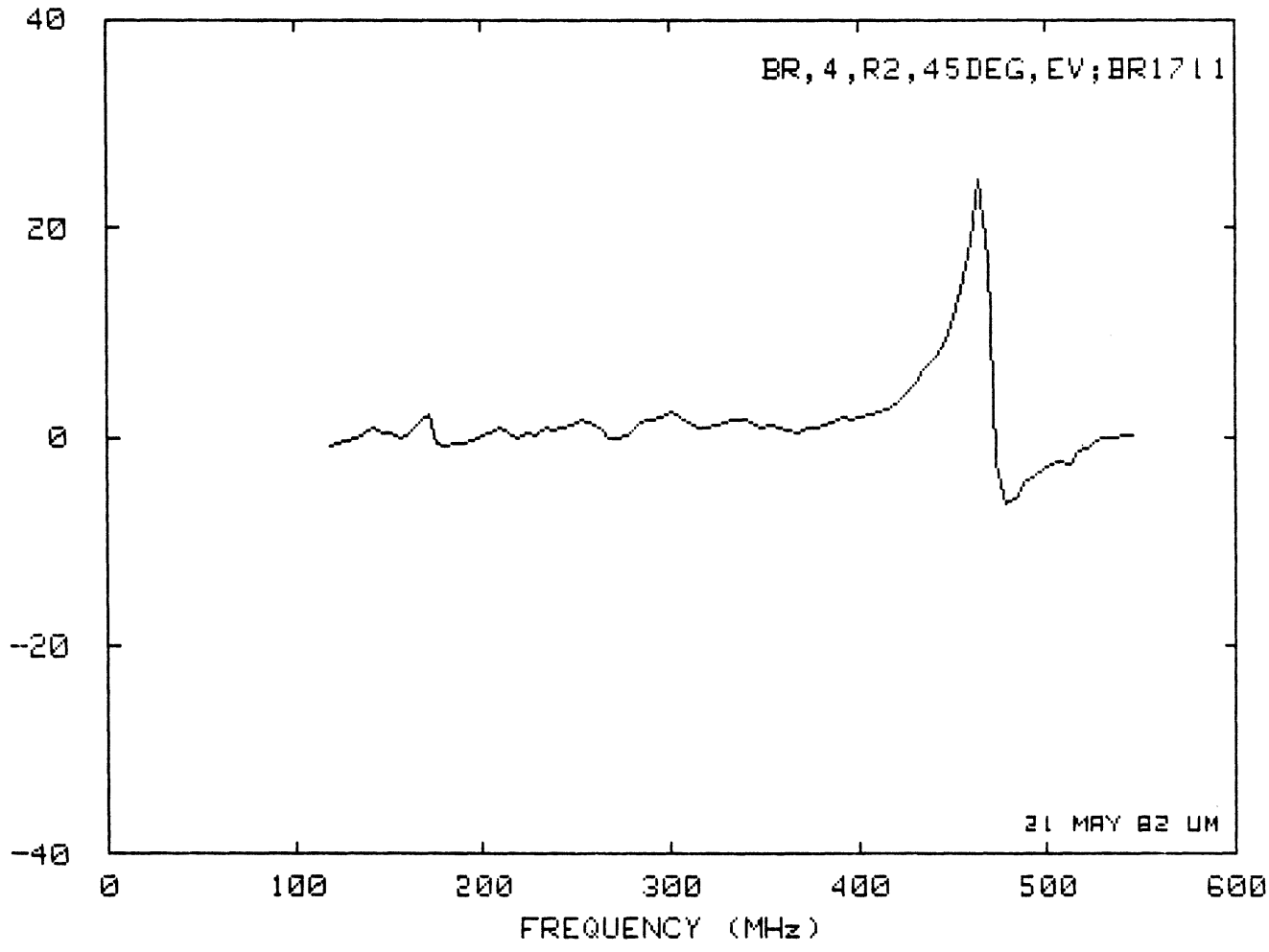
BR,4,R2,45DEG,EV;BR1711
21 MAY 82 UM
40
20
0
-20
-40
0
100
200
300
400
500
600
FREQUENCY (MHz)

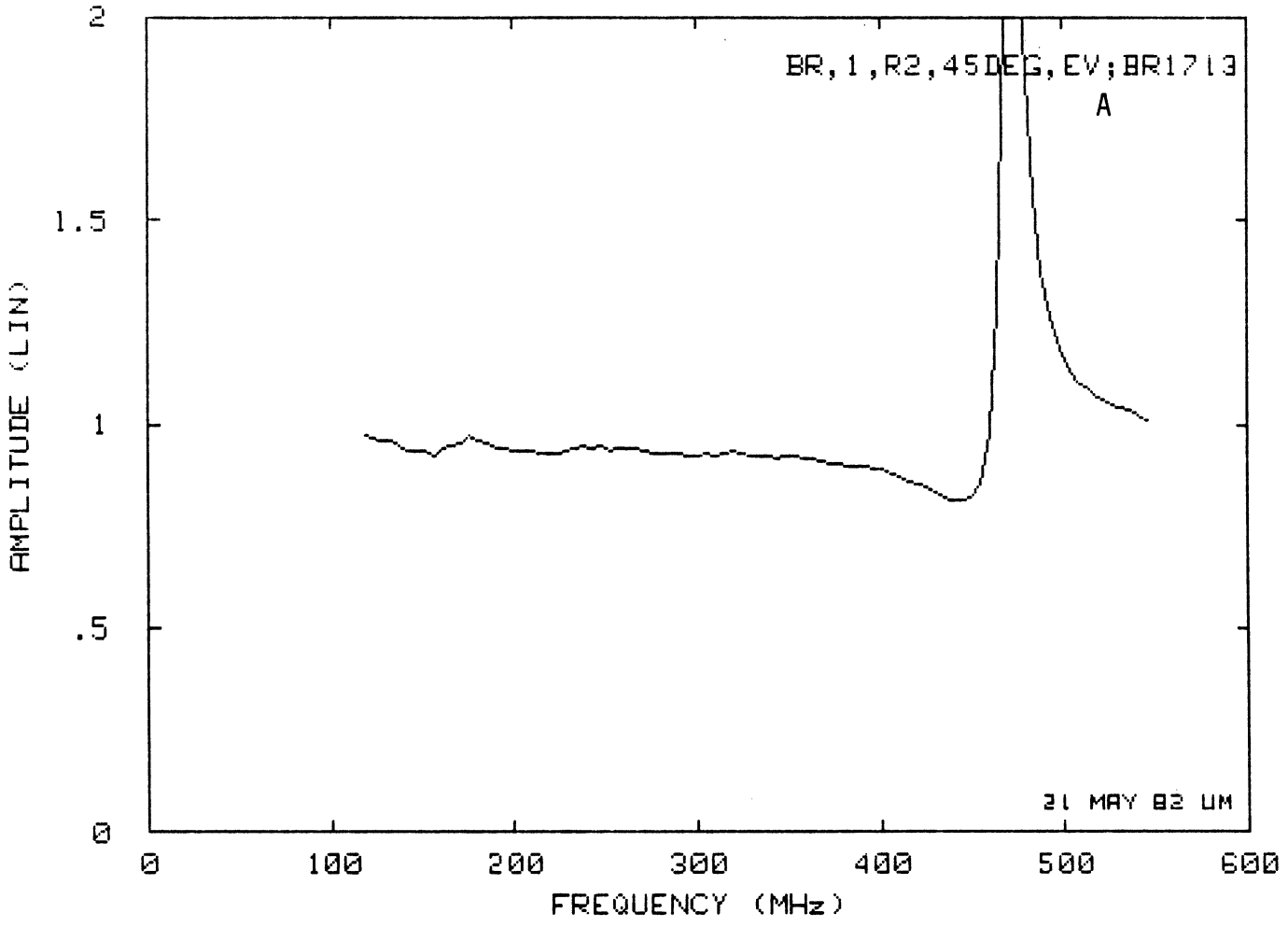
BR,1,R2,45DEG,EV;BR1713
A
21 MAY 82 UM
AMPLITUDE (LIN)
2
1.5
1
.5
0
0
100
200
300
400
500
600
FREQUENCY (MHz)

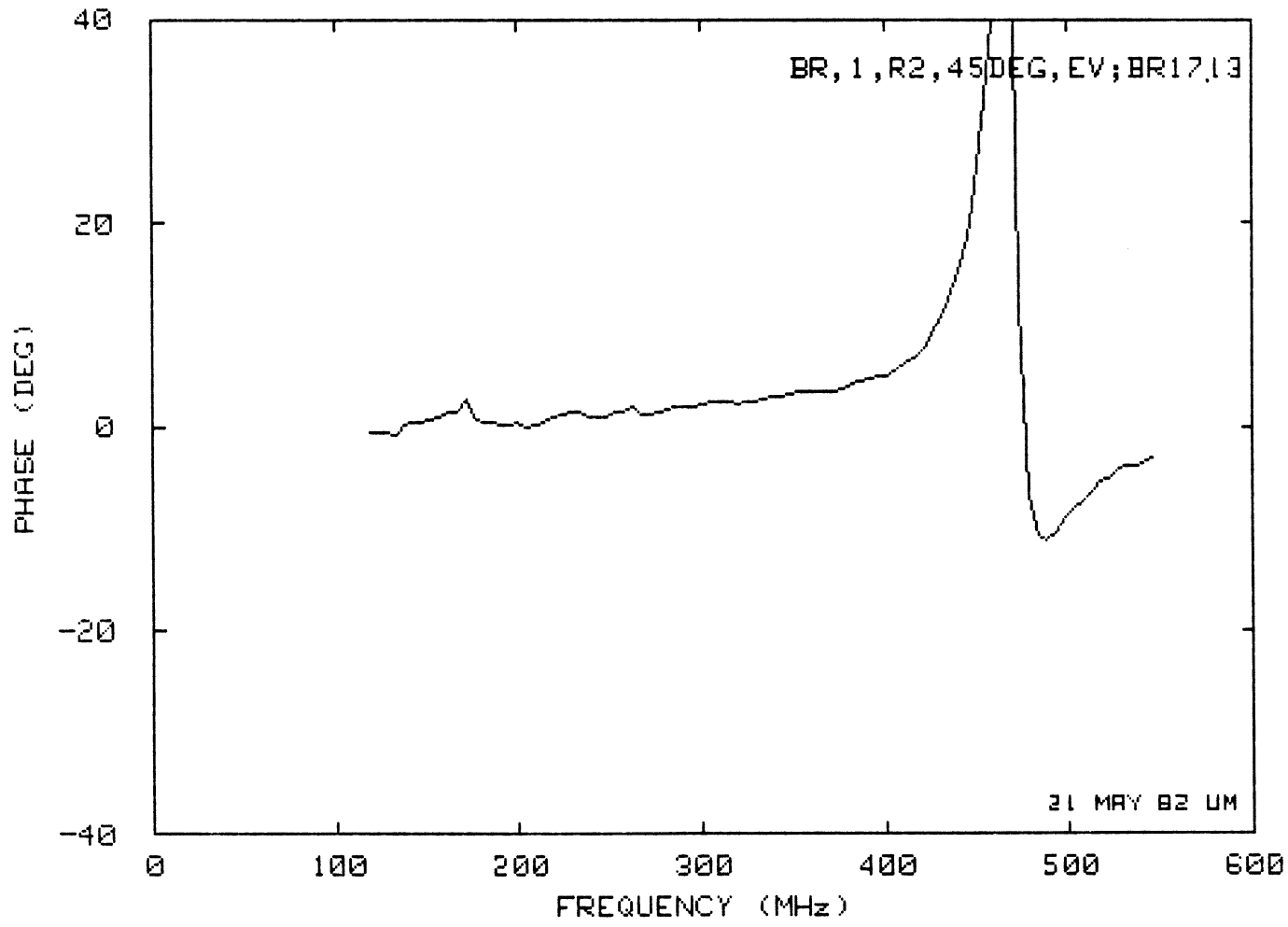
BR,1,R2,45DEG,EV;BR1713
21 MAY 82 UM
PHASE (DEG)
40
20
0
-20
-40
0
100
200
300
400
500
600
FREQUENCY (MHz)

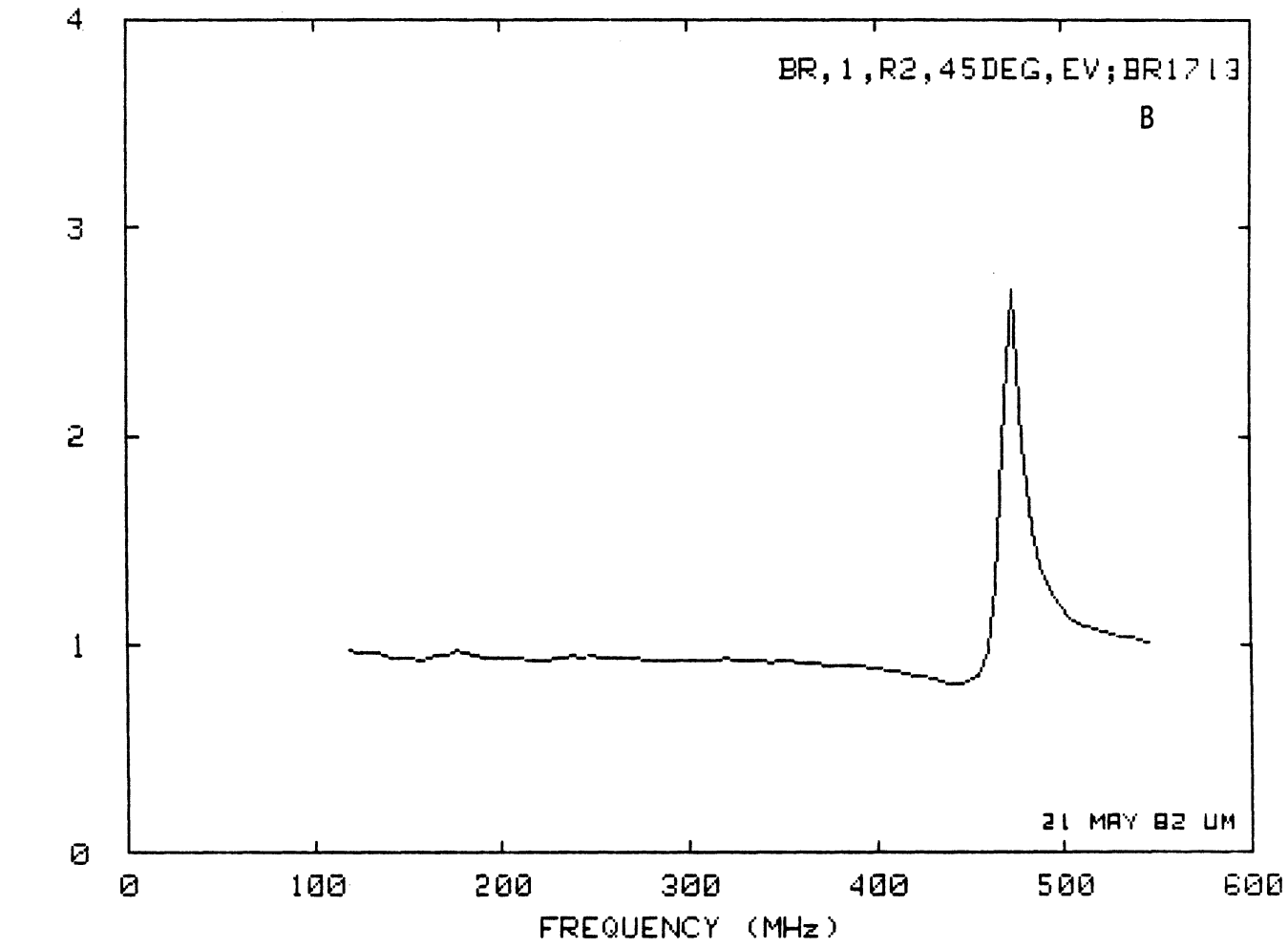
BR,1,R2,45DEG,EV;BR1713
B
21 MAY 82 UM
4
3
2
1
0
0
100
200
300
400
500
600
FREQUENCY (MHz)

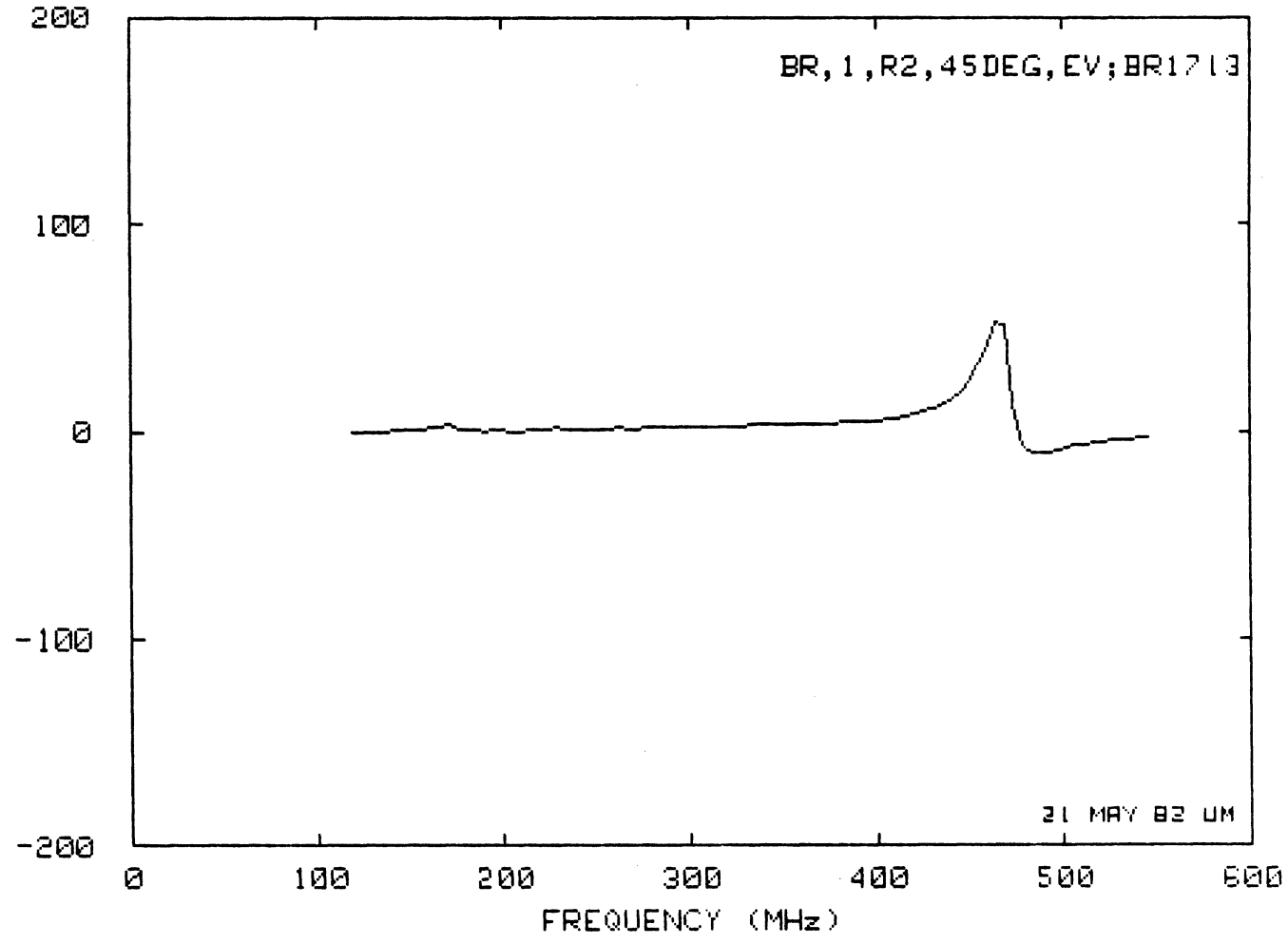
BR,1,R2,45DEG,EV;BR1713
21 MAY 82 UM
200
100
0
-100
-200
0
100
200
300
400
500
600
FREQUENCY (MHz)

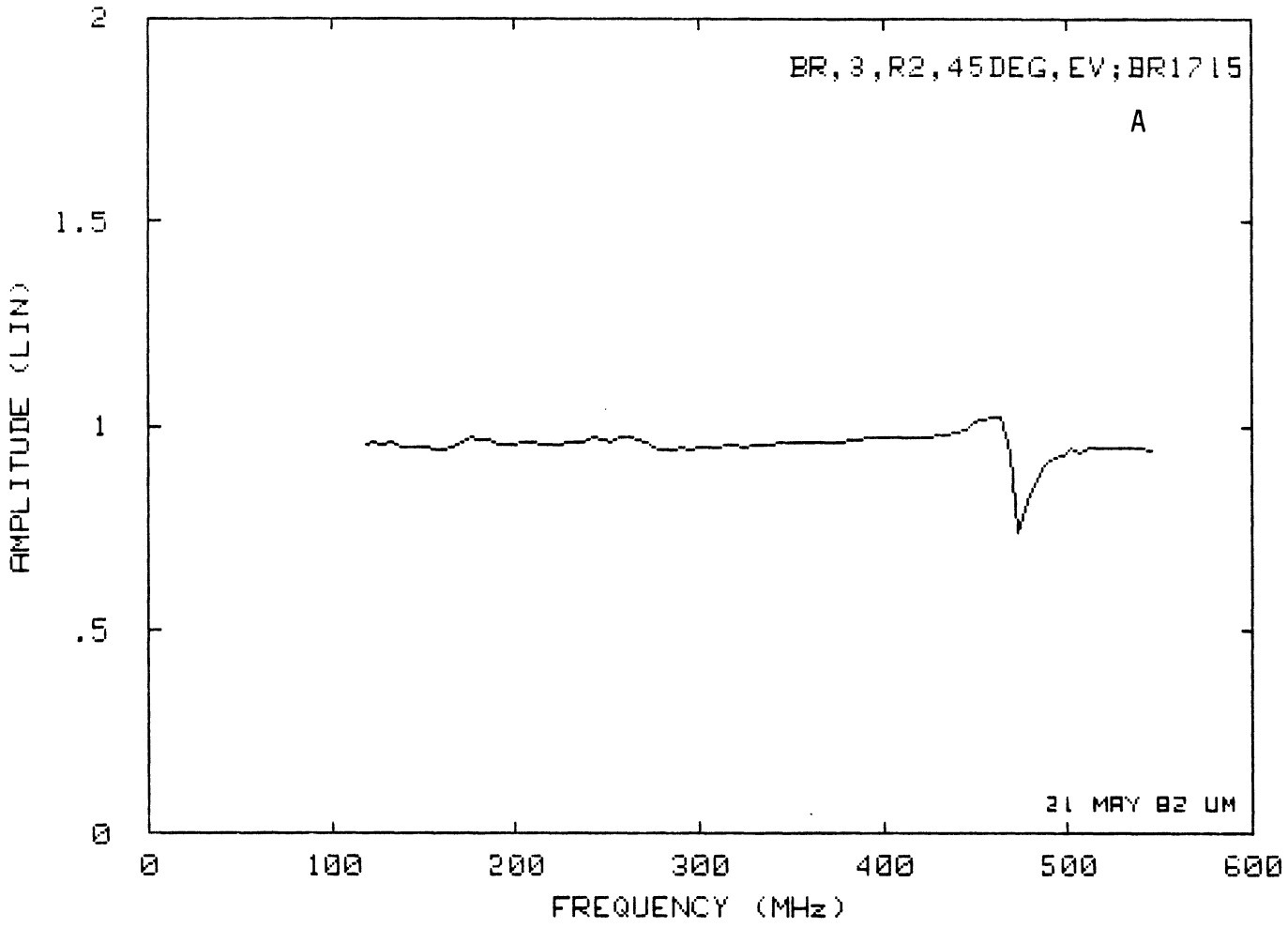
BR,3,R2,45DEG,EV;BR1715
A
21 MAY 82 UM
AMPLITUDE (LIN)
2
1.5
1
.5
0
0
100
200
300
400
500
600
FREQUENCY (MHz)

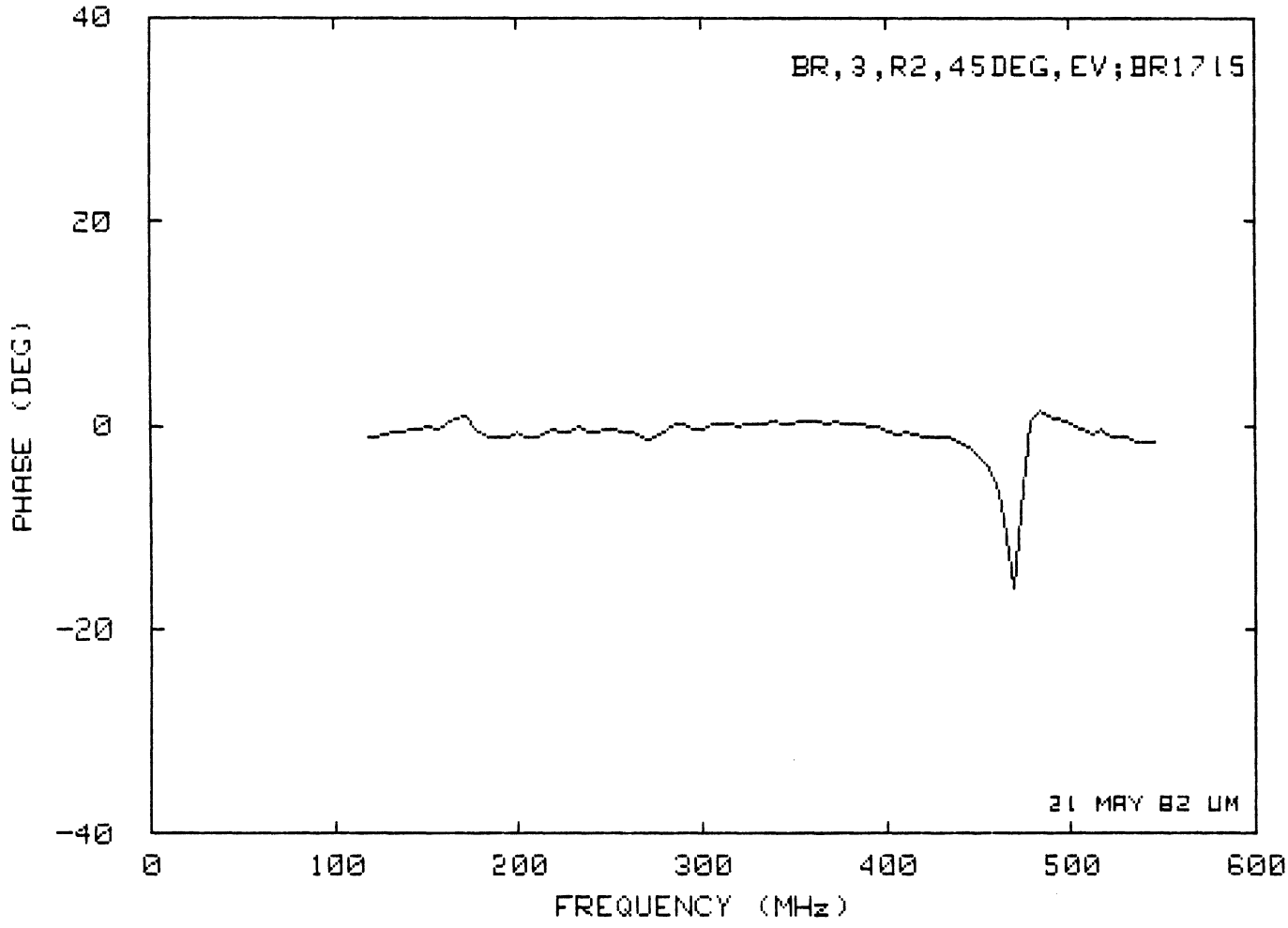
BR,3,R2,45DEG,EV;BR1715
21 MAY 82 UM
PHASE (DEG)
40
20
0
-20
-40
0
100
200
300
400
500
600
FREQUENCY (MHz)

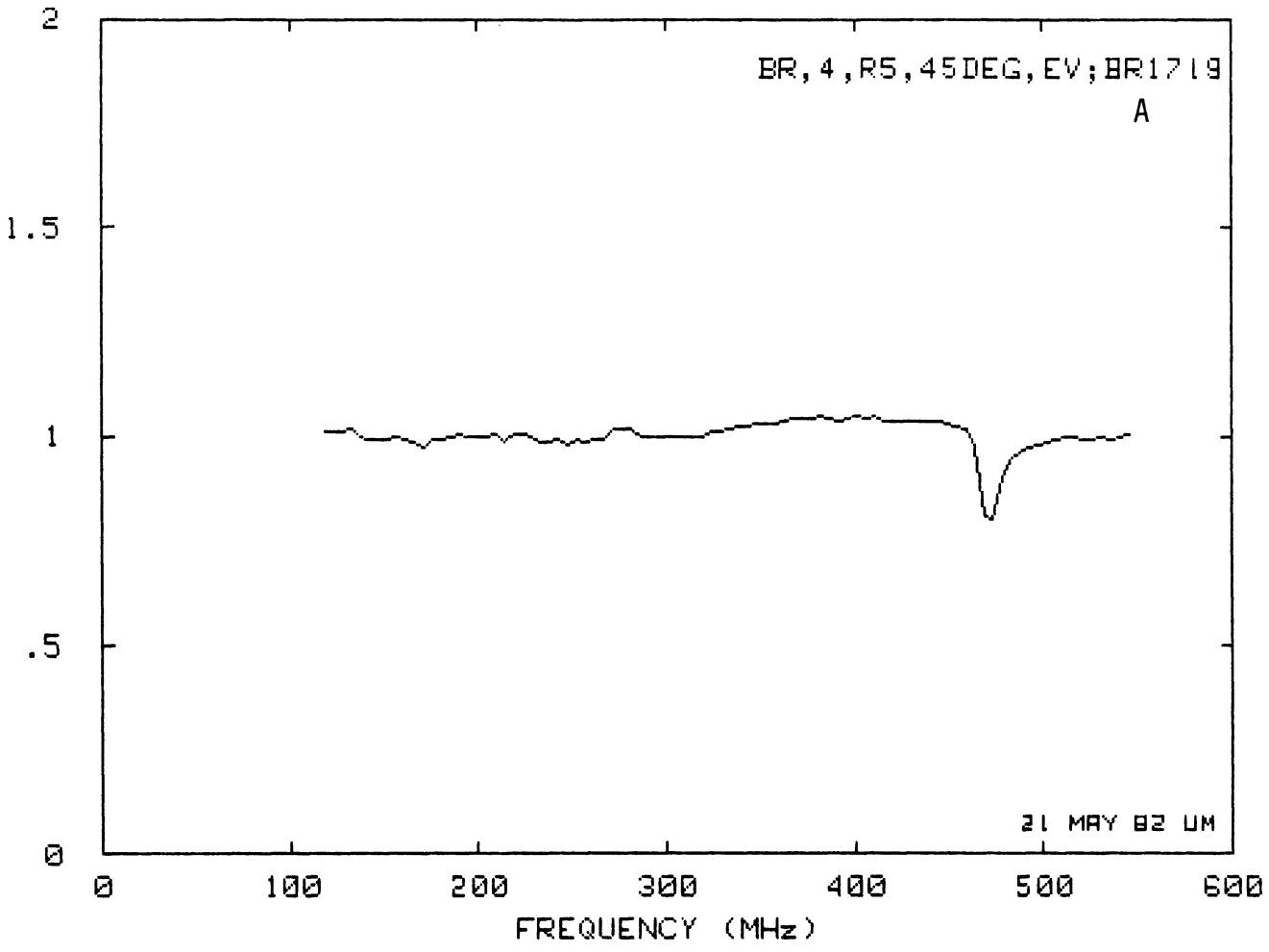
BR,4,R5,45DEG,EV;BR1719
A
21 MAY 82 UM
2
1.5
1
.5
0
0
100
200
300
400
500
600
FREQUENCY (MHz)

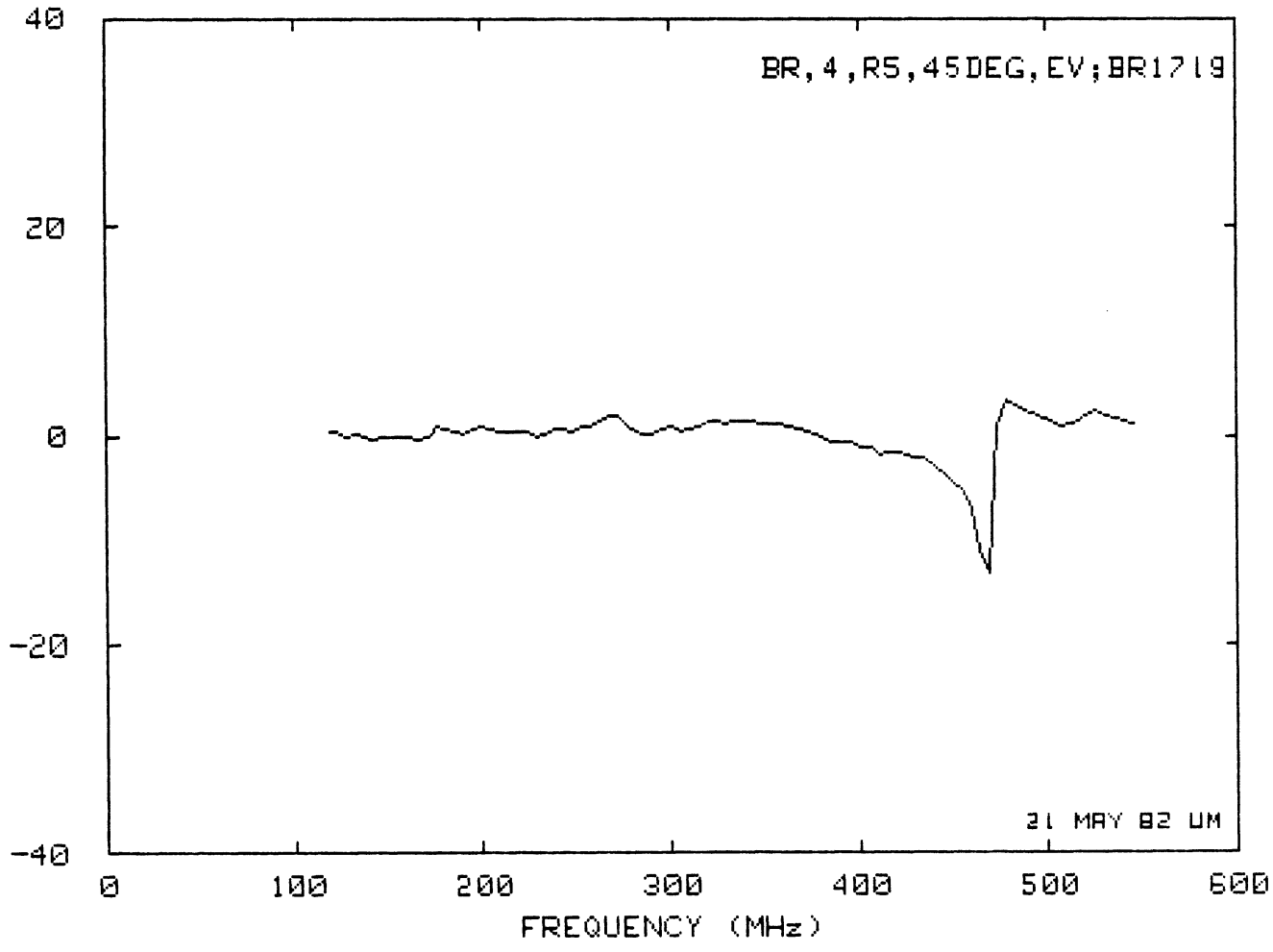
BR,4,R5,45DEG,EV;BR1719
21 MAY 82 UM
40
20
0
-20
-40
0
100
200
300
400
500
600
FREQUENCY (MHz)

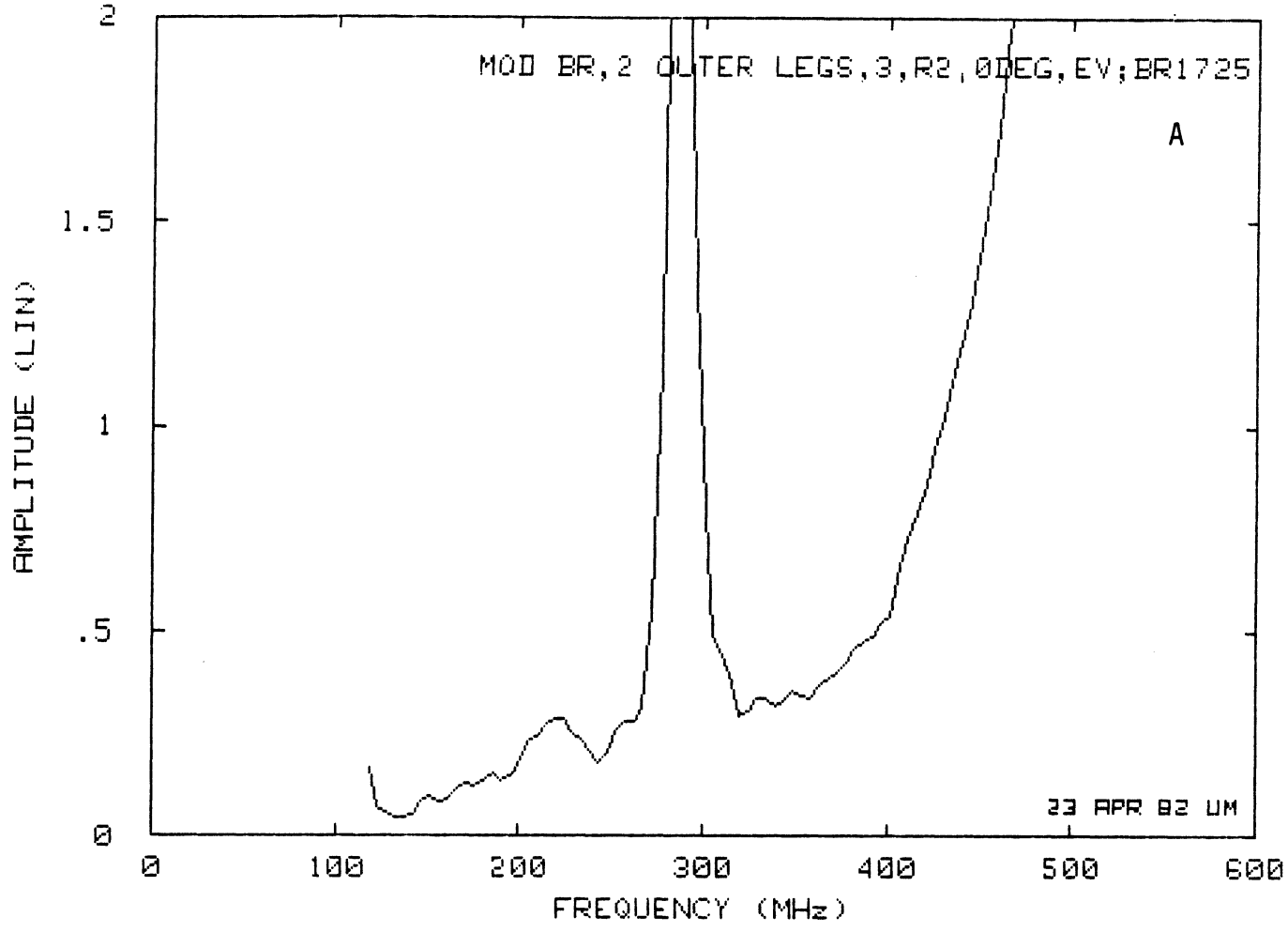
MOD BR,2 OUTER LEGS,3,R2,0DEG,EV;BR1725
A
23 APR 82 UM
AMPLITUDE (LIN)
2
1.5
1
.5
0
0
100
200
300
400
500
600
FREQUENCY (MHz)

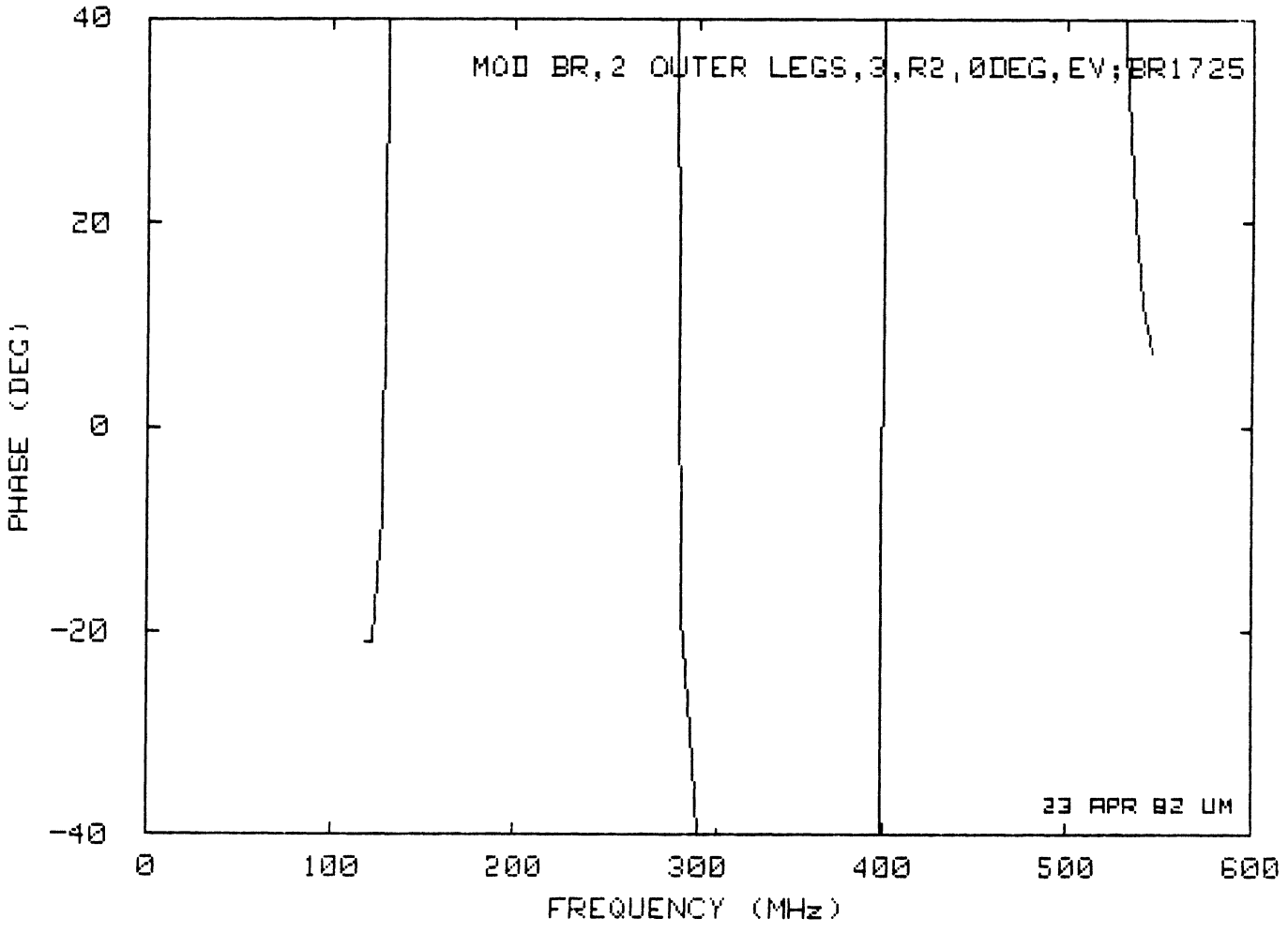
MOD BR,2 OUTER LEGS,3,R2,0DEG,EV;BR1725
23 APR 82 UM
PHASE (DEG)
40
20
0
-20
-40
0
100
200
300
400
500
600
FREQUENCY (MHz)

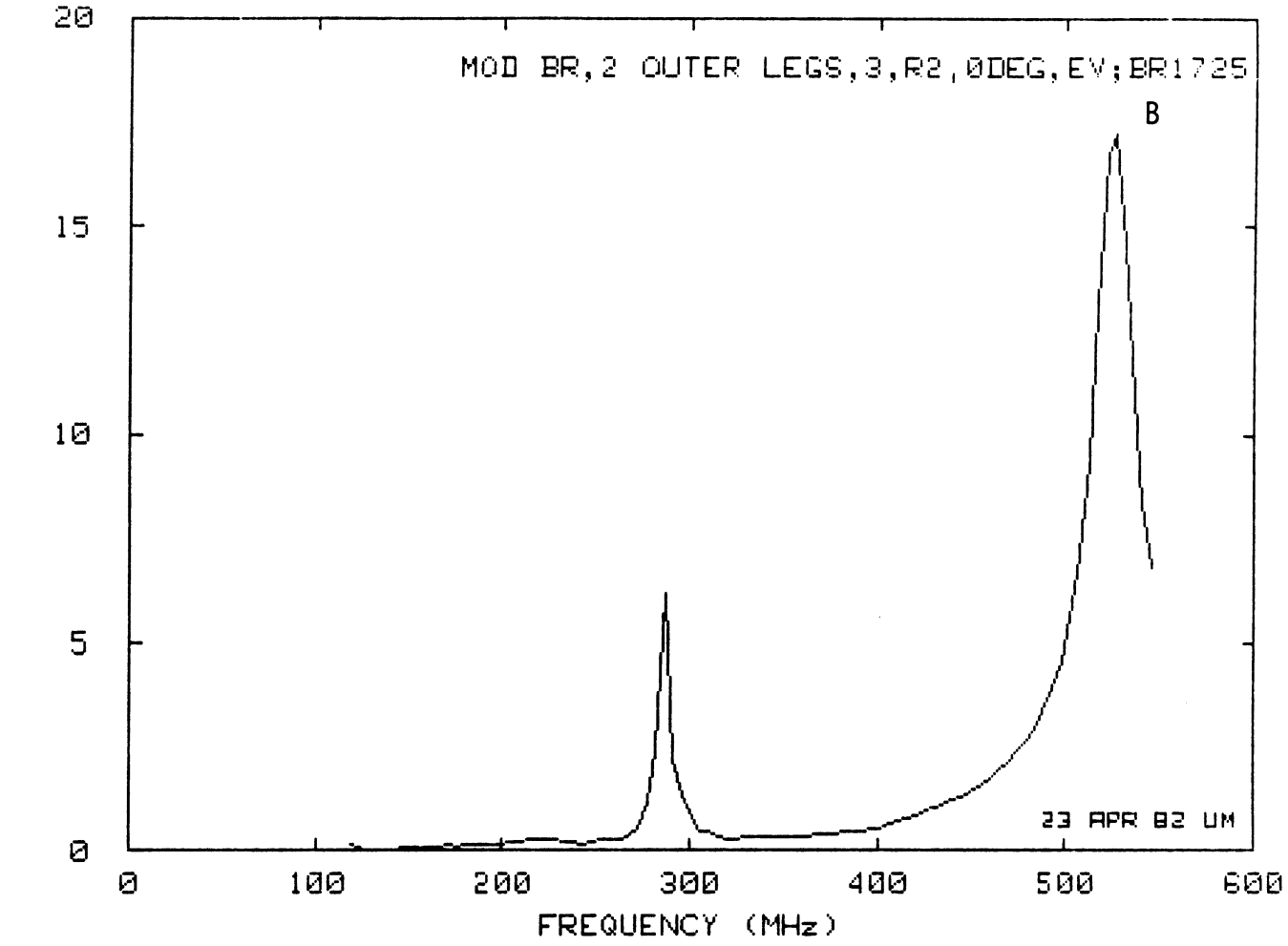
MOD BR,2 OUTER LEGS,3,R2,0DEG,EV;BR1725
B
23 APR 82 UM
20
15
10
5
0
0
100
200
300
400
500
600
FREQUENCY (MHz)

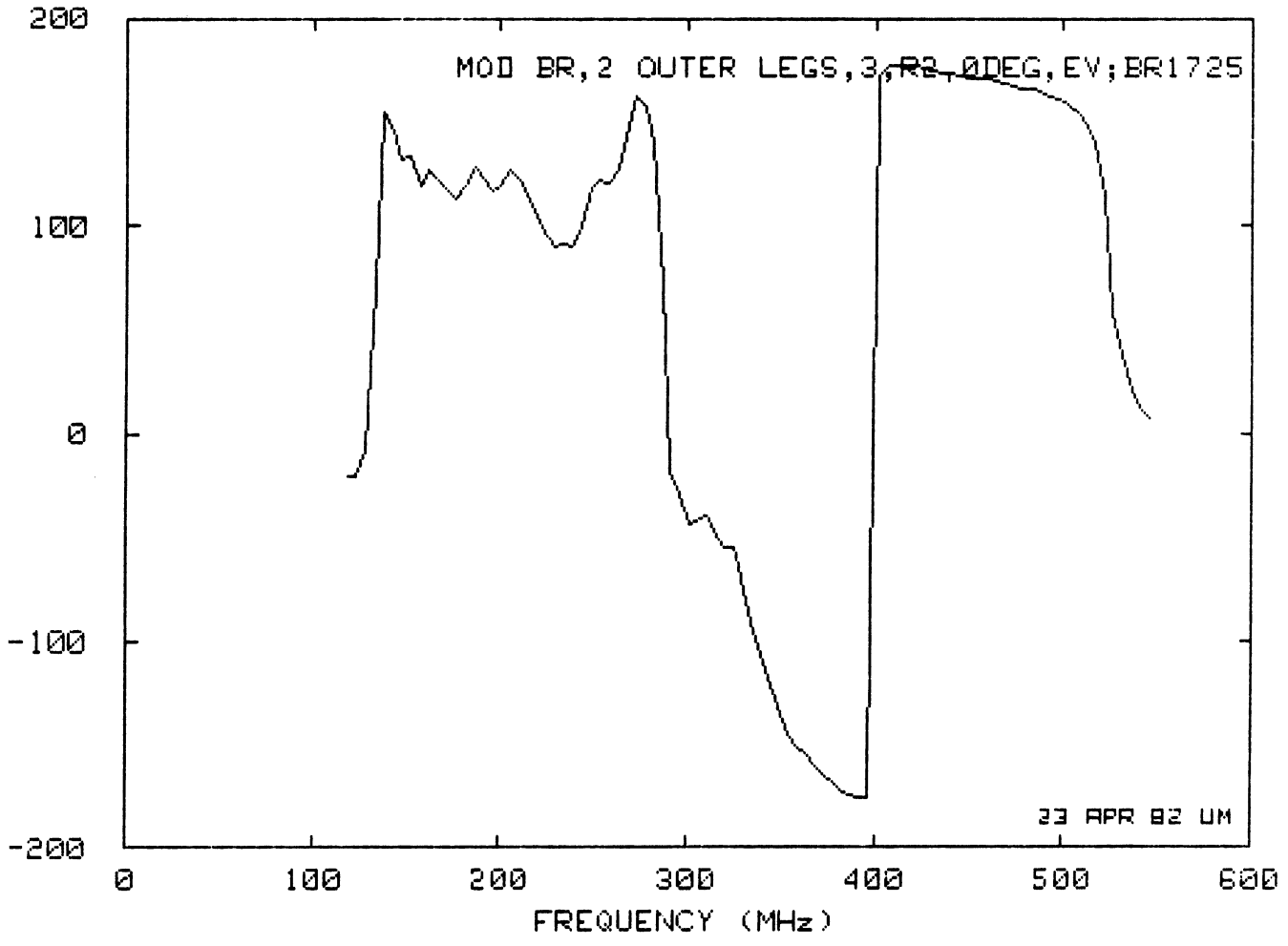
MOD BR,2 OUTER LEGS,3,R2,0DEG,EV;BR1725
23 APR 82 UM
200
100
0
-100
-200
0
100
200
300
400
500
600
FREQUENCY (MHz)

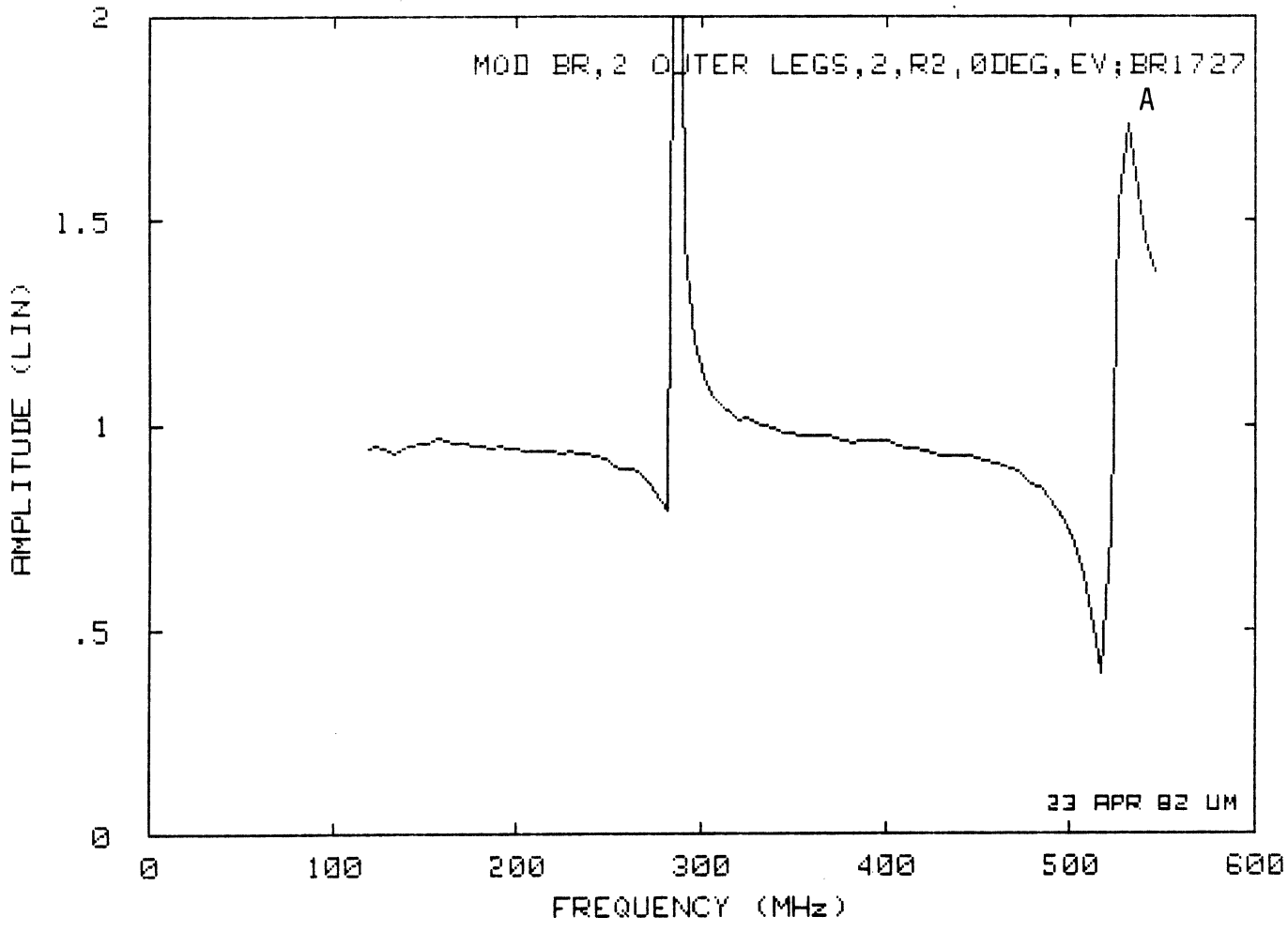
MOD BR,2 OUTER LEGS,2,R2,0DEG,EV;BR1727
A
23 APR 82 UM
AMPLITUDE (LIN)
2
1.5
1
.5
0
0
100
200
300
400
500
600
FREQUENCY (MHz)

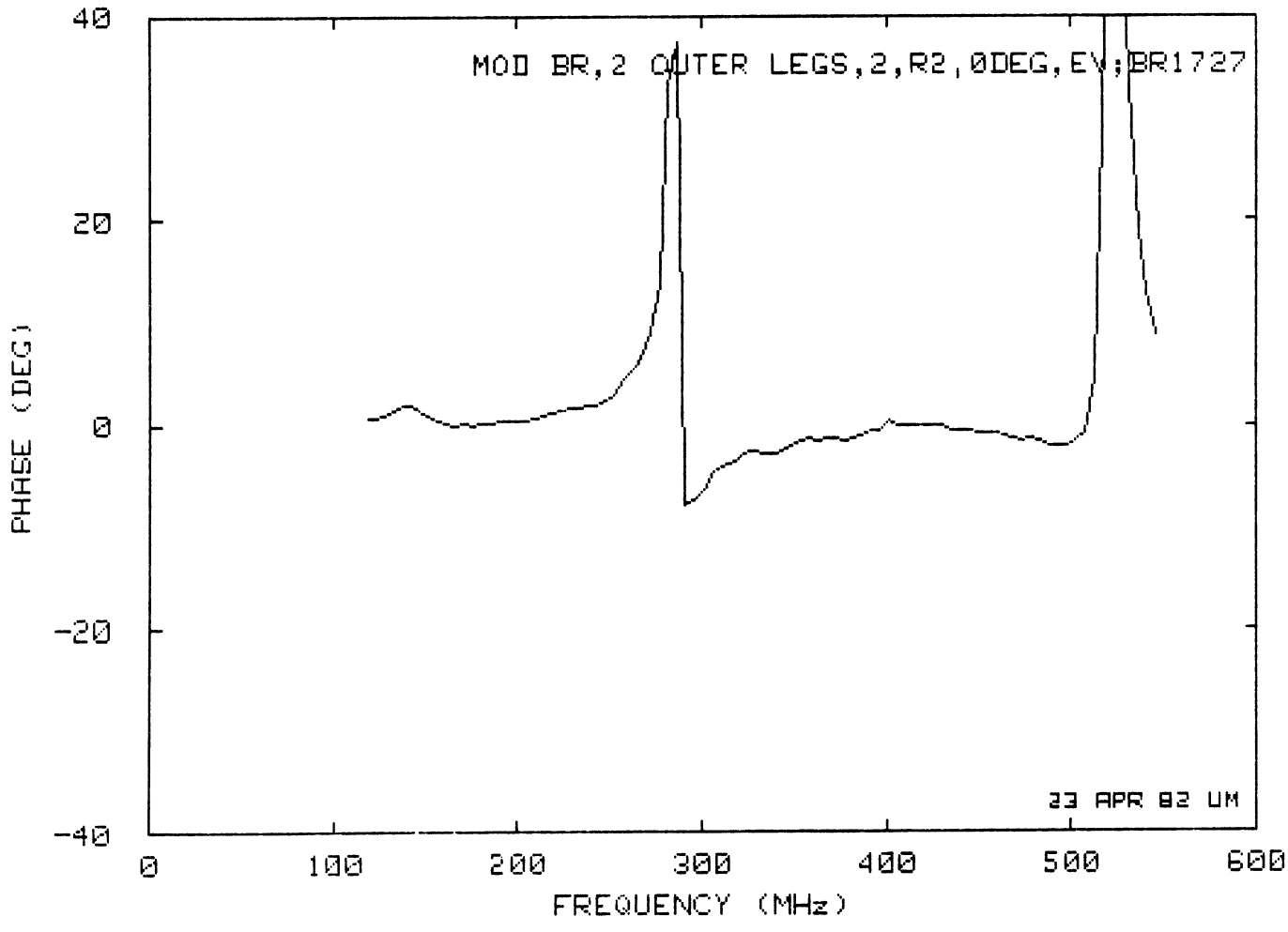
MOD BR,2 OUTER LEGS,2,R2,0DEG,EV;BR1727
23 APR 82 UM
PHASE (DEG)
40
20
0
-20
-40
0
100
200
300
400
500
600
FREQUENCY (MHz)

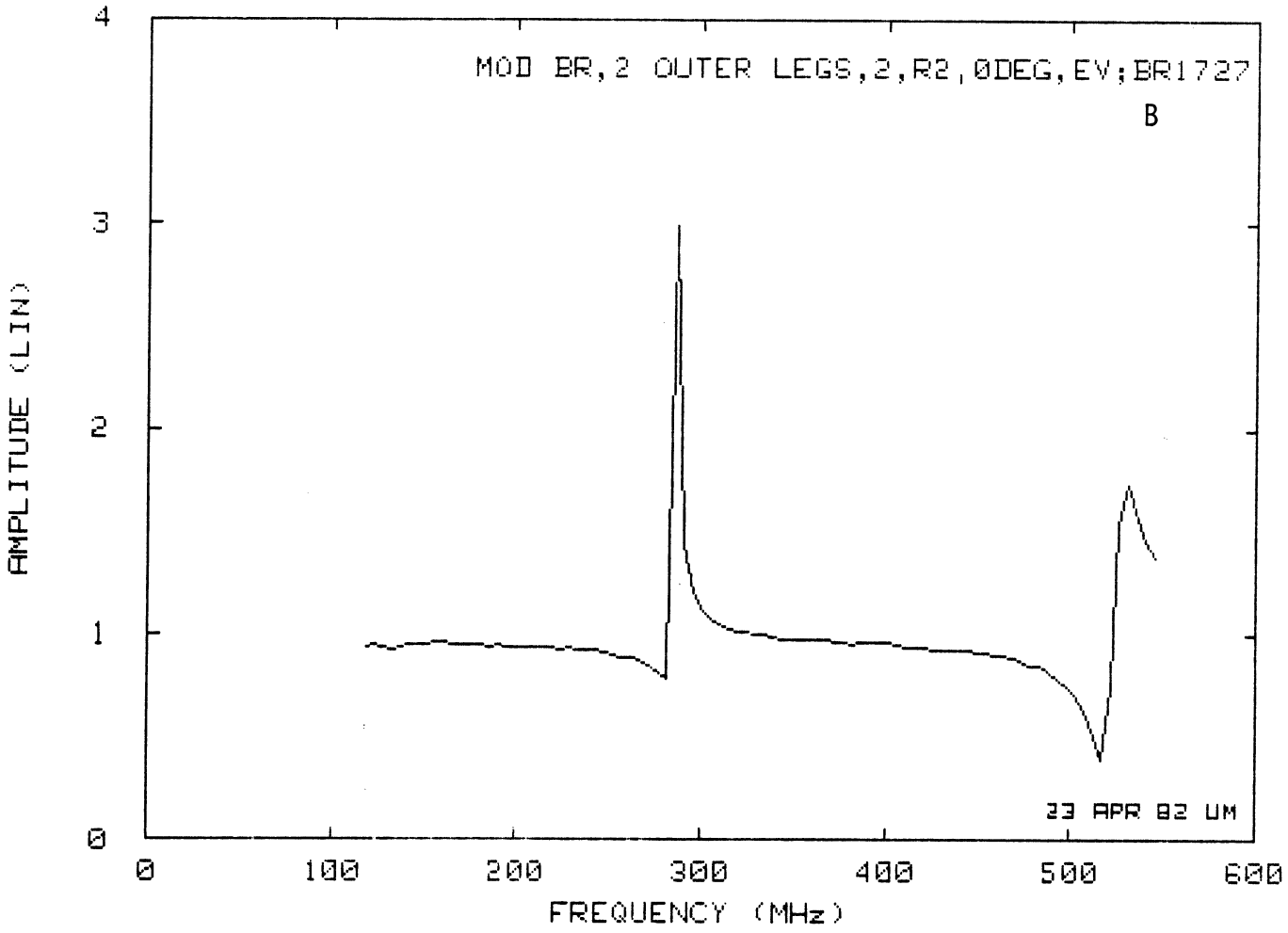
MOD BR,2 OUTER LEGS,2,R2,0DEG,EV;BR1727
B
AMPLITUDE (LIN)
4
3
2
1
0
23 APR 82 UM
0
100
200
300
400
500
600
FREQUENCY (MHz)

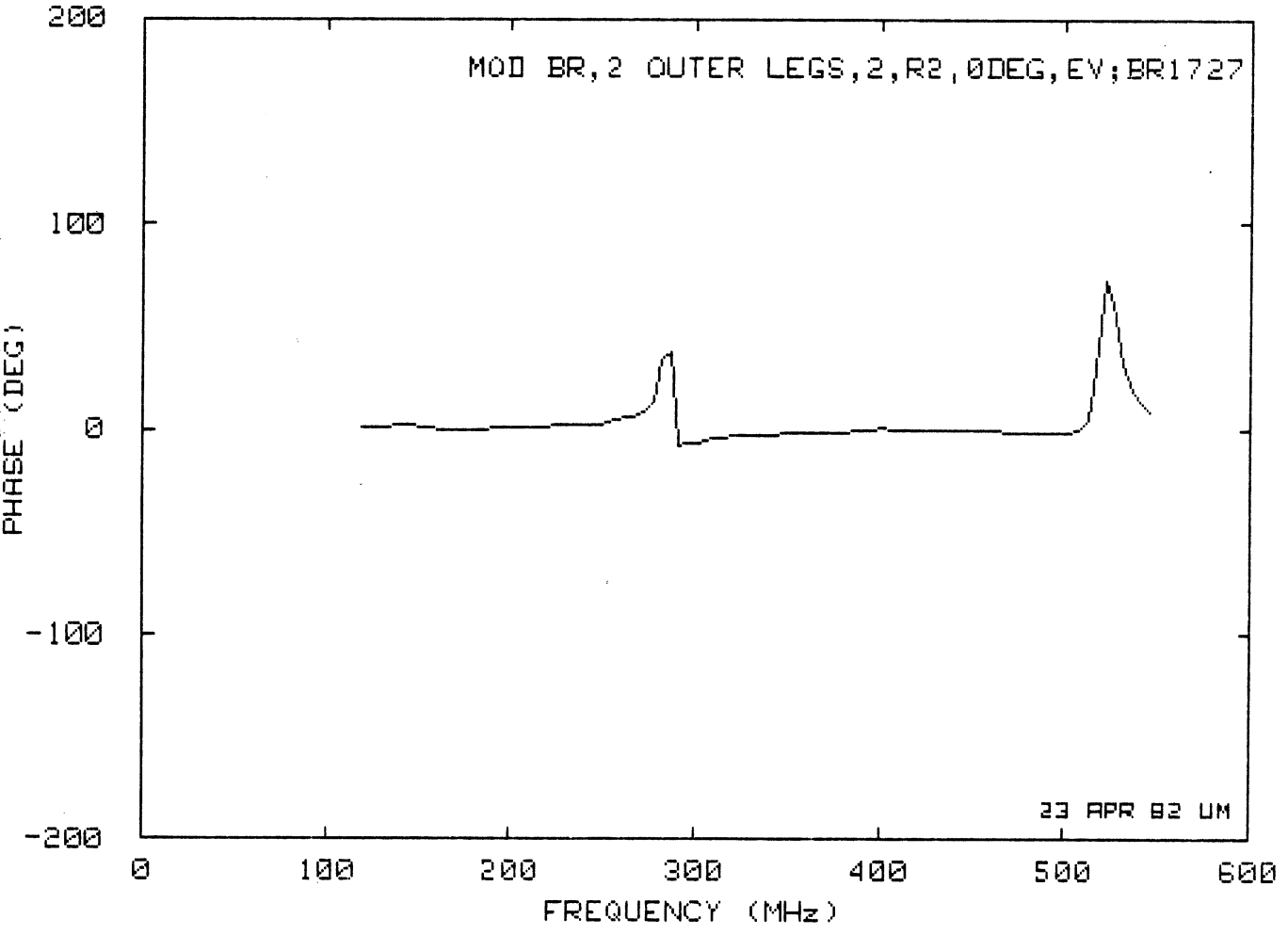
MOD BR,2 OUTER LEGS,2,R2,0DEG,EV;BR1727
PHASE (DEG)
200
100
0
-100
-200
23 APR 82 UM
0
100
200
300
400
500
600
FREQUENCY (MHz)

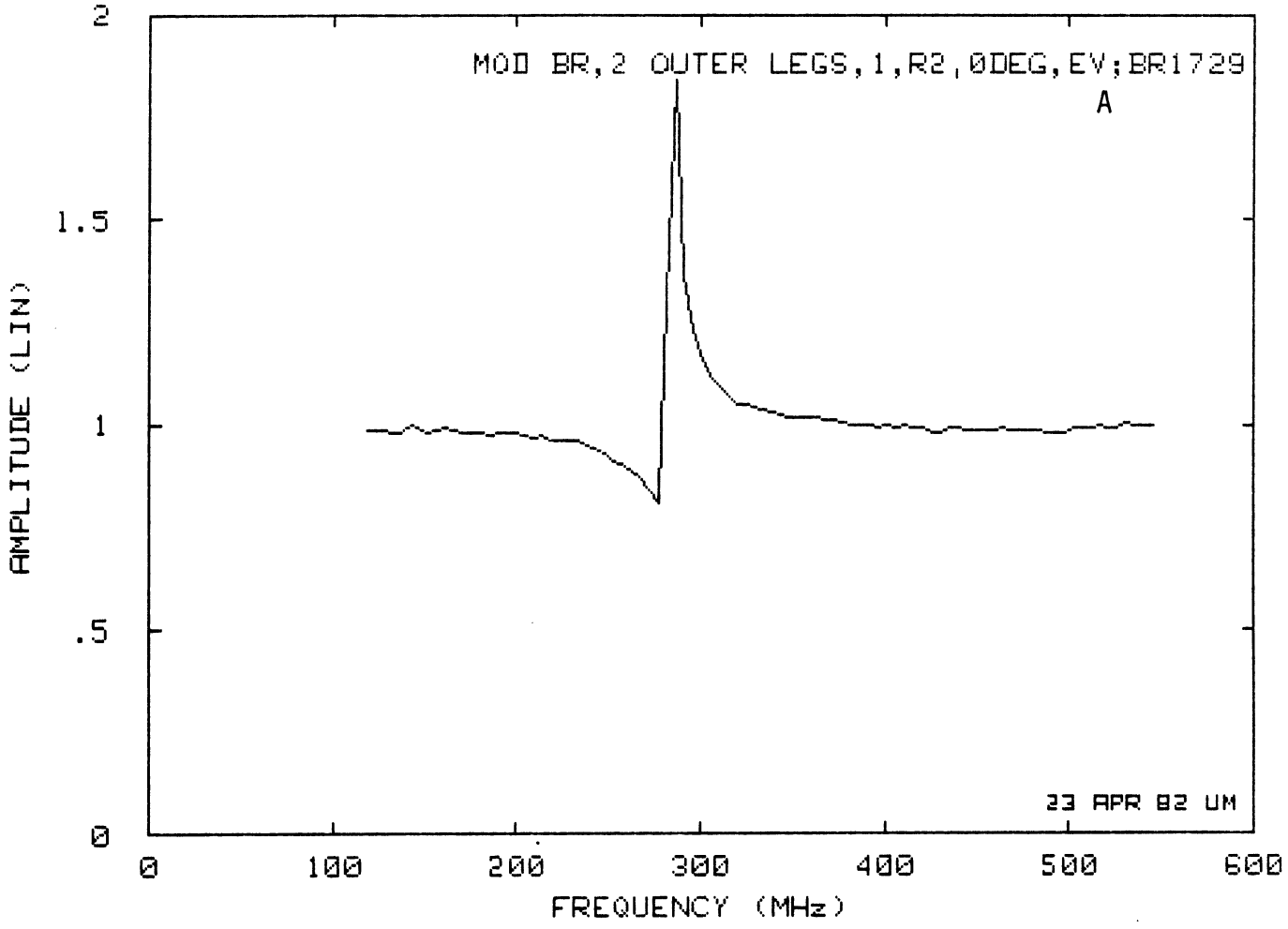
MOD BR,2 OUTER LEGS,1,R2,0DEG,EV;BR1729
A
23 APR 82 UM
AMPLITUDE (LIN)
2
1.5
1
.5
0
0
100
200
300
400
500
600
FREQUENCY (MHz)

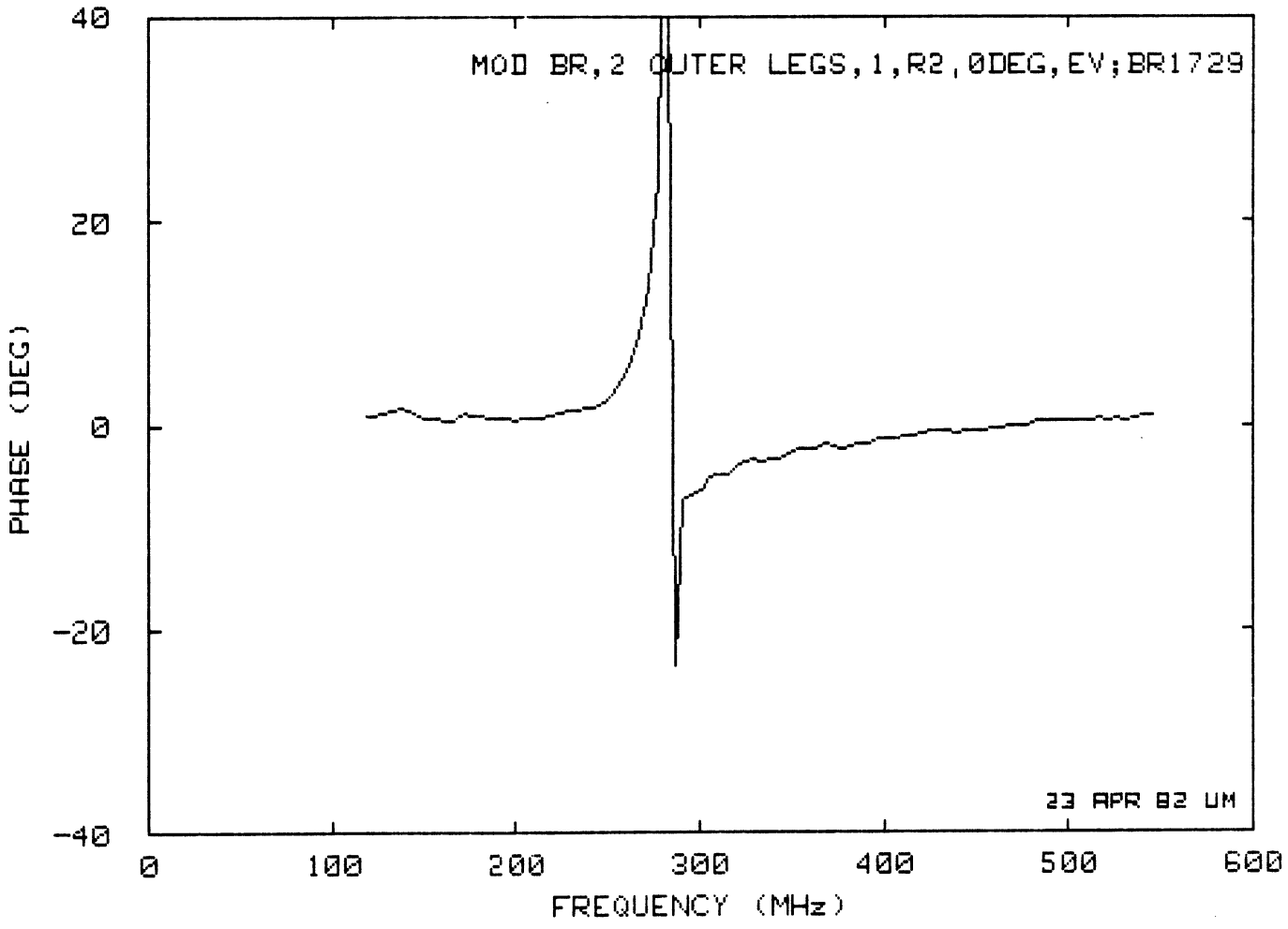
MOD BR,2 OUTER LEGS,1,R2,0DEG,EV;BR1729
23 APR 82 UM
PHASE (DEG)
40
20
0
-20
-40
0
100
200
300
400
500
600
FREQUENCY (MHz)

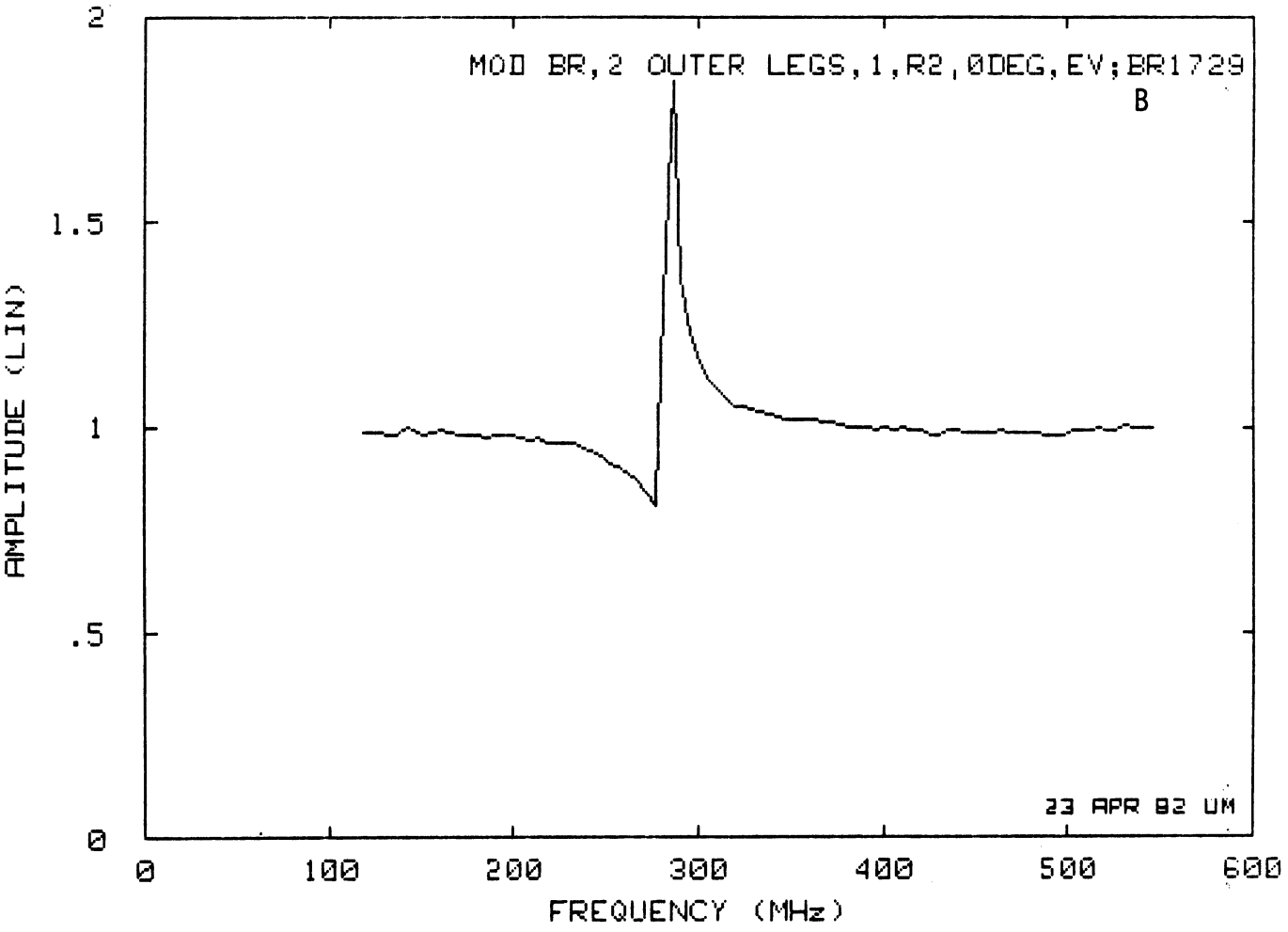
MOD BR,2 OUTER LEGS,1,R2,0DEG,EV;BR1729
B
23 APR 82 UM
AMPLITUDE (LIN)
2
1.5
1
.5
0
0
100
200
300
400
500
600
FREQUENCY (MHz)

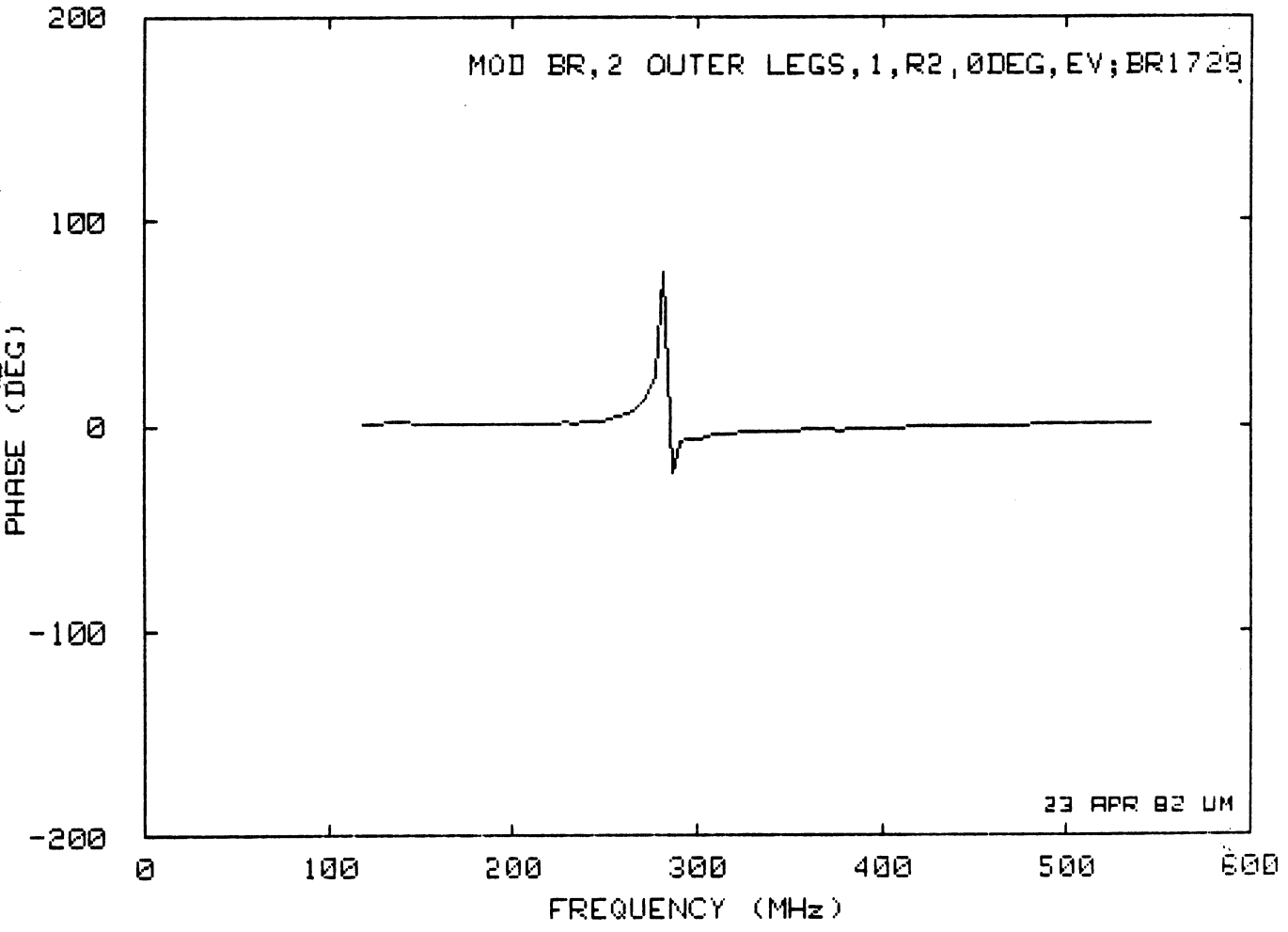
MOD BR,2 OUTER LEGS,1,R2,0DEG,EV;BR1729
23 APR 82 UM
PHASE (DEG)
200
100
0
-100
-200
0
100
200
300
400
500
600
FREQUENCY (MHz)

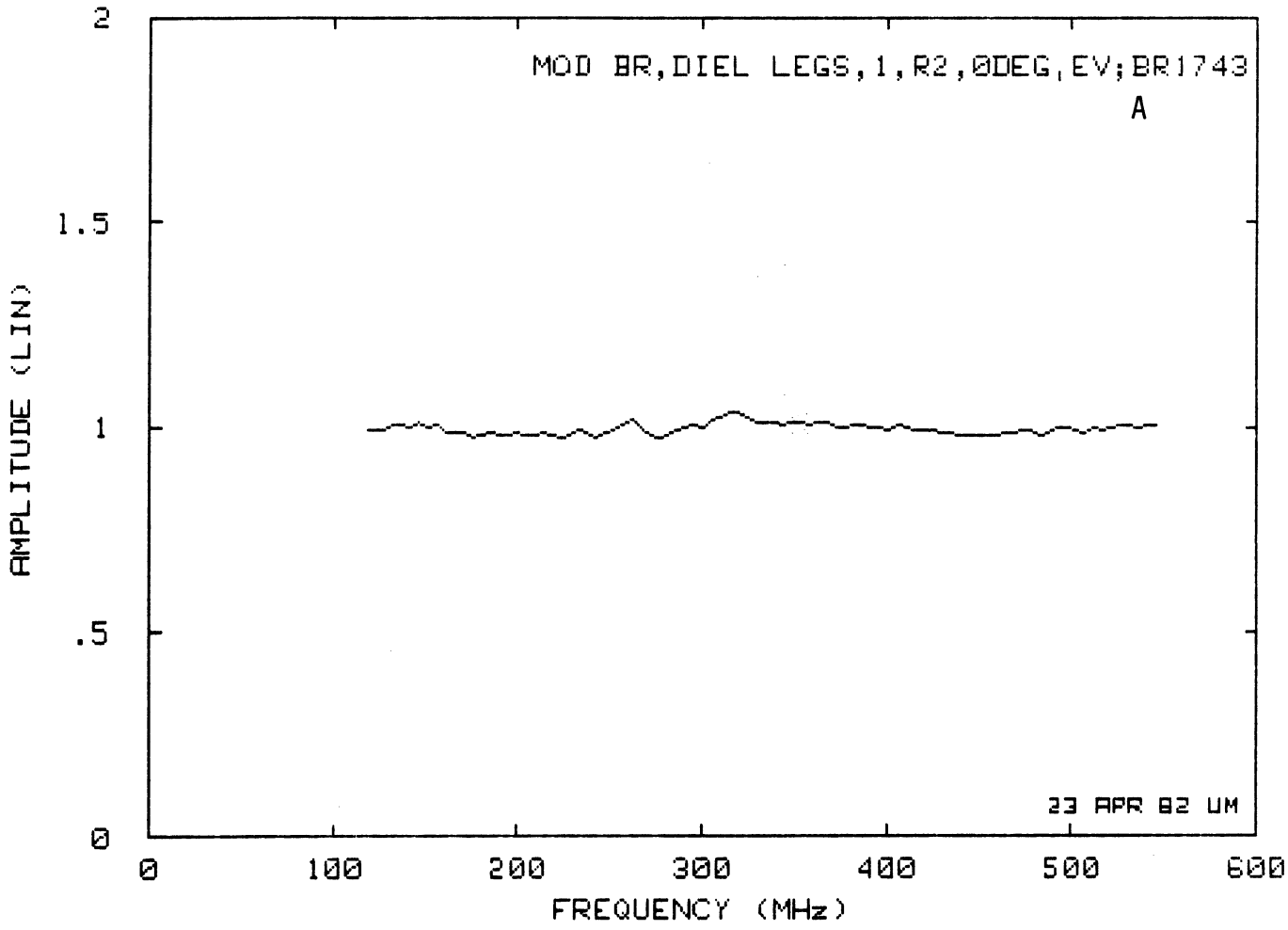
MOD BR,DIEL LEGS,1,R2,0DEG,EV;BR1743
A
23 APR 82 UM
AMPLITUDE (LIN)
2
1.5
1
.5
0
0
100
200
300
400
500
600
FREQUENCY (MHz)

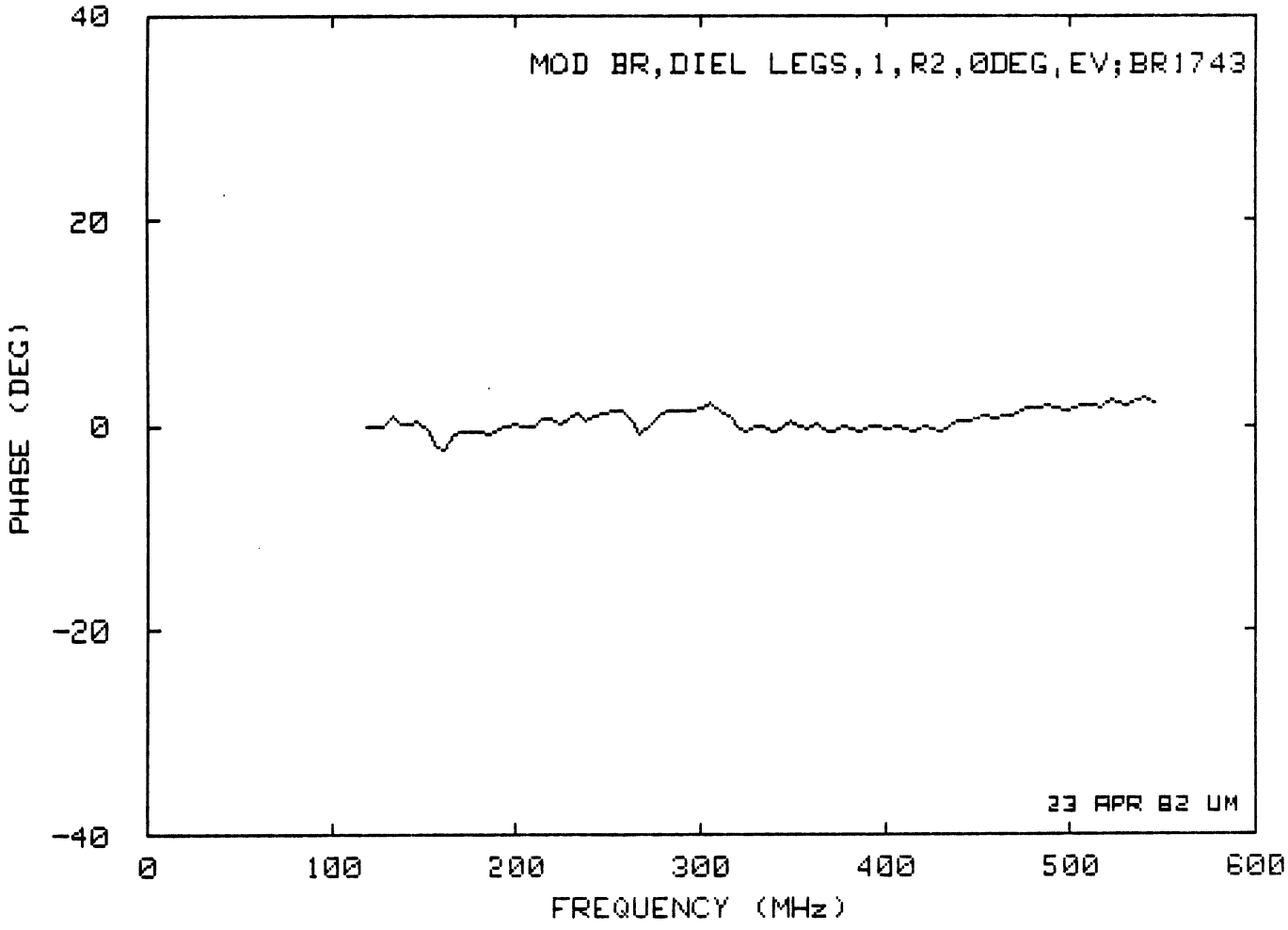
MOD BR,DIEL LEGS,1,R2,0DEG,EV;BR1743
23 APR 82 UM
PHASE (DEG)
40
20
0
-20
-40
0
100
200
300
400
500
600
FREQUENCY (MHz)

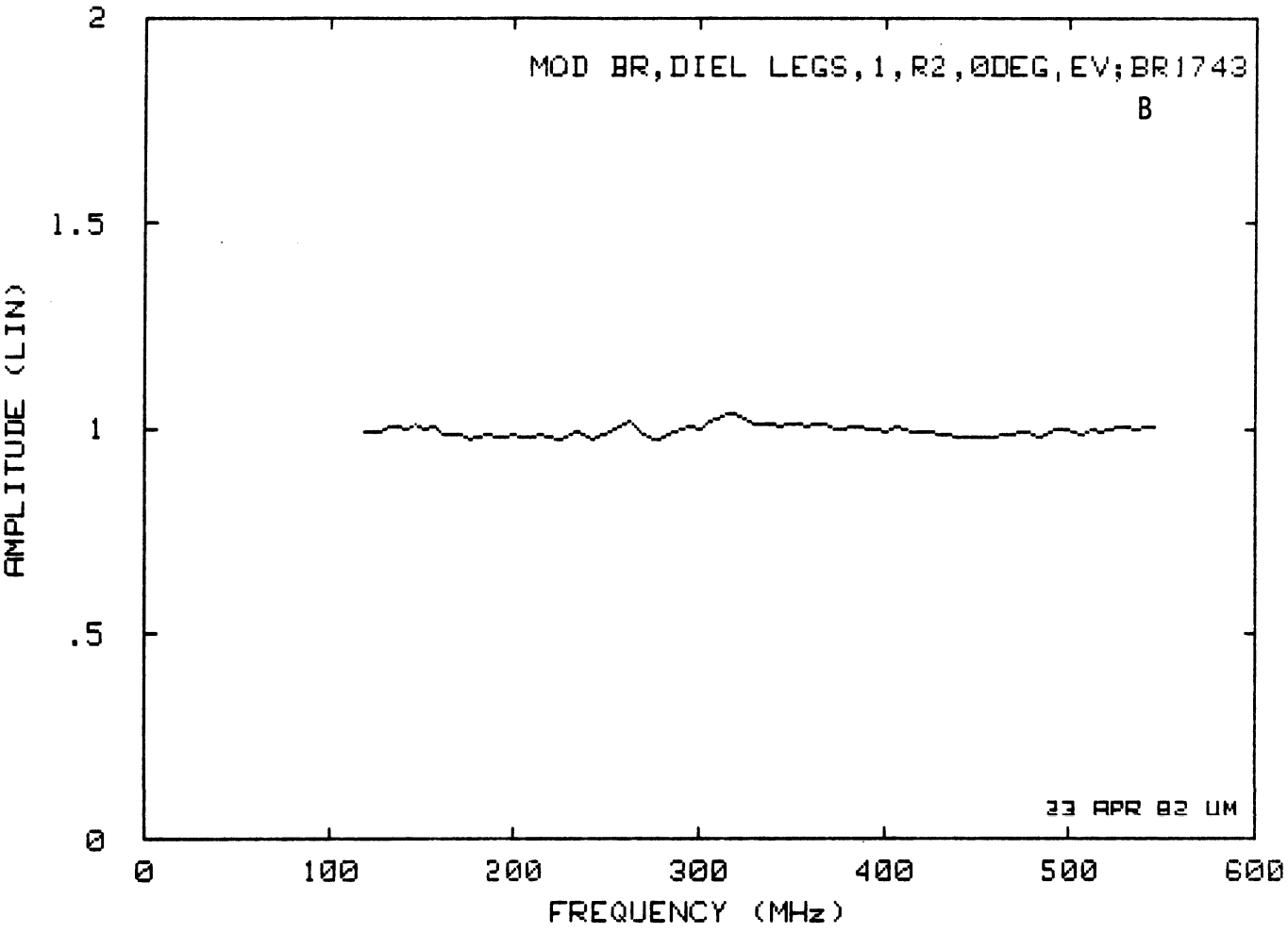
MOD BR,DIEL LEGS,1,R2,0DEG,EV;BR1743
B
23 APR 82 UM
AMPLITUDE (LIN)
2
1.5
1
.5
0
0
100
200
300
400
500
600
FREQUENCY (MHz)

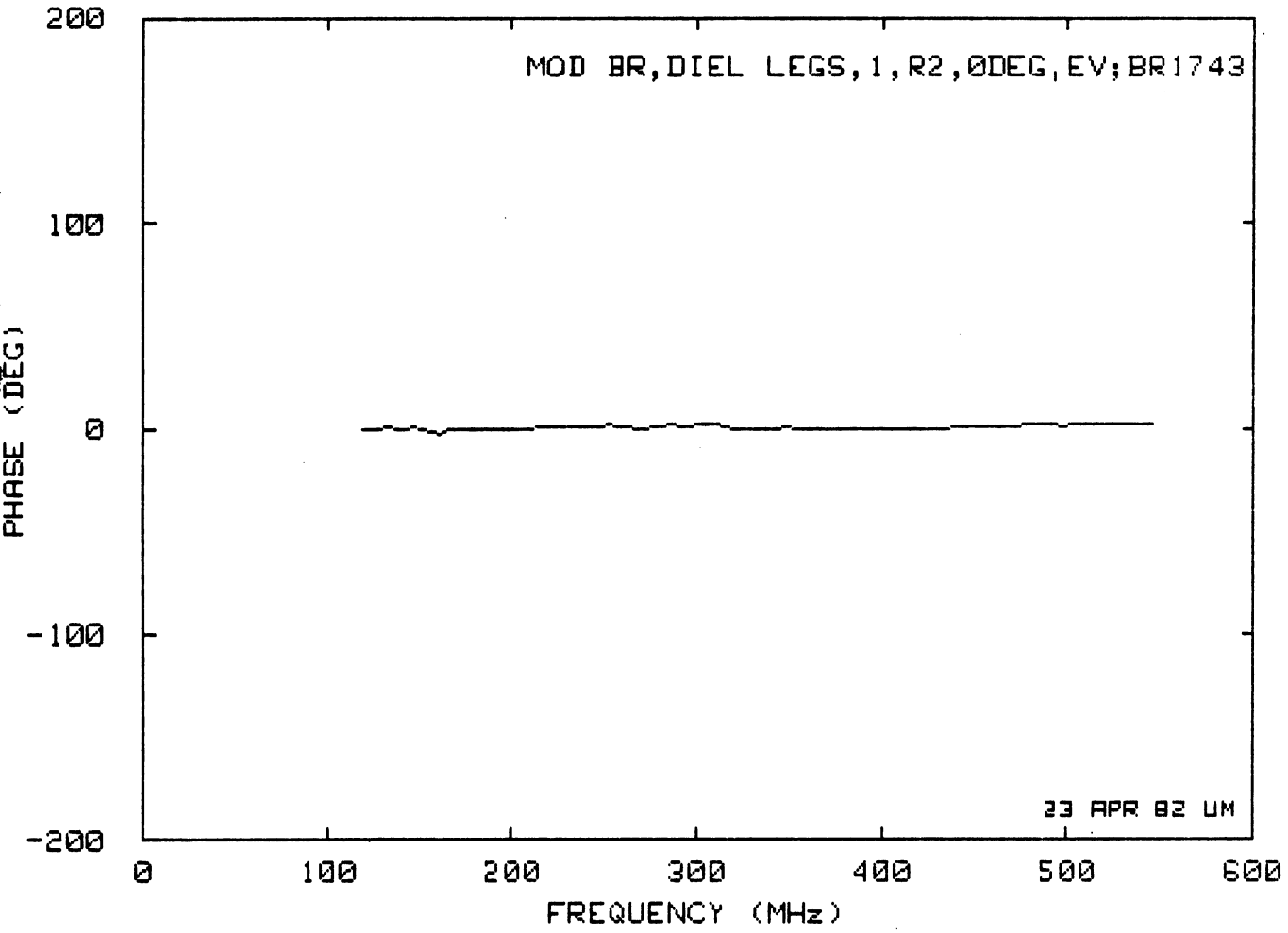
MOD BR,DIEL LEGS,1,R2,0DEG,EV;BR1743
23 APR 82 UM
PHASE (DEG)
200
100
0
-100
-200
0
100
200
300
400
500
600
FREQUENCY (MHz)

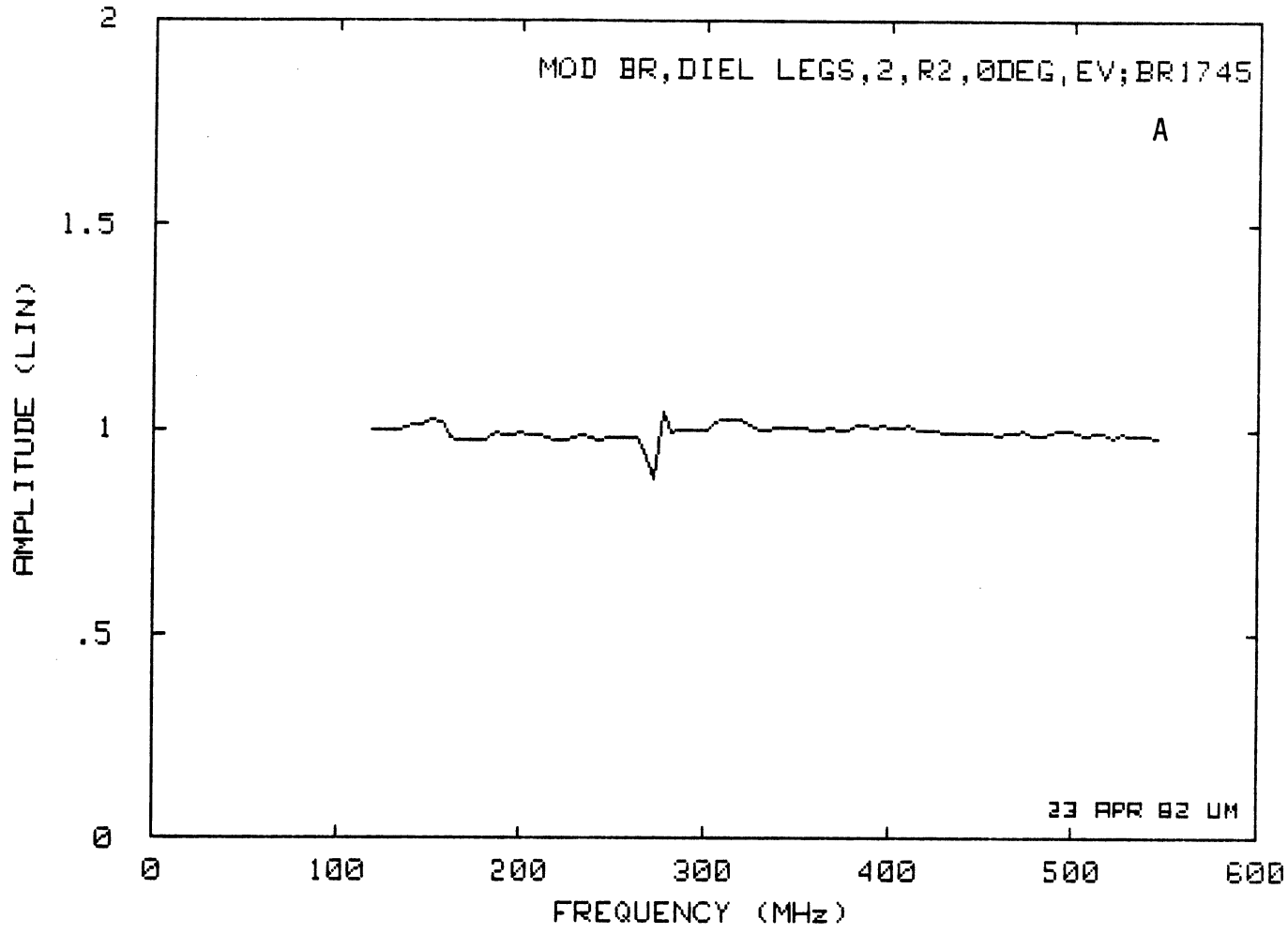
MOD BR,DIEL LEGS,2,R2,0DEG,EV;BR1745
A
23 APR 82 UM
AMPLITUDE (LIN)
2
1.5
1
.5
0
0
100
200
300
400
500
600
FREQUENCY (MHz)

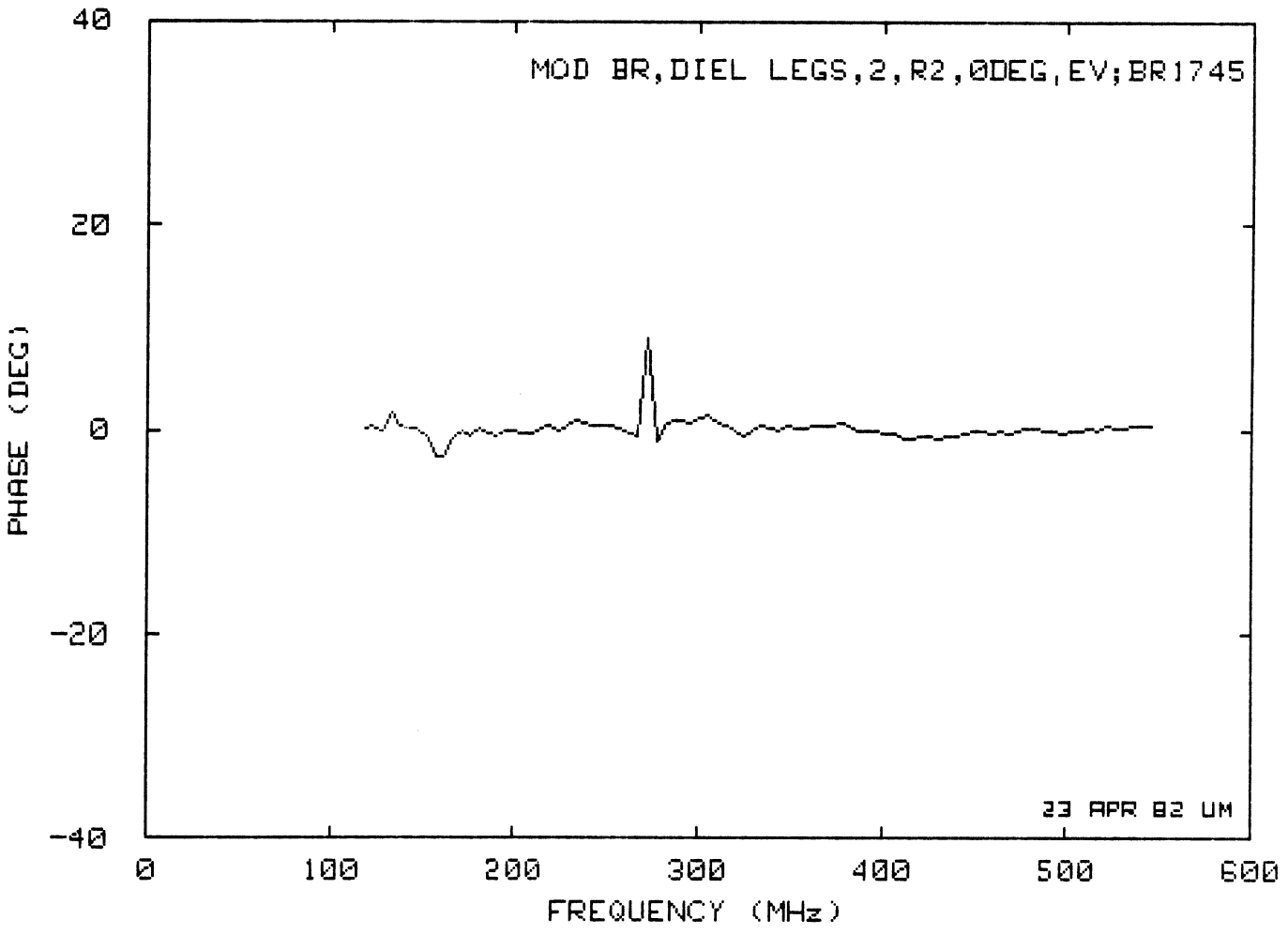
MOD BR,DIEL LEGS,2,R2,0DEG,EV;BR1745
23 APR 82 UM
PHASE (DEG)
40
20
0
-20
-40
0
100
200
300
400
500
600
FREQUENCY (MHz)

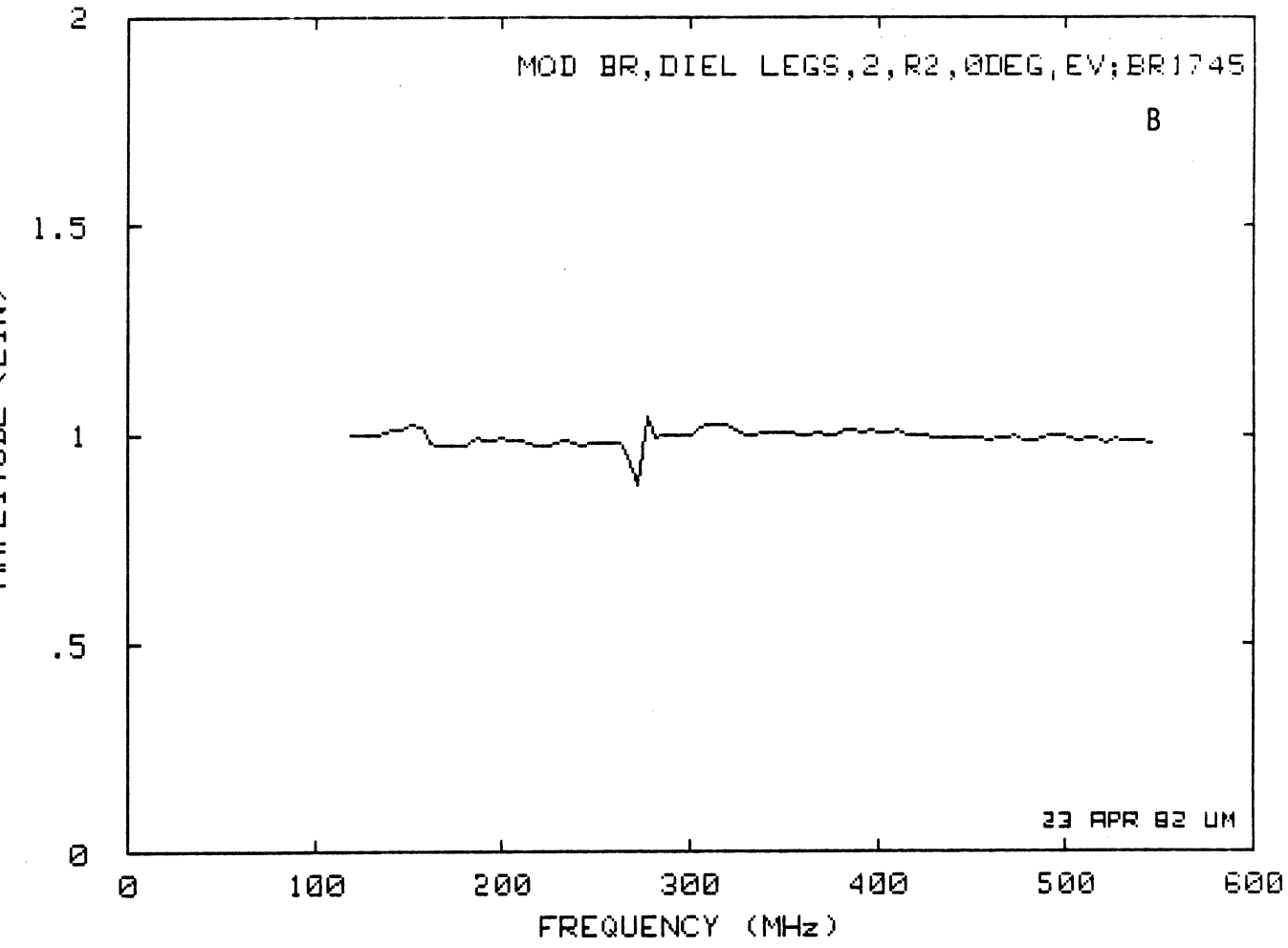
MOD BR,DIEL LEGS,2,R2,0DEG,EV;BR1745
B
23 APR 82 UM
2
1.5
1
.5
0
0
100
200
300
400
500
600
FREQUENCY (MHz)

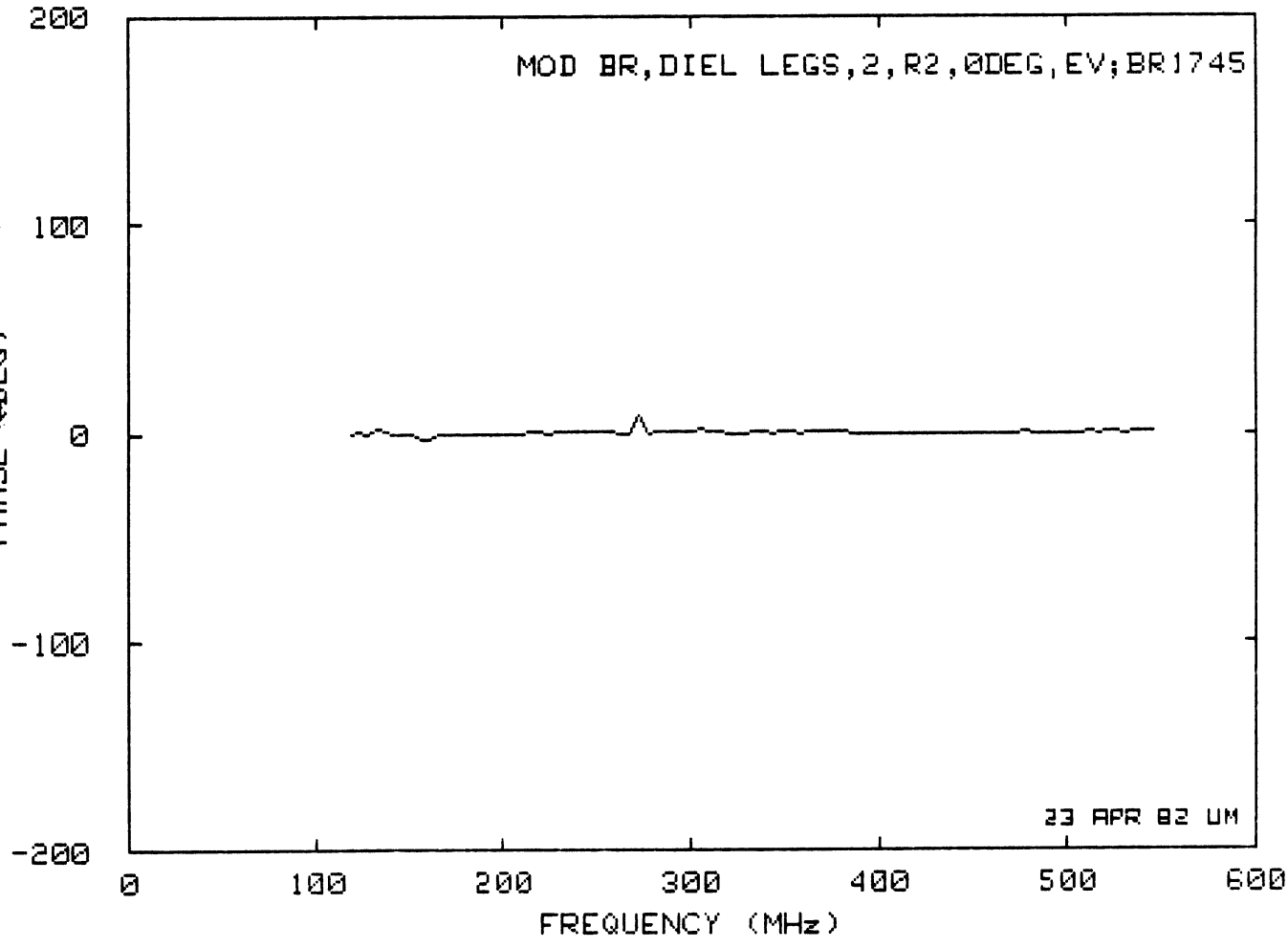
MOD BR,DIEL LEGS,2,R2,0DEG,EV;BR1745
23 APR 82 UM
200
100
0
-100
-200
0
100
200
300
400
500
600
FREQUENCY (MHz)

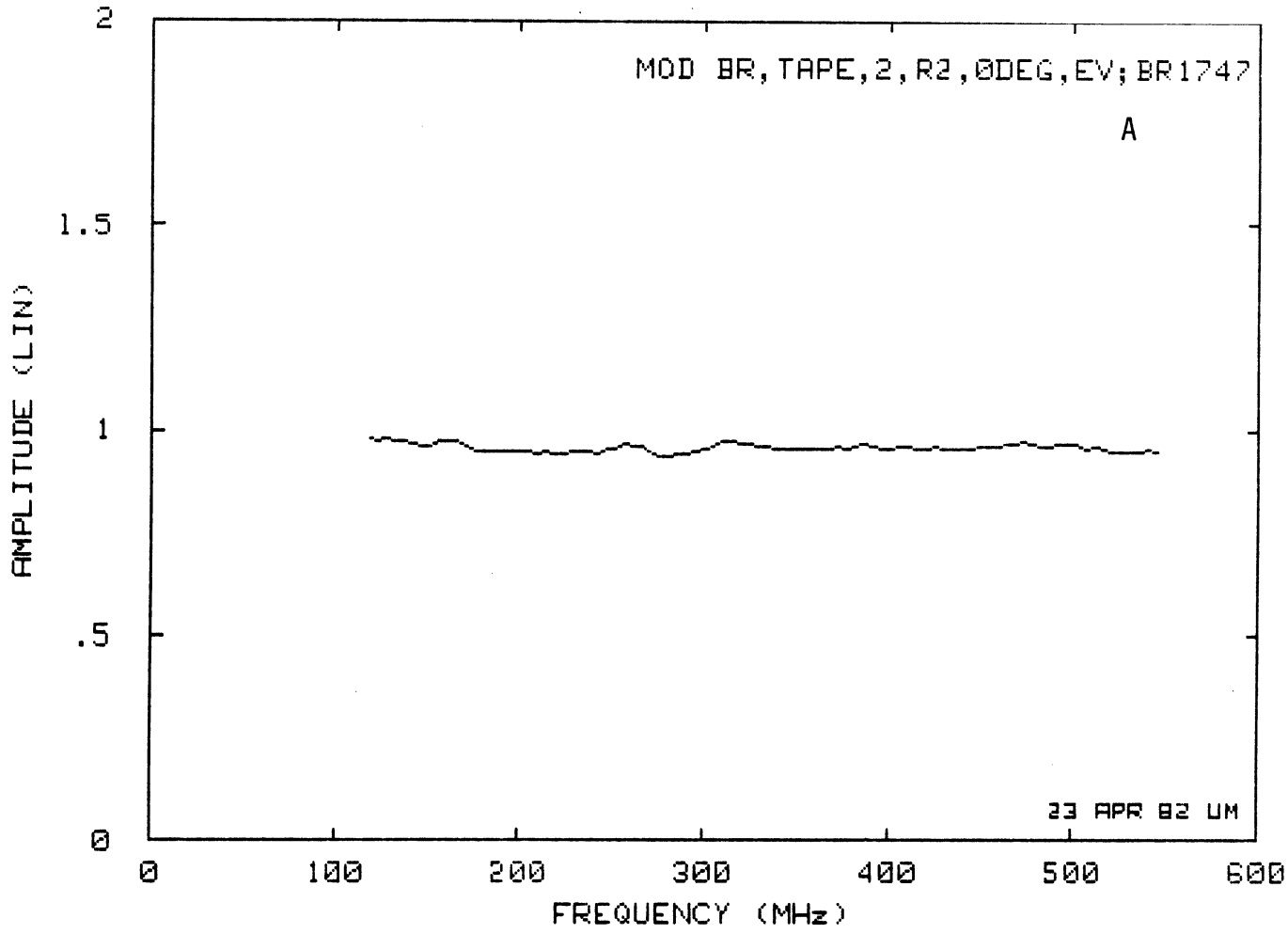
MOD BR,TAPE,2,R2,0DEG,EV;BR1747
A
23 APR 82 UM
AMPLITUDE (LIN)
2
1.5
1
.5
0
0
100
200
300
400
500
600
FREQUENCY (MHz)

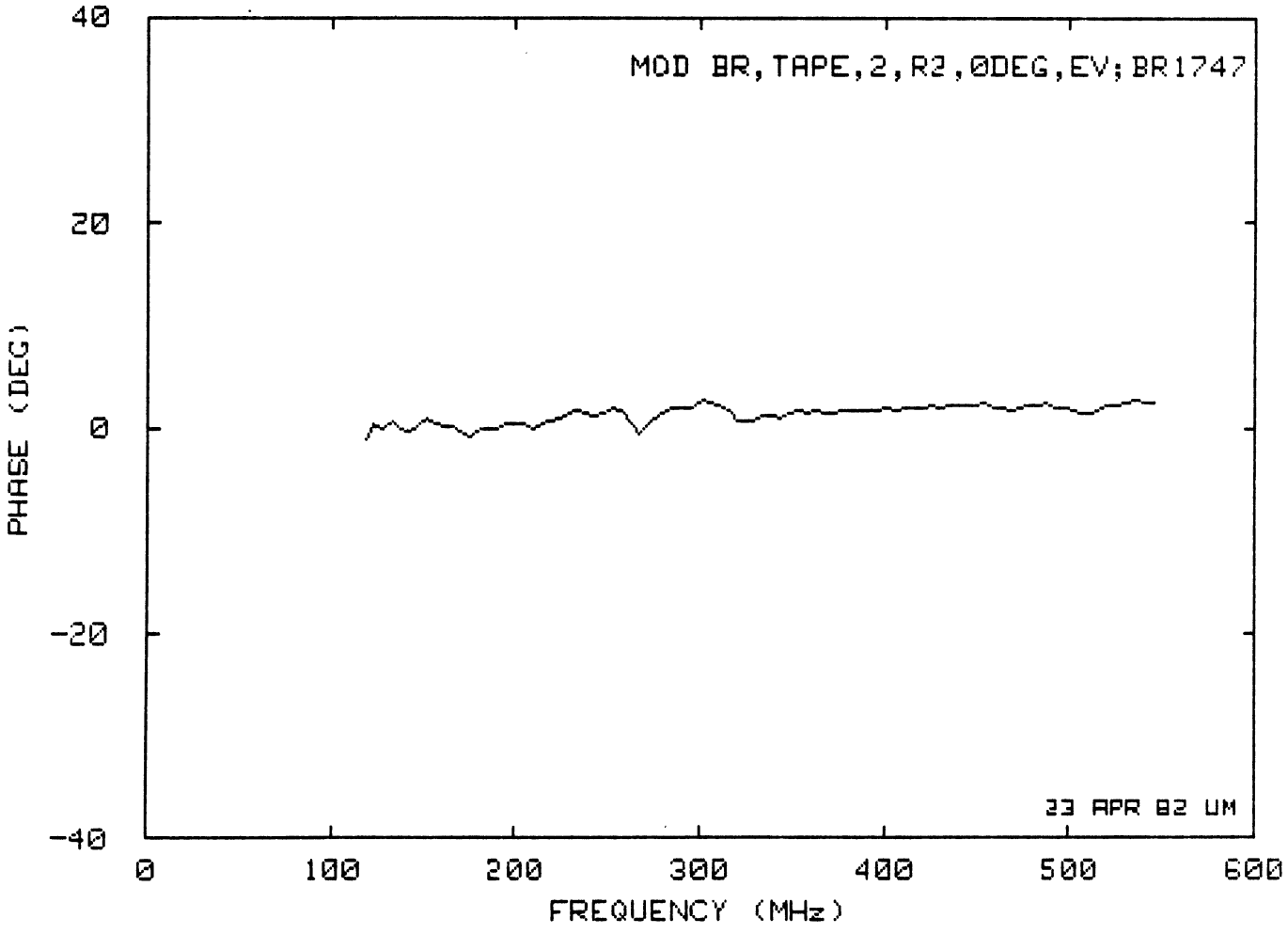
MOD BR,TAPE,2,R2,0DEG,EV;BR1747
23 APR 82 UM
PHASE (DEG)
40
20
0
-20
-40
0
100
200
300
400
500
600
FREQUENCY (MHz)

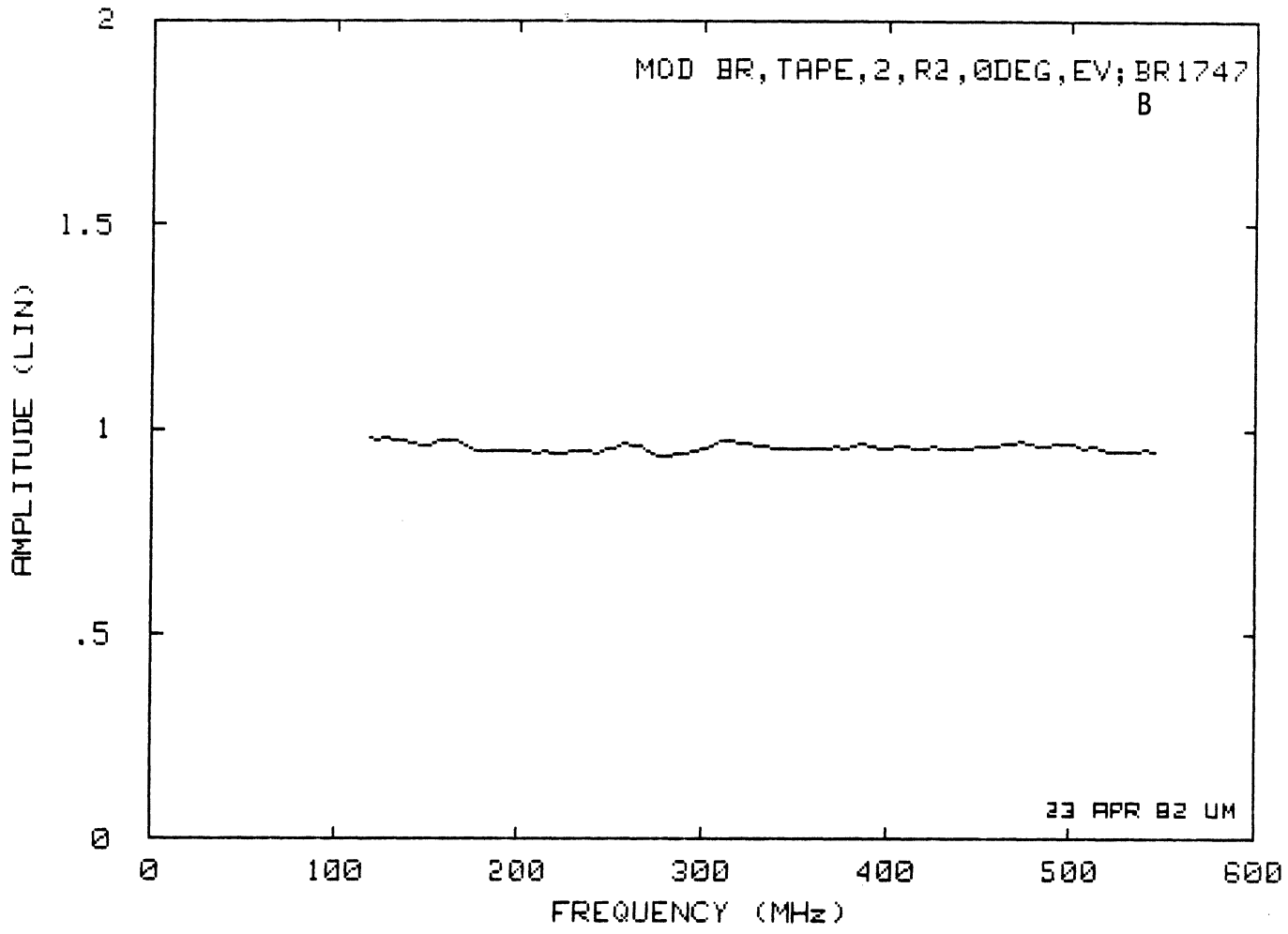
MOD BR,TAPE,2,R2,0DEG,EV;BR1747
B
23 APR 82 UM
AMPLITUDE (LIN)
2
1.5
1
.5
0
0
100
200
300
400
500
600
FREQUENCY (MHz)

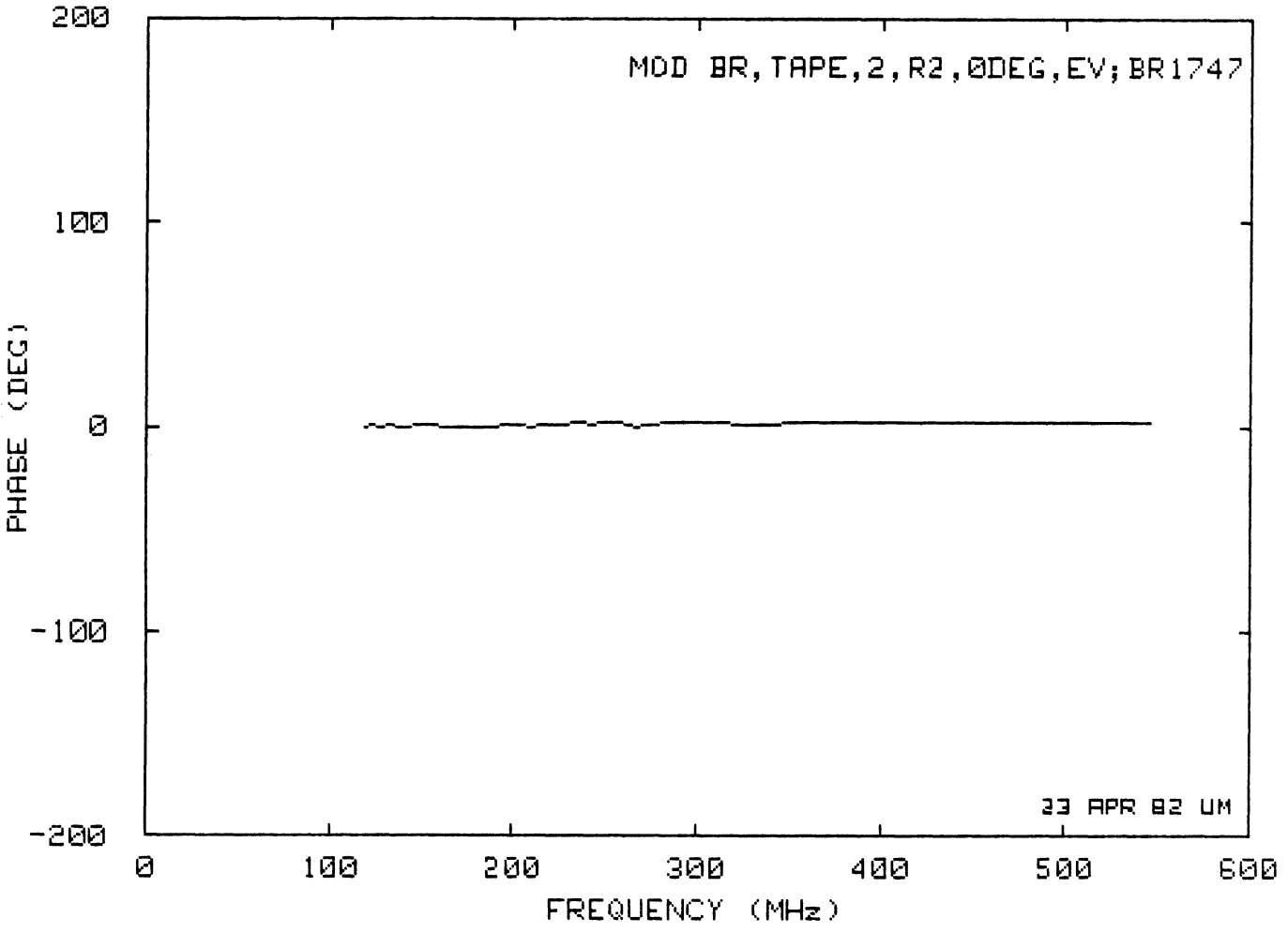
MOD BR,TAPE,2,R2,0DEG,EV;BR1747
23 APR 82 UM
PHASE (DEG)
200
100
0
-100
-200
0
100
200
300
400
500
600
FREQUENCY (MHz)

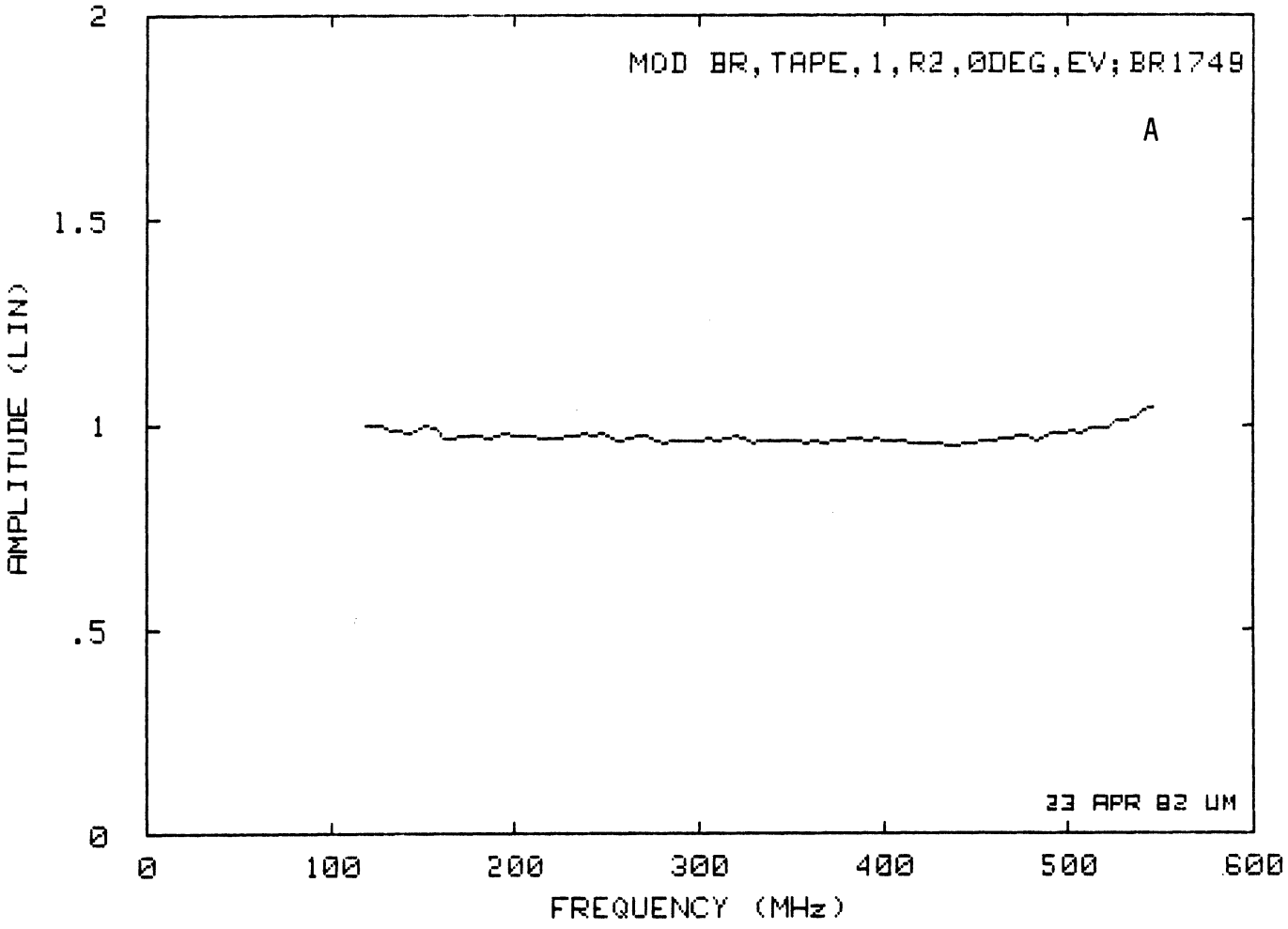
MOD BR,TAPE,1,R2,0DEG,EV;BR1749
A
23 APR 82 UM
AMPLITUDE (LIN)
2
1.5
1
.5
0
0
100
200
300
400
500
600
FREQUENCY (MHz)

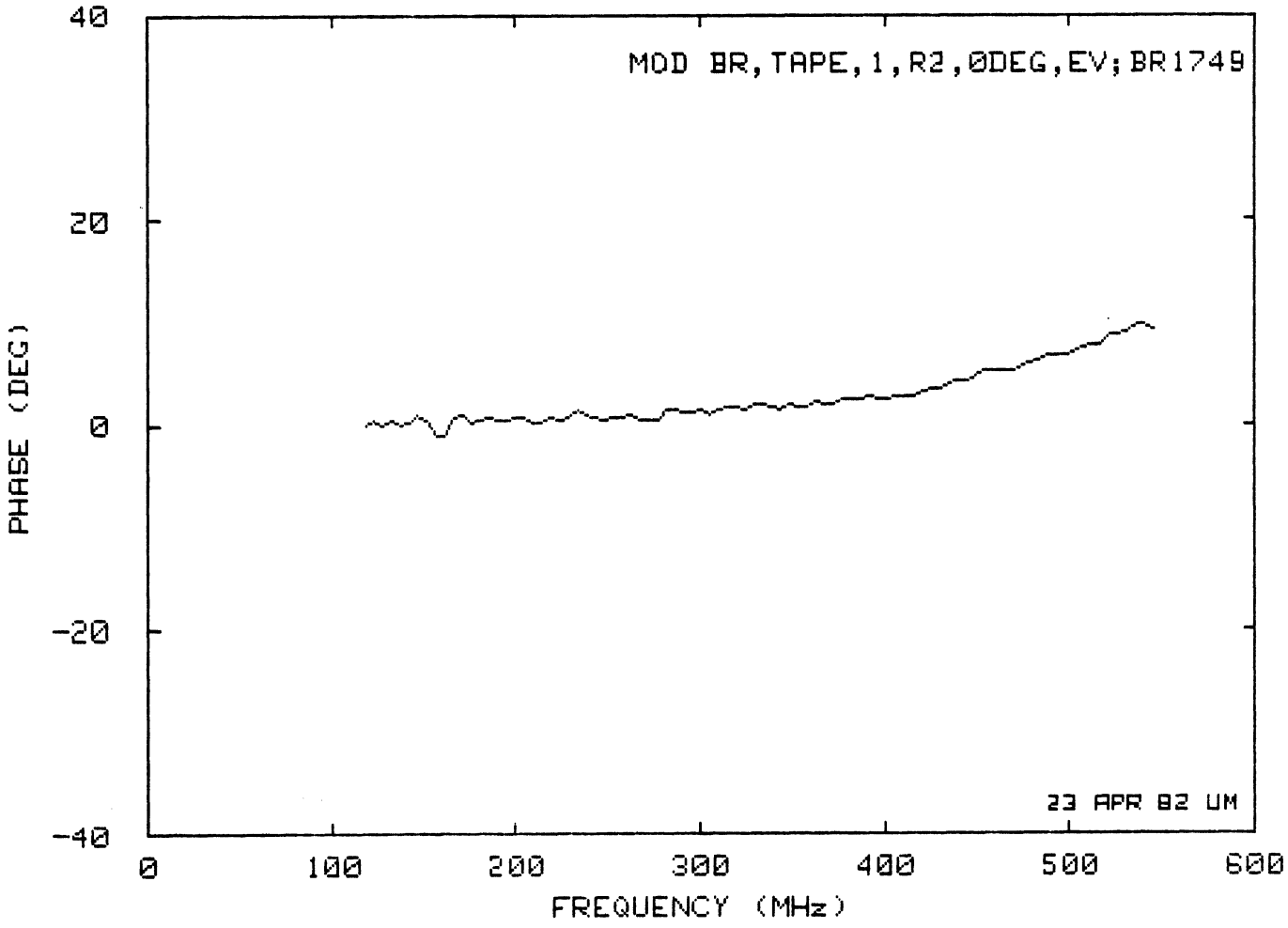
MOD BR,TAPE,1,R2,0DEG,EV;BR1749
23 APR 82 UM
PHASE (DEG)
40
20
0
-20
-40
0
100
200
300
400
500
600
FREQUENCY (MHz)

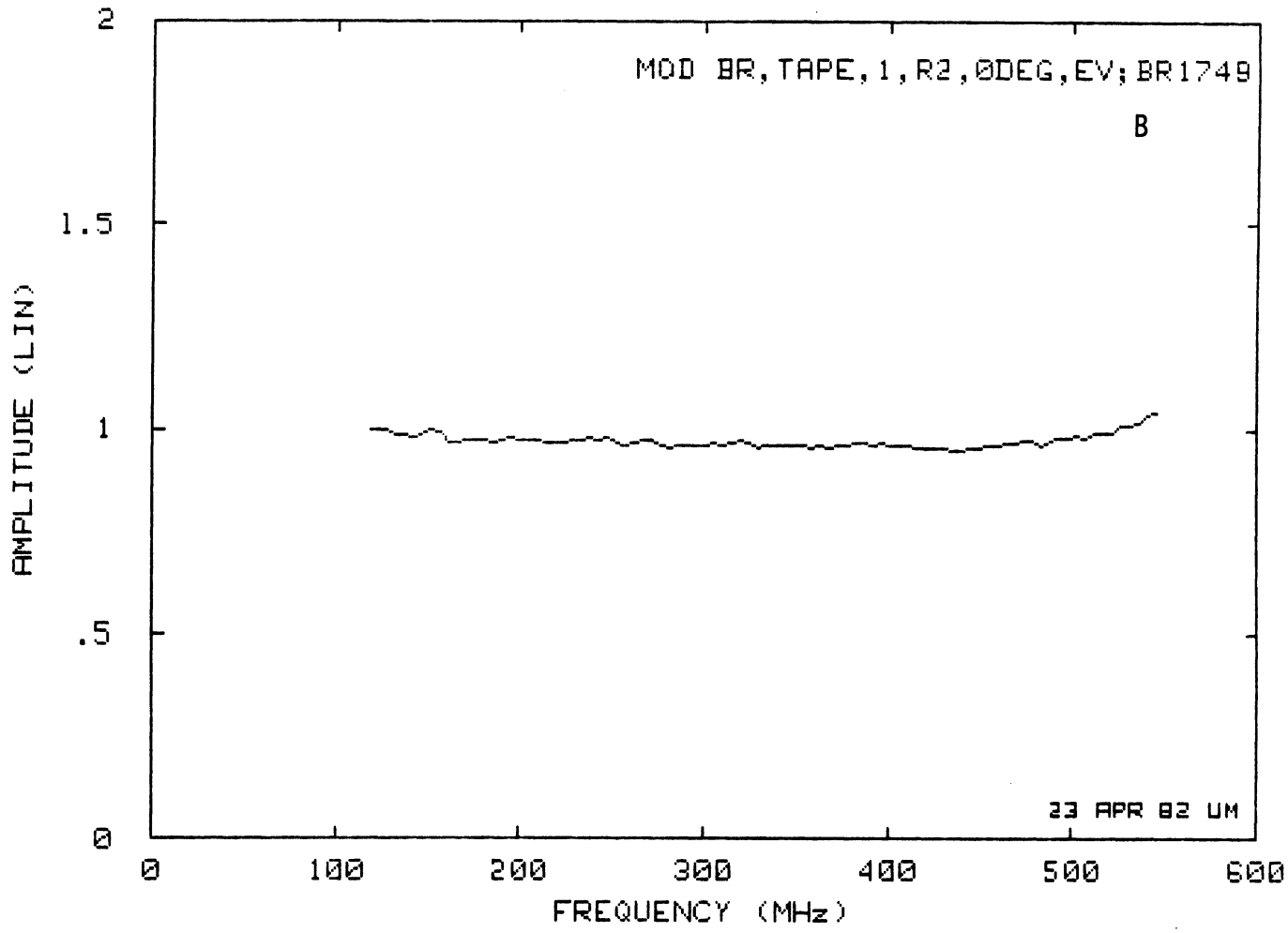
MOD BR,TAPE,1,R2,0DEG,EV;BR1749
B
23 APR 82 UM
AMPLITUDE (LIN)
2
1.5
1
.5
0
0
100
200
300
400
500
600
FREQUENCY (MHz)

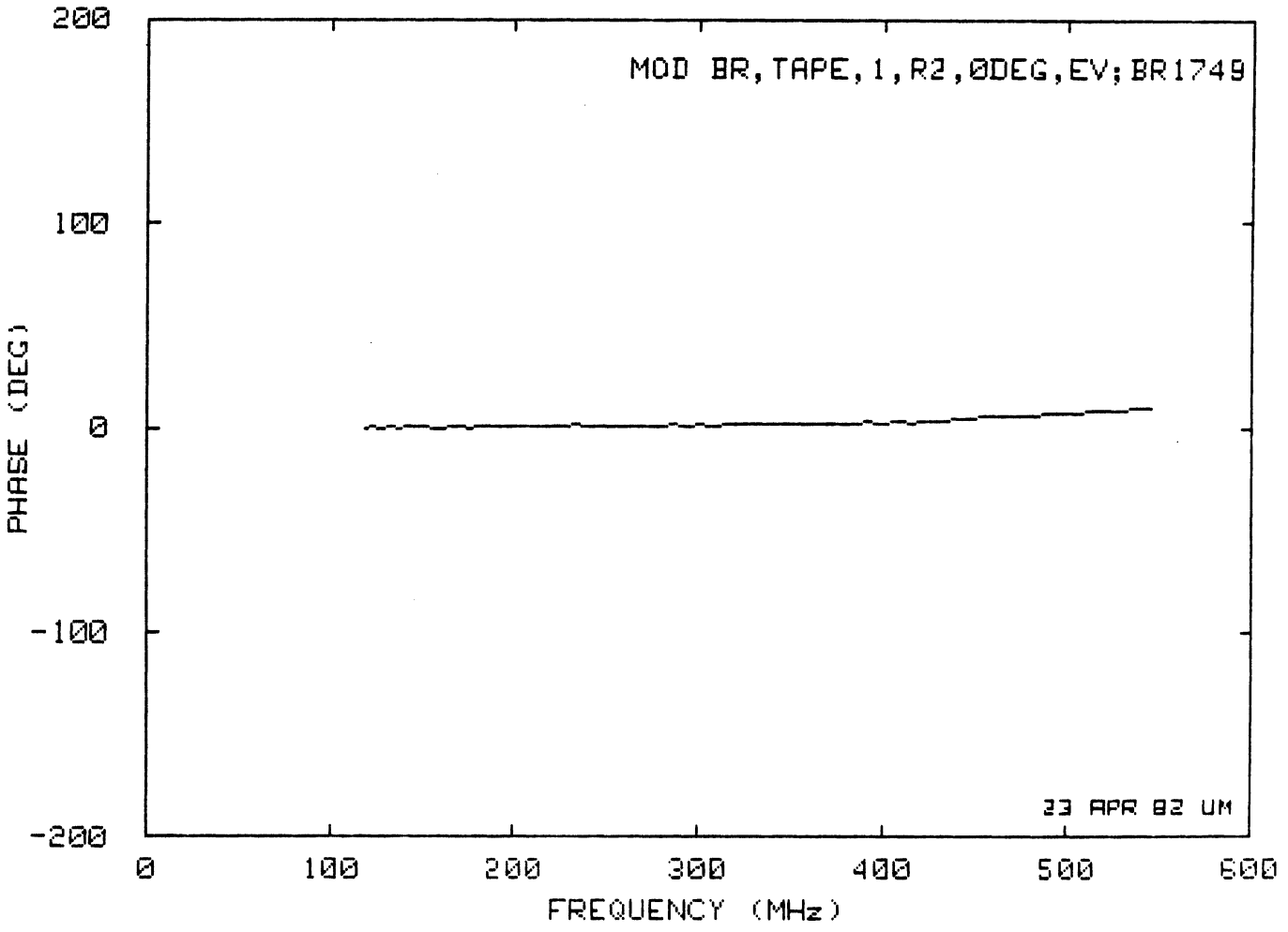
MOD BR,TAPE,1,R2,0DEG,EV;BR1749
23 APR 82 UM
PHASE (DEG)
200
100
0
-100
-200
0
100
200
300
400
500
600
FREQUENCY (MHz)

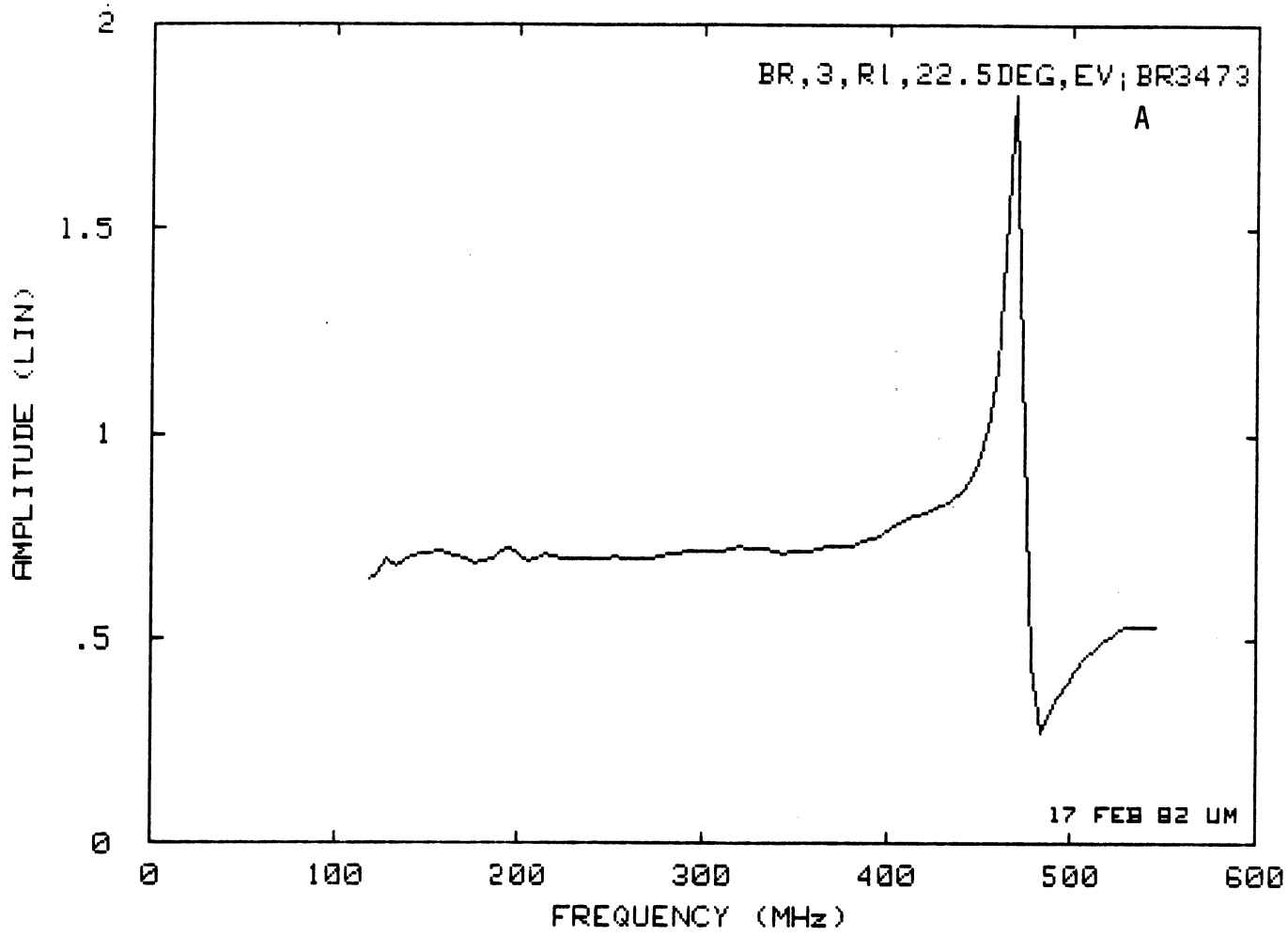
BR,3,R1,22.5DEG,EV;BR3473
A
17 FEB 82 UM
AMPLITUDE (LIN)
2
1.5
1
.5
0
0
100
200
300
400
500
600
FREQUENCY (MHz)

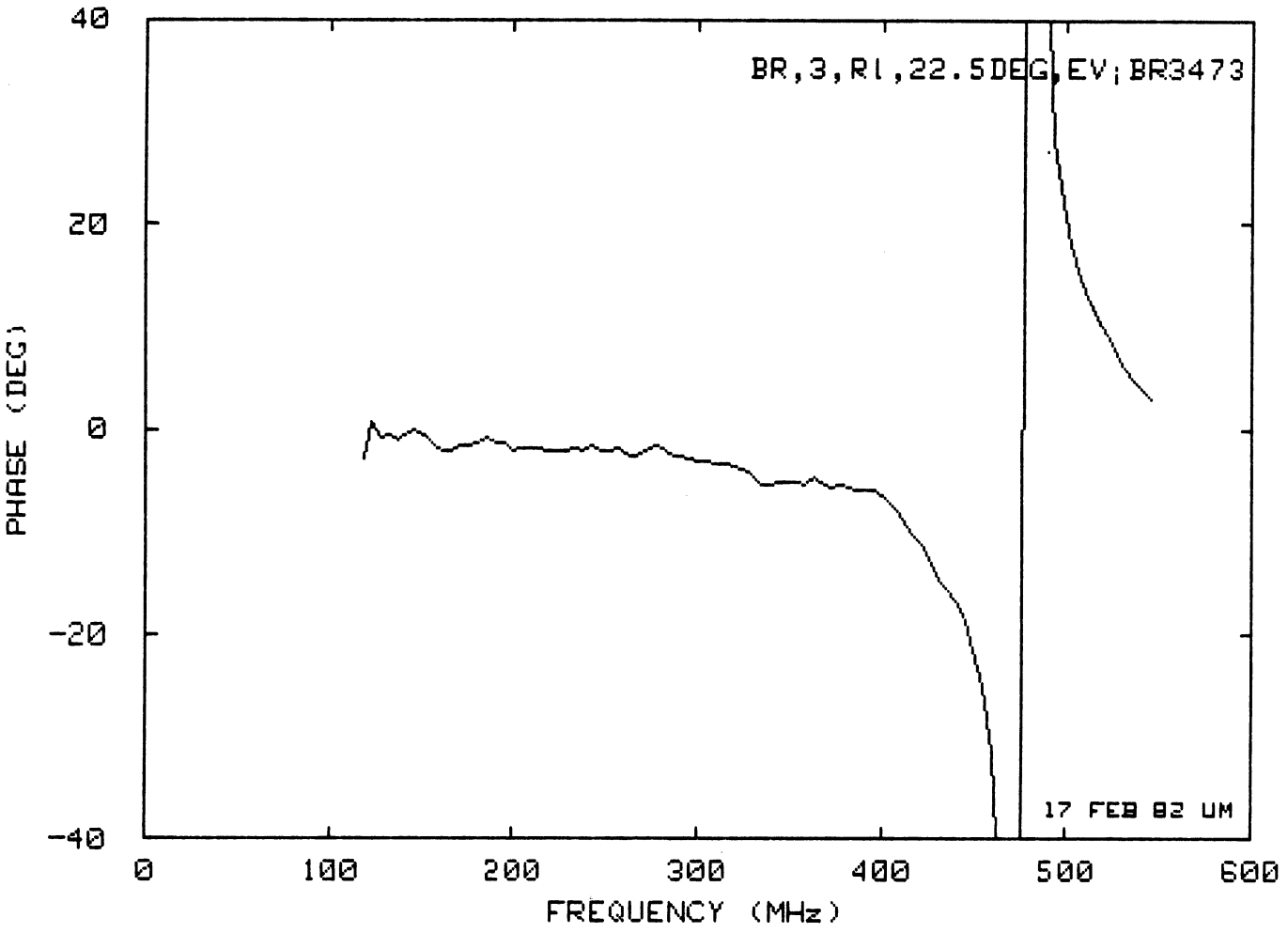
BR,3,R1,22.5DEG,EV;BR3473
17 FEB 82 UM
PHASE (DEG)
40
20
0
-20
-40
0
100
200
300
400
500
600
FREQUENCY (MHz)

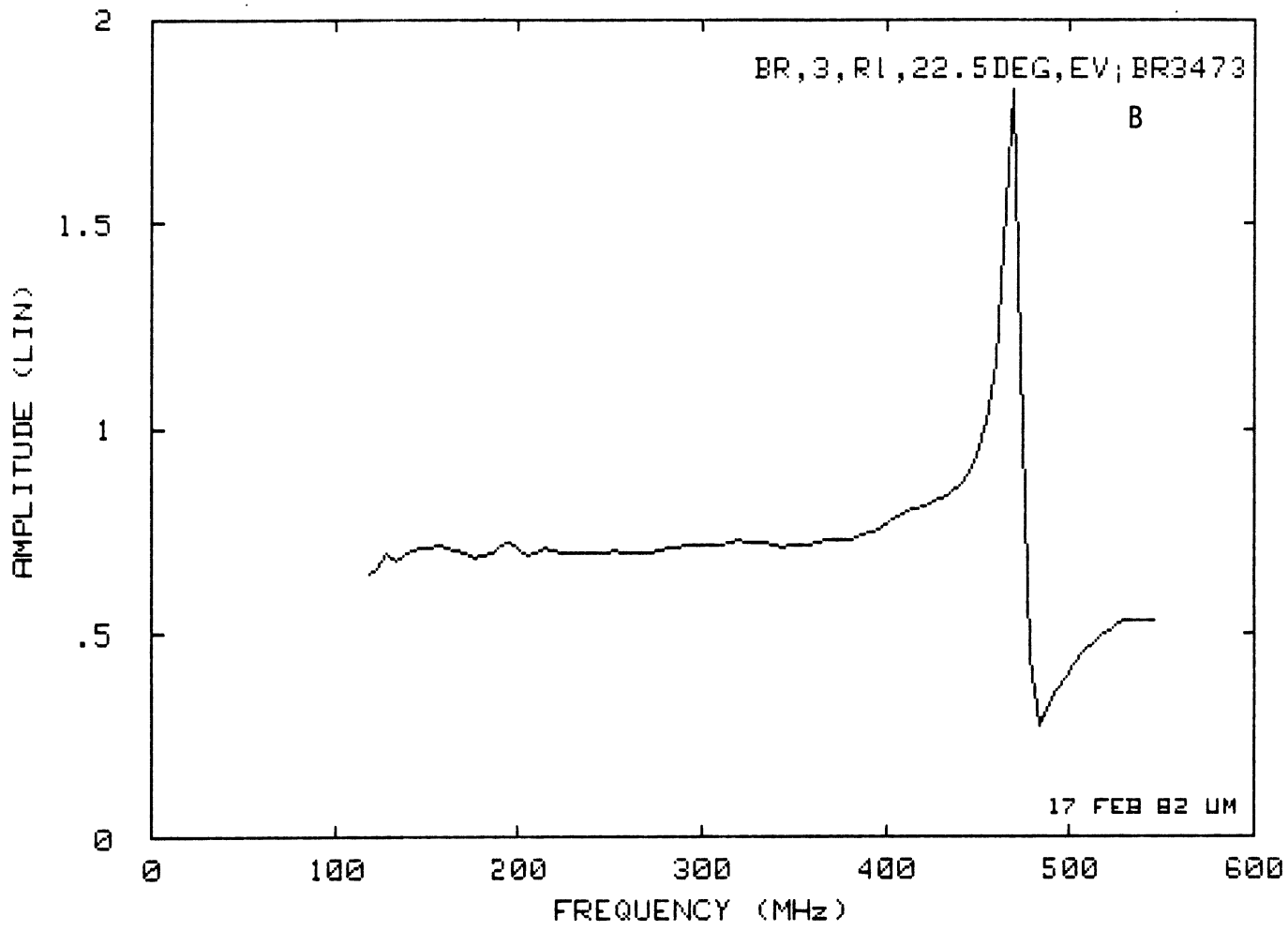
BR,3,RI,22.5DEG,EV;BR3473
B
17 FEB 82 UM
AMPLITUDE (LIN)
2
1.5
1
.5
0
0
100
200
300
400
500
600
FREQUENCY (MHz)

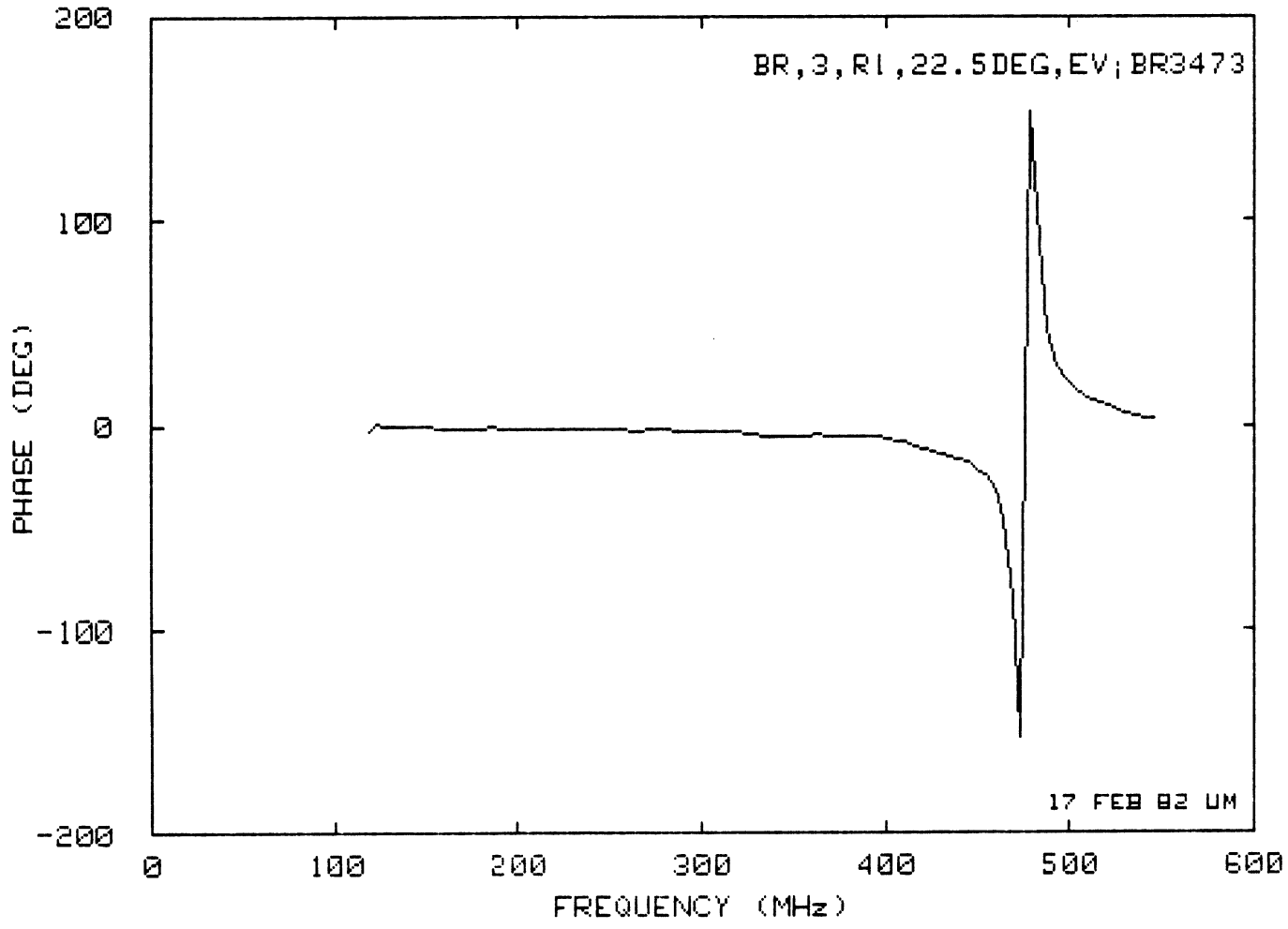
BR,3,RI,22.5DEG,EV;BR3473
17 FEB 82 UM
PHASE (DEG)
200
100
0
-100
-200
0
100
200
300
400
500
600
FREQUENCY (MHz)

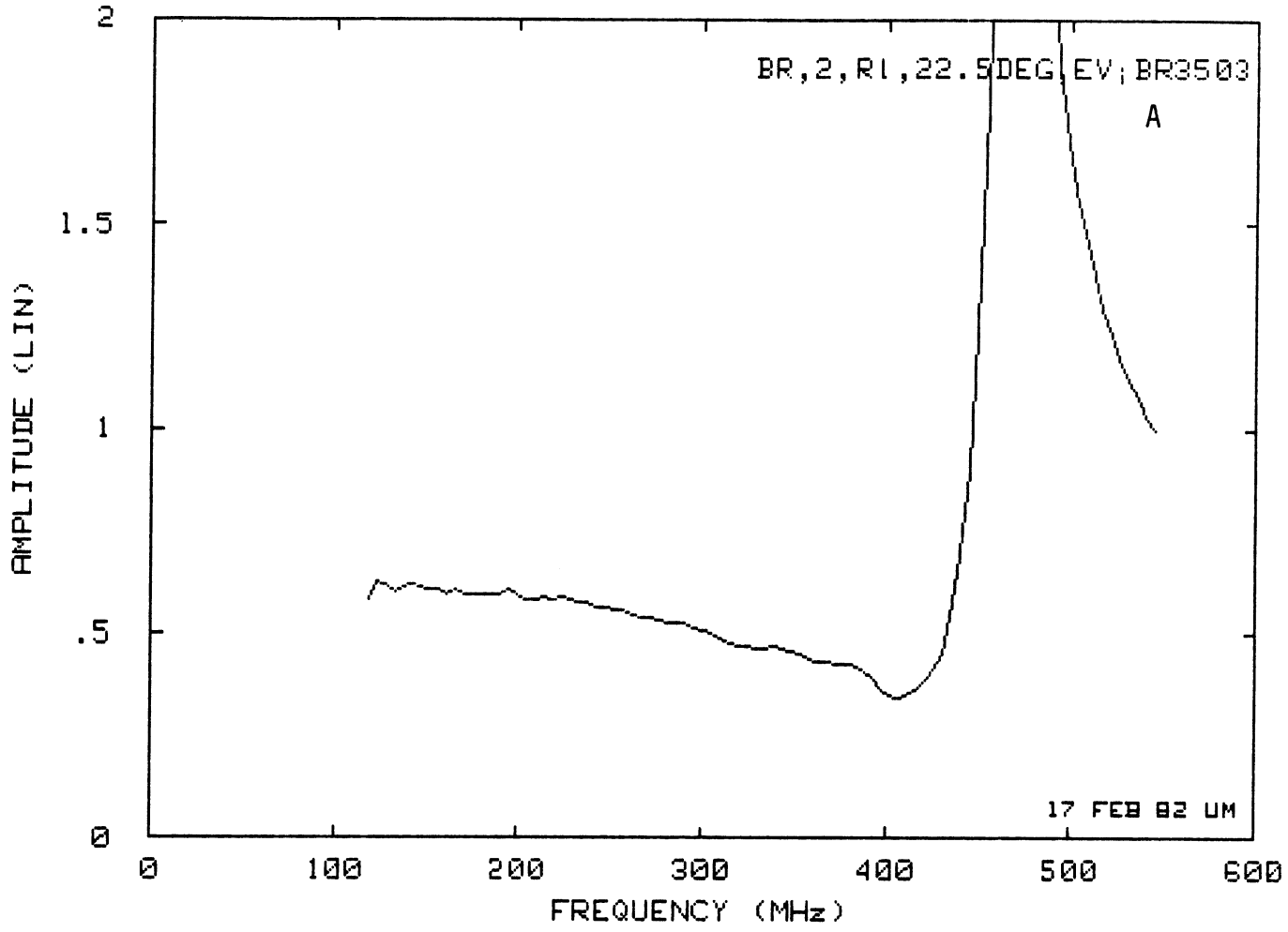
BR,2,RI,22.5DEG,EV;BR3503
A
17 FEB 82 UM
AMPLITUDE (LIN)
2
1.5
1
.5
0
0
100
200
300
400
500
600
FREQUENCY (MHz)

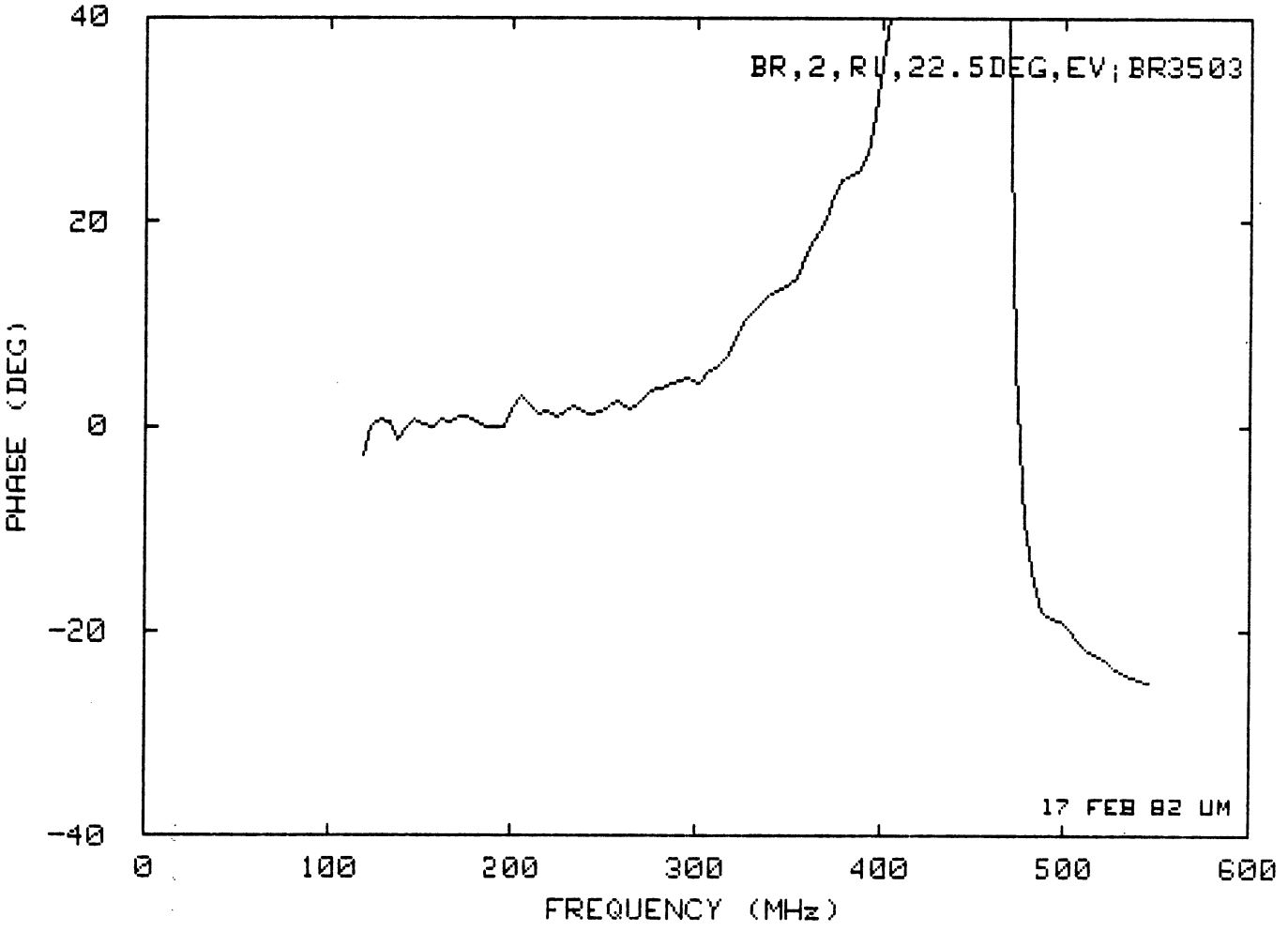
BR,2,RI,22.5DEG,EV;BR3503
17 FEB 82 UM
PHASE (DEG)
40
20
0
-20
-40
0
100
200
300
400
500
600
FREQUENCY (MHz)

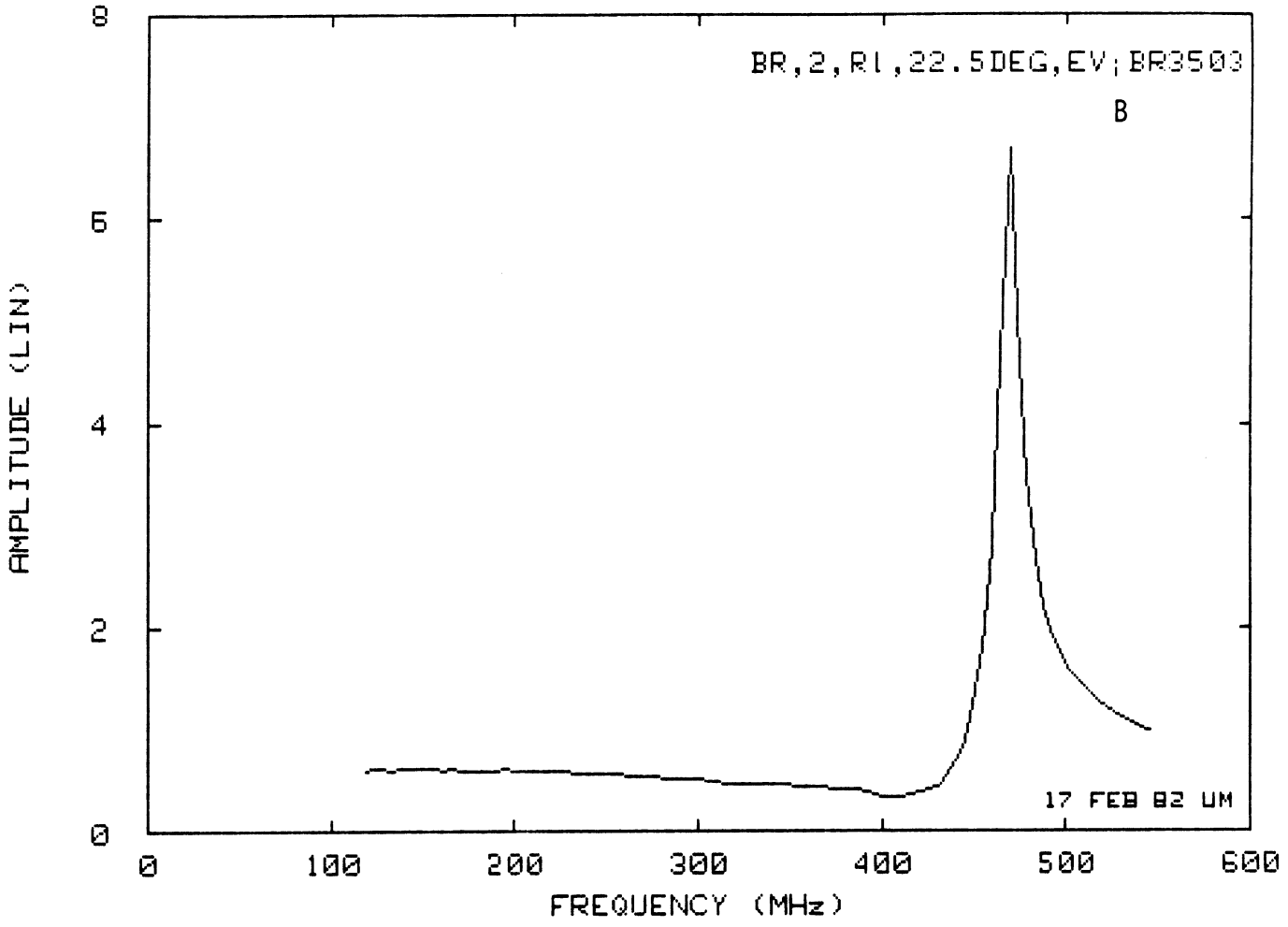
BR,2,RI,22.5DEG,EV;BR3503
B
17 FEB 82 UM
AMPLITUDE (LIN)
0
2
4
6
8
0
100
200
300
400
500
600
FREQUENCY (MHz)

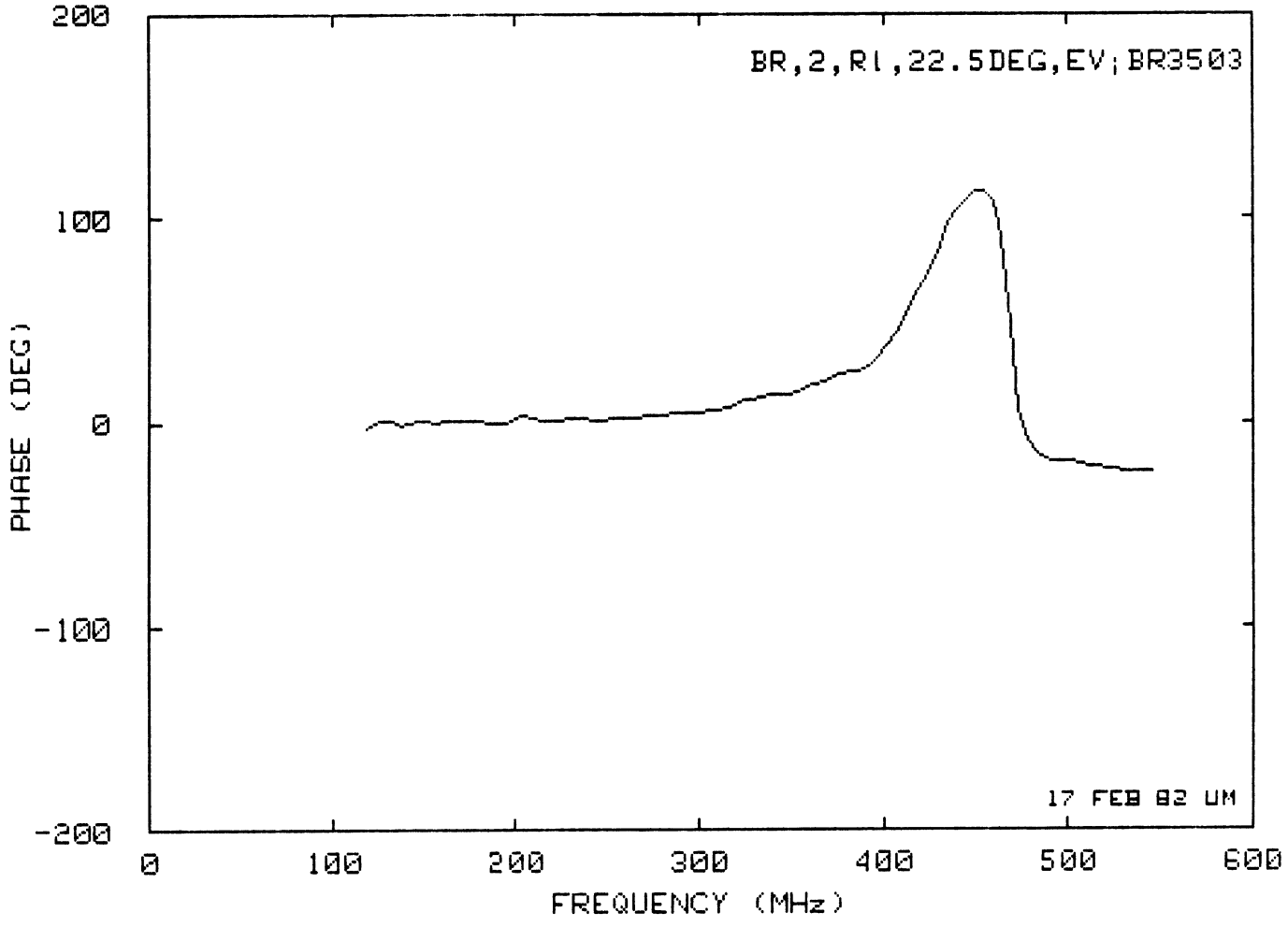
BR,2,RI,22.5DEG,EV;BR3503
17 FEB 82 UM
PHASE (DEG)
200
100
0
-100
-200
0
100
200
300
400
500
600
FREQUENCY (MHz)

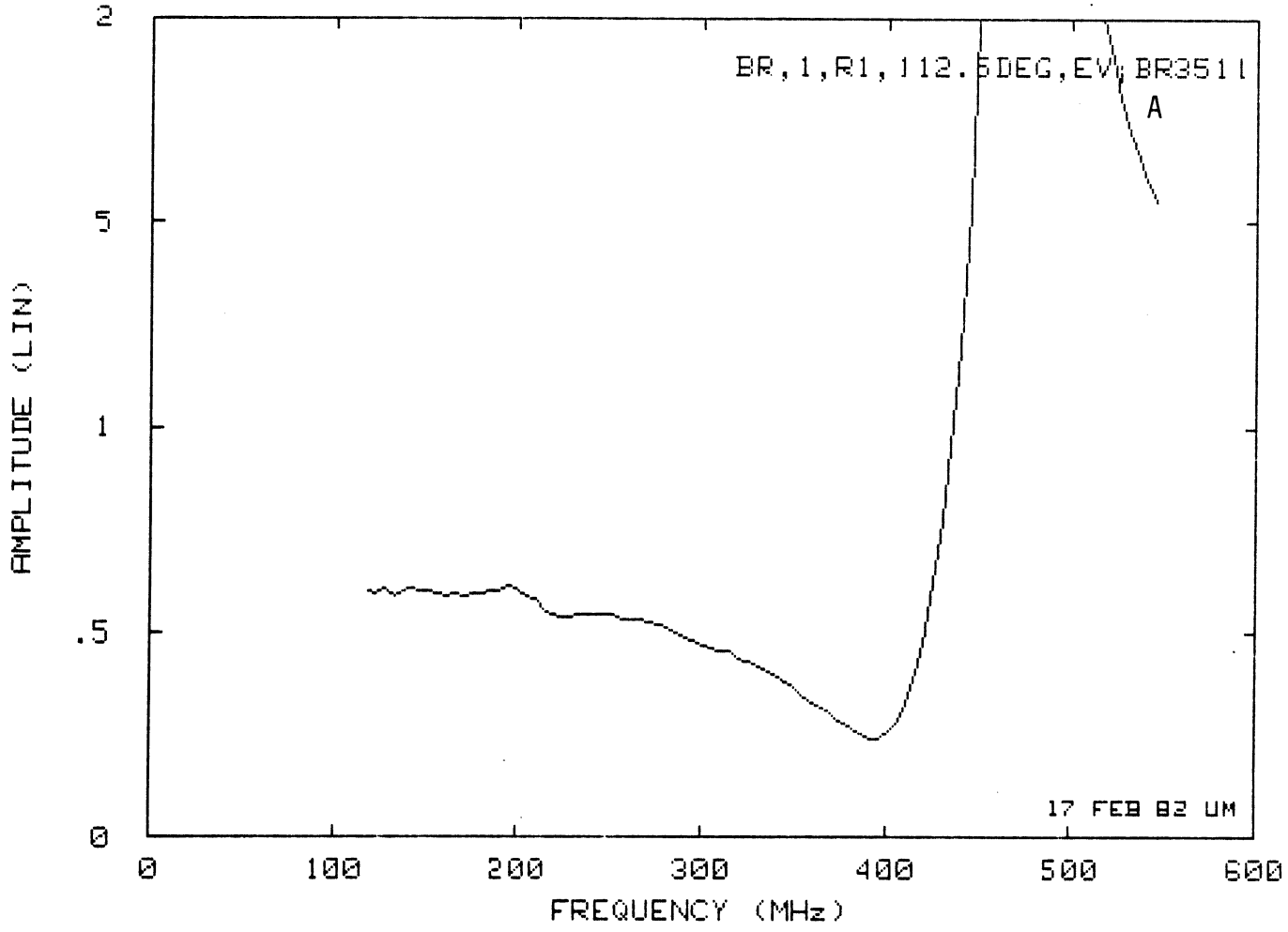
BR,1,R1,112.5DEG,EV;BR351(
A
17 FEB 82 UM
AMPLITUDE (LIN)
2
5
1
.5
0
0
100
200
300
400
500
600
FREQUENCY (MHz)

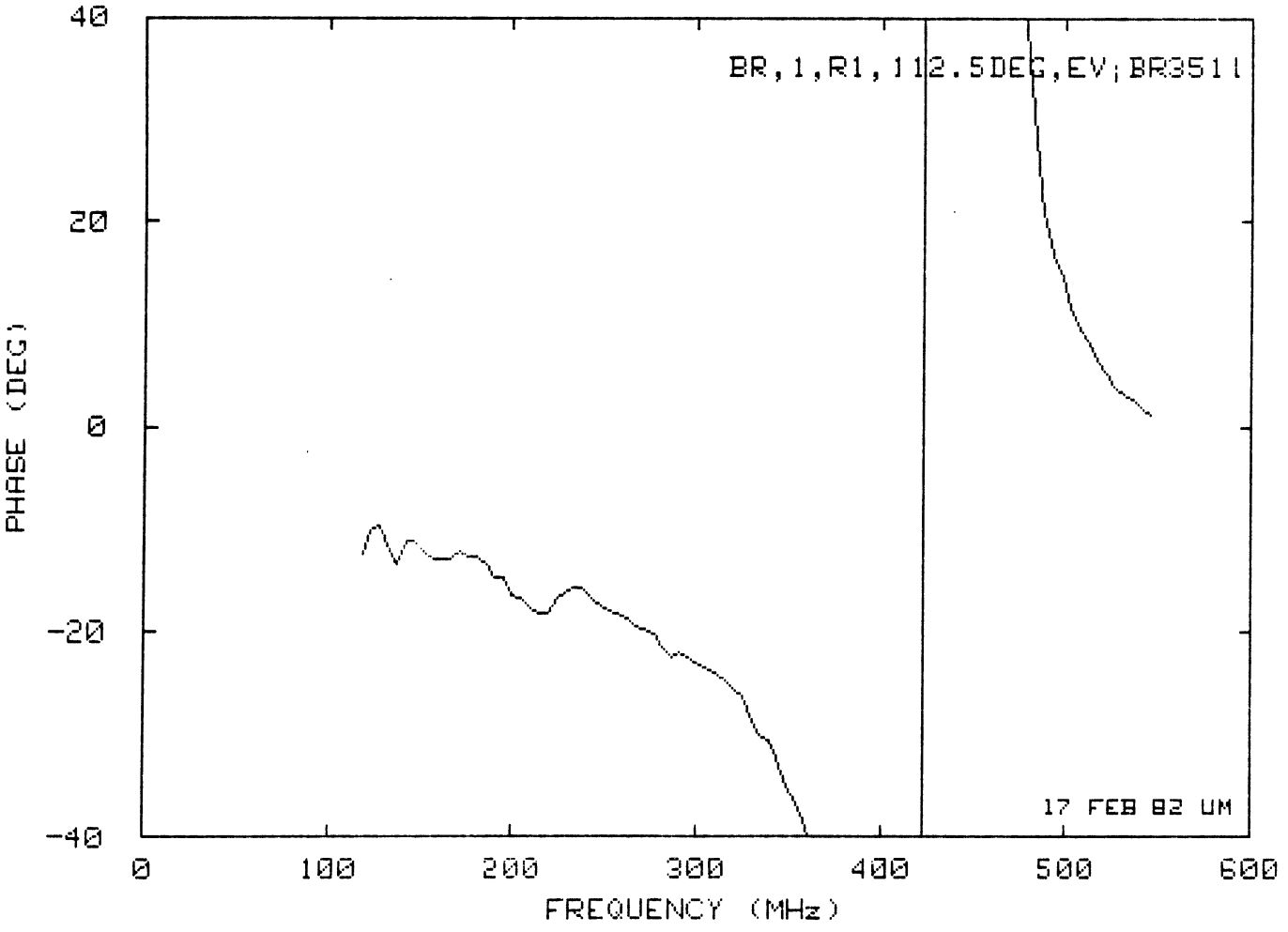
BR,1,R1,112.5DEG,EV;BR351(
17 FEB 82 UM
PHASE (DEG)
40
20
0
-20
-40
0
100
200
300
400
500
600
FREQUENCY (MHz)

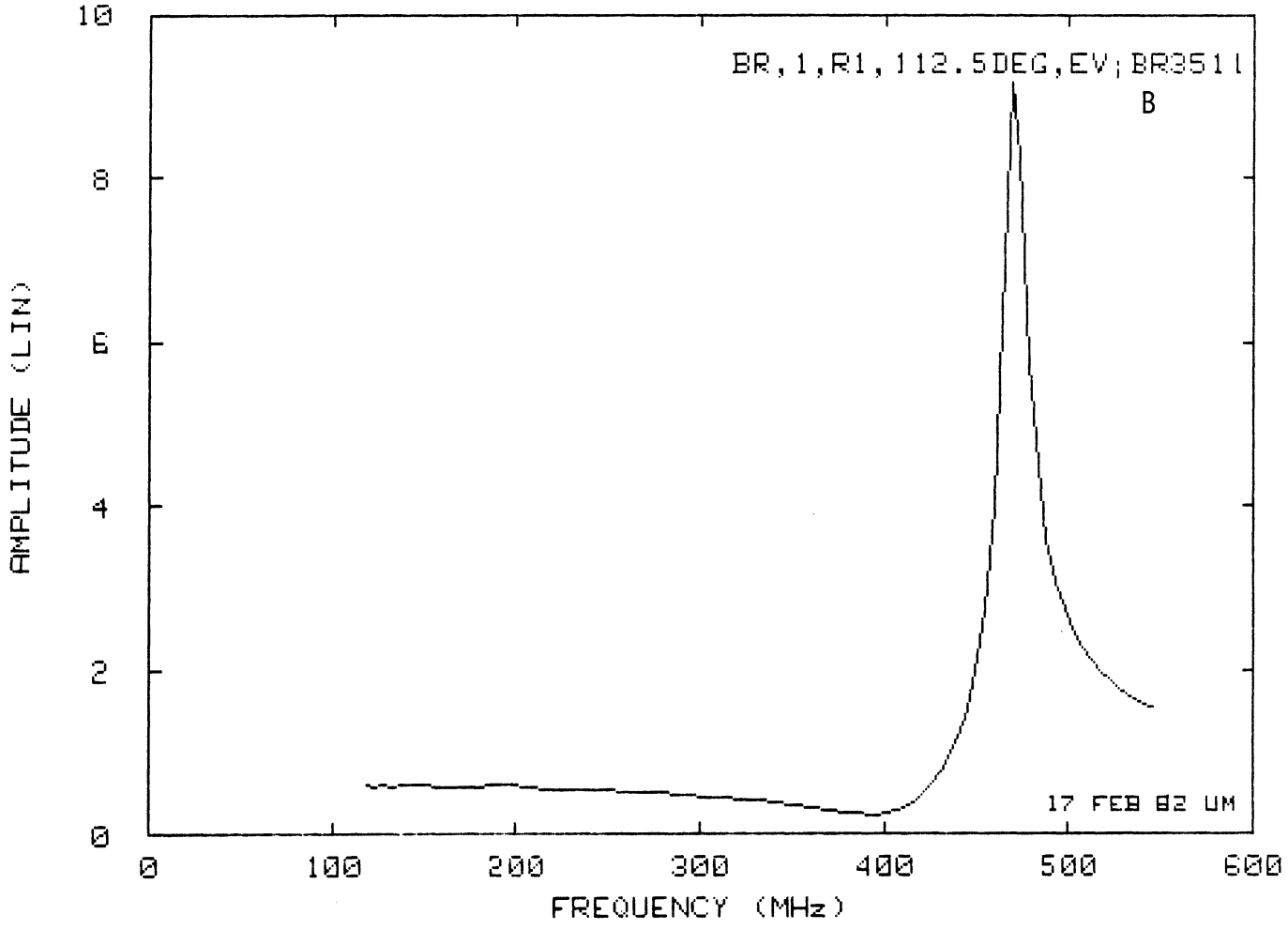
BR,1,R1,112.5DEG,EV;BR351
B
17 FEB 82 UM
AMPLITUDE (LIN)
10
8
6
4
2
0
0
100
200
300
400
500
600
FREQUENCY (MHz)

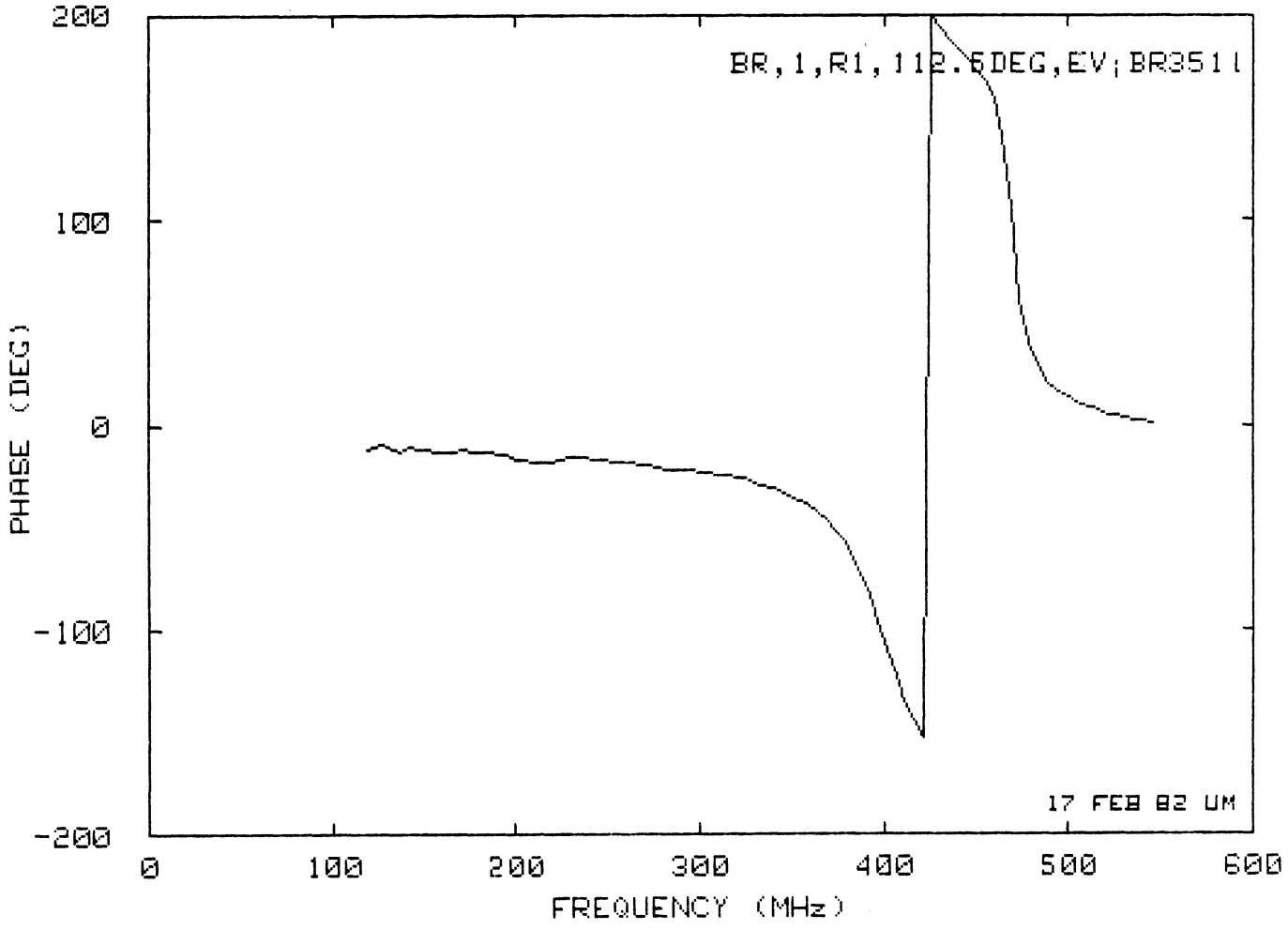
BR,1,R1,112.5DEG,EV;BR351
17 FEB 82 UM
PHASE (DEG)
200
100
0
-100
-200
0
100
200
300
400
500
600
FREQUENCY (MHz)

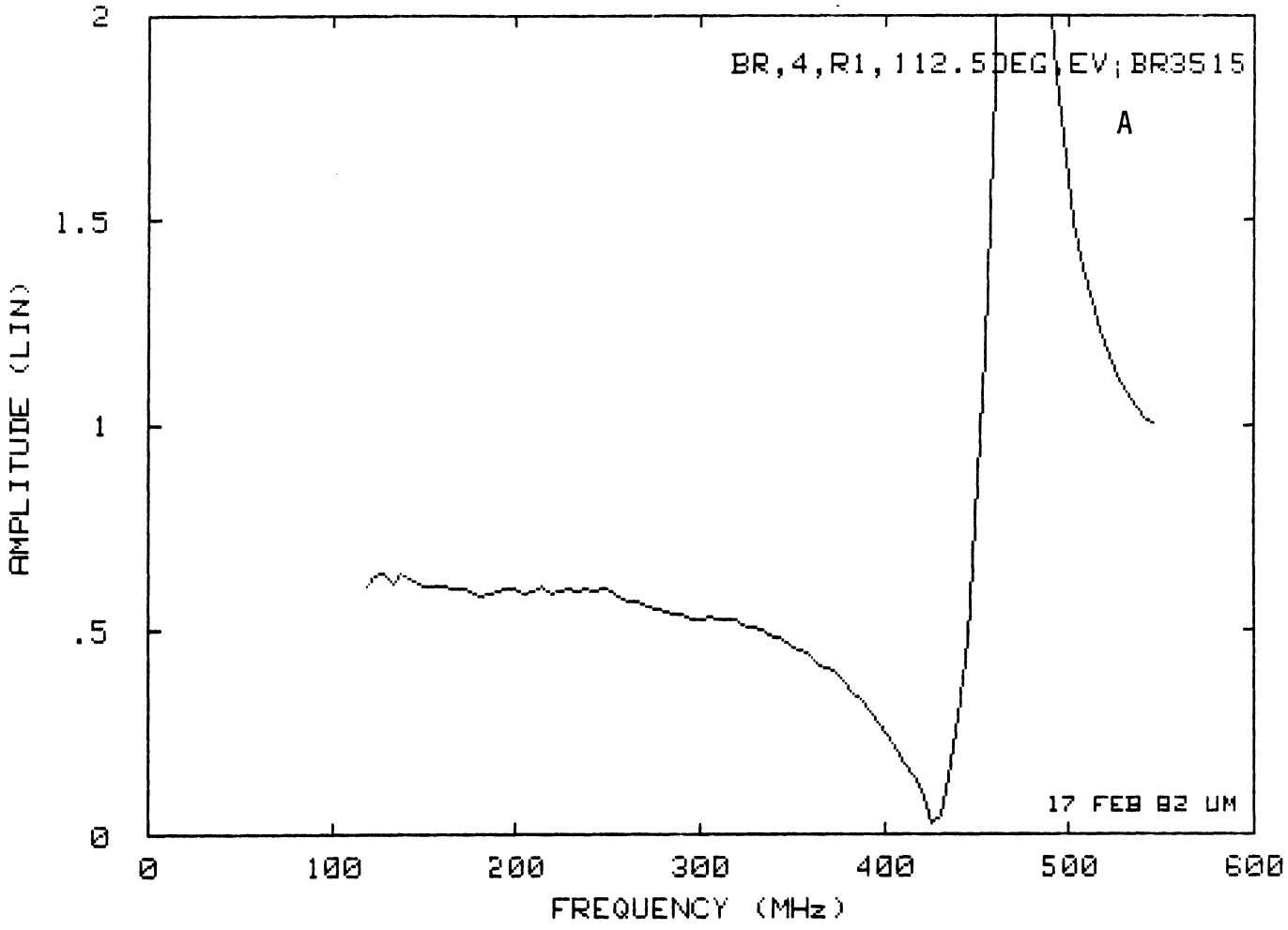
BR,4,R1,112.5DEG,EV;BR3515
A
17 FEB 82 UM
AMPLITUDE (LIN)
2
1.5
1
.5
0
0
100
200
300
400
500
600
FREQUENCY (MHz)

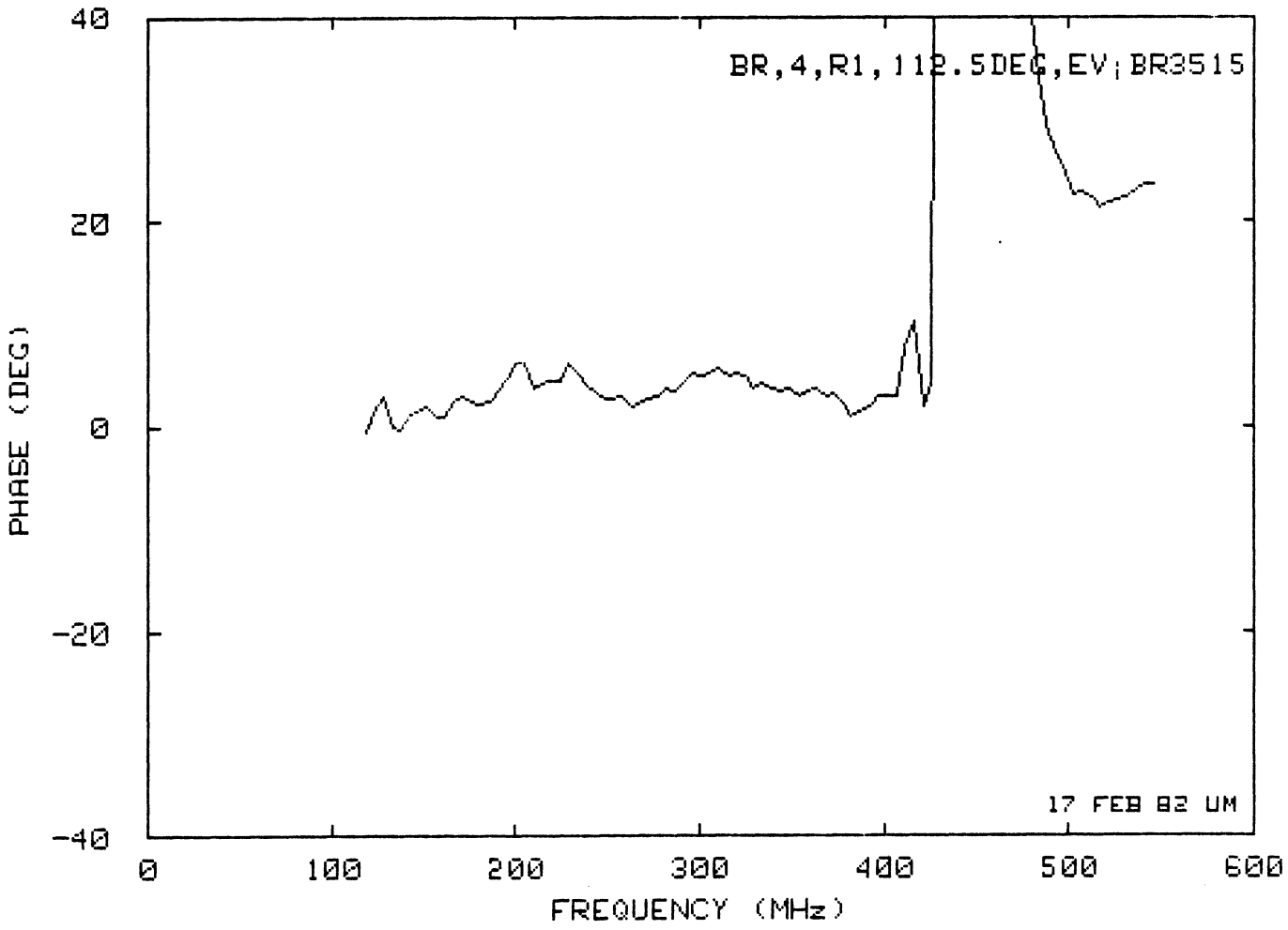
BR,4,R1,112.5DEG,EV;BR3515
17 FEB 82 UM
PHASE (DEG)
40
20
0
-20
-40
0
100
200
300
400
500
600
FREQUENCY (MHz)

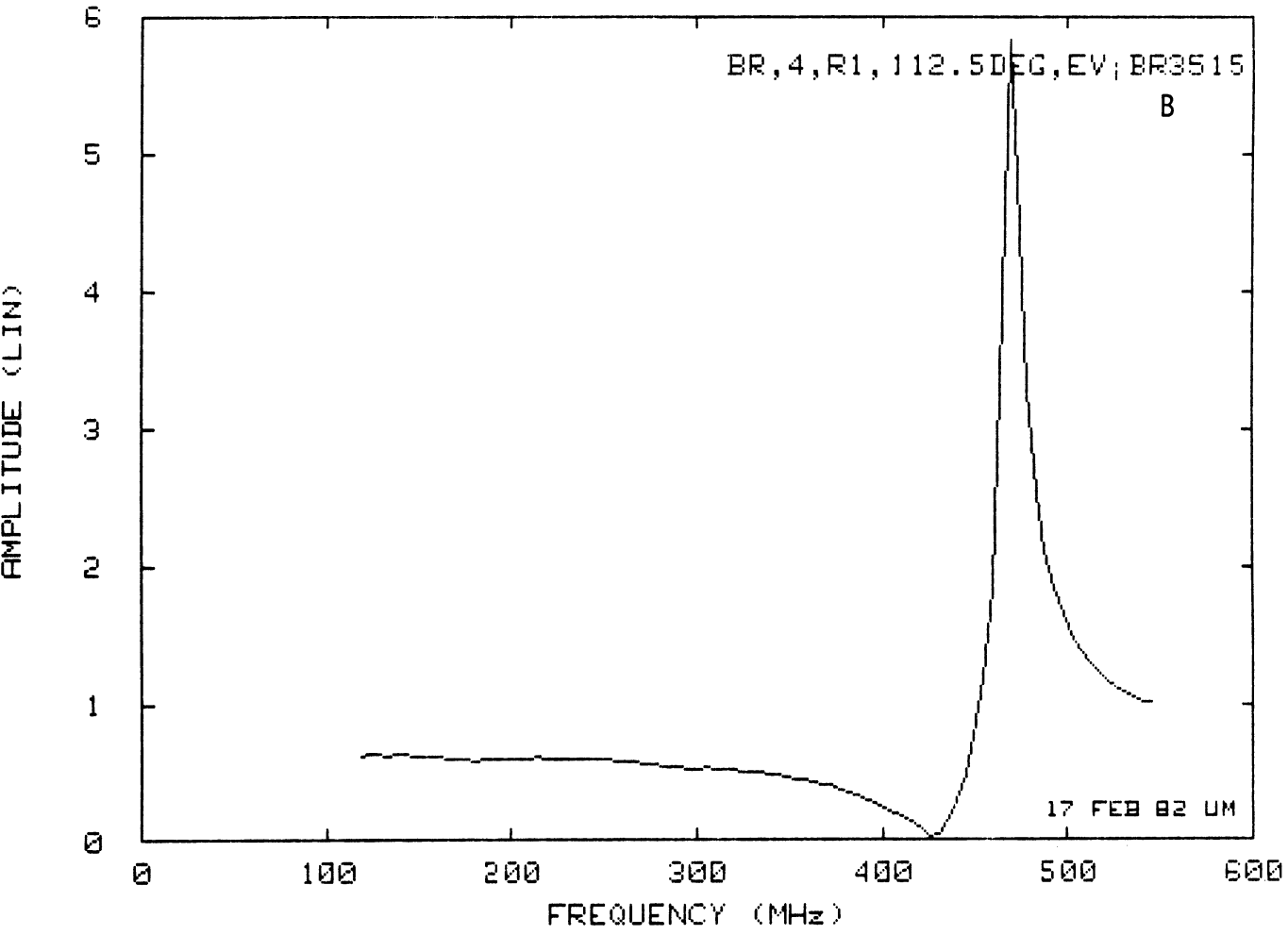
BR,4,R1,112.5DEG,EV;BR3515
B
17 FEB 82 UM
AMPLITUDE (LIN)
FREQUENCY (MHz)
0
1
2
3
4
5
6
0
100
200
300
400
500
600

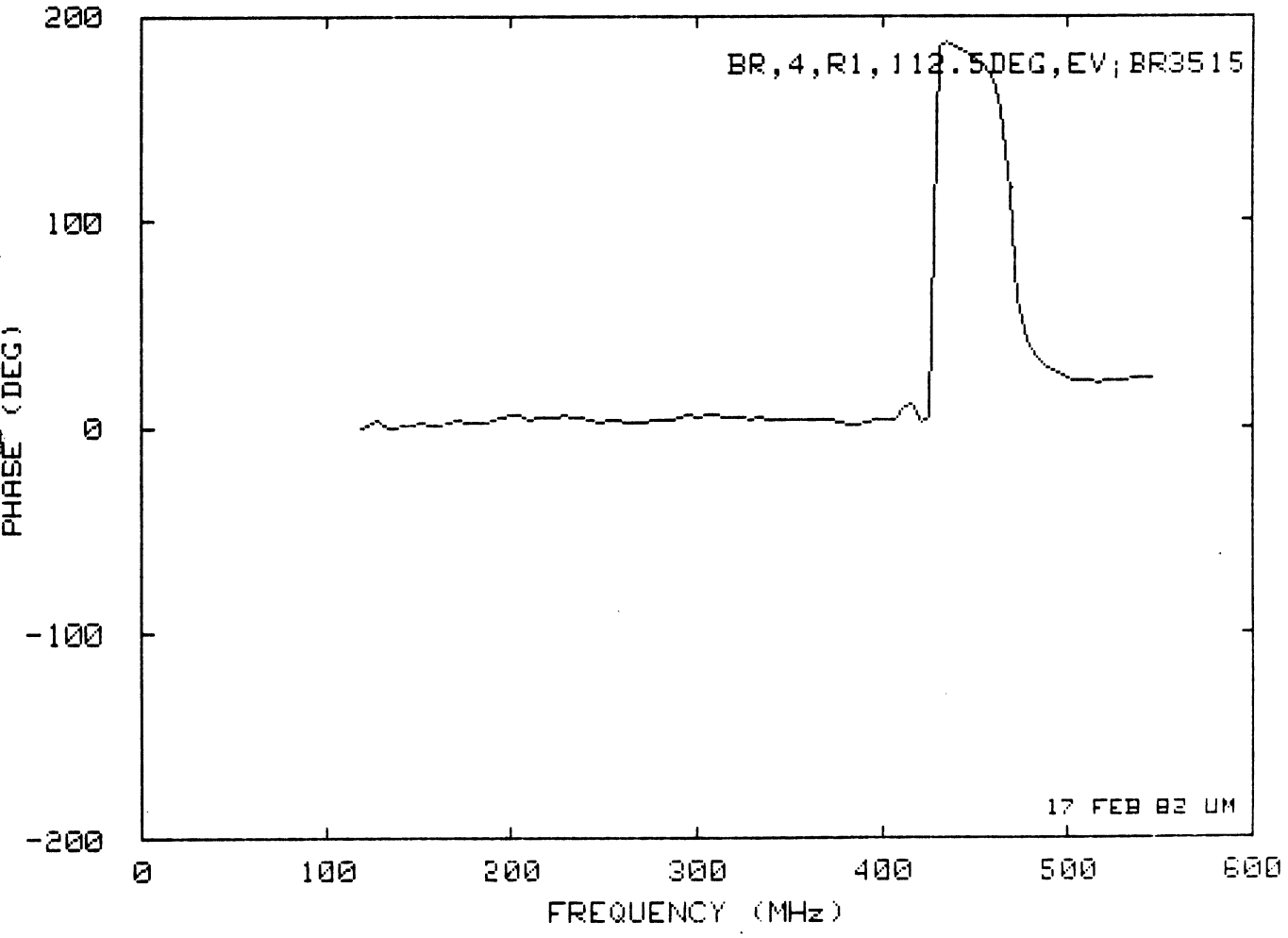
BR,4,R1,112.5DEG,EV;BR3515
17 FEB 82 UM
PHASE (DEG)
FREQUENCY (MHz)
200
100
0
-100
-200
0
100
200
300
400
500
600

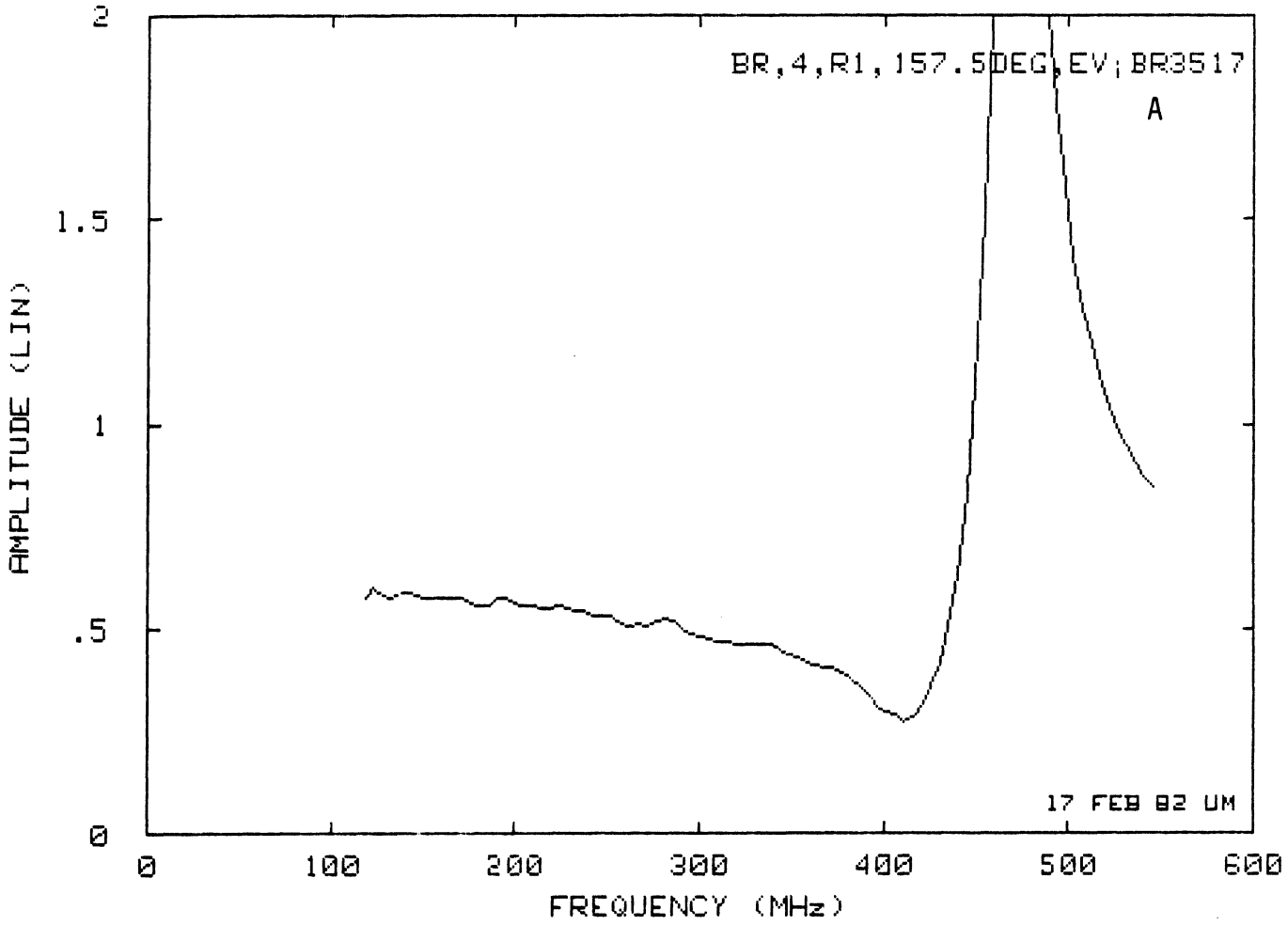
BR,4,R1,157.5DEG,EV;BR3517
A
17 FEB 82 UM
AMPLITUDE (LIN)
2
1.5
1
.5
0
0
100
200
300
400
500
600
FREQUENCY (MHz)

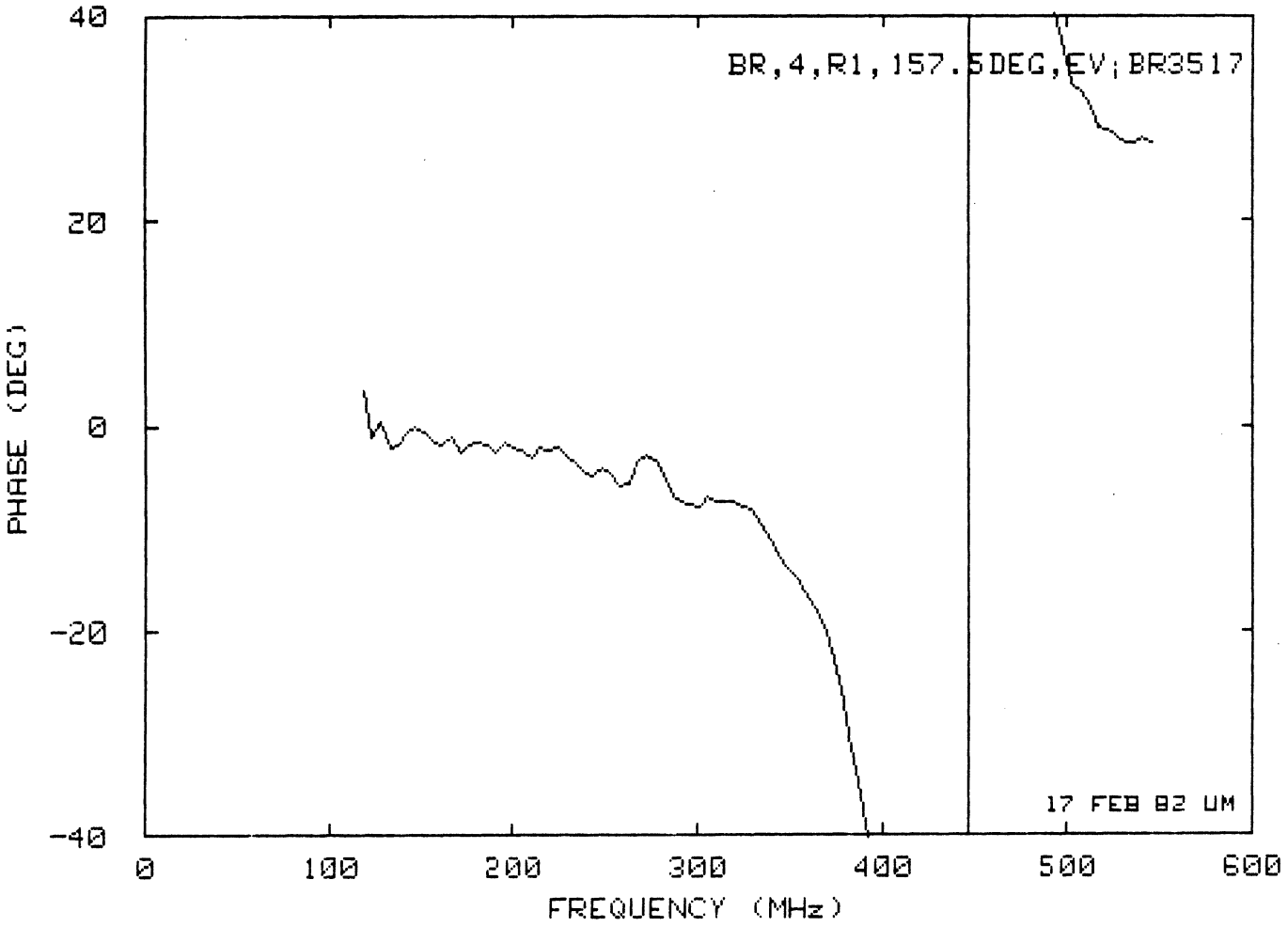
BR,4,R1,157.5DEG,EV;BR3517
17 FEB 82 UM
PHASE (DEG)
40
20
0
-20
-40
0
100
200
300
400
500
600
FREQUENCY (MHz)

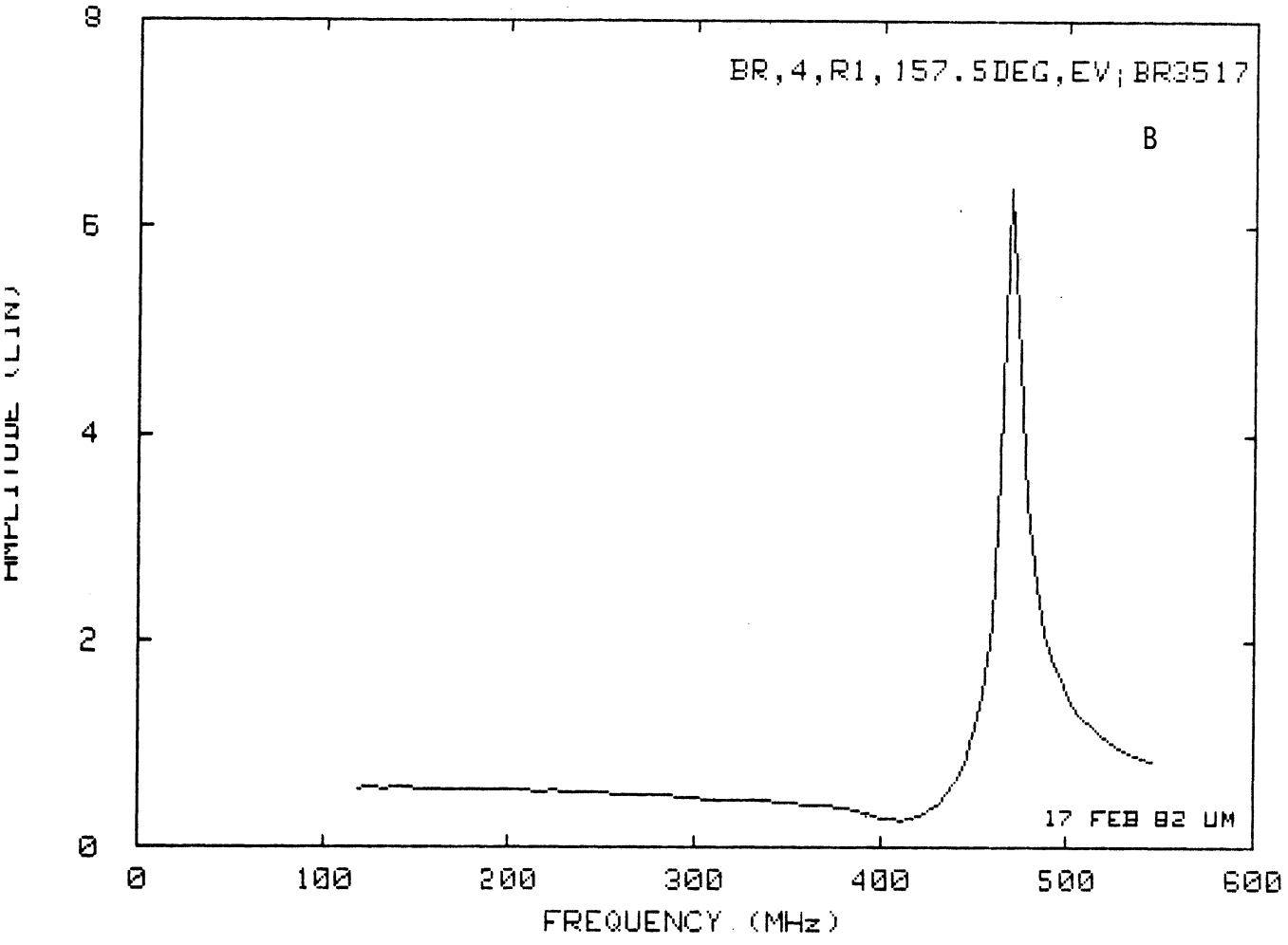
BR,4,R1,157.5DEG,EV;BR3517
B
17 FEB 82 UM
AMPLITUDE (LIN)
0
2
4
6
8
0
100
200
300
400
500
600
FREQUENCY (MHz)

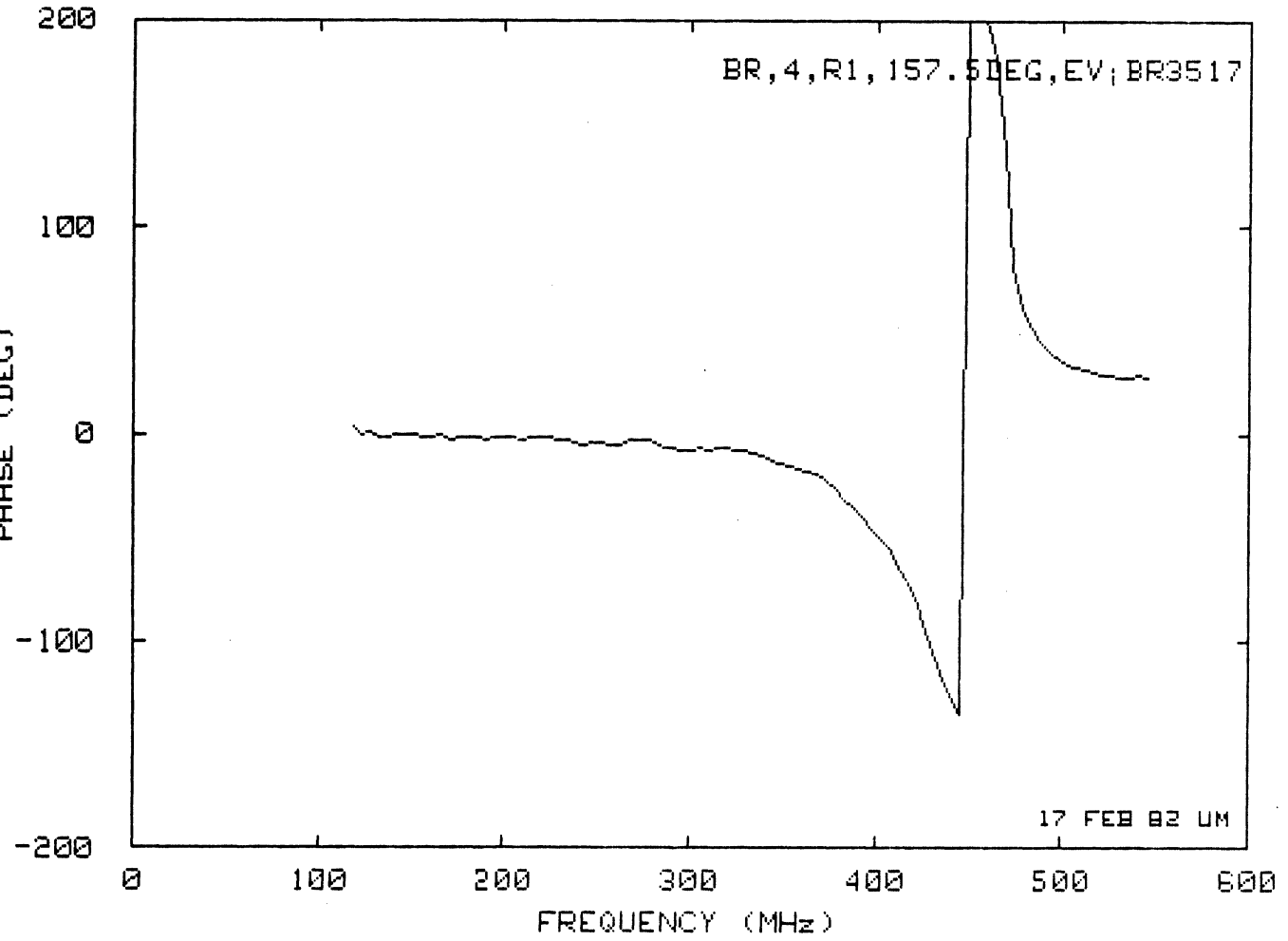
BR,4,R1,157.5DEG,EV;BR3517
17 FEB 82 UM
PHASE (DEG)
200
100
0
-100
-200
0
100
200
300
400
500
600
FREQUENCY (MHz)

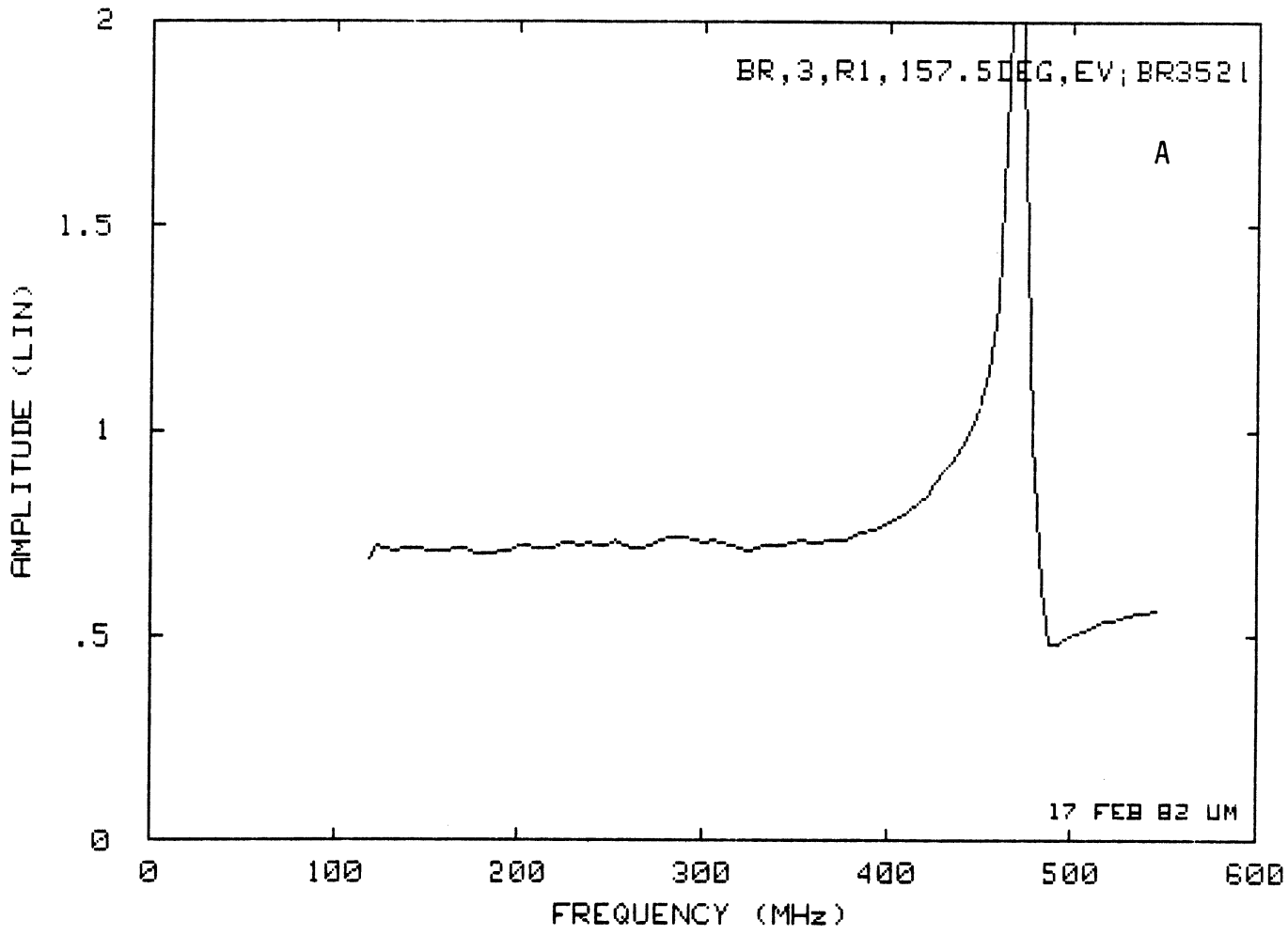
BR,3,R1,157.5DEG,EV;BR352l
A
17 FEB 82 UM
AMPLITUDE (LIN)
2
1.5
1
.5
0
0
100
200
300
400
500
600
FREQUENCY (MHz)

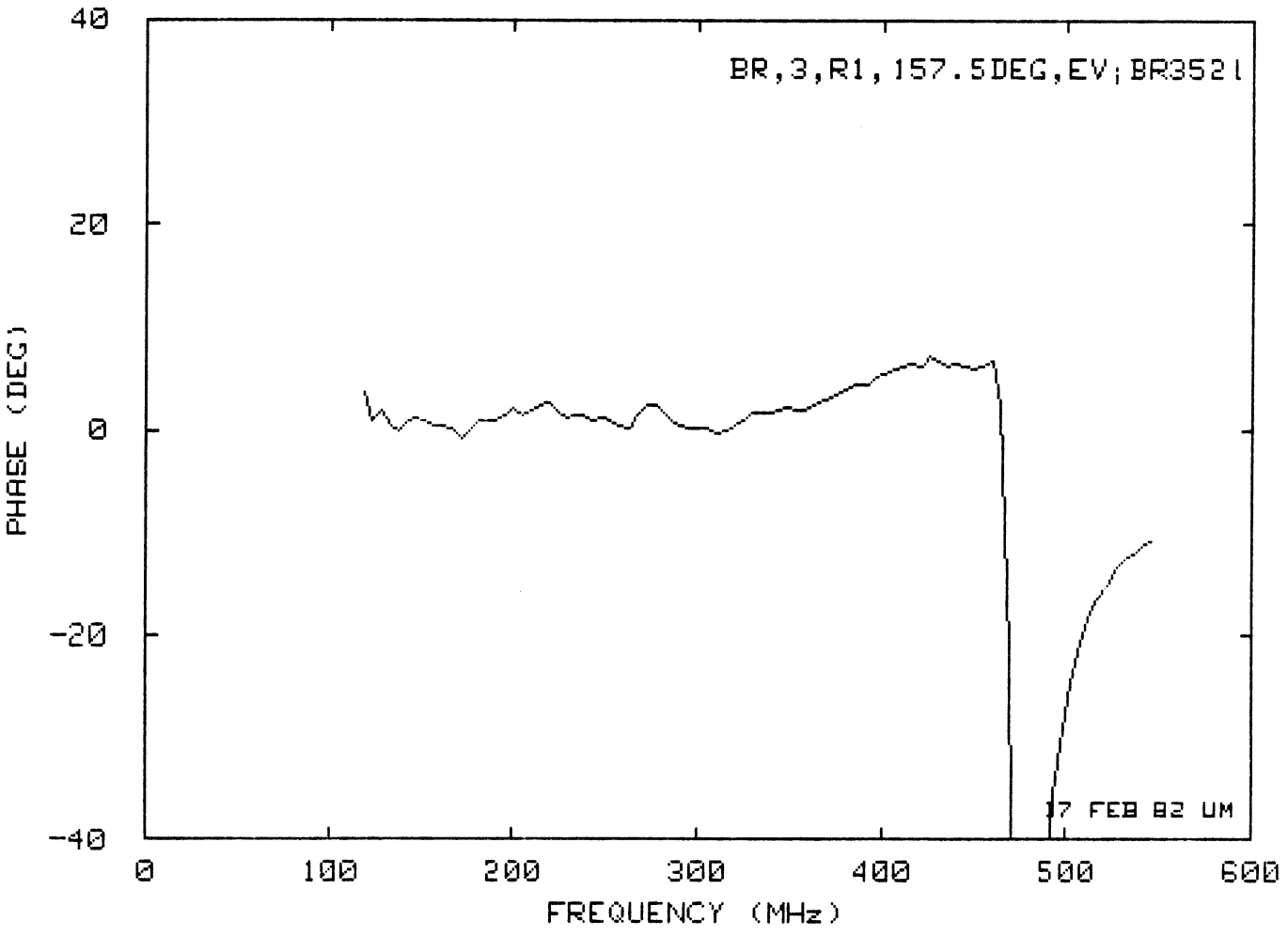
BR,3,R1,157.5DEG,EV;BR352l
17 FEB 82 UM
PHASE (DEG)
40
20
0
-20
-40
0
100
200
300
400
500
600
FREQUENCY (MHz)

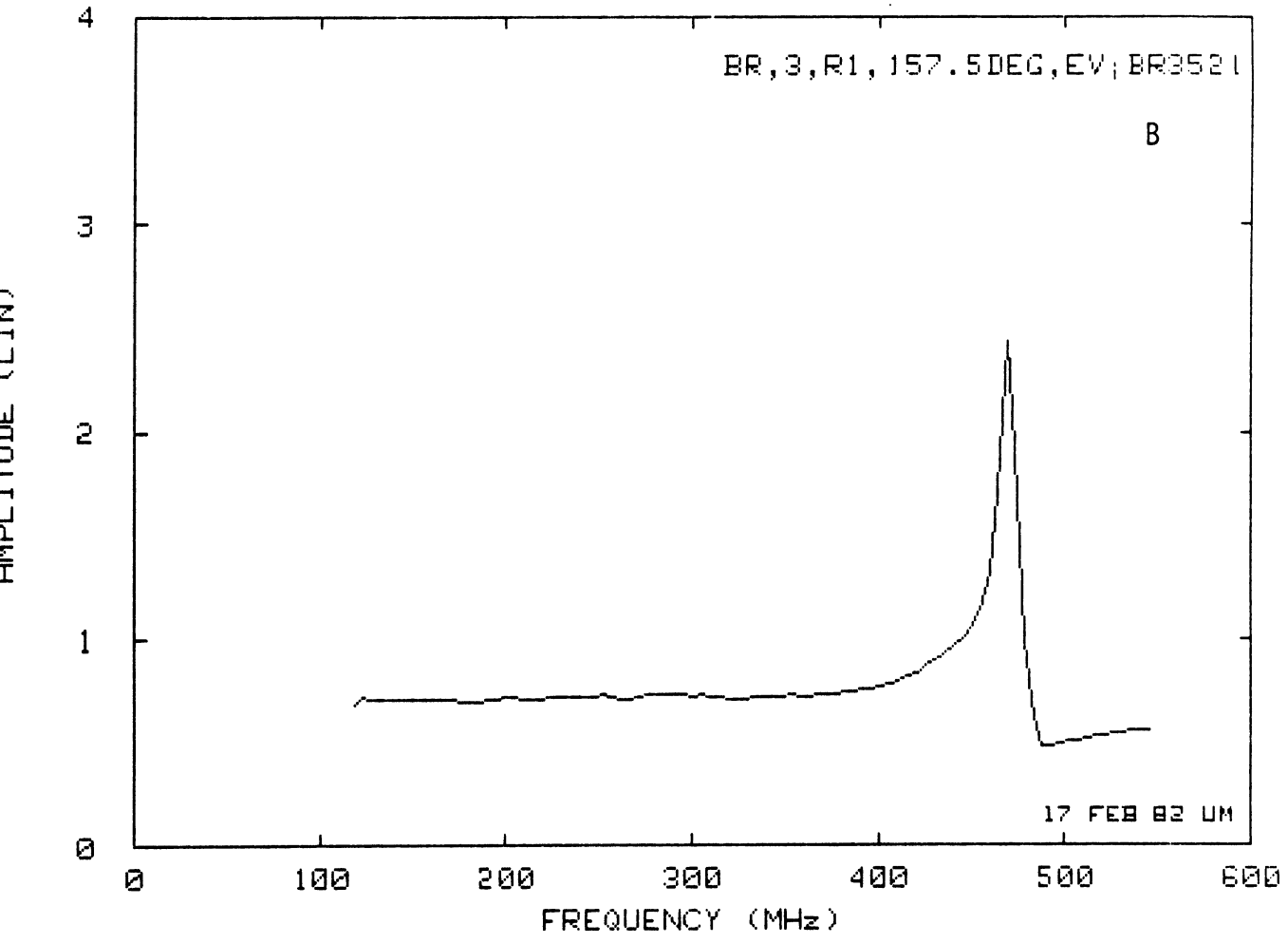
BR,3,R1,157.5DEG,EV;BR352(
B
17 FEB 82 UM
AMPLITUDE (LIN)
0
1
2
3
4
0
100
200
300
400
500
600
FREQUENCY (MHz)

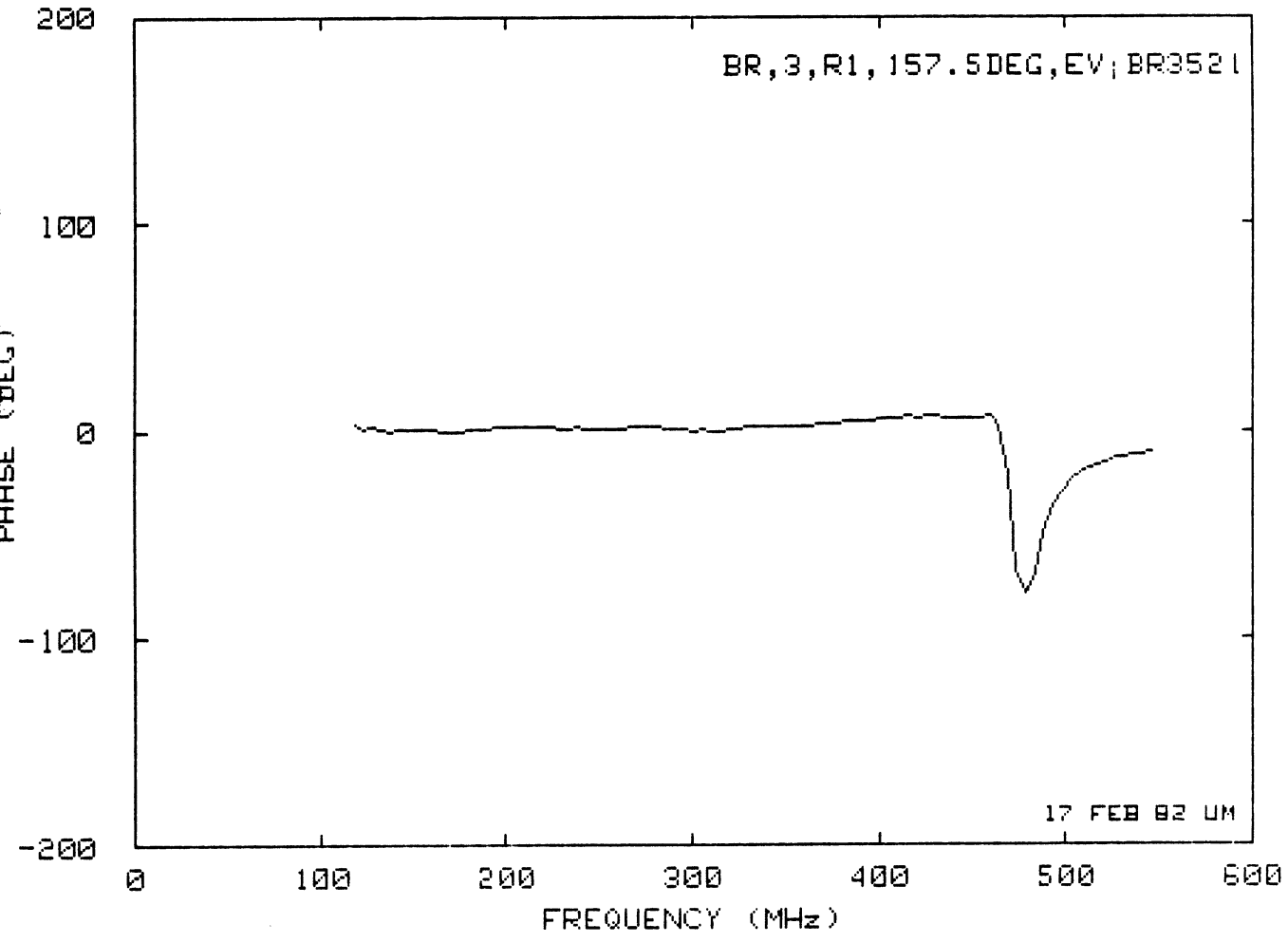
BR,3,R1,157.5DEG,EV;BR352(
17 FEB 82 UM
PHASE (DEG)
200
100
0
-100
-200
0
100
200
300
400
500
600
FREQUENCY (MHz)

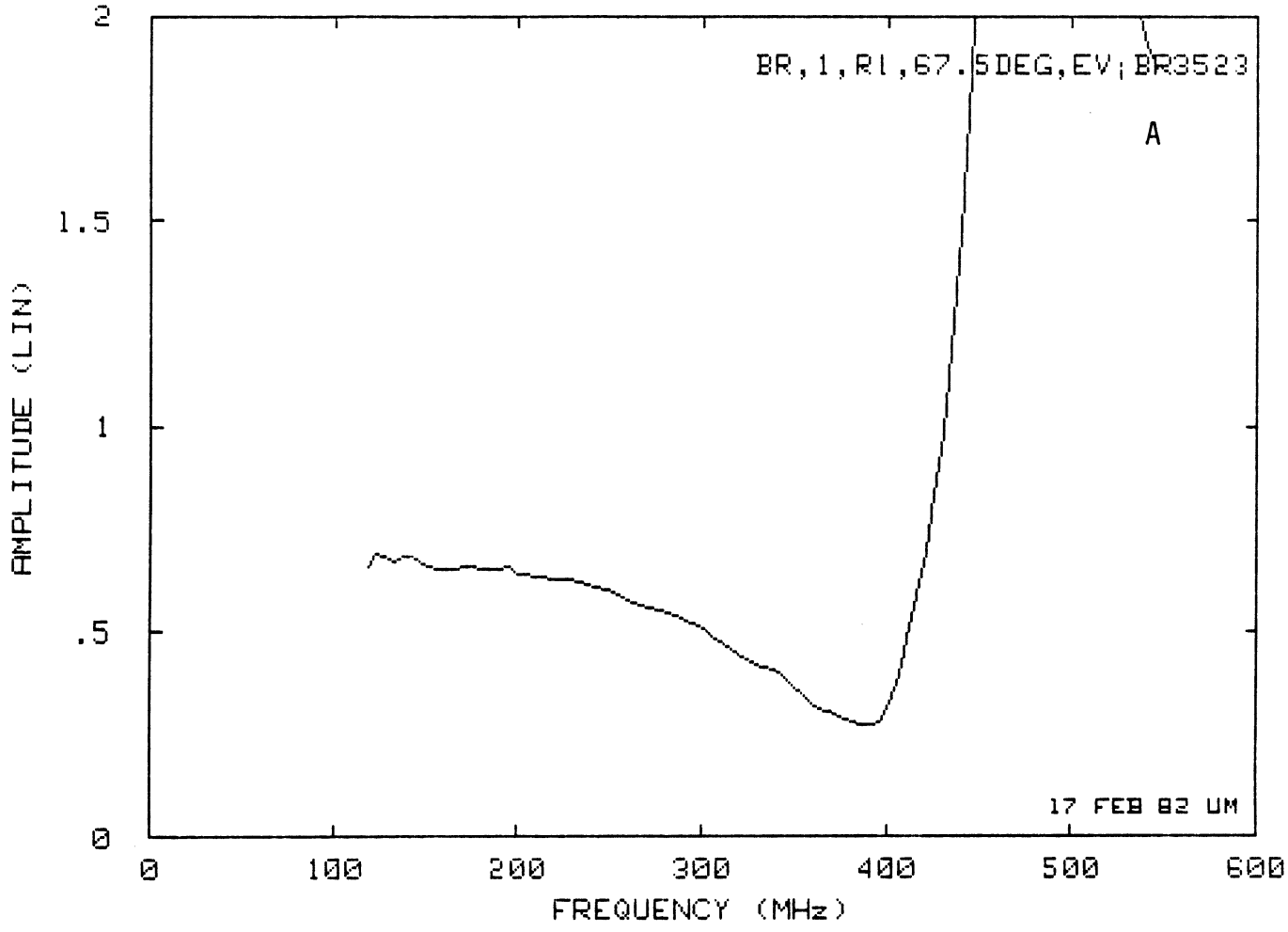
BR,1,R1,67.5DEG,EV;BR3523
A
17 FEB 82 UM
AMPLITUDE (LIN)
2
1.5
1
.5
0
0
100
200
300
400
500
600
FREQUENCY (MHz)

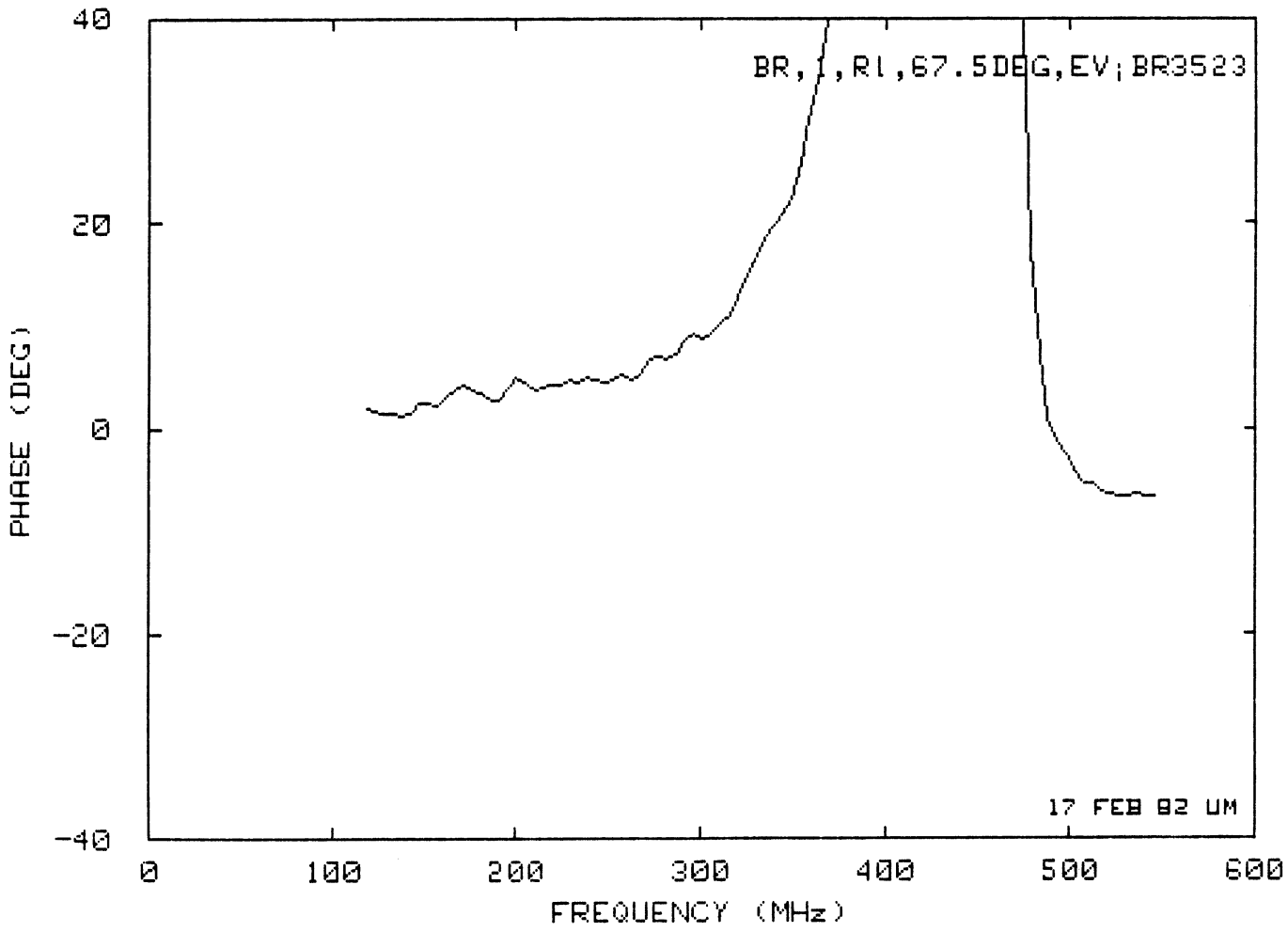
BR,1,R1,67.5DEG,EV;BR3523
17 FEB 82 UM
PHASE (DEG)
40
20
0
-20
-40
0
100
200
300
400
500
600
FREQUENCY (MHz)

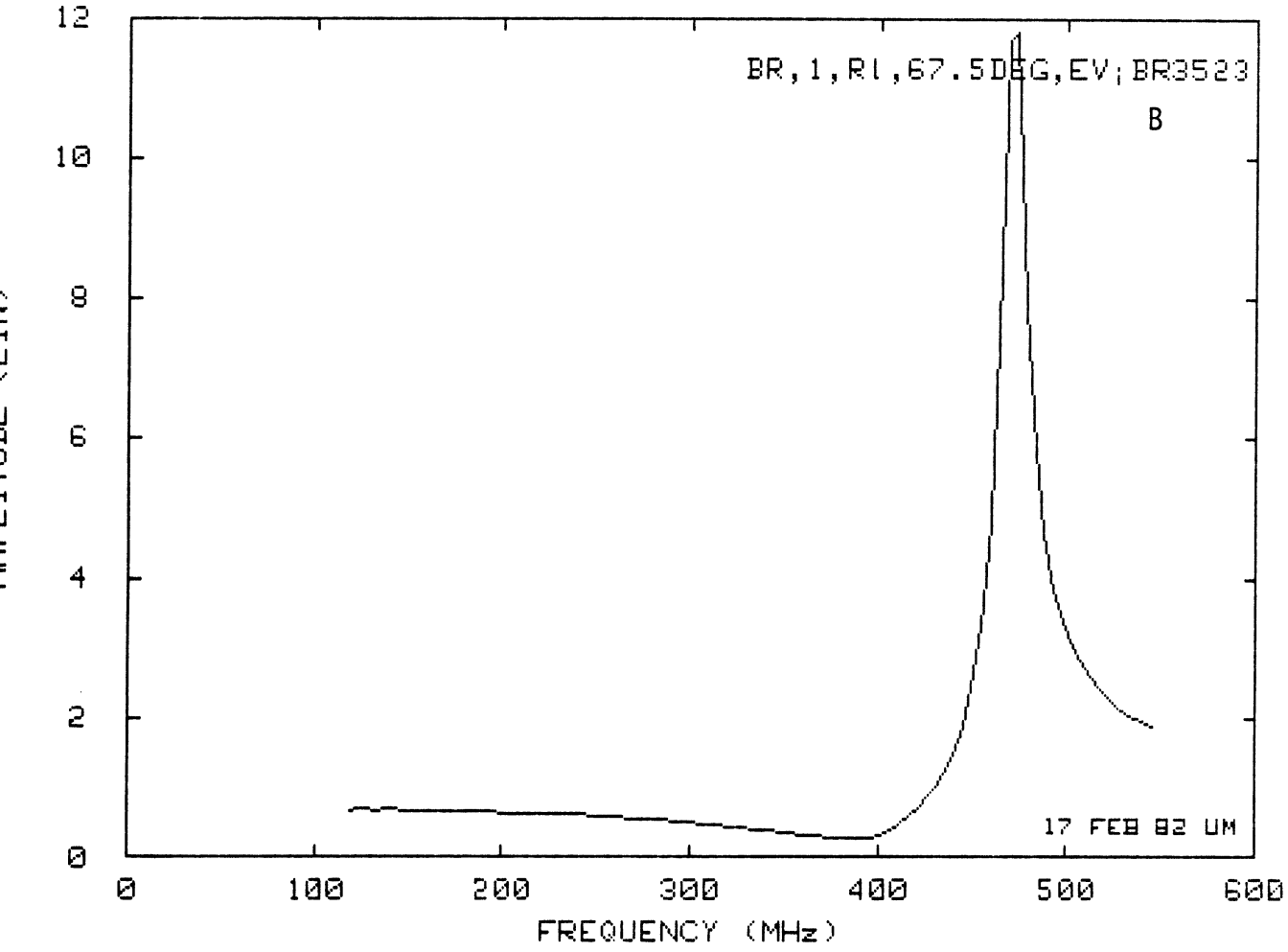
BR,1,R1,67.5DEG,EV;BR3523
B
17 FEB 82 UM
12
10
8
6
4
2
0
0
100
200
300
400
500
600
FREQUENCY (MHz)

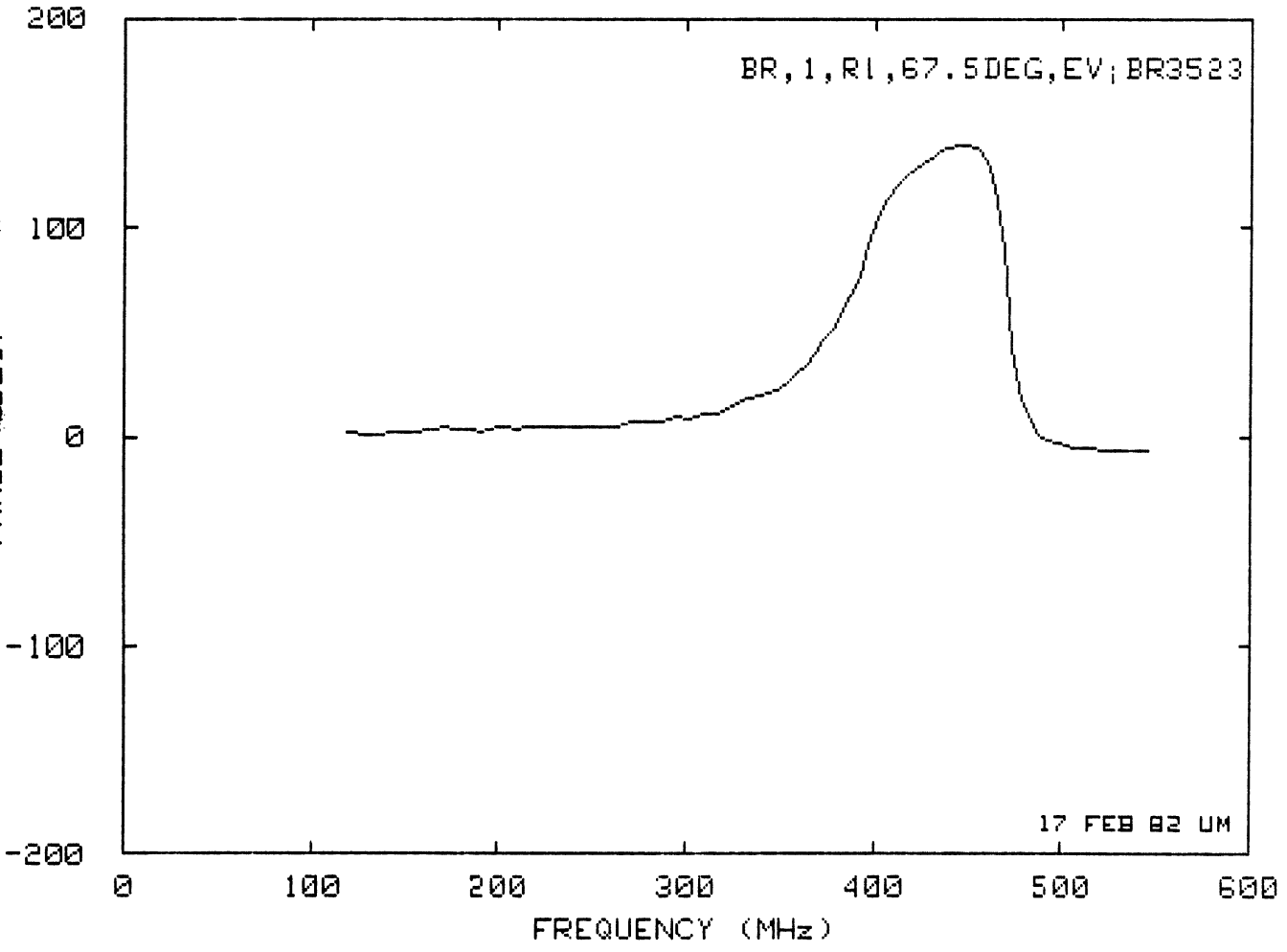
BR,1,R1,67.5DEG,EV;BR3523
17 FEB 82 UM
200
100
0
-100
-200
0
100
200
300
400
500
600
FREQUENCY (MHz)

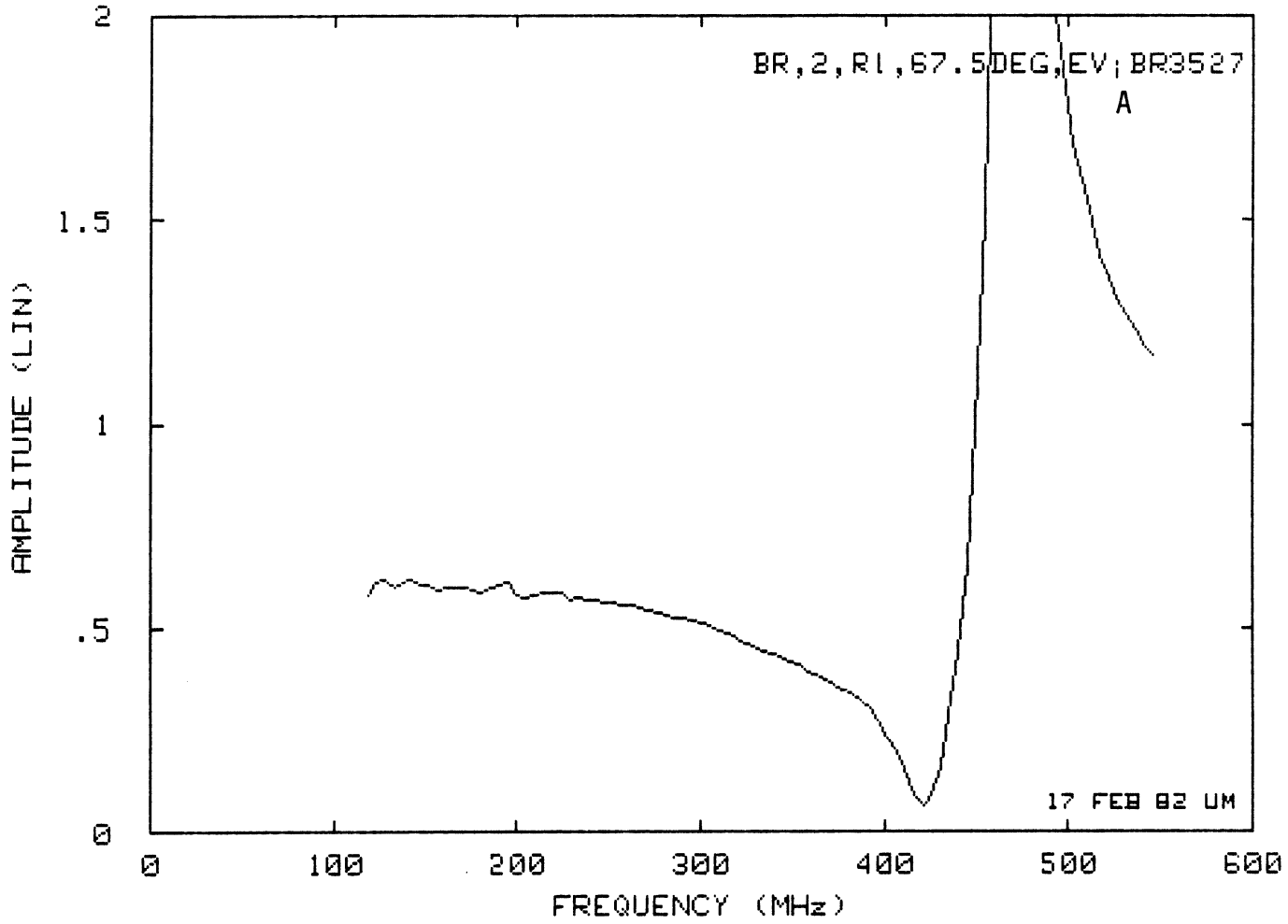
BR,2,R1,67.5DEG,EV;BR3527
A
17 FEB 82 UM
AMPLITUDE (LIN)
2
1.5
1
.5
0
0
100
200
300
400
500
600
FREQUENCY (MHz)

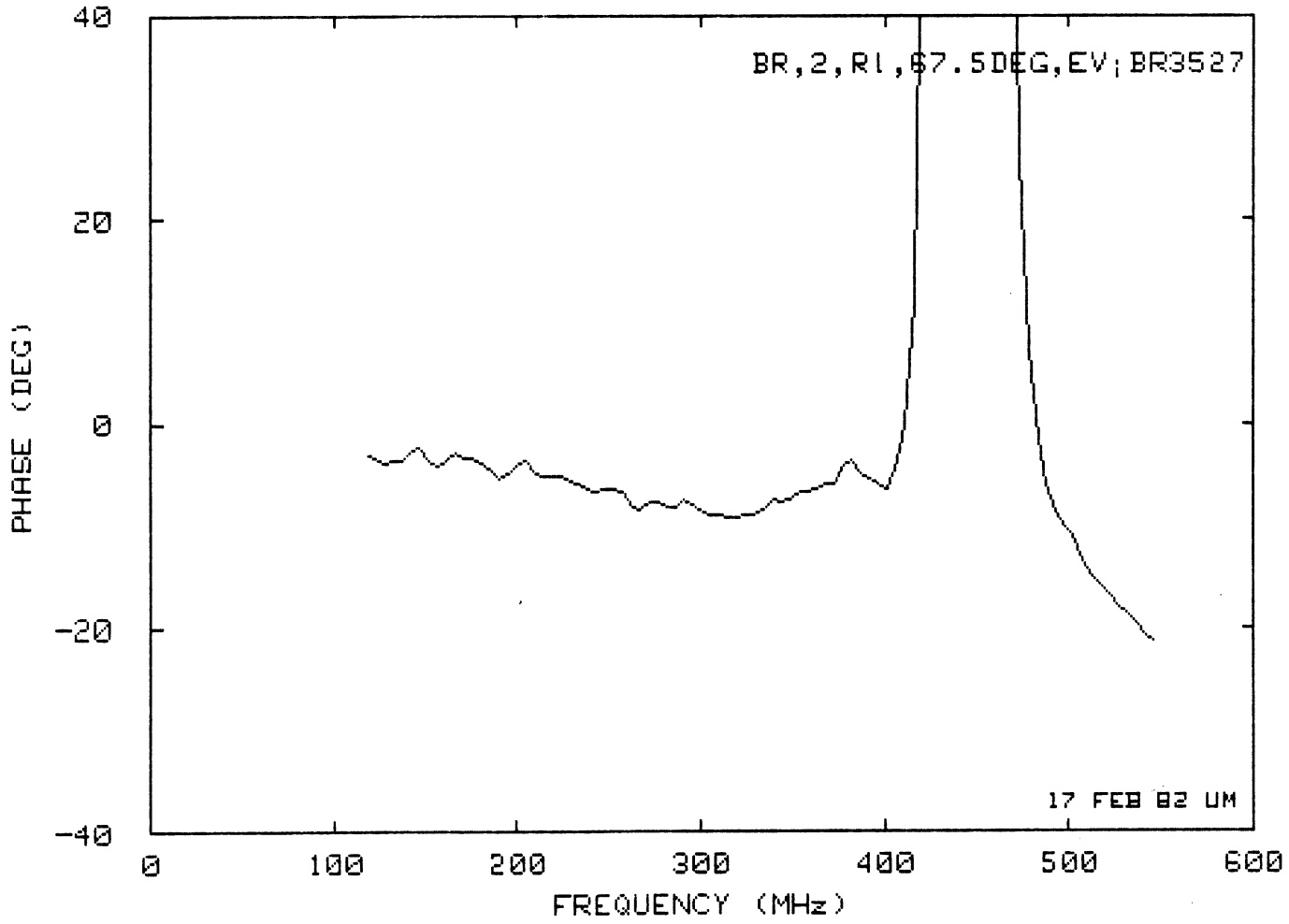
BR,2,R1,67.5DEG,EV;BR3527
17 FEB 82 UM
PHASE (DEG)
40
20
0
-20
-40
0
100
200
300
400
500
600
FREQUENCY (MHz)

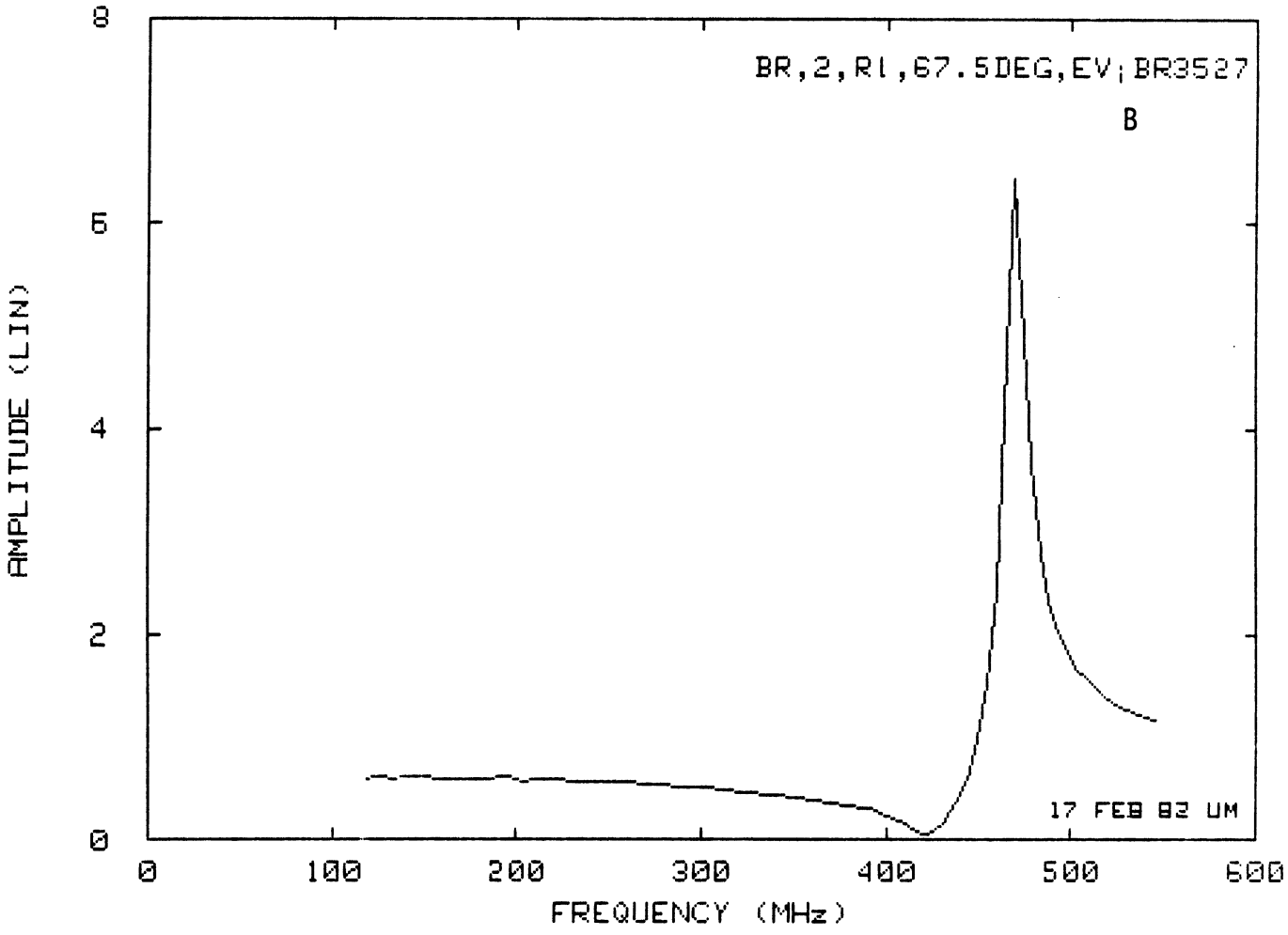
BR,2,R1,67.5DEG,EV;BR3527
B
17 FEB 82 UM
AMPLITUDE (LIN)
0
2
4
6
8
0
100
200
300
400
500
600
FREQUENCY (MHz)

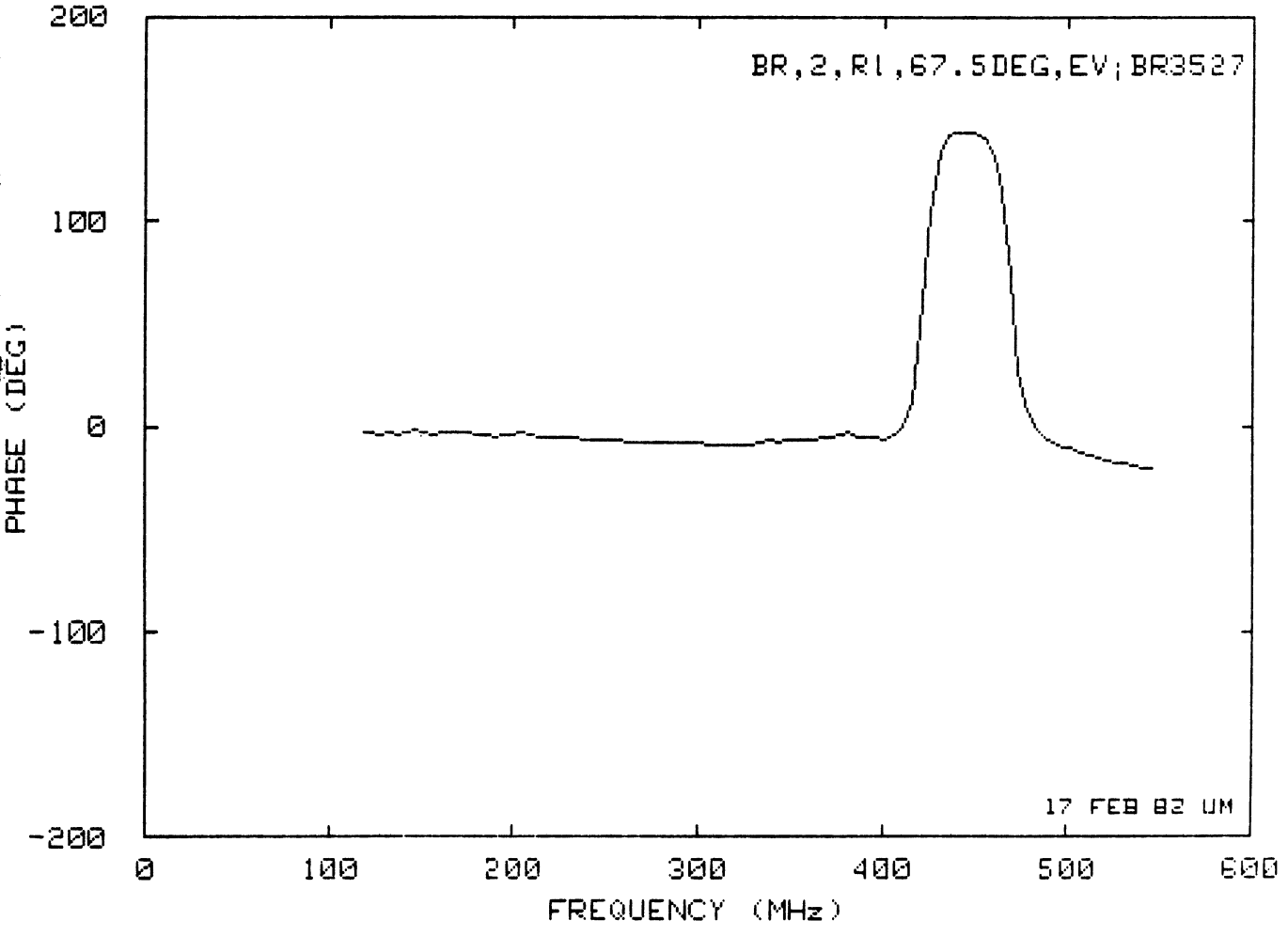
BR,2,R1,67.5DEG,EV;BR3527
17 FEB 82 UM
PHASE (DEG)
200
100
0
-100
-200
0
100
200
300
400
500
600
FREQUENCY (MHz)

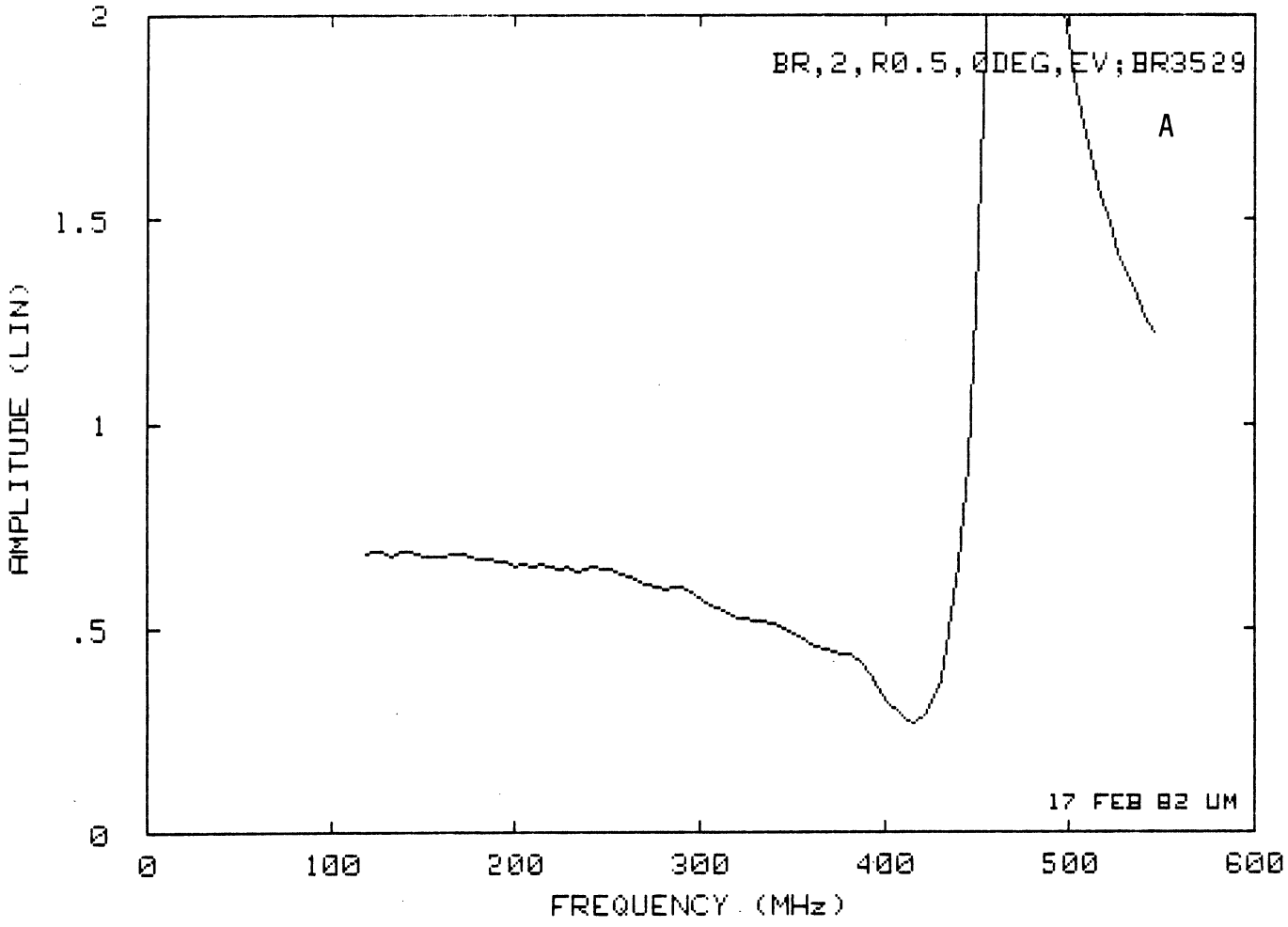
BR,2,R0.5,0DEG,EV;BR3529
A
17 FEB 82 UM
AMPLITUDE (LIN)
2
1.5
1
.5
0
0
100
200
300
400
500
600
FREQUENCY (MHz)

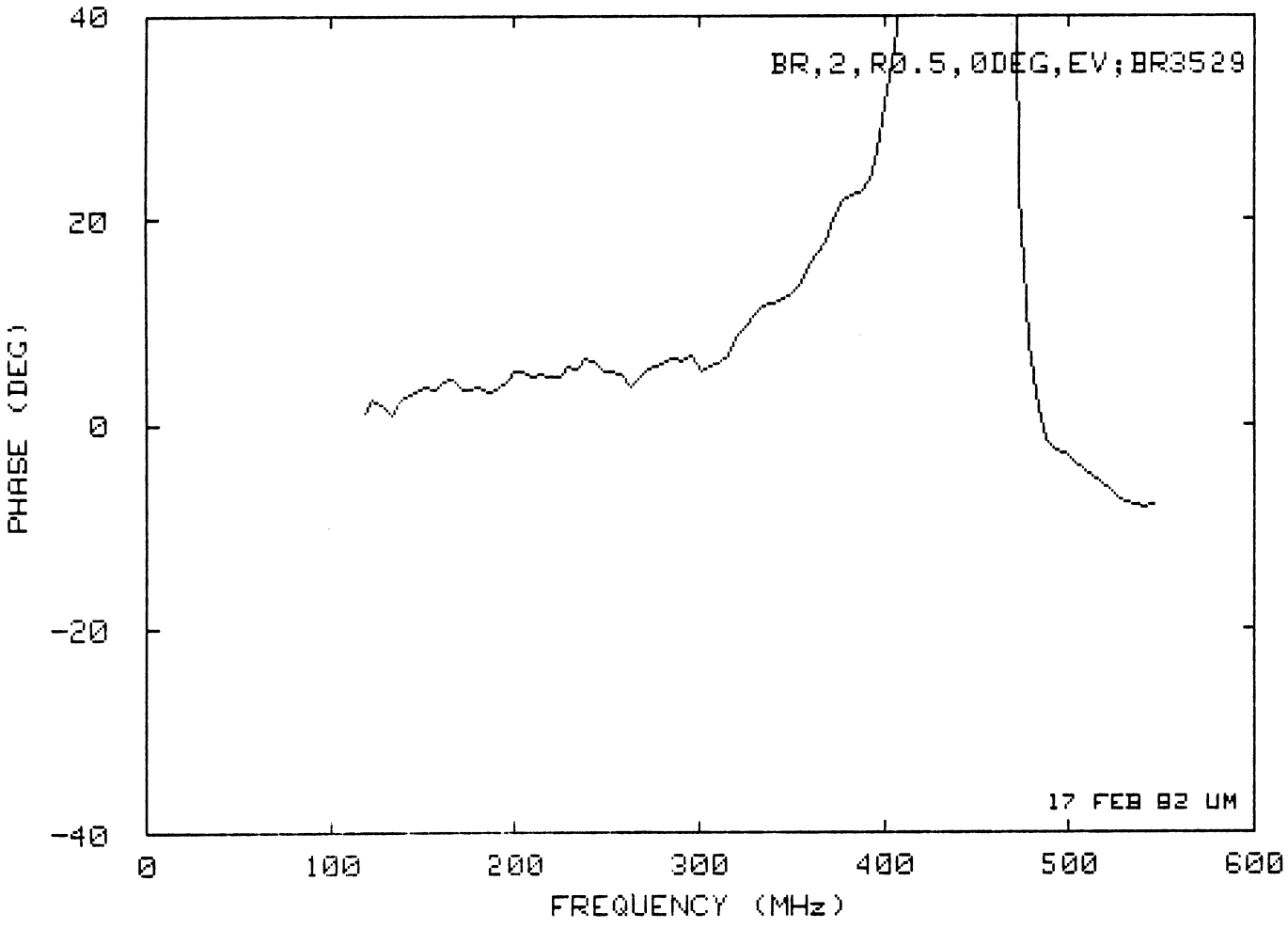
BR,2,R0.5,0DEG,EV;BR3529
17 FEB 82 UM
PHASE (DEG)
40
20
0
-20
-40
0
100
200
300
400
500
600
FREQUENCY (MHz)

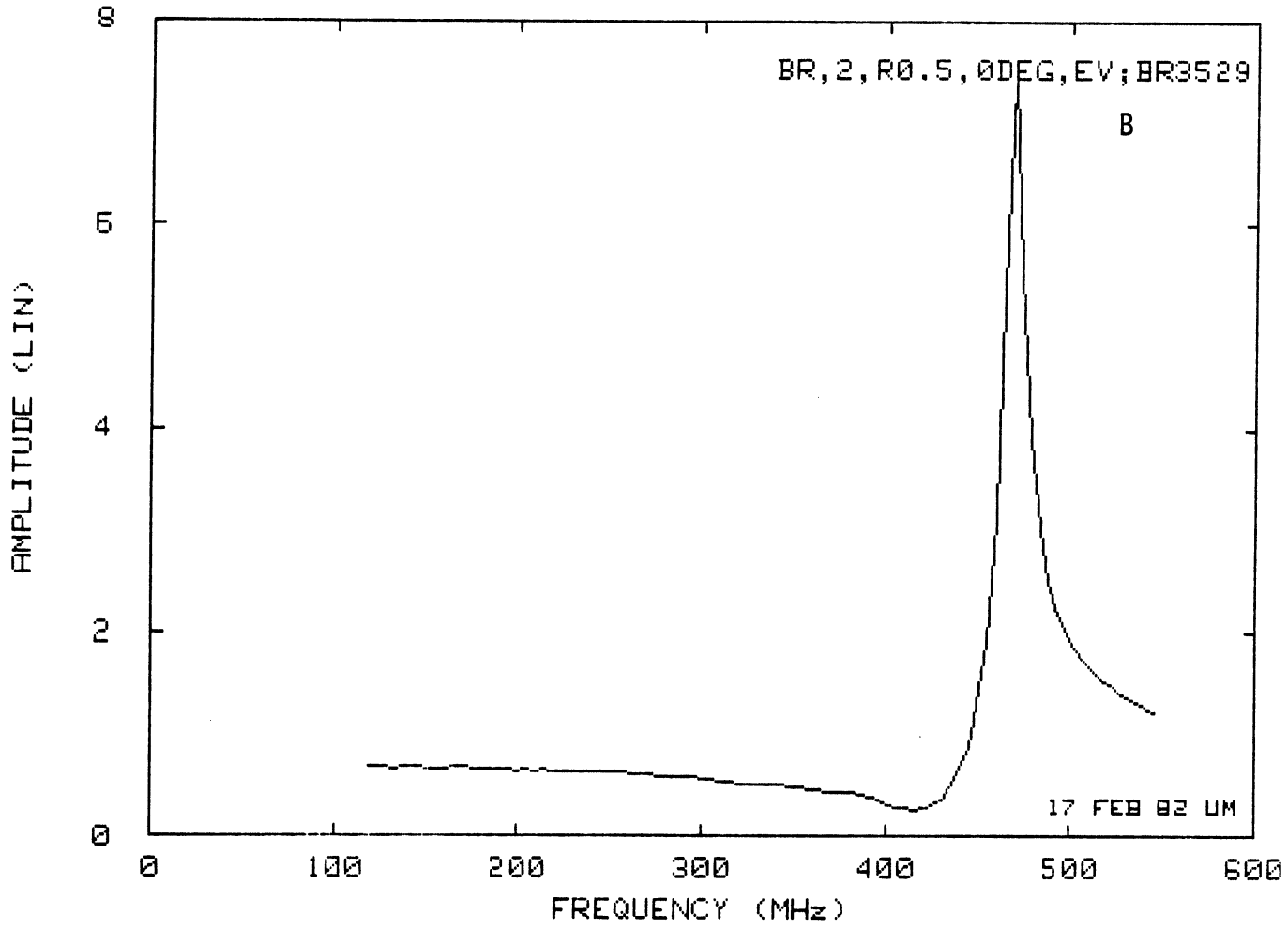
BR,2,R0.5,0DEG,EV;BR3529
B
17 FEB 82 UM
AMPLITUDE (LIN)
8
6
4
2
0
0
100
200
300
400
500
600
FREQUENCY (MHz)

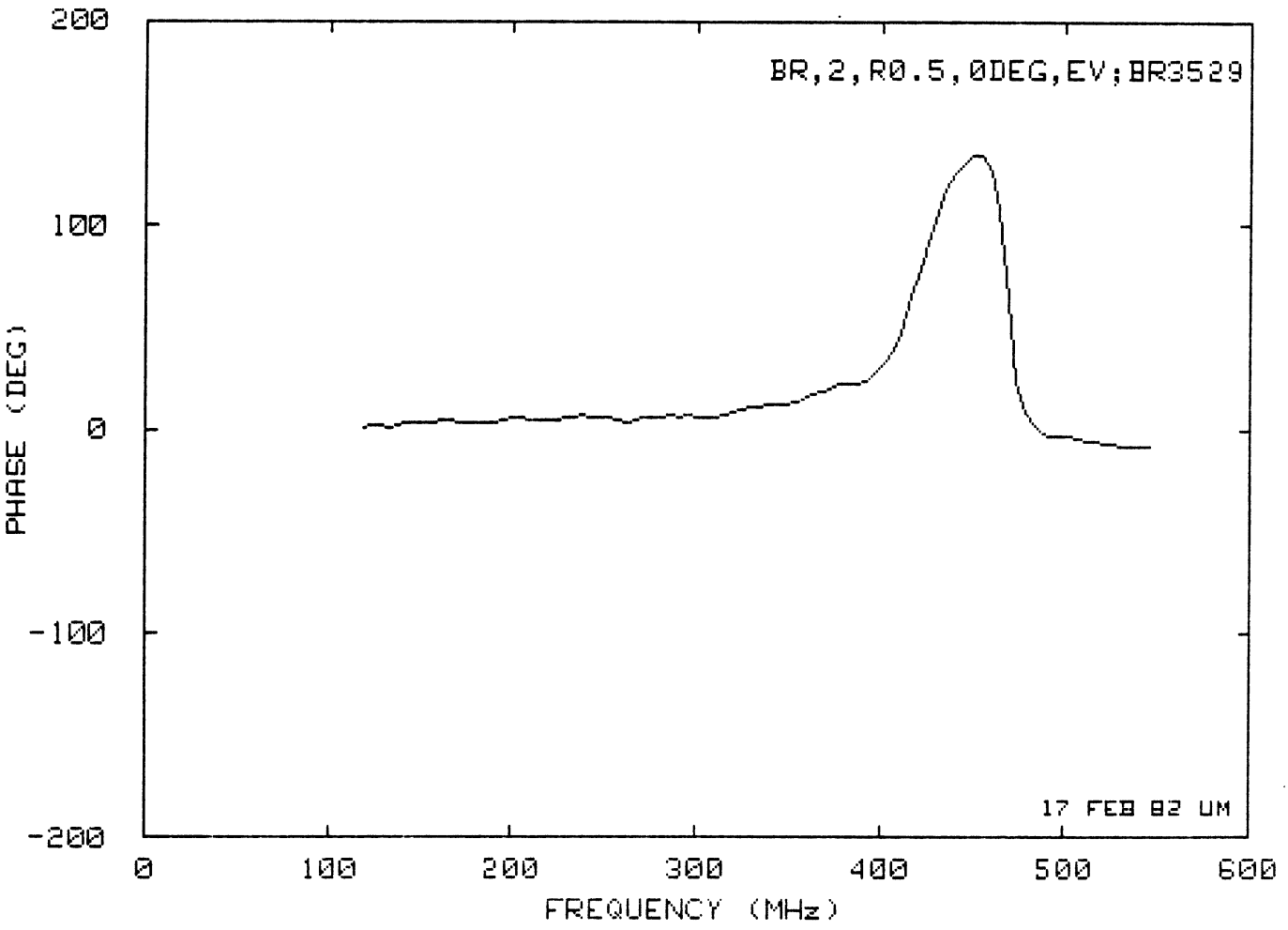
BR,2,R0.5,0DEG,EV;BR3529
17 FEB 82 UM
PHASE (DEG)
200
100
0
-100
-200
0
100
200
300
400
500
600
FREQUENCY (MHz)

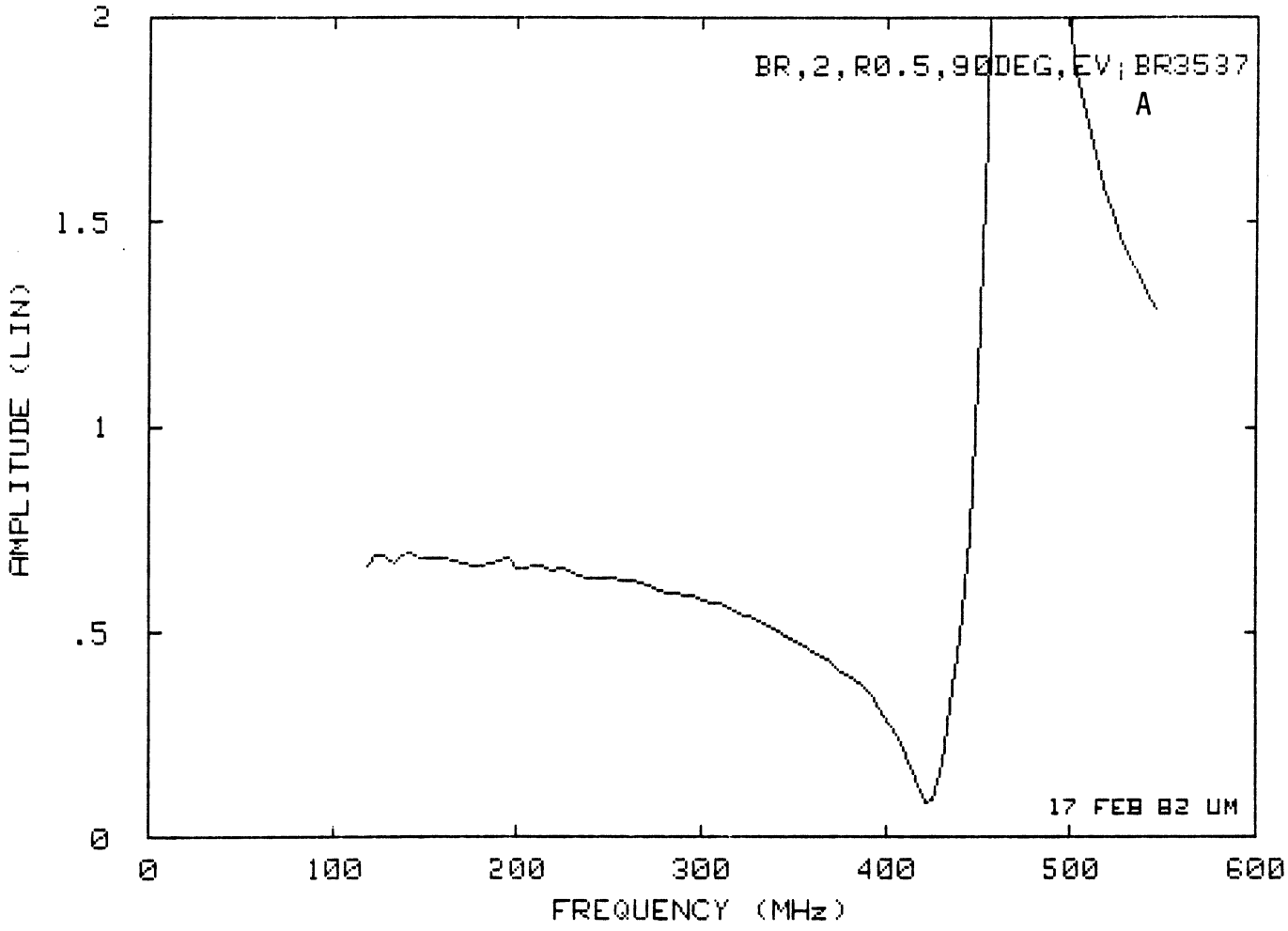
BR,2,R0.5,90DEG,EV;BR3537
A
17 FEB 82 UM
AMPLITUDE (LIN)
2
1.5
1
.5
0
0
100
200
300
400
500
600
FREQUENCY (MHz)

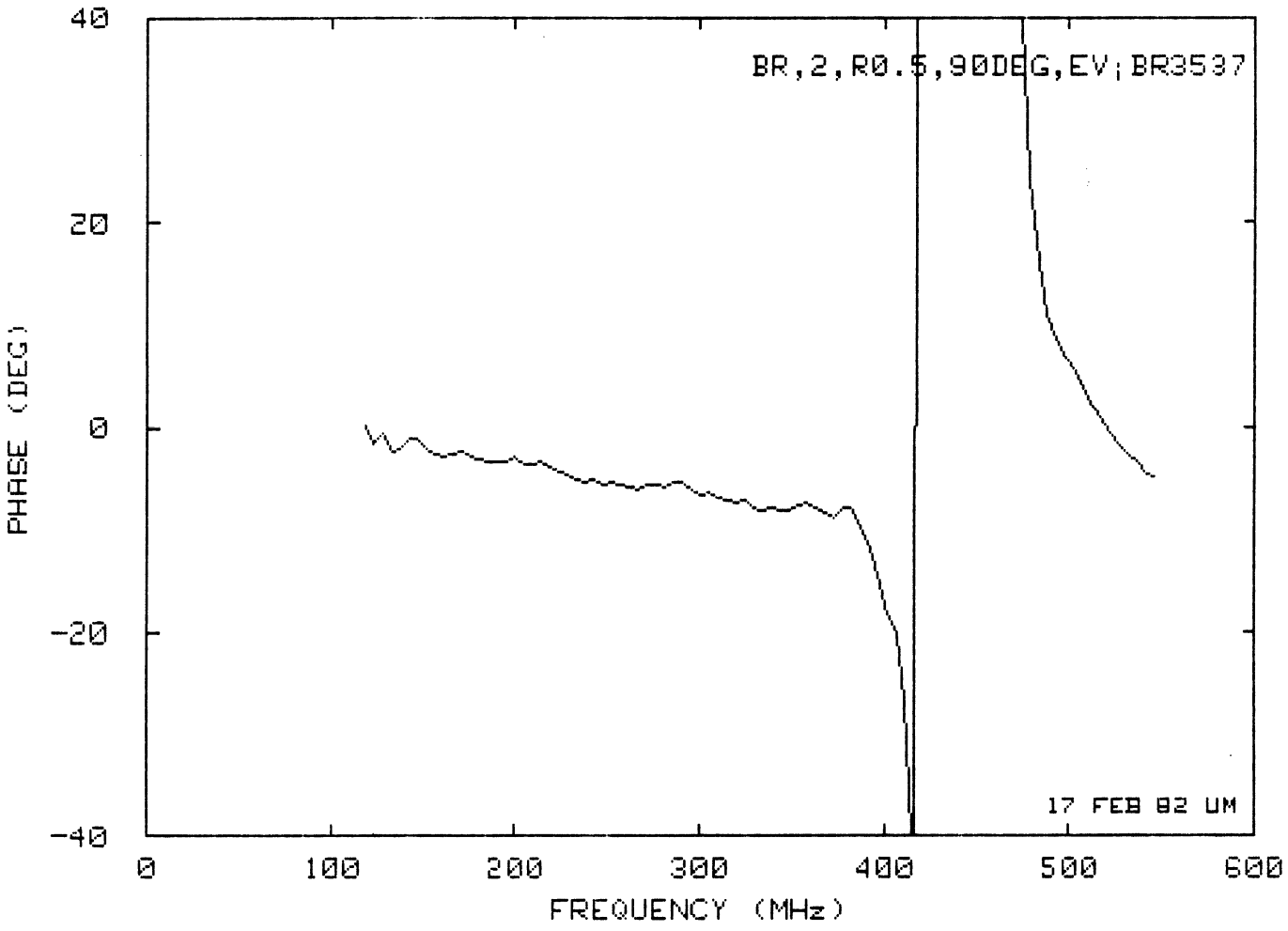
BR,2,R0.5,90DEG,EV;BR3537
17 FEB 82 UM
PHASE (DEG)
40
20
0
-20
-40
0
100
200
300
400
500
600
FREQUENCY (MHz)

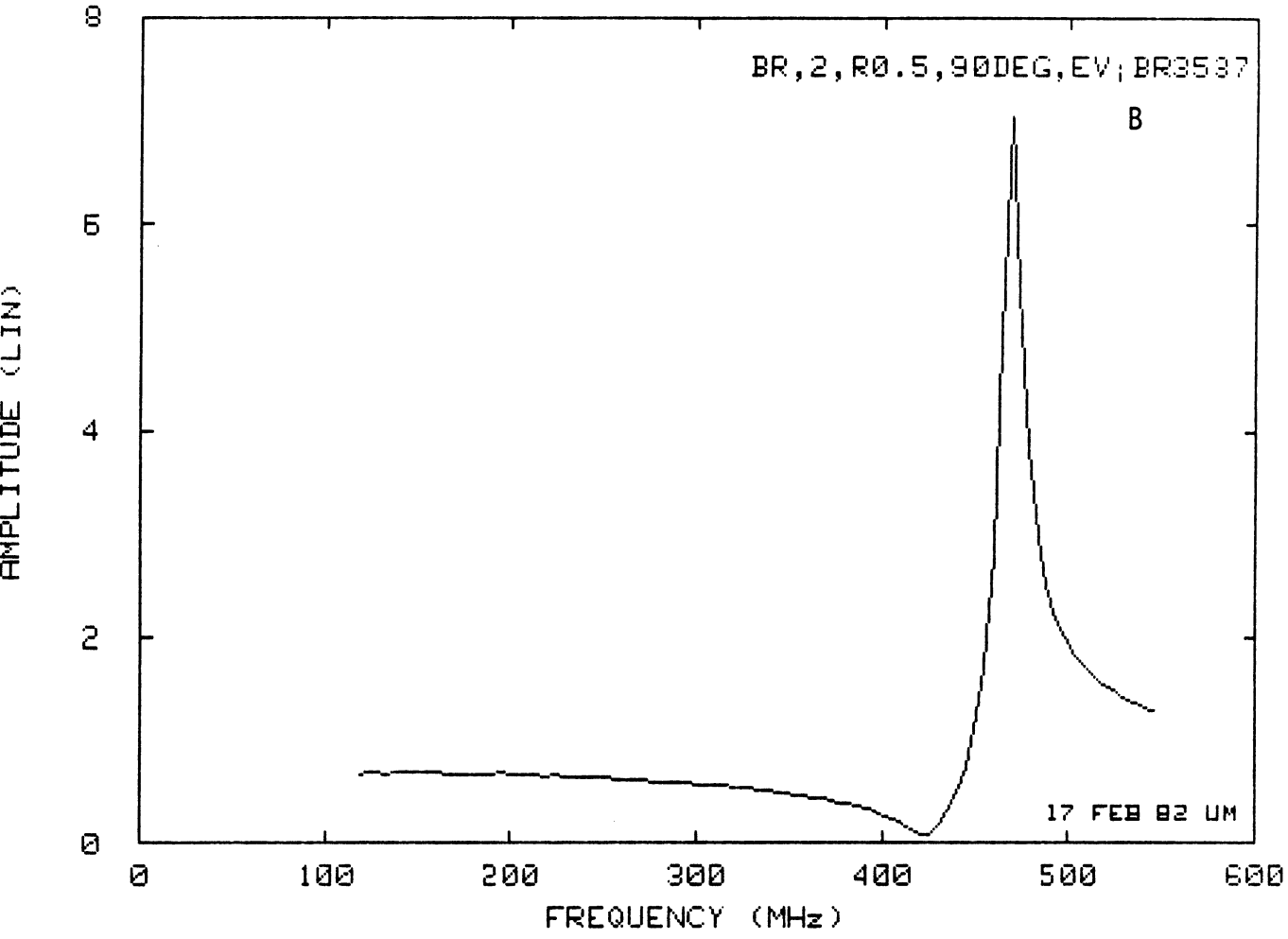
BR,2,R0.5,90DEG,EV;BR3537
B
17 FEB 82 UM
AMPLITUDE (LIN)
0
2
4
6
8
0
100
200
300
400
500
600
FREQUENCY (MHz)

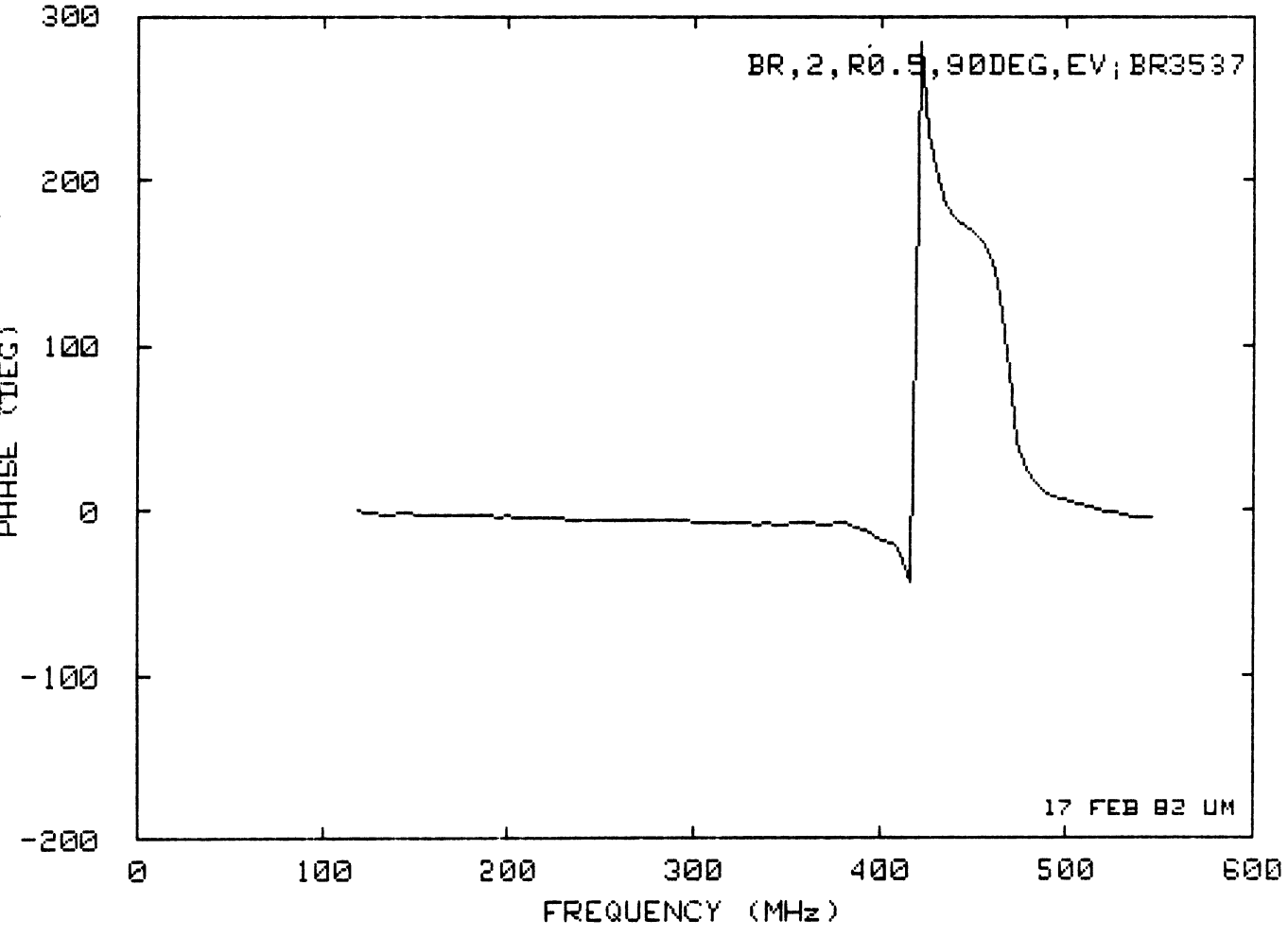
BR,2,R0.5,90DEG,EV;BR3537
17 FEB 82 UM
PHASE (DEG)
300
200
100
0
-100
-200
0
100
200
300
400
500
600
FREQUENCY (MHz)

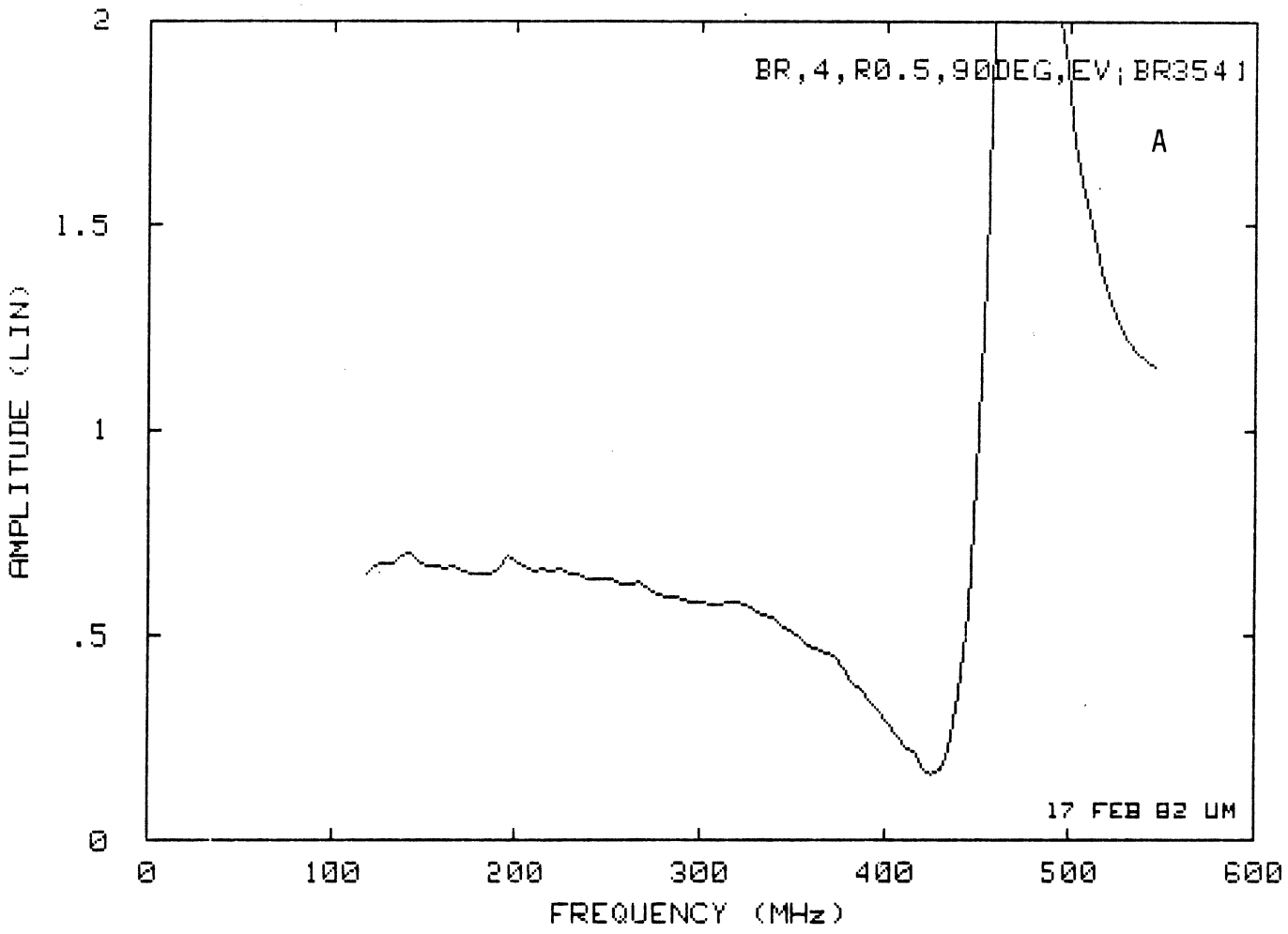
BR,4,R0.5,90DEG,EV;BR3541
A
17 FEB 82 UM
AMPLITUDE (LIN)
2
1.5
1
.5
0
0
100
200
300
400
500
600
FREQUENCY (MHz)

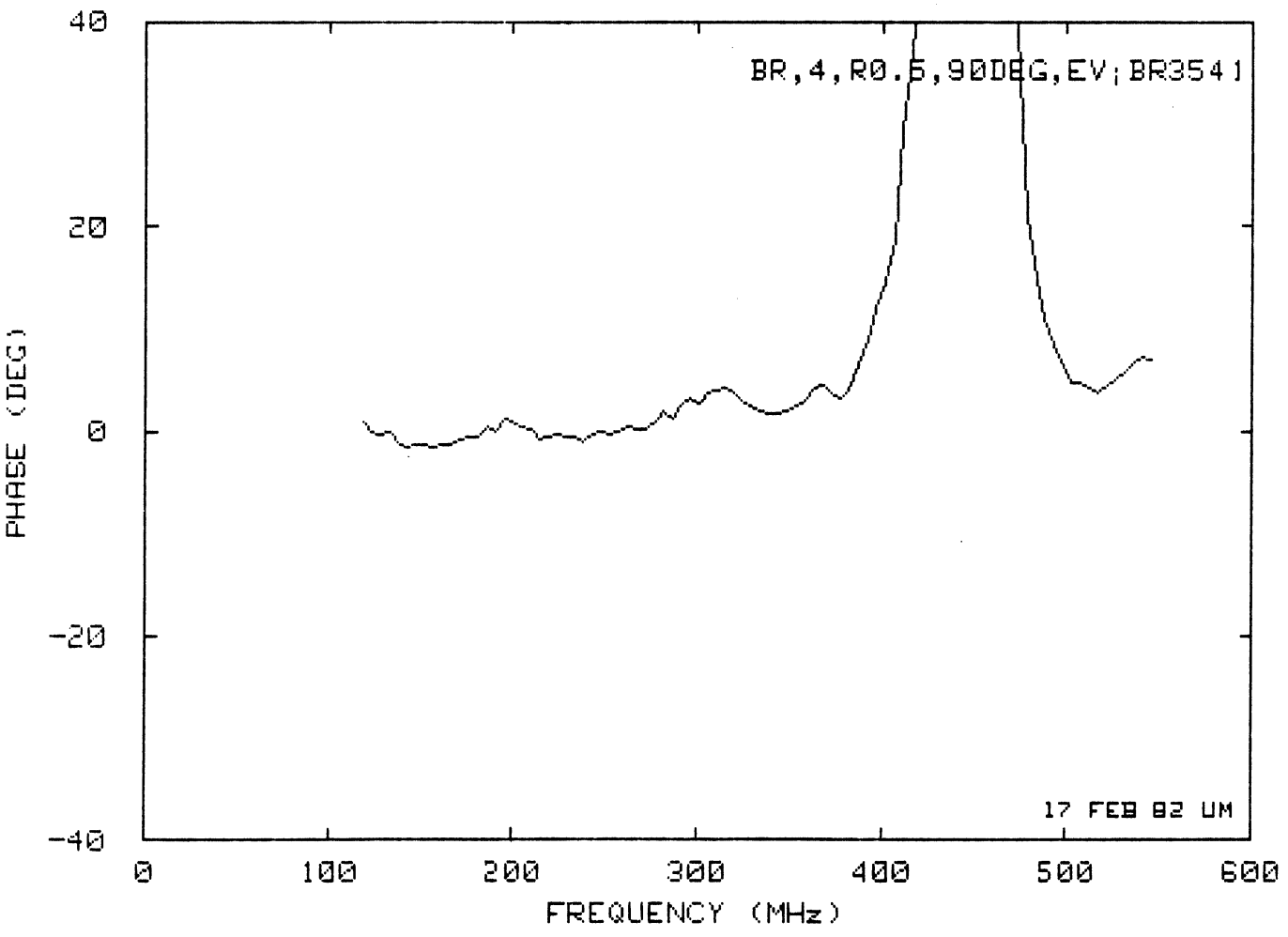
BR,4,R0.5,90DEG,EV;BR3541
17 FEB 82 UM
PHASE (DEG)
40
20
0
-20
-40
0
100
200
300
400
500
600
FREQUENCY (MHz)

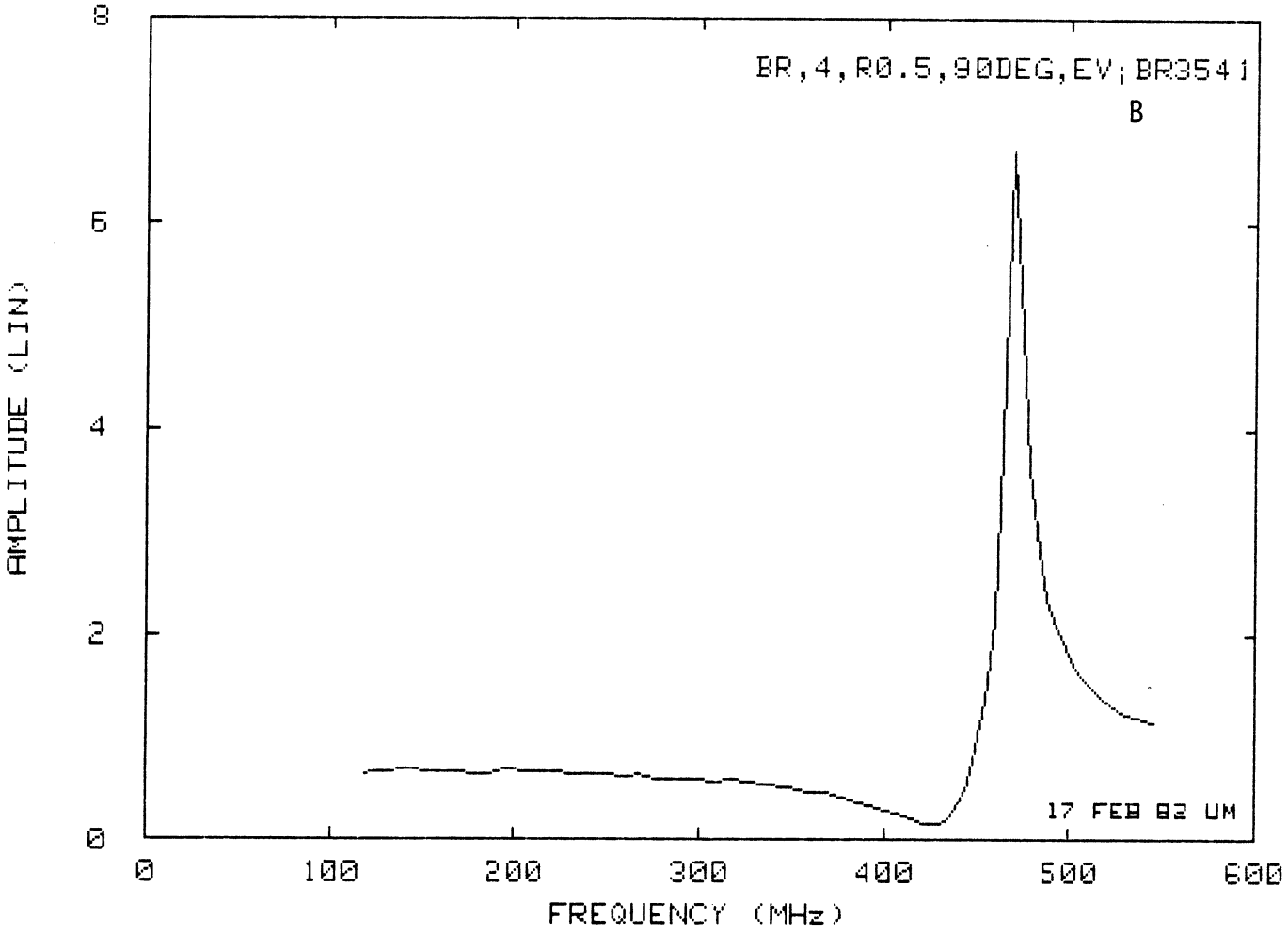
BR,4,R0.5,90DEG,EV;BR3541
B
17 FEB 82 UM
AMPLITUDE (LIN)
0
2
4
6
8
0
100
200
300
400
500
600
FREQUENCY (MHz)

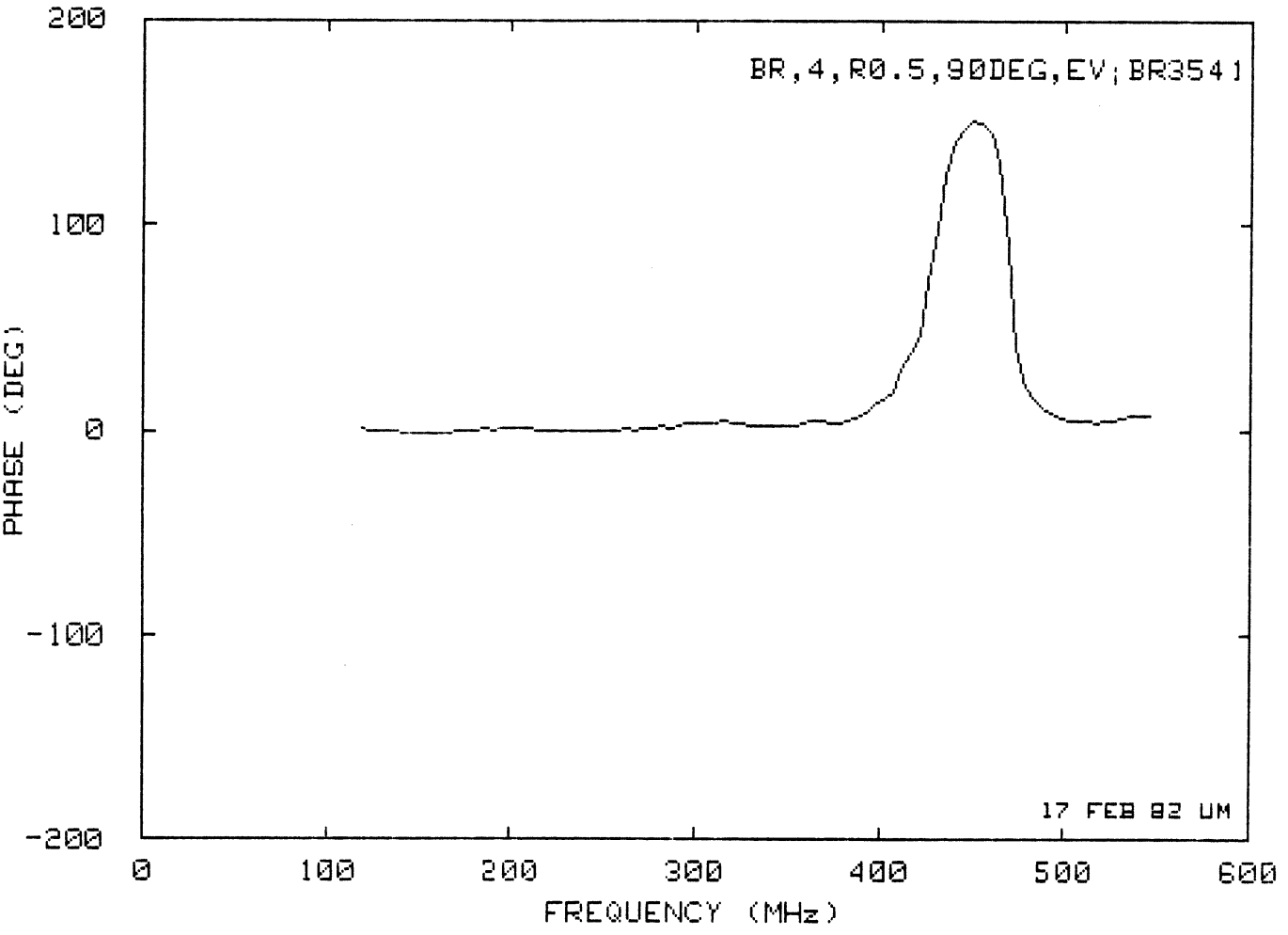
BR,4,R0.5,90DEG,EV;BR3541
17 FEB 82 UM
PHASE (DEG)
200
100
0
-100
-200
0
100
200
300
400
500
600
FREQUENCY (MHz)

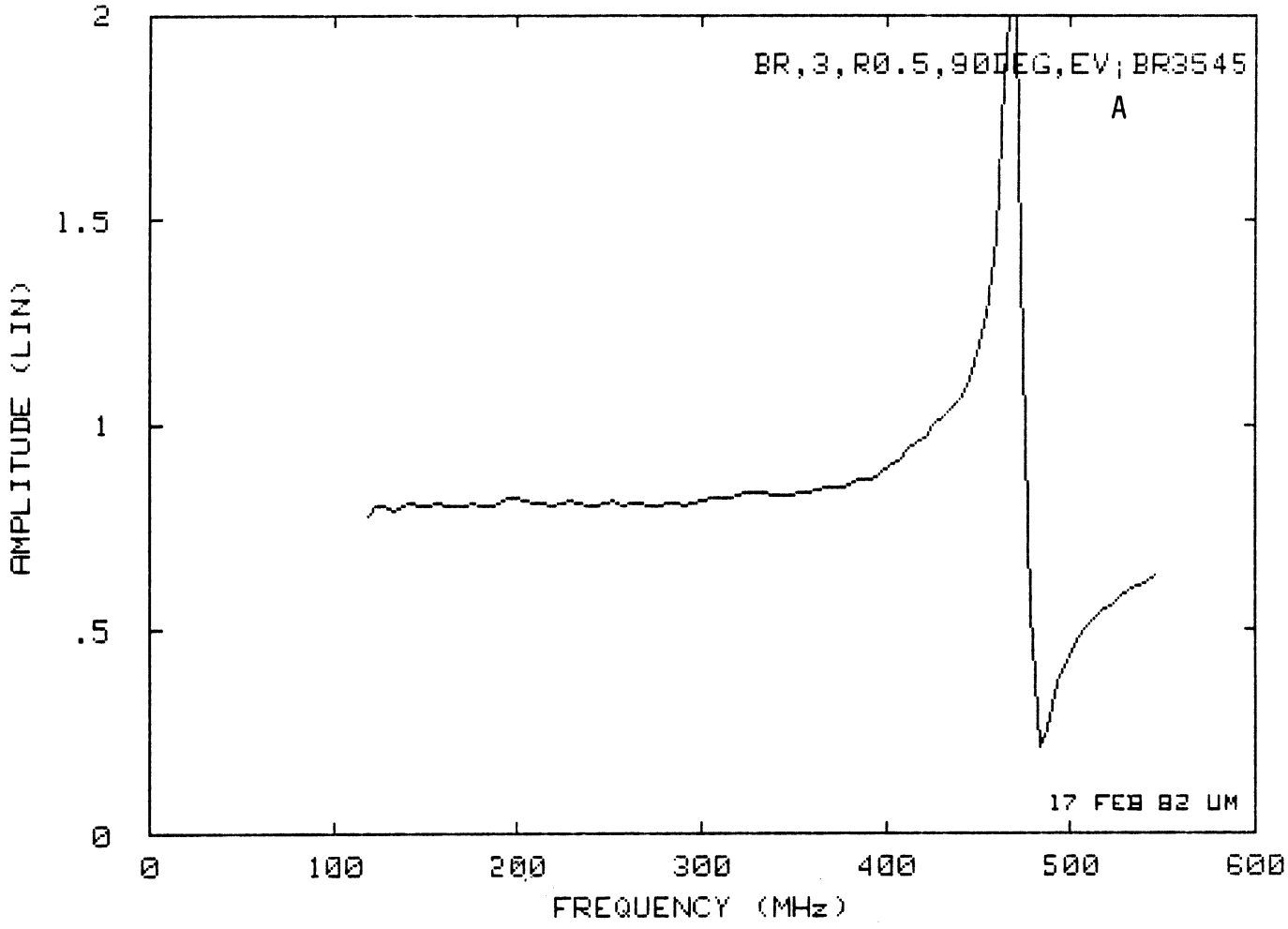
BR,3,R0.5,90DEG,EV;BR3545
A
17 FEB 82 UM
AMPLITUDE (LIN)
2
1.5
1
.5
0
0
100
200
300
400
500
600
FREQUENCY (MHz)

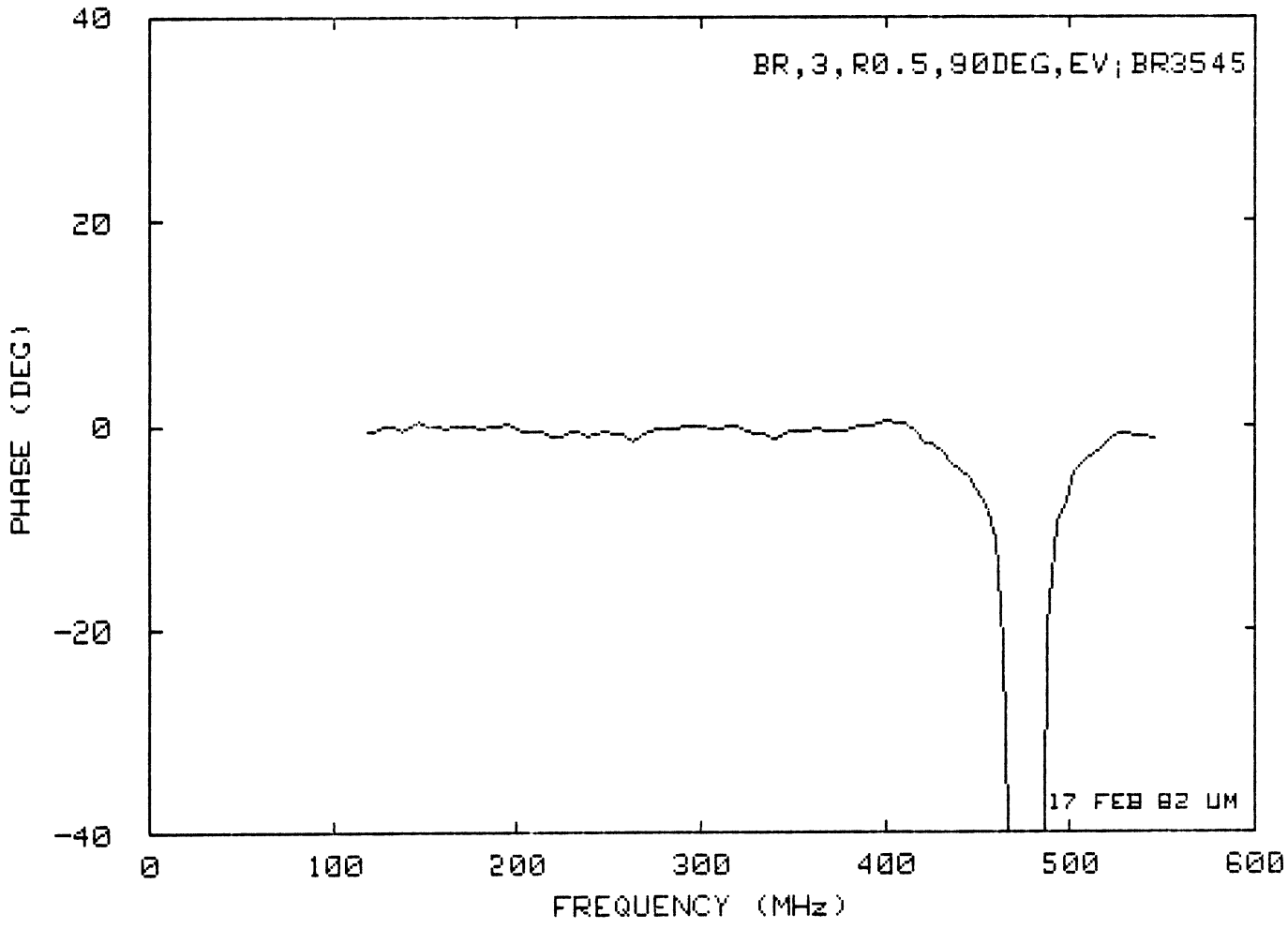
BR,3,R0.5,90DEG,EV;BR3545
17 FEB 82 UM
PHASE (DEG)
40
20
0
-20
-40
0
100
200
300
400
500
600
FREQUENCY (MHz)

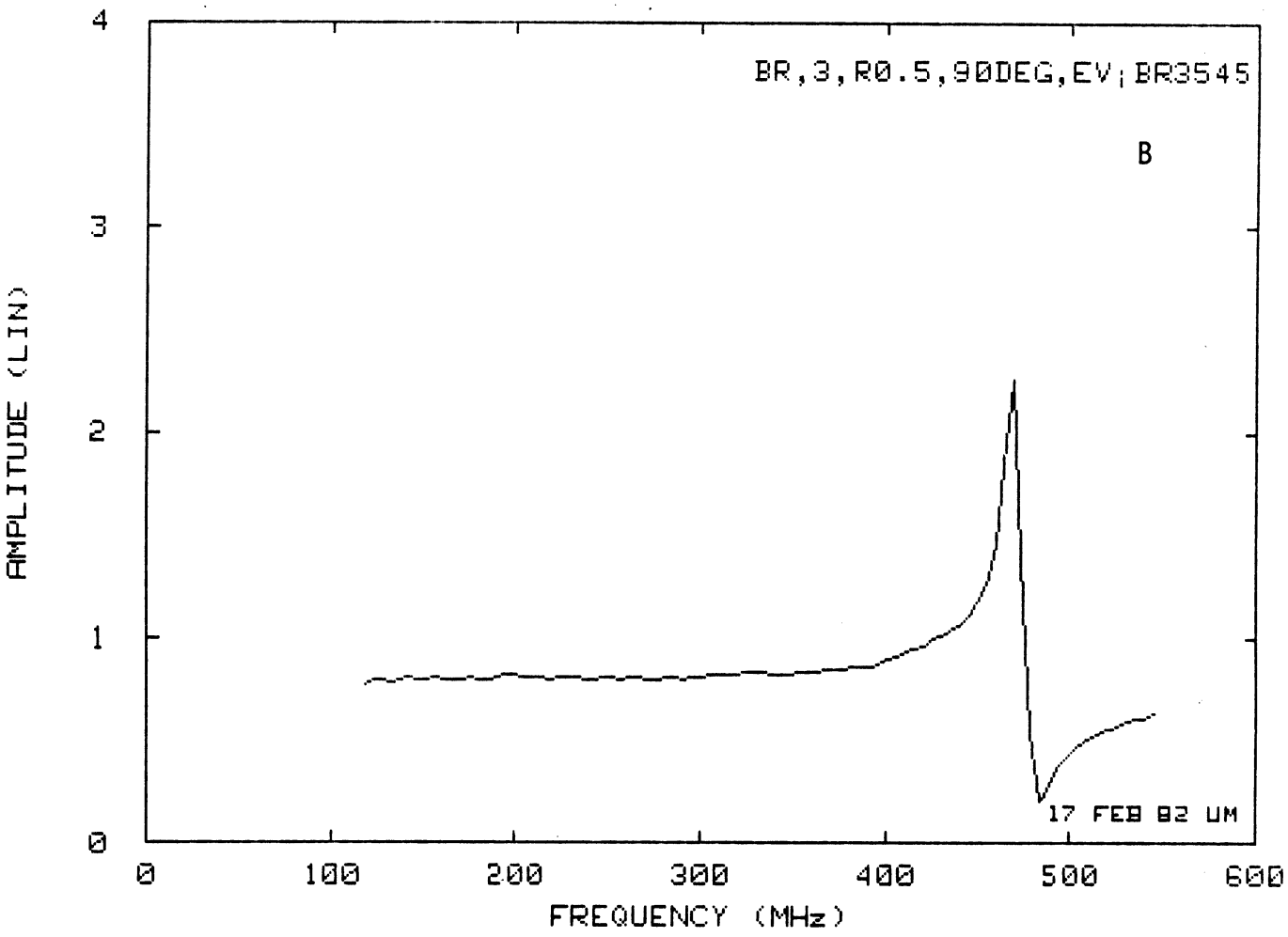
BR,3,R0.5,90DEG,EV;BR3545
B
17 FEB 82 UM
AMPLITUDE (LIN)
FREQUENCY (MHz)
0
1
2
3
4
0
100
200
300
400
500
600

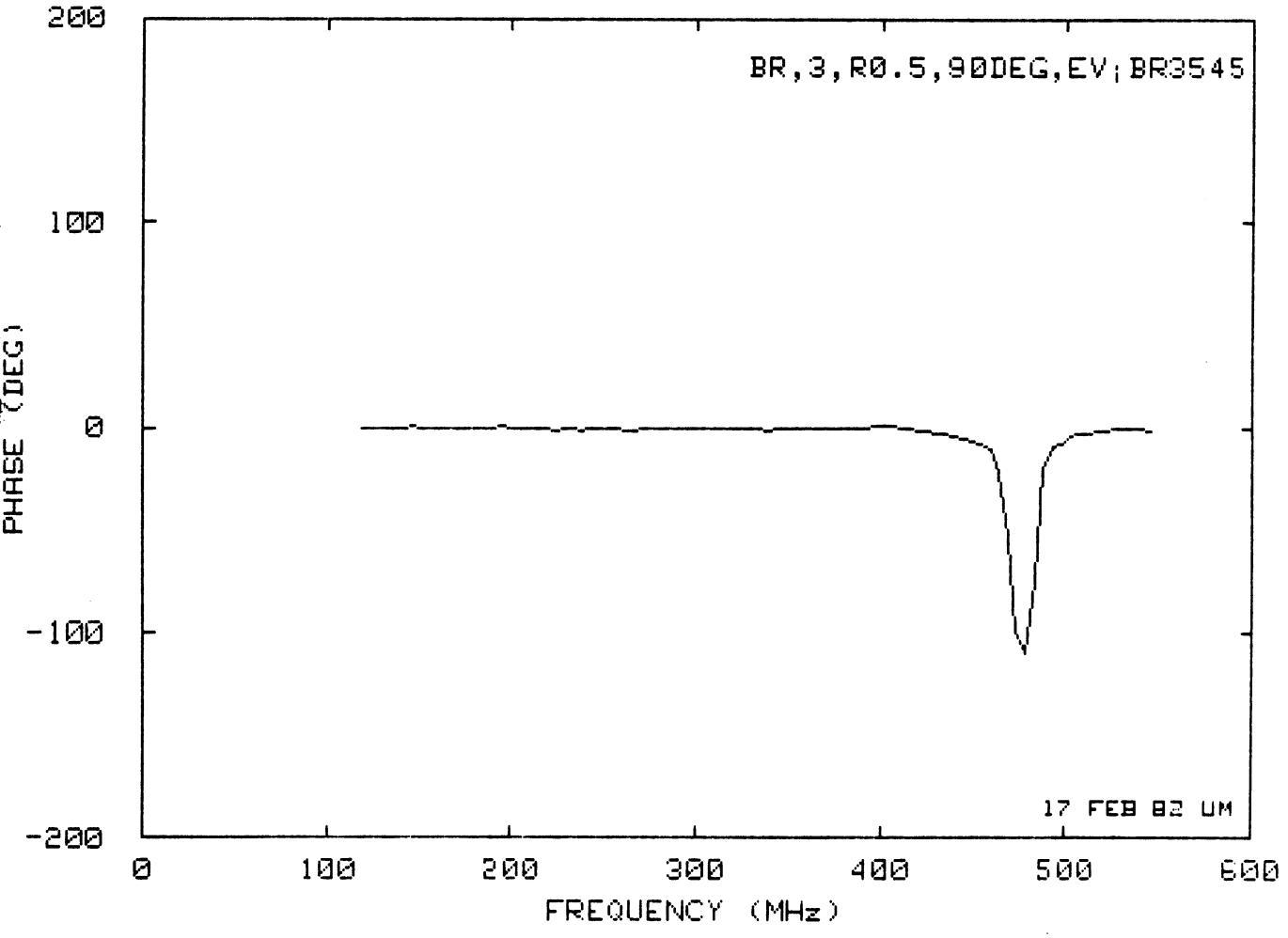
BR,3,R0.5,90DEG,EV;BR3545
17 FEB 82 UM
PHASE (DEG)
FREQUENCY (MHz)
200
100
0
-100
-200
0
100
200
300
400
500
600

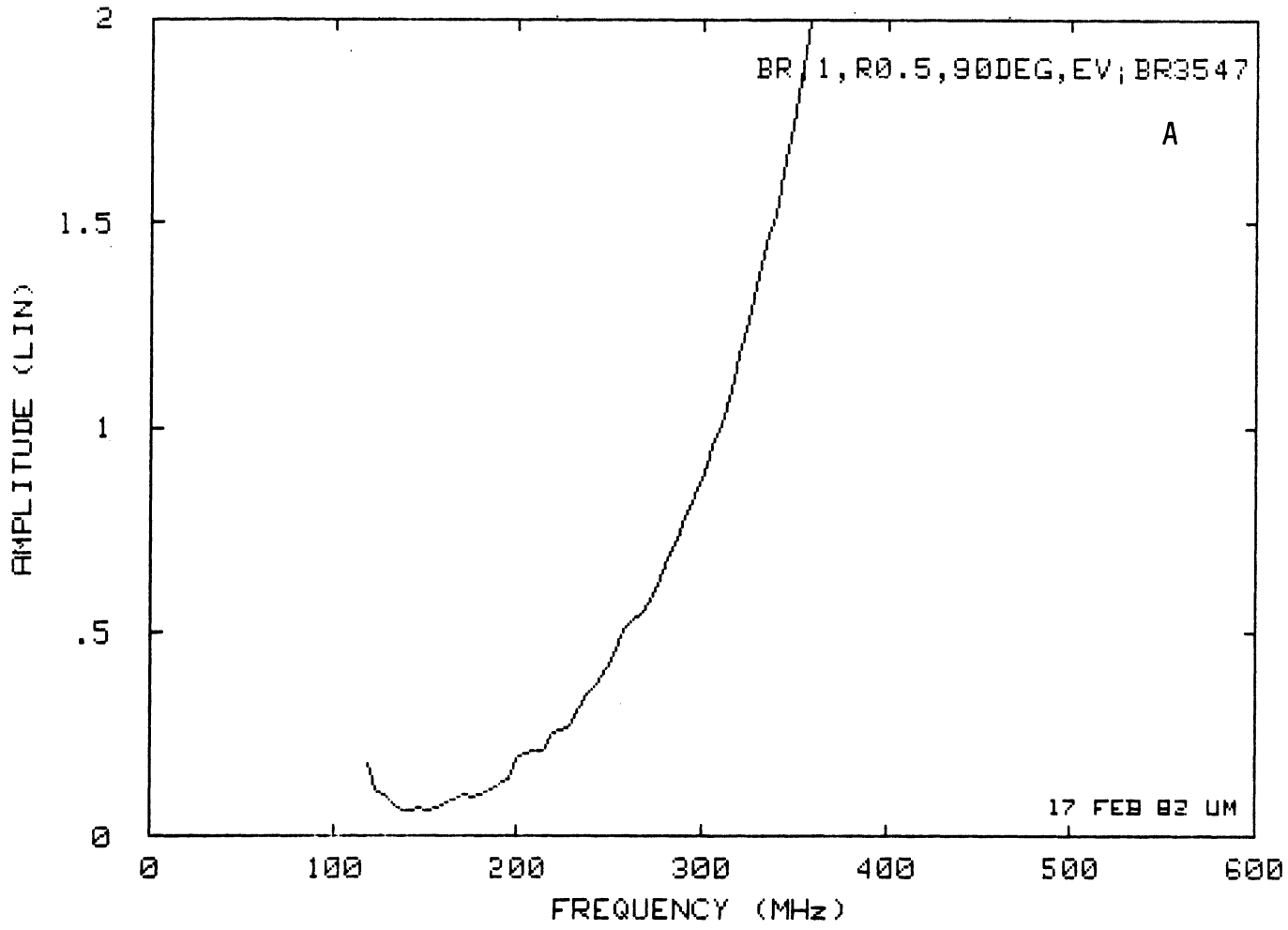
BR,1,R0.5,90DEG,EV;BR3547
A
17 FEB 82 UM
AMPLITUDE (LIN)
2
1.5
1
.5
0
0
100
200
300
400
500
600
FREQUENCY (MHz)

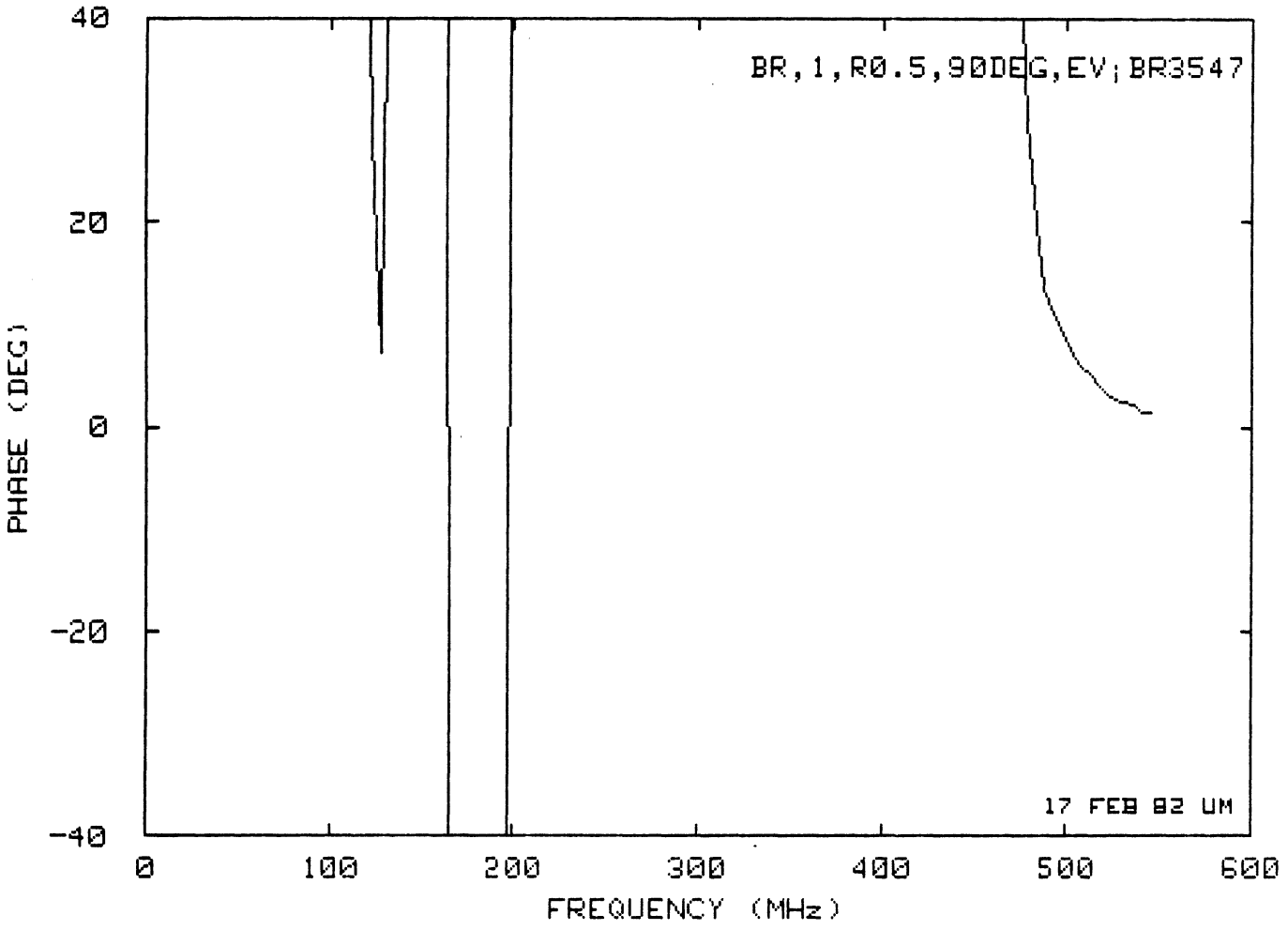
BR,1,R0.5,90DEG,EV;BR3547
17 FEB 82 UM
PHASE (DEG)
40
20
0
-20
-40
0
100
200
300
400
500
600
FREQUENCY (MHz)

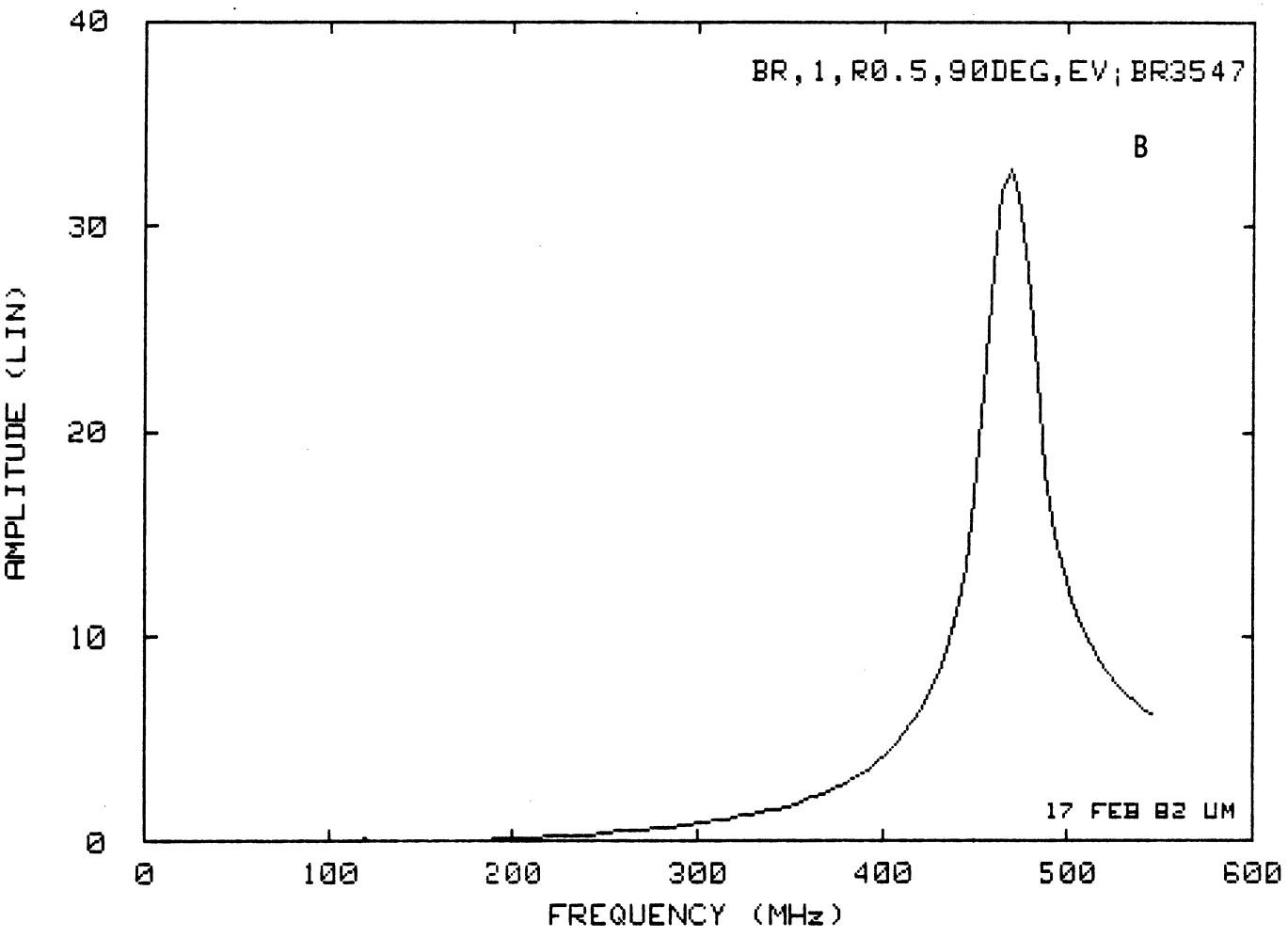
BR,1,R0.5,90DEG,EV;BR3547
B
17 FEB 82 UM
AMPLITUDE (LIN)
40
30
20
10
0
0
100
200
300
400
500
600
FREQUENCY (MHz)

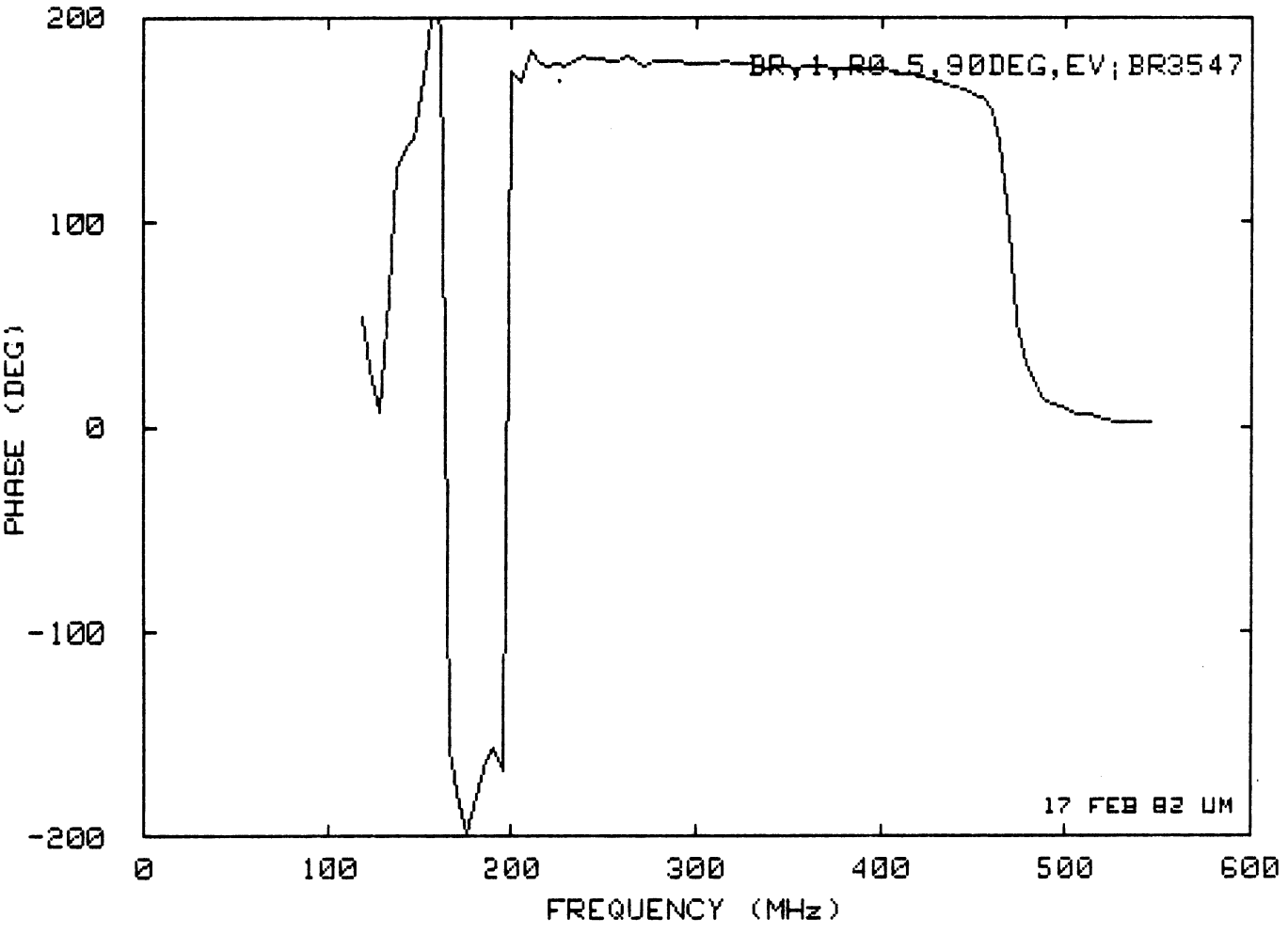
BR,1,R0.5,90DEG,EV;BR3547
17 FEB 82 UM
PHASE (DEG)
200
100
0
-100
-200
0
100
200
300
400
500
600
FREQUENCY (MHz)

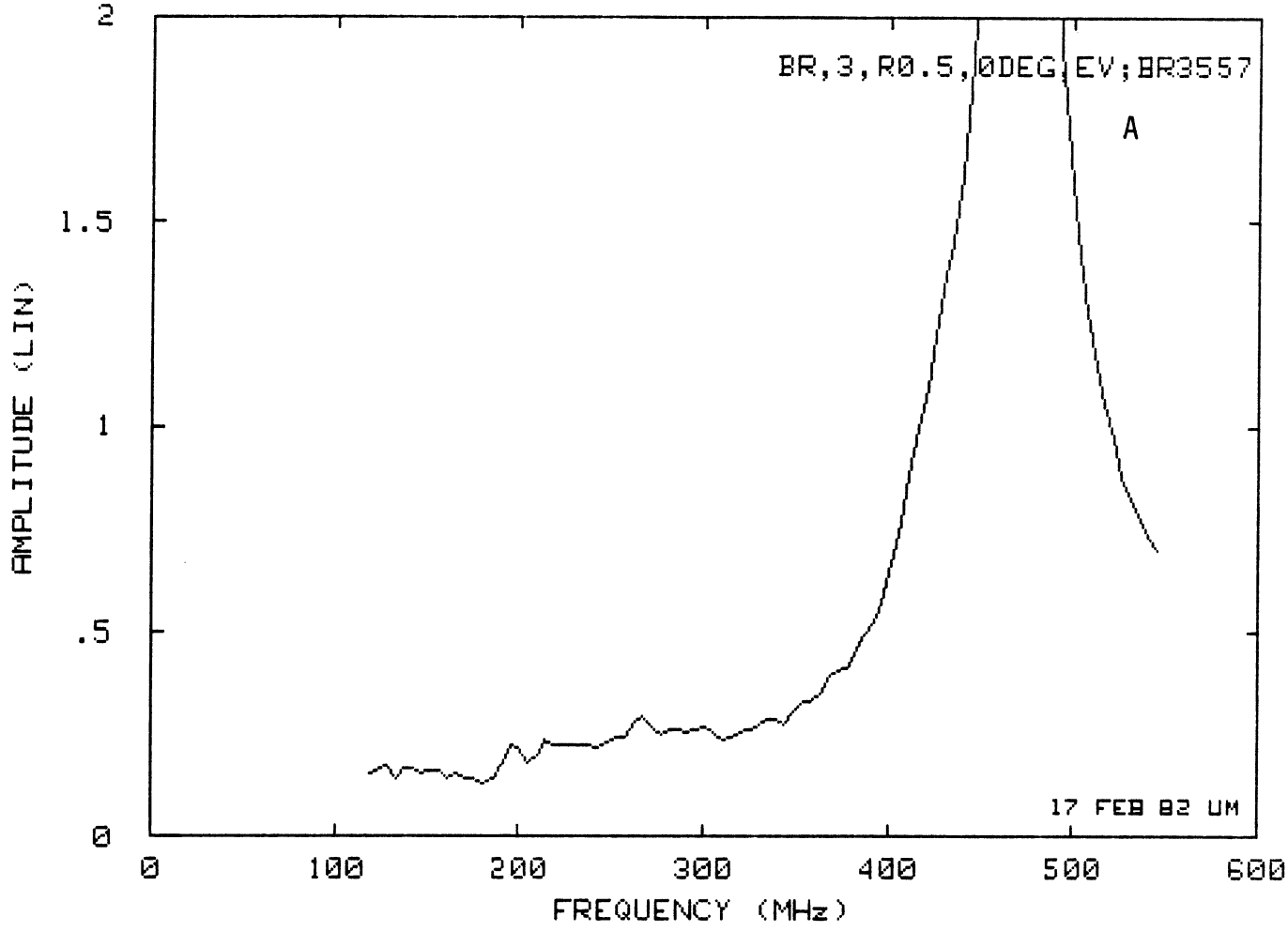
BR,3,R0.5,0DEG,EV;BR3557
A
17 FEB 82 UM
AMPLITUDE (LIN)
2
1.5
1
.5
0
0
100
200
300
400
500
600
FREQUENCY (MHz)

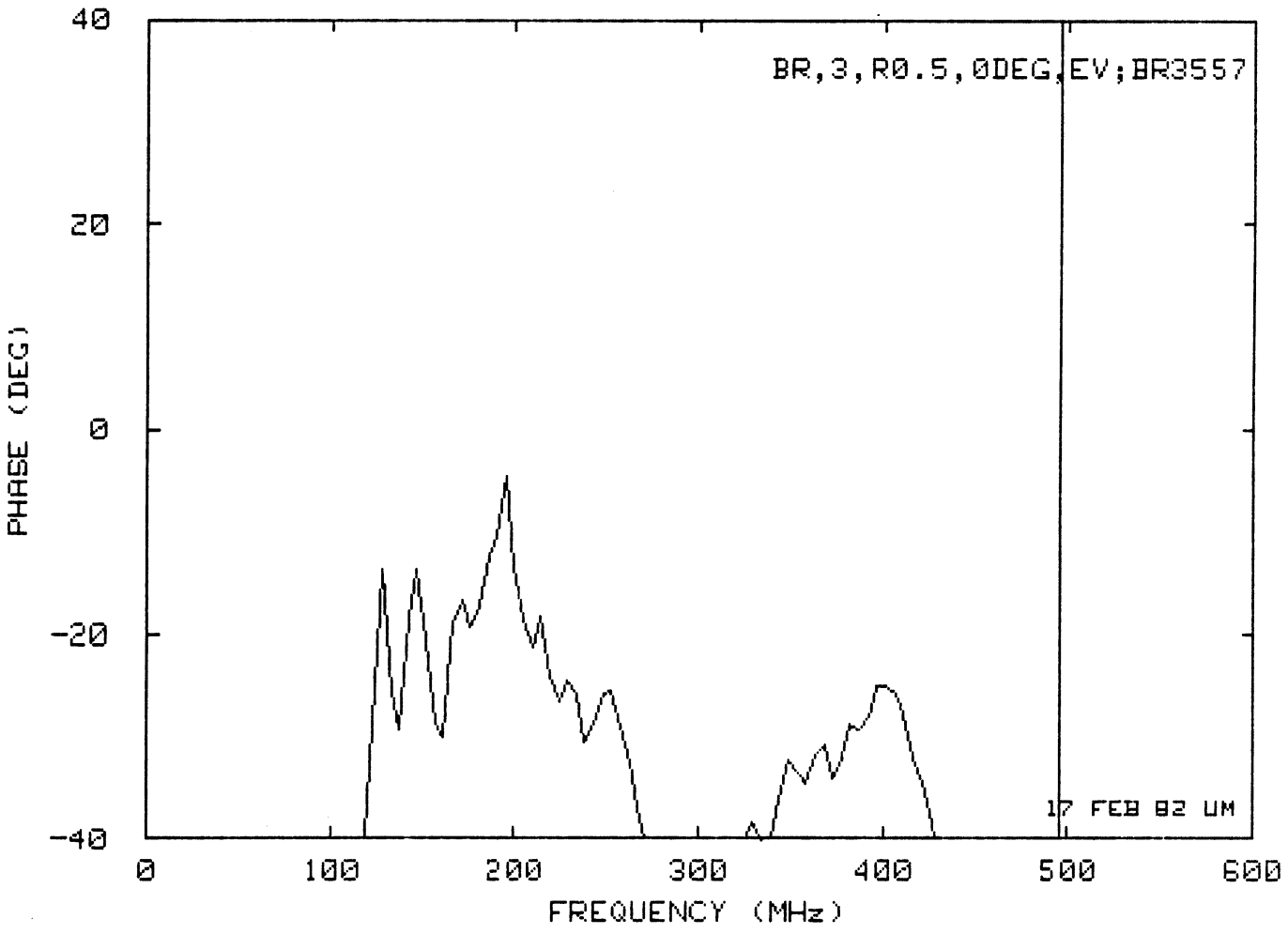
BR,3,R0.5,0DEG,EV;BR3557
17 FEB 82 UM
PHASE (DEG)
40
20
0
-20
-40
0
100
200
300
400
500
600
FREQUENCY (MHz)

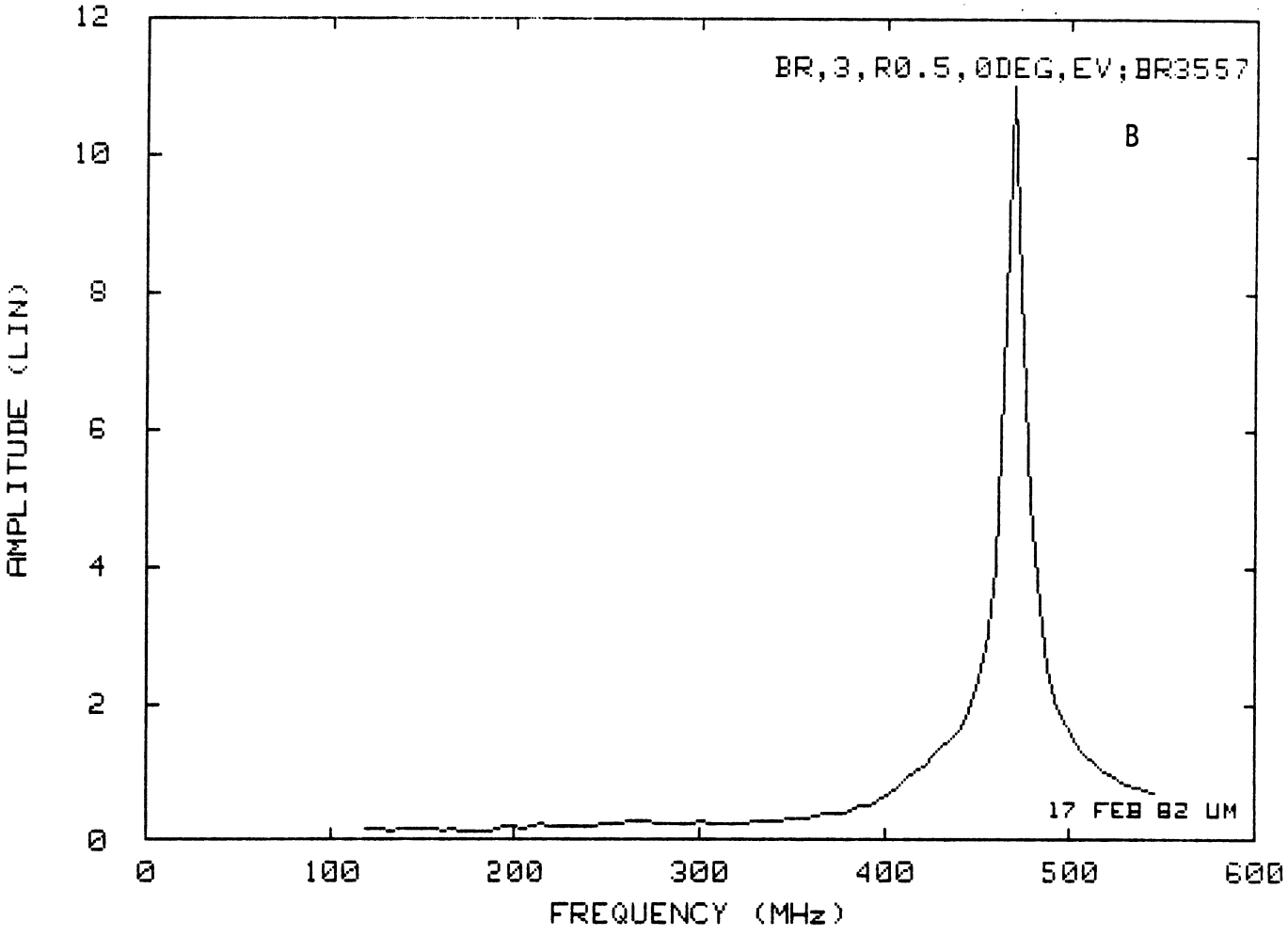
BR,3,R0.5,0DEG,EV;BR3557
B
17 FEB 82 UM
AMPLITUDE (LIN)
FREQUENCY (MHz)
0
2
4
6
8
10
12
0
100
200
300
400
500
600

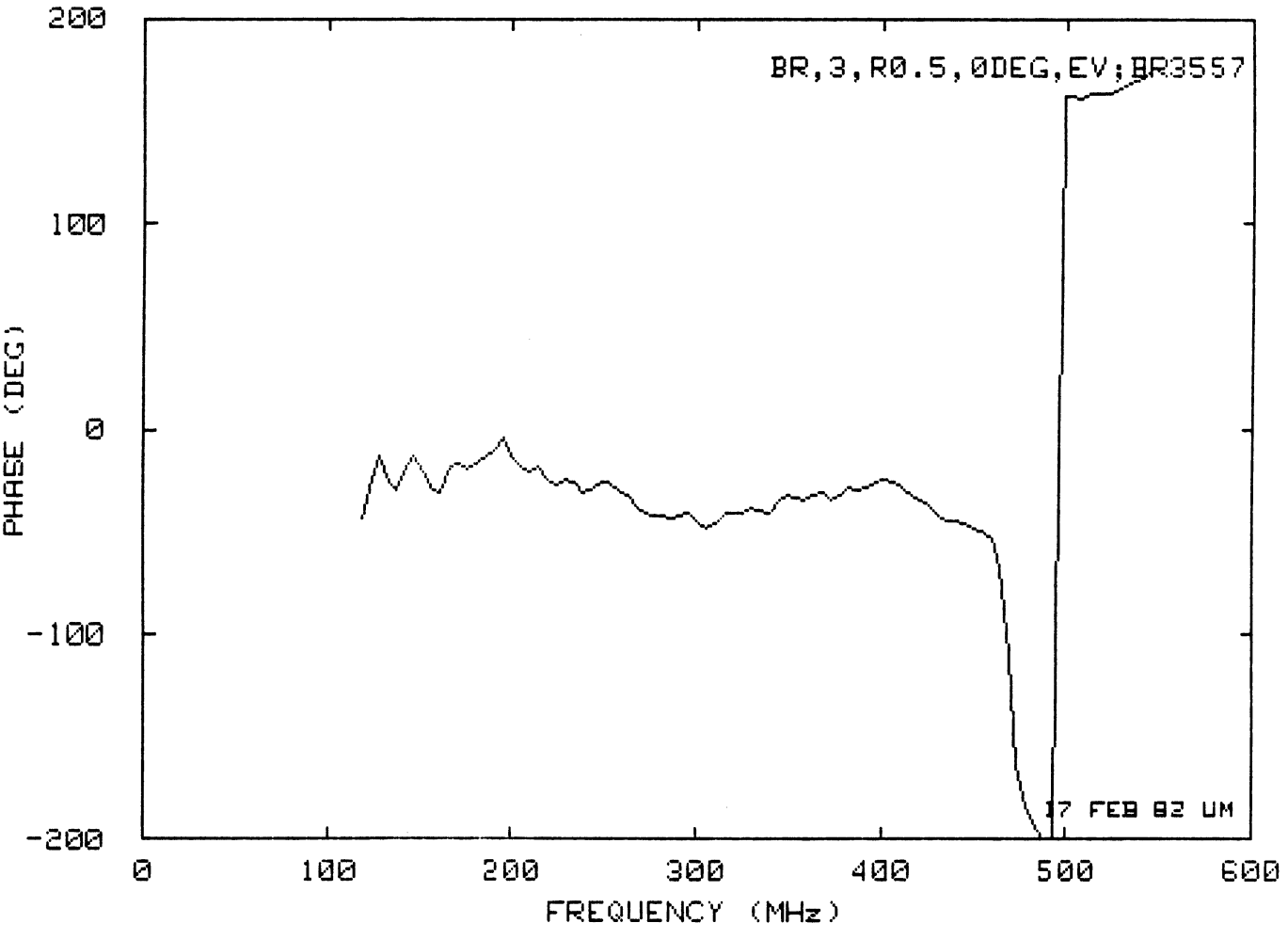
BR,3,R0.5,0DEG,EV;BR3557
17 FEB 82 UM
PHASE (DEG)
FREQUENCY (MHz)
200
100
0
-100
-200
0
100
200
300
400
500
600

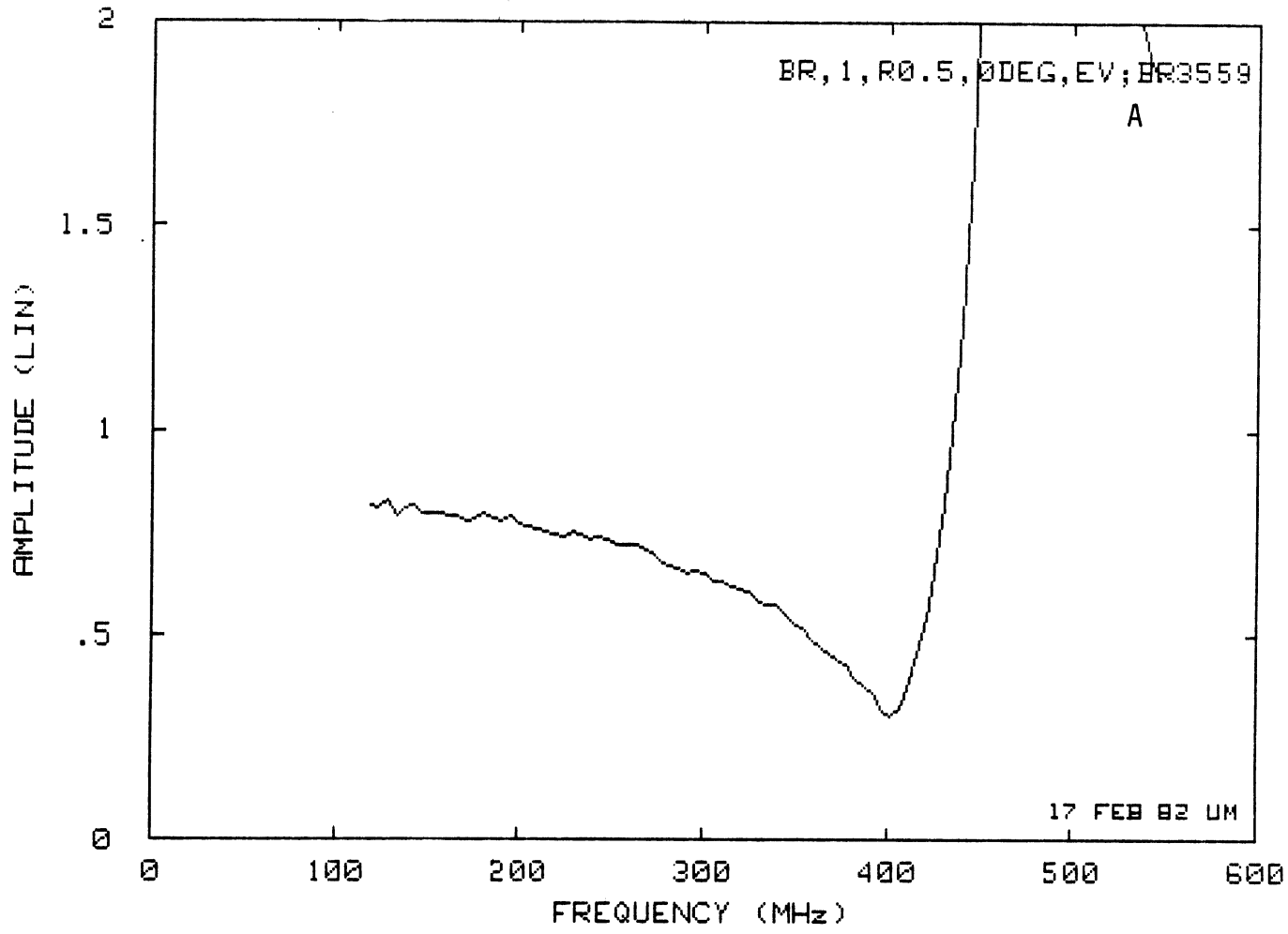
BR,1,R0.5,0DEG,EV;BR3559
A
17 FEB 82 UM
AMPLITUDE (LIN)
2
1.5
1
.5
0
0
100
200
300
400
500
600
FREQUENCY (MHz)

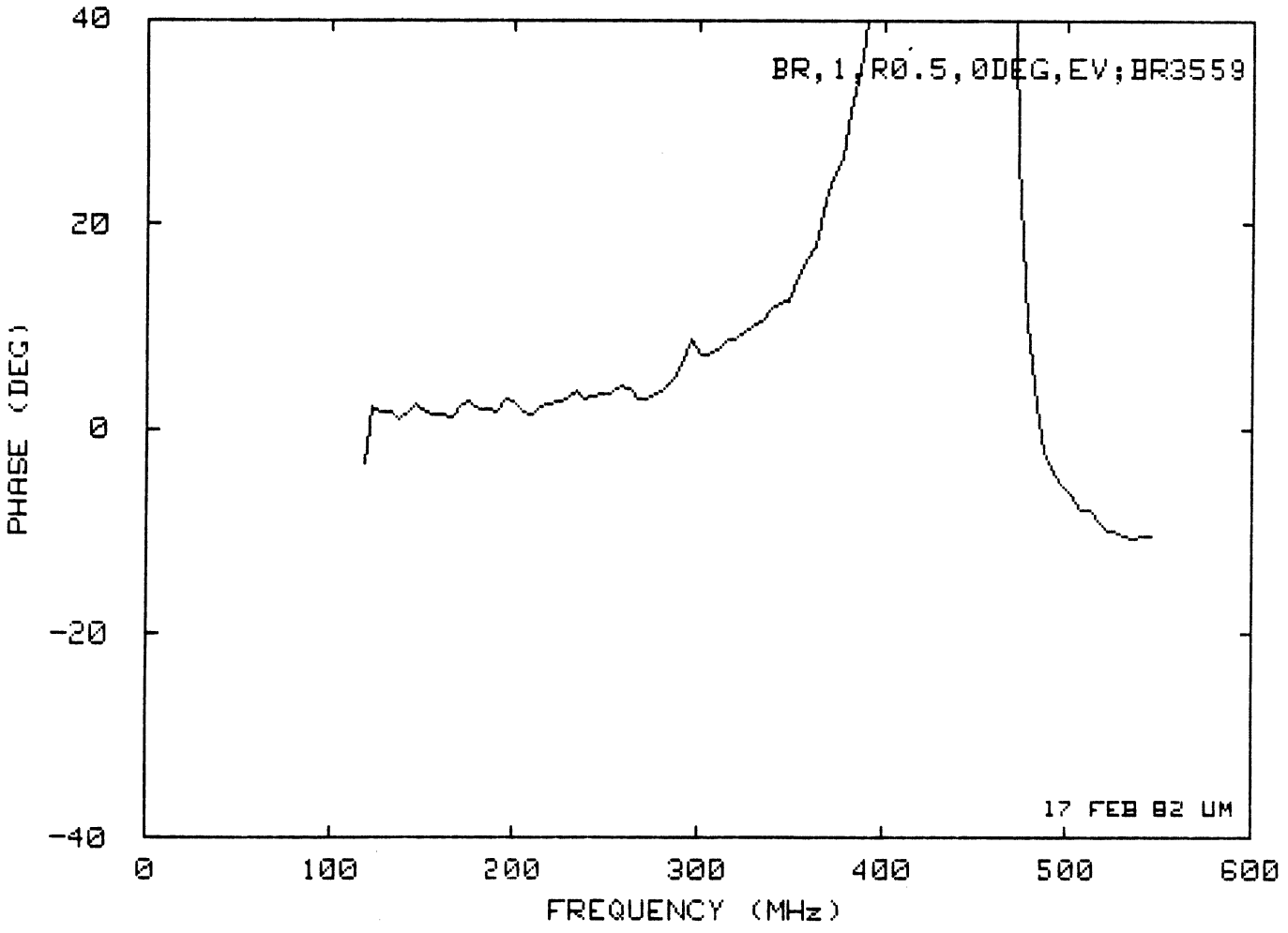
BR,1,R0.5,0DEG,EV;BR3559
17 FEB 82 UM
PHASE (DEG)
40
20
0
-20
-40
0
100
200
300
400
500
600
FREQUENCY (MHz)

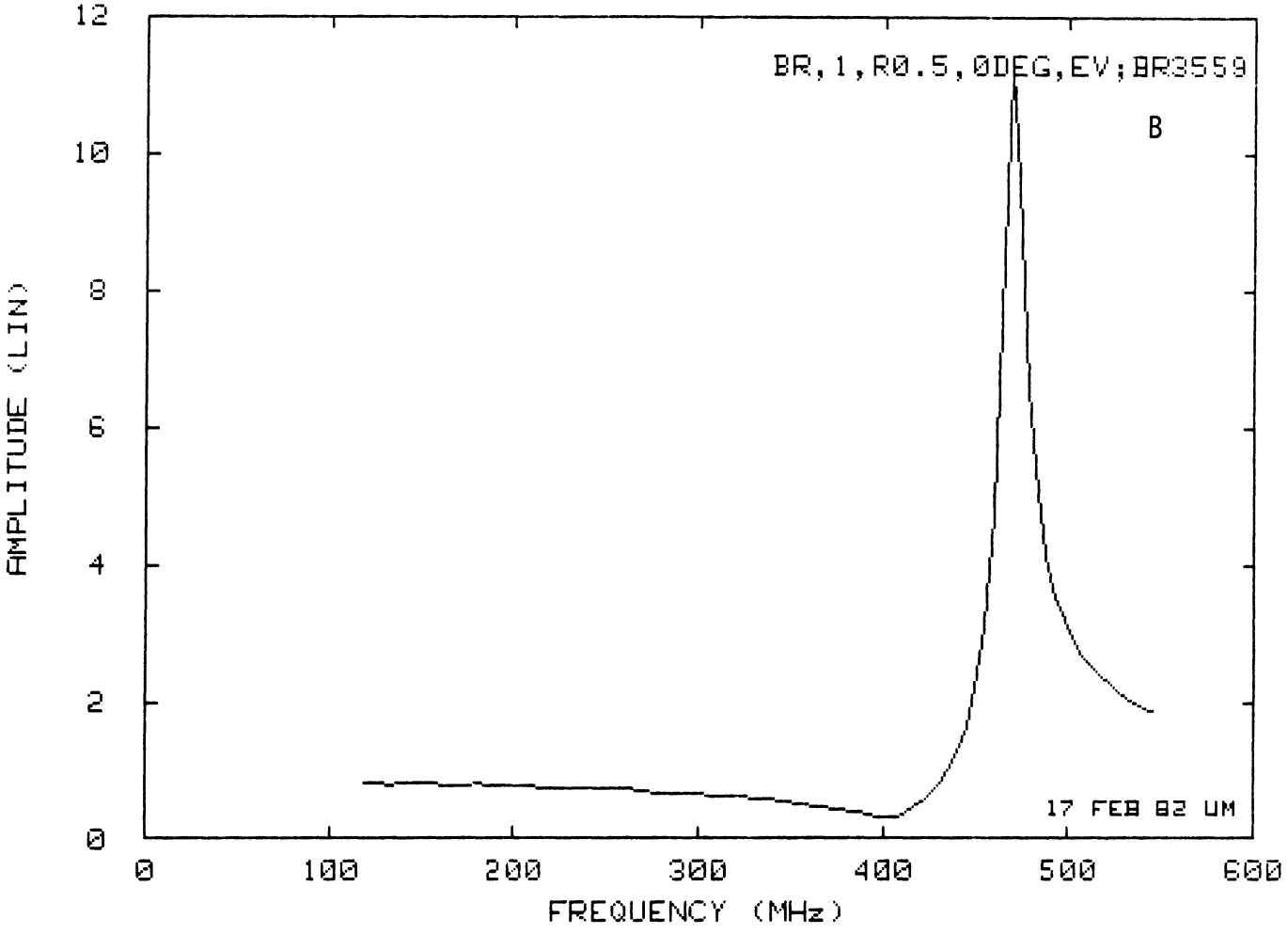
BR,1,R0.5,0DEG,EV;BR3559
B
17 FEB 82 UM
AMPLITUDE (LIN)
12
10
8
6
4
2
0
0
100
200
300
400
500
600
FREQUENCY (MHz)

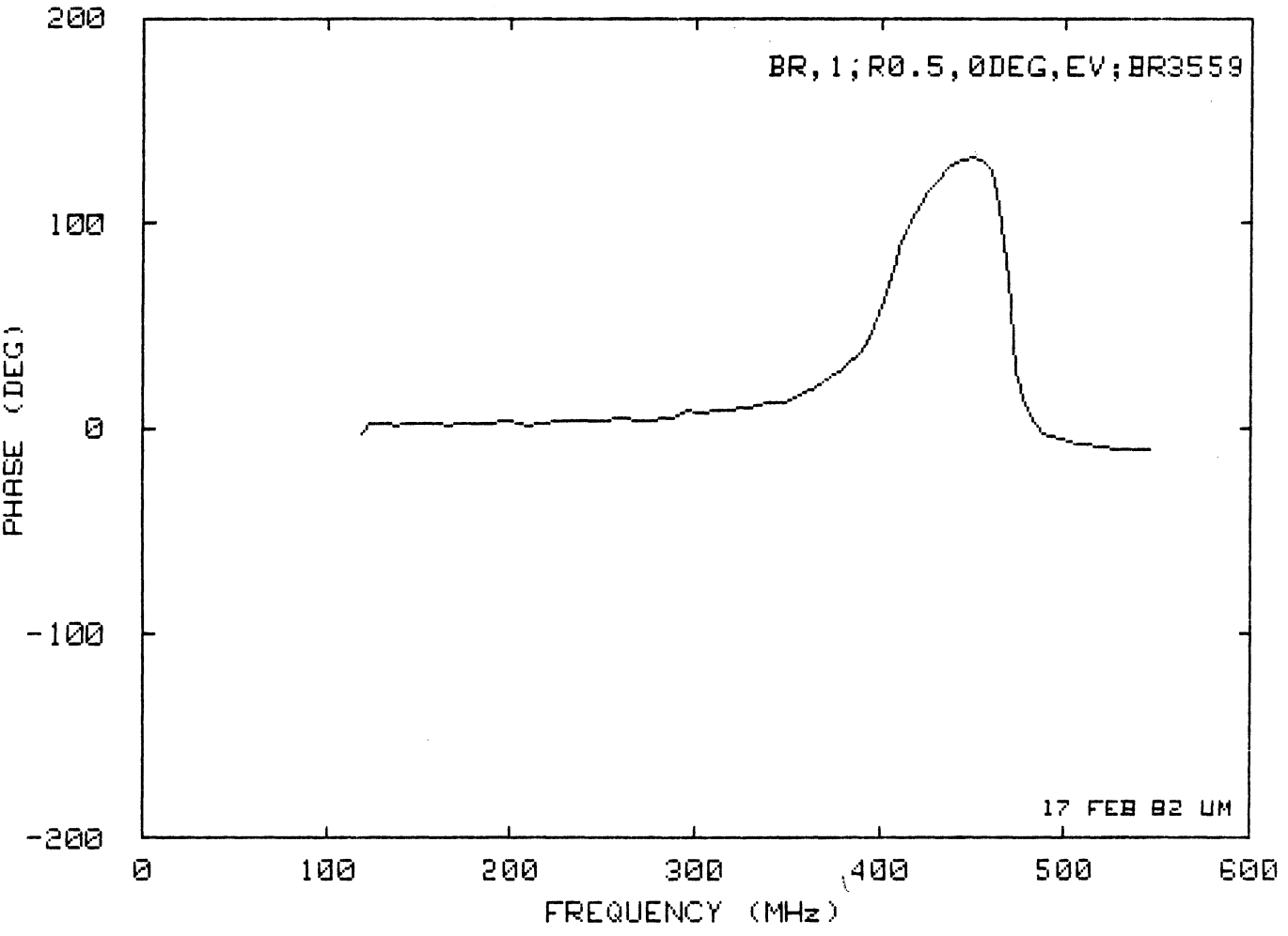
BR,1;R0.5,0DEG,EV;BR3559
17 FEB 82 UM
PHASE (DEG)
200
100
0
-100
-200
0
100
200
300
400
500
600
FREQUENCY (MHz)

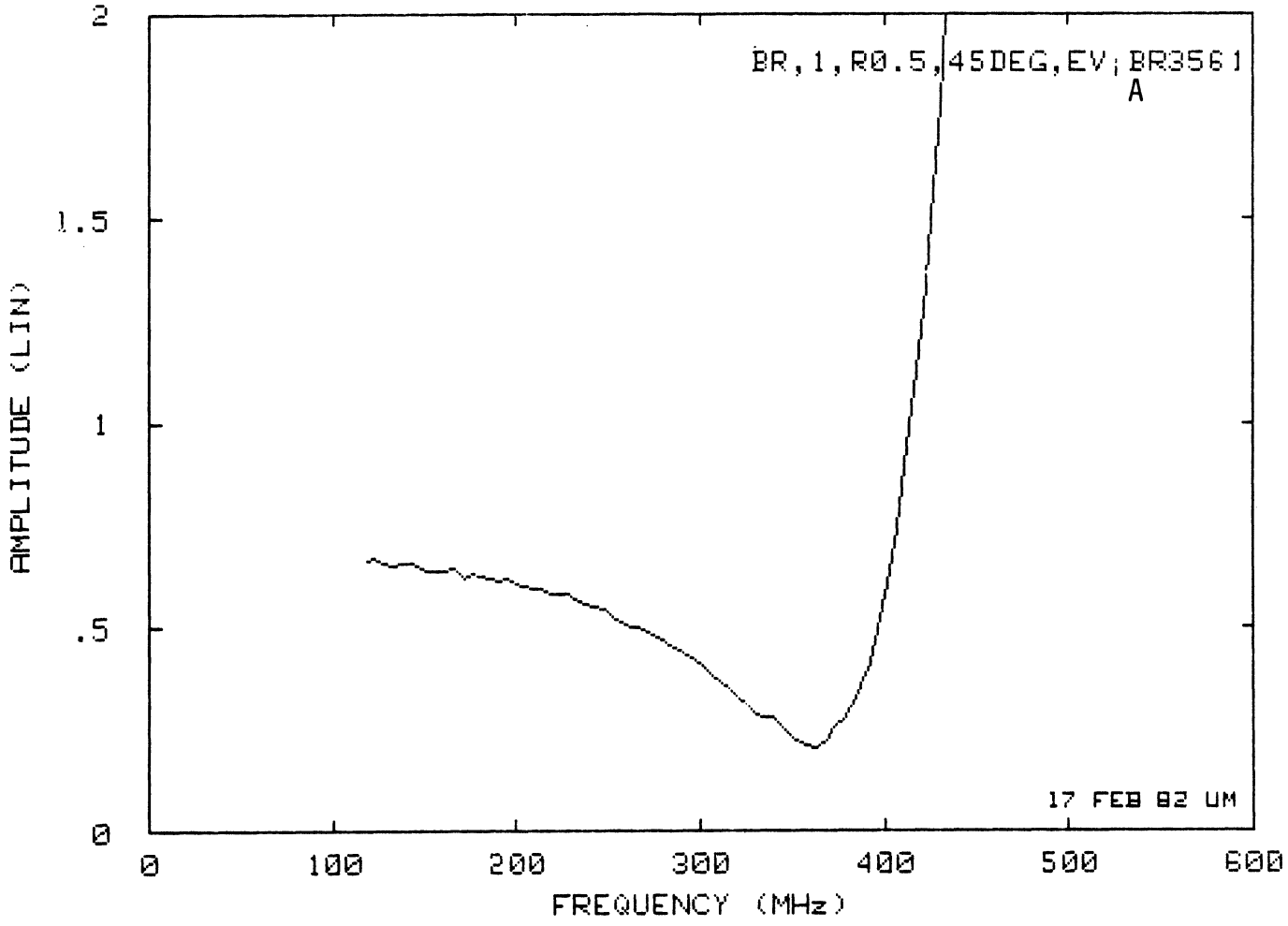
BR,1,R0.5,45DEG,EV;BR3561
A
17 FEB 82 UM
AMPLITUDE (LIN)
2
1.5
1
.5
0
0
100
200
300
400
500
600
FREQUENCY (MHz)

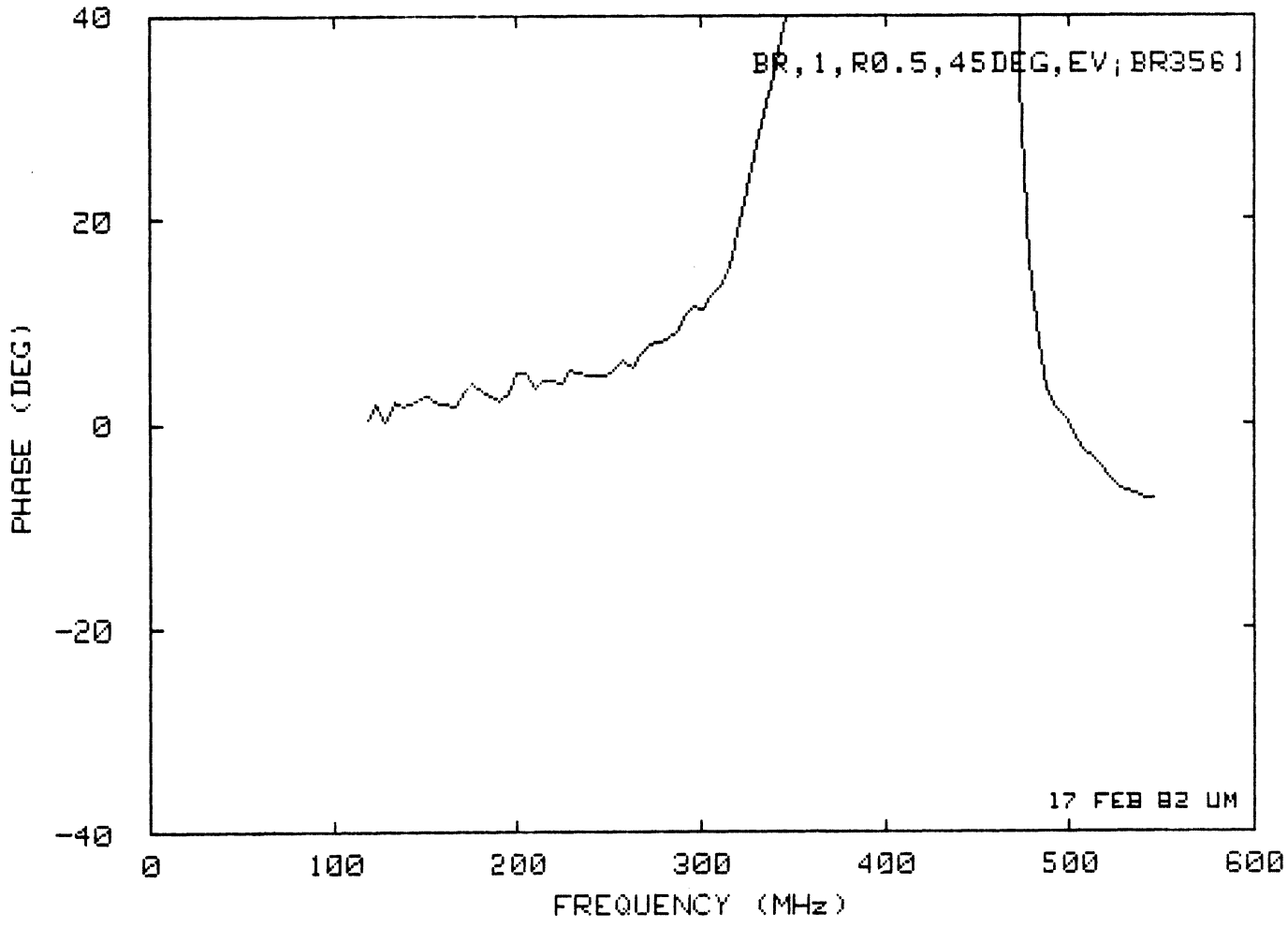
BR,1,R0.5,45DEG,EV;BR3561
17 FEB 82 UM
PHASE (DEG)
40
20
0
-20
-40
0
100
200
300
400
500
600
FREQUENCY (MHz)

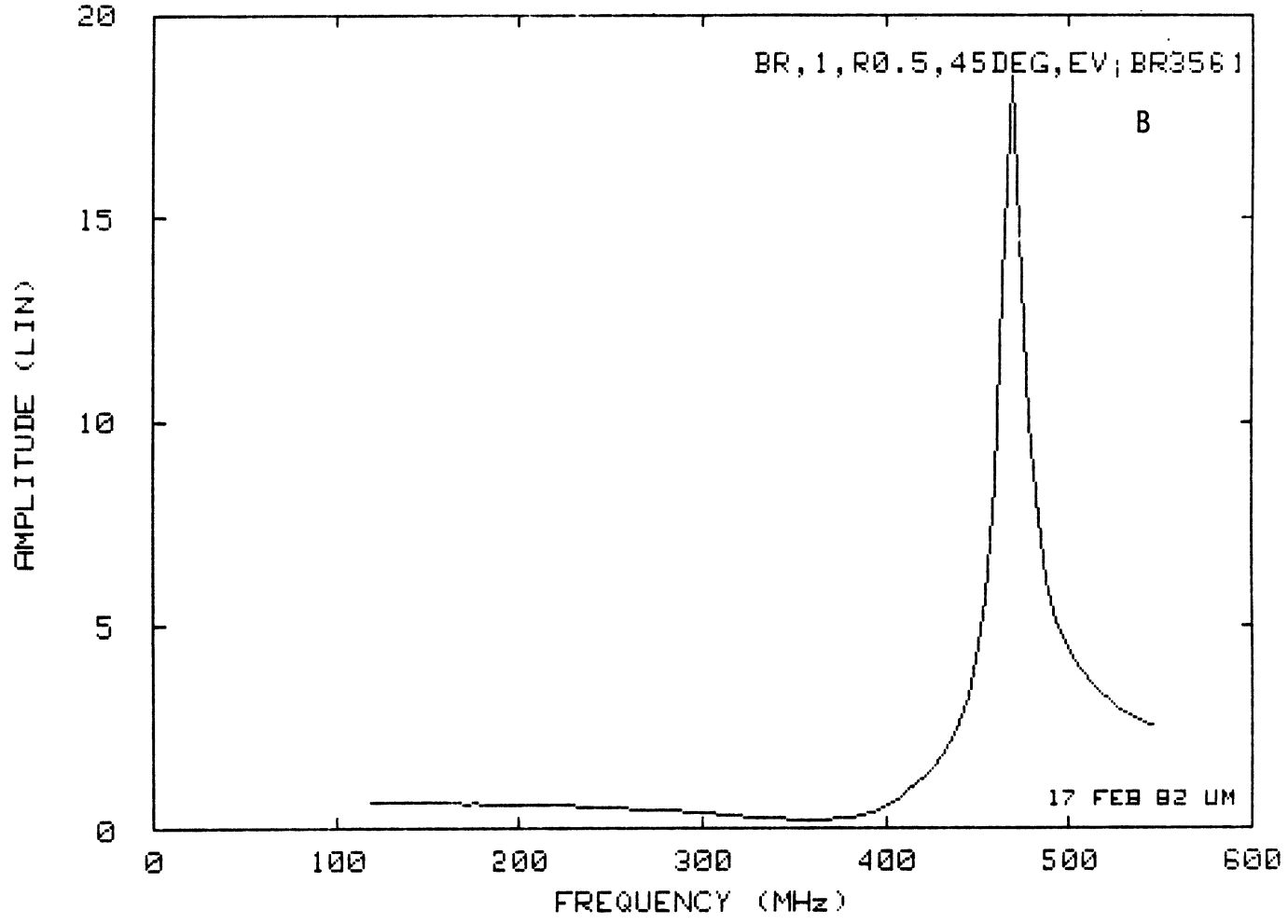
BR,1,R0.5,45DEG,EV;BR3561
B
17 FEB 82 UM
AMPLITUDE (LIN)
20
15
10
5
0
0
100
200
300
400
500
600
FREQUENCY (MHz)

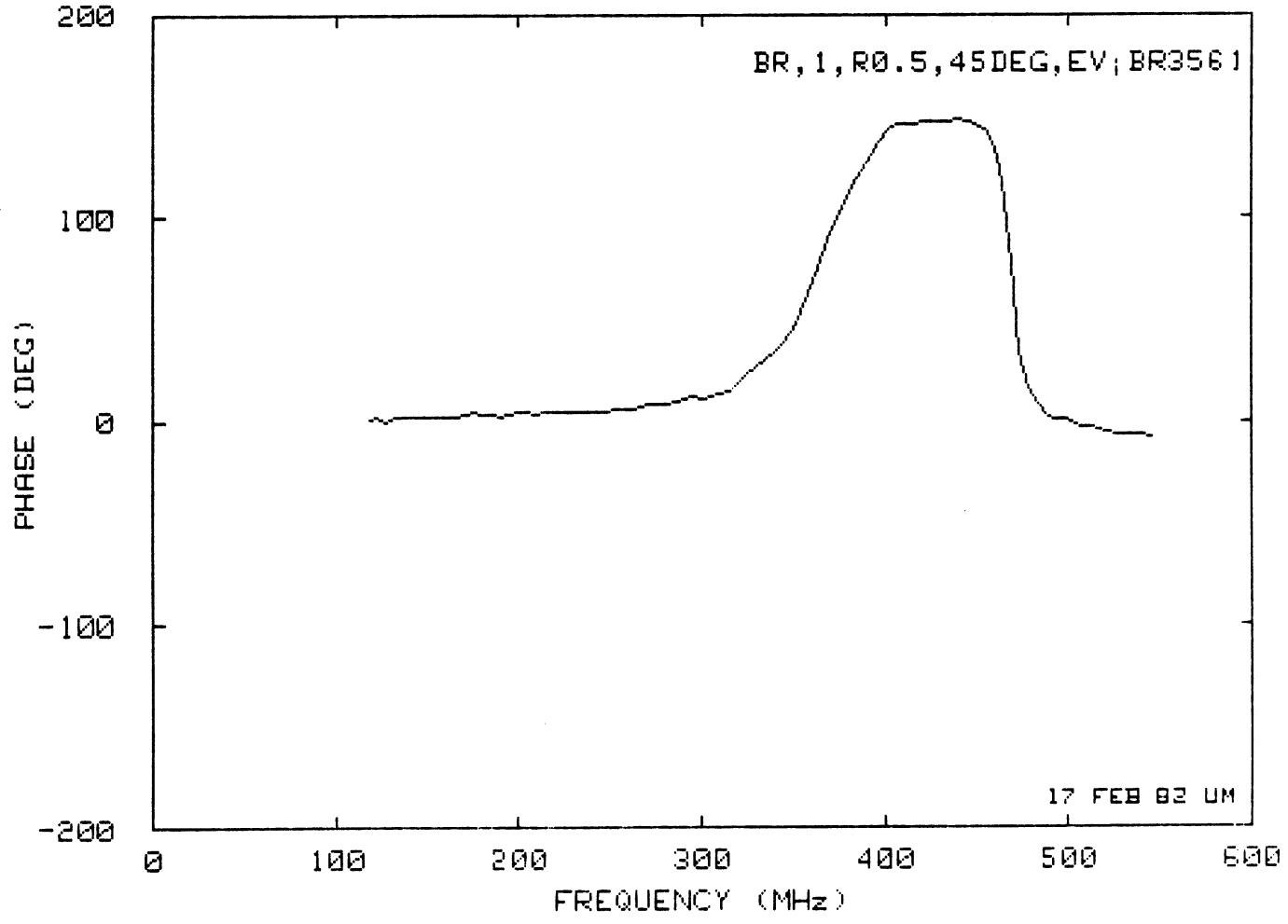
BR,1,R0.5,45DEG,EV;BR3561
17 FEB 82 UM
PHASE (DEG)
200
100
0
-100
-200
0
100
200
300
400
500
600
FREQUENCY (MHz)

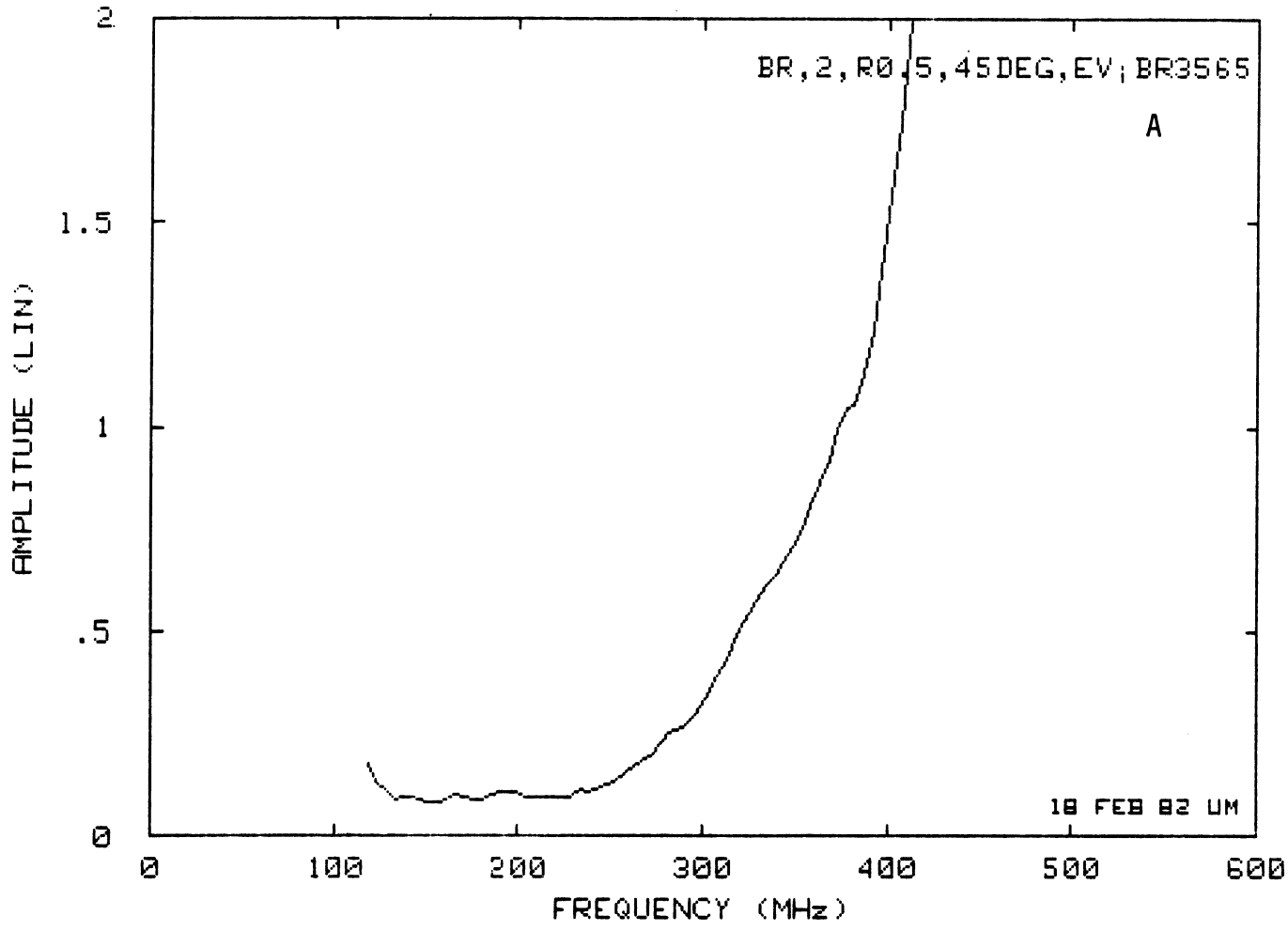
BR,2,R0.5,45DEG,EV;BR3565
A
18 FEB 82 UM
AMPLITUDE (LIN)
2
1.5
1
.5
0
0
100
200
300
400
500
600
FREQUENCY (MHz)

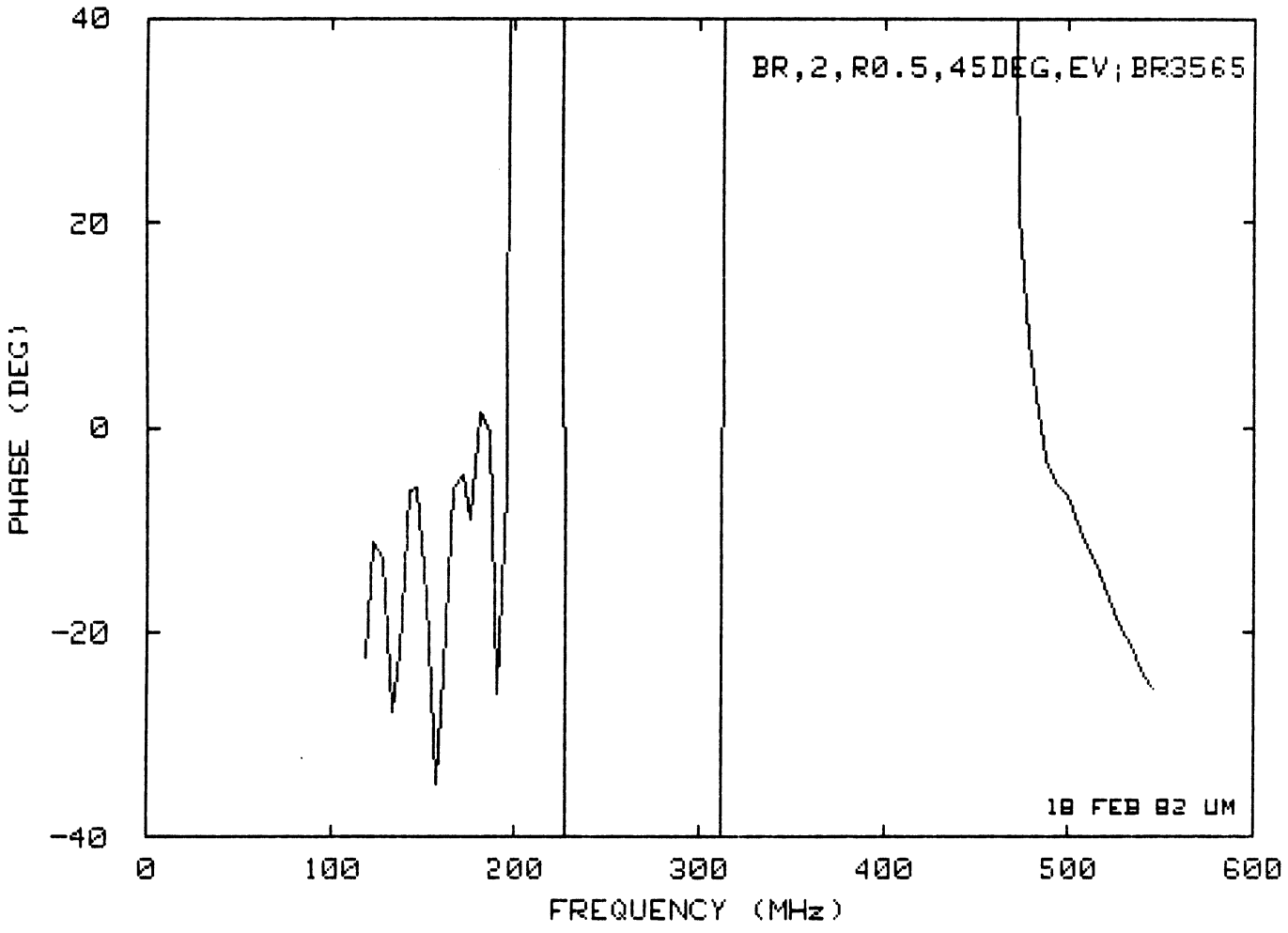
BR,2,R0.5,45DEG,EV;BR3565
18 FEB 82 UM
PHASE (DEG)
40
20
0
-20
-40
0
100
200
300
400
500
600
FREQUENCY (MHz)

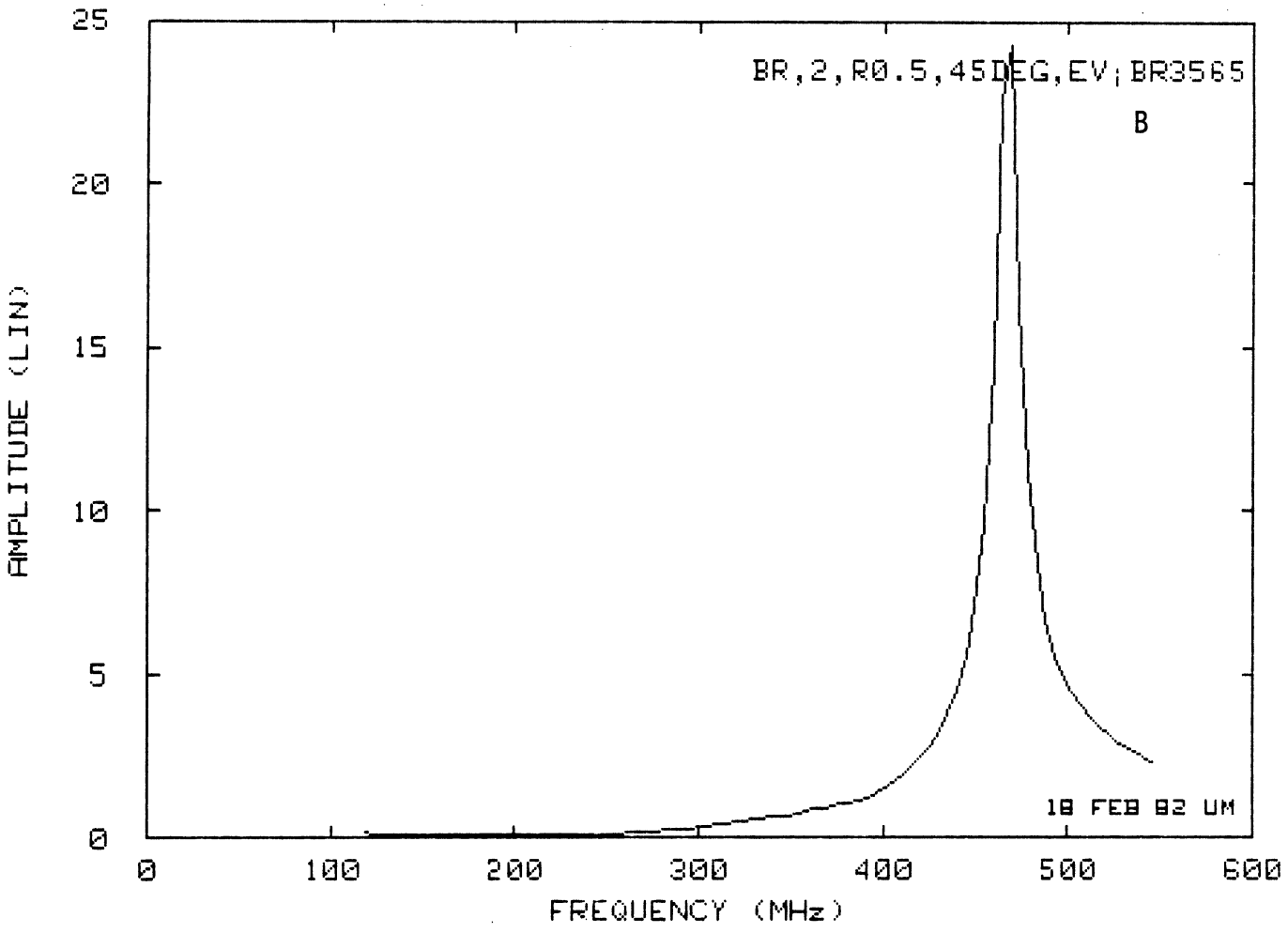
BR,2,R0.5,45DEG,EV;BR3565
B
18 FEB 82 UM
AMPLITUDE (LIN)
25
20
15
10
5
0
0
100
200
300
400
500
600
FREQUENCY (MHz)

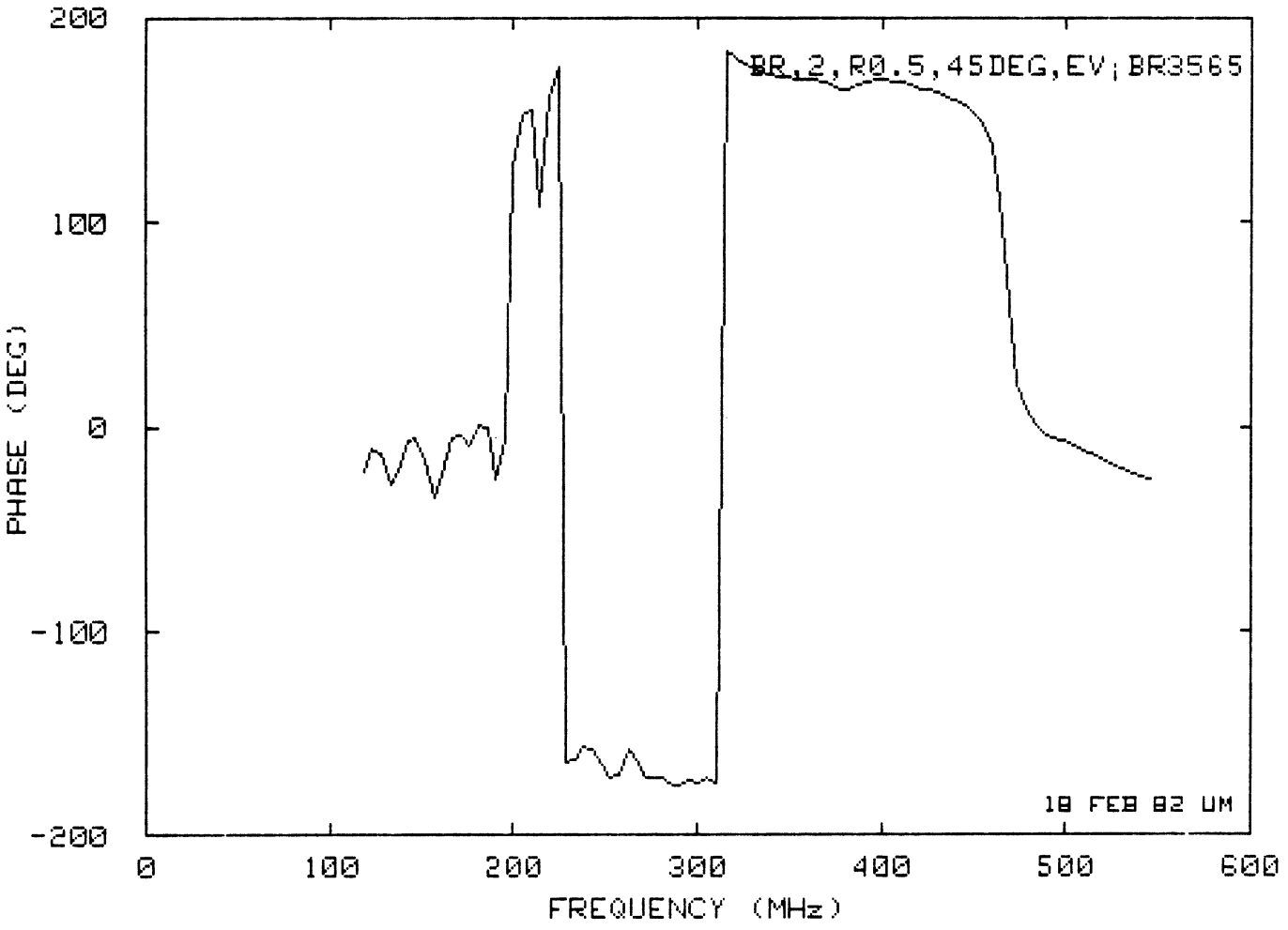
BR,2,R0.5,45DEG,EV;BR3565
18 FEB 82 UM
PHASE (DEG)
200
100
0
-100
-200
0
100
200
300
400
500
600
FREQUENCY (MHz)

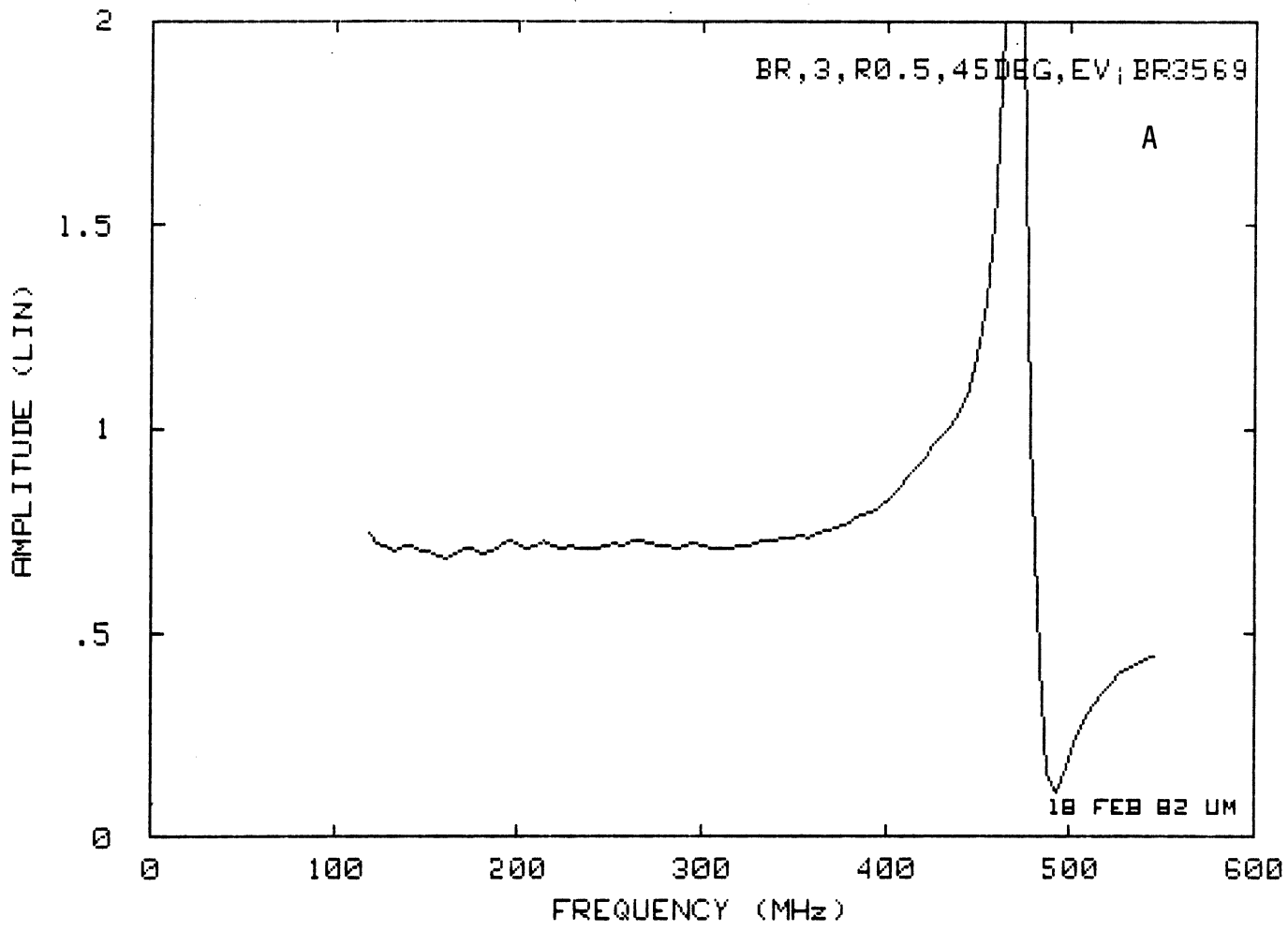
BR,3,R0.5,45DEG,EV;BR3569
A
18 FEB 82 UM
AMPLITUDE (LIN)
2
1.5
1
.5
0
0
100
200
300
400
500
600
FREQUENCY (MHz)

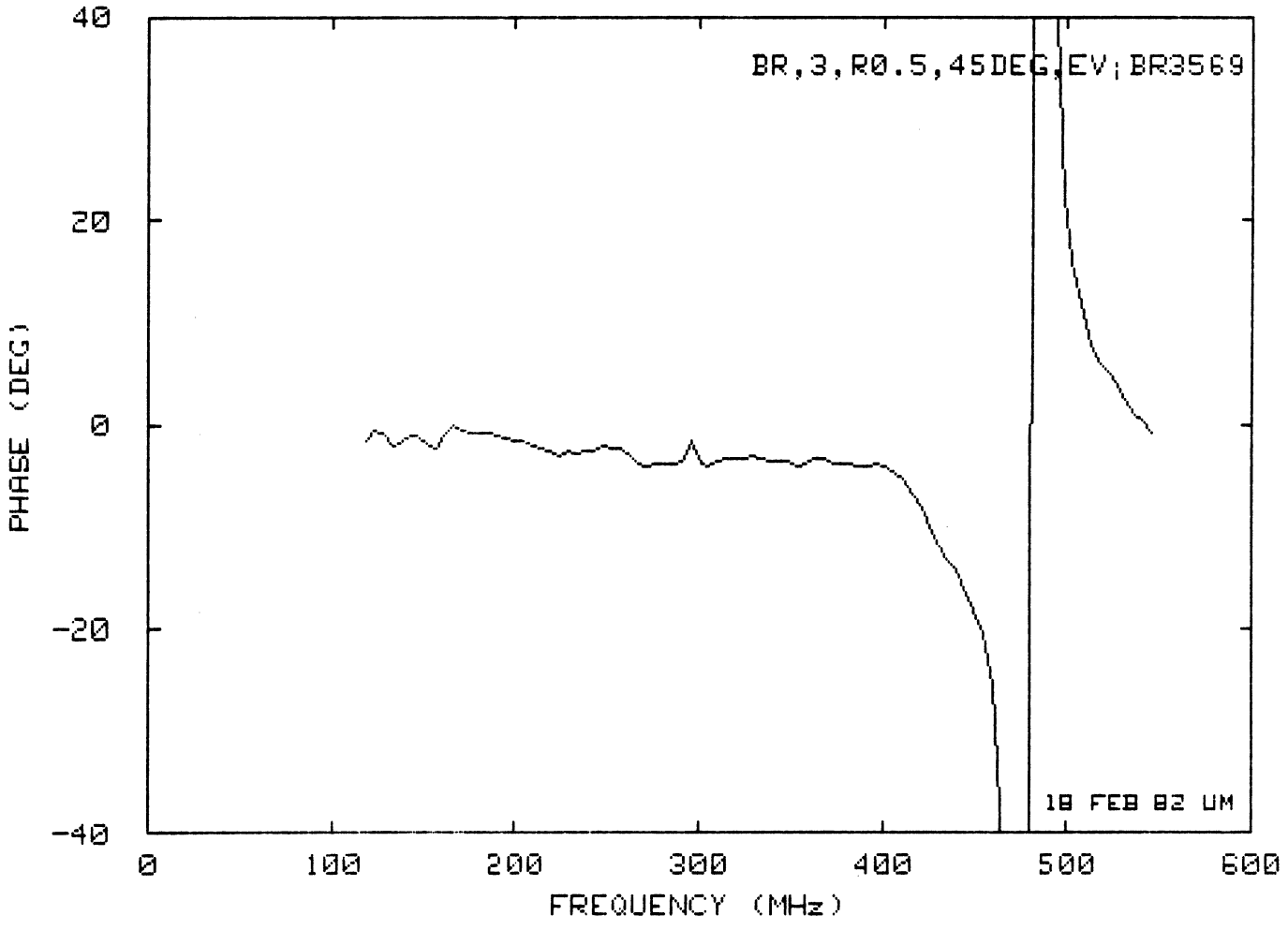
BR,3,R0.5,45DEG,EV;BR3569
18 FEB 82 UM
PHASE (DEG)
40
20
0
-20
-40
0
100
200
300
400
500
600
FREQUENCY (MHz)

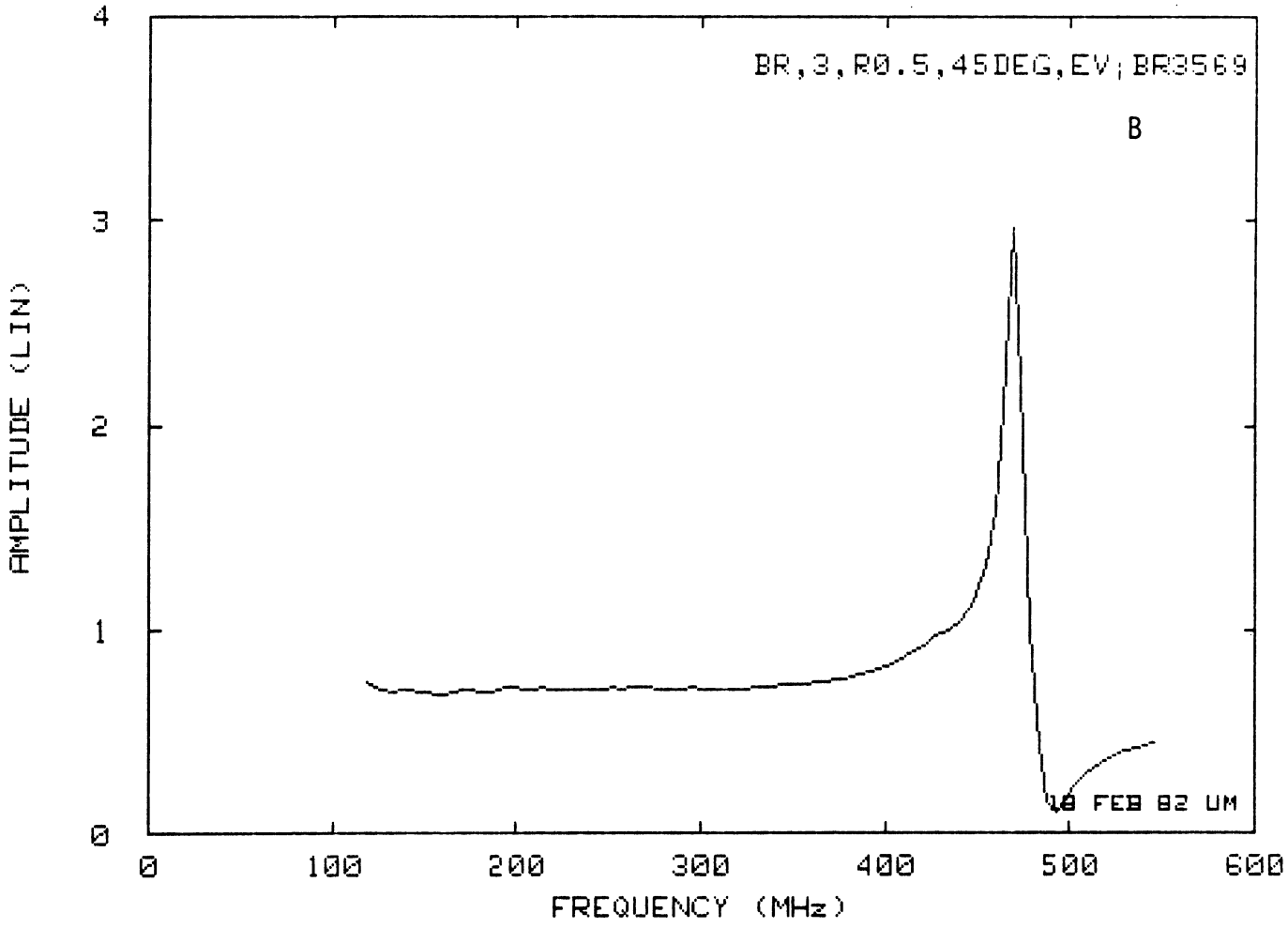
BR,3,R0.5,45DEG,EV;BR3569
B
18 FEB 82 UM
AMPLITUDE (LIN)
FREQUENCY (MHz)
0
1
2
3
4
0
100
200
300
400
500
600

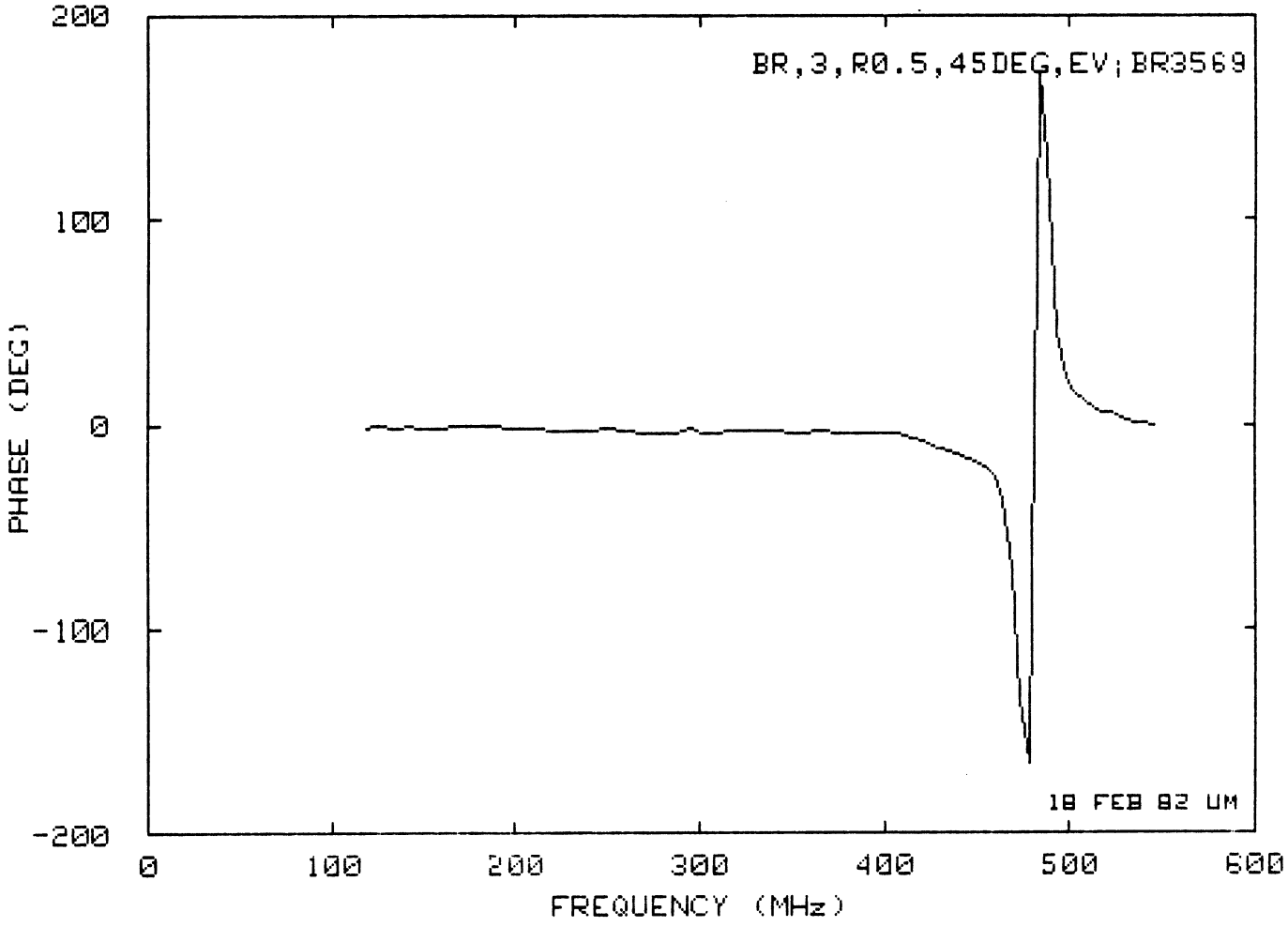
BR,3,R0.5,45DEG,EV;BR3569
18 FEB 82 UM
PHASE (DEG)
FREQUENCY (MHz)
200
100
0
-100
-200
0
100
200
300
400
500
600

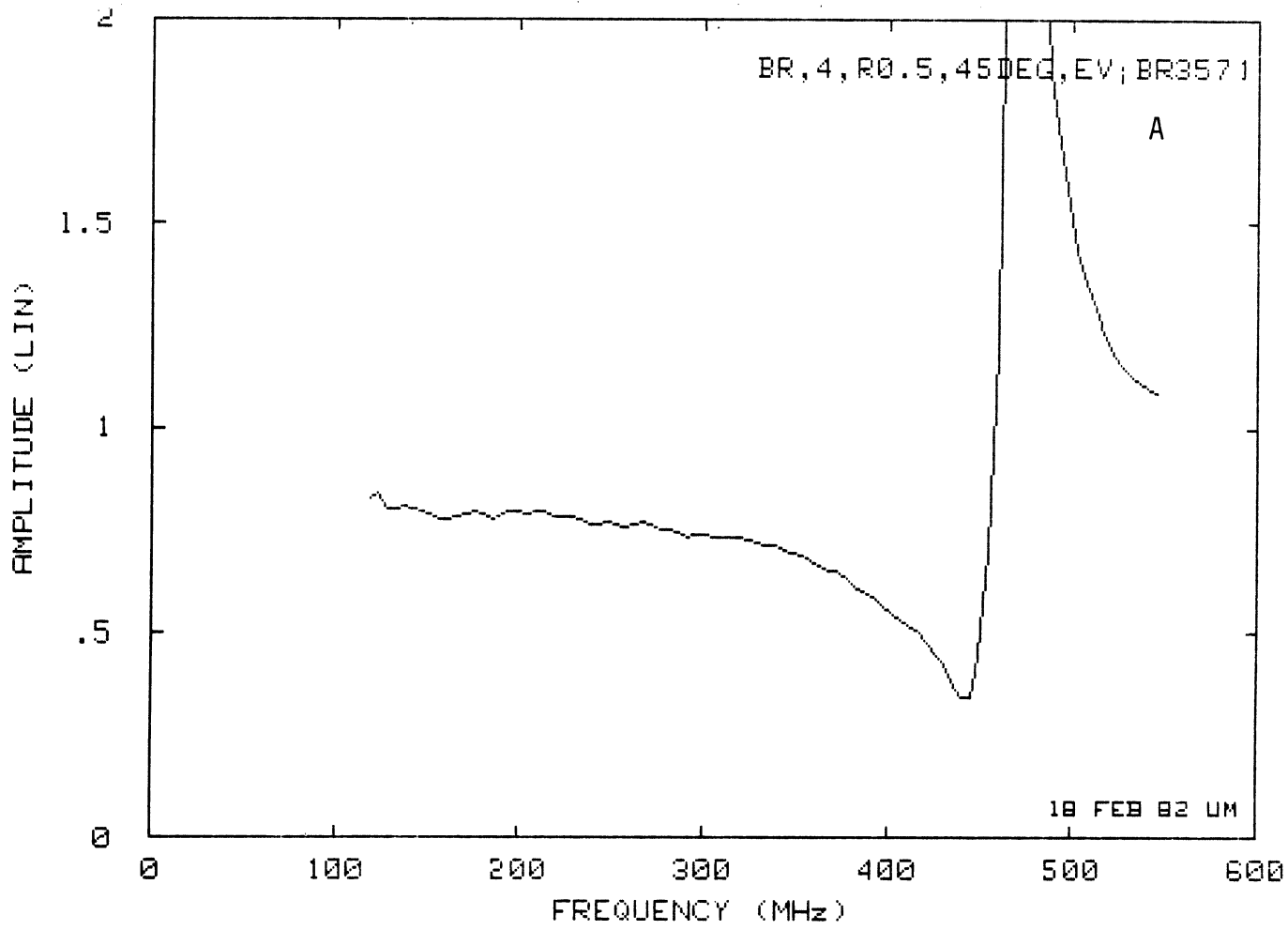
BR,4,R0.5,45DEG,EV;BR3571
A
18 FEB 82 UM
AMPLITUDE (LIN)
2
1.5
1
.5
0
0
100
200
300
400
500
600
FREQUENCY (MHz)

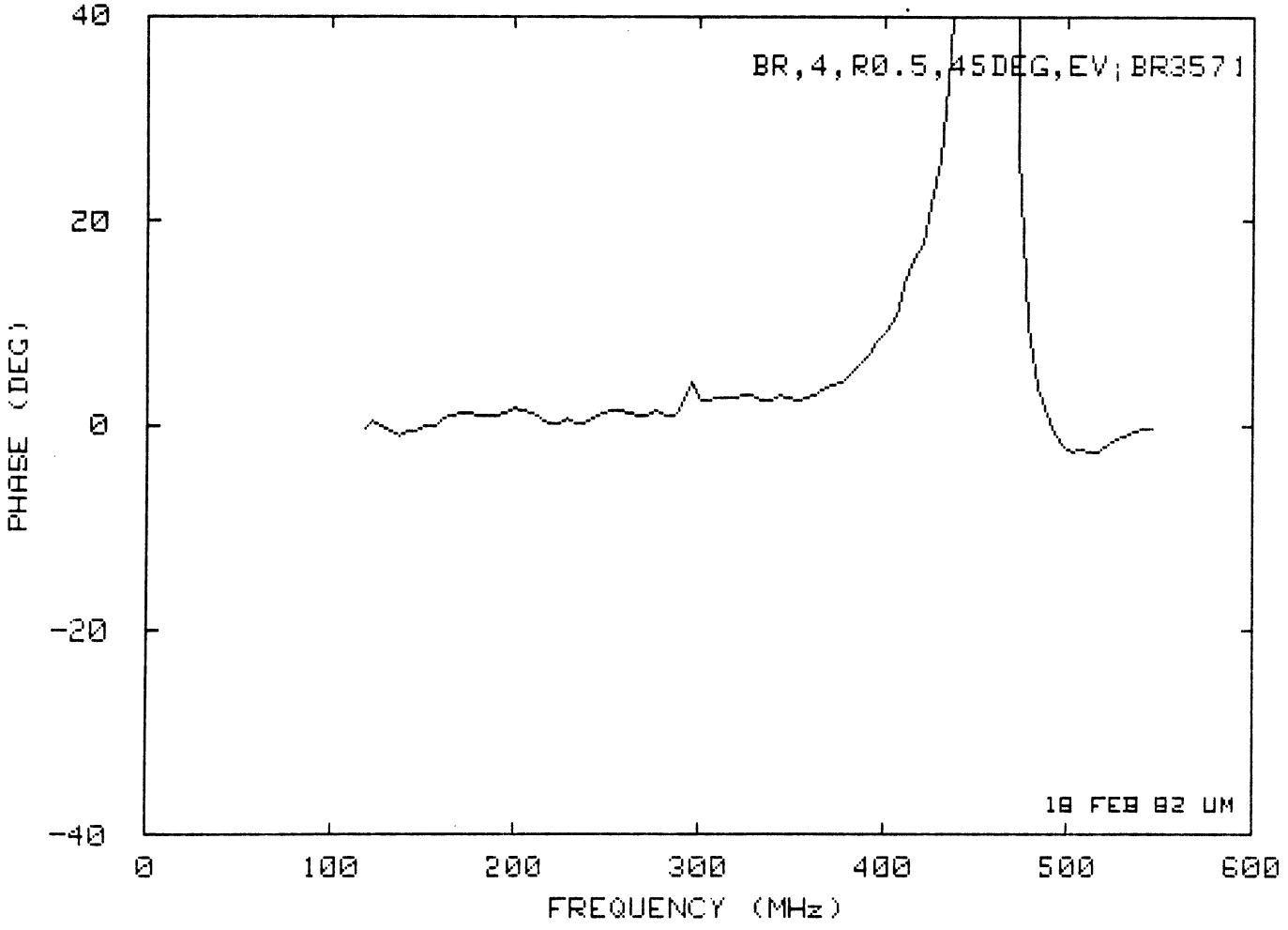
BR,4,R0.5,45DEG,EV;BR3571
18 FEB 82 UM
PHASE (DEG)
40
20
0
-20
-40
0
100
200
300
400
500
600
FREQUENCY (MHz)

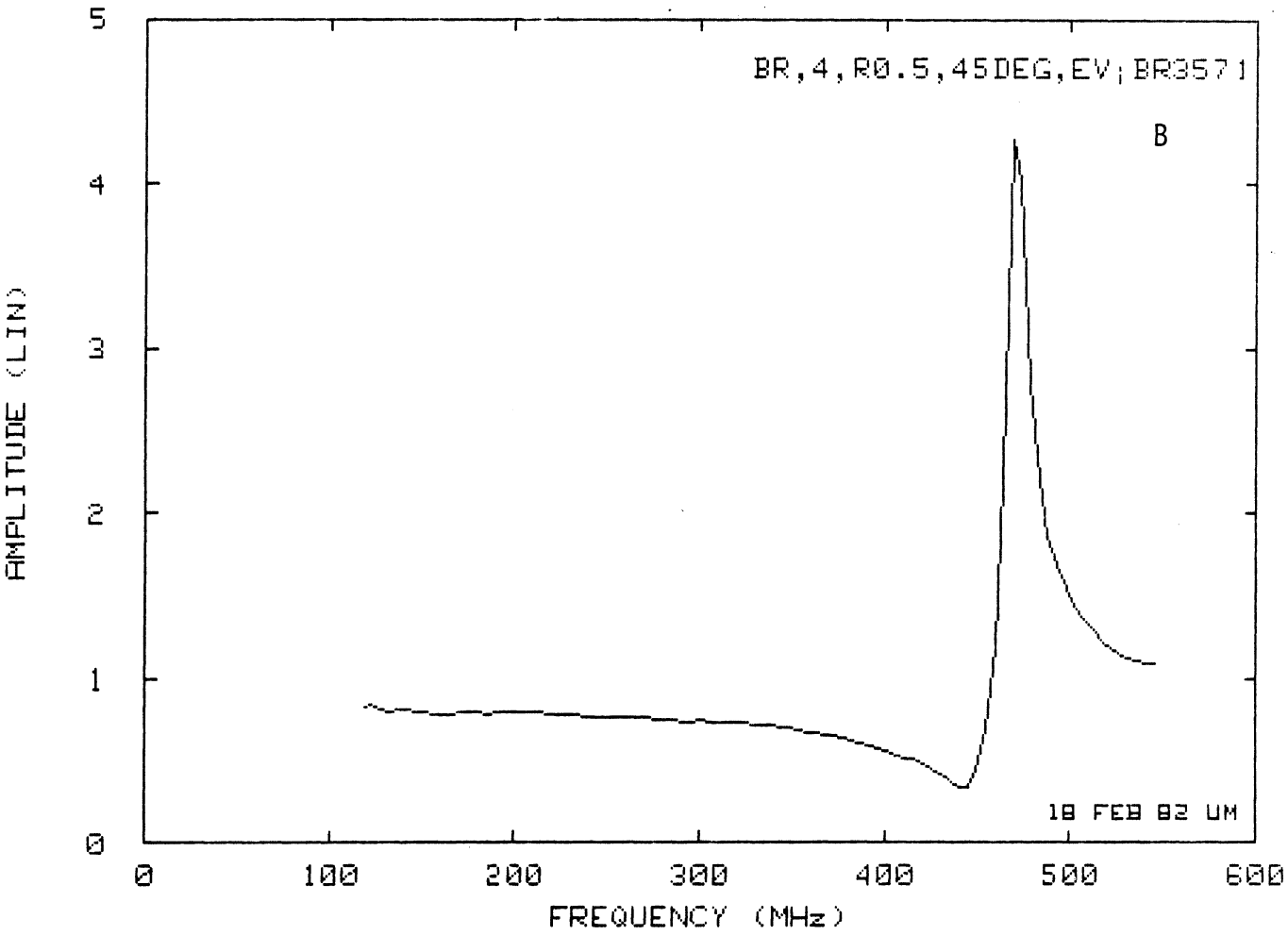
BR,4,R0.5,45DEG,EV;BR3571
B
18 FEB 82 UM
AMPLITUDE (LIN)
0
1
2
3
4
5
0
100
200
300
400
500
600
FREQUENCY (MHz)

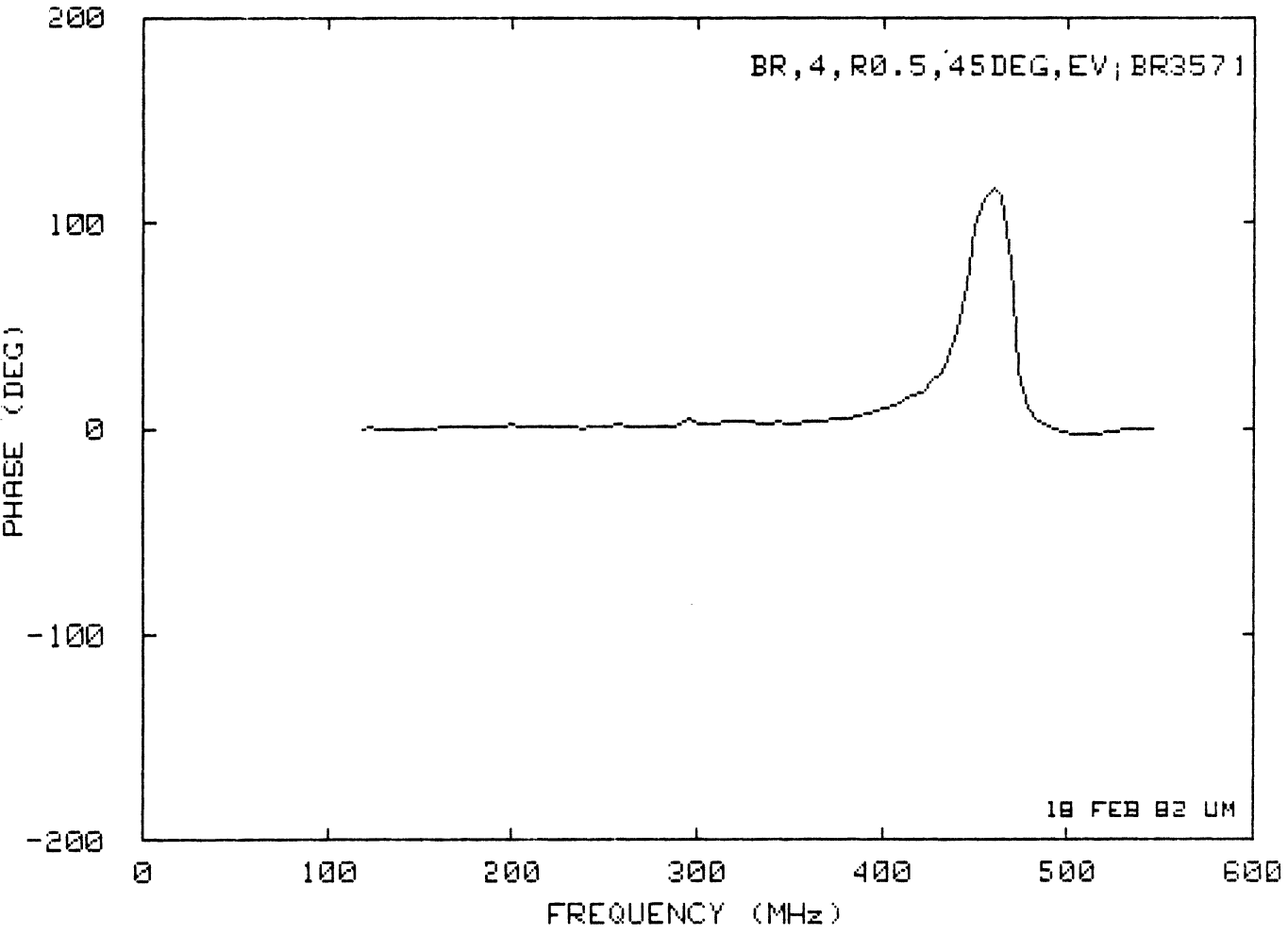
BR,4,R0.5,45DEG,EV;BR3571
18 FEB 82 UM
PHASE (DEG)
200
100
0
-100
-200
0
100
200
300
400
500
600
FREQUENCY (MHz)

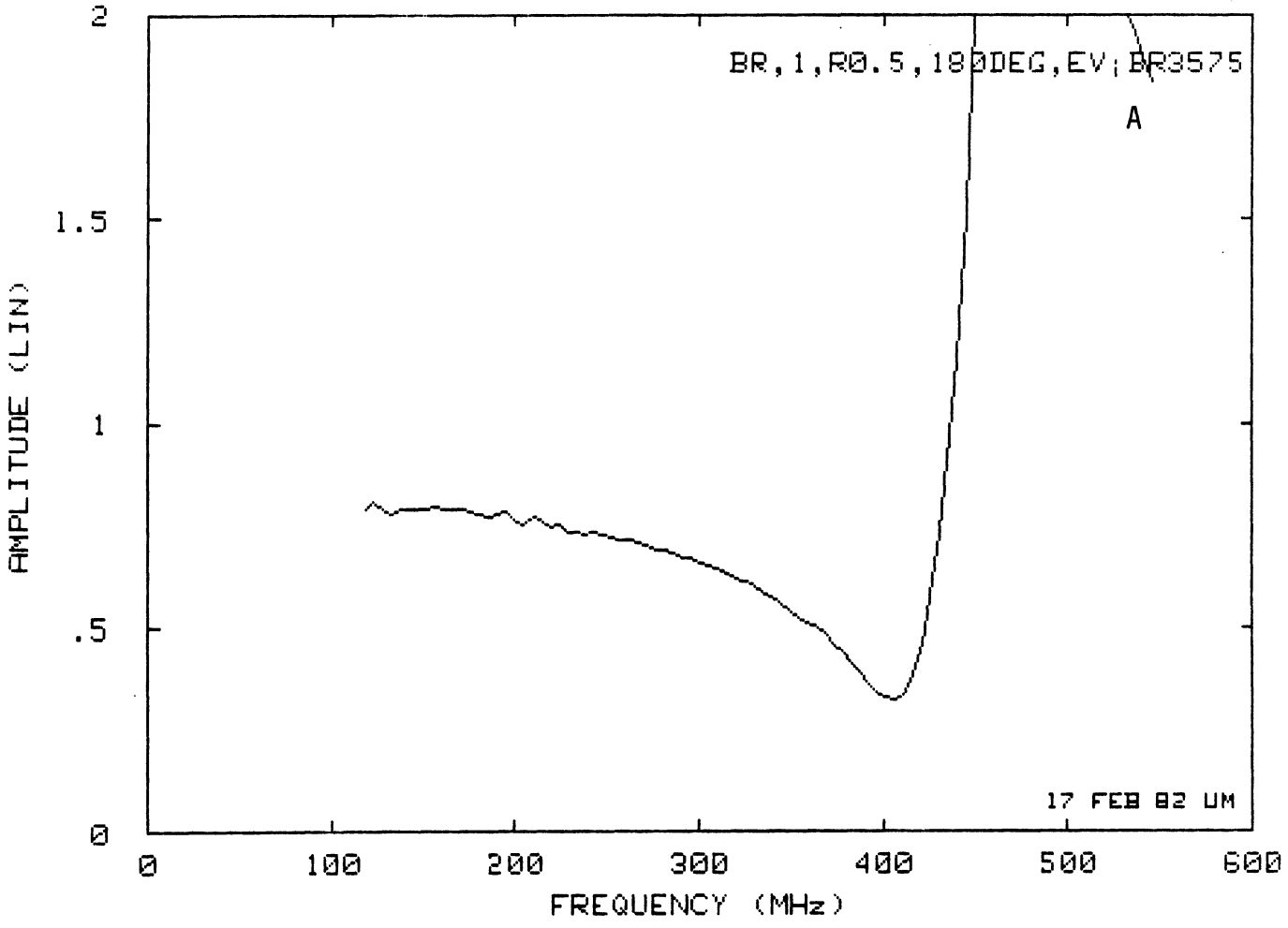
BR,1,R0.5,180DEG,EV;BR3575
A
17 FEB 82 UM
AMPLITUDE (LIN)
2
1.5
1
.5
0
0
100
200
300
400
500
600
FREQUENCY (MHz)

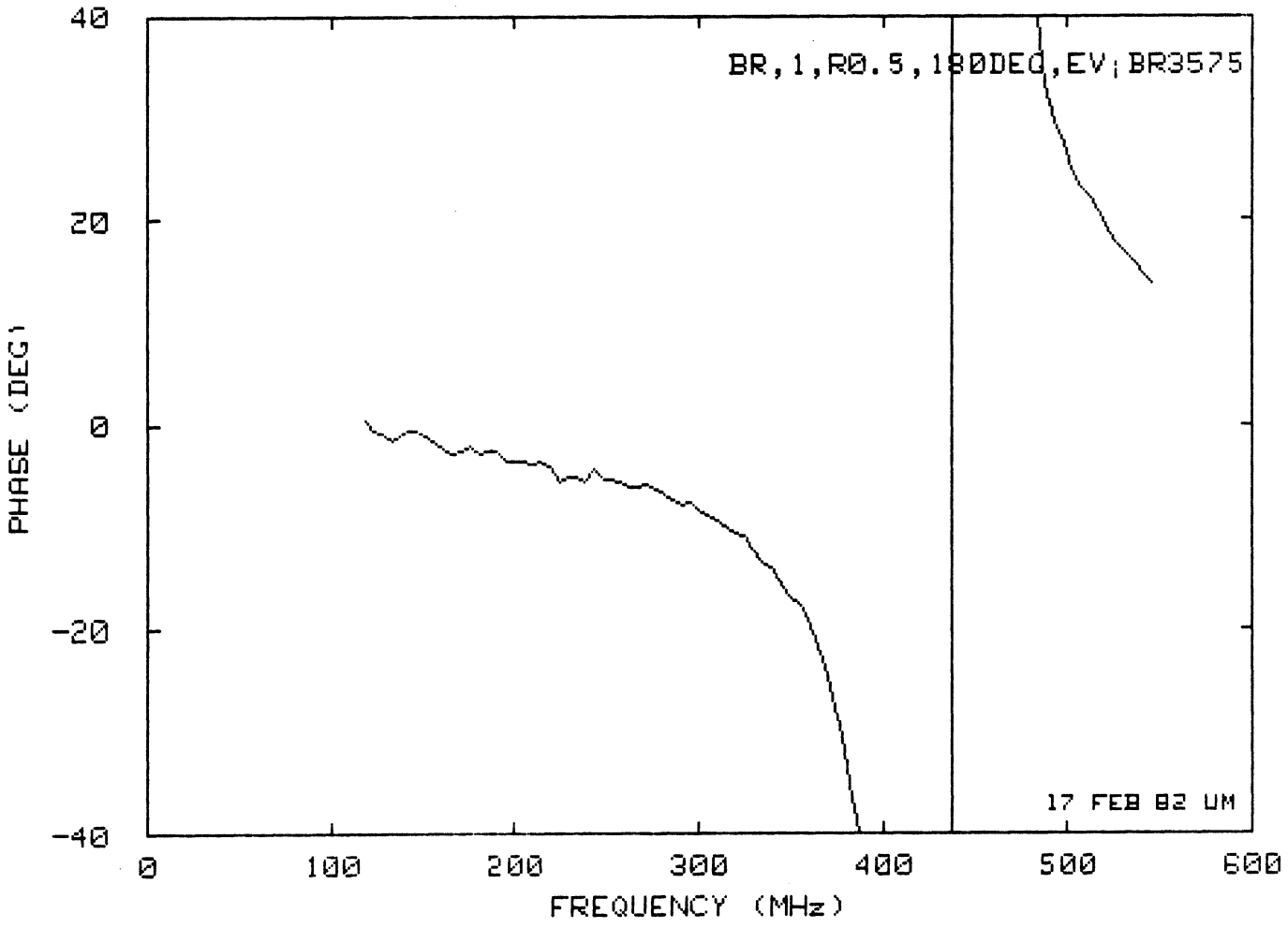
BR,1,R0.5,180DEG,EV;BR3575
17 FEB 82 UM
PHASE (DEG)
40
20
0
-20
-40
0
100
200
300
400
500
600
FREQUENCY (MHz)

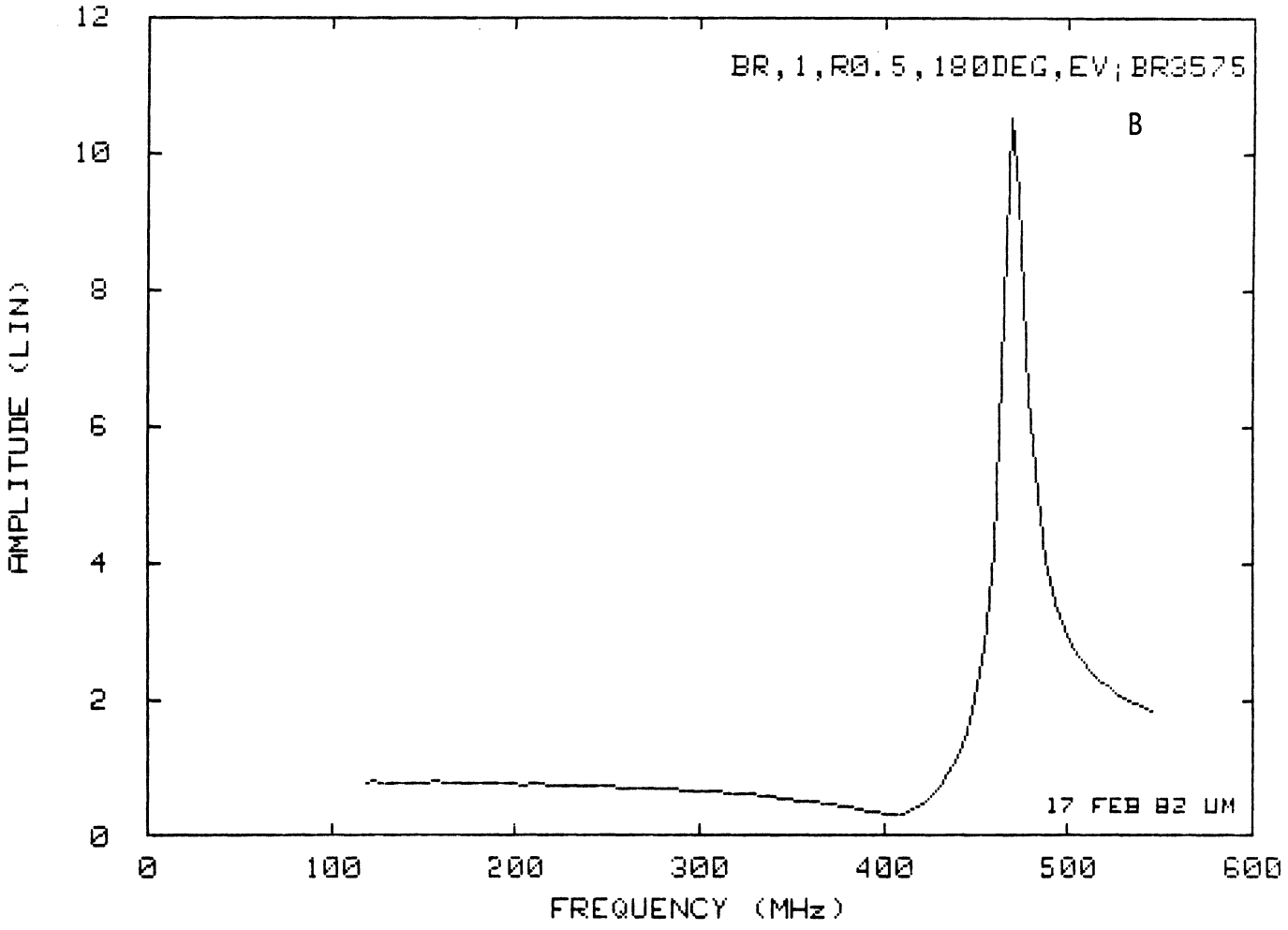
BR,1,R0.5,180DEG,EV;BR3575
B
17 FEB 82 UM
AMPLITUDE (LIN)
12
10
8
6
4
2
0
0
100
200
300
400
500
600
FREQUENCY (MHz)

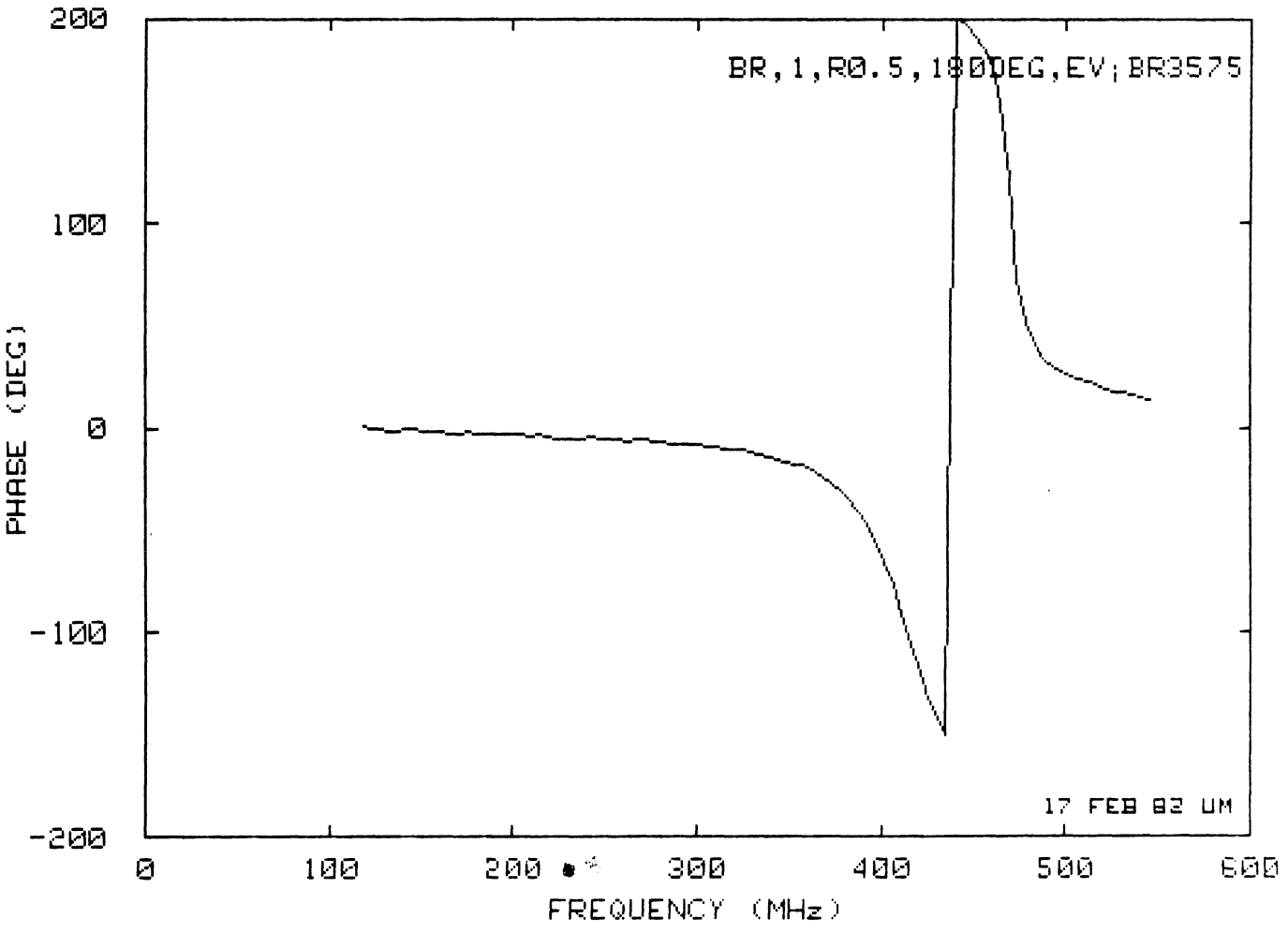
BR,1,R0.5,180DEG,EV;BR3575
17 FEB 82 UM
PHASE (DEG)
200
100
0
-100
-200
0
100
200
300
400
500
600
FREQUENCY (MHz)

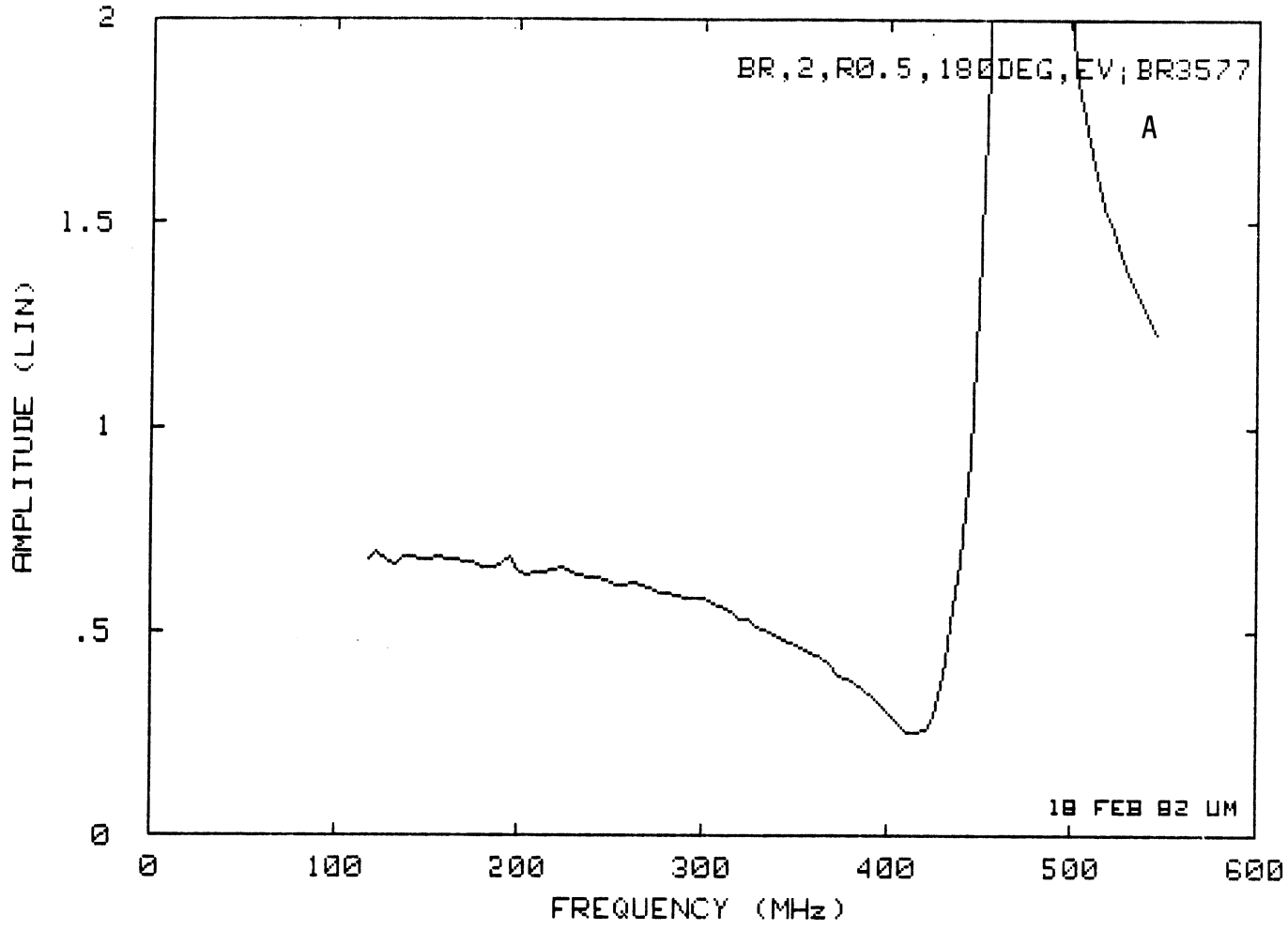
BR,2,R0.5,180DEG,EV;BR3577
A
18 FEB 82 UM
AMPLITUDE (LIN)
2
1.5
1
.5
0
0
100
200
300
400
500
600
FREQUENCY (MHz)

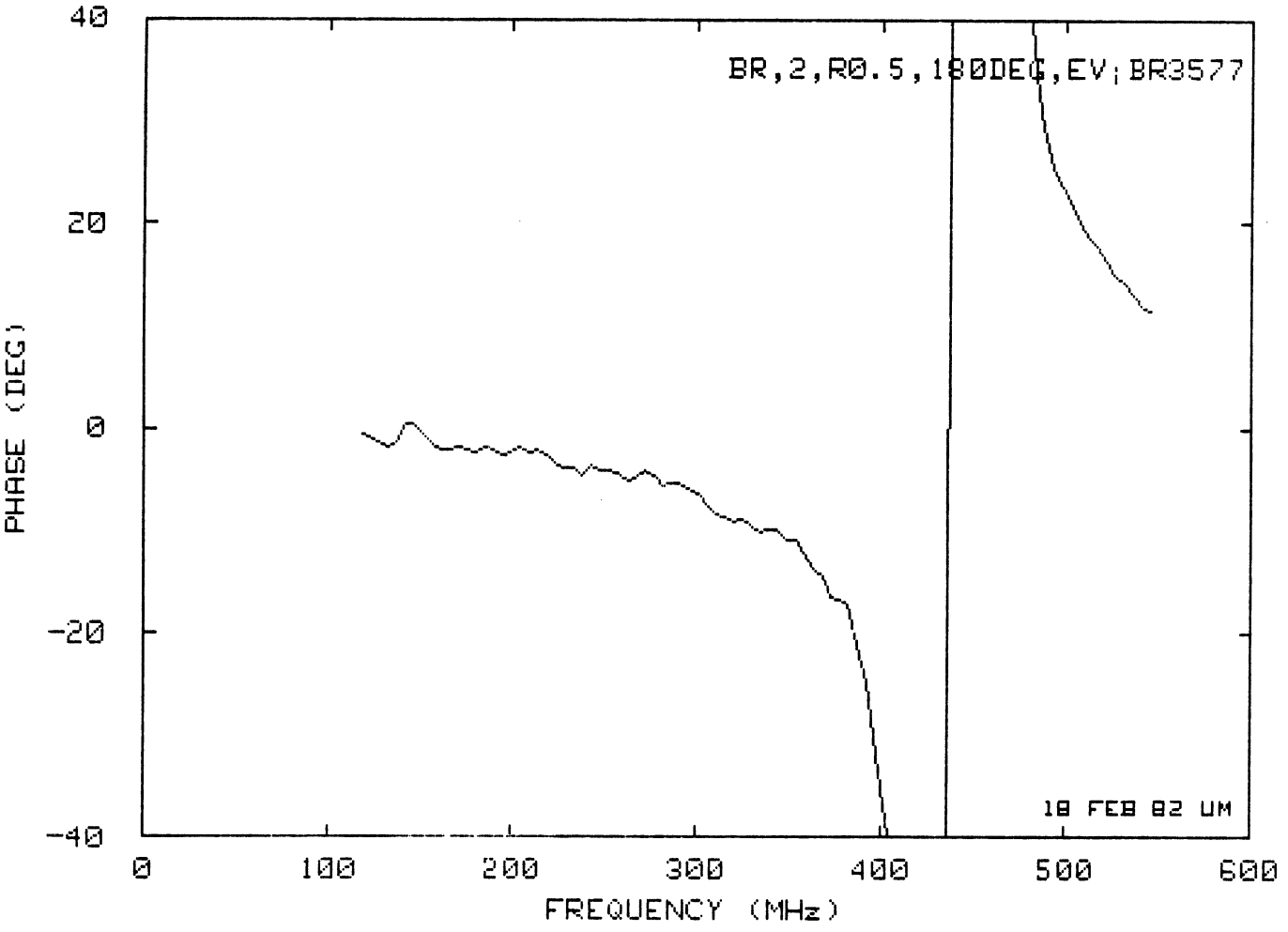
BR,2,R0.5,180DEG,EV;BR3577
18 FEB 82 UM
PHASE (DEG)
40
20
0
-20
-40
0
100
200
300
400
500
600
FREQUENCY (MHz)

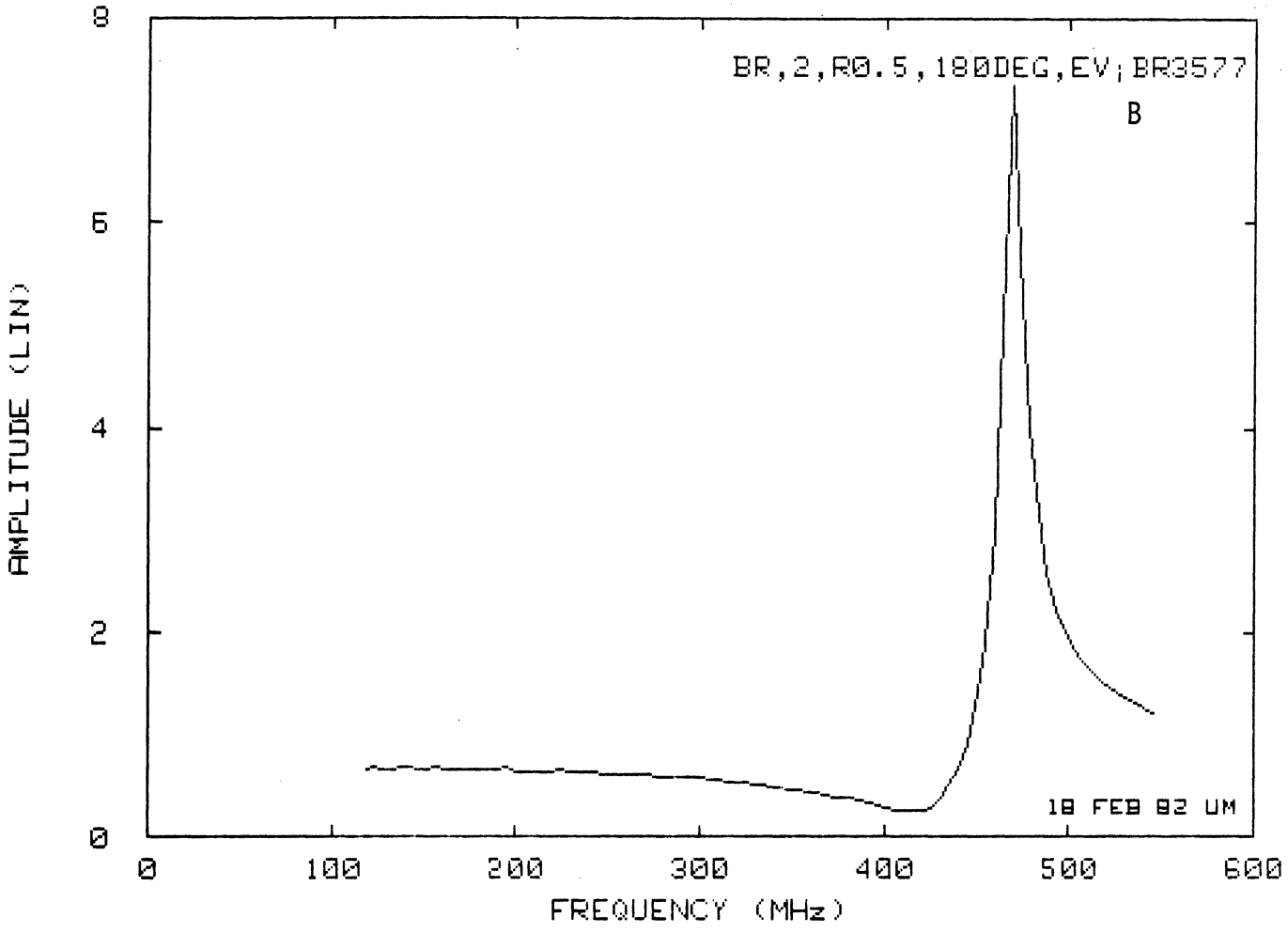
BR,2,R0.5,180DEG,EV;BR3577
B
18 FEB 82 UM
AMPLITUDE (LIN)
0
2
4
6
8
0
100
200
300
400
500
600
FREQUENCY (MHz)

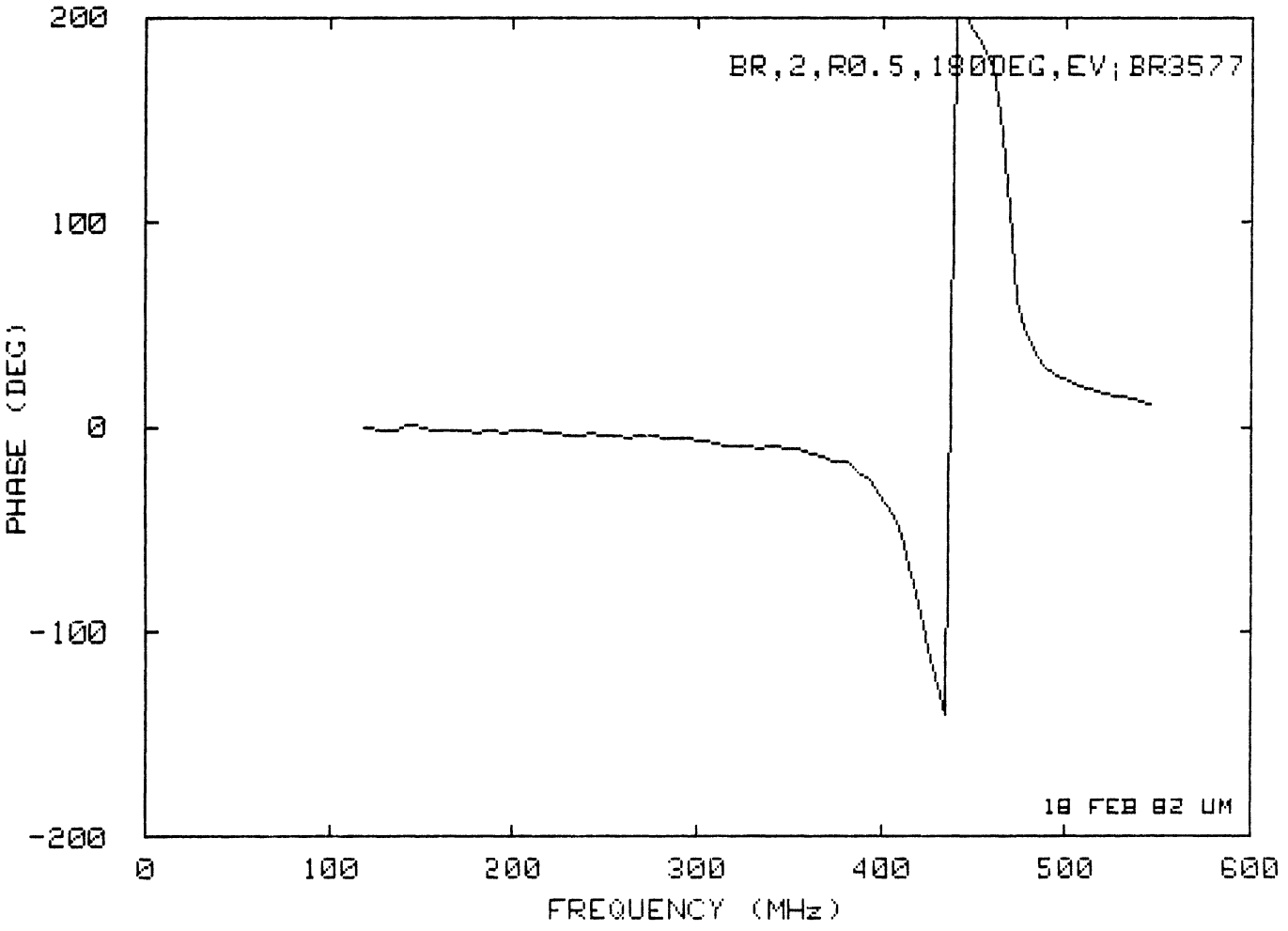
BR,2,R0.5,180DEG,EV;BR3577
18 FEB 82 UM
PHASE (DEG)
200
100
0
-100
-200
0
100
200
300
400
500
600
FREQUENCY (MHz)

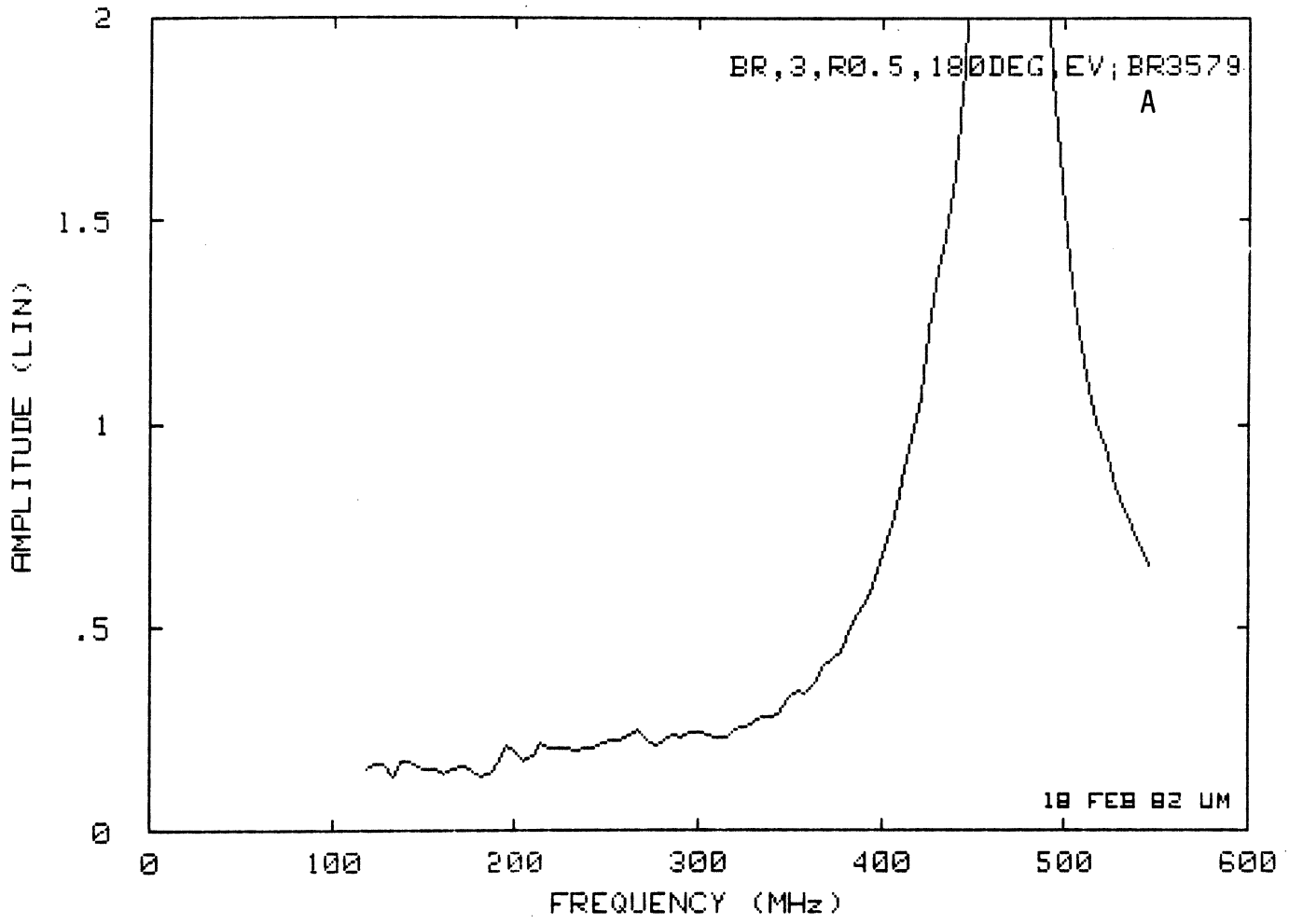
BR,3,R0.5,180DEG,EV;BR3579
A
18 FEB 82 UM
AMPLITUDE (LIN)
2
1.5
1
.5
0
0
100
200
300
400
500
600
FREQUENCY (MHz)

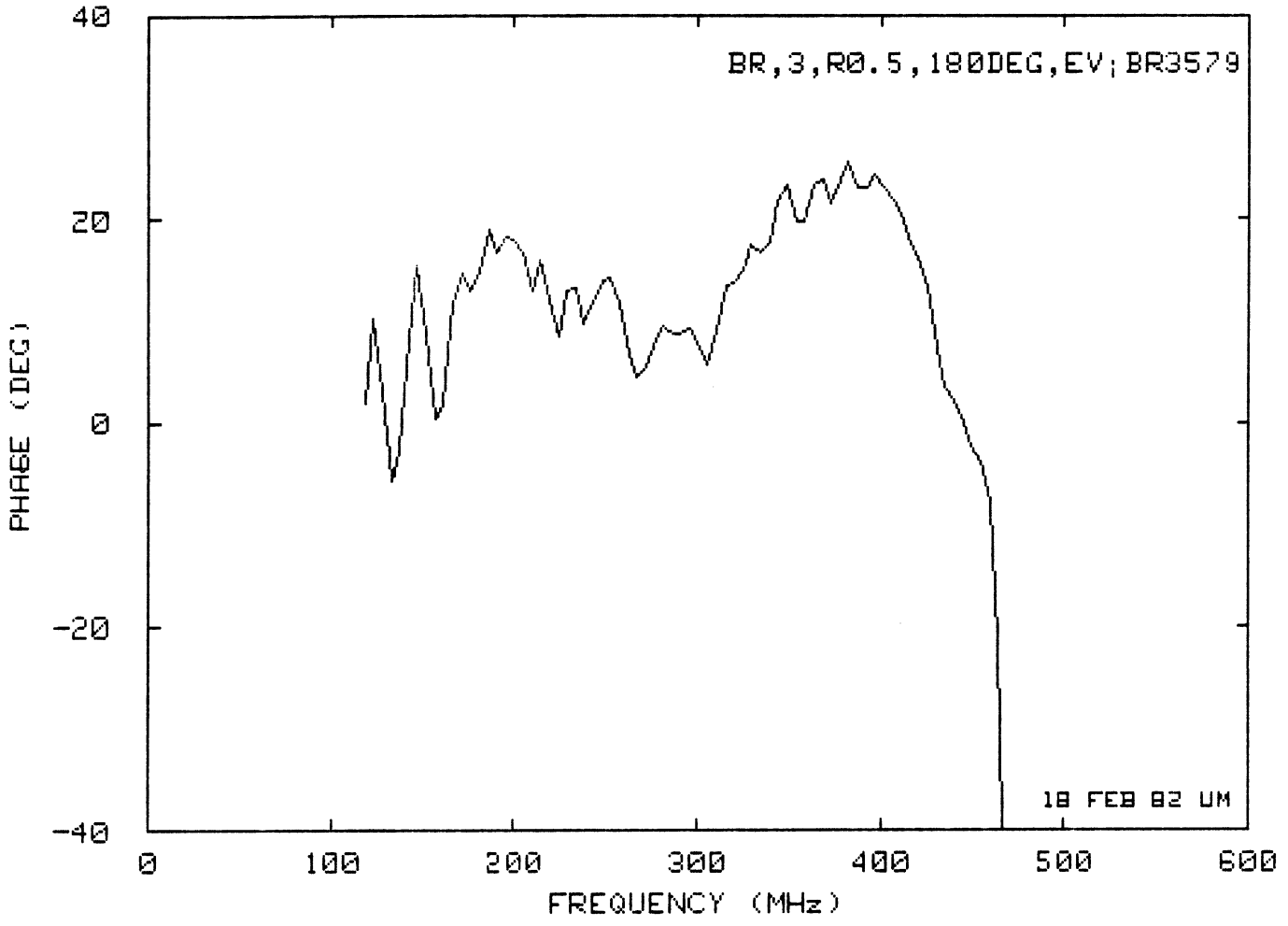
BR,3,R0.5,180DEG,EV;BR3579
18 FEB 82 UM
PHASE (DEG)
40
20
0
-20
-40
0
100
200
300
400
500
600
FREQUENCY (MHz)

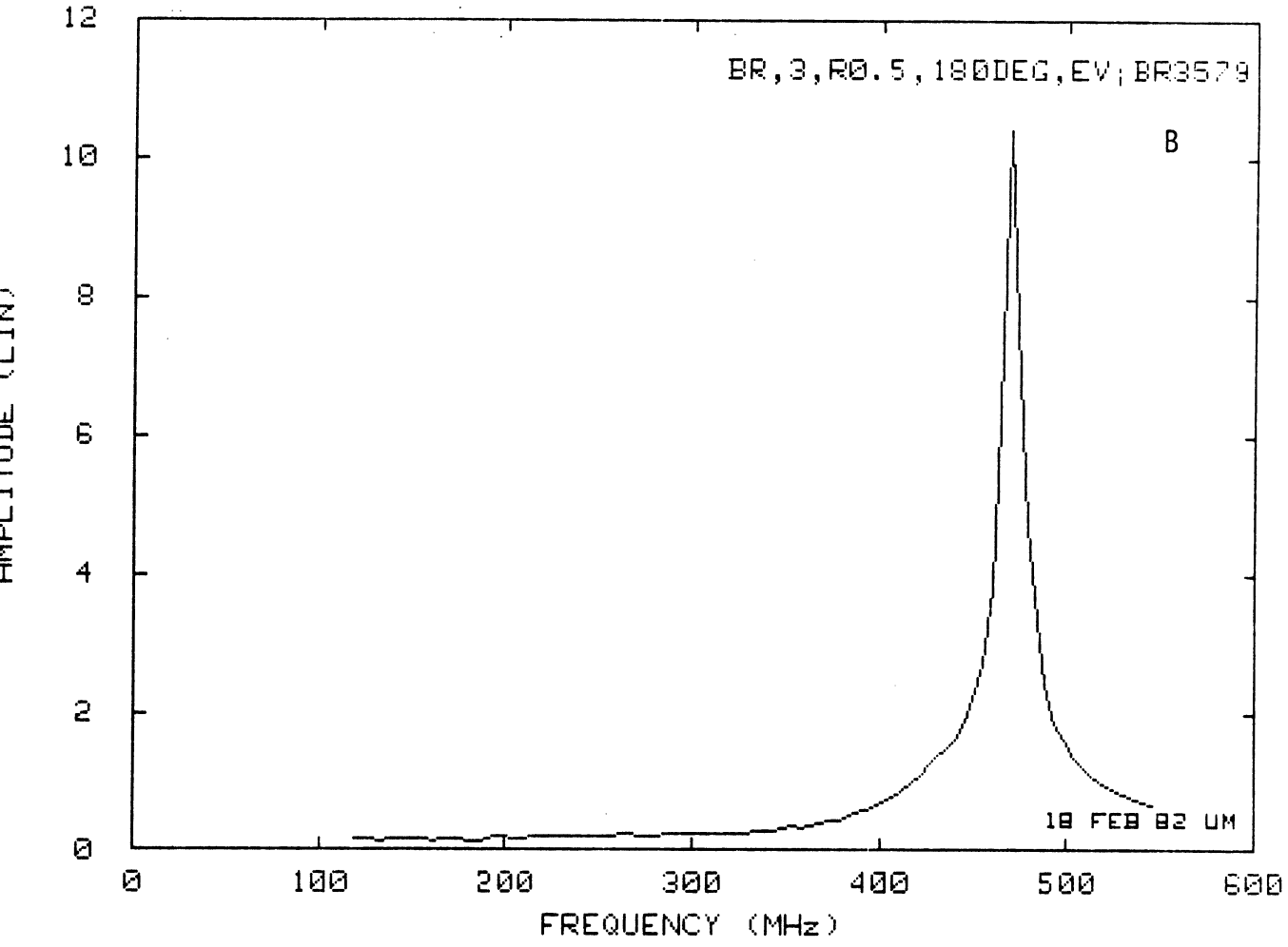
BR,3,R0.5,180DEG,EV;BR3579
B
18 FEB 82 UM
AMPLITUDE (LIN)
12
10
8
6
4
2
0
0
100
200
300
400
500
600
FREQUENCY (MHz)

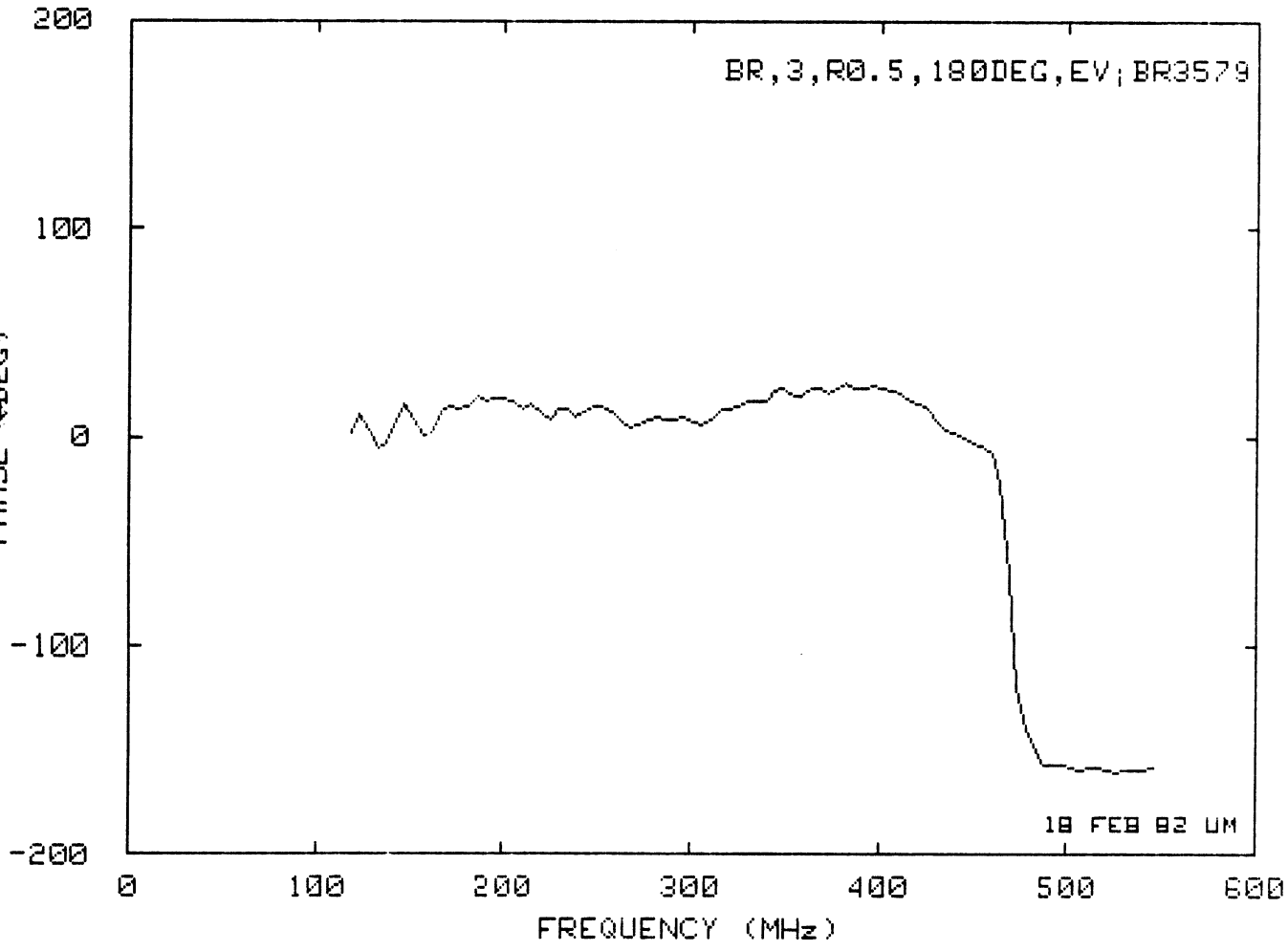
BR,3,R0.5,180DEG,EV;BR3579
18 FEB 82 UM
200
100
0
-100
-200
0
100
200
300
400
500
600
FREQUENCY (MHz)

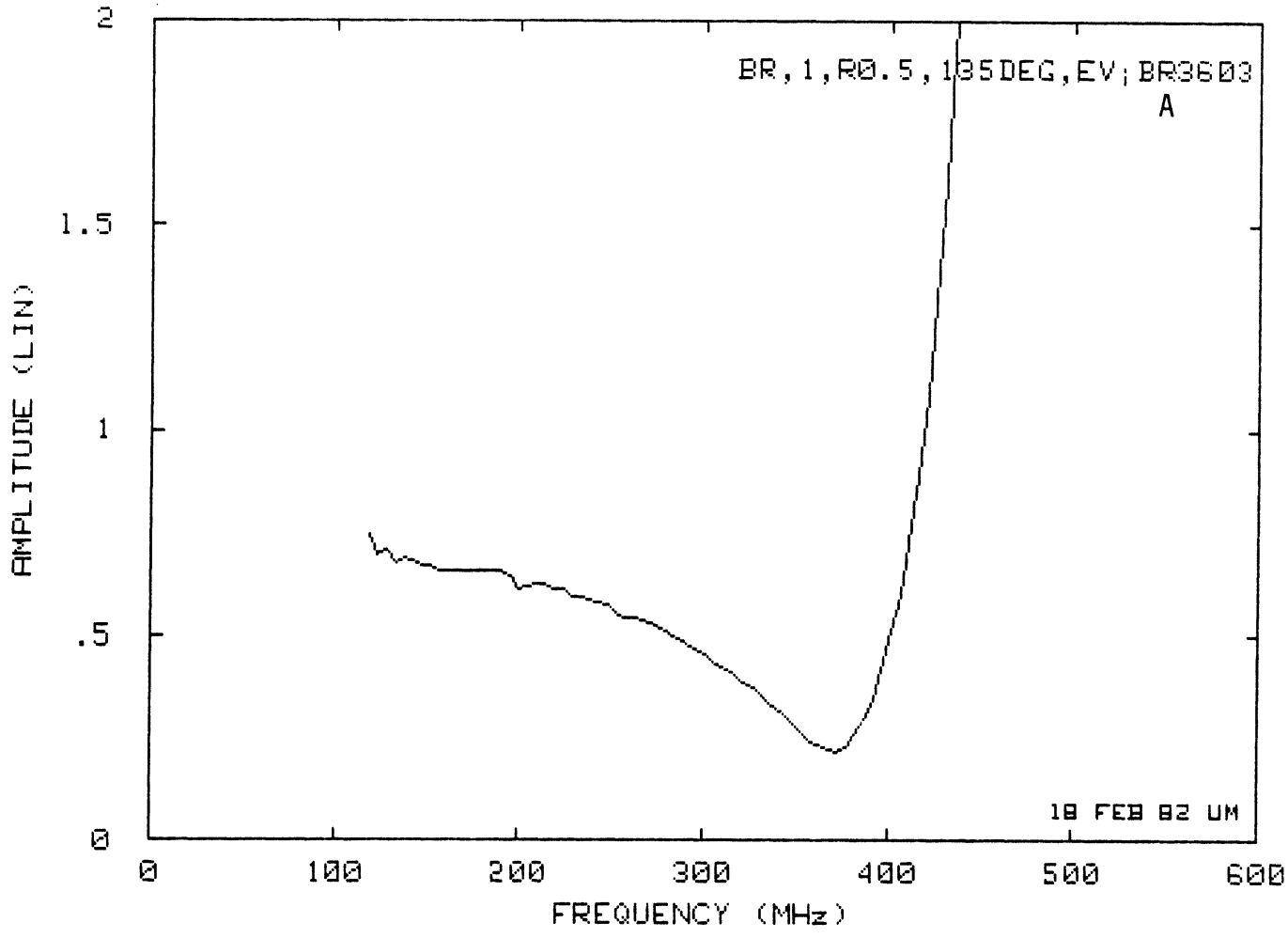
BR,1,R0.5,135DEG,EV;BR3603
A
18 FEB 82 UM
AMPLITUDE (LIN)
2
1.5
1
.5
0
0
100
200
300
400
500
600
FREQUENCY (MHz)

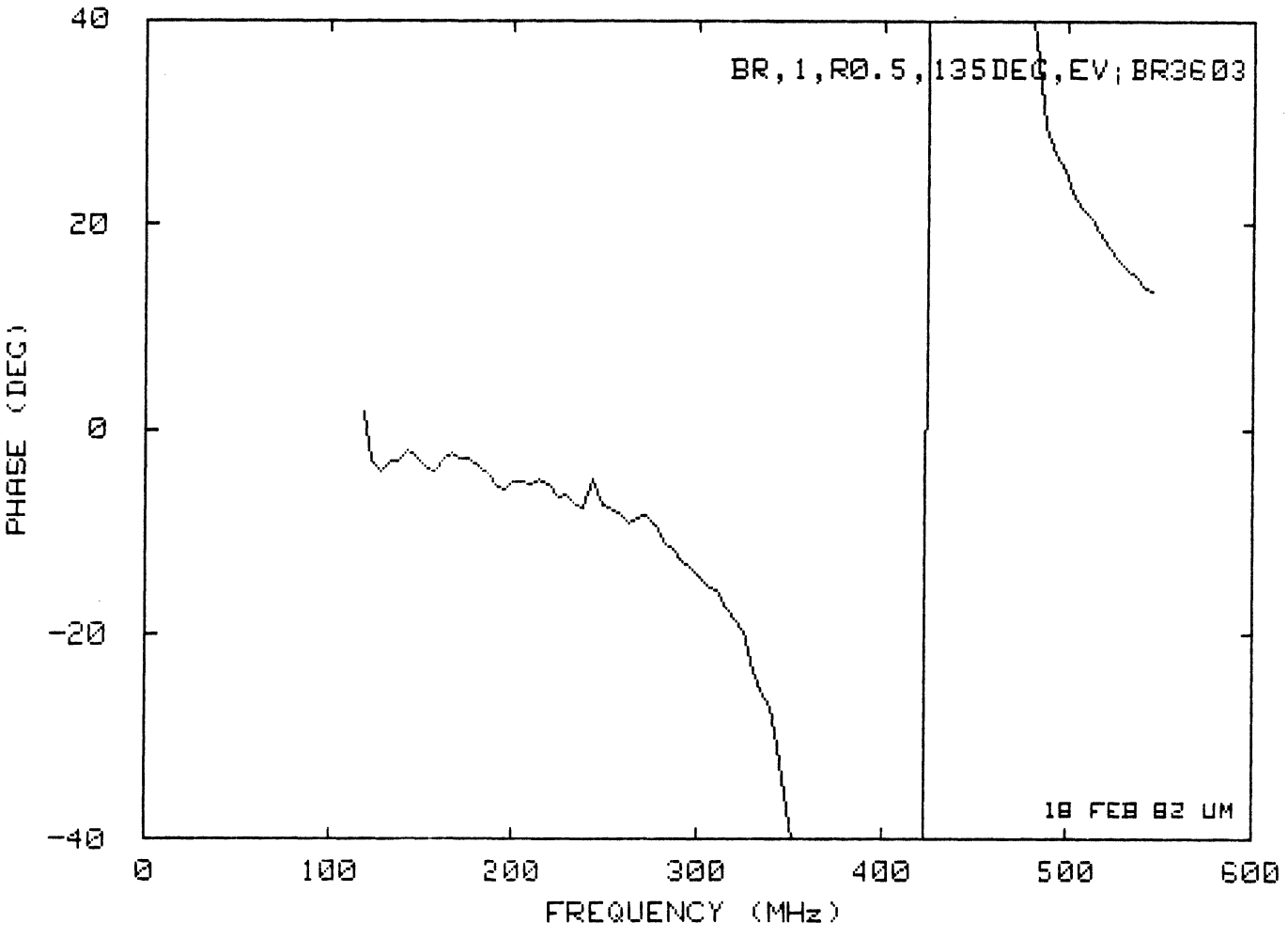
BR,1,R0.5,135DEG,EV;BR3603
18 FEB 82 UM
PHASE (DEG)
40
20
0
-20
-40
0
100
200
300
400
500
600
FREQUENCY (MHz)

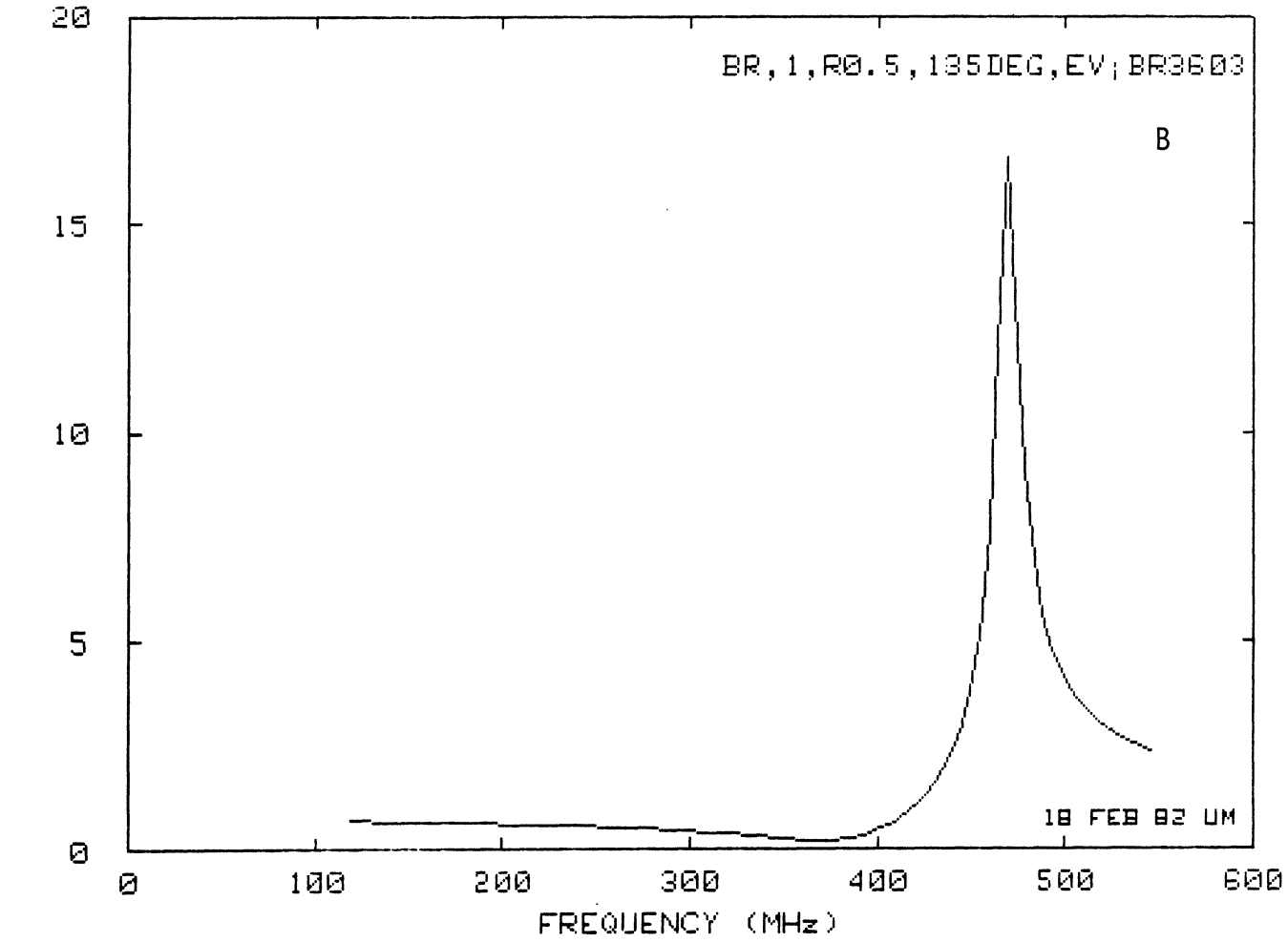
BR,1,R0.5,135DEG,EV;BR3603
B
18 FEB 82 UM
20
15
10
5
0
0
100
200
300
400
500
600
FREQUENCY (MHz)

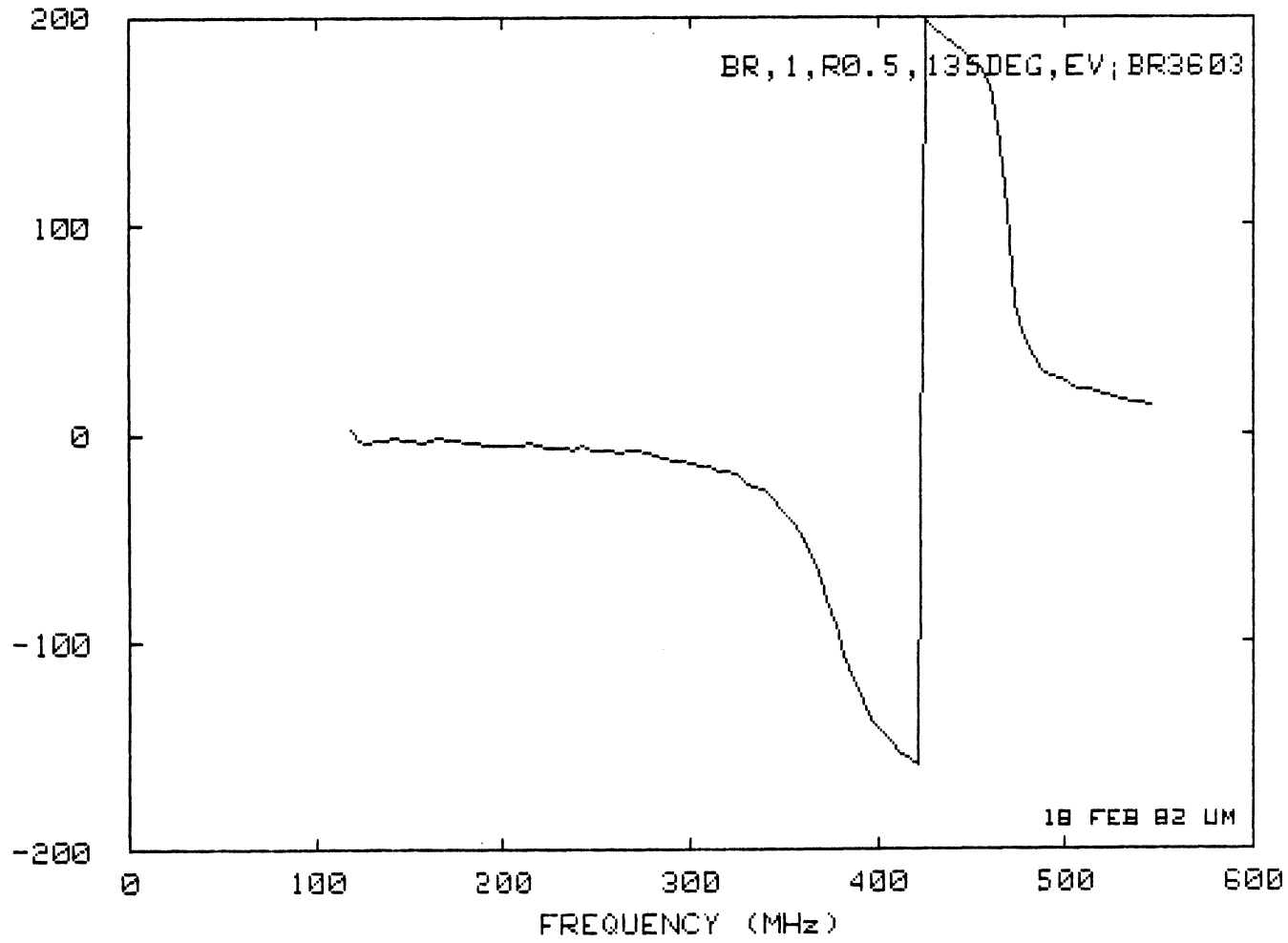
BR,1,R0.5,135DEG,EV;BR3603
18 FEB 82 UM
200
100
0
-100
-200
0
100
200
300
400
500
600
FREQUENCY (MHz)

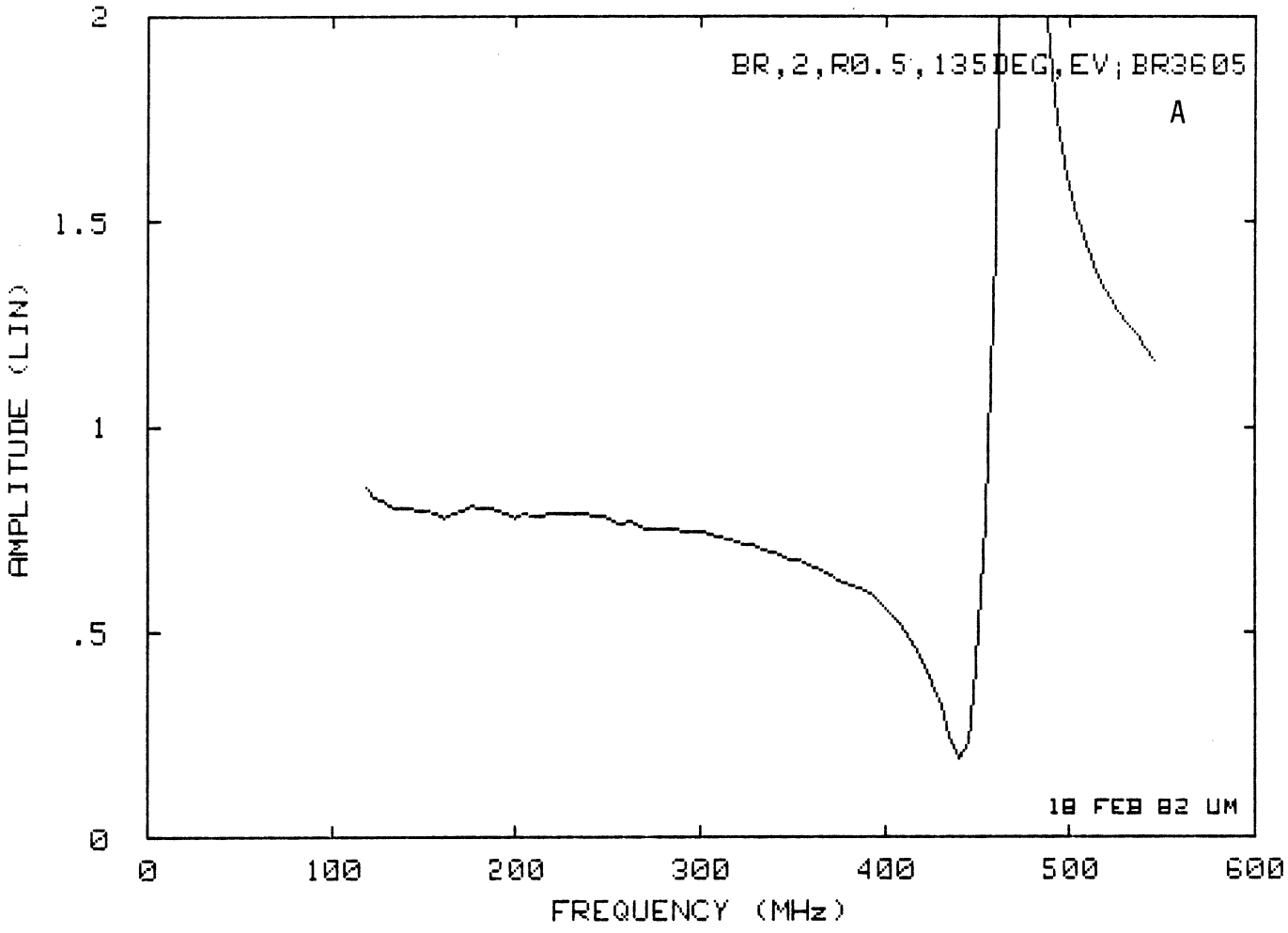
BR,2,R0.5,135DEG,EV;BR3605
A
18 FEB 82 UM
AMPLITUDE (LIN)
2
1.5
1
.5
0
0
100
200
300
400
500
600
FREQUENCY (MHz)

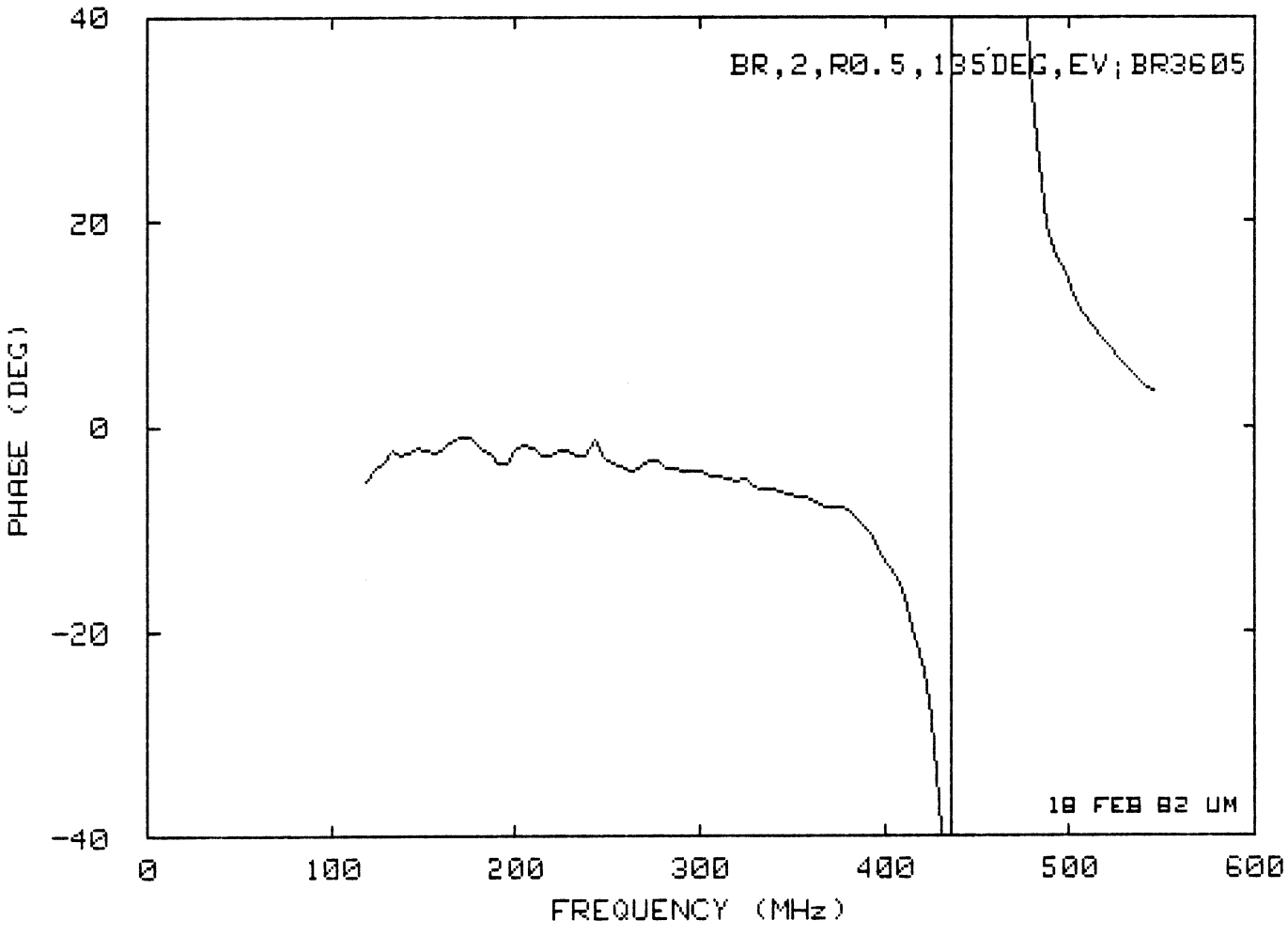
BR,2,R0.5,135DEG,EV;BR3605
18 FEB 82 UM
PHASE (DEG)
40
20
0
-20
-40
0
100
200
300
400
500
600
FREQUENCY (MHz)

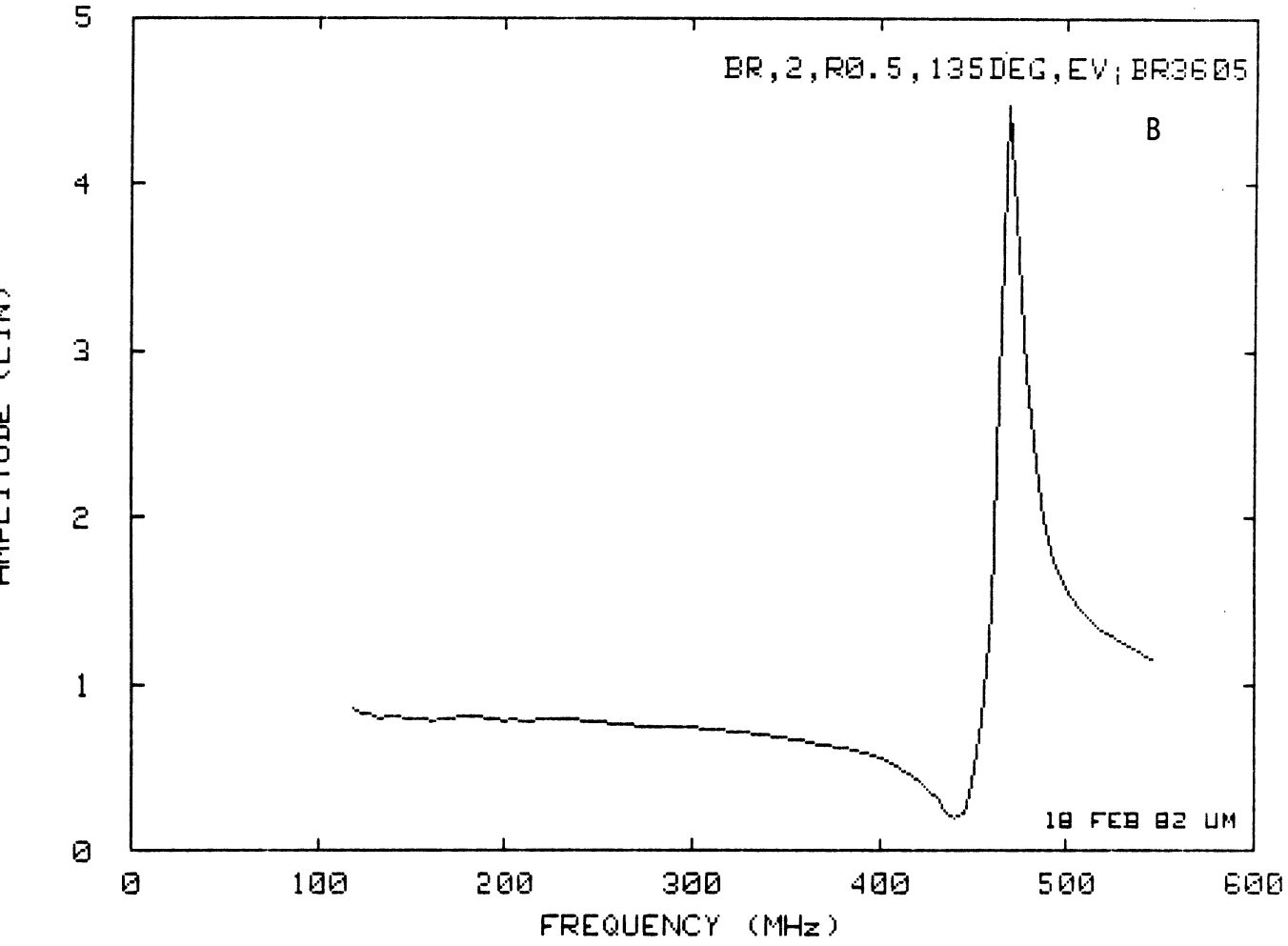
BR,2,R0.5,135DEG,EV;BR3605
B
18 FEB 82 UM
AMPLITUDE (LIN)
0
1
2
3
4
5
0
100
200
300
400
500
600
FREQUENCY (MHz)

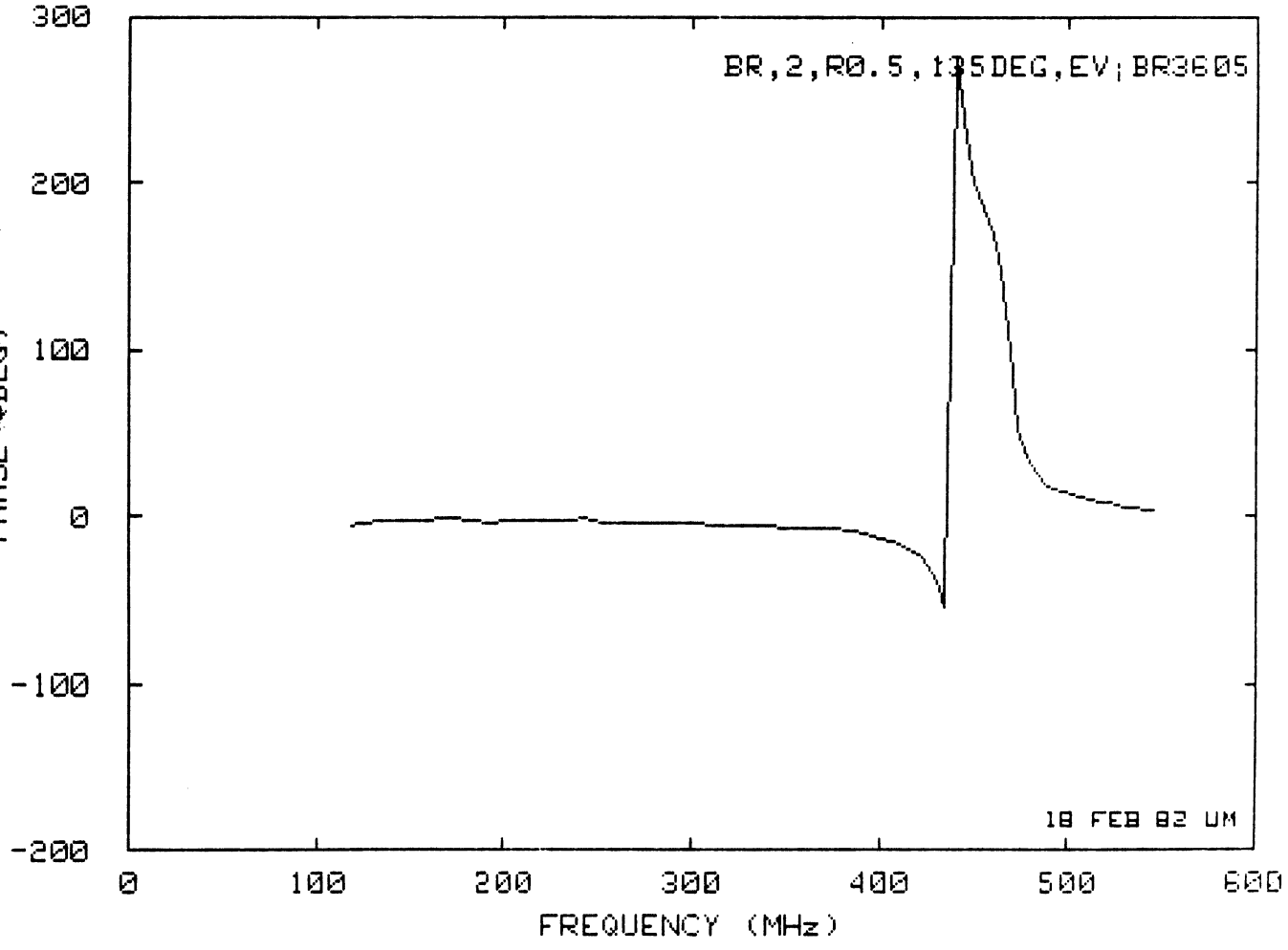
BR,2,R0.5,135DEG,EV;BR3605
18 FEB 82 UM
-200
-100
0
100
200
300
0
100
200
300
400
500
600
FREQUENCY (MHz)

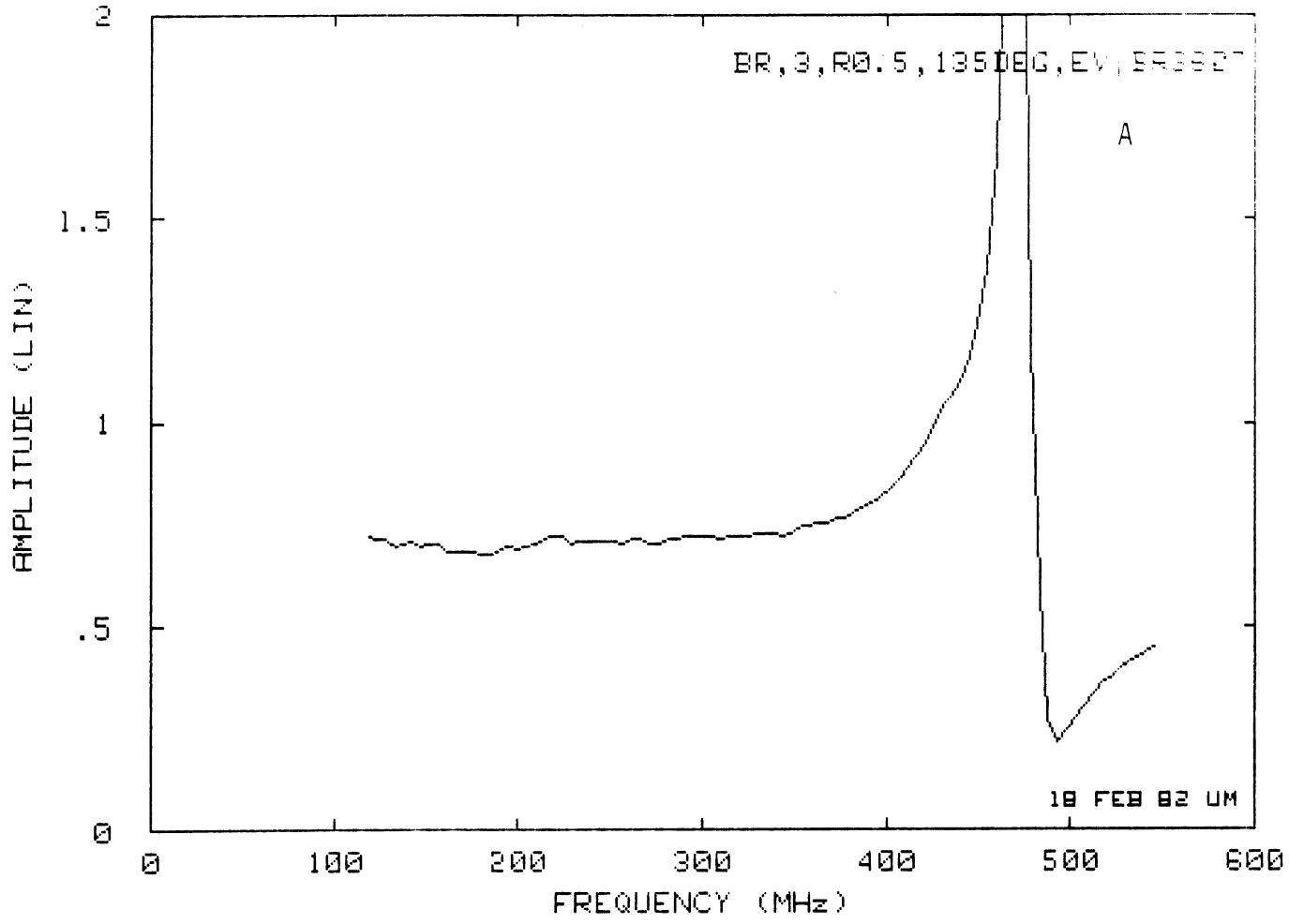
BR,3,R0.5,135DEG,EV;BR3607
A
18 FEB 82 UM
AMPLITUDE (LIN)
2
1.5
1
.5
0
0
100
200
300
400
500
600
FREQUENCY (MHz)

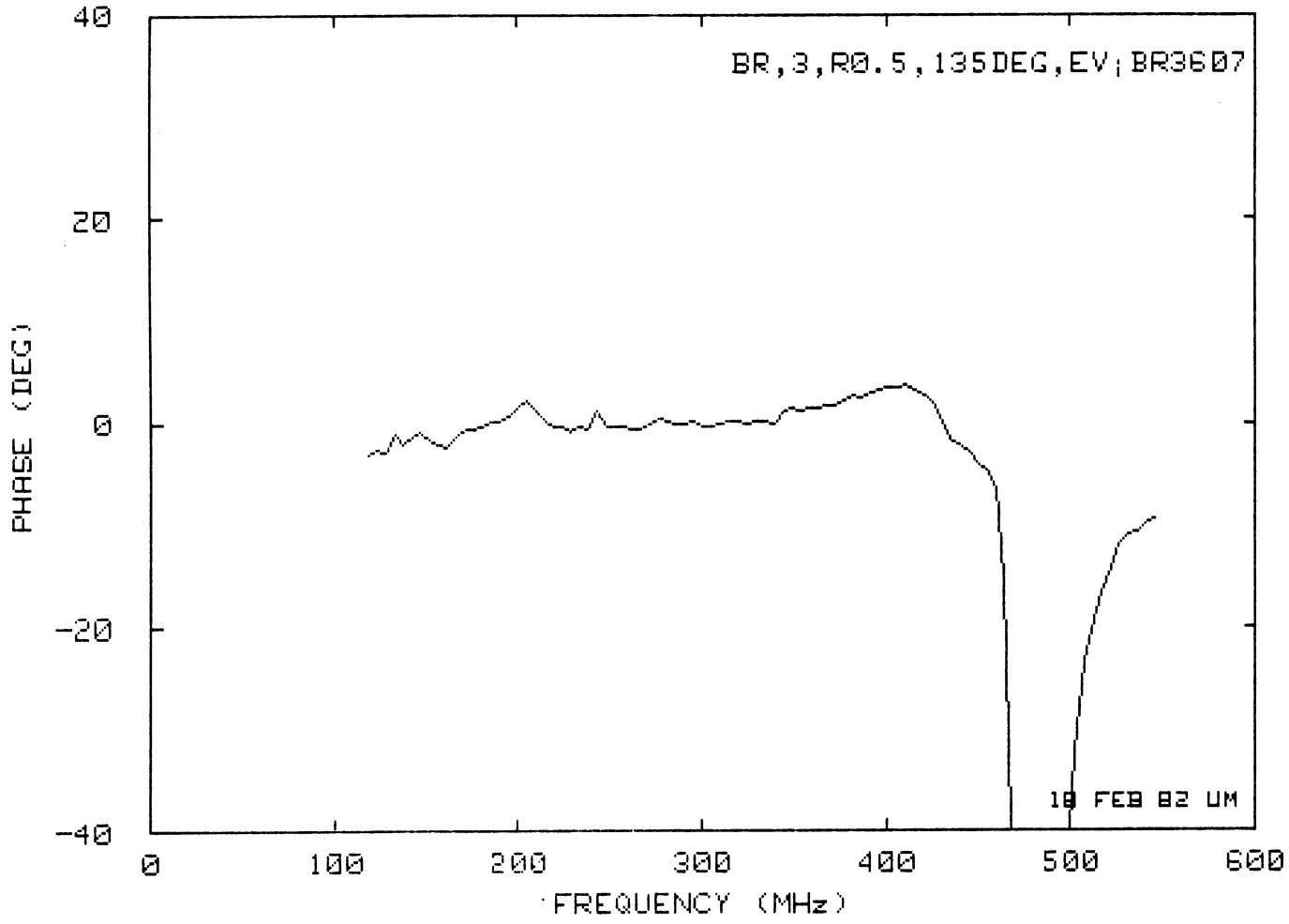
BR,3,R0.5,135DEG,EV;BR3607
18 FEB 82 UM
PHASE (DEG)
40
20
0
-20
-40
0
100
200
300
400
500
600
FREQUENCY (MHz)

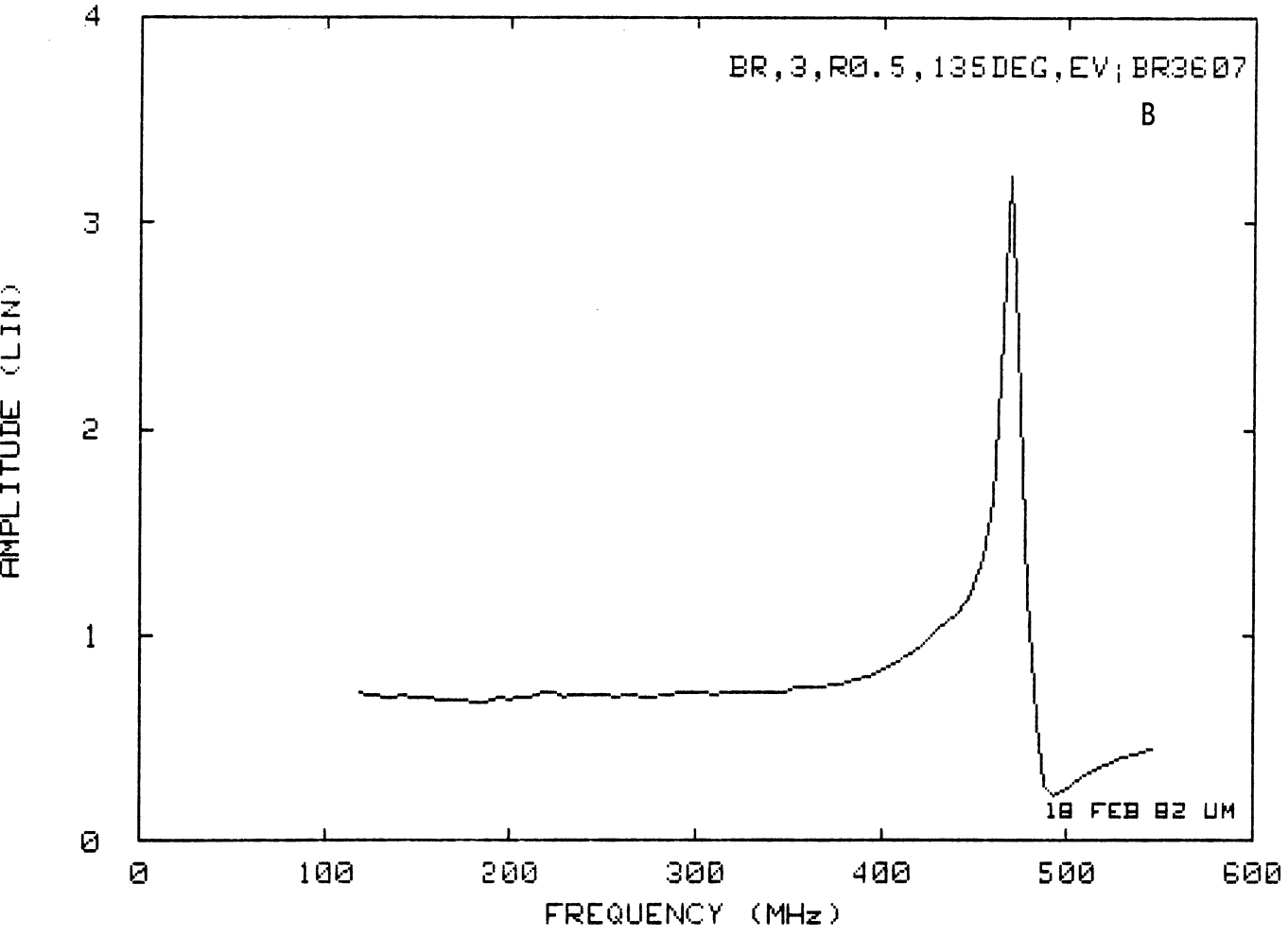
BR,3,R0.5,135DEG,EV;BR3607
B
18 FEB 82 UM
AMPLITUDE (LIN)
4
3
2
1
0
0
100
200
300
400
500
600
FREQUENCY (MHz)

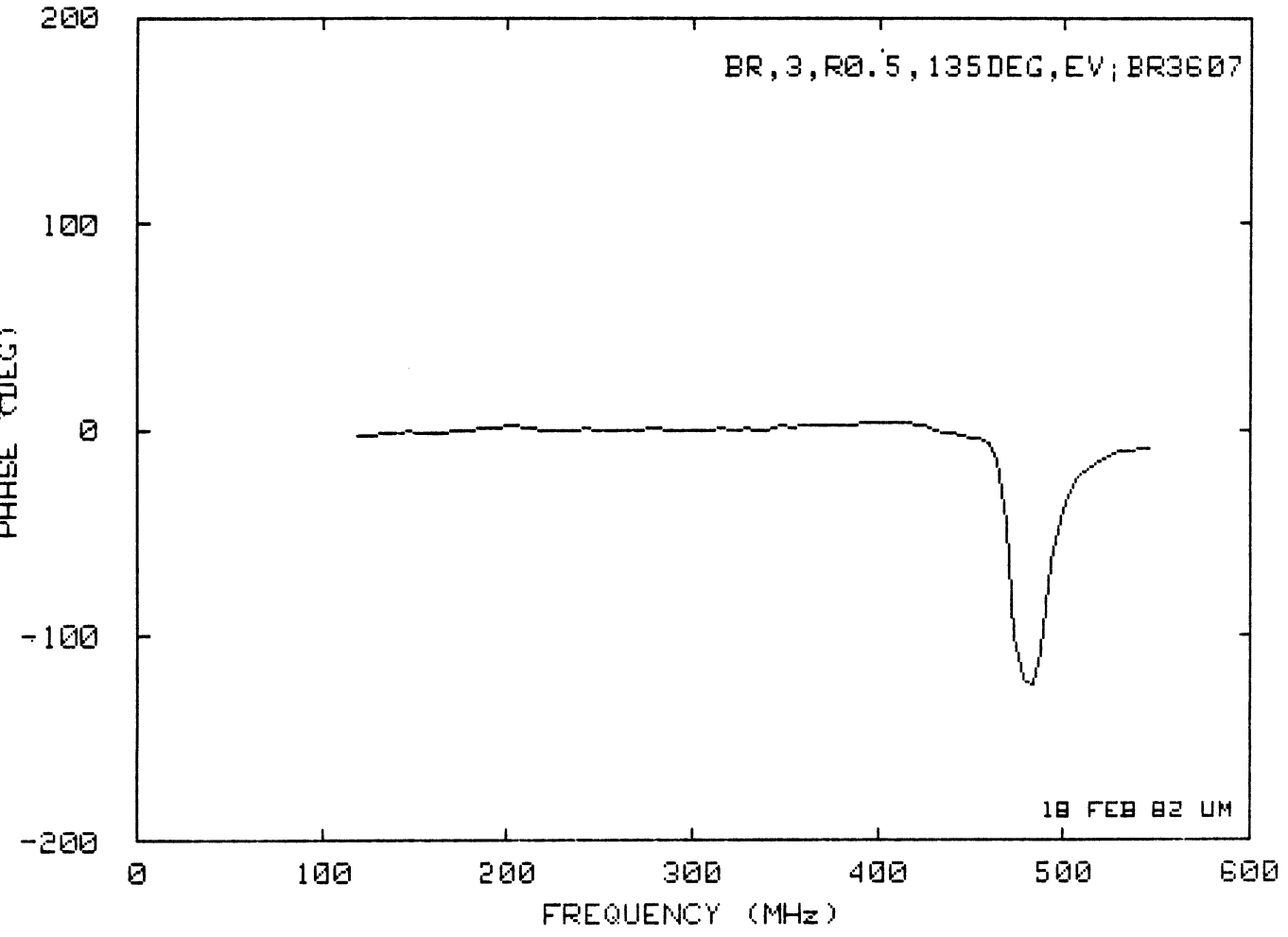
BR,3,R0.5,135DEG,EV;BR3607
18 FEB 82 UM
PHASE (DEG)
200
100
0
-100
-200
0
100
200
300
400
500
600
FREQUENCY (MHz)

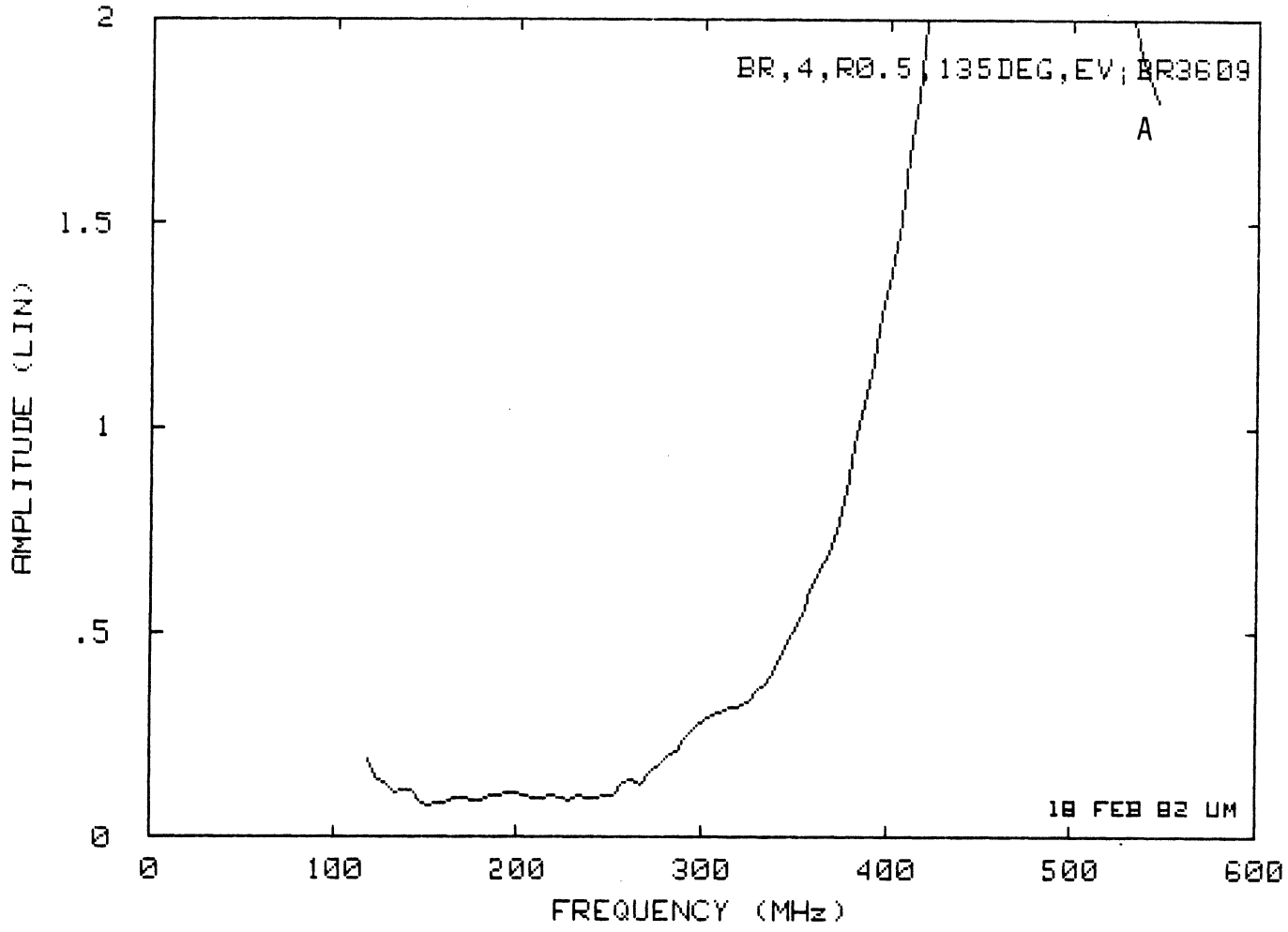
BR,4,R0.5,135DEG,EV;BR3609
A
18 FEB 82 UM
AMPLITUDE (LIN)
2
1.5
1
.5
0
0
100
200
300
400
500
600
FREQUENCY (MHz)

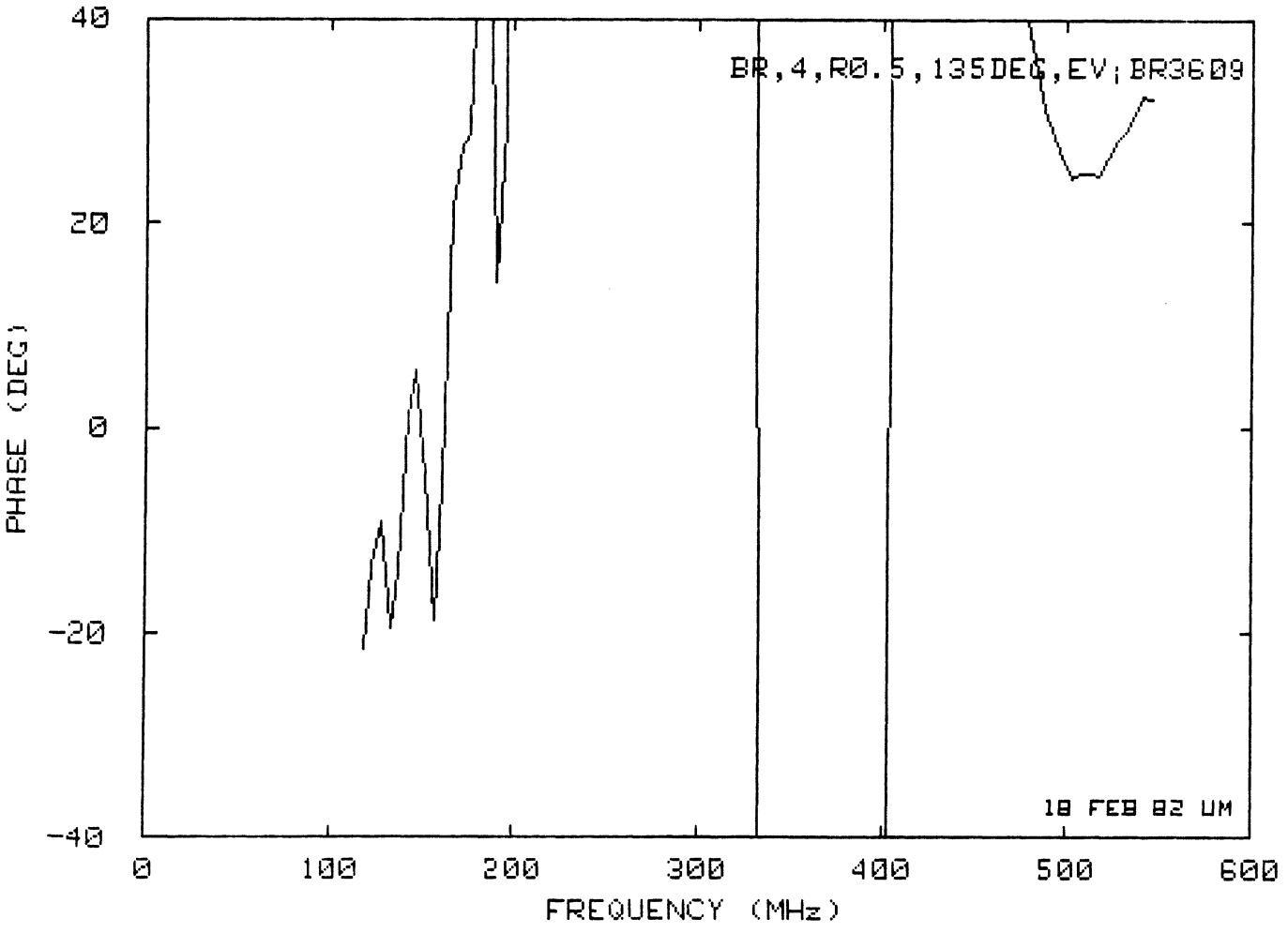
BR,4,R0.5,135DEG,EV;BR3609
18 FEB 82 UM
PHASE (DEG)
40
20
0
-20
-40
0
100
200
300
400
500
600
FREQUENCY (MHz)

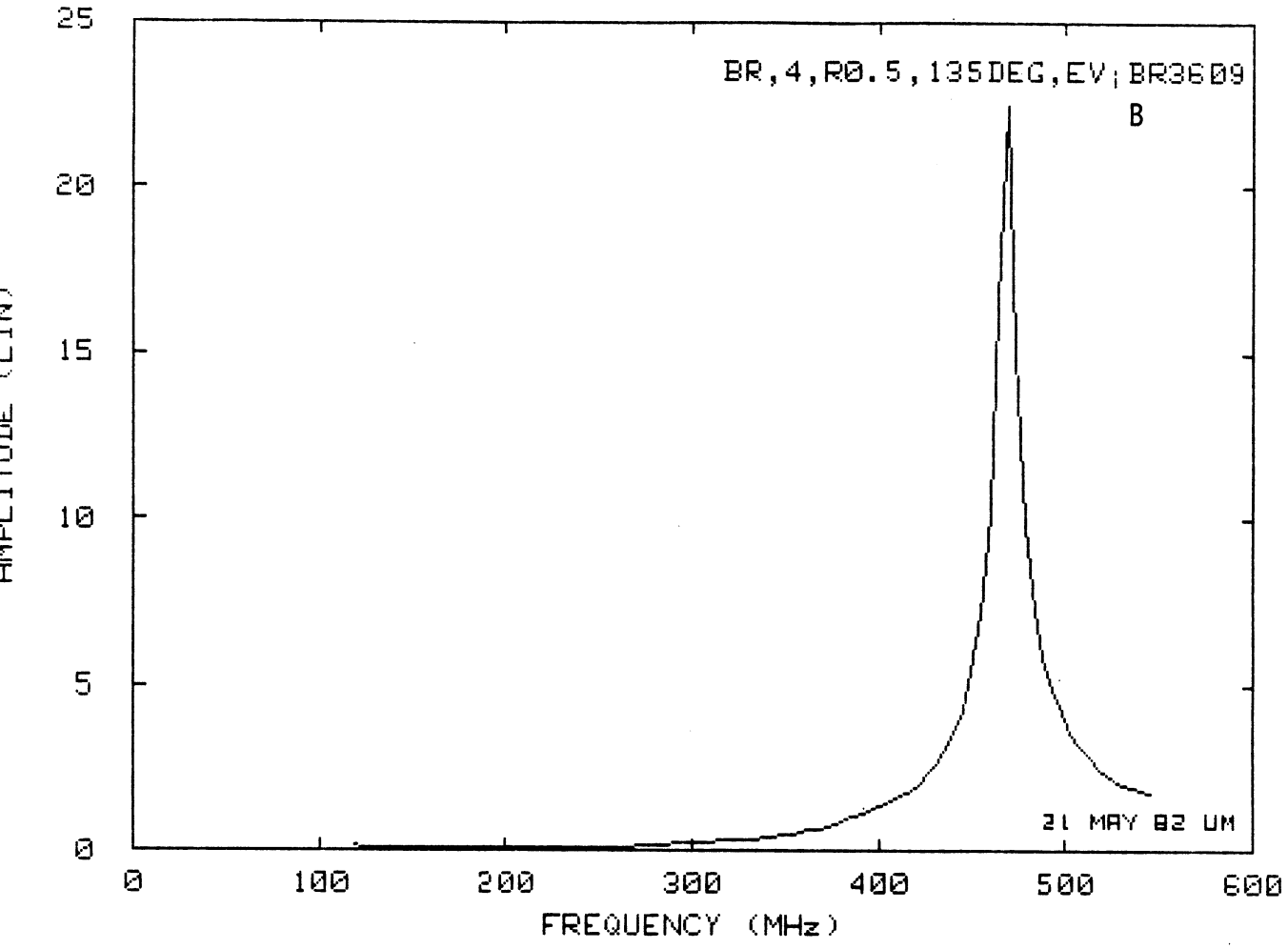

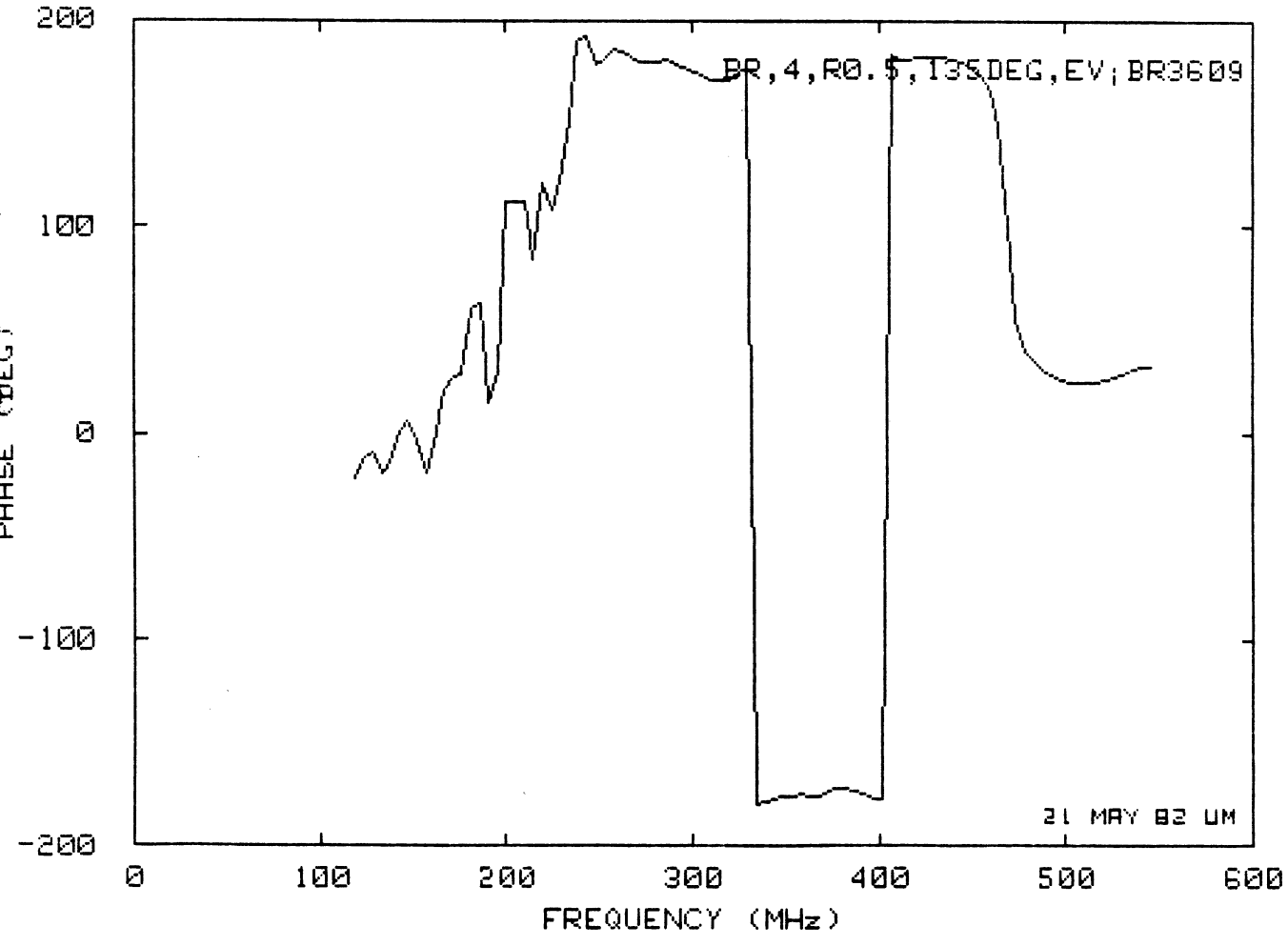

*U.S. GOVERNMENT PRINTING OFFICE: 1982 522-046/8594 1-3